

Propellants Manufacture, Hazards, and Testing

Propellants Manufacture, Hazards, and Testing

A symposium sponsored by
the Division of Industrial
and Engineering Chemistry
at the 153rd Meeting of the
American Chemical Society,
Miami Beach, Fla.,
April 10-11, 1967.

Carl Boyars and Karl Klager,

Symposium Chairmen

Library
American Chemical Society

ADVANCES IN CHEMISTRY SERIES

88

AMERICAN CHEMICAL SOCIETY
WASHINGTON, D. C. 1969

Coden: ADCSHA

Copyright © 1969

American Chemical Society

All Rights Reserved

Library of Congress Catalog Card 75-87208

PRINTED IN THE UNITED STATES OF AMERICA

American Chemical Society
Library
1155 16th St., N.W.
Washington, D.C. 20036

In Propellants Manufacture, Hazards, and Testing; Boyars, C., et al.;
Advances in Chemistry; American Chemical Society: Washington, DC, 1969.

Advances in Chemistry Series

Robert F. Gould, *Editor*

Advisory Board

Frank G. Ciapetta

William von Fischer

Frederick M. Fowkes

Edwin J. Hart

F. Leo Kauffman

Stanley Kirschner

John L. Lundberg

William E. Parham

Edward E. Smissman



AMERICAN CHEMICAL SOCIETY PUBLICATIONS

FOREWORD

ADVANCES IN CHEMISTRY SERIES was founded in 1949 by the American Chemical Society as an outlet for symposia and collections of data in special areas of topical interest that could not be accommodated in the Society's journals. It provides a medium for symposia that would otherwise be fragmented, their papers distributed among several journals or not published at all. Papers are refereed critically according to ACS editorial standards and receive the careful attention and processing characteristic of ACS publications. Papers published in ADVANCES IN CHEMISTRY SERIES are original contributions not published elsewhere in whole or major part and include reports of research as well as reviews since symposia may embrace both types of presentation.

PREFACE

On October 3, 1957 the first successful artificial satellite began to orbit the earth. The breathtaking advances in space flight since then are evidence of the rapid development of propellant technology. This development was able to proceed rapidly because a strong propellant technology based on military requirements already existed.

This volume is the result of a request by the American Chemical Society's Division of Industrial and Engineering Chemistry that we organize a symposium on propellants for the 153rd ACS national meeting in April 1967. The chapters are, for the most part, selected from those papers invited for the meeting; other papers were solicited later to provide more complete coverage of important areas. This volume is intended to introduce chemists and chemical engineers (and other scientists and engineers) to modern propellant technology; it is also intended to broaden the view of those already engaged in this field.

In organizing the symposium, we made the usual division into solid and liquid rocket propellants. Most readers no doubt already know the relative merits of solid *vs.* liquid systems—*viz.*, the instant readiness of solids (compared with cryogenic liquids), their higher density (important in volume-limited systems), and the relative simplicity of rocket construction; liquids offer easy variation in thrust level and the attainment of higher specific impulses, the latter because physical separation permits the use of fuels and oxidizers that would be incompatible if premixed.

Solid propellants utilize polymers, often with plasticizers, and often providing a matrix to contain other ingredients which participate in the combustion. The polymer-plasticizer combination provides the mechanical properties required and allows processing of the propellant into the desired shape and dimensions. Polymer and plasticizer may in themselves be energetic (capable of undergoing internal oxidation-reduction, exothermic, gas-forming decomposition) or may serve as fuels for suspended oxidizer particles. The first three chapters in this volume deal with solid propellants whose processing involves solution-gelation of the polymer. The next four chapters cover propellants in which the matrix is formed by *in situ* polymerization. These are followed by chapters on mechanical properties, combustion mechanism, and hazards. The volume concludes with chapters on liquid propellants, their properties, and their combustion mechanism.

We thank the authors and reviewers of each of the papers. We also express our appreciation to the myriad chemists and chemical engineers who have contributed and will continue to contribute to progress in all aspects of rocket propulsion—propellants, structural materials, insulation, adhesives, igniters, process control, and safety.

Silver Spring, Md.
Sacramento, Calif.
February 1969

CARL BOYARS
KARL KLAGER

Manufacture of Cast Double-Base Propellant

R. STEINBERGER and P. D. DRECHSEL

Explosives and Chemical Propulsion Department, Hercules, Inc.,
Wilmington, Del. 19899

The cast double-base process has been developed into a highly versatile technique for manufacturing solid rocket charges. Propellants manufactured by this process provide a wide range of energies, burning rates, and mechanical properties. Free-standing and case-bonded charges are manufactured routinely for many military and space applications, varying in size from ounces to several tons. The process consists of two basic steps: (1) "casting powder" is manufactured, consisting of nitrocellulose, plasticizers, and any solid ingredients; (2) casting powder is combined in a mold with "casting solvent," consisting of the remainder of the plasticizer. When this mixture is heated to moderate temperatures, a monolithic propellant grain is formed by plasticizer diffusion. A mathematical model of casting and curing has been evolved which relates processing conditions and material properties to the structural behavior of the propellant grain throughout the process.

The cast double-base process is a technique for forming solid propellant charges (grains) based on nitrocellulose as the polymeric binder and nitroglycerin or other high energy liquids as plasticizers. The process consists of two essential steps:

(1) Manufacture of casting powder: a product containing all the nitrocellulose and solid ingredients and a portion of the plasticizer is made in the form of a right circular cylinder approximately 1 mm. in diameter and length.

(2) Casting and curing: casting powder is loaded into a mold; the interstices between the granules are filled with a casting solvent consisting of the remainder of the plasticizer. On heating to moderate temperatures, interdiffusion of polymer and plasticizer occurs and knits the two-component system into a single monolithic grain.

Propellant Composition. In principle, any solid ingredient which is chemically compatible with nitrate esters can be introduced into the propellant by way of the casting powder. Any liquid ingredient used in the formulation must also be a plasticizer or co-plasticizer for nitrocellulose. In practice, three major families of compositions have been developed, differing in the composition of the casting powder (*see* Table I for typical compositions):

(1) Single-base casting powder: the casting powder consists of nitrocellulose, stabilizer, solid additives for ballistic modification, and a small amount of plasticizer. The normal ratio of casting powder to casting solvent, 2:1 by volume, yields a final composition of approximately 60% nitrocellulose.

(2) Double-base casting powder: this differs from single-base casting powder in that a significant amount of nitroglycerin is incorporated in the casting powder. The resultant propellant is more highly plasticized and more energetic than that made from single-base casting powder.

(3) Composite-modified casting powder: significant amounts of crystalline oxidizer and metallic fuel can be incorporated in double-base casting powder, yielding highly energetic propellant compositions. The nitrocellulose is even more plasticized in these compositions than in those made with double-base casting powder.

Table I. Typical Propellant Compositions

<i>Ingredient</i>	<i>Single Base, %</i>		<i>Double Base, %</i>		<i>Composite, %</i>	
	<i>C.P.^a</i>	<i>Prop.^b</i>	<i>C.P.</i>	<i>Prop.</i>	<i>C.P.</i>	<i>Prop.</i>
Nitrocellulose	88.0	59.0	75.0	50.2	30.0	22.3
Plasticizer	5.0	36.0	17.0	44.0	10.0	32.8
Ballistic Additives	5.0	3.4	6.0	4.0	—	—
Solid Oxidizer	—	—	—	—	28.0	20.8
Solid Fuel	—	—	—	—	29.0	21.6
Stabilizer	2.0	1.6	2.0	1.8	3.0	2.5

^a Casting powder.

^b Propellant.

From the manufacturing point of view these three classes of compositions differ mainly in terms of safety precautions, necessitated by incorporating nitroglycerin and/or solid oxidizers and reflected in equipment differences, remote operations, etc. The drying time for single-base casting powder is longer than for double-base and composite casting powders.

History. The cast double-base process was developed under U.S. Government auspices during World War II, the initial work being done by Kincaid and Shuey (7). The process filled a need for rocket charges significantly larger than those conveniently made by the then existing extrusion processes.

The early work was done with single-base casting powder in producing cartridge grains for such applications as aircraft JATO's, sounding rockets, and guided missiles. The success of the cast double-base approach was attributed in great part to the development of a ballistically attractive family of "plateau" propellants (8, 9) which utilized various lead salts of organic acids (*e.g.*, lead stearate) to create low temperature coefficients and low sensitivity of burning rate to pressure.

As the need for higher energy became pressing, double-base casting powders were developed which maintained the excellent ballistic properties of the earlier propellants. Moreover, since these compositions were more heavily plasticized, they were more suitable for case-bonded applications in which the propellant is cast directly into the motor and bonded to the wall; such applications demand a low modulus of elasticity and a high strain capability in preference to high strength. Case-bonded double-base propellants were first used in space launch vehicles—*e.g.*, Project Vanguard and Scout.

Another substantial increase in delivered energy was obtained by incorporating substantial amounts of solid oxidizer (*e.g.*, ammonium perchlorate) and metallic fuel (*e.g.*, aluminum) in the casting powder. The resulting family of composite-modified double-base (CMDB) propellants has found widespread use in ballistic missiles and space motors.

Accompanying the development of propellants has been an evolution of more complex grain designs demanding ever-increasing sophistication in tooling and casting techniques. Early examples of cast double-base propellants were straight cylindrical charges cast into cellulose acetate inhibitors and featuring star-shaped perforations for maintaining a constant burning surface (Figure 1). To accommodate the requirement for high thrusts and short burning times of larger charges with propellants having low burning rates, the multiperforated charge design evolved. In principle, this consisted of concentric rings of propellant connected by struts; in practice, it involved a complex array of arc-shaped mold cores held in place by appropriate base plates and spiders, still inside a cylindrical inhibitor tube. At the same time, the slotted tube design was introduced for longer burning applications.

The straight cylindrical configuration was appropriate for cartridge-loaded motors—*i.e.*, motors which permit the separate manufacture of propellant grains and subsequent loading into the chambers. More efficient designs, in terms of volumetric loading and mass fraction of propellant, are possible in case-bonded motors. This approach was first used with cast double-base propellants in the Altair motor for Project Vanguard, Scout, Delta, and other space missions. In such designs, it became appropriate to fill both domes of the motor with propellant and to work through relatively small openings at either end of the motor case

for introducing mold components and propellant. Star perforations and slots were still used for ballistic control; however, the geometric design problem shifted from a predominantly two-dimensional to a three-dimensional one. An added degree of complexity was introduced with the development of multinozzle configurations (typically four), demanding appropriately shaped channels leading to each nozzle.

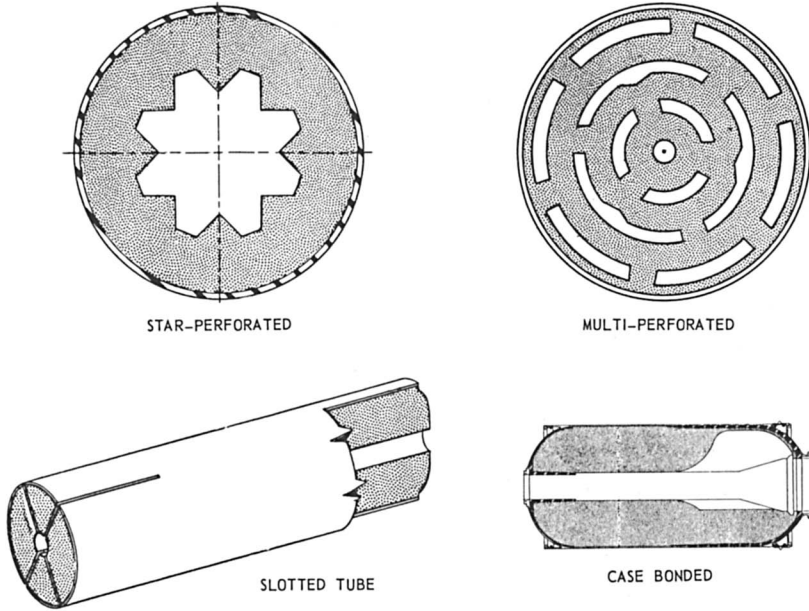


Figure 1. Propellant grain design

Manufacture of Casting Powder

Casting powder consists of right circular cylinders with a length-to-diameter ratio (L/D) of approximately unity; the casting powder comprises the polymeric binder (nitrocellulose), all other solid ingredients, and a fraction of the plasticizer and stabilizer intended for the final composition. The manufacturing process borrows heavily from that used for smokeless powder intended for guns, differing only where the incorporation of new ingredients demands special techniques.

Process Steps. Casting powder manufacture is basically a plastics-forming operation, utilizing a volatile solvent to impart mobility to the polymeric binder. The process is shown schematically in Figure 2 in terms of the major equipment used. For discussion, the process may be divided conveniently into the following operations:

(1) **Mixing.** All ingredients are blended in the presence of solvent to produce an extrudable dough.

(2) **Granulating.** The dough is shaped into right circular cylinders by extrusion into strands which are then cut.

(3) **Drying.** Volatile solvent is removed by exposure to a circulating hot fluid.

(4) **Finishing.** The granules are glazed with graphite, blended into large homogeneous lots, and screened to remove clusters, dust, and foreign material.

Many variations are practiced in each of these steps, depending on the composition, the facilities available, and the individual experience of the manufacturer. Since space is not available to treat each of these variations here, we shall describe a particular set of techniques used at one plant. For a more complete treatment of smokeless powder manufacturing techniques, we refer the reader to Refs. 2 and 3.

MIXING. Nitrocellulose is introduced into the process as alcohol-wet material in a lumpy condition. Depending on the needs of the subsequent process, it may be subjected to agitation in heavy duty mixers to reduce the size of the lumps.

For convenience in introducing nitroglycerin, a solution of nitroglycerin in a volatile solvent (typically acetone) is blended with the nitrocellulose in a Schrader bowl, a low shear mixer with large clearances. This is called premixing. The resulting premix serves as a feed stock for the final mixer, a heavy duty, horizontal, sigma-blade mixer. The mixer is jacketed to provide for circulation of hot or cold water during various stages in the mixing operation.

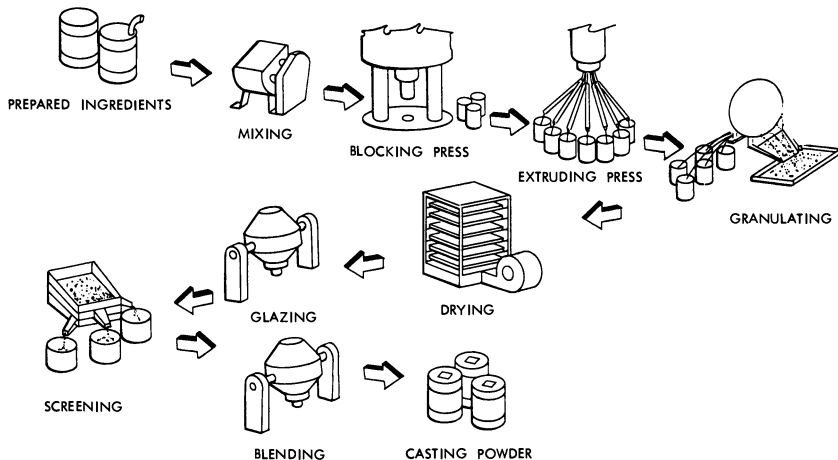


Figure 2. Casting powder manufacturing process

The mixer serves three purposes. First, it blends all the ingredients to provide uniform distribution in the final propellant. Second, it provides time, heat, and contact for solvation of all or part of the nitrocellulose by the volatile solvent and plasticizer. Third, it provides mechanical energy to disrupt nitrocellulose fibers and expose them to solvation. Solvated nitrocellulose is the matrix which bonds the rest of the material together and eventually gives strength and elasticity to the finished propellant.

At this stage many parameters control the uniformity and subsequent extrusion and handling characteristics of the product—*e.g.*,

(1) Solvent composition. Mixtures of ether or acetone and alcohol are commonly used as solvents.

(2) Solvent amount. The amount is largely determined by the amount of nitrocellulose in the composition. Figure 3 provides an example of the effect of solvent composition and amount on density.

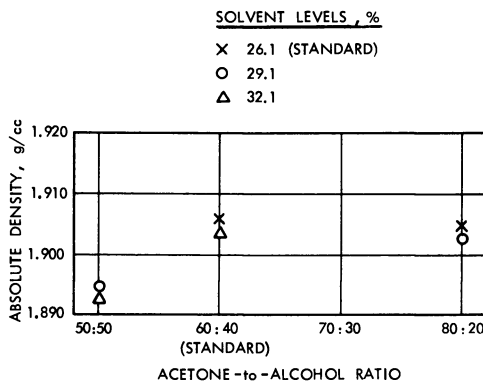


Figure 3. Effect of processing solvent on density of casting powder

(3) Order of adding ingredients. It is usually advantageous to provide for partial solvation of nitrocellulose first, thus establishing a viscous matrix which helps distribute the remaining ingredients.

(4) Temperature. Temperature is maintained just above the boiling point of the solvent to displace air without excessive loss of solvent.

(5) Time. An example of the breakup of agglomerates of solid oxidizer as a function of mixing time is given in Figure 4.

(6) Direction of blade rotation. (Blade speed is normally kept constant.)

(7) Solvent removal. When dough is oversolvated for any reason, the mixer lid is opened and/or air is circulated over the mixer charge to remove excess solvent.

Quantitative techniques are not commonly used for characterizing the dough at the conclusion of the mix cycle. Appearance of the mix and manual evaluation of consistency form the basis for determining whether the dough is mixed adequately and suitable for extrusion. Some progress has been made, however, in the use of a test pressing. In this test, a portion of the charge is loaded into a press, extruded at a standard rate, and the resulting pressure noted. This technique has been quite successful in providing mix-to-mix uniformity once the proper test pressure has been established empirically for a particular formulation.

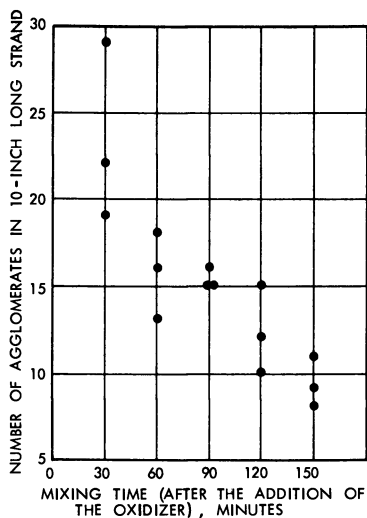


Figure 4. Effect of mixing time on breakup of agglomerates

In the mixing operation, it is standard practice to utilize as part of the ingredient feedstock a standard percentage of remix material, such as press heels, waste strands, etc., which has gone through the process once. Aside from the obvious economic advantage, the remix supplies presolvated nitrocellulose, giving better distribution of ingredients in the mix and thus improving mechanical and ballistic properties in the final propellant product.

As an added mixing step, a so-called "macaroni" operation is frequently used. It consists of preblocking the dough and extruding it through a set of large dies. In addition to the mechanical work input provided by this operation, it also serves to remove, *via* a screen placed in front of the die, some of the nitrocellulose agglomerates which resist blending into strands. The "macaroni" strands serve as feedstock for the granulation sequence.

GRANULATING. The shaping or granulating operation proceeds in three steps: preparing the dough for extrusion (blocking), extruding, and cutting. Blocking consists of loading the dough (in strands if the macaroni step was used) into a press and subjecting it to moderate pressure for a relatively short time. This prepares the feedstock in a form convenient for loading into a second press for extrusion. Moreover, blocking removes most of the occluded air with a resulting beneficial effect on casting powder density. Other desirable effects are improved consolidation, solvation, and homogenization of the charge. The temperature of the blocking press is maintained at the same level as that of the extrusion press.

An extrusion is comprised of a basket (cylinder) to contain the mix and a hydraulically actuated piston to press the mass through multiple extrusion dies. The baskets are jacketed for temperature control and contain internal screens to retain large agglomerates. Since the casting powder strands are unperforated, the dies are simple cylindrical barrels with conical lead-in sections. Extrusion rates are normally controlled by orifices in the hydraulic supply line; however, constant-rate positive displacement devices are also used. As they extrude, the strands are collected separately in suitable containers.

Extrusion parameters, such as basket temperature, extrusion rate, and die design, can be adjusted to suit a particular formulation and granule size. This is an empirical process based on experience. Extrusion characteristics represent an intimate interplay between press parameters and dough properties, the latter predominating. What is wanted is maximum production rate of a smooth, dense, homogeneous strand; of these qualities, smoothness is perhaps most sensitive to extrusion conditions.

After extrusion, the strands are cut using standard small arms, powder cutting machines which feature multiple blades on a circular cutting head. Several strands are cut at once. Length and perpendicularity of cut are controlled by synchronizing the feeding mechanism with the cutting head. Quality of cut is important since a ragged or slanted cut produces uneven edges or "tails" on the powder granule which leads to poor screen loading density (*SLD*). Meticulous attention is paid, therefore, to sharpness and adjustment of the blades. The plasticity of the strand also influences the neatness of the cut.

Precise control of L/D is complex since it depends on shrinkage characteristics during drying, which normally are anisotropic. Thus, the cutting operation must be conducted with full awareness of dimensional changes to be expected in the extrusion operation preceding it and the drying operation following it. Some typical dimensional changes are shown in Table II.

Table II. Dimensional Changes during Granulation

	Single-Base, inch	Double-Base, inch	CMDB, inch
Die diameter	0.049	0.053	0.122
Green strand diameter	0.041	0.044	0.118
Dried granule diameter	0.034	0.036	0.108
Length as cut	0.040	0.036	0.137
Dried granule length	0.035	0.035	0.129

In some instances it is advantageous to finish off the shaping task with a "green tumbling" operation, in which the solvent-wet (green) cut powder is tumbled in a barrel. A slight increase in *SLD* results, presumably by reducing the number of "tails" and by a slight rounding of the granules.

DRYING. A considerable amount of volatile solvent is removed by evaporation during the latter stages of mixing and by flashing from the strands at the extrusion and cutting steps. The remainder must be removed in the drying operation.

Single-base powder is considerably more difficult to dry than double-base or composite modified double-base (CMDB) compositions because more nitrocellulose, plasticized to a much lesser degree, is present, thus reducing the diffusion rate of volatiles. Therefore, single-base powder goes through a water dry operation, consisting of leaching in a hot water bath for several days. This heat transfer mechanism avoids premature drying and case hardening of the granule surface, thus promoting complete diffusion of solvent out of the interior of the granule. Solvent and water removal are completed in a stream of hot air. Even with vigorous drying, it is difficult to reduce the total volatile content below 1%.

Double-base and CMDB powders are loaded on shallow trays which are stacked in dry houses and subjected to a stream of hot air (140°F.) for several days. Results of a typical drying run for a double-base casting powder are shown in Figure 5. Initial drying is quite rapid; however, extended cycles are required to get consistent values below the specification maximum, in this case 0.50% total volatiles (TV).

The effect of TV on *SLD* can be surprisingly significant as shown in Figure 6 for CMDB formulation. Clearly, neither the change in *SLD* nor the corresponding change in absolute density can be accounted for by the change in composition. The *SLD* change possibly reflects a change in surface characteristics which makes the granules more susceptible to smoothing during the subsequent glazing and blending.

FINISHING. After casting powder has been dried, several operations are required to make it suitable for use. The first is glazing, which reduces the electrostatic charge which may accumulate in a moving mass of powder and promotes easy flow. A small amount (typically 0.05%) of

graphite is added to the powder in a tumbling barrel and is distributed over the surface of the granules by slow rotation of the barrel; a typical glazing cycle consists of five revolutions per minute over a period of 2 hours. This process increases the conductivity of a dry bed of casting powder by a factor of almost a million.

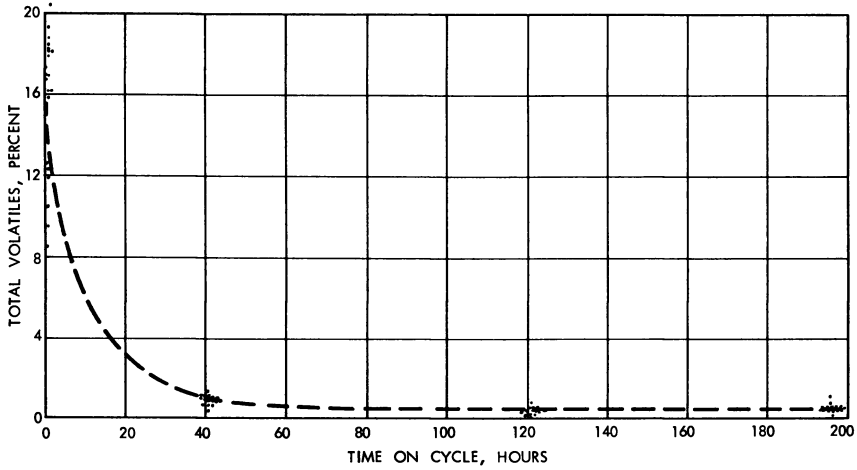


Figure 5. Total volatiles vs. drying time

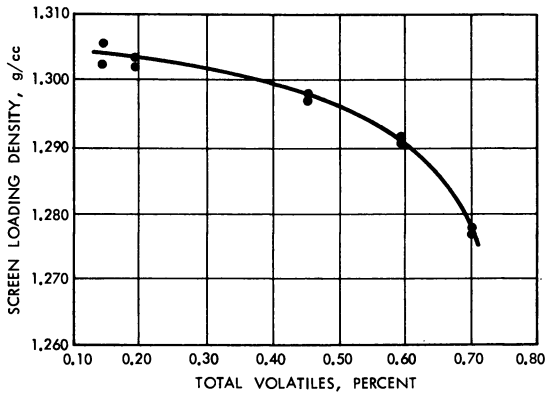


Figure 6. Effect of percent total volatiles on the screen loading density of casting powder

Since the tumbling barrel has a capacity of approximately 5000 lbs., glazing constitutes the first step of the blending operation where casting powder lots of any size (1 million lbs. is not uncommon), representing many mixer loads and many days of operation, are combined as homogeneous lots. This practice of blending large lots of casting powder provides the basis for the high level of reproducibility in cast double-base

propellants. Minor variations in material and processing conditions during casting powder manufacture are evened out by this technique; since the properties of the final cast propellant are determined largely by the properties of the casting powder, reproducibility is assured.

The blending step can also be used to provide precise adjustment in propellant properties, based on the measured properties of sublots. Figure 7 shows the effect of blending two sublots, the resulting burning rate in this case reflecting a disproportionate influence of the higher rate subplot. Similar adjustments in mechanical properties, *SLD*, etc., are feasible.

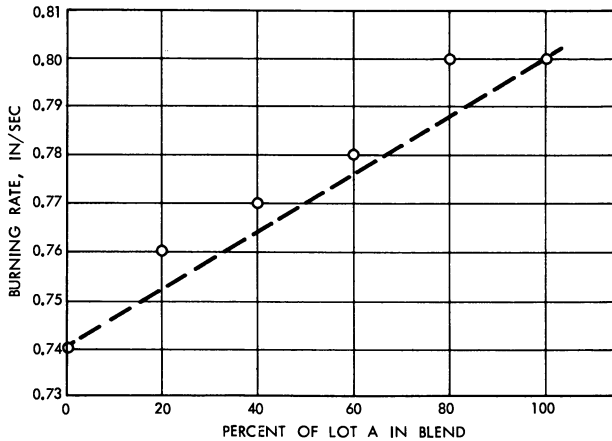


Figure 7. Burning rate of casting powder blends

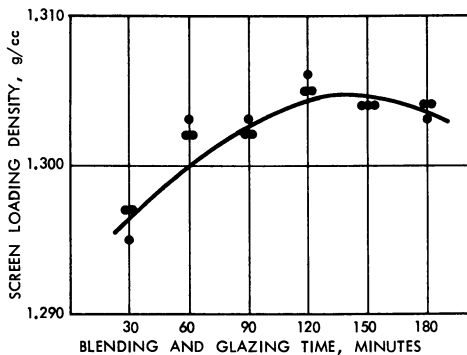


Figure 8. Effect of tumbling time on screen loading density

An important side effect of the glazing and blending operations is an increase in *SLD*, traceable to a general smoothing of the granule surfaces by attrition. A typical set of data is given in Figure 8.

Finally, the casting powder is screened to remove clusters and foreign material and then packed into containers typically holding 150 lbs.

Casting Powder Parameters. The steps in the foregoing description of casting powder manufacture are designed to yield certain characteristics in the final product. The properties desired in casting powder and the significance of these properties are described below.

DENSITY. The density of the casting powder should be the highest possible, normally higher than 97% of theory. Deviations arise from two sources: voids and volatiles. Voids represent air which may not disappear during final processing of the propellant and may, therefore, lead to pits or porosity in the grain. The resulting ballistic effects can be severe, depending on motor design and inherent ballistic properties of the propellant. Mechanical properties will also be degraded. Volatiles, such as moisture and processing solvent, are always present to a certain extent. Complete elimination by drying is not feasible. Volatiles act as plasticizers and coolants, and their presence is taken into account in the normal evaluation of a propellant. Excess amounts, however, will alter mechanical properties and curing characteristics, paralleling the effect of excess inert plasticizer. Minor ballistic changes will also result.

MOISTURE AND VOLATILES. These are measured as independent quantities, largely as an indication of the efficiency of the drying process. Possible undesirable side effects were mentioned above. As nitrocellulose is slightly hygroscopic, casting powders will often pick up small percentages of moisture from the atmosphere (*see* Figure 9). Normal total volatile contents range from 0.5 to 1.0%.

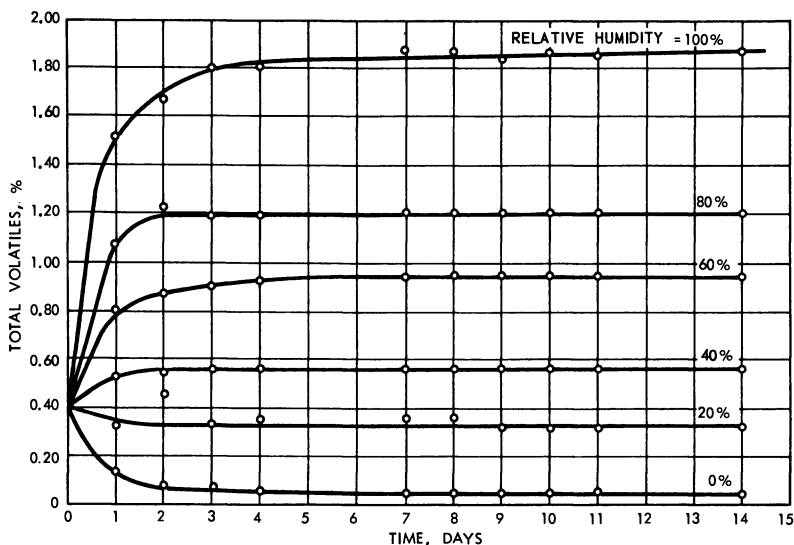


Figure 9. Moisture gain and loss of casting powder

SCREEN LOADING DENSITY (*SLD*). The packing fraction of the casting powder as loaded into a mold will determine the final composition as it controls the ratio of casting powder to casting solvent (*P/S*) and thus directly affects all propellant properties. This is demonstrated in Figure 10 where tensile strength is shown to be a highly sensitive property. As a relative measure of packing fraction, the parameter *SLD* is used, referring to a standard technique for obtaining a quantitative value. It consists of filling a standard container with casting powder through a standard screen which acts as a distributor and weighing the amount loaded. *SLD* is sensitive to variations in density and *L/D* as well as to imperfections in the surface characteristics of the granules, ragged cuts (tails), poor glazing, etc. For uniformity of final propellant properties over a long production run, maximum *SLD* is desired.

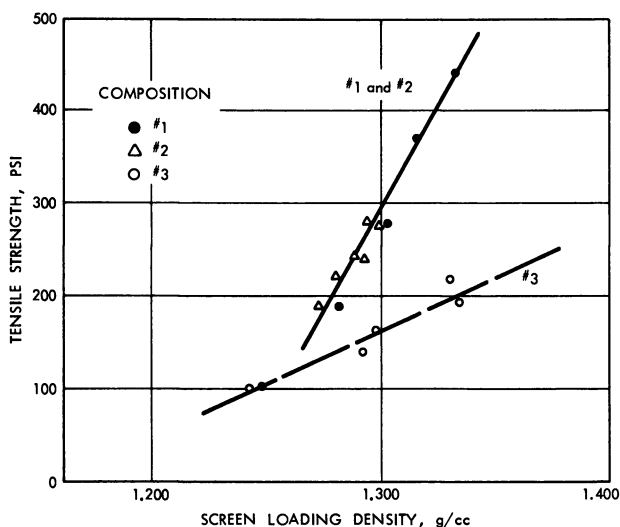


Figure 10. Effect of casting powder *SLD* on tensile strength of propellant

UNIFORMITY. For optimum properties and highest degree of reproducibility, all ingredients should be distributed uniformly throughout the casting powder granule. This is particularly true of the ballistic modifiers since burning rates can vary dramatically, depending on uniformity of distribution. Mechanical properties depend critically on the availability of nitrocellulose for plasticization. Therefore, it is important that a significant fraction of the original nitrocellulose fibers be disrupted and that a homogeneous matrix of partially plasticized nitrocellulose be present

throughout the granule. In some compositions of high nitrocellulose content, some of the fibrous structure is maintained, and these particles end up acting as filler rather than binder. Unfortunately, no quantitative measure of uniformity has been developed. Some qualitative information can be gained from microscopic examination.

SWELLING CHARACTERISTICS. The rate and uniformity with which casting powder granules are plasticized by casting solvent are critical in determining the proper cure conditions and the properties of the final propellant. Swelling characteristics are measured by dilatometric and microscopic techniques described in detail later.

Propellant Charge Manufacture

Steps in Propellant Grain Manufacture. The manufacture of a propellant charge proceeds by the steps depicted in Figure 11.

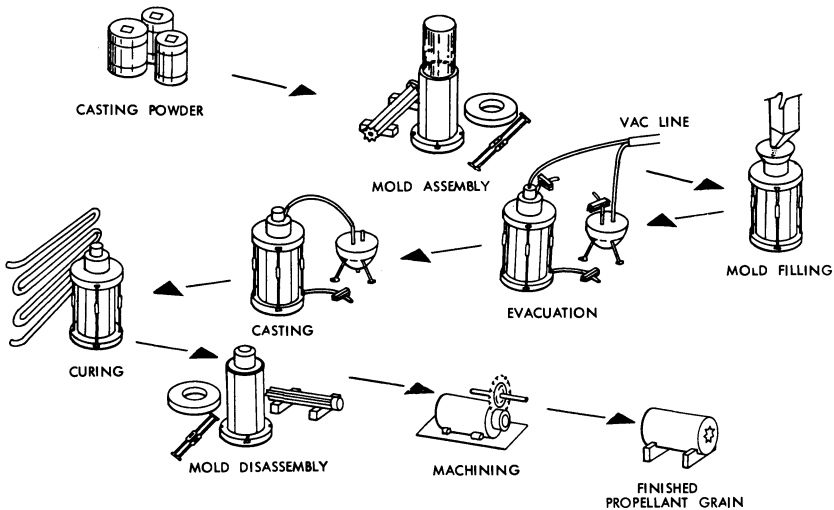


Figure 11. Propellant grain manufacturing process

MOLD FILLING. The first basic step is to fill a mold or the motor case with casting powder. Ideally, the technique selected to fill the mold is one which results in maximum reproducible loading density. Simple dumping or pouring yields low packing density and results that are not very reproducible. In well-loaded units, the packing density is such that 68 vol. % of the container is occupied by casting powder. Simple dumping might lead to only 57%.

Early in the history of the cast double-base process, the principle of screen loading was discovered. In essence, it was found that an evenly

distributed "rain" of powder granules falling 2 or more feet at a controlled rate would pack a vertical cylindrical mold densely and uniformly. Cylindrical cartridge-loaded propellant charges are normally made by loading molds using a screen loading adapter. This is a full-diameter tube fitted with an upper distributor plate with comparatively large evenly spaced holes and a lower screen dispersion plate with holes approximately twice the powder diameter. Powder flows from a hopper through the distributor plate to the screen plate which, in turn, disperses the powder evenly onto the powder bed.

With the advent of dome-ended, case-bonded units like Altair, the restricted end-openings of these motors prevented proper distribution and packing by the early screen-loading technique. Mold-filling studies showed that chambers with restricted openings and complicated core configurations could be filled satisfactorily if the powder granules were accelerated by air moving through tubes at relatively high velocities and then dispersed and/or deflected into the chamber at the proper angle (see Figure 12). This method known as the "air dispersion powder filling technique" has proved to be equal or superior to the standard screen-loading method.

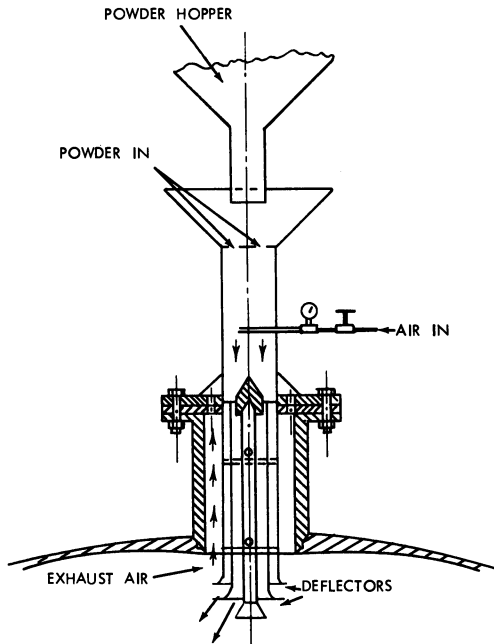


Figure 12. Air dispersion powder filling apparatus

In combination with the above techniques, vibration has also been used to achieve maximum bulk density in mold or motor. The powder bed is usually vibrated by externally mounted, pneumatic vibrators. Variable results have been obtained in the studies of the effectiveness of vibration in full-scale units. In some instances, bulk density has been improved; in others no improvement has been noted. Even with a given motor and mold-filling apparatus, the effectiveness of vibration may depend upon the particular type of casting powder.

Table III summarizes the results of a laboratory-scale investigation of these various powder-loading techniques. Except for simple pouring, the differences between various filling techniques may be relatively minor. In practice, the method selected depends upon the casting powder type and the geometry of the charge to be manufactured.

Table III. Relative Bulk Densities by Various Mold-Filling Techniques

<i>Mold Filling Method</i>	<i>% Standard Laboratory, SLD</i>
Pouring	88.5
Screen load	101.0
Screen load (vibration)	101.6
Air load	101.9
Air load (vibration)	102.2

EVACUATION. After the mold or motor is filled with casting powder, it is subjected to a vacuum (< 10 mm. Hg) to remove volatiles, especially air. This is commonly carried out in a vacuum bell for periods ranging from 16 to 40 hours, depending on the size of the casting powder granules.

Before casting, the casting solvent is usually evacuated in a desiccator for at least 16 hours, maintaining the pressure below 10 mm. Hg. To increase the efficiency of removing volatiles, the casting solvent is often agitated by allowing a small stream of dry air to bubble up from the bottom of the solvent desiccator.

CASTING. The casting step consists of filling the interstitial space in the powder bed with casting solvent, a mixture of nitrocellulose plasticizers. The casting solvent may be introduced to the bed from the top of the mold, from the bottom, or radially from perforated cores. Both bottom and top castings are commonly used today. Figure 13 shows a typical arrangement for bottom casting under vacuum. Here, solvent is forced up through the powder bed by applying pressure to the surface of the casting solvent desiccator. Some types of casting powder are best cast under vacuum for maximum freedom from porosity. However, many

full-scale units are successfully cast with the powder bed kept at atmospheric pressure during casting.

CURING. When the mold or motor is completely filled, the propellant mass consists of two macroscopic phases, powder and solvent, and pressure is applied independently to each phase. One arrangement which permits this is shown in Figure 14. In the motor shown, a piston (ram) applies pressure to the bed through a column of powder which extends out through one or more of the motor openings. Perforations in the piston face permit hydraulic pressure to be applied to the casting solvent phase independently during the early stages of cure. Solvent pressures up to 60 p.s.i.g. and ram pressure up to 200 p.s.i.g. have been used during the cure.

Frequently, the curing process is carried out during two distinct periods: an ambient rest period in which the unit is simply stored one or

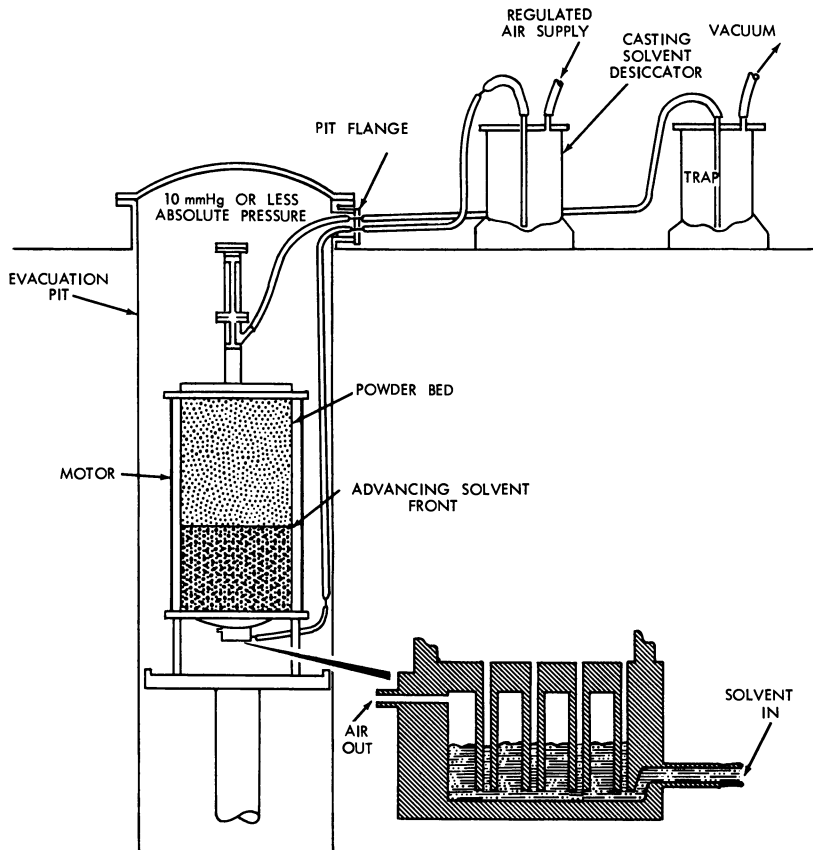


Figure 13. Arrangement for pressure-vacuum casting

more days at 80°F. and a second period in a cure bay at 120°–140°F. for a longer period.

After several days to 2 weeks at the elevated cure temperature, the propellant has been converted to a macroscopically homogeneous mass by mutual diffusion of nitrocellulose and plasticizers. The propellant charge is then permitted to cool to room temperature, casting fixtures are disassembled, cores are extracted, and finally the propellant end surfaces are machined to conform to required dimensions.

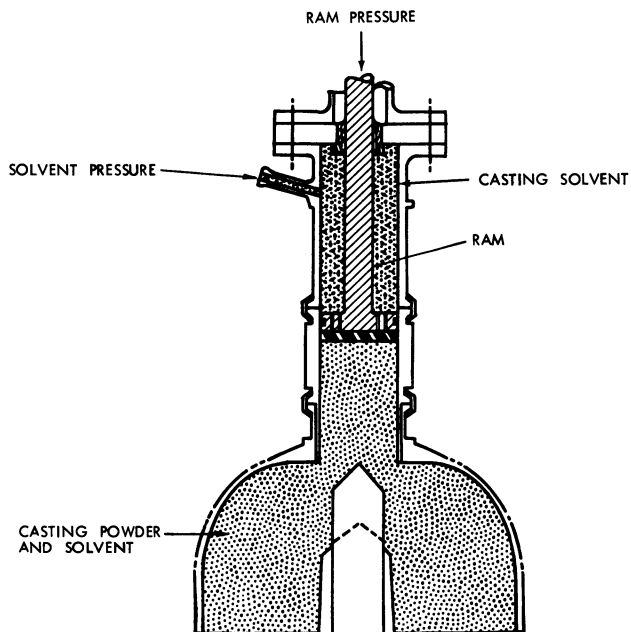


Figure 14. Curing fixtures for applying ram and solvent pressure

Theory of Casting and Curing. **CASTING.** As mentioned above, casting is essentially the process of causing plasticizer to flow through and fill the interstices of a bed of casting powder. A knowledge of the height of casting or the distance that the solvent front moves through the bed in a given period of time is essential in designing casting equipment and selecting casting procedures.

Laminar flow of a fluid in a packed bed may often be described by the Carman-Kozeny Equation (6):

$$\bar{V} = \frac{dL}{dt} = \frac{g\sqrt{2}D^2}{180\mu} \left(\frac{\epsilon}{1-\epsilon} \right) \left(\frac{\Delta P}{L} \right) \quad (1)$$

where:

- ΔP = pressure drop through the bed
- L = length of bed
- ϵ = volumetric void fraction of bed
- μ = fluid viscosity
- V = average fluid velocity through bed
- D = granule diameter
- Ψ = granule shape factor
- g = gravitational constant
- t = time

In applying this equation to the casting of a propellant charge, remember that both the bed and the fluid characteristics are changing with time. When casting solvent and powder are brought into contact and begin to cure, the granules swell and the viscosity increases as nitrocellulose begins to dissolve in the casting solvent. During the time required for casting (usually less than an hour), casting powder granules change very little in size; however, even small changes may cause a relatively large change in ϵ , the void fraction of the bed. The viscosity of casting solvent may increase threefold in just 20 minutes contact time with casting powder (see Figure 15). By substituting empirical time-dependent expressions for $(\epsilon/1 - \epsilon)^2$ and μ , it is possible to arrive at an integrated form of the Carman-Kozeny Equation which is applicable to the casting of a propellant charge:

$$L = 277 D\Psi \sqrt{\frac{\Delta P a_o}{\mu_o (b - m)} e^{(b-m)t} - 1} \quad (2)$$

where:

- a_o, b = empirically determined casting powder swelling constants
- μ_o = initial casting solvent viscosity
- m = empirical constant in viscosity *vs.* contact-time expression

The empirical constants a_o , b , and m are a function of composition and casting powder granule dimensions. The modified form of the Carman-Kozeny Equation (8) can indeed be used to predict the height of casting *vs.* time for various propellant formulations. Figure 16 illustrates that the predicted curves agree moderately well with those obtained experimentally. Actually, the agreement is virtually as good if the equation used ignores the time dependence of ϵ and accounts only for the viscosity change with time, using μ_o and m .

At present there are two practical approaches in the design of casting equipment and procedures for a propellant with unfamiliar characteristics. One can measure directly height of casting *vs.* time in a long cylindrical experimental casting, or the solvent viscosity may be determined as a

function of contact time and used in conjunction with the modified Carman-Kozeny Equation. Until recently the former approach was used exclusively. In the future, the latter approach is likely to find application because it can yield more information.

CURING. The curing process of a double-base propellant converts a bed of casting powder granules whose interstices are filled with casting solvent to a macroscopically homogeneous mass of propellant. It is convenient to discuss the theory of curing on a microscale and on a macro-scale separately.

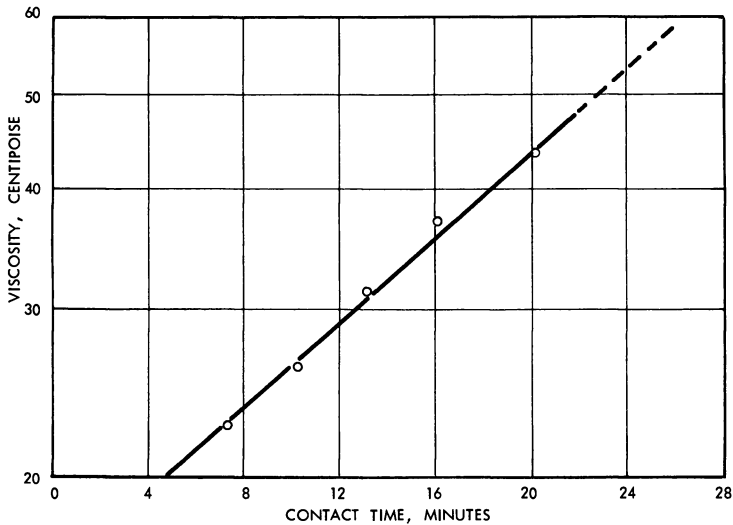


Figure 15. Casting solvent viscosity during cure at 77°F.

Microscale. When a casting powder granule is brought into contact with casting solvent, the polymeric binder of the casting powder and the casting solvent begin to dissolve in one another by mutual diffusion. Since the nitrocellulose molecules are relatively large, the transport of plasticizer from casting solvent into the casting powder binder is intrinsically more rapid than that of nitrocellulose in the reverse direction. Consequently, a hydrostatic pressure tends to build upon the polymer side of the powder-solvent interface, and swelling of the granule takes place in proportion to the volume of plasticizer sorbed.

From a practical standpoint, a system is considered cured when mechanical and ballistic properties show no further change with storage at cure temperature. However, propellant that is "fully cured" does not exhibit a perfectly homogeneous distribution of ingredients.

Transmission radiography (soft x-rays) of thin propellant slices has indicated that the relative concentration of filler solids may be approxi-

mately 40% lower at granule boundaries than at granule centers in "fully cured" production propellant. Autoradiography of cured propellant made with ^{14}C tagged plasticizer shows that the plasticizer/NC ratio may be roughly 10% greater at the interstices than at granule centers.

A three-dimensional mathematical analysis of diffusion in a curing cast double-base system has not yet been developed. However, general diffusion theory suggests a relation between cure time and granule dimensions. In the early stages of cure, equivalent cure times for a given composition might be expected to be proportional to the square of the granule diameter. This rule of thumb appears to be a reasonable approximation even for fully cured propellants.

The diffusion coefficients of nitroglycerin and triacetin in double-base propellant have been measured at 77° – 140°F . Activation energies for diffusion ranged from 10 to 13 kcal./mole. Thus, cure rates for a given propellant composition can be expected approximately to double in going from 120° to 140°F .

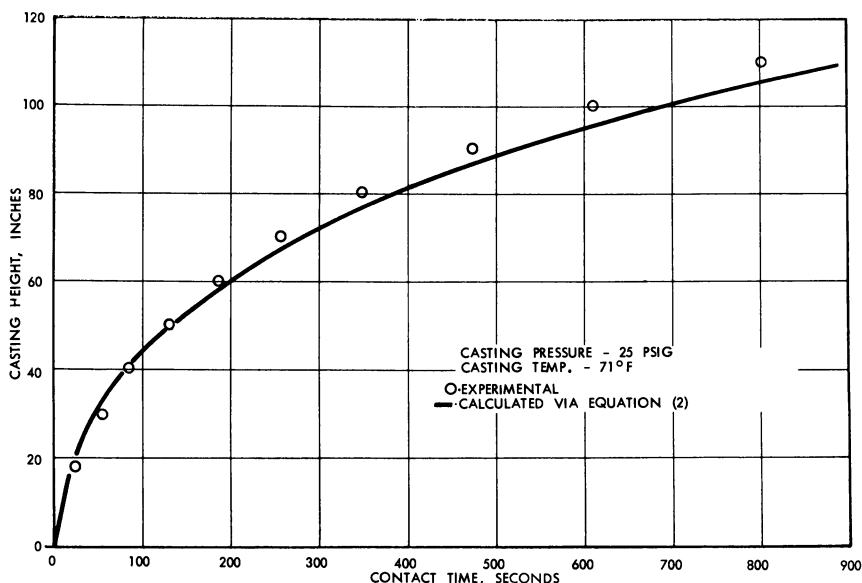


Figure 16. Height of casting

Macroscale. Immediately after casting, a propellant charge consists of two phases on a macroscopic scale: a discontinuous solid phase of casting powder granules in contact, and a continuous interconnected fluid phase of casting solvent. During this post-cast stage of curing the mechanical and rheological behavior of the propellant charge is that of

porous media, like wet soil or gravel. After this stage the propellant enters a precure stage during which it may be considered a quasi-continuum; casting powder granules have been markedly softened, and the interstices are approaching the viscosity of the softened granules. Finally, the macroscopic mechanical properties exhibit no further change, and the propellant has entered the cured stage.

In the past, specifications for cast double-base propellant charge manufacture had been selected on the basis of experience and trial-and-error. If grain defects such as fissures, separations, porosity, or soft spots were encountered during the early stages of a motor development program, process parameters (solvent and ram pressure, ambient rest periods, etc.) were varied until defect-free charges were produced consistently. During the past two years, a mathematical model of casting and curing double-base propellant has been under development to place the process on a sound engineering basis.

The mathematical model attempts to describe the deformations and stresses in a grain during all stages of its manufacture. In principle, deformations and stresses calculated with the aid of the model together with useful failure or defect criteria would permit a prediction of grain integrity through the entire process. Such calculations would provide direct guidance in the specification of optimum manufacturing conditions for defect-free grains.

Established methods for the structural analysis of cured propellant charges can be applied to the precured stage provided the material properties during the last stages of cure are available. Recently, a structural analysis approach has been developed (10) for the post-cast stage of the process when the grain is a two-phase powder-solvent mixture. Since linear viscoelasticity theory is not sufficiently general to predict the effect of solvent and ram pressure, Biot's theory (4, 5) of porous media has been used. To handle the complex geometry of a solid propellant grain, the theory of porous media was combined with an existing finite element computer program (1) for the stress analysis of cured propellant charges. The mathematical model used thus far has not included the effects of viscoelasticity or irreversible deformations.

To predict the mechanical integrity of any body, three things must be known in addition to an adequate analytical technique:

- (1) The loads sustained by the body
- (2) The mechanical properties of the system
- (3) A useful definition of failure (loss of integrity)

The loads on a propellant charge are generally known and recorded as the process variables (pressures), or they can be calculated from temperature and thermal and mechanical properties of the system. Until recently, the required mechanical properties and failure criteria were

not known for a propellant charge during the post-cast or the precure stages of cure.

MATERIAL PROPERTIES. The elementary form of the analysis used requires the following properties of propellant during cure: tensile modulus, effective bulk modulus, and propellant volume change. Each of these properties changes with temperature and time elapsed since casting. Because of the unusual nature of the material (sticky, wet, explosive, "gravel"), special tests, equipment, and techniques were developed for these measurements.

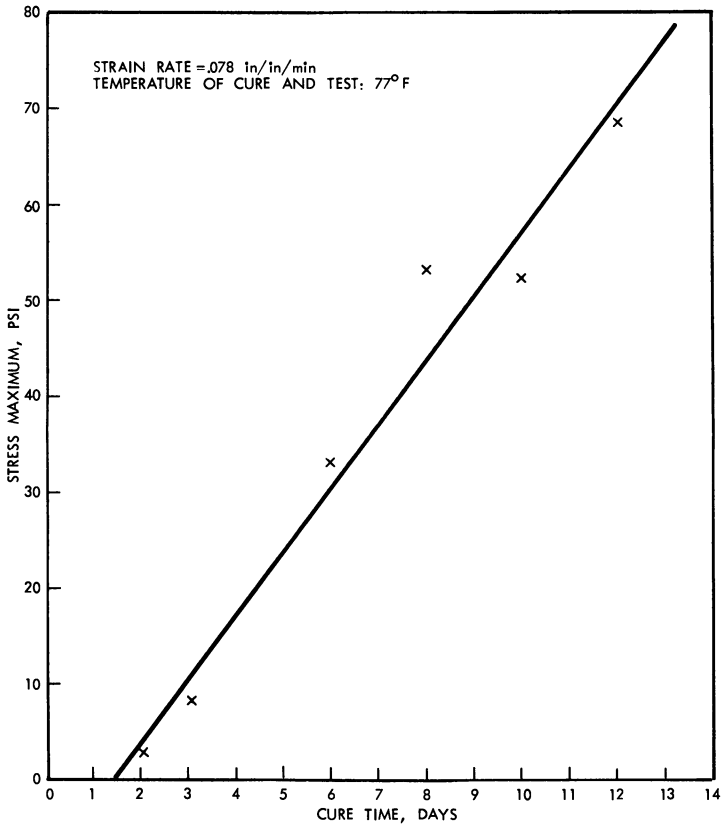


Figure 17. Development of tensile strength during ambient cure

A special split tensile specimen mold was made to measure tensile properties of propellant during cure. A miniature casting is made in a dumbbell-shaped mold. The gage section of the mold is split axially so that it can be removed to expose the partially cured propellant. The mold is placed in a tensile tester, and the specimen is pulled with the end parts in place. Figure 17 shows that during the early stages of cure

the propellant possesses only a small fraction of the strength of the fully cured material. A fully cured specimen of the same propellant would yield a tensile strength of 110 p.s.i.g. at the indicated strain rate.

The effective bulk modulus and volume changes during cure are determined in a specially designed dual dilatometer apparatus (*see* Figure 18). To make these measurements, a 1-inch-diameter casting of propellant is made in a flexible polyethylene septum held in a rigid-walled vessel containing a fixed quantity of water. A capillary tube is connected to the casting solvent phase to monitor the solvent which enters or leaves the bed during cure. The corresponding volume change is termed the bed sorption. Volume changes of the casting powder bed are monitored with the aid of a second capillary tube connected to the water phase. The algebraic sum of the volume changes indicated by these two capillaries is the total volume change of the system.

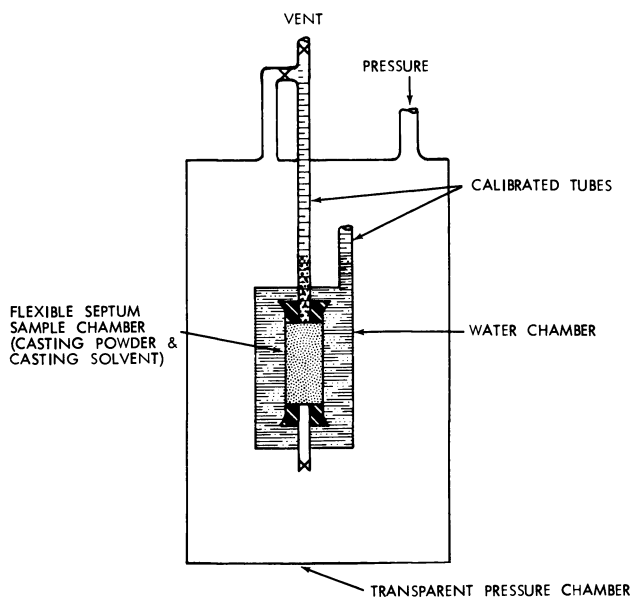


Figure 18. Dual dilatometer

Pressure tests are performed in an external pressure chamber by applying equal pressure to both solvent and water phase (powder bed) to simulate solvent pressure in an actual casting. Ram pressure is simulated by applying a differential positive pressure across the septum which acts on the powder bed. Thus, bed volume change, bed sorption, and total volume change can be followed during cure as a function of time, temperature, solvent pressure, and ram pressure.

This same apparatus permits estimates to be made of the so-called jacketed compressibility (the reciprocal of the effective bulk modulus) during early cure. This is accomplished by applying momentary pressure to the bed alone (ram pressure) and observing the corresponding bed volume change in the water meniscus.

The dilatometric behavior of cast double-base propellant reveals much concerning the nature of the cure process. As an illustrative example, Figure 19 shows the curing behavior at constant temperature, 80°F., for a casting powder which has a porosity of about 2.7% based on the total propellant volume.

When a plot of maximum total volume change *vs.* percent theoretical casting powder density is extrapolated to 100% of theoretical density, the total volume change is usually less than 0.1%. Thus, during cure of a double-base propellant, the volume change caused simply by mixing polymer and solvent is small.

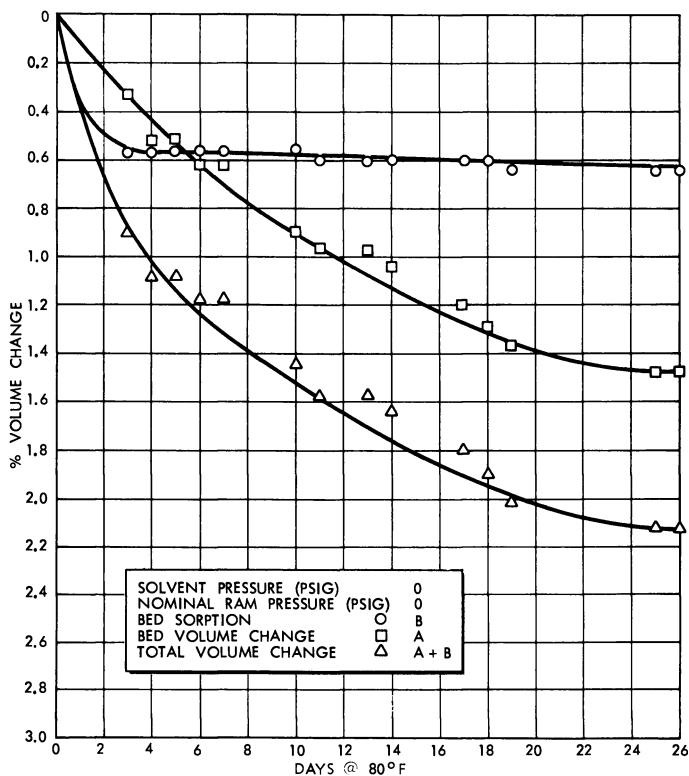


Figure 19. Dual dilatometer: typical isothermal propellant cure

The total volume change recorded in Figure 19 must be attributed largely to hole-filling of the casting powder pores. Although the nominal ram pressure is zero, the actual average pressure on the bed is about 1 p.s.i.g. owing to septum stress. Nevertheless, it is sufficient to decrease the bed volume by $\sim 1.4\%$. The marked sensitivity of bed volume to ram pressure is illustrated in Figure 20 which shows the maximum bed volume change (at time = ∞) as a function of ram pressure.

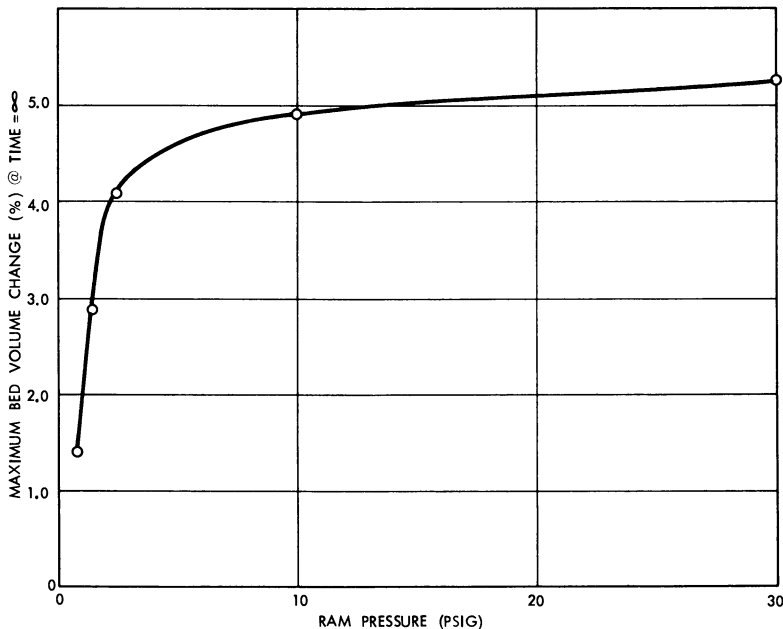


Figure 20. Effect of ram pressure on maximum bed volume change during cure at 80°F.

Figure 21 shows that the relatively large bed volume change observed for 30-p.s.i.g. ram pressure are accounted for by solvent expressed from the bed, and the total volume change is actually much less than the bed volume change.

At first sight the above results might suggest that enormous inward travel of rams would be observed in full-scale units using 30 p.s.i.g. or more ram pressure during cure. Such is not the case. During the early stages of cure, ram pressure is rapidly dissipated a relatively short distance from the end of the ram piston face. Consequently, compaction of the powder bed owing to ram pressure is confined to the immediate vicinity of the ram face—*i.e.*, in the powder column and just inside the

motor. In some motors, this may produce a desirable set of properties in the vicinity of the powder column. In other motors such localized compaction by the ram actually would be detrimental.

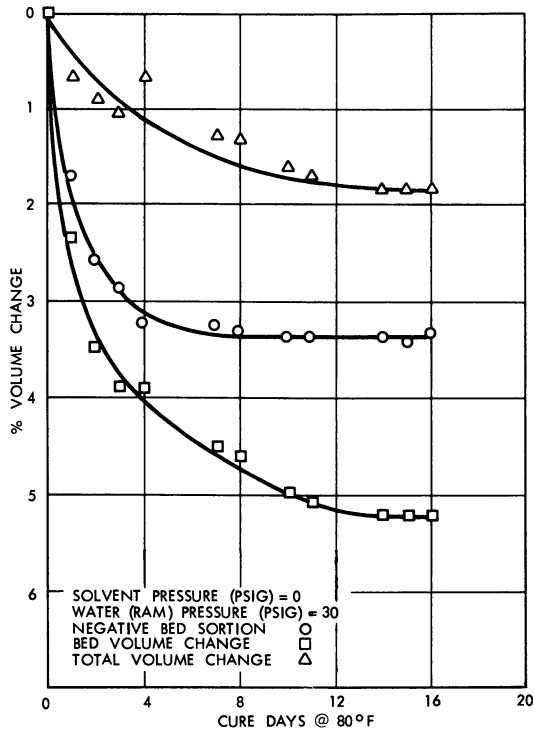


Figure 21. Dual dilatometry: effect of ram pressure on isothermal propellant cure

MATHEMATICAL MODEL. Initial attempts have been made to apply the least sophisticated form of the mathematical model of the curing process to some actual problems. Thus far, the results have served merely to provide qualitative guidance to the selection of the process variables for a limited number of new motor development programs. Sufficient experience with the use of the mathematical model has not yet been accumulated to provide quantitative verification of its validity.

Literature Cited

- (1) Anderson, J. M., *AIAA Paper No. 65-175* (1965).
- (2) Ball, A. M., Army Material Command Pamphlet, **AMCP 706-175** (1961).
- (3) Ball, A. M., *Chem. Eng. Progr.* **57**, 80, 106 (1961).
- (4) Biot, M. A., *J. Appl. Phys.* **12**, 155 (1941).

- (5) Biot, M. A., Willis, D. G., *J. Appl. Mech.*, 594-601 (Dec. 1957).
- (6) Foust, A. S., *et al.*, "Principles of Unit Operations," p. 473, Wiley, New York, 1960.
- (7) W. A. Noyes, Jr., ed., "Science in World War II—Chemistry," pp. 178-8, Little, Brown, Boston, 1948.
- (8) Preckel, R. F., *ARS J.* **31**, 1286 (1961).
- (9) Preckel, R. F., *AIAA J.* **3**, 346 (1965).
- (10) Thacher, J. H., *CPIA Publ.* **119**, **1**, 457 (1966).

RECEIVED April 10, 1967.

Nitrocellulose Plastisol Propellants

ALBERT T. CAMP

Development and Technology Department, Naval Ordnance Station,
Indian Head, Md.

Slurry-cast, filled nitrocellulose plastisols offer a variety of easily processed compositions with high performance potential as solid propellants. As a fully available vehicle for beryllium fuel, which offers the highest potential of any metal in an oxygen oxidizing environment, these plastisols are unexcelled. Processing hazards have justified the development of a non-mechanical, inert-carrier process for safer mixing. High quality, low cost, fine-particle spheroidal nitrocellulose is the key ingredient for successful application of this system on a large scale. Many different nitrate ester plasticizers and conventional stabilizers have been used successfully. Fillers consist of perchlorate salts, nitramine compounds, and certain light metals and hydrides.

Colloided nitrocellulose-base compositions which attain their final form essentially without the aid of volatile solvents meet the general definition for plastisols. In this sense the history of nitrocellulose plastisols dates back to the early work of the last century on blasting gelatins. Here, a small proportion of fibrous nitrocellulose is dispersed in nitroglycerin, and the mixture is gelatinized and partially desensitized by diffusion of the nitroglycerin into the nitrocellulose fibers. This diffusion tends to be too rapid, even at room temperature, to allow the practical use of fibrous nitrocellulose in a highly filled pourable slurry. Therefore, a great deal of effort has been directed since 1945 toward developing approaches which would allow real control over the rate of diffusion of high energy plasticizers into the nitrocellulose macrostructure. The chapter by R. Steinberger and Paul Drechsel (12) describes 20 years of progress with the extruded casting powder and casting solvent, or "interstitial-filling," approach.

The present paper deals with the intrinsically simpler, pourable slurry approach which has been studied for about as long but applied to only a limited extent in flight-type rockets.

The key to the successful application of high performance, pourable nitrocellulose plastisols lies in a reasonably priced, high quality source of fine-particle, at least partially colloided, spheroidal nitrocellulose. Here we are speaking of particles much finer than the well-known ball powder, produced by the Olin Mathieson Chemical Co. for small arms for over 30 years (7). Actually, particles on the order of 5–50 μ diameter appear to be required to assure a reasonable continuum of uniformly plasticized nitrocellulose binder in a propellant containing 45% or more of combined crystalline oxidizer and powdered metal fuel. Such a continuum of binder is necessary to assure acceptable mechanical properties and reproducible burning characteristics of the finished propellant. Preincorporation of a certain content of the water-insoluble solids within the nitrocellulose microspheres is an effective means of helping to assure this continuum of binder and alleviates the requirements for extremely small ball size. The use of a total of 45% or more of crystalline oxidizer and (generally) metal fuel is essential if the propellant is to be competitive with other modern propellants now in service.

Discussion

Table I gives a range of typical ingredient types and percentages for potentially useful nitrocellulose plastisol propellants.

Table I. Typical Ingredients for Nitrocellulose Plastisol Propellants

<i>Ingredients</i>	<i>Weight %</i>
Spheroidal nitrocellulose (12.2 or 12.6% nitrogen)	5–20
Nitrate ester plasticizers	25–40
Desensitizing plasticizers	0–10
Stabilizers	0.5–2.0
Oxidizers	40–50
Metallic fuels	0–20

Nitroglycerin, pentaerythritol trinitrate, 1,1,1-trimethylolethane (metriol) trinitrate, 1,2,4-butanetriol trinitrate, diethylene glycol dinitrate, and triethylene glycol dinitrate are typical energetic plasticizers. Glycerol triacetate is a typical desensitizing plasticizer for nitroglycerin. Stabilizers include *sym*-diethyldiphenylurea (ethyl centralite), 2-nitrodiphenylamine, and other phenyl compounds capable of scavenging —NO_2 radicals evolved in the slow decomposition of nitrate esters. Crystalline oxidizers

include ammonium perchlorate, potassium perchlorate, and cyclic methylene nitramines. Aluminum, beryllium, and compatible metal hydrides are typical energetic fuels.

Since 1958 Picatinny Arsenal has reported moderate success with high density-impulse, smokeless-burning, nitrocellulose plastisols containing crystalline nitramines (1). However, by far the greatest effort in the United States and Great Britain has been directed toward the most energetic versions of this system containing, in the double-base matrix, ammonium perchlorate, aluminum or beryllium, and often a nitramine oxidizer. Most U.S. propellant research and development groups have worked on these high energy systems at some time since 1956 because of their high performance potential and simplicity of manufacture. Patent applications have been filed by some of these organizations, and two or more have been granted to the respective inventors (4, 14).

During the past 10 years great strides have been made in the development and service application of highly loaded, synthetic rubber-base and interstitially-cast double-base composite-modified propellants. Largely for this reason and for economic and logistic reasons as well, the slurry-cast nitrocellulose plastisols have been relegated to a secondary role.

The foregoing trends have placed increasing demands on the quality of spheroidal nitrocellulose and have, for some applications, necessitated serious attention to chemical crosslinking of the nitrocellulose. More than 10 years ago investigators at the Naval Ordnance Test Station attempted to crosslink nitrocellulose with pentaerythritol trinitrate (PETriN) through the use of a diisocyanate. These attempts proved impractical because the reaction rate of isocyanate with the hydroxyl group in PETriN was much faster than that with the nitrocellulose hydroxyl groups. The resultant dimer of PETriN, formed with diisocyanate, further proved to be a poor plasticizer for nitrocellulose. Eventually it was discovered that PETriN alone was an effective gelatinizing agent for spheroidal (10μ) nitrocellulose and imparted a degree of mechanical strength and dimensional stability to the resultant binder, which has apparently not been duplicated by other castable combinations of nitrocellulose and plasticizers. It was postulated that opportunities for hydrogen bonding existed in the PETriN-nitrocellulose system which could account for its remarkable dimensional stability and physical strength. High viscosity of the slurry, poor low temperature properties of the binder, and certain economic and logistic considerations have combined to prevent serious exploitation of this scientifically interesting discovery.

In more recent years investigators at Picatinny Arsenal, Hercules, Inc., and elsewhere have succeeded in developing practical crosslinked

nitrocellulose binders using diisocyanates and other bifunctional reactants. These are attractive where the nitrocellulose content must be less than about 10% to permit high solids loading and high content of more energetic nitrate ester plasticizer. Reactivity of isocyanates with residual moisture in the propellant ingredients has contributed to the difficulty of using this route for crosslinking.

Sources of Spheroidal Nitrocellulose

Olin Mathieson ball powders of various particle-size distributions have been evaluated since about 1947 as the source of nitrocellulose for interstitially cast, as well as slurry-cast, propellants (3, 9). By 1959 the Naval Ordnance Test Station (NOTS) and the Naval Ordnance Section at Indian Head, Md. (NOSIH), applying earlier work by the Atlantic Research Corp. (11), had developed a reasonable process for producing an essentially pure, stabilized spherical nitrocellulose with an average particle size of about 10μ . Though expensive, this product has proved to be a good standard for comparison with spheroidal nitrocelluloses developed by the du Pont Co., Hercules, Inc. (13), and Olin Mathieson. The NOTS-NOSIH-ARC process involves complete solution of the nitrocellulose in nitromethane and dispersion in water with the aid of a colloid mill and an emulsifying agent. The Olin process is also a lacquer emulsion-in-water approach described for gun granulations in the literature in 1946 (6) and again in 1956 (8). The relatively small 50–60 μ "fluid-ball" size used as a base for rocket propellants is achieved in the emulsion and solvent distillation stage (3, 9). The du Pont process (2) and the Hercules process appear to differ from the other two in that they do not involve complete solution of the nitrocellulose. The du Pont patent reveals the use of special emulsifying agents and a crosslinked coating of neutralized polyacrylic acid and allyl sucrose. All four sources of spheroidal nitrocellulose share the important property of having a resistant shell which is not penetrated quickly at room temperature by the commonly used energetic and conventional plasticizers already mentioned. Only Olin Mathieson provides both single- and double-base commercial forms of spheroidal nitrocellulose, but both Olin and Hercules have provided extensive tailoring services to government and industry by incorporating oxidizers and burning rate modifiers to meet special requirements. All four sources are still under consideration by U.S. propellant development groups, choice being governed by solids loading required (higher solids loading generally requiring the finer, average particle size), cost, propellant mixing equipment available, other ingredients to be employed, and preference of the user.

Processing Techniques and Equipment

The processes and equipment used for making pourable nitrocellulose plastisol rocket propellants are generally simpler and of lighter construction, respectively, than those used for other propellant types. In 1959 Grand Central Rocket Co. (now Lockheed Propulsion Co.) introduced a process based on the use of open polyethylene mixing vessels and air-powered turbine agitators. The process is still used and offers a low investment cost for remote, pilot-scale operations with especially hazardous and/or toxic compositions. More conventional vertical planetary mixers, produced by several U.S. and British manufacturers, have also proved effective. Mixers with submerged bearings are not recommended and have proved dangerous. Vacuum mixing is unnecessary because of the ease of deaeration in a subsequent transfer step. It is also potentially much more hazardous than atmospheric pressure mixing because of the extremely rapid deflagration characteristics of the foamed propellant during deaeration if it should become ignited by friction or some malfunction in the mixing apparatus.

In the slurry process, as conventionally conducted, spheroidal nitrocellulose is first gently dispersed in a solution of plasticizers and stabilizers; this is followed by dispersion of metal powder (if used), burning rate modifiers, and oxidizers in the same vessel. Mix temperature is generally maintained below 85°F. to avoid excessive gelatinization and viscosity increase. Mix viscosity is generally from 1/10th to 1/100th that of typical rubber-based composite propellants. This accounts for the low power requirements during mixing and the feasibility of efficient, rapid deaeration during the subsequent vacuum transfer and/or casting steps. Curing is accomplished at 100°–140°F. over a few days, time and temperature depending on composition and size of the propellant charge. Pressure curing is commonly used to overcome the effects of shrinkage.

Inert Diluent Process

The unusual sensitivity of some composite-modified double-phase propellants before curing has justified intensive effort to exploit a non-mechanical mixing process. First introduced in about 1959 as the "quick-mix" process by Rocketdyne Division of North American Aviation (5, 10), the inert diluent process has been developed at the Naval Ordnance Station, Indian Head, Md. for application to a variety of propellant compositions. Separate streams of solids, slurried in heptane, and an emulsion of plasticizers in heptane, are combined in a non-mechanical mixing chamber. The complete propellant slurry is allowed to settle, and the heptane is separated and recycled in a continuous operation. Figure 1

shows the various elements and steps in the process. Various double-base and composite modified double-base compositions have been successfully processed at the 300-lb./hr. scale in a demonstration plant. A larger, fully continuous, remotely controlled, closed-cycle plant is under construction at the Naval Ordnance Station (Indian Head, Md.). It is expected that fluorocarbon-based composites, as well as the complete family of slurry cast, plastisol double-base propellants, will be processible in this facility.

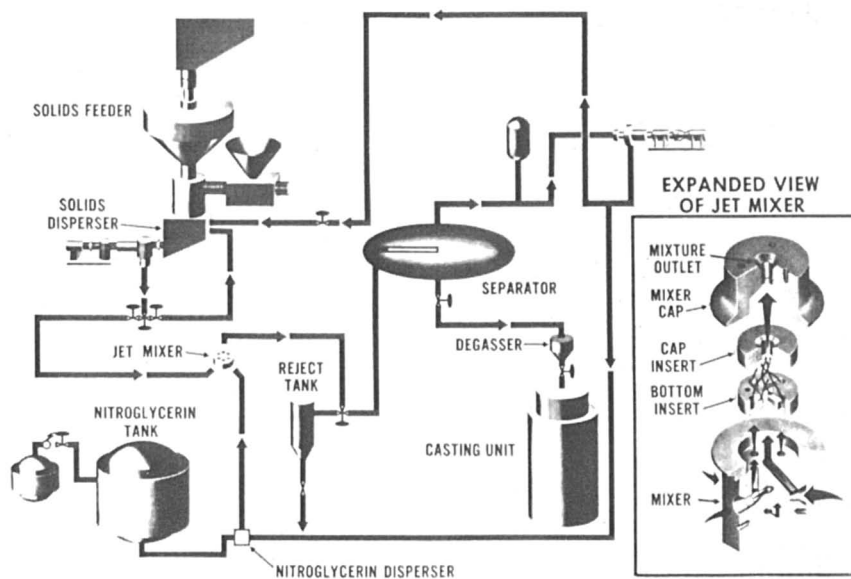


Figure 1. Inert diluent process flow diagram

Adhesives for Case Bonding

The advanced applications for nitrocellulose plastisol propellants require that they be integrally bonded to the motor case. Successful case bonding for the multiyear storage life of a rocket calls for special adhesives and liners which are completely compatible with these highly plasticized propellants. Best results have been obtained with a combination of an impervious rubber liner and a crosslinked adhesive system with a limited affinity for the plasticizers used in the propellants. Examples of effective liners are silica-filled butyl rubber and chlorinated synthetic rubber. Epoxy polyamides, isocyanate-crosslinked cellulose esters, and combinations of crosslinked phenol-formaldehyde and polyvinyl formal varnishes have proved to be effective adhesives between propellant and impervious liners. Pressure curing of the propellants helps

to assure satisfactory bonding, forces to produce hydraulic pressures of 30–70 p.s.i.g. are commonly employed during the early stages of curing.

Literature Cited

- (1) Baumann, Robert, *Picatinny Arsenal Tech. Rept. 2601* (March 1959) (classified).
- (2) Bergman, R. C., U. S. Patent **3,200,092** (Aug. 10, 1965).
- (3) Cook, R. L., Andrew, E. A., U. S. Patent **2,888,713** (1959).
- (4) Godfrey, J. N., U. S. Patent **3,290,190** (Dec. 1966).
- (5) Kramer, Frank B., U. S. Patent **3,022,149** (Feb. 20, 1962).
- (6) Olive, Theodore, *Chem. Eng.* **53** (12), 92, 136 (1946).
- (7) Olsen, Fred, Tibbitts, G. C., Kerone, E. B. W., U. S. Patent **2,027,114** (Jan. 7, 1936).
- (8) O'Neil, J. J., *Ordnance* (Sept.-Oct. 1956).
- (9) Reinhardt, C. M., U. S. Patent **2,919,181** (1959).
- (10) Sheeline, R. D., *Chem. Eng. Progr.* (Feb. 1965).
- (11) Sloan, A. W., Mann, D. J., U. S. Patent **2,891,055** (June 16, 1959).
- (12) Steinberger, R., Drechsel, P., *ADVAN. CHEM. SER.* **88**, 1 (1969).
- (13) Voris, R. S., U. S. Patent **2,843,582** (1958).
- (14) Weil, L. L., U. S. Patent **2,967,098** (Jan. 3, 1961).

RECEIVED March 17, 1967.

3

Poly(vinyl chloride) Plastisol Propellants

KEITH E. RUMBEL¹

Atlantic Research Corp., a Division of The Susquehanna Corp.,
Alexandria, Va. 22314

Poly(vinyl chloride) (PVC) plastisol propellants consist of fine solid oxidizer, and sometimes powdered metal, uniformly dispersed in cured PVC plastisol. Their characteristics and manufacture are reviewed. Information is given on composition, uncured propellant flow, curing time, variation of physical properties with temperature of cure and use, combustion products, safety characteristics, and manufacturing techniques. Effects of oxidizer content (ammonium or potassium perchlorate) on specific impulse, flame temperature, density, and burning rate are shown. Burning rate is correlated with oxidizer particle size. Wide variation of burning rate by use of additives and fine metal wires is demonstrated. The effects of aluminum and magnesium on specific impulse and burning rate are covered. PVC plastisol propellants are used in control motors, sounding rockets, and tactical weapons.

In many ways plastisol propellants are similar to the many composite propellants which have binders comprised of polyesters, acrylates, epoxies, polysulfides, polyurethanes, or polybutadiene-acrylic acid. They all contain 75–80% by weight of finely divided inorganic solids uniformly dispersed in a continuous matrix of organic elastomeric binder. They all utilize the same inorganic oxidizer (normally ammonium perchlorate) and the same powdered metals (usually aluminum) to enhance performance, and they all are made by thoroughly mixing the solid ingredients into a nonvolatile liquid to form a viscous slurry, deaerating the mixed slurry to remove entrapped air or other gases, casting the deaerated slurry into molds of the desired shape, and solidifying the mass.

¹ Present address: 11517 Waples Mill Rd., Oakton, Va. 22124.

It is in the technique of solidifying the mass that plastisol propellants differ so markedly from composite propellants. In composite propellants, the nonvolatile liquid is comprised of monomers or low molecular weight prepolymers. Solidification is accomplished by completion of the polymerization reactions. Much attention must be given to the degree of completion of these reactions during manufacture so as to minimize changes in physical properties as a consequence of continued slow polymerization, or so-called "post-cure," following manufacture.

In plastisol propellants, however, all polymerization reactions are complete before propellant manufacture begins. Solidification is accomplished through solvation (or solution) of the solid resin (or polymer) particles in the nonvolatile liquid, which has been selected to be a plasticizer for the resin. Solvation or "curing" is accomplished by heating to a temperature at which the resin particles dissolve rapidly (within a matter of a few minutes) in the plasticizer to form a gel which on returning to room temperature has the characteristics of a rubbery solid.

The resin used to manufacture plastisol propellants must be dispersion grade. The resin particles should be spherical (18) (or nearly so), preferably a maximum diameter of about 30μ or less (14, 17), free from porosity (14), and have a clean surface (15). This will permit the formation of a smooth, creamy plastisol when mixed with approximately an equal weight of the usual plasticizers for the polymer in question. Further, the plastisol of the resin and plasticizer must be capable of being heavily loaded with oxidizer and other fine solids to permit the formulation of a useful propellant composition.

In the plastisol propellant process, it is essential that the resin particles not solvate too rapidly at processing temperature since a rapid increase in viscosity of the propellant mix interferes with the mixing and casting operation. There must be adequate "pot life" of the mixed propellant. The resin-plasticizer system itself is the dominating influence on pot life, and for this reason certain combinations cannot be used in the plastisol process.

The first successful static firing of plastisol propellant took place late in 1950 as part of a broad program conducted by Atlantic Research Corp. to investigate and evaluate plastisol propellants and methods for their manufacture (16). Major attention was directed to poly(vinyl chloride), cellulose acetate, and nitrocellulose, although other polymers were tested for their suitability (17). Patent applications were filed for plastisol propellant compositions and manufacturing processes, based on poly(vinyl chloride) (PVC) (19) and on nitrocellulose (18). The commercial availability of dispersion grade PVC enabled work with this resin to advance rapidly. The balance of this paper is devoted to a discussion of PVC plastisol propellants and their manufacture.

Composition of PVC Plastisol Propellants

Basically, PVC plastisol propellants are systems of binder, oxidizer, and metallic fuel (if used). Minor ingredients, normally comprising less than 2% of the total, consist of wetting agent, stabilizer, opacifier, and burning rate modifier. The composition of three typical PVC plastisol propellants is shown in Table I.

Any one of several commercially available PVC paste resins may be used. [Exon 654 (Firestone) and QYNV (Union Carbide) are used in the formulations given in Table I; Geon 121 (Goodrich) has also been used (17, 19).] The various resins may not yield identical values for some of the propellant properties such as fluidity of uncured propellant, and the physical properties and thermal stability of the cured propellant,

Table I. Composition of Typical PVC Plastisol Propellants

Composition, wt. %	Arcite 368 ^a	Arcite 373D	Arcite 386
PVC	8.44	8.62	11.67
Plasticizer	9.90 ^b	10.79 ^c	11.67 ^c
Ammonium perchlorate	81.03	58.90	73.93
Aluminum	—	21.10	0.99
Wetting agent ^d	0.25	0.25	0.25
Stabilizer	0.33 ^e	0.34 ^f	0.47
Carbon black	0.05	—	0.05
Harshaw copper chromite	—	—	0.97

^a Arcite, a registered trademark of Atlantic Research Corp., is used to designate solid propellants having a PVC plastisol binder.

^b Plasticizer is dibutyl sebacate.

^c Plasticizer is 2-ethylhexyl adipate.

^d British Detergent: equal parts of glycerol monooleate, pentaerythritol dioleate, and dioctyl sodium sulfosuccinate.

^e Ferro 1203, Ferro Corp.

^f Equal parts BC 74 and XE 82, Advance Chemical Co.

but these variations are readily determined by laboratory formulation testing. For example, DeFries and Godfrey (3) mention the use of Taliani-type tests in gas evolution studies utilized to evaluate propellant ingredients.

There are several plasticizers for PVC that may be used in propellants. Weil (19) mentions sebacates, phthalates, adipates, and glycol esters of higher fatty acids as being desirable. Dibutyl sebacate, dioctyl sebacate, and 2-ethylhexyl adipate are all good. The plasticizer has a most important effect on the physical properties of the cured propellant and the variation of these properties with temperature. Long chain, aliphatic plasticizers impart improved low temperature flexibility, and hence are preferable to aromatic plasticizers such as the phthalates. An increase in plasticizer viscosity leads to an increase in viscosity of the mixed pro-

pellant, but the variation of propellant viscosity with solids loading depends on the choice of plasticizer. Burning rate is changed little by selection from among certain of the acceptable plasticizers and by modest variation from the customary equal parts by weight of PVC and plasticizer.

The wetting agent in the propellant composition is used to facilitate the mixing of ingredients and to reduce the viscosity of mixed propellant so that it is more easily cast. The wetting agent listed in Table I was also used by Rossen and Rumbel (9).

PVC plastisol propellants cure in the temperature range 300°–350°F. Only a few minutes' residence time at curing temperature is required for complete solvation (or solution) of the PVC resin in the plasticizer. Since the propellant has the low thermal conductivity characteristic of plastics, however, several hours may be required to raise the central portion of a propellant grain to curing temperature by heat conducted from an external source. During this time, those portions of the grain closest to the source of heat may remain at curing temperature for several hours. Stabilizer is added to the formulation to retard the decomposition of PVC during cure. It does so by absorbing hydrogen chloride which may be liberated by PVC during the heating and which would otherwise cause further polymer decomposition (19). The formation of double bonds by dehydrochlorination provides sites for crosslinking with the resultant loss of mechanical flexibility of the propellant binder. DeFries and Godfrey (3) report the quantitative effects of stabilization on the reduction of gas evolution at curing temperatures. Normal concentrations of stabilizer are from 0.25 to 0.50%. Barium ricinoleate (19), mixed barium and cadmium soaps (3) and "a mixture of polyfunctional epoxy compound and an organic barium compound" (9) have been reported as stabilizers for PVC plastisol propellants.

Flow Characteristics of Uncured PVC Plastisol Propellant

Viscosity of PVC plastisol propellant is conveniently in the range 500–1000 poise. The usable range of viscosity is limited at the low end by a tendency for solid ingredients (such as oxidizer or metallic fuel) to separate from the uncured PVC plastisol liquid phase in processing or storage steps between the mixing operation and solidification of the mass during cure. Normally, however, this presents no problem because of the typical desire to maximize specific impulse of the propellant, which is accomplished by reducing binder content, which, in turn, simultaneously increases viscosity of uncured propellant. The upper limit of the usable viscosity range is the usual one encountered. It is here that wetting agent becomes a useful addition to the composition to decrease viscosity.

The upper limit depends quantitatively on the viscosity that can be processed through the casting fixtures in reasonable time. Too high a viscosity may also lead to problems under certain flow conditions as, for example, when propellant folds over on itself to form a void space which may remain as a defect in the cured grain. If the propellant grain is to be formed and cured by screw extrusion, however, somewhat higher viscosities can be handled. A viscosity of 1600 poise has been reported (9) for a PVC plastisol propellant processed this way.

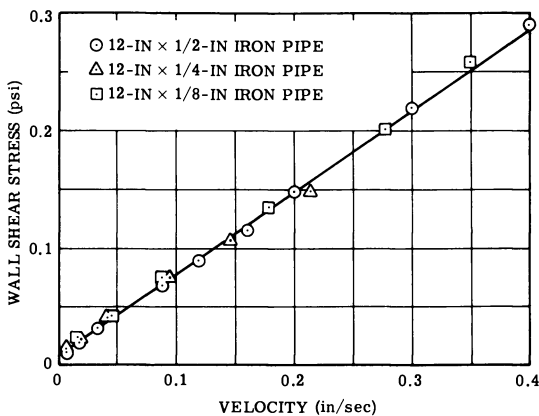


Figure 1. Flow of uncured PVC plastisol propellant in pipes at $70 \pm 2^\circ\text{F}$. (17)

Flow of uncured PVC plastisol propellant in pipes at low velocities occurs by slippage at or near the wall (17). As is characteristic of such a flow mechanism, velocity of flow is proportional to shear stress at the wall and is independent of pipe diameter. This is shown in Figure 1 (taken from Ref. 17). A single straight line (with slight curvature near the origin) correlates the data for three pipe diameters on coordinates of shear stress at the wall *vs.* velocity of flow. (Shear stress at wall = $PD/4L$ where P is the pressure drop causing the flow through a pipe of diameter, D , and length, L .) These data are typical for PVC formulations having 25% binder. Mixed propellant slowly increases in viscosity when stored at room temperature. Figure 2 (also from Ref. 17) illustrates this effect. The data of Figures 1 and 2 are correlated satisfactorily by the equation:

$$S_w = PD/4L = 0.01 + (0.350 + 0.0170 A)V$$

where S_w is shear stress at the pipe wall, P is the pressure drop causing flow through the pipe of diameter D and length L , A is age (in days) of propellant since being mixed, and V is velocity of flow (in inches per

second) in the pipe. The units of S_w and P are pounds per square inch; the units of D and L are inches. A pseudo-yield stress of 0.01 p.s.i.g. is indicated by the data.

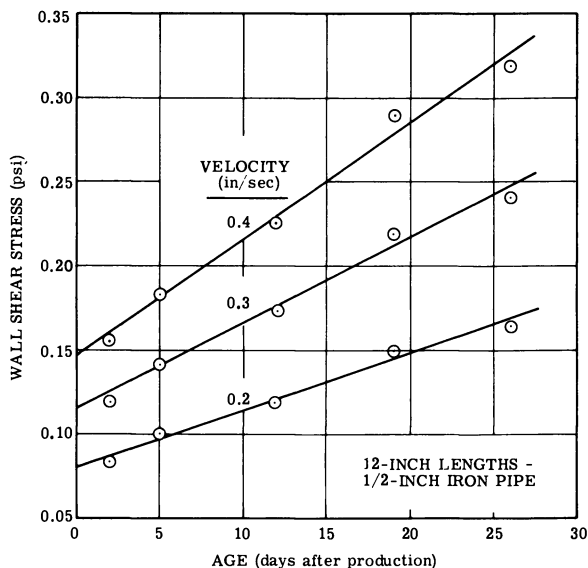


Figure 2. Effect of age on flow properties of uncured PVC plastisol propellant (17)

Curing of PVC Plastisol Propellant

A unique characteristic of PVC plastisol propellants, and one which is often overlooked by those unfamiliar with this propellant system, is the very rapid cure rate once the plastisol binder has reached curing temperature. This is graphically shown in Figure 3 in which the effect of curing time on the tensile strength of PVC plastisol binder is illustrated for various curing temperatures (17). Full tensile strength is developed after only five minutes or less at temperatures of 300°F. or higher.

The effect of curing temperature on a typical PVC plastisol formulation having 25% binder, Arcite 103, is shown in Figure 4 as given by Weil *et al.* (17). [Arcite 103 has the following percentage composition (17): PVC (Geon 121), 12.4; dibutyl sebacate, 12.4; ammonium perchlorate, 74.6; stabilizer (equal parts Ferro 121 and 221), 0.5; carbon black, 0.1.] Ultimate elongation and ultimate stress at rupture are essentially fully developed by 20 minutes curing time at 325°F. or higher.

Since no chemical reactions are involved in curing PVC plastisol propellant, the heat required to raise the propellant to curing temperature

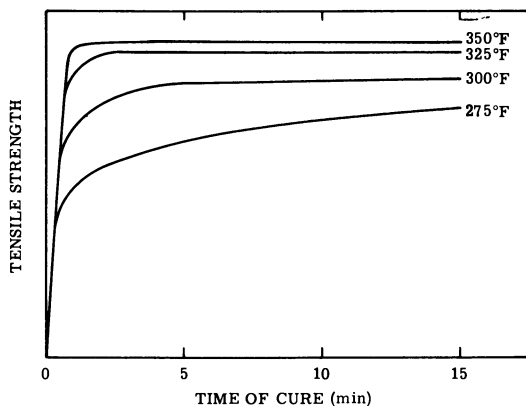


Figure 3. Effect of curing time on tensile strength of a PVC plastisol for various curing temperatures (17)

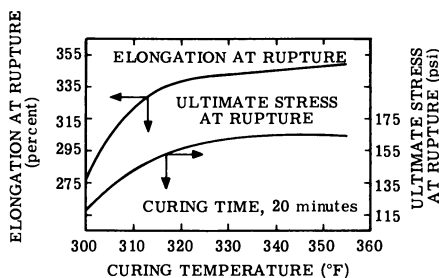


Figure 4. Effect of curing temperature on tensile characteristics of a typical PVC plastisol propellant (17)

must be supplied externally. In the continuous screw extrusion process of forming and curing grains, the working of the propellant by the screw in the barrel of the extruder can provide the required heat, the heating medium circulated through the jacket surrounding the barrel simply providing for heat loss (9). Dielectric heating also generates heat internally in the propellant owing to the rapid reorientation of the molecular dipole under the influence of the alternating electric field. This method of curing PVC plastisol propellant has been investigated (17). More commonly, however, the heat required to raise the propellant grain to curing temperature is simply transferred by conduction through the propellant mass from an external source. Weil *et al.* (17) give curves of the time required to raise the midplane temperature of slabs of PVC plastisol propellant to 310°, 330°, or 350°F. when both slab surfaces are maintained at 360°F. and initial slab temperature is 70°F. These curves can be linearized by

plotting heating time *vs.* the square of slab thickness as shown in Figure 5. Further generalization encompassing other initial temperatures, final center temperatures, and shapes is possible with the aid of the Williamson-Adams chart (20) for midplane or midpoint of various solid shapes having negligible resistance to heat transfer at their surface (8). This chart is dimensionless, the logarithm of unaccomplished temperature change at the center, $(t_a - t_m)/(t_a - t_b)$, being plotted *vs.* dimensionless time, θ/r_m^2 , where t_a is surface temperature, t_b is initial uniform propellant temperature, t_m is temperature of midplane or midpoint, α is thermal diffusivity, θ is time from start of heating, and r_m is the *minimum* distance from surface to center. Using the value of $\alpha = 0.0138$ sq. in./min. derived from the data of Weil *et al.* (17) and the Williamson-Adams chart given by McAdams (8), one can develop a semilogarithmic plot of unaccomplished temperature change at the center *vs.* the ratio θ/r_m^2 , with dimensions of minutes/sq. inch. Such a plot for several shapes is given in Figure 6.

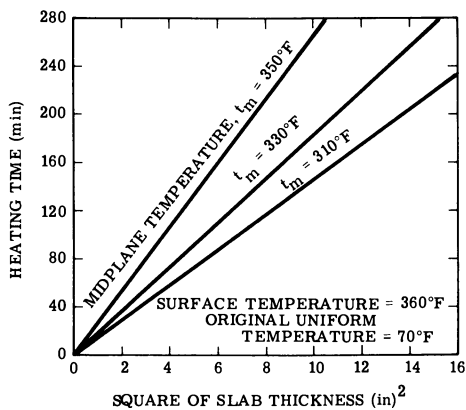


Figure 5. Time to heat slabs of PVC plastisol propellant to various curing temperatures by conduction

The effect of prolonged heating at curing temperature (for periods of up to several days) is to destroy the elastomeric properties of PVC propellant. Brittleness temperature increases from its normal value of -10° to -15°F. , degree of crosslinking increases, ultimate elongation decreases, but ultimate stress and yield stress are not greatly changed. The change is more rapid as curing temperature increases from 300° to 350°F. , and the extent of change depends on both curing temperature and the length of time the propellant is heated. DeFries and Godfrey (3) give quantitative data on these effects.

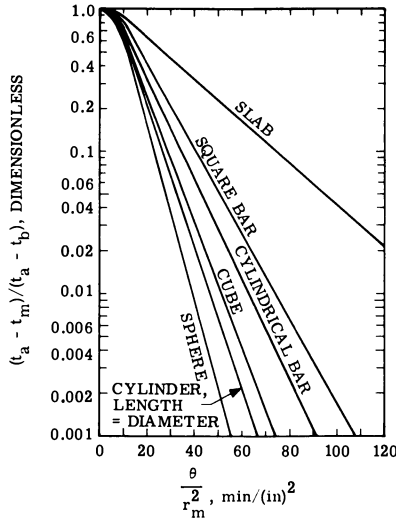


Figure 6. Unaccomplished temperature change of midplane or midpoint of various shapes in curing PVC plastisol propellant by conduction

Variation of Physical Properties with Temperature

In use, solid rocket propellants are called upon to function effectively over an extended temperature range. The effect of temperature on the physical properties of cured PVC propellant is, therefore, of major importance. DeFries and Godfrey (3) give data which illustrate the variation of physical properties of a typical PVC plastisol propellant over a wide temperature range, from -60° to 300°F . (the threshold of curing). Figure 7 (from Ref. 3), shows these trends. Young's modulus, ultimate stress, and yield stress increase regularly as temperature is decreased. Ultimate elongation, however, reaches a sharp maximum at about 200°F .

Yield stress is crucial in design applications since when yield stress is exceeded, separation or dewetting takes place between the PVC binder and the oxidizer or other solids in the propellant (3). The burning surface progresses abnormally rapidly into zones of such overstress causing an excessive rate of gasification and consequent abnormal pressure-time and thrust-time curves. Specific data are normally developed, therefore, to support the design application of each formulation.

Formulation of PVC Plastisol Propellants

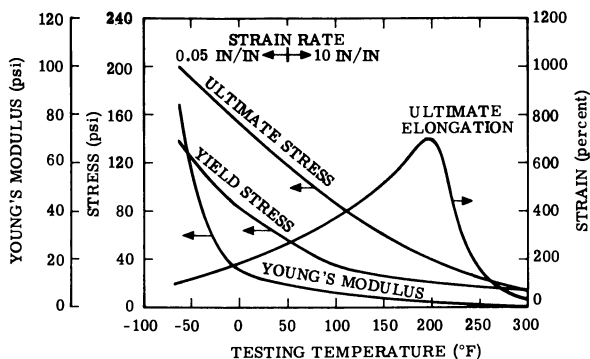
The propellant formulator is faced with the task of balancing compositional variables in such a way as to result in desirable properties of both

the cured and uncured propellant. An adequate fluidity of the mixed propellant must be achieved so that it can be processed satisfactorily. At the same time, it is important to achieve specific levels of several properties of the cured propellant. Specific impulse, density, burning rate, suitable physical properties, and safety characteristics are usually important. The following factors have been noted (3) as necessary considerations when formulating specific compositions for use in rockets.

(a) Solids loading has a significant effect on [physical] properties since the propellant tends to become stiffer, weaker, and less extensible as solids are increased, although the yield strength may be somewhat improved.

(b) Particle size and particle-size distribution of solids control uncured viscosity. Strength is affected, higher strength being attained with smaller particle sizes.

(c) Resin-plasticizer ratio affects viscosity and strength greatly, with formulations rich in plasticizer more easily processed but somewhat deficient in strength and rigidity.



SPE Journal

Figure 7. Physical properties of a typical PVC plastisol propellant at various temperatures (3)

In the simple two-component system of PVC binder and oxidizer, the important propellant properties of specific impulse, density, adiabatic flame temperature, and burning rate increase with an increase in solids loading. This is shown in Figure 8, where theoretical calculated values of specific impulse, adiabatic flame temperature, and density are given for a range of oxidizer content for PVC plastisol propellants comprised of only binder and oxidizer. [Calculated values of specific impulse reported throughout this paper are for adiabatic combustion at a rocket chamber pressure of 1000 p.s.i.a. followed by isentropic expansion to 1 atm. pressure with the assumptions that during the expansion process chemical compo-

sition does not change and that condensed phases (if present) are at the temperature and velocity of the gaseous phase (except in Figure 16 where values are also reported for the assumption of shifting chemical composition during the expansion process so as to maintain chemical equilibrium).] The binder in this case is equal parts PVC and dibutyl sebacate; the oxidizer is either ammonium perchlorate or potassium perchlorate. The effect of solids loading is pronounced, higher oxidizer content increasing flame temperature and specific impulse (because the composition more closely approaches the stoichiometric composition) and density. At a fixed oxidizer content, the use of potassium perchlorate as oxidizer (rather than ammonium perchlorate) leads to a more fully oxidized composition, slightly higher flame temperature, markedly higher density, and markedly lower specific impulse. The volumetric specific impulse or product of specific impulse and density, is nearly the same for the two oxidizers at the higher levels of oxidizer content.

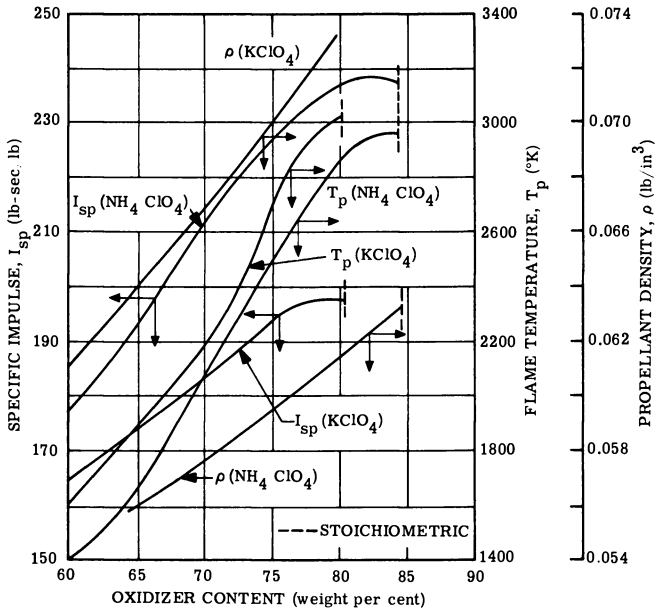


Figure 8. Effect of oxidizer-content on specific impulse, flame temperature, and density (equal parts PVC and dibutyl sebacate) (10)

As might be expected from its effect on flame temperature, increased oxidizer content also increases the burning rate. [All burning rates reported in this paper were measured by the strand-burning technique in a nitrogen atmosphere. Propellant strands, in a vertical position, approximately 4 mm. square (or 4 mm. in diameter), and inhibited by dip-coating

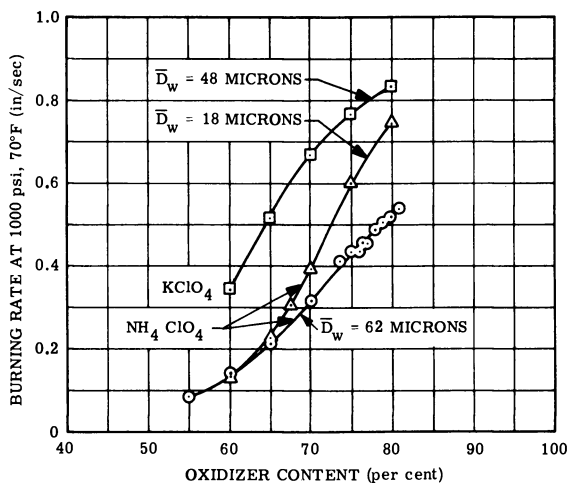


Figure 9. Effect of oxidizer content and type on burning rate (equal parts PVC and dibutyl sebacate) (10)

in a solvent solution of plasticized PVC, were ignited at their upper ends by an electrically energized hot wire which passed through the strand. Burning rate was determined from the time required for the burning surface to melt two small wires of fuze-metal alloy which pierced the strand a measured 3.50 in. apart.] The higher flame temperature results in a higher rate of heat transfer from the hot flame zone to the burning propellant surface which, in turn, increases the rate of gasification of the unburned propellant. Quantitative trends are shown in Figure 9 for the simple two-component system of PVC binder (equal parts PVC and dibutyl sebacate) and oxidizer. Burning rate at 1000 p.s.i.a. and 70°F. is shown as a function of oxidizer content with potassium perchlorate or ammonium perchlorate as oxidizer. The divergent curves at higher contents of ammonium perchlorate are the result of another variable—oxidizer particle size—which is discussed subsequently. Oxidizer particle size for the three curves in Figure 9 is noted thereon as weight-average particle size expressed in microns. [Particle-size analysis for the potassium perchlorate is given in Appendix A. The ammonium perchlorate of $\bar{D}_w = 62\mu$ was a blend of equal parts Grind A and Grind B or Grind D and Grind E, particle-size analysis of which is in Appendix A. The ammonium perchlorate of $\bar{D}_w = 18\mu$ was “through 400 mesh.” To determine \bar{D}_w for oxidizer through 400 mesh or through 325 mesh, the Gaudin-Yavasca relation (5) was used in accordance with Ref. 10. This yields the relation $\bar{D}_w = D_{max}/2$, where D_{max} is the size of the largest particle (assumed equal to the smallest opening through which the oxidizer was passed).] Weight-average particle size, which has been found empirically

to correlate burning rate of PVC plastisol propellants, is defined by the expression:

$$\bar{D}_w = \frac{\int Ddw}{\int dW}$$

where W is the weight percent of particles of size less than D . Some of the data on which Figure 9 is based are shown in Figure 10 for potassium perchlorate oxidizer and in Figure 11 for ammonium perchlorate oxidizer.

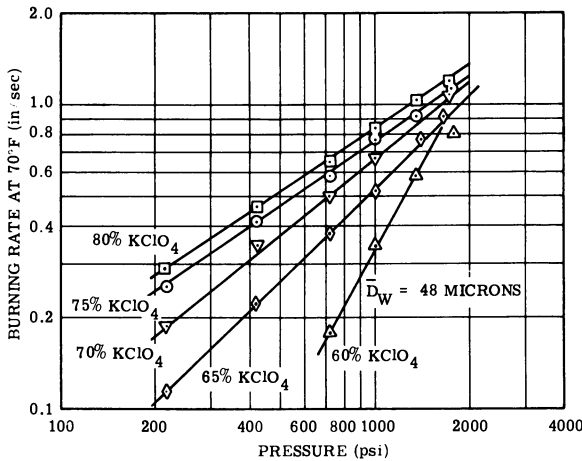


Figure 10. Burning rate of PVC plastisol propellant oxidized with potassium perchlorate (equal parts PVC and dibutyl sebacate) (10)

The complete replacement of ammonium perchlorate with potassium perchlorate markedly increases the burning rate at higher pressures (greater than 500 p.s.i.a.) but has little or no effect at lower pressures. As a result, there is a large increase (from approximately 0.4 to approximately 0.7) in the burning rate pressure exponent (in the relation $r = bP^n$, where r is linear burning rate, b is a constant, and P is pressure). The reason for the higher pressure exponent with potassium perchlorate oxidizer is not known, but its effect is persistent. Even when most of the potassium perchlorate is replaced with ammonium perchlorate, the disadvantage of the higher pressure exponent is not ameliorated. Figure 12 shows the results of such a study in which the weight-average particle size of both oxidizers was held approximately constant at about 50μ .

There is an unmistakable tendency in PVC plastisol propellants oxidized with ammonium perchlorate for the burning rate to become more or less insensitive to pressure in the pressure interval 200–700 p.s.i.a. when

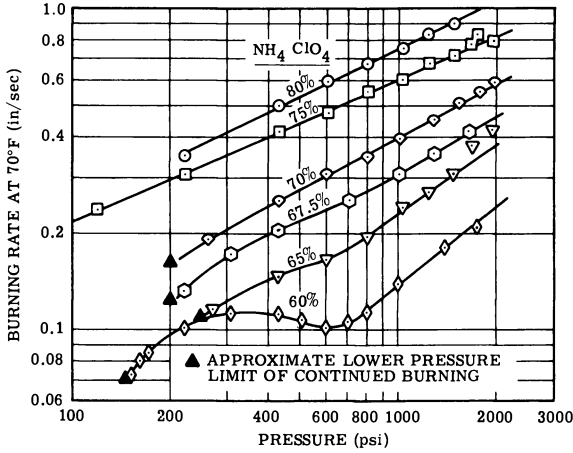


Figure 11. Burning rate of PVC plastisol propellant oxidized with ammonium perchlorate (equal parts PVC and dibutyl sebacate, 18- μ oxidizer) (10)

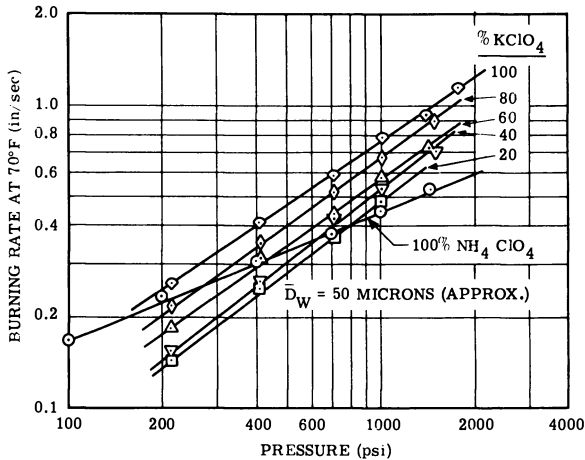


Figure 12. Replacement of potassium perchlorate with ammonium perchlorate (equal parts PVC and dibutyl sebacate, 75 wt. % oxidizer) (10)

the oxidizer content is low (10). This is evidenced in Figure 11 at 60% oxidizer and again in Figure 13 at 60 and 65% oxidizer with the coarser oxidizer particle size. [The ammonium perchlorate of $\bar{D}_w = 62\mu$ was a blend of equal parts Grind A and Grind B or Grind D and Grind E of Appendix A. Particle-size distribution for $\bar{D}_w = 134\mu$ is shown in Appendix A, Grind C.] Only a slight residual of this effect remains at an

oxidizer level of 70%, and it is not observed at higher oxidizer contents. This phenomenon is not well understood.

Not only does particle size of the solids affect uncured viscosity and cured strength, as pointed out by DeFries and Godfrey in the above quotation, it also has an important effect on burning rate. On the micro scale at which the combustion reactions take place, PVC propellants are heterogeneous. An examination of the details of the burning propellant surface reveals oxidizer particles of various sizes surrounded by the PVC binder. Obviously, the oxygen-rich and fuel-rich gases evolved from the burning surface must mix before the combustion reactions can be completed. Gas-phase mixing is therefore an important rate-controlling process in the propellant burning. From this it follows that the more intimately the fuel (binder) and oxidizer are mixed in the solid phase (such as by decreasing oxidizer particle size at constant oxidizer percentage), the less the mixing resistance to combustion and the faster the burning rate. Experimental data confirm this view. Correlation of burning rate at 1000 p.s.i.a. and 70°F. for the simple propellant system comprised of equal parts PVC and dibutyl sebacate as the binder, the balance being either ammonium perchlorate or potassium perchlorate, is shown in Figure 14. This correlation of burning rate with weight-average particle size was found empirically after concluding that specific surface is not the particle-size parameter affecting burning rate (10). Description of the particle-size distribution of the ammonium perchlorate used in obtaining the data correlated in Figure 14, together with the precise values of burning rate, pressure exponent, and \bar{D}_w , are given in Appendix B. No correlation of pressure exponent with particle size is apparent.

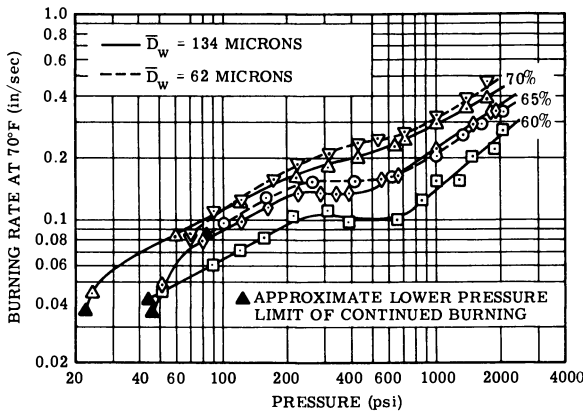


Figure 13. Plateaus in burning rate curves (equal parts PVC and dibutyl sebacate, ammonium perchlorate oxidizer) (10)

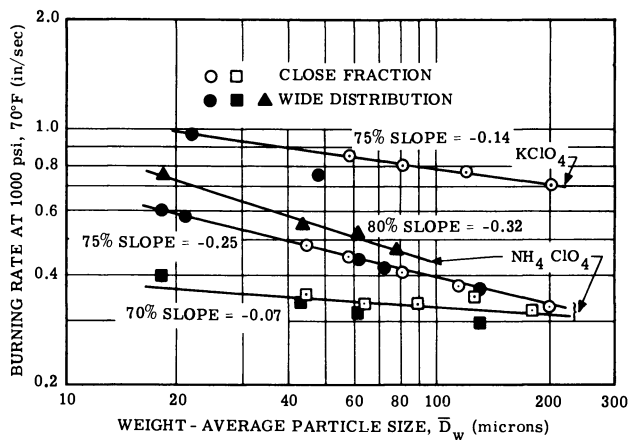


Figure 14. Effect of oxidizer particle size on burning rate (equal parts PVC and dibutyl sebacate)

A Metal as an Ingredient

Scurlock, Rumbel, and Rice (13) have shown that specific impulse of PVC plastisol propellants is substantially increased by incorporating aluminum or magnesium in the formulation. An illustration of what can be accomplished is indicated in Figure 15. Specific impulse is plotted as a function of organic fuel (or binder) content, the computations having been made for 5, 10, and 15 wt. % of aluminum or magnesium added to a metal-free composition of 25% binder and 75% oxidizer. Results from a more general study of the improvement in specific impulse that can be obtained with various amounts of aluminum and binder are given in Figure 16. For this study, the binder was assumed to be 43.1% PVC and 56.9% 2-ethylhexyl adipate, the oxidizer being ammonium perchlorate. Two sets of curves are shown. The lower set was calculated on the same basis as the other values of specific impulse reported elsewhere in this paper—*i.e.*, on the assumption of “frozen chemical composition” during expansion. The upper set was calculated on the different assumption that chemical equilibrium is maintained during the expansion process—*i.e.*, there is “shifting chemical composition” during expansion. Comparison of these two sets shows that they tend to diverge as aluminum content is increased, up to the level corresponding to maximum specific impulse, and that maximum specific impulse occurs at slightly higher aluminum content when the assumption of shifting chemical composition is made. At a level of 20% aluminum, the two assumptions regarding chemical composition during expansion lead to a difference of 10 lb.-sec./lb. in

calculated specific impulse. Maximum specific impulse falls in the range of 18 to 22% aluminum.

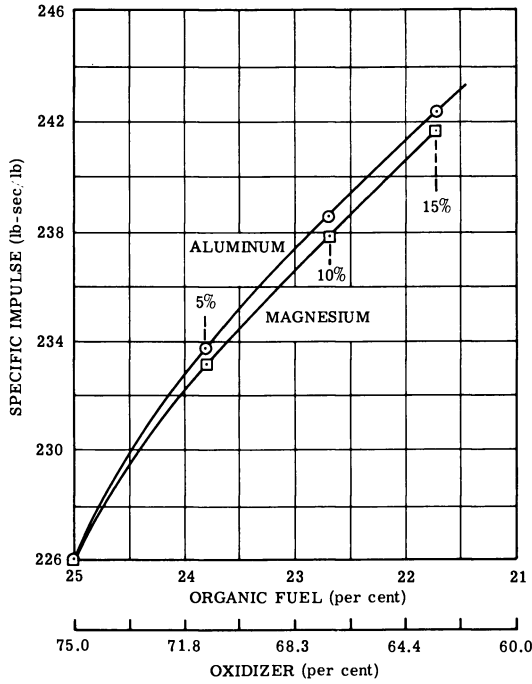


Figure 15. Increase in specific impulse by adding aluminum or magnesium (13)

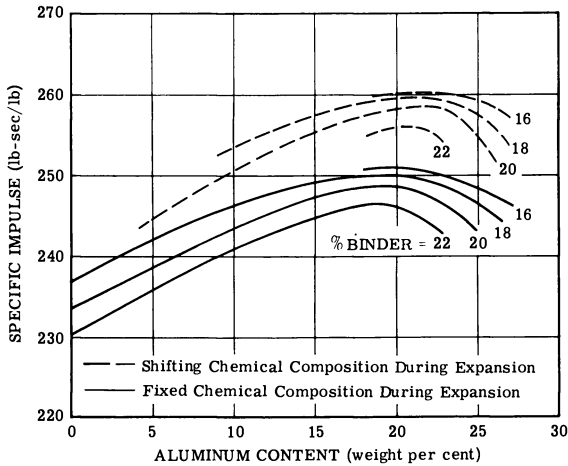


Figure 16. Increased specific impulse by using aluminum

With binder content held constant, an increase in aluminum content is obtained at the expense of ammonium perchlorate content. Since aluminum has a greater density (2.70 gm./cu. cm.) than ammonium perchlorate (1.95 gm./cu. cm.), this exchange can greatly increase the fluidity of the mixed propellant, particularly if the aluminum which is used is spherical or spheroidal in contrast to the shape of ground ammonium perchlorate.

Burning rate is increased and pressure exponent is slightly decreased by the addition of either finely divided aluminum or magnesium to standard Arcite in an amount equal to the molar equivalent of the chlorine contained in the propellant. This is illustrated in Figure 17 for metal powders that were of a size 100% passing through a 325-mesh screen. The effect of other levels of magnesium content is shown in Figure 18 for spherical metal particles of a size through 325 mesh but retained on 400 mesh. Standard Arcite is a formulation of the following composition which has been used as "the point of departure" in studies of the burning rate of PVC plastisol propellants (10):

<i>Ingredient</i>	<i>Wt. %</i>
PVC	12.5
Plasticizer (dibutyl sebacate)	12.5
Oxidizer (ammonium perchlorate, equal parts of Grind D and Grind E, $\bar{D}_{50} = 62$ microns)	75.0
Stabilizer (Ferro 121-221, added) "	0.4

" Ferro Corp.

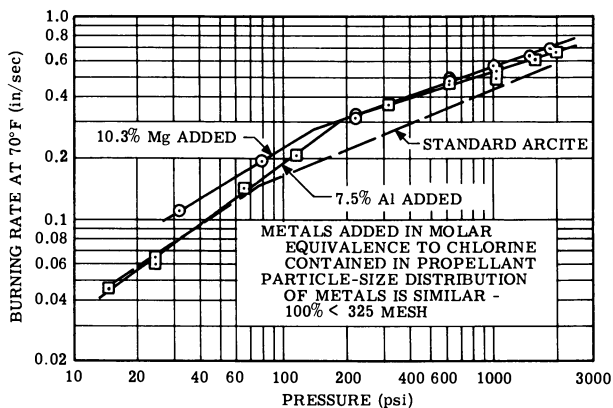


Figure 17. Addition of equimolar quantities of aluminum and magnesium to standard Arcite (10)

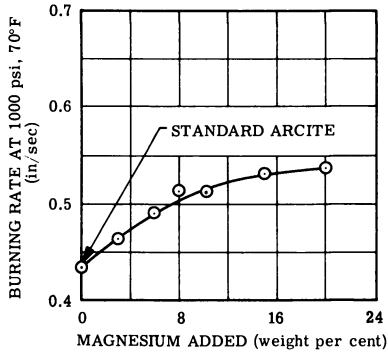


Figure 18. Effect of magnesium on burning rate (magnesium spheres, 325-400 mesh) (10)

The same coordinates that were found to correlate the effect of oxidizer particle size on burning rate also satisfactorily correlate the effect on burning rate of metal particle size when 10.3% of closely screened, spherical magnesium is added to standard Arcite. This is shown in Figure 19. At this level of metal added, burning rate is increased by magnesium particle size less than approximately 250μ but is decreased by larger particle size.

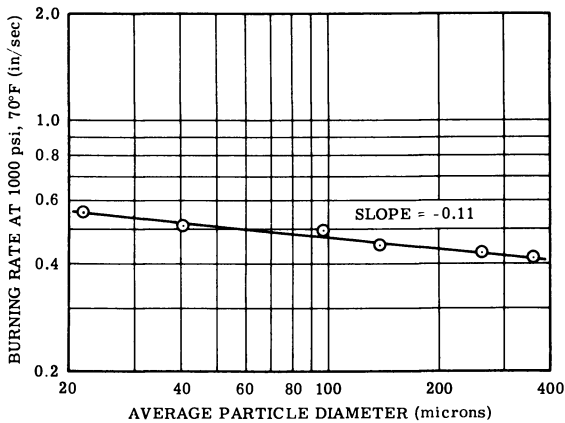


Figure 19. Effect of magnesium particle size on burning rate (10.3 added to standard Arcite) (10)

Additives for Altering Burning Rate

Additives for altering burning rate are always of interest to the propellant formulator in his efforts to meet the ballistic needs of the rocket

designer. The universal hope is for a selection of additives which can be used in small quantities, controllably to increase or decrease burning rate, to decrease the sensitivity of burning rate to pressure or temperature, or to accomplish some combination of these changes. The ideal additives would have negligible effect on fluidity of the mixed propellant, physical properties of the cured propellant, thermal stability, storage stability, or safety characteristics. Few are ideal, but some are useful, nevertheless.

Several materials have been examined as potential burning-rate additives for PVC plastisol propellants (10). The addition to standard Arcite of 1% carbon black, ammonium dichromate, or hydrazine sulfate has negligible effect on burning rate. [All results are reported for the effect of the additives on burning rate at 1000 p.s.i.a. and 70°F.] A 10% increase is obtained by adding 2% ferric oxide, or 1% chromic oxide, copper oxide, magnesium carbonate, or magnesium oxide, whereas a 10% decrease is obtained by adding 1% oxamide or calcium carbonate. A 20% increase is obtained by adding 1% Prussian blue or 2% of a mixture of equal parts copper oxide and magnesium oxide. Copper chromite (Cu-0202P from Harshaw Chemical Co.) is more effective. As little as 0.2% increases the burning rate 25% (10). More data on the effectiveness of copper chromite at two levels of oxidizer particle size and on oxamide and calcium carbonate are shown in Figure 20.

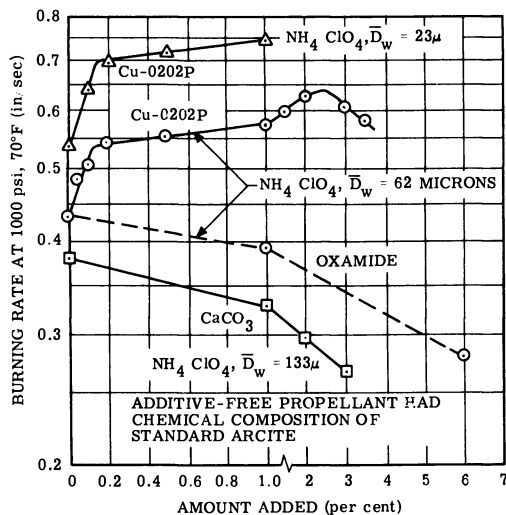


Figure 20. Effect of additives on burning rate

Copper chromite has proved to be the most useful additive for increasing the burning rate, and in addition, it has a persistent tendency to lower the pressure exponent.

Metal Wires to Increase Burning Rate

One of the advantages of PVC plastisol propellant is its compatibility with the use of fine metal wires to increase burning rate. In this technique, metal wires are embedded in the propellant grain before cure. Then, when the propellant is burned, the wires extend from the unburned propellant into the flame zone. The metal wires have considerably higher thermal diffusivity than the gases between the unburned propellant surface and the flame, so they provide paths for rapid heat transfer to the burning surface. As a result, the propagation of the burning surface along each wire is much faster than the normal burning rate. The burning surface adjacent to each wire recesses to form a cone with the wire at its apex. This increases the area of the burning surface, with a corresponding increase in mass burning rate or effective linear burning rate of the propellant. The rate of propagation of the burning surfaces along each wire is uniform, and the inverted cone formed around each wire continues to expand in base diameter until it intersects an edge of the propellant grain or other cones centered on neighboring wires. A steady state is thus readily established.

Table II. Burning Rates Along 5-mil Wires of Various Metals Embedded in PVC Plastisol Propellant

Wire	Burning Rate Along Wire, in./sec.	Ratio of Burning Rate Along Wires to Standard Rate ^a	Properties of the Metal	
			Thermal Diffusivity at 650° C., sq. cm./sec.	Melting Temperature, °C.
Silver	2.65	5.3	1.23	960
Copper	2.32	4.6	0.90	1083
Tungsten	1.82	3.6	0.67	3370
Platinum	1.46	2.9	0.35	1755
Aluminum	1.16	2.3	0.94	660
Magnesium ^b	0.96	1.9	0.66	651
Steel ^c	0.80	1.6	0.064	1460 ^d

^a Normal burning rate of the propellant material = 0.50 in./sec.

^b A square filament cut from 0.005-in. magnesium sheet was used.

^c Music wire.

^d Estimated.

A five-fold increase in effective burning rate is possible by using 0.005-in diameter silver wires. The degree of increase that can be obtained with wires of various metals is apparently determined by the thermal diffusivity and melting temperatures of the metal. This is illustrated in Table II (12). The burning rate at 1000 p.s.i.a. and 70°F.

measured along 0.005-in. diameter wires of various metals embedded in PVC plastisol propellant is shown together with the thermal diffusivity (at 650°C.) and melting temperature of the metal. The increase of burning rate with wire melting temperature, thermal diffusivity remaining constant, is demonstrated by a comparison of the results obtained with copper *vs.* those obtained with aluminum. A similar comparison can be made with tungsten and magnesium. That higher burning rate is associated with higher thermal diffusivity of the wire is shown by comparing the results for aluminum with those for magnesium. These two metals have essentially the same melting temperature. In comparing the efficacy of copper and silver for increasing burning rate, it is apparent that the lower melting temperature of silver is more than overbalanced by its higher thermal diffusivity.

The use of solid, end-burning grains containing axially oriented wires is a particularly attractive way of utilizing the technology of fine metal wires to increase burning rate.

Combustion Products

The temperature and composition of propellant combustion products are of interest to those concerned with materials of construction and insulation for the combustion chamber and nozzle of the rocket motor. These values are readily computed from basic thermodynamic data for the specific propellant composition and operating pressure of interest with the aid of today's large-scale digital computers. By way of illustration, however, the products of combustion computed this way for the three typical plastisol propellants given in Table I are shown in Table III for a combustion pressure of 1000 p.s.i.a. Approximate propellant composition is also shown for convenient reference.

The major gaseous combustion products are CO, CO₂, HCl, H₂, H₂O, and N₂. Comparing Arcite 386 and 368, one can see the increased oxidation of CO and H₂ as oxidizer content is increased from 74 to 81%. Flame temperature increased 600°F., and moles of gas per unit weight of propellant decreased 5%. The effect of replacing oxidizer with aluminum can be seen from a comparison of Arcite 368 and 373D. Flame temperature is increased some 800°F., CO₂ and H₂ are reduced, and moles of gas per unit weight of propellant are decreased about 9%. In addition, the concentration of N₂ and HCl in the combustion products is less with Arcite 373D since the ammonium perchlorate oxidizer is the only source of nitrogen and the major source of chlorine in the formulation. A total of 84% of the aluminum in Arcite 373D appears as liquid Al₂O₃ in the combustion products.

Table III. Combustion Temperature and Products of Typical PVC Plastisol Propellants

	<i>Arcite 368</i>	<i>Arcite 373D</i>	<i>Arcite 386</i>
Propellant Composition, wt. %			
Binder	19	20	24
Oxidizer (NH ₄ ClO ₄)	81	59	74
Aluminum	—	21	1
Burning rate modifier	—	—	1
Combustion Pressure, p.s.i.a.	1000	1000	1000
Combustion Temperature, °F.	4697	5523	4085
Combustion Temperature, °K.	2865	3324	2525

Combustion Products, gram moles/100 grams propellant

Al	—	0.002	—
AlCl	—	0.058	—
AlCl ₂	—	0.057	—
AlCl ₃	—	0.002	—
AlOCl	—	0.006	—
Al ₂ O	—	0.001	—
CO	0.421	0.936	0.799
CO ₂	0.454	0.014	0.288
Cl	0.029	0.022	0.005
H	0.011	0.104	0.005
HCl	0.794	0.435	0.809
H ₂	0.204	1.414	0.559
H ₂ O	1.529	0.166	1.241
NO	0.003	0.0	0.0
N ₂	0.343	0.250	0.315
O	0.001	0.0	0.0
OH	0.025	0.005	0.003
O ₂	0.003	0.0	0.0
Total Gases	3.817	3.472	4.024
Al ₂ O ₃ (liquid)	—	0.329	0.028

Motor Firings

The temperature coefficient of motor chamber pressure, π_K , has been reported (17) to be about 0.09%/°F. in the static firing of small motors loaded with 2-in. diameter tubular grains (inside-outside burning). Measured specific impulse was reported to be 90% of theoretical. Higher percentages of theoretical specific impulse are obtained in larger motors.

Motor applications of PVC plastisol propellants have been notably free of unstable burning problems.

Safety Characteristics

PVC plastisol propellants are quite safe to work with. Binder ingredients are nonexplosive and nontoxic. Ammonium perchlorate, the principal

oxidizer, is ground and handled in quantity safely, common-sense attention being given to its segregation from organic materials and explosives and to the avoidance of (1) static buildup, (2) accumulation of ammonium perchlorate dust in work areas and on machinery and equipment, (3) introduction of organic matter into the perchlorate, and (4) subjecting perchlorate to overheating caused by sliding friction or otherwise. The powdered metals, often used as high energy ingredients, can also be handled safely with due regard to the usual precautions taken with combustible dusts.

The three propellants listed in Table I have been tested in the cured state and classed propellant explosive (solid) Class B by the Interstate Commerce Commission (6). The aluminized formulation, Arcite 373D, gave the same test results when uncured. In addition, Arcite 373D and Arcite 386, both cured and uncured, tested zero cards in the standard Naval Ordnance Laboratory card-gap test (1, 2).

Nevertheless, PVC plastisol propellants are high energy materials and should not be handled frivolously. For example, subjecting the propellant to frictional pressure, a blow, or local overheating can cause ignition with resultant rapid gas evolution, which, if not adequately vented, can lead to a serious accident. Blind-tapped screw or bolt holes are to be avoided in all equipment used in propellant manufacturing. All propellant mixing, extrusion, curing, and machining is customarily carried out behind suitable barricades by remote control.

PVC plastisol propellant having the chemical composition of standard Arcite (composition given above) ignites at 540° to 550°F. when its temperature is increased about 30°F./min. (16, 17). Thus, there is an ample margin of safety between the autoignition temperature and the curing temperature, which is about 200°F. lower (19).

Manufacture of PVC Plastisol Propellants

In the manufacture of PVC plastisol propellants, the usual care is taken to assure that all ingredients meet specifications for chemical composition, dryness, and particle size. Since PVC plastisol propellants do not involve chemical reaction in their curing process, however, the presence of certain impurities in the ingredients is far less critical than with those propellant systems that are solidified by polymerization reaction. Ammonium perchlorate, the most common oxidizer, can normally be procured from the supplier with the required low moisture content. If not, it is dried immediately before use. Tray dryers or other drying means may be used, depending upon the quantity of material. Normally, some or all of the oxidizer must be ground to achieve the desired mean particle size and particle-size distribuion. High speed hammer mills have proved

quite satisfactory for the grinding of ammonium perchlorate. The ingredients are batch weighed and then thoroughly mixed in high shear mixers. Typical of the mixing equipment used is the double-blade mixer shown in Figure 21. Mixing is carried out under vacuum to obtain an air-free mixed propellant.

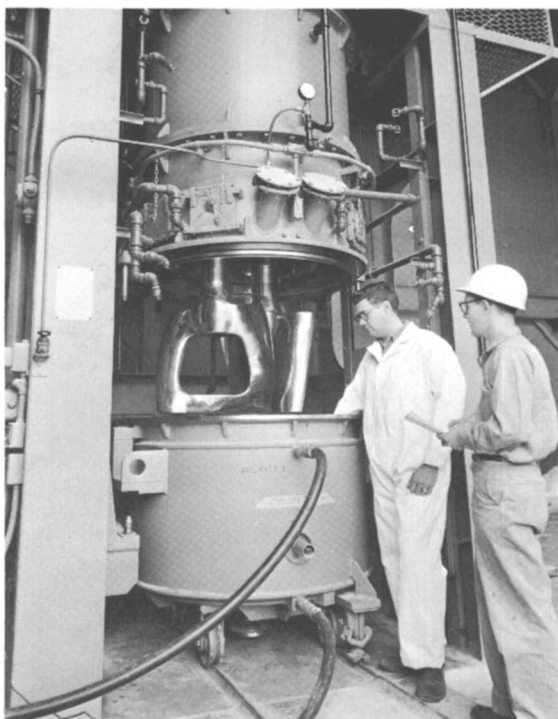


Figure 21. Propellant mixer

After mixing, the propellant is transferred into a casting pot, a container in which it may be held and from which it may be cast. The long pot life of mixed PVC plastisol propellant permits it to be held almost indefinitely to meet the convenience of the production schedule. The long pot life also makes possible the full characterization of a batch of mixed propellant, by extensive tests on batch samples, before the batch is committed to further processing.

PVC plastisol propellant may be formed into the required size and shape to make the desired grains either by screw extrusion or by casting into molds. No exotherm or volume change is observed as a result of curing (16). Molds are normally bottom-filled, the propellant being forced into them from a pressurized casting pot. Heat to raise the propellant to curing temperature may be supplied by many means. The filled

mold may be heated in a circulating hot-air oven, in a steam-filled autoclave, or the mold may be of a double-wall construction so that hot heat-transfer fluid or steam under pressure may be circulated through its interstices. Judge (7) has described the manufacture of Redeye grains (solid, end-burning grains approximately 2.5 in. in diameter) by Atlantic Research Corp. and has pictured a multimold autoclave used in their cure. If a grain with central perforation is being cured, there is often an opportunity to supply heat to the mandrel, which forms the perforation, by circulating a heating medium through it. This can substantially reduce curing time for some grain shapes because the rate-limiting process in curing PVC plastisol propellant is the time required to heat all portions of the grain to curing temperature. Figure 6 can be used as a guide in estimating the reduction in curing time. Because of greater thermal contraction of the propellant compared with that of the metal molds, the cured propellant tends to shrink away from the mold as the mold and propellant are returned to room temperature following cure. Release of propellant from the mold is aided by Teflon lining the mold.

Continuous screw extrusion is another way to form PVC plastisol propellant into the desired size and cross-sectional shape. Simultaneous curing of the propellant is also accomplished. This process has been described fully by Rossen and Rumbel (9) and is only summarized here. Mixed propellant is fed from a casting pot into the feed end of a continuous worm-screw extruder which is fitted at the discharge end of the screw with a device for constricting propellant flow. The action of the

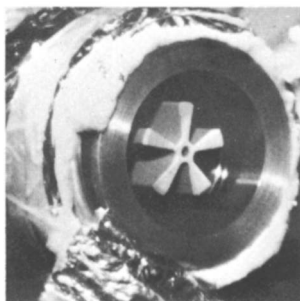


Figure 22. Star mandrel in extruder die

screw against the discharge pressure creates back flow of propellant through the small clearance between the lands of the screw and the extruder barrel. This working of the propellant, which has a viscosity of approximately 1600 poise as it is introduced into the extruder (9), heats the mass uniformly as it passes through the extruder. Circulation of heating medium through the extruder barrel also augments heating of

the propellant, if needed, as well as provides for heat loss to the surroundings. Since solvation of dispersion grade PVC resin in the plasticizer is rapid at curing temperature, propellant curing actually takes place within the extruder. The cured propellant, which is thermoplastic, passes from the discharge end of the extruder through a heated die which shapes the thermoplastic mass into the desired cross-section. A mandrel may be centered in the die, as shown in Figure 22, if a central-perforated grain is desired. The hot extrudate emerging from the die passes in succession through a diameter-sensing device, a section in which the propellant is cooled, and traction belts for pulling the extrudate from the die at a rate determined by the diameter-sensing device. Precise control of finished-grain diameter is obtained in this way. Finally, the continuous extrudate is cut into pieces approximately the finished grain length. These are

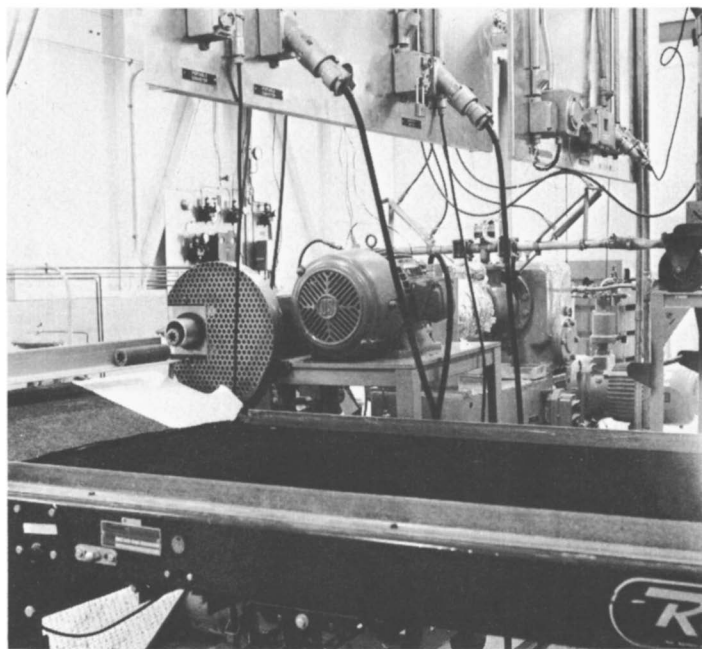


Figure 23. Extruding PVC plastisol propellant

removed from the extruder by conveyer belt. A general view of an extruder, showing propellant supply from casting pot (at upper right), grain emerging from cut-off saw (at left), and conveyer belt for removal of cut grain (at lower right) is shown in Figure 23.

Regardless of whether they are formed by casting or extrusion, cured grains are trimmed to final dimensions; inspected dimensionally, radiographically, and otherwise, as may be required; inhibited, if required;

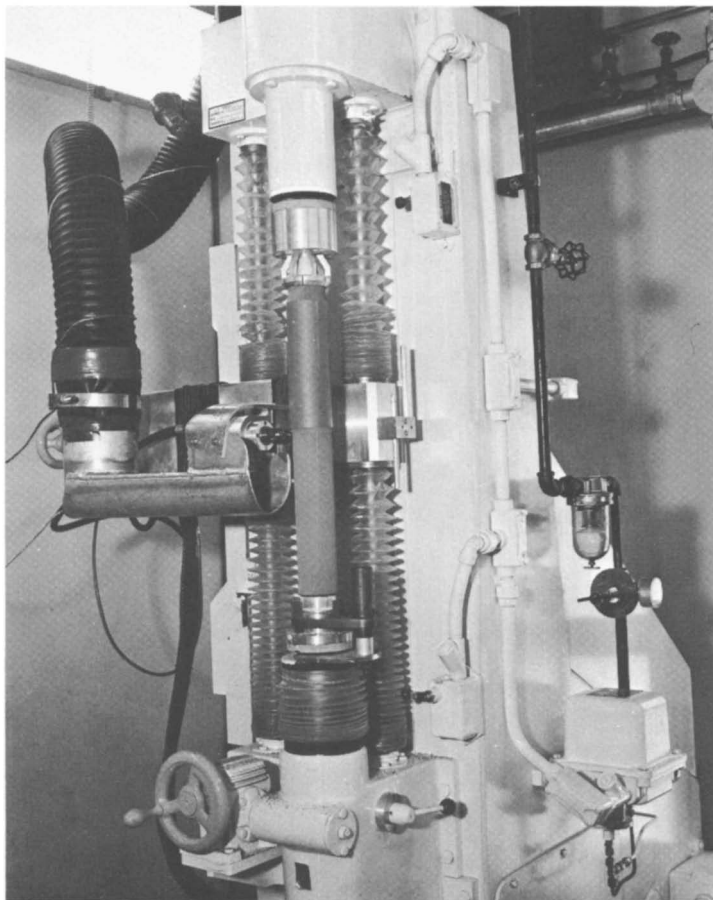


Figure 24. *Machining cured grain*

and cartridge-loaded into motor hardware. A typical inhibitor is the reinforced epoxy inhibitor described by DeFries *et al.* (4). Machining operations are readily performed. Close dimensional tolerances have been held in the machining of PVC plastisol propellant grains by sawing, sanding, milling, turning, and with rotating cutters approaching the fixed grain. Machining of a Redeye grain in a vertical tracer lathe is shown in Figure 24. Both fixed and rotating cutting tools have been used successfully. In any propellant machining, of course, attention must be given to safe removal and disposal of propellant chips and dust.

Applications of PVC Plastisol Propellant

PVC plastisol propellant has found wide use in control rockets for large missiles where precise increments of thrust or impulse are required

with a high level of reliability. Some of the specific applications have been in the Vanguard, Tiros, Mercury, Athena, Minuteman, and Polaris programs. In addition, PVC plastisol propellant is extensively used in sounding rockets, most notably in the Iris and the Arcas and their boosters. The control rockets and sounding rockets have covered a range of total impulse from 1.5 to 210,000 lb.-sec. Finally, PVC plastisol propellant is used in tactical missiles; in the sustainer motor of the Terrier ship-launched missile, and in both the booster and sustainer of the shoulder-fired Redeye, an air-defense guided-missile system.

Appendix

A. Particle-Size Distribution of Various Grinds of Oxidizer

U.S. Sieve Series		Cumulative Wt. % Through					
Mesh	Opening, μ	$KClO_4$	NH_4ClO_4 Grind A	NH_4ClO_4 Grind B	NH_4ClO_4 Grind C	NH_4ClO_4 Grind D	NH_4ClO_4 Grind E
400	37	—	—	—	20.6	22.2	60.8
325	44	49.6	33.2	62.8	22.4	31.9	64.8
270	53	—	—	—	27.2	41.3	73.6
200	74	84.1	51.6	86.6	32.9	53.5	82.5
170	88	91.0	64.0	91.2	—	—	—
140	105	—	—	—	45.5	71.2	90.6
100	149	99.3	90.0	97.2	63.1	90.1	97.2
70	210	—	—	—	82.1	98.3	99.6
60	250	99.8	99.2	99.2	—	—	—
50	297	—	—	—	96.9	100.0	100.0
40	420	—	—	—	99.9	—	—
\bar{D}_w (μ)		48	80	45	134	79	44

B. Ballistic Data and Oxidizer Size for PVC Plastisol Propellants Oxidized with Ammonium Perchlorate

Oxidizer Size (see Appendix A)	Ballistic Data at 1000 p.s.i.a. and 70°F.		\bar{D}_w μ
	Burning Rate, in./sec.	Pressure Exponent	
80% Oxidizer			
Grind E	0.55	0.42	44
< 400 mesh	0.75	0.49	18
50% Grind D/50% Grind E	0.52	0.42	62
Grind D	0.47	0.40	79
75% Oxidizer			
< 60 > 100 mesh	0.34	0.40	200

Appendix B. Continued

<i>Oxidizer Size</i> (see Appendix A)	<i>Ballistic Data at</i> <i>1000 p.s.i.a. and 70° F.</i>		\bar{D}_w μ
	<i>Burning Rate,</i> <i>in./sec.</i>	<i>Pressure</i> <i>Exponent</i>	
< 100 > 170 mesh	0.37	0.40	118
< 170 > 200 mesh	0.41	0.42	81
< 200 > 325 mesh	0.45	0.40	59
< 325 mesh	0.58		22
50% Grind A/50% Grind B	0.44	0.43	62
54% < 60 > 100 mesh/ 20% < 100 > 200 mesh/ 26% < 325 mesh	0.37	0.40	134
50% < 100 > 200 mesh/50% < 200 mesh Grind C	0.36	0.41	134
< 400 mesh	0.60	0.44	18
< 270 > 400 mesh	0.48	0.44	45
70% Oxidizer			
< 400 mesh	0.40	0.55	18
< 270 > 400 mesh	0.36	0.49	45
< 200 > 270 mesh	0.34	0.46	64
50% Grind A/50% Grind B	0.32	0.37	62
< 140 > 200 mesh	0.34	0.49	89
< 100 > 140 mesh	0.35	0.46	127
< 70 > 100 mesh	0.32	0.53	180
Grind C	0.30	0.51	134
Grind E	0.34	0.47	44

Literature Cited

- (1) Amster, A. B., Beaugard, R. L., Bryan, G. L., Lawrence, E. K., NAVORD Rept. 5788 (Feb. 3, 1958).
- (2) Amster, A. B., Noonan, E. C., Bryan, G. L., ARS J. 30, 960 (1960).
- (3) DeFries, Myron G., Godfrey, John N., SPE J. 19, 637 (1963).
- (4) DeFries, Myron G., Macri, Bruno J., Rice, Alvist V., Robinson, Courtland N., Madden, Dale A., U. S. Patent 3,108,433 (Oct. 29, 1963).
- (5) Gaudin, A. M., Yavasca, AIME Tech. Publ. 1819 (May 1945).
- (6) George, T. C. (Agent), "Tariff No. 19, Interstate Commerce Commission Regulations for Transportation of Explosives and Other Dangerous Articles by Land and Water in Rail Freight Service and by Motor Vehicle (Highway) and Water," Part 73.88, (f) Propellant Explosives, Class B, Note 2, Bureau of Explosives, Association of American Railroads, New York, N. Y. (August 5, 1966).
- (7) Judge, John F., Technol. Week 29 (Oct. 24, 1966).
- (8) McAdams, W. H., "Heat Transmission," 3rd ed., p. 43, McGraw-Hill, New York, 1954.
- (9) Rossen, Joel N., Rumbel, Keith E., U. S. Patent 3,155,749 (Nov. 3, 1964).
- (10) Rumbel, K. E., Grover, J. H., Cohen, M., Scurlock, A. C., Army-Navy-Air Force Solid Propellant Meeting, 9th (May 11, 1953).

- (11) Rumbel, Keith E., Cohen, Melvin, U. S. Patent **2,997,375** (Aug. 22, 1961).
- (12) Rumbel, Keith E., Cohen, Melvin, Nugent, Robert G., Scurlock, Arch C., U. S. Patent **3,140,663** (July 14, 1964).
- (13) Scurlock, Arch C., Rumbel, Keith E., Rice, Millard Lee, U. S. Patent **3,107,186** (Oct. 15, 1963).
- (14) Sloan, Arthur W., Mann, David J., U. S. Patent **2,891,055** (June 16, 1959).
- (15) Stewart, William D., Poindexter, Edward, Jr., Wachtel, William L., U. S. Patent **2,915,519** (Dec. 1, 1959).
- (16) Weil, L. L., Herron, D. P., Army-Navy-Air Force Solid Propellant Meeting, 7th (April 16-18, 1951).
- (17) Weil, L. L., Sloan, A. W., Scurlock, A. C., Army-Navy-Air Force Solid Propellant Meeting, 8th (June 4-6, 1952).
- (18) Weil, Lester L., U. S. Patent **2,967,098** (Jan. 3, 1958).
- (19) Weil, Lester L., U. S. Patent **2,966,403** (Dec. 27, 1960).
- (20) Williamson, E. D., Adams, L. H., *Phys. Rev.* **14**, 99 (1919).

RECEIVED May 4, 1967.

Chemistry of Propellants Based on Chemically Crosslinked Binders

WILLIAM F. ARENDALE

University of Alabama in Huntsville, P. O. Box 1247, Huntsville, Ala. 35807

Chemically crosslinked polymers synthesized during in-situ polymerization in the presence of other propellant ingredients and often with the combustion chamber of the rocket motor as the reaction vessel have been the subject of extensive research during the past 20 years. The requirements for energy, physical properties, and processing characteristics have been reported and are also the subject of other chapters in this volume. In this paper chemical principles related to propellant chemistry are discussed using examples rather than attempting to provide an encyclopedia of specific materials and/or propellant formulations. Chemists and chemistry have made significant contributions to propellant science. Each subdiscipline has shared in the success. Some of the successes of each are discussed.

The essential ingredients of a composite propellant are a crosslinked binder (usually an organic polymer) and an oxidizer (usually finely divided ammonium nitrate or ammonium perchlorate). In addition, most useful propellant formulations contain a stabilizer, ballistic modifiers, high energy fuel additives, a wetting agent and/or plasticizers or other additives to adjust physical properties. The synthesis of a single crosslinked molecule that might perform all of these functions, although far from theoretically impossible, has not been successfully achieved. However, the tremendous successes of chemists in synthesizing molecules for specific purposes can be illustrated by developments in propellant chemistry as well as in other areas of application. These successes make the study of the history of 20 years of research on composite propellants containing chemically crosslinked binders most interesting.

The requirements, manufacturing procedures, designs of case-bonded solid propellant rockets, and the performance characteristics of a useful

propellant formulation have been described (1, 2, 22). This presentation focuses on the achievements of chemists and the chemical principles related to the crosslinked polymers that have made possible solid propellant rockets containing over a million pounds of propellant with combustion and manufacturing characteristics sufficiently flexible that the ballistic properties of the propellant formulations can be tailored to specific uses.

Propellant chemistry includes examples from many fields of chemistry—*e.g.*, polymer chemistry, surface chemistry, thermochemistry, and catalysis. References (3, 4, 6, 8, 9, 19, 20, 23, 24, 26) to several standard works that discuss the theory related to these disciplines are included in the Literature Cited. It is assumed that the reader has some acquaintance with these works, and individual references have not been attempted. Likewise, individual propellant formulations have not been given. Selection of a formulation for a particular application depends on the ballistic and physical property requirements, and the technology regarding the selection of a formulation is not the purpose of this paper. This task should be performed by scientists experienced in the technology.

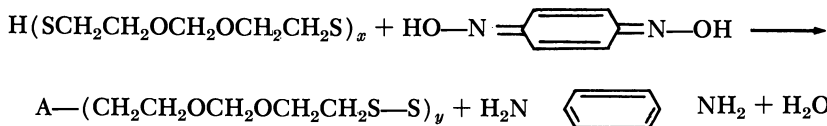
The First Composite Propellants

The first composite propellants were the early asphalt propellants containing potassium perchlorate (75%) as an oxidant with asphalt (25%) as a binder. The high molecular weight asphalt, containing little effective crosslinking, softens sufficiently at reasonable temperatures that finely ground potassium perchlorate can be incorporated into the mixture of hydrocarbons, leaving sufficient fluidity that the propellant formulation can be formed into the desired shape in the pressure vessel that will later form the combustion chamber. Some success was achieved in modifying the properties of the binder, for improved processing characteristics, by incorporating hydrocarbon oils in the formulation. Since the average molecular weight and molecular weight distribution of the binder are modified by adding the oil, the softening point and the fluidity of the binder are more desirable from the processors viewpoint. True elastomeric properties were not achieved.

Propellants Containing Crosslinked Binders

Chemistry of Polysulfide Polymers. Propellant chemistry based on chemically crosslinked binders had its beginning at the Jet Propulsion Laboratory in the winter of 1946 when potassium and/or ammonium perchlorate were mixed into Thiokol LP-3 polysulfide liquid polymer, to which had been added an oxidative curative, *p*-quinone dioxime. This polysulfide polymer, as described by Jorczak and Fettes (13), is prepared

by the reaction of 98 mole % dichloroethyl formal and 2 mole % trichloropropane with sodium polysulfide. An excess of sodium polysulfide is used to form a high molecular weight rubber dispersion. Treatment of the aqueous dispersion with sodium hydrosulfide and sodium sulfite allows controlled cleavage of the high molecular weight polymers to liquid polymers of lower molecular weight terminated with mercaptan groups. To regain the high polymer weight rubber, the mercaptan groups are oxidized back to disulfide groups by an oxidant. In the example above, *p*-quinone dioxime is used, which in turn is reduced to *p*-phenylenediamine or polymeric derivatives of *p*-phenylenediamine.



The Thiokol LP-3 polymer has an average molecular weight of approximately 1000, a viscosity of 7.0–12.0 poise, and a specific gravity of 1.27. The end groups, A, of the cured polymer are small in number and may be residual hydroxyl groups from the manufacturing process or other groups formed during the final polymerization process by substitution or cleavage reactions.

The flexibility inherent in the polymer manufacturing procedure allowed for the synthesis of many variations of polymer. The examination of these materials in propellant formulations by scientists at the Jet Propulsion Laboratories, Thiokol Chemical Corp., and later other propellant companies not only resulted in many useful solid propellant formulations but laid a significant portion of the foundation on which the propellant chemists of today continue to build.

In addition to the historic position in the development of a science of propellants, experiences with the chemistry of polysulfide polymers and propellants will be presented in greater detail than the other types of propellants because of the clarity with which the areas of chemistry can be described.

EFFECT OF PREPOLYMER MOLECULAR WEIGHT. Thiokol LP-3 as described above has an average molecular weight of 1000. Two other polymers of similar chemical composition are available; these polymers have average molecular weights of 4000 and 300. Processability of a propellant formulation is related to the fluidity of the mixed propellant formulation. If additional fluidity can be obtained by varying any of the propellant ingredients, this fluidity may result in fewer defects in the finished product, or the propellant scientist may be able to incorporate additional solids for higher energy or solid ballistic modifiers for better performance. Early experiments were related to the effects of the molecu-

lar weight of the polymer on the processing characteristics of the propellant. Figure 1 shows the variation of viscosity of Thiokol LP-2 (molecular weight 4000) with temperature. The viscosity reaches about 60 poise at 160°F. with smaller reductions with higher temperatures. This might indicate a processing temperature of 160°F. However, the 1000-molecular weight polymer has the same chemical composition but a viscosity of 10 poise at 80°F. The lower molecular weight polymer would be chosen on the basis of ability to process at a lower temperature. On the basis of viscosity alone, a still lower viscosity polymer could have been chosen. The final choice represents a compromise. A point is reached where the solids will not remain homogeneously suspended in the liquid. Also, the lower the molecular weight of the prepolymer, the greater the chance of incomplete reactions or significant effects being caused by impurities acting as chain stoppers during the cure of the propellant formulation. A polysulfide polymer with viscosity of 15 poise at ambient temperatures was most frequently chosen.

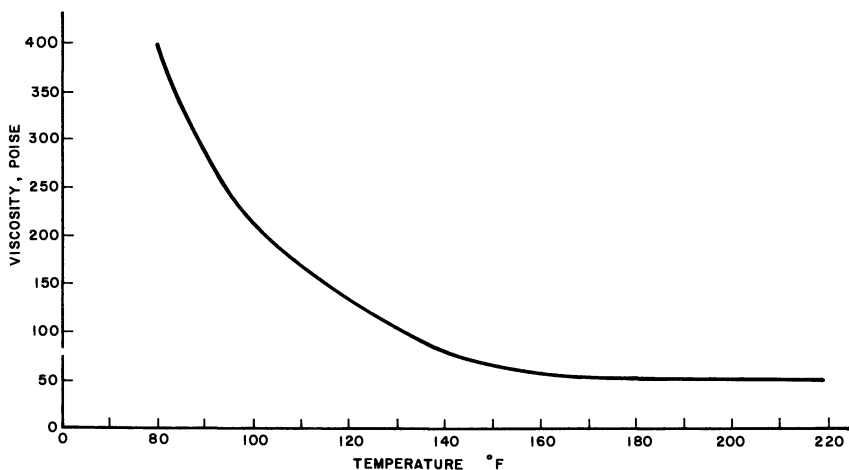


Figure 1. Viscosity vs. temperature for Thiokol LP-2

EFFECT OF INCOMPLETE POLYMERIZATION. Since the polymer forms the continuous phase in composite propellants, it is not surprising that the final molecular weight of the polymer has a significant effect on the physical properties of the propellant. The qualitative relationships between molecular weight and properties of a polymer are discussed in most texts on polymer chemistry. As the molecular weight of a linear molecule is increased, the properties progress from those of a liquid that flows readily, to a liquid that may support its own weight and flow slowly, to a stretchy material with significant resistance to deformation, to a solid deforming slowly over a period of years (creep). Since the continuous

phase of a propellant begins as a liquid, significant increases in molecular weight must take place (joining of 50 to 100 or more units). This chemical reaction takes place in the presence of up to 90% other material. Reproducibility of physical properties demands that the same molecular weight be achieved in each batch of propellant. Much chemistry can be involved in determining the effect of the major propellant ingredients and even small amounts of impurities on the extent of polymerization and the time-temperature history required to reach the final state. If the reaction is interrupted before the ultimate molecular weight is obtained, unfavorable physical properties may result as the solid propellant motor is later aged, particularly at elevated temperatures. A convenient method of evaluation of possible lot-to-lot differences is an "inert" cure. The polymer and required curing agents are mixed with carbon black or other fillers, and the physical properties are measured. If the ultimate molecular weight is too high as indicated by a low ultimate elongation-to-strength ratio, adjustments are made. A convenient method of process control for polysulfide propellants was the manufacture of a liquid polymer capable of oxidation to too high a strength and modifying it by adding a monofunctional mercaptan—*e.g.*, benzyl mercaptan as a chain stopper. Since this material is monofunctional, it limits the molecular weight. The limiting molecular weight is adjusted during polymer manufacture by removing fewer of the $-\text{S}-\text{CH}_2\text{CH}_2\text{OH}$ and $-\text{S}-\text{CH}_2\text{CH}_2\text{-OCH}_2\text{OCH}_2\text{CH}_2\text{OH}$ end groups. During manufacture, these materials are more soluble in the aqueous phase than the corresponding mercaptans, and their presence can be controlled through the number of aqueous washes. The inclusion of a chain stopper in adjustable amounts in the propellant formulations provides an excellent means of obtaining polymer lot-to-lot reproducibility during propellant manufacture.

EFFECT OF CROSSLINKS IN THE POLYMER. An uncrosslinked or linear polymer has the highest extensibility but will yield when placed under long time stresses (creep). A completely three-dimensional polymer structure is brittle, seldom exhibits but a few percent elongation, and shatters when stressed at high rates of strain. The chemistry of the adjustment of crosslink density in polysulfide prepolymers centered around the use of trichloropropane as a trifunctional material in the recipe for polymer manufacture. Polymers manufactured with 0.5 mole % of trichloropropane in the initial charge of raw materials were found to require less benzyl mercaptan (chain stopper) and to be more reproducible in prepolymer production and in propellant manufacture than polymers containing 2 mole % trichloropropane. Qualitatively, monofunctional and trifunctional material may be added in small quantities in the same mole % without significant change on ultimate properties. The optimization of crosslinking *vs.* polymer length *vs.* branched chain

structure is the concern of the propellant chemist. Extensive test procedures and experienced interpretation of the results have made the difference between good and excellent solid propellant motor performance. Procedures for measuring physical properties, values for individual propellant formulations, and a discussion of interpretation and applicability of physical properties in the design of rocket motors are the subjects of separate papers (10, 15, 16) and portions of this volume.

EFFECT OF PLASTICIZER. The composite propellants discussed here differ from the propellants discussed in Chapters 2 and 3 by the manufacturing procedure. In the previous propellants the high polymer was produced in a chemical plant; for the propellants of interest here, the high molecular weight polymer is produced in the pressure vessel. However, plasticizers can be used for the same effects as discussed in the previous papers. The only additional requirement, for the polymers under discussion, is that the plasticizer be inert to the chemical reactions forming the high molecular weight polymer. Plasticizers can be used to modify the physical properties, particularly the low temperature properties, and are often used to increase the fluidity of the uncured propellant. When using plasticizers, it is important to choose a material that is sufficiently soluble in the gel structure formed by the polymer and yet sufficiently high in molecular weight to be nonvolatile. When working with plasticizers, one must consider the entire rocket system. The plasticizer may be more soluble in the inert liner surrounding the propellant, and migration will take place to the liner degrading the properties of the liner. Disastrous results can occur if the plasticizer concentrates at the interface of the propellant and liner. Should the plasticizer have significant vapor pressure, plasticizer may be distilled from the propellant, causing a change in physical properties of the propellant or equally undesirable changes in the properties of the propellant surface where strains may be greatest. Even with the possibilities of these undesirable effects, plasticizers remain one of the useful tools available to the propellant scientist for attaining desirable properties in propellant formulations. However, when it is necessary to use plasticizers, experimental plans must be more extensive and include observation for longer periods of time.

EFFECTS OF CHEMICAL REACTION ON SPECIFIC VOLUMES. When small molecules undergo condensation reactions to form larger molecules, a decrease in specific volume often occurs. For Thiokol LP-3, the decrease is approximately 5%. Since the polymer may represent only 15–30% of the formulation, this amounts to a small percent decrease in propellant volume. Decreases in some polymer systems can be so great as to make processing of the propellant in case-bonded rocket systems very difficult. This change must be considered in developing the processing procedure, and its effect is included in the discussion of volume change below.

EFFECTS OF EXOTHERMIC CURING REACTIONS. Most chemical reactions are exothermic, and reaction rates increase with increasing temperature. The effects of this chemical principle on the processing procedures and final propellant properties must be considered. During the mix cycle if the exothermic reaction progresses rapidly, two effects may be observed: (1) a rise in processing temperature resulting from inability to remove the heat; hence, different size propellant batches may exhibit different processing characteristics; (2) generation of heat indicates reaction is taking place. If a nonreproducible extent of reaction occurs before the propellant is placed in the final containers, problems may occur with batch-to-batch reproducibility of physical properties, particularly with batches of different sizes. These effects probably represent one of the greatest concerns to the processing engineer and can result in significant cost for time-temperature and environmental controls.

During cure, care must be exercised to prevent the formation of cracks and voids caused by shrinkage during solidification of the propellant. Shrinkage may be a result of temperature drop (thermal shrinkage) or to the decrease in polymer volume described above. A typical thermal shrinkage problem is depicted in Figure 2. The temperature of the propellant when cast is usually below the temperature of the curing oven. The heat of polymerization is being generated within the propellant. If the heat is generated faster than it can be removed from the propellant by conduction and radiation, as illustrated, the heat of polymerization warms the propellant above oven temperature. As the reaction approaches completion and the rate of heat generation decreases, the temperature recedes. Mechanical strength is developed only near the end of the curing process, and the propellant must pass through a critical stage in which it still has little strength but too few bonds remain to be formed and the propellant is incapable of healing across a plane of shear. To prevent permanent defects, therefore, volume changes and resulting deformation must be restricted within narrow limits during the critical stage. Specific processing conditions are obviously required for each propellant formulation, each rocket size, and specific design.

Again, the propellant scientist has several tools from which to choose. Since reaction rates usually double for each 10°C., mixing may be done well below the final cure (oven) temperature. The propellant will then receive heat from the oven as heat is generated within. At no time will the temperature of the propellant exceed the temperature of the oven. It is often advantageous to program a rise in oven temperature as the temperature of the propellant increases. Low heats of reaction or specific propellant configurations may prevent consideration of this method. A method of greater applicability is the addition of catalyst or other additives to the formulation to control reaction rate. Diphenylguanidine was

used in polysulfide propellant formulation for this purpose. Another useful material was finely divided magnesium oxide. The magnesium oxide, in addition to forming the apparently necessary alkaline environment, gave considerable improvements in physical properties. The activity and surface properties of the magnesium oxide were particularly important, and the description of the desired materials was a significant contribution of chemists.

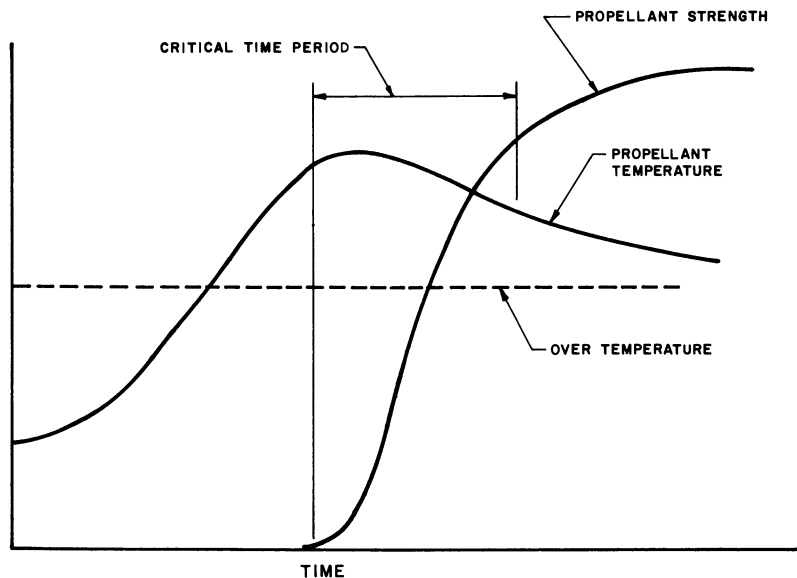


Figure 2. Propellant strength and temperature as a function of cure time

Ammonia is generated by the reaction of diphenylguanidine and magnesium oxide with ammonium perchlorate. The cure rate of polysulfide propellant formulations can be a function of the amount of ammonia removed during the mix cycle. Frequently, a vacuum is placed on uncured propellant to remove entrapped air. Too long a vacuum mix cycle, with polysulfide propellants, can remove excess ammonia changing the reaction condition during cure.

An obvious formulation change to provide different reaction rates is a change in the cure reagents. In the case of polysulfide polymers, unless active inorganic oxides or hydroxide are used, the curing agent does not enter the polymer chain. Hence, many peroxides, organic nitro compounds, and other oxidizing agents can be considered. Each will impart its own special characteristics to the processing conditions and final propellant properties.

EFFECT OF WETTING OF SOLIDS BY THE POLYMER. Much work has been done on the effect of a filler on a rubbery material, using materials

such as carbon black and titanium dioxide. Since the oxidizer and other solids represent from 65–90% of the propellant formulation, the forces developed between the polymer and solids are important in determining the final physical properties. If the solids are not wet by the polymer, when the material is strained, the polymer will separate from the solids, leaving small holes. When this happens, little additional stress is required to produce significant strains in a propellant of this type. The opposite effect can also be achieved. Significant attractive forces can be developed between polymers and oxidizers to give the propellant the physical properties of a highly crosslinked brittle polymer rather than the desired viscoelastic material. The conditions obtained when a pressure-sensitive adhesive is used between two materials is probably representative of the desired effect.

In addition to the effects on physical properties, an effect on ballistic properties may also be observed. If the polymer does not fill the entire space not occupied by the solids, when ignited the flame front may proceed by connected voids to yield an uncontrolled combustion condition. A porous condition can have an effect on the sensitivity to detonation as discussed in Chapter 10. The attractive forces between polymer and solids are probably the major contributing factor that causes differences in physical properties of propellant and causes one polymeric or polymer-plus-plasticizer system to be preferred over another.

EFFECT OF STRUCTURE ON LOW TEMPERATURE PROPERTIES. The second-order transition or brittle temperature of a polymer is determined by its structure. Since most organic halides and particularly chlorides can be used in the process for manufacturing polysulfide polymers, systematic investigation of the relationship of polymer structure to low temperature propellant properties was one of the most interesting and rewarding investigations. Investigations included the saturated aliphatic chain from ethylene to hexamethylene, as well as several specialty halides. The dibutyl formal disulfide polymer became the polymer of choice when high strain capacity at low temperature was required and is the primary polymer in many useful propellant formulations.

Crystallization of the polymer when the propellant formulation is subjected to low temperatures can be annoying (12). Formation of additional periodic attractions between molecules has the same effect as additional crosslinking. Upon crystallization, the propellant becomes hard and brittle with low strain capability. If the effect is caused by crystallization of the polymer, the original physical properties are obtained when the propellant is heated above the melting point of the polymer. These effects are time-temperature dependent and can have a significant effect on the selection of operating and storage temperatures

and conditions. Since these effects in polymers have been the subject of many investigations, the path of investigation is well characterized. Because of the time-temperature dependency, the investigations can be difficult and annoying, but sometimes the most difficult can be the most rewarding.

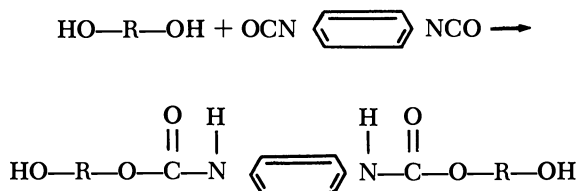
EFFECTS OF CHEMICAL CHANGES ON STORAGE CHARACTERISTICS. Propellant formulations are the result of many chemical reactions and the utilization of many engineering principles. Successful efforts have often resulted and continue to result in many useful solid propellant units for military and scientific uses. Probably nothing is more discouraging than to see a useful item fail to function after being placed in storage awaiting use. The propellant scientist in many cases can only wait for time to tell to be completely sure. However, there are a number of techniques that can be used to attempt to predict behavior on storage. Probably, the most universal test is storage under aggravated conditions. The propellant and often the entire solid propellant unit is kept at temperatures above reasonably expected operating conditions. Analysis of results is usually based on a hypothesis of an increase in reaction rate or an increase in solubility with temperature. If the selected cure reaction is one that does not go to completion, then higher temperatures may accelerate the reaction and decrease the time required to reach ultimate properties. This test can be useful when chemical reactions creating crosslinks are used. The number of effective crosslinks compared with chain-stopping reactions may increase rapidly near the end. The opposite effect is also observed. This principle can be illustrated from experience with polysulfide polymers containing formal groups where the formal group is a weak link in the chain with respect to thermal and hydrolytic degradation processes at elevated temperatures. At a temperature where the decomposition reactions involving scission of the formal link becomes important, the molecular weight of the chain decreases. The higher the temperature, the faster the reaction. Studies of aggravated aging can result in misleading results if the chemist interprets his results improperly.

If a volatile component is present in the cured propellant, another effect must be considered. In polysulfide formulations a molecule of water is generated each time a polysulfide bond is formed. The vapor pressure of the ammonium perchlorate propellant formulation becomes that of an ammonia-ammonium perchlorate saturated solution. Ammonia and water can be driven from the formulation, and the water condenses on cold surfaces. If the condensate returns to the propellant surface, perchlorate is leached from the surface of the propellant. This perchlorate may later recrystallize on the surface. A surface void of perchlorate is very difficult to ignite, while a perchlorate-rich surface produces the

Crosslinks can be controlled by the number of unsaturated sites in the polyester prepolymer. Theoretically if each molecule has only two reaction sites, then infinite, almost linear, chains could be obtained. Hence, average functionality and molecular weight distribution in the prepolymer are extremely important. Plasticizers can be used to advantage in adjusting the average properties of the binder as obtained in the solid propellant formulation.

Some of the more difficult technical problems were the inability to obtain the desired propellant strain capability required for case bonded solid rocket designs, the volatility and explosive limits of styrene, the control of the peroxide cure catalyst activity, and control of the exotherms during mixing and curing cycles. The formulation had excellent stability to further reaction on aging and good energy levels. A number of acceptable propellant formulations were obtained, particularly by Aerojet General Corp.

CHEMISTRY OF POLYURETHANES. A binder system capable of many permutations results from the reaction of difunctional alcohols with diisocyanates to form polyurethanes (5, 14).

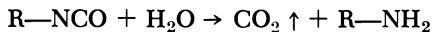


Hydroxyl terminated polymers obtained by the polymerization of ethylene and propylene oxides have been commercially available as solvents for a number of years. These materials can be obtained in any molecular weight range, many distributions of molecular weight, and have nearly pure difunctionality. Isocyanates react readily with high selectivity with the hydroxyl group. Toluene diisocyanate has been commercially available for a number of years. The crosslinking can be controlled by using trifunctional alcohols. Crosslinking can be delayed by taking advantage of the fact that isocyanates react more readily with primary alcohols than secondary or tertiary alcohols if crosslinks are formed only on reaction with a tertiary alcohol.

The reaction of isocyanates with alcohol is strongly exothermic. A portion of this heat can be removed and better quality control achieved by forming a prepolymer with half of the alcohol and the diisocyanate. The new prepolymer has isocyanate terminals and can be used with the remaining quantities of the difunctional and/or the trifunctional alcohol in the propellant mix. In recent years isocyanate-terminated polymers

have been commercially available. The alcohols used in forming these polymers may be different from those used in the propellant formulation.

A strong consideration of the chemist and process engineer interested in these system has been the control of moisture in the propellant ingredients and during processing.



The carbon dioxide is not appreciably soluble in the other propellant ingredients or the polymer. Carbon dioxide that is generated during cure creates a spongy, undesirable propellant. Control of ingredient quality and processing conditions to overcome this reaction can result not only in control of carbon dioxide generation but in the additional benefit of excellent batch-to-batch reproducibility. The general applicability of this cure mechanism, the availability of many synthesis routes to hydroxyl-terminated systems, the availability of diisocyanates in the urethane plastic field, all have led to investigation of many different polyurethane systems in propellants.

The propellant scientist has always been interested in getting more fuel value in the polymer, or greater self-contained energy into the binder so that more metallic fuels and high energy solids could be incorporated into the formulation. Excellent work (7) has been accomplished particularly by Aerojet-General Corp. in incorporating nitro groups into the prepolymer, the isocyanate, and the trifunctional alcohols. These have been converted into excellent high energy propellant formulations.

Several of the urethane polymers are known for their thermal stability. Probably related to the thermal stability are the slow burning rates that have been obtained with some of the propellant formulations based on polyurethanes.

The constant awareness that the propellant chemist must keep for small amounts of impurities can be illustrated by the effects of the small quantities of peroxide that can be found in the polyoxide polymers. Small quantities of peroxide lead to chain scission at elevated temperatures and result in depolymerization.

Probably in no other propellant binder system will one find the number of excellent examinations of propellant failure criteria as have been carried out on the urethane propellants. This can be partly attributed to dewetting of the oxidizer that occurs when many of these formulations are strained, the high ultimate elongations that have been obtained on many of them, and because of the large number of binder ingredient permutations that can be made. The development of propellant science owes much to the many investigations performed on these materials.

CHEMISTRY OF POLYESTERS. As new applications for solid propellants were demonstrated and as the development of propellant science accel-

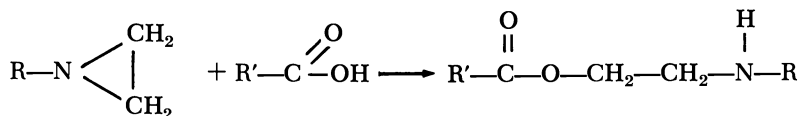
erated, the chemists began to consider the synthesis of polymers specifically for use in propellants. The desire for high fuel value suggested hydrocarbon polymers. The tremendous background available on elastomeric 1,4-butadiene copolymers suggested that one of the starting materials should be butadiene. Many vinyl compounds containing functional groups will copolymerize with butadiene. A copolymer that has found considerable interest is that of butadiene with acrylic acid. It can be made by bulk polymerization or in aqueous emulsions. Most of the polymers of interest in propellants are made by the latter process. The difference in the solubility in water of butadiene and acrylic acid allows adjustment of emulsion stability to control the kinetics and hence the amount of acrylic acid that enters the polymer. The copolymer can be manufactured in a wide range of molecular weights, molecular weight distributions, average functionability per molecule, water content and residual impurities (11, 21). A number of difunctional epoxides, such as the diglycidyl ether of bisphenol A, in a number of molecular weight ranges and purities are available as curing agents. With a knowledge of additives, plasticizers, effects of polymer variations, the propellant scientist has tailored many successful propellant formulations. More pounds of propellant have been made from this type system than any other.

A terpolymer of butadiene, acrylonitrile, and acrylic acid can be made by similar procedures developed for the copolymer. Substitution of this terpolymer in propellant formulation results in a higher modulus and a greater resistance to creep without appreciable sacrifice of strain capability except at temperatures below ambient.

Since these polymers vary in average functionability, primary and secondary carboxyl groups, 1-2 and 1-4 addition product, and chain-branching products, it is not surprising that excellent control must be exercised during manufacture of the prepolymers and during propellant production.

The reaction of epoxides with carboxylic acids in the presence of ammonium perchlorate can be very slow. The search for a catalyst to accelerate the cure rate for a particular formulation can be particularly rewarding. The slowness of the reaction can lead to a disadvantage of the system if not carefully investigated. If cure is stopped before all of the epoxide groups have been consumed, cure will continue at a rate which depends on storage temperature. The epoxide can continue to react with carboxyl groups rapidly at elevated temperatures, or very, very slowly at ambient temperature, to yield highly crosslinked propellant systems with low strain capability.

Similar systems have been developed using di- and/or trifunctional derivatives of aziridines as curing agents.



The curing rates are somewhat faster. The aziridines do not react with the secondary amines formed during the cure as the epoxides react with the hydroxyl groups. Hence, side reactions are avoided. The difficulties in producing di- and trifunctional materials of high purity have hindered the wide acceptance of aziridines except in speciality formulations.

A hydrocarbon prepolymer containing terminal carboxyl groups (28) is available to the propellant chemist. These polymers were synthesized to eliminate some of the variables found in the copolymers. The carboxyl groups can be made of the same types with like reactivity. These linear non-branched polymers impart greater extensibility to elastomeric formulations. The chemistry in propellants is similar to the random functionality polymer. As 20 years of the chemistry of crosslinked propellant binders is reviewed, one familiar with the art cannot fail to predict solid propellant formulations using these polymers tailored to the specific requirements of the solid rocket design with the confidence that any discipline of science can be practiced.

Miscellaneous Topics

This discussion has been concerned primarily with the chemistry of the polymer in filled crosslinked elastomer formulations. Since the purpose of these formulations is to produce a gas with high enthalpy, thermochemistry is important. The heat of combustion of the components and the effect of the nature and molecular weight of the gaseous products are included in several literature references. The increase in enthalpy that can be obtained by adding finely divided metals to the formulations makes the use of these materials desirable in many applications. Their presence has catalyzed many excellent studies on two-phase gas flow particularly during expansion in a nozzle.

Since realization of the expected performance depends on rate of combustion and combustion efficiency, many studies have been made on catalysis. The studies of iron oxide have been particularly fruitful. The activity, amount and particle size of the iron additive can be an important tool in adjusting the performance of a propellant formulation. In many propellant formulations, performance can be improved by using soluble catalysis.

When a cured propellant formulation is transparent to radiation from the flame front, adjustment of the opaqueness by using carbon black can yield valuable changes in performance.

Compatibility of ingredients is always important. Particularly important to safe handling is the autoignition temperature and friction sensitivity of the propellant. Small changes in the formulation can often effect these important properties. An example is the sensitivity of some propellant formulations to extremely small amounts of chlorate. Safety precautions must always include consideration of the chemistry. By following this practice, the propellant industry has experienced an excellent safety record while making unusual progress in the application of viscoelastic materials in case-bonded solid propellant rockets.

Summary

Applications of scientific principles have resulted in removing the "black magic" that characterized the early applications of solid propellants. In 25 years of existence, solid composite propellants have become a major industrial product. The achievements of the solid propellant scientists give a real feeling of confidence in the use of this product when designed and developed by a competent and experienced scientific team. Exciting new advances in the state-of-the-art will be built on the sound foundation that has been established.

Literature Cited

- (1) Arendale, W. F., *Ind. Eng. Chem.* **48**, 725 (1956).
- (2) Arendale, W. F., Neely, T. A., "Encyclopedia of Chemical Technology," 2nd suppl. ed., Interscience, New York, 1960.
- (3) Billmeyer, F. W., "Textbook of Polymer Chemistry," Interscience, New York, 1962.
- (4) Bueche, F., "Physical Properties of Polymers," Interscience, New York, 1962.
- (5) Burns, E. A., *Anal. Chem.* **35**, 1270 (1963).
- (6) Fettes, E. M., Ed., "High Polymers," Vol. XIX, Interscience, New York, 1964.
- (7) Fischer, J. R., U. S. Patent 3,087,961 (1963).
- (8) Flory, P. J., "Principles of Polymer Chemistry," Cornell University Press, Ithaca, 1953.
- (9) Glassman, I., *Am. Scientist* **53**, 508 (1965).
- (10) Groetzinger, W. H., III, *ARS J.* **30**, 498 (1960).
- (11) Gustavson, C., Woychesin, E. A., *Ind. Eng. Chem., Prod. Res. Develop.* **5**, 314 (1966).
- (12) Hunter, W. E., Foster, E. T., Mangum, G. F., *ARS Publ.* **1594-61** (1961).
- (13) Jorczak, J. S., Fettes, E. M., *Ind. Eng. Chem.* **43**, 324 (1951).
- (14) Klager, K., Geckler, R. D., Parrette, R. L., U. S. Patent 3,132,967 (1964).
- (15) Kruse, R. B., *AIAA Paper* **65-147** (1965).
- (16) Landel, R. F., Smith, T. L., *ARS J.* **31**, 599 (1961).

- (17) Lawrence, R. W., U. S. Patent **3,000,175** (1961).
- (18) *Ibid.*, **3,000,715** (1961).
- (19) Meares, P., "Polymers, Structure and Bulk Properties," Van Nostrand, London, 1965.
- (20) Penner, S. S., "Chemistry Problems in Jet Propulsion," Pergamon, New York, 1957.
- (21) Quacchia, R. H., De Milo, A. J., *Ind. Eng. Chem., Prod. Res. Develop.* **5**, 351 (1966).
- (22) Ritchey, H. W., *Astronautics* **39** (Jan. 1958).
- (23) Roberts, R. F., U. S. Patent **3,031,288** (1962).
- (24) Sarner, S. F., "Propellant Chemistry," Reinhold, New York, 1966.
- (25) Sutton, G. P., "Rocket Propulsion Elements," 2nd ed., Wiley, New York, 1963.
- (26) Taylor, James, "Solid Propellant and Exothermic Compositions," Interscience, New York, 1959.
- (27) *Technol. Week* **19**, 42 (1966).
- (28) *Thiokol Bull.* **RP-3** (1966).

RECEIVED May 4, 1967.

Polyurethane-Based Propellants

A. E. OBERTH and R. S. BRUENNER

Research and Technology Department, Aerojet-General Corp.,
Sacramento, Calif.

Solid propellant technology as pertaining to polyurethane-based propellants is presented. Particular emphasis has been placed on the newer developments as well as the fundamental knowledge gained in the field. Much of this knowledge is not restricted to solid propellant technology but is of general nature. This includes contributions to kinetics and mechanism of the urethane reaction, metal catalysis, the effect of fillers on mechanical properties of filled elastomers, tear phenomena in composite materials, the importance of the interface between solid particle and matrix on physical properties, and the mechanism of filler reinforcement. Progress pertaining more directly to propellant technology includes such topics as catalyst modification to increase the potlife of propellant batches, calculation of mix viscosities of multimodal dispersions, mechanism and prevention of moisture embrittlement, and others.

The need for dimensionally stable composite propellants led to the replacement of asphalt as a binder by polymerizable liquid compounds, such as unsaturated polyesters, styrene, and acrylates, which after mixing with the solid ingredients were converted to a rigid matrix by radical induced polymerization (21). Case-bonded motors demanded an increased strain capability of the propellant grain which was first met by polysulfide binder systems (1, 4, 19, 23). Large rocket motors with higher ballistic performance and stringent mechanical requirements led to the development of polyurethane propellants which made their debut in the mid-1950's (11, 24). This paper is mainly concerned with the newer technological developments, particularly the advances made in improving the mechanical properties.

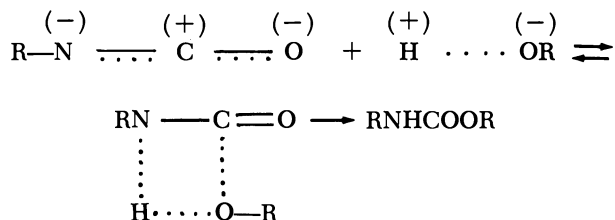
Polyurethane propellants derive their name from a rubbery matrix which is formed through the reaction of organic, hydroxyl-carrying

molecules with isocyanates. As in all solid propellants the matrix keeps oxidizer, metallic fuel, and other solid components dispersed. Further, it provides the necessary exhaust gases on combustion and imparts mechanical strength to the propellant. The backbone structure of the matrix may consist of polyethers, polyesters, or a mixture of both, which may or may not contain ester-type plasticizers. More recently, hydroxy-terminated polybutadienes and their hydrogenated versions have been added to the list (22).

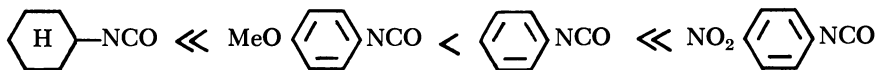
The solids content of propellants ranges between 70 and 90%. The higher limit is dictated by processability. Propellants with less than 70% solids are rare since the specific impulse of such combinations is unduly low. Ammonium perchlorate is the preferred oxidizer and takes the largest percentage in the composition. For special formulations ammonium nitrate or other oxidizing agents may be encountered. Aluminum powder is the most frequently used additive to boost specific impulse and may be found in quantities up to 25%.

The Urethane Reaction

The urethane reaction is particularly useful for solid propellant applications because of its quantitative nature, convenient rate which can be adjusted by proper choice of catalysts, and the availability of many suitable hydroxyl compounds which permit the tailoring of propellant mechanical properties. Despite the quantitative nature and apparent simplicity of the urethane reaction: $R'NCO + ROH \rightarrow R'NHCOOR$, its exact course has not been fully explored yet. It does not follow simple second-order kinetics as the above formula would suggest since its second-order rate constant depends on many factors, such as concentration of reactants and the nature of the solvent. Baker and co-workers (2) proposed that the reaction is initiated through the attack of an alkoxide ion on the carbon atom of the isocyanate group



Thus, any substitution of the isocyanate molecule which renders this carbon atom more positive should increase the reactivity of the isocyanate. This was verified by Baker (3), who showed that reactivity greatly increased in the following order:



In addition, compounds favoring the formation of alkoxide ions should accelerate the reaction, as shown by Farkas and Strohm (14) and by Oberth and Bruenner for metal as well as base catalysts (7, 26, 27). This latter view on catalysis is recent—earlier investigators assumed activation of the isocyanate (38)—but is gaining increasing acceptance (18). The hypothesis also explains differences of reactivity among the individual alcohols as well as the effects of solvents on the rate of reaction (26), as shown by the good correlation between the energy of the hydrogen bond and the reactivity of the respective alcohol or alcohol-solvent pair. In uncatalyzed reaction mixtures the strongest polarization of the oxygen-hydrogen bond (favoring the formation of the alkoxide ion) occurs in self-associated or so-called polymeric alcohol (energy of the bond 4–5 kcal./mole). Hence, the reaction rate constant is highest in systems where this species predominates—*e.g.*, in concentrated mixtures and in solution in weak solvents. Conversely, dilute solutions in strong solvents like ethers, nitriles, and esters contain the alcohol almost exclusively as the very weakly hydrogen-bonded single bridge dimer with correspondingly low reactivity (bond energy, *ca.* 1 kcal./mole). According to this classification monomeric alcohol should be the slowest reacting alcoholic species, but since monomeric alcohol occurs only in equilibrium with the polymeric form or alcohol solvent complexes, experimental verification has not been obtained yet. The energy of the hydrogen bond in amine-alcohol complexes attains values of 10 kcal./mole and thus accounts readily for the catalysis by organic bases (3, 14, 26). Finally, alkoxoacids formed from the metal catalysts and the alcohol (7, 27), contain the alcohol in completely ionized form, which could explain the particularly high activity of some catalysts. For example, the reaction between butyl isocyanate and butanol in dioxane is accelerated up to 10^7 times by addition of small quantities of ferric acetylacetonate. The latter is the preferred catalyst in polyurethane propellant formulations.

Reactions of the Urethane Group

Thermal Cleavage. Urethanes derived from aliphatic primary or secondary alcohols are rather stable even at elevated temperatures. They will decompose above 200°C. in contrast to urethanes derived from tertiary alcohols or phenols, which decompose at lower temperatures. The presence of certain catalysts may also accelerate the thermal decomposition—*e.g.*, catalysts used in the preparation of the urethane (39). Thermal decomposition yields a variety of products from several possible reactions

which can occur simultaneously. Some known reactions are the dissociation into isocyanate and alcohol (6, 12) (the back reaction of the urethane formation) and the breakdown of the urethane into a secondary amine and carbon dioxide or into a primary amine, an olefin, and carbon dioxide (12). To obtain the good thermal stability of urethanes, it was found necessary to inactivate the cure catalysts or other such impurities at a later stage. For example, sulfur will deactivate ferric acetylacetonate at high temperatures or over extended periods of time, but it will not affect significantly the catalyst during cure (short time and moderately elevated temperature).

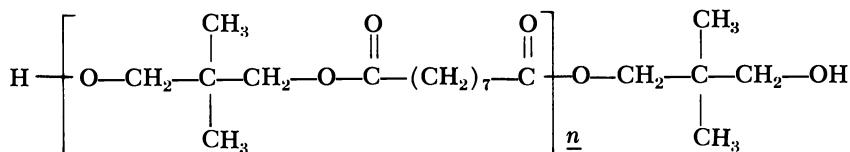
Hydrolytic Cleavage. As a derivative of carbonic acid the urethane group can be cleaved hydrolytically but only under rigorous conditions (40). It is more stable than an ester group but can react similarly with alcohols and amines (20, 35). However, such conditions are unlikely to prevail in a propellant.

Propellant Binder Components

In principle any diol/triol mixture which reacts with a diisocyanate will yield a network. However, to be useful as propellant binder, additional requirements must be met. The most important are low cure shrinkage, low reaction exotherm, rubbery characteristics down to arctic temperatures, good aging stability, and ease of handling during propellant manufacture.

Many of these requirements are fulfilled by long chain diols as the main building block for the polymeric network. This keeps the isocyanate concentration at low levels, avoiding the problems of excessive cure shrinkage, exotherm and hard, non-rubbery properties. All of the presently used diols, forming the bulk of the binder matrix are polymers with molecular weights up to 10,000 carrying terminal hydroxyl groups. According to the backbone structure they may be subdivided into polyesters, polyethers, and polybutadienes. Of the polyethers a few high molecular weight triols exist also, which find application in solid propellants.

Polyesters. Of the great variety of potential candidates only poly-(neopentylglycol azelate) (NPGA), a liquid material of approximately 2000 molecular weight, is still used in modern propellants. Its chemical structure is shown below.



Polyesters are not desirable because of the lower specific impulse than those obtained with polyether or polybutadiene matrixes at practical solids loadings (*cf.* Figures 17–19) and their comparatively high viscosity. This high viscosity is caused at least in part by a wide distribution of the molecular weight in the prepolymers. Because the low temperature properties obtained with NPGA are not outstanding, it is used in combination with polyether diols to which it imparts better tensile properties at the higher and ambient temperature regions. Other polyesters which may be found in older propellant formulations are poly(neopentyl glycol sebacate) and poly(neopentyl glycol-6-nitro sebacate).

Polyethers. Three structurally different polyether diols are mainly used: poly(1,2-oxypropylene) diol (PPG), poly(1,2-oxybutylene) diol (B-2000), both terminated essentially by secondary hydroxyl groups, and poly(1,4-oxybutylene) diol, a considerably more reactive component owing to primary hydroxyl termination. Of these the poly(oxypropylenes) (PPG) are offered in a wide range of molecular weights. Triols are also available with this backbone. The main advantages of the polyethers are their availability in large quantities, low viscosity, and proper rate of cure. With respect to impulse, polyethers stand between polyesters and polybutadienes over which they have the advantage of greater aging stability. Although polyethers are known to absorb oxygen and form peroxides which decompose at elevated temperatures causing chain cleavage, addition of aromatic amine type antioxidants easily corrects this disadvantage. Thus, propellants have been made which were aged several years at elevated temperatures (150°–180°F.) without significant loss of mechanical properties. Poly(1,2-oxypropylenes) and poly(1,2-oxybutylenes) have low glass transition temperatures (T_g) and are therefore suitable for the manufacture of propellants which are to be operational over a wide temperature range.

The most widely used compound is PPG with approximately 2000 molecular weight. High molecular weight triols, such as trimethylolpropane-initiated poly(oxypropylene) glycols with molecular weights up to 5000, are also frequently encountered in propellant binders. B-2000, a 2000 molecular weight poly(1,2-butylene glycol) (Dow Chemical Co.), gives outstanding low temperature properties and does not suffer from moisture embrittlement (*see* below). Poly(1,4-oxybutylene) of approximately 1000 molecular weight (LD-124, duPont) and its higher analogs (*e.g.*, T-30 approx. 3000 MW, duPont) have found limited application in some propellants. Although these latter two prepolymers produce very strong binders, their high T_g value precludes use as propellant matrixes where low temperature performance is required. They have found extensive use in liner formulations (*see* below).

Other polyethers which have found limited application are poly(ethylene oxides) and some mixed polyester-polyethers such as Peedo-120 (Union Carbide), a diester of poly(1,4-butylene oxide)diol and azelaic acid.

Polybutadienes. Hydroxyl-terminated polybutadienes are comparatively late comers and are still in the development stage. They combine the high specific impulse of the well-proved carboxy-terminated polybutadienes with the clean, stoichiometric urethane reaction yielding propellants with unsurpassed mechanical properties.

The hydroxyl-terminated polybutadienes are the only prepolymers which have been specifically prepared as prepolymers for propellant binders. Because of the high reactivity of the hydroxyl group in an all-hydrocarbon environment these materials have to be processed carefully to avoid premature curing (potlife). Depending on the manufacturing process, their functionality is not always well defined. As with all polybutadienes they are subject to air oxidation with subsequent hardening. Partial or total hydrogenation solves this problem but introduces others—*e.g.*, high viscosities and higher T_g values with consequent poor low temperature properties.

Depending on the catalyst and process used, the microstructure of the polymer can be varied from a low to a high vinyl content (20–80%). Increasing vinyl content raises viscosity and T_g and therefore should be kept low. Typical microstructure data for some prepolymer candidates are shown in Table I.

Table I. Microstructure Data for Prepolymers

Polymer	Source	Process	Initiator	Percent		
				Cis	Trans	Vinyl
Butarez	Phillips Petrol.	anionic	organolithium	34	39	27
Telagen	General Tire	anionic	organolithium	34	41	25
Hycar	B. F. Goodrich	free radical	azobis(cyano-pentanoic acid)	29	51	20

Polyfunctional OH Components (Crosslinkers). For crosslinking, trifunctional alcohols are used mainly. Some are of the same type as the difunctional prepolymers—*e.g.*, polyethers derived from trifunctional initiators (glycerol, trimethylolpropane, 1,2,6-hexanetriol) and propylene or butylene oxide—and are preferred. Low molecular weight alcohols are used also. Examples are the ones listed above and glycerol monoricinoleate, glycerol triricinoleate and amino alcohols like triethanolamine.

Tetrafunctional crosslinkers are rarely used. An example is tetra-(2-hydroxypropyl)ethylenediamine.

Isocyanates. The most common isocyanates encountered in polyurethane propellants are 2,4-tolylene diisocyanate, TDI, and hexamethylene diisocyanate, HDI. 3-Nitrazapentane diisocyanate has also been used in high density propellants. In some polyurethane liners Adiprene L (duPont), a NCO-terminated condensation product of poly(1,4-oxybutylene)diol and TDI is used, as well as some of the more highly functional isocyanates, such as polymethylenepolyphenyl isocyanate (Papi, Carwin Chemical Co.).

Plasticizers. The desirable effects which plasticizers impart are lower mix viscosity and improved low temperature properties (lower T_g). Sometimes a lower elastic modulus of the propellant, also a consequence of plasticization, is desired. Table II lists some of the more frequently used plasticizers.

Other Additives. Additives are sometimes required to improve processing or handling of solid propellants. These include antifoaming agents, antioxidants, and other stabilizing and desensitizing agents. Their function is to stabilize and maintain the desired mechanical properties, and to ensure processing characteristics that facilitate mixing and casting, while other additives serve as curing accelerators or as burning rate modifiers. Some are inorganic salts, and others are organic liquids. Table III lists some commonly used chemicals.

Table II. Plasticizers Used in Solid Propellants

	<i>Boiling Point, °C.</i>	<i>Melting Point, °C.</i>	<i>Density at 25°C. grams/cc.</i>	<i>Viscosity, cp.</i>
Isodecyl pelargonate (2.5 mm. Hg)	150	-80	0.855-0.866	1.38, 100°C.
Dioctyl sebacate (4 mm. Hg)	248	-55	0.910-0.913	19.9, 20°C.
Dioctyl adipate (5 mm. Hg)	214	-70	0.919-0.924	13.7, 20°C.
Oronite 6 (Standard Oil of California)	—	-50 to -56 ^a	0.830 (15.5° / 15.5°C.)	1.66-5.0, 100°C.
Bisdinitropropyl acetal/ Bisdinitropropyl formal (1:1)	—	0	1.383-1.397	18.5, 25°C.
Circo Light Oil (Sun Oil Co.)	—	-34 ^a max	0.920-0.928	62, 25°C.
Di(butylcarbitol) formal (5 mm. Hg)	195-197	—	0.96-0.97	6, 20°C.

^a Pour point.

Table III. Modifiers and Additives

<i>Stabilizers</i>	<i>Processing Aids</i>	<i>Fillers</i>	<i>Ballistic Modifiers</i>
Diphenylamine	lecithin	carbon black	metal oxides
Phenyl-naphthylamine	sodium laurylsulfate	dyestuffs	alkaline earth carbonates
Magnesium oxide	silicone oils	metal wire	alkaline earth sulfates

Processing Characteristics of Polyurethane Propellants

Compatibility. Owing to the high reactivity of the isocyanate group, polyurethane propellants require a more sophisticated processing technique than the rather foolproof, carboxy-terminated polybutadiene aziridine and/or epoxy-cured propellant systems. Processing is even more complicated if "bonding agents" (*see below*) are present, which are used to bolster mechanical properties in practically any modern propellant.

All binder components must be completely miscible, except the bonding agents which need not be soluble in the binder components. Further, it is advantageous if the hydroxyl groups on the diols and triols have about equal reactivity to obtain a uniform distribution of crosslinks in the final network. Some materials, usually low molecular weight diols, become sparingly soluble when they react partially with an isocyanate and may precipitate during cure. Such a binder will become heterogeneous and exhibit poor mechanical properties.

Finally, the prepolymers forming the binder network as well as the plasticizers should not possess any solvating power for the ammonium perchlorate. For example, poly(ethylene oxides) besides being hygroscopic, dissolve too much oxidizer leading to extremely viscous, non-mixable, propellant batches.

Much the same happens if the prepolymers contain basic (tertiary) amino groups—*e.g.*, diols based on primary amines extended with propylene and ethylene oxide and similar materials. The amine nitrogen reacts with the oxidizer, releasing ammonia, and is itself converted to the ammonium ion. Ensuing ionic interaction raises the viscosity of the batch to the point where it becomes unmixable (*see also* later section on moisture embrittlement).

Mix Process. Usually all liquid components (except the diisocyanate), antioxidants, ballistic additives, bonding agents, and metallic fuel are blended together and transferred to the mixer, a jacketed stainless steel vessel with provisions for vacuum mixing. This mixer is not much different from those found in the bread-baking industry, from which, in fact, this one was derived. Depending on the type of propellant, the

temperature of mixing ranges from ambient to 150°F. With the mixer blades in action, oxidizer is added from a hopper. After completion of the oxidizer addition, the batch is agitated in vacuum to remove dissolved gases which otherwise would cause porosity in the cured propellant. The vacuum mix cycle is followed by the addition of the curative, HDI or TDI in which the cure catalyst, ferric acetylacetonate, or other metal catalysts are dissolved. Addition of the curative is followed by the final vacuum mix. The liquid propellant batch is then either cast directly into prefabricated and lined rocket chambers or transferred to the casting station, where the casting of large rocket motors, requiring more than one propellant batch, takes place. Before casting, quality control tests are conducted on the liquid propellant which ensure that the properties of the cured propellant will fall within specification.

Potlife. Batch qualification and casting usually take several hours during which time the propellant must stay fluid. This time is called potlife and obviously depends on such factors as catalyst level and temperature of the propellant batch. Reduction of the catalyst concentration to obtain an acceptable potlife is not always advisable because it may prolong unduly the time for complete cure. Further, unreacted hydroxyl and/or isocyanate groups tend to undergo undesirable side reactions.

A practical solution to this problem has been worked out as a direct consequence of studying the mechanism of metal chelate catalysis (7, 28). It was found that the catalytic activity of metal acetylacetonates was reduced upon adding small quantities of acetylacetone, HAA (Figure 1). Acetylacetone is fairly reactive and is consumed slowly by the metallic fuel or other propellant ingredients. Thus, the catalytic activity of the metal acetylacetonate is restored. The proper ratio of $\text{Fe}(\text{AA})_3/\text{HAA}$ depends on the propellant binder system—*e.g.*, a molar ratio of 1:2 will usually give satisfactory potlife in binder systems using diols with secondary hydroxyl groups. This method has been found particularly useful for processing propellants containing bonding agents (*see below*).

Processing in the Presence of Bonding Agents. Propellant batches containing bonding agents exhibit the unique phenomenon of a “dry mix” before the addition of the isocyanate. The batch has no fluidity whatsoever, and its consistency ranges from a wet, clay-like lump to a dry powder, depending on solids content and the chemical nature of the binder. This condition is probably caused by hydrogen bonding between the hydroxyl groups of the bonding agents enveloping the oxidizer particles and the diol and triol compounds of the matrix. Bonding agents for polyurethane propellants are small, highly polar, organic diols or triols (*e.g.*, triethanolamine), which accumulate on the surface of the oxidizer particle, yielding a dense layer of hydroxyl group. Upon adding the diisocyanate and cure catalyst the comparatively fast-reacting hydroxyl

groups of the bonding agents are converted into NCO-terminated moieties having much less hydrogen-bonding ability (26). This causes the "physical network" to collapse and restores the fluidity of the propellant batch. The potlife-prolonging $\text{Fe}(\text{AA})_3$ -HAA method is particularly useful here since fluidity of the propellant batch depends on partial reaction of the hydroxyl group. Thus, only catalyst and diisocyanate are added, and mixing continues until the propellant batch has reached its maximum fluidity. Addition of acetylacetone slows further polymerization, thus ensuring optimum castability combined with good potlife.

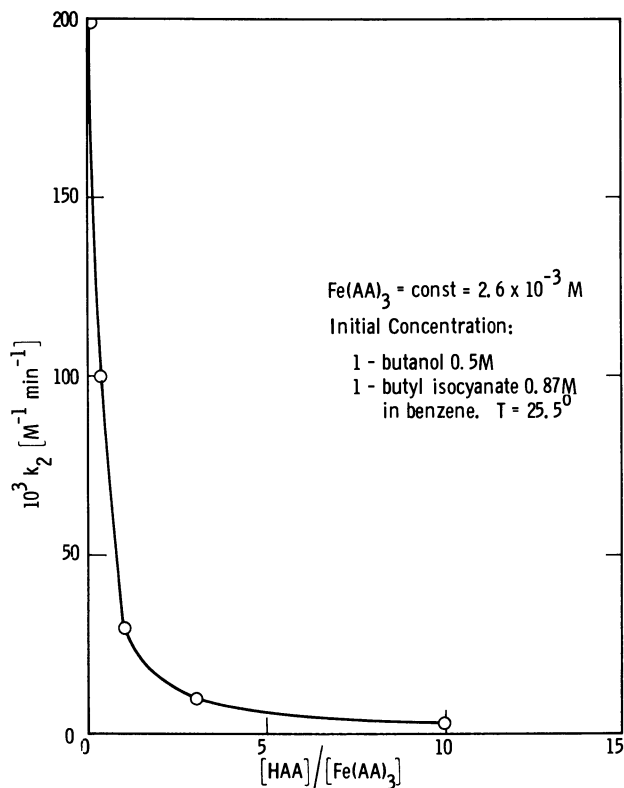


Figure 1. Dependence of the rate of the $\text{Fe}(\text{AA})_3$ -catalyzed urethane reaction on HAA addition

Quality Control and Reproducibility

Analytical Tests. The properties of the binder network and thus the mechanical properties of the final propellant depend largely on the stoichiometry of the urethane reaction. Reproducibility requires a host of analytical tests such as the determination of hydroxyl number, acid

number, and water content. Similarly, the propellant batch is monitored by such tests as density determinations (indicating the correct composition), viscosity buildup (indicating the expected cure profile), a rapid cure test (showing whether the propellant should be cast or not), and others. The last is probably the most important of these three. These tests are well established throughout the propellant industry and need no further comment. With the advent of the more sophisticated hydroxyl-terminated polybutadiene prepolymers, functionality and functionality distribution became a new problem.

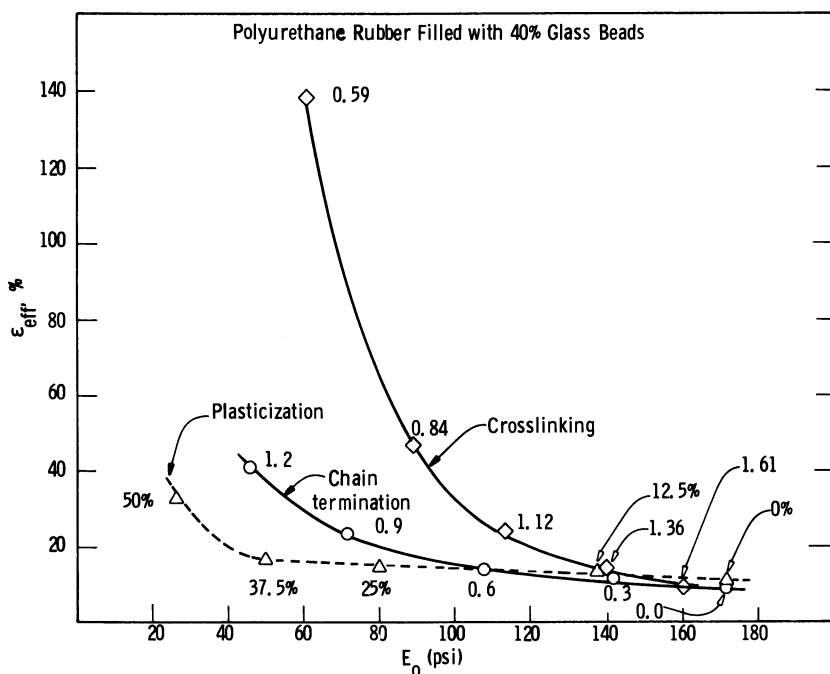


Figure 2. Effect of crosslinking, chain termination, and plasticization on effective strain. Numbers on points refer to percent plasticizer, moles of chains $\times 10^4$ /cc. or moles of chains $\times 10^4$ /cc. dangling, respectively

Functionality and Functionality Distribution of Prepolymers. It is customary to use the initial modulus of a propellant as a guide number for the expected strain capability. Therefore, propellant moduli are held between certain specific limits. As long as the prepolymers used in these propellants are manufactured in well established technical processes, such specifications are adequate. In new propellant developments, where different prepolymers stemming from the various vendors are screened,

the initial modulus no longer suffices as criterion. The same propellant modulus, for example, can be achieved in three different ways (not altering the solid content). Chain termination, changing plasticizer content, and using different crosslinker to chain extender ratios will affect the initial modulus but do not impart equivalent strain capability to the final network. Only the last method yields acceptable binders with high "effective strain" values (Figure 2). The "effective strain" is defined here as the strain at the point where the extrapolated straight line-portion of the volume-increase curve intersects the strain axis (Figure 3); it may be interpreted as the strain at which significant propellant dilatation commences. Investigation of the dilatational behavior of many solid propellants indicated good correlation between the effective strain and the strain-cycling capability of propellants.

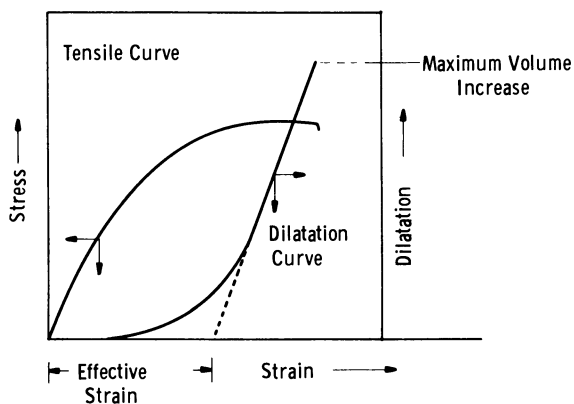


Figure 3. *Representative dilatation curve*

Usually the propellant chemist would not adjust the modulus by introducing chain termination into an otherwise over-crosslinked binder. However, the problem is that involuntary chain termination is omnipresent. The two main culprits are poor functionality of the binder prepolymers and deviations from stoichiometry during the cure reaction. Thus, it is of prime interest to ascertain the exact functionality and functionality distribution of prepolymers. One method which has been worked out and found to give good values for the over-all functionality is shown in Figure 4. The equilibrium modulus of a number of elastomers prepared from some representative prepolymers with differing concentrations of crosslinker (in this case CTI = cyclohexanetriisocyanate) is plotted against the quotient of weight fraction and the molecular weight of the crosslinker. Presumably at zero crosslink density the equilibrium modulus

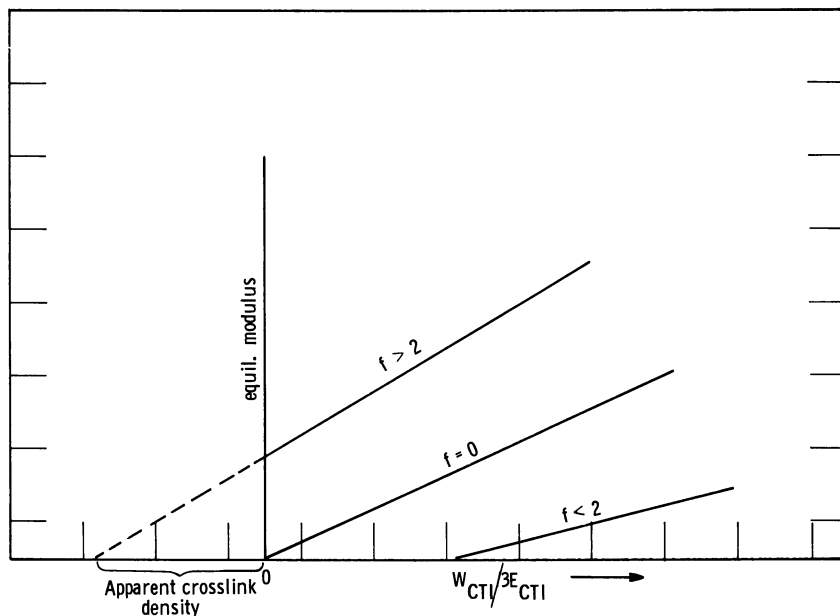


Figure 4. Equilibrium modulus vs. functionality of prepolymers as ascertained for elastomers prepared with increasing quantities of CTI (cyclohexane triisocyanate)

is also zero. From the intercept with the abscissa, the functionality can be calculated if the theoretical crosslink density ν_{th} of the binder is given by

$$\nu_{th} = \frac{3d}{2} \sum_{i=1}^n \frac{(f_i - 2)}{f_i} \frac{W_i}{E_i}$$

where d is the density of the cured rubber, f_i is the functionality of the i th component in the binder and may assume values between 1 and 3, W_i is its weight fraction, and E_i is the analytically determined equivalent weight. The equation is based on the following considerations. Of an f -functional compound two functions are used for chain propagation. Therefore, $(f - 2)/f$ represents the fraction of the functional groups which is available for crosslinking. The crosslink density will be proportional to the weight fraction of the particular component and inversely proportional to its equivalent weight. Only those prepolymers contribute to the over-all crosslink density whose functionality differs from 2.0. Plasticizers ($f = 0$) are to be excluded since they are not part of the rubber network. However, they modify the weight fraction of the functional components. The factor $3d/2$ converts the crosslink density from "moles branch points/gram" to the more familiar "moles chains/cc."

Thus, at zero equilibrium modulus we can write for a three-component binder consisting of a known crosslinker (assume $f = 3.0$), a known diisocyanate (assume $f = 2.0$) and a prepolymer of unknown functionality f :

$$0 = \frac{2\nu_{th}}{3d} = \frac{W_{CTI}}{3E_{(CTI)}} + \frac{(f-2)W_p}{fE_p},$$

where W_p and E_p are weight fraction and equivalent weight of the prepolymer of unknown functionality. Since all quantities except f are known, f can be evaluated. It can be shown that the average functionality, f , so obtained is identical with the quotient of the sum of all equivalents/sum of all moles.

An average functionality of 2 does not necessarily mean that the binder prepolymer is of good quality. For example, an average functionality of 2 can be easily obtained by blending mono-, di-, and tri-functional binder constituents. However, such a practice would not be conducive to good mechanical properties of the cured propellant binder.

Stress decay (relaxation) measurements of propellant binders are a way to obtain insight into the network structure of binder systems (29). In addition, high hysteretical losses appear to be associated with good tensile properties. Figure 5 shows a normalized stress-decay *vs.* time plot of a polyurethane elastomer. If the reference stress, σ_R , is chosen at a time which is long compared with the time it took to stretch the speci-

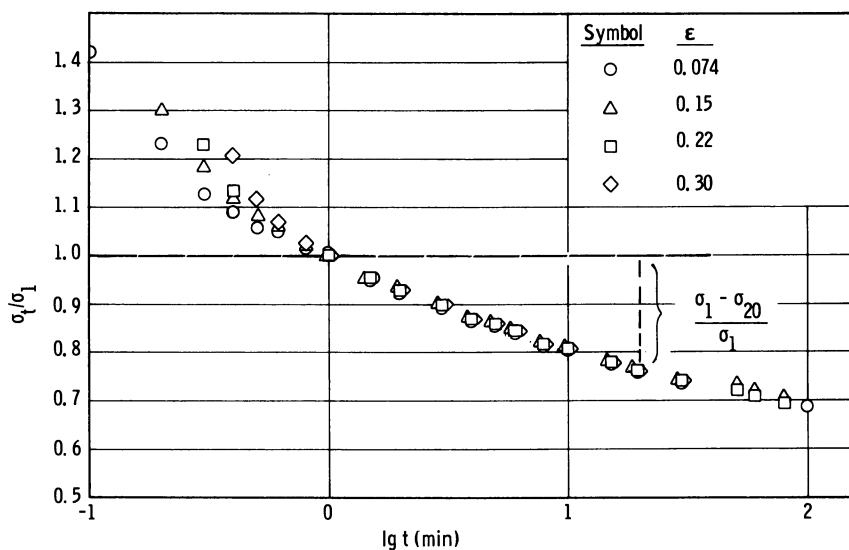


Figure 5. Normalized stress-relaxation *vs.* time plot of an LD-124, PPG-IDP-HDI elastomer pulled to different strains. $T = 25^{\circ}\text{C}.$; $\dot{\epsilon} = 0.74 \text{ min.}^{-1}$

men, then the relative stress decay D_R defined as $D_R = (\sigma_R - \sigma_t)/\sigma_R$, where σ_t is the stress at time t , becomes independent of the degree of deformation, or gage length of the specimen. One and 20 minutes were chosen for σ_R and σ_t , respectively. Figure 6 shows a plot of D_{20} vs. the molecular weight between crosslinks at three temperatures for a polybutadiene-polyurethane rubber. As long as the elastomer is in the rubbery region—*i.e.*, follows at least qualitatively the predictions of the theory of elasticity—its stress decay increases with increasing molecular weight between crosslinks, M_c . Adjustment of M_c by changing the ratio of crosslinker to chain extender maintains proportionality between M_c and the length of the chain between crosslinks, M_l . If chain scission is used to increase M_c , M_l will lag behind M_c . All propellant binder systems tested showed that chain scission yielding long unconnected chain ends did not raise D_{20} significantly. Chain termination can be produced experimentally by introducing monoisocyanates, not using enough diisocyanates, and so forth. A typical experiment is shown in Figure 7. Unconnected chain ends do not contribute to the tensile properties of a

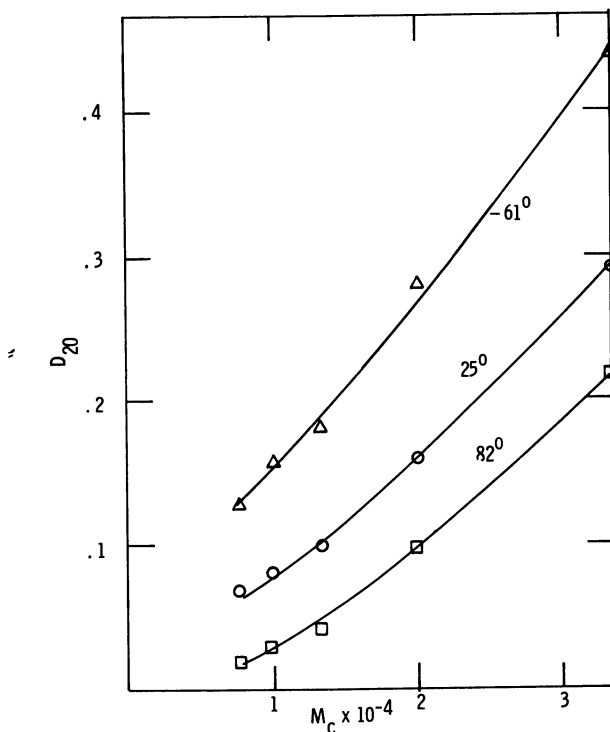


Figure 6. Relative stress decay vs. molecular weight between crosslinks of polybutadiene-polyurethane rubber at three temperatures

propellant and hence are unnecessary ballast from the standpoint of good mechanical properties. Stress relaxation, at least qualitatively, provides a way to detect such useless structures.

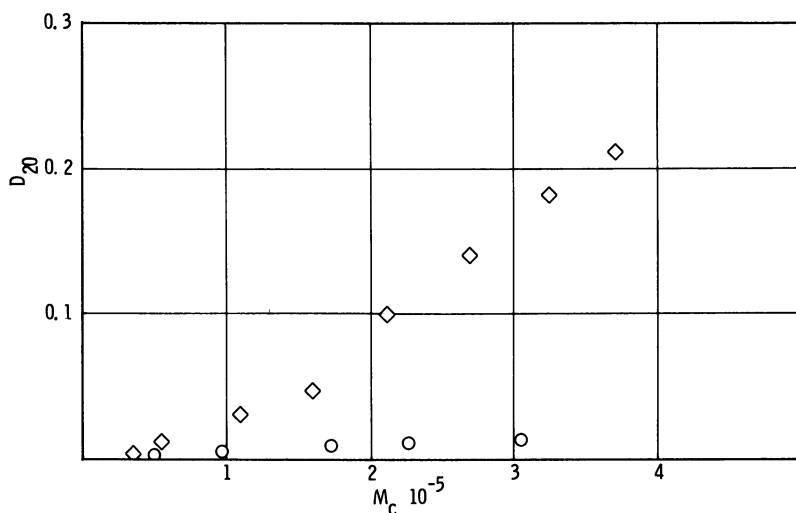


Figure 7. D_{20} at 25°C. vs. M_c of poly(1,2-oxypylene)-polyurethane rubbers prepared by proper crosslinking (\diamond) and chain termination (\circ)

Mechanical Properties

In most modern solid rocket motors the propellant grain is bonded to the motor case by using a special rubbery material between steel wall and solid propellant (liner). This design minimizes the quantity of heat-insulating material, thereby greatly increasing the payload or range of the rocket. The unburned propellant itself acts as heat shield between the flame and chamber wall. The price of this design is higher flexibility demanded from the propellant grain, which has to be maintained over an extended temperature range. An example for this are the air-to-air missiles positioned under the wings of supersonic aircraft. Since steel wall and propellant grain have different thermal coefficients of expansion, strains are induced which might lead easily to cracking of the grain with disastrous consequences upon ignition. A propellant chemist spends most of his time obtaining a formulation for a propellant with adequate mechanical properties and satisfactory storage life.

Tensile properties of a propellant depend mainly on the tensile properties of the matrix, concentration, particle size, and particle size distribution of the solids, and the quality of the interphase between solid

particles and binder matrix. Changes of environmental pressure also affect the properties.

Influence of Matrix. The most important single parameter pertaining to the mechanical properties of solid propellants is their strain capability, which depends strongly on the crosslink level of the binder matrix. Figure 8 shows the effect of crosslink level on the dilatational behavior of glass-filled polybutadiene-polyurethanes. With increasing crosslink density the effective strain moves towards shorter elongations. Not all manipulations which reduce crosslink density are equivalent with respect to strain-cycling ability. Chain scission will reduce crosslink density and initial modulus, but the effective strain is improved only moderately (Figure 2). Detailed investigation of the dilatational behavior in filled systems indicated internal tearing to be the source of the volume increase; hence, volume increase is affected in the same manner as tearing in the unfilled rubber. Thus, a filled rubber of low crosslink density, because of its better tear resistance, will show less internal tearing than its more highly crosslinked counterpart. Plasticizers in an amorphous, nonassociated rubber do not alter greatly the resistance to tear and hence do not improve significantly the effective strain of such composites. Increasing strain rate increases the stress at which tearing commences in the unfilled rubbers, but elongation is slightly decreased usually. The same pattern is followed by dilatation in filled rubbers. These examples may suffice to point out that good strain capability of propellants is intimately linked to high tear resistance of the propellant matrix. Thus, the optimum performance of a binder system with a given chemical backbone structure should lie at low crosslink levels, where the latter have been obtained by choosing a proper crosslinker-chain extender ratio.

The chemical nature of the backbone probably is significant also with respect to tear properties. Unfortunately, it is in this area that information is scanty. Further, it is well known that those elastomers exhibit the highest resistance to tear which are partially crystalline or at least show the phenomenon of strain crystallization. Such elastomers, however, have a comparatively high elastic modulus which rapidly increases with decreasing temperature. This makes such elastomers unsuitable for propellants which are to remain elastic even at arctic temperature. Table IV shows a comparison between binder modulus at -61°C . and propellant modulus and elongation at the same temperature. The binders were prepared by using the same concentration of crosslinker (TP-4040) and ester-type plasticizer but varying the ratio of (noncrystallizing) poly(1,2-oxybutylene)diol/(crystallizing) poly(1,4-oxybutylene)diol in such a way that the urethane group concentration was kept constant. The latter was achieved by using a mixture of poly(oxytetramethylene)diols having the

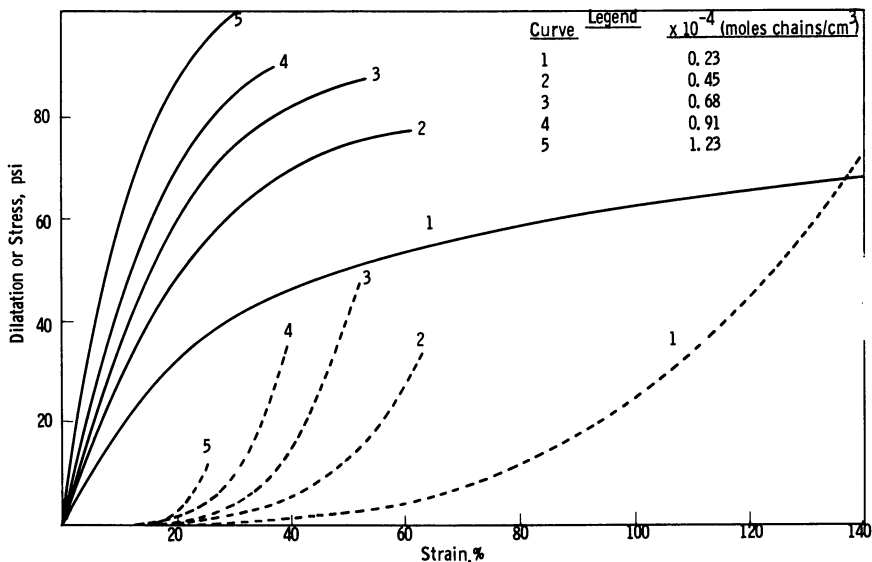


Figure 8. Tensile properties and dilatation vs. crosslink density. Binders filled with 40% glass beads ($\sim 35\mu$ average). $\dot{\epsilon} = 0.74 \text{ min.}^{-1}$; $T = 25^\circ\text{C}$.

same average equivalent weight as the poly(1,2-oxybutylene)diol. Table IV indicates that to obtain propellants with good strain capability at low temperatures, binders are required which possess very low elastic moduli at low temperatures. Most elastomers which yield strong tough rubbers at ambient temperatures do not qualify at low temperatures. One more thought might be injected here. The strength of elastomers depends on the degree of chain interaction (van der Waals bonds, hydrogen bonds, etc.). Thus, these types of materials usually display a high viscosity, even in the form of comparatively low molecular weight prepolymers. Such viscous materials pose an additional mixing problem, making it virtually impossible to incorporate the quantity of solids required for maximum ballistic performance.

Table IV. Effect of Elastic Modulus of Binder on Propellant at -61°C .

Binder		Propellant	
E_0 , p.s.i.g.	ϵ , %	E_0 , p.s.i.g.	ϵ , %
2800	>700	54,000	4
620		20,000	17
101		11,100	43
32		7300	57
20		5500	72

^a Strain rate is 0.74 min.^{-1} .

Thus essentially three different backbone structures remain for consideration. These are poly(1,2-oxypropylenes), poly(1,2-oxybutylenes) and the various polybutadienes.

Moisture Embrittlement. Early polyurethane propellants frequently lost their low temperature strain capability after being exposed to an atmosphere of high relative humidity. A typical example is presented in Table V for "embrittling" and "nonembrittling" polyurethane rubbers filled with ammonium perchlorate. A detailed study of this phenomenon indicated that some of the prepolymers, essentially those containing the propylene oxide moiety, are capable of dissolving large quantities of NH_4ClO_4 in the presence of water (30). The peculiar solubility characteristics of PPG are shown in Tables VI and VII. These solutions have

Table V. Effect of 6-Days Exposure of JANAF Bars to 90% RH at 77°F. on Low Temperature Mechanical Properties^a of Two Polyurethane Binders Filled with 75% NH_4ClO_4 at -40°F . and with $\dot{\epsilon} = 0.74 \text{ min.}^{-1}$

Type	H_2O Absorbed,	Condition	σ_b , p.s.i.g.	ϵ_b , %	E_o , p.s.i.g.
	%				
Embrittling	none	dry	390	110	1400
	0.25	wet	1100	1	150,000
Nonembrittling	none	dry	390	110	1100
	0.15	wet	160	108	960

^a Properties: σ_b = tensile strength at break; ϵ_b = elongation at break; E_o = Young's modulus.

a strong negative temperature coefficient of viscosity probably caused by ensuing ion-dipole interactions. The increase of the low temperature modulus after soaking polyoxypropylene binder bars in various electrolyte solutions is shown in Table VIII. The "non-embrittling" poly(1,2-oxy-

Table VI. Solubility of AP and H_2O in Binder Components

Binary Systems				
Solvent ^a	Solute	% Dissolved	T, °C.	Specific Resistance, Ω
PPG	H_2O	2.3	22	$>3 \times 10^7$
PPG	H_2O	infinite	0	$>3 \times 10^7$
LD-124	H_2O	2.4	22	$>3 \times 10^7$
B-2000	H_2O	0.5	22	$>3 \times 10^7$
PPG	NH_4ClO_4	0.66	22	1.6×10^6
PPG	NH_4ClO_4	4.57	0	1.0×10^6

^a PPG = poly(1,2-oxypropylene)diol; LD-124 = poly(1,4-oxybutylene)diol; B-2000 = poly(1,2-oxybutylene)diol.

butylenes) do not show a modulus increase after immersion in saturated, aqueous ammonium perchlorate. Additional, similar experimentation on the various binder systems in use has shown that moisture embrittlement will occur and is peculiar to those propellant binders where the absorption of water in the binder phase greatly increases the solubility of the electrolyte filler causing ion-dipole interaction which stiffens the network. This stiffening becomes particularly pronounced at low temperatures owing to the strong negative temperature coefficient of solubility as well as ion-dipole interaction. Drying restores the original (dry) properties because the dehydrated binder cannot hold the ammonium perchlorate in solution. Moisture embrittlement is of concern only in those propellants in which NH_4ClO_4 is dispersed in a binder system having a polyoxypropylene backbone. Since polyoxybutylenes are less polar than PPG and hence absorb less water, they no longer show moisture embrittlement. Polybutadienes, of course, are also not affected.

Moisture embrittlement must be distinguished from other forms of embrittlement. Brittleness of propellants at low temperatures is normally caused by binders which stiffen excessively with decreasing temperatures, owing to partial crystallization of the binder matrix (*e.g.*, copolymers of butadiene with acrylonitrile, some hydrogenated polybutadienes, etc.). Such propellants are brittle at low temperatures whether they have been exposed to moisture or not.

Table VII. Solubility of AP and H_2O in Binder Components

Ternary Systems: Binder Component, Salt, H_2O					
Binder Component	Salt	% Dissolved		T, °C.	Specific Resistance, Ω
		Salt	H_2O		
PPG	NH_4NO_3	0.69	4.1	22	3×10^6
		0.04	2.4	22	$>3 \times 10^7$
	NH_4ClO_4	11.8	4.5	45	—
		14.3	15.8	22	1000
		13.8 ^a	23.2	0	1700
		11.8 ^a	23.2	0	100
		9.9 ^a	72.9	0	32
LD-124	NH_4ClO_4	1.94	0.6	45	—
		2.7	9.9	22	4500
B-2000	NH_4ClO_4	0.07	0.66	22	$>3 \times 10^7$
		0.1	0.53	0	$>3 \times 10^7$
Bis(ethylhexyl)-hexamethylene dicarbamate	NH_4ClO_4	0.29	1.4	22	1×10^6

^a Concentration of dissolved NH_4ClO_4 depends on H_2O /PPG ratio.

Another form of embrittlement, akin to moisture embrittlement, is encountered where the oxidizer (*e.g.*, LiClO_4) possesses marked solubility in the binder phase even without the aid of water. Such systems also exhibit a comparatively poor processability (high mix viscosity).

Table VIII. Effect of the Absorption of Electrolyte Solution on the Low Temperature Modulus of a PPG Propellant Binder

JANAF Dumbbell Specimens

<i>Saturated Aqueous Electrolyte^a</i>	<i>Immersed at Room Temperature, days</i>	E_0 at -75°F . <i>p.s.i.g.</i> $\dot{\epsilon} = 0.74 \text{ min.}^{-1}$
None	0	67
H_2O	13	45
LiClO_4	13	55,000
NaClO_4	13	6700
NH_4ClO_4	13	4800
KClO_4	13	67
AgClO_4	13	55,000
$\text{Mg}(\text{ClO}_4)_2$	13	50,000
LiI	7	1010
NaI	7	1280
KI	13	125

^a NH_4BF_4 , NH_4Br , NH_4NO_3 , LiNO_3 , MgSO_4 , KCl , KBr , $\text{Ca}(\text{NO}_3)_2$, $\text{Cu}(\text{NO}_3)_2$, and $\text{Cr}(\text{NO}_3)_3$ showed no effect.

Effect of Solids on Mechanical Properties. CHEMICAL EFFECTS. Since chemical interactions between binder and filler are highly undesirable, they are avoided as much as possible. If they do occur, corrective measures must be taken. However, some bonding agents of the type of alkanol amines utilize their reactivity with AP to become adsorbed (chemisorbed) onto the surface of the crystal, where they are later converted to a tough polymeric shell enveloping the particle. An undesirable reaction sometimes occurring during the developmental stages of a propellant is the soft-center cure reaction, so named because the propellant grain possesses a hard, apparently well-cured surface with a soft or even liquid interior. The cause has been traced to the reaction between aluminum particles and alcoholic hydroxyls. During some prolonged mixing under certain adverse conditions the oxide layer on the aluminum particle is abraded. The freshly exposed metal surface will react with the alcoholic hydroxyl groups with formation of aluminum alkoxides and liberation of hydrogen. This depletes the hydroxyl-group concentration causing an abundance of NCO groups, which cannot find a partner. Thus, the propellant remains uncured, except on exposed surfaces where moisture

will effect linking of the isocyanate-terminated chains through urea formation:



There are many solutions for the above problem. Usually changes in mix procedure, particle size of ingredients, etc., take care of the situation. In particularly bad cases, addition of binder soluble oxidants, like $\text{Na}_2\text{Cr}_2\text{O}_7$, which immediately reoxidizes the aluminum surface, solves the problem.

PHYSICAL EFFECTS OF FILLER. Dispersion of any hard particulate matter in a soft matrix will yield a composite with quite different properties. The two main causes for these effects are load sharing of the filler particles and strain dilatation of filled elastomers.

LOAD SHARING OF FILLER PARTICLES. Comparison of ultimate strength of a propellant and its unfilled binder matrix almost always shows that the propellant has up to several times the tensile strength of the matrix. This "filler reinforcement" is presently thought to stem from additional "crosslinks" formed between filler particles and the network chains of the binder matrix (5, 8, 9, 34). Effective network chains are defined as the chain segments between crosslinks. From the classical theory of elasticity, the strength and/or modulus of an elastomer is proportional to the number of effective network chains per unit volume, N , or

$$\sigma = NkT \left(\alpha - \frac{1}{\alpha^2} \right)$$

where σ is the stress, α is the extension ratio l/l_0 , k is Boltzmann's constant, and T is the absolute temperature. According to this concept one would expect a strong effect of particle size on strength and modulus because the quantity of "new crosslinks" should depend on the available surface area. This is qualitatively true for tensile strength if tests are conducted under ambient atmospheric pressure, but the modulus is independent of particle size (31). However, if tensile tests are carried out under superimposed pressure, both coarse and fine fillers yield about the same tensile properties (31). It might also be mentioned that the modulus is increased much more than tensile strength by the incorporation of solid particles. The effect of solids on the elastic modulus has been studied by many investigators. One of the best fitting equations has been derived by Eilers and Van Dyck (13) and was adapted to filled elastomers by Smith and Landel (25):

$$E/E_0 = \{1 + K \phi / (1 - S' \phi)\}^2$$

where E and E_0 are modulus of filled and unfilled matrix, ϕ is the volume

fraction of filler, and K and S' are empirical constants. A good review on this subject has recently been given by Payne (33).

It was known for some time that a filler having a wide particle size distribution caused less increase of modulus than the same quantity having a narrow range of particle sizes. Farris (15) and Schwarzl (41) showed that good agreement with experimental data can be obtained if one treats the dispersion of fine particles as a homogeneous new phase having a viscosity which can be calculated from some appropriate expression—*e.g.*, the equation above. The coarse phase is then dispersed in this “composite liquid” yielding the final viscosity. This model was extended to account for multimodal systems.

While modulus or viscosity of suspensions are described adequately by existing theories, the tensile reinforcement is still subject to considerable controversy and far from a quantitative assessment. A recent hypothesis (31) which appears to be in agreement with most observed effects on solid propellants assumes that the solid particles are sharing a disproportionately larger portion of the load than the comparatively soft matrix. The idea is best illustrated by a model of a hard fiber embedded in a soft elastomer. If the aggregate is strained by the amount ϵ , the stress buildup in the fiber, σ_f , is proportional to its modulus, E_f , or $\sigma_f = E_f \cdot \epsilon$. Similarly the stress in the matrix σ_m , equals $E_m \cdot \epsilon$. Hence, if $E_f \gg E_m$, $\sigma_f \gg \sigma_m$. Since the total load on the composite is unchanged and acting on any cross-section, the soft matrix bears a comparatively small portion of the over-all load. Consequently, a higher load on the composite is necessary before the failure stress of the weaker matrix is reached. By experimental stress analyses it was shown that this principle could be applied also to particulate fillers embedded in a matrix.

Predictions of the mechanical response of filled elastomers are further aggravated by the phenomenon of strain dilatation. As soon as dilatation commences, the tensile stress lag behind elongation, the degree of dilatation for a given composite being roughly a measure for the deviation from the expected mechanical response. Dilatation increases with particle size and volume fraction of filler—it decreases somewhat if the filler is bonded to the matrix. Farris (16, 17) showed that dilatation can account well for the mechanical behavior of solid propellants and his equation:

$$\sigma = E \epsilon \left(\exp - \beta \frac{\Delta v}{v_0 \epsilon} \right),$$

where β is a material constant and $\Delta v/v_0$ is the volume increase, is in good agreement with experimental data.

Binder-Filler Interaction. A strong bond between binder and filler is important for obtaining high tensile strength. In Figure 9 the tensile properties obtained from two different filler materials are compared. The

epoxy resin yields the stress-strain curve characteristic for reinforcing fillers, while the glass beads are considered nonreinforcing for obvious reasons. The difference between the two types of bonding is also brought out by swelling experiments shown in Figure 10. The matrix expands through uptake of solvent. Because the filler particle does not expand, the matrix breaks loose and forms halos, unless very strong bonds between matrix and filler prevent dewetting. A consequence of the uneven swelling around firmly bound particles is the appearance of stress gradients which become visible with polarized light and also cause distortion of halos near resin particles.

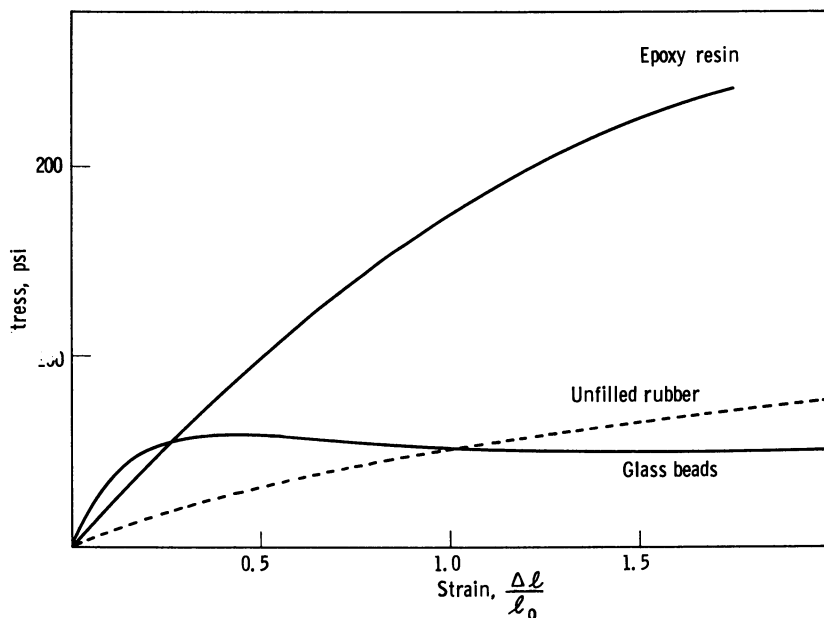


Figure 9. Reinforcing and nonreinforcing filler (volume fraction = 0.5) in poly(1,2-oxypropylene)-type polyurethane rubber. $\dot{\epsilon} = 0.74 \text{ min.}^{-1}$; $T = 25^\circ\text{C}$.

The formation of halos could be interpreted as failure of the adhesive bond. However, further investigation of the course of "adhesive failure" around solid particles in elastomeric matrixes showed that before dewetting, tiny voids were created next to the filler particle (Figure 11) but distinctly located in the matrix, away from the filler surface. Only after further straining did these voids coalesce and merge in the well-known vacuoles (*cf.*, Figure 14) exposing the filler surface. Stress analysis of a spherical inclusion in an elastomeric matrix indicates that the highest stress is located a little away from the surface in the matrix (Figure 12)

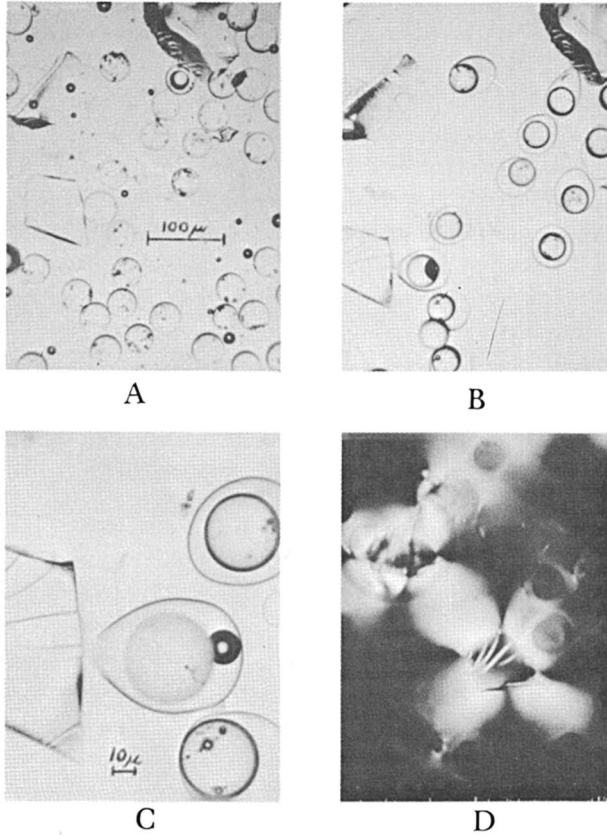


Figure 10. Glass beads and epoxy resin in swollen polyurethane rubber

A: Non-swollen

B: Halos have formed around glass spheres; resin is chemically bonded and does not dewet

C: Distortion of halo around glass sphere in the stress field of the non-releasing resin particle

D: Stress patterns around resin particles under polarized light

exactly where the first voids appear. Consequently, the conclusion seems to be that the first stage of failure is an internal tearing of the matrix—*i.e.*, cohesive failure (32). This conclusion is further substantiated by experimental data showing that the stress where these first voids appear is a function of the elastic modulus and is practically independent of the chemical nature of elastomer or filler (Figure 13). The ensuing “adhesive failure” (also called dewetting or vacuole formation) is most likely

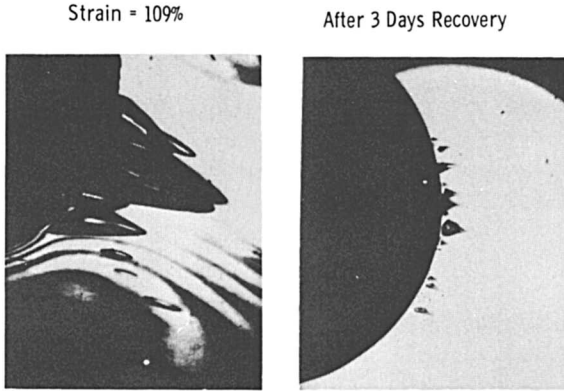


Figure 11. Internal tearing around bonded steel sphere in polyurethane rubber

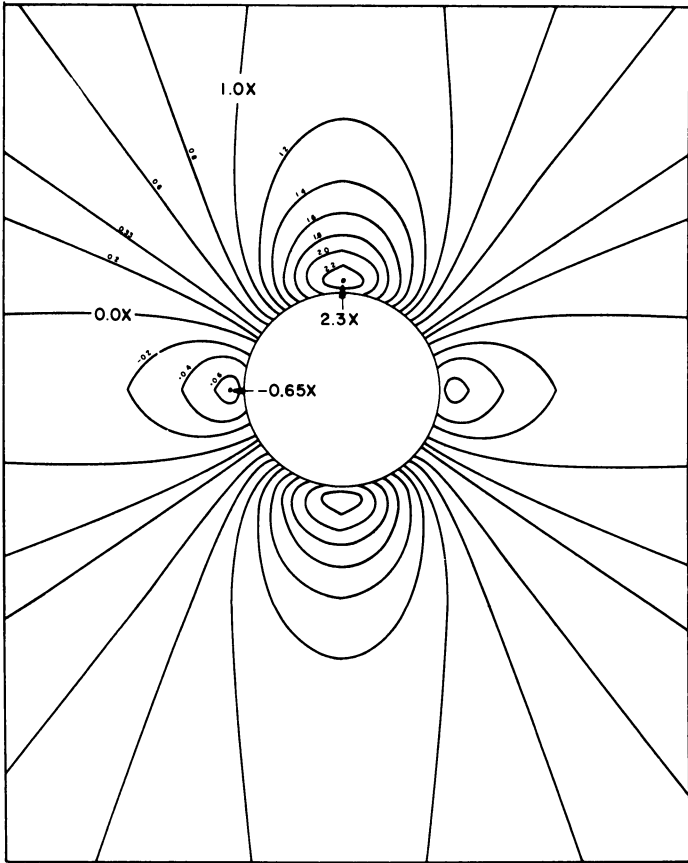


Figure 12. Binder stresses around filler particle (loading vertical)

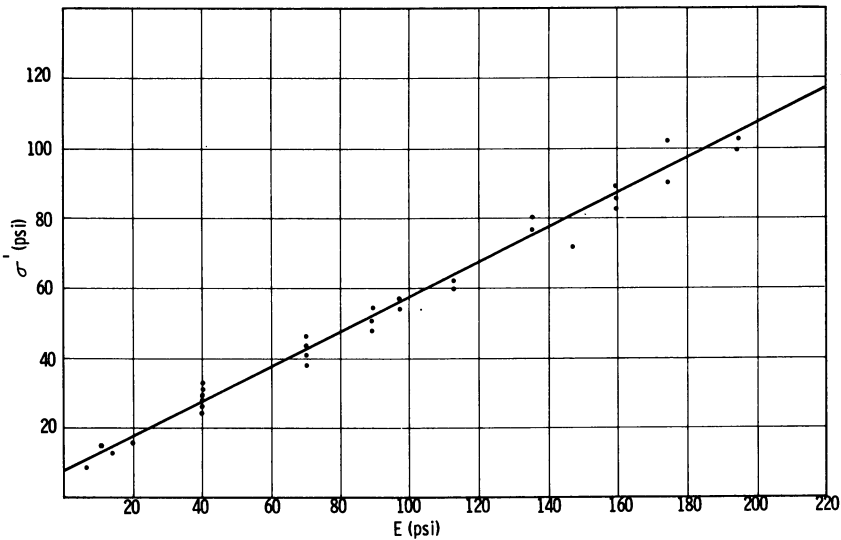


Figure 13. Critical stress (σ') vs. Young's modulus of elastomers containing spherical inclusions. $\dot{\epsilon} = 0.74 \text{ min.}^{-1}$; $T = 25^\circ\text{C}$.

a peel process, caused by the tremendous stress concentration created at the point where the void reaches the filler surface (32). The observed stress dependence of void formation on the elastic modulus suggests that if a high modulus layer of elastomeric material surrounds the solid particle, the locus of void formation will be pushed further into the matrix phase. Furthermore, if this high modulus layer has a strong tear resistance, the void will be hindered from reaching the filler surface but will grow in the opposite direction. Since the filler particle is not dewetted, it continues to share the load, and the effect of dilatation on mechanical properties is less than if dewetting takes place (31, 32). The two kinds of vacuole growth are shown in Figure 14. The cavity around the bonded particle has its biggest opening away from the oxidizer crystal, sort of forming a figure 8, whereas the dewetted particle shows the typical eye-texture characteristic for "nonreinforcing" fillers. Bonding agents added to the propellants appear to provide this high modulus layer. Evidence for this is ample and is given below.

(a) Bonding agents either are reacting chemically with the oxidizer (alkanol amines) or are being physically adsorbed. In any case they are quite polar compounds which are usually good solvents for AP and are not too soluble in the binder phase. Compounds which are chemisorbed to the AP do not need to be sparingly soluble. These characteristics make it plausible that bonding agents will aggregate on the oxidizer surface during the mix process.

(b) Bonding agents must be capable of conversion into a polymer—*i.e.*, their HO functionality must be 2 or greater if this conversion is

achieved *via* reaction with a diisocyanate. This is best illustrated by the following series of compounds:

<i>Compound</i>	<i>Effectiveness as Bonding Agent</i>
$ \begin{array}{c} \text{CH}_3 \quad \text{BF}_3 \\ \diagdown \quad / \\ \text{N} \quad \text{---} \quad \text{CH}_2\text{CH}_2\text{---} \text{OC} \begin{array}{c} \text{O} \\ \end{array} \text{---} \text{CH}_3 \\ / \\ \text{CH}_3 \end{array} $	Inactive
$ \begin{array}{c} \text{CH}_3 \quad \text{BF}_3 \\ \diagdown \quad / \\ \text{N} \quad \text{---} \quad \text{CH}_2\text{CH}_2\text{OH} \\ / \\ \text{CH}_3 \end{array} $	Inactive
$ \begin{array}{c} \text{CH}_3 \quad \text{BF}_3 \\ \diagdown \quad / \\ \text{N} \quad \begin{array}{l} \text{---} \text{CH}_2\text{CH}_2\text{OH} \\ \text{---} \text{CH}_2\text{CH}_2\text{OH} \end{array} \\ / \end{array} $	Good
$ \begin{array}{c} \text{CH}_2\text{CH}_2\text{OH} \\ \text{F}_3\text{B}:\text{N} \quad \begin{array}{l} \text{---} \text{CH}_2\text{CH}_2\text{OH} \\ \text{---} \text{CH}_2\text{CH}_2\text{OH} \end{array} \\ \text{CH}_2\text{CH}_2\text{OH} \end{array} $	Good

(c) The bonding agent must be capable of forming chemical links with the binder matrix. For example, compounds which are highly effective in a polyurethane cure system are not effective in carboxy-terminated aziridine propellants.

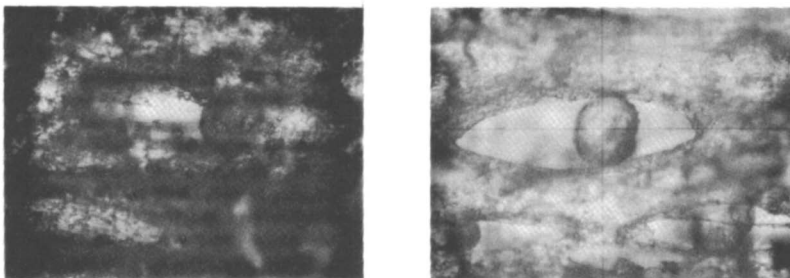


Figure 14. Cavity formation around NH_4ClO_4 crystals in polyurethane elastomers. $100\times$

Left: Bonded to rubber
Right: Non-bonded

Small quantities of these compounds improve the mechanical properties of propellants significantly (Figure 15 and Table IX).

Aging Stability of Polyurethane Propellants

The shelf life required of solid propellants varies from 24 months to more than 10 years, depending on the mission and the exposure to which

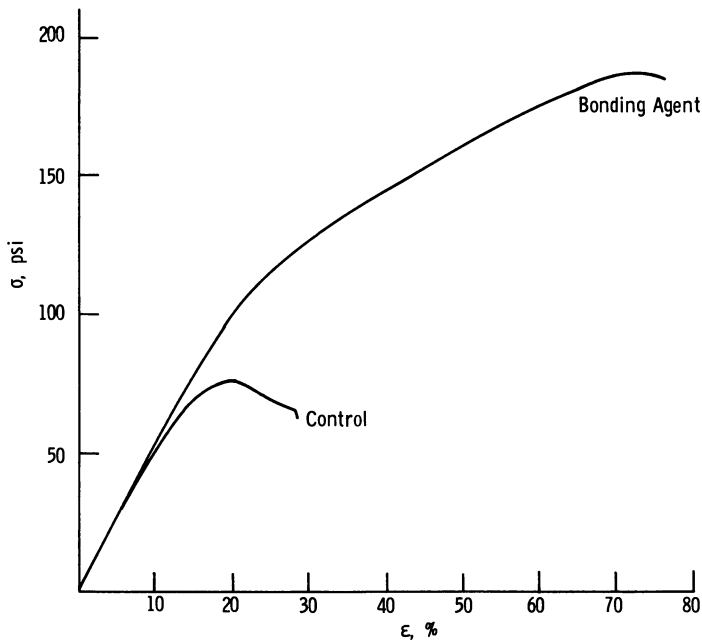


Figure 15. Effect of 0.35 wt. % of a bonding agent on physical properties of a polyurethane propellant. $T = 25^{\circ}\text{C.}$; $\dot{\epsilon} = 0.74 \text{ min.}^{-1}$

Table IX. Effect of Bonding Agent on Propellant Mechanical Properties^a

Temperature, °F.	Bonding Agent	σ_m , p.s.i.g.	ϵ_m , %	E_o , p.s.i.g.
180	yes	86	26	440
	no	61	15	460
77	yes	185	75	510
	no	75	19	520
0	yes	285	89	720
	no	180	22	860
-40	yes	420	72	2530
	no	276	21	1870
-75	yes	820	35	8100
	no	610	14	6300

^a Properties: σ_m = stress at nominal maximum; ϵ_m = strain at nominal maximum stress.

the missile is subjected. During this time mechanical properties, ballistic properties, as well as the bond between propellant and liner must remain between narrowly specified limits.

Generally one distinguishes between humidity and thermal aging of propellants.

Humidity Aging. So far no polymeric binder material has been found which prevents moisture from diffusing into the interior of the propellant grain. Although moisture at ordinary temperatures does not undergo chemical reaction to any significant degree with the components of the propellant, nevertheless, it affects the mechanical properties strongly. Tensile strength, elongation, and modulus are often lowered drastically (Figure 16). This degradation of properties is caused by the accumulation of moisture on the surface of the oxidizer crystal, thus creating a low modulus (liquid) layer which envelops the particle. In essence, this means that the "bond" between oxidizer and binder is destroyed, and dewetting will commence at low stress levels with commensurate loss of mechanical properties. Small quantities of absorbed moisture (0.1% and less) cause this effect. Redrying of the propellant restores the original dry properties. As discussed before, some propellants will, in addition, exhibit the phenomenon of moisture embrittlement.

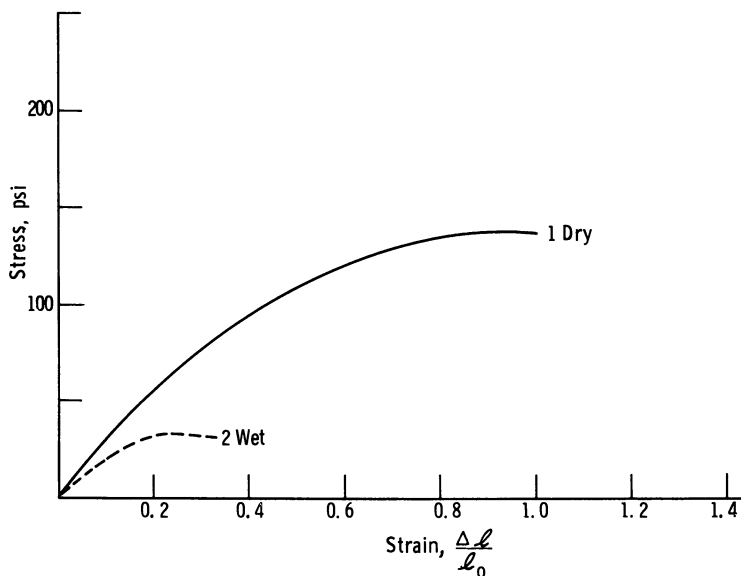


Figure 16. Effect of moisture on uniaxial tensile properties. Dumb-bell specimen exposed 14 days to 95% relative humidity, during which time the propellant absorbed 0.31% water. $T = 25^\circ\text{C}$.; $\dot{\epsilon} = 0.74 \text{ min.}^{-1}$

There have been unsuccessful efforts to design or find propellant systems which are invariant to moisture. Although the rate of moisture penetration depends somewhat on the chemical nature of the binder backbone, being slightly larger in polyether systems than in polybutadienes, there is little difference with respect to the effect on mechanical properties of propellants utilizing different matrixes. This is because the water will collect on the oxidizer surface to a degree depending only on the relative humidity of the atmosphere and not at all on the chemistry of the binder, provided equilibrium moisture absorption has been reached. Whether the binder also dissolves marked quantities of water is of little significance, since the properties of the elastomer are hardly altered by the small amounts of water. The best solution to the moisture problem is a seal on rocket chambers. Often this is further aided by including bags containing drying agents.

Thermal Aging. Probably all missiles will experience changes in temperature during their storage life. Even if the propellant is not exposed to higher temperatures, there are slow chemical reactions occurring which may cause the propellant to harden excessively, eventually resulting in cracked grains. Other propellant binders soften instead, which causes slumping of the grain or insufficient rigidity to withstand acceleration after launching. Debonding between propellant and liner or liner and insulation is also encountered sometimes.

Therefore, it is of utmost importance to develop realistic tests which indicate whether a new propellant formulation will have an acceptable shelf life. Since no propellant development program has the duration required from the developed product, accelerated aging tests are conducted, usually at elevated temperatures, the results of which are then extrapolated by various empirical methods to the life expectancy under the conditions the missile is likely to encounter. One inherent disadvantage of accelerated aging tests is that degradative reactions occurring at higher temperatures are not necessarily the same which cause harm at low temperatures and long duration. The correlation of data from accelerated tests with long term, low temperature aging data is constantly revised and upgraded as new information becomes available. These correlations are obtained from various sources. The services may store missiles in various positions, usually upright as well as horizontally, and fire them at appropriate time intervals. Firings are often conducted at the extremes of temperature between which the rocket is to be operational. Decrease of ballistic performance below specification or the incidence of failures above tolerable limits establishes the useful life of the propellant. Some accelerated aging data for a polyether-polyurethane propellant are presented in Table X.

Liners

In some applications the propellant can be cast directly on the primed chamber wall; in most cases, however, the propellant is bonded to the wall or to the heat insulation through an intermediate layer—the liner (36).

The liner may combine the function of a heat insulator and an adhesive to bond to the propellant, but in practice these two functions are assigned to different materials. For heat insulation, most commonly a silica-filled nitrile rubber (NBR) is used; it chars when exposed to high temperatures. The propellant must adhere strongly to this rubber so that the bond strength exceeds the cohesive strength of the propellant. Direct bonding to insulation is possible only with some propellants—*e.g.*, polyether–polyurethane propellants containing nitroplasticizers such as bis(2,2-dinitropropyl) formal or acetal. Most propellants are bonded to the rubber through a liner.

Table X. Mechanical Properties of Polyether–Polyurethane Propellant^a after Accelerated Aging

Uniaxial Instron Data: Strain Rate 0.74 min.⁻¹

Test Temp., °F.		Uniaxial Instron Data: Strain Rate 0.74 min. ⁻¹					
		Unaged	8 Days 220°F.	14 Days 220°F.	1 Month 180°F.	4 Months 180°F.	3 Months 150°F.
150	σ_m , p.s.i.g.	107	94	112	106	121	112
	ϵ_m , %	21	23	40	28	33	29
	σ_b , p.s.i.g.	102	89	112	100	121	110
	ϵ_b , %	26	29	41	37	34	33
	E_o , p.s.i.g.	872	883	636	817	809	873
77	σ_m , p.s.i.g.	173	184	180	205	207	205
	ϵ_m , %	45	48	54	52	53	42
	σ_b , p.s.i.g.	172	184	180	205	207	205
	ϵ_b , %	48	48	54	52	54	43
	E_o , p.s.i.g.	1020	867	697	875	997	1120
-40	σ_m , p.s.i.g.	432	373	314	389	354	434
	ϵ_m , %	69	73	73	73	66	73
	σ_b , p.s.i.g.	423	367	310	376	354	431
	ϵ_b , %	74	79	78	86	70	77
	E_o , p.s.i.g.	2650	3510	3010	3250	3850	2650

^a Composition (wt. %): NH₄ClO₄ 67; aluminum 17; CuO2O₂, a burning rate accelerator 0.1; sulfur, stabilizer 0.1; *N*-phenyl-naphthylamine, stabilizer 0.1; Fe(AA)₃ 0.015; HAA 0.009; polyether–polyurethane binder containing 25% isodecyl pelargonate 15.68%.

In selecting a liner one must consider the required strength as known from grain stress analyses data as well as the type and composition of the propellant to be bonded. In general, the liner is also a castable and curable composition and of the same type of elastomer as the propellant binder—*i.e.*, for a polyether–polyurethane propellant the liner would also be a polyether–polyurethane although its constituents may be different from the propellant binder. In particular it will contain prepolymers, which make a tough rubber with high tensile strength—*e.g.*, poly(1,4-oxybutylene) glycol. For further reinforcement it may be filled. The filler at the same time serves as a thickening (thixotropic) agent to confer desired flow characteristics upon the uncured liner for brushing, spraying, spinning, and other methods of application. Examples for such fillers are colloidal silica, certain metal oxides like ferric oxide or titanium dioxide, and fibrous materials like potassium titanate.

To ensure a strong bond between liner and insulation as well as propellant to liner, it is necessary that liner as well as propellant cure well at the interfaces. This means that in many cases the rubber insulation must undergo some treatment to remove substances which may interfere with the liner cure. Such substances are usually low molecular weight compounds and can often be removed by heating—*e.g.*, water, which would otherwise react with isocyanate in a polyurethane liner. In addition the insulation and/or the cured liner surface may be washcoated with a cure catalyst which will increase the reaction rate of alcoholic hydroxyl groups over the rate of reaction of water with isocyanate to such an extent that the latter reaction can no longer compete with the cure reaction.

Another means to achieve better bonding is to increase the contacting surface area. Finally, the aging stability of liners has to be at least as good as that of the propellants with which it is used.

Ballistic Considerations

Thermodynamic Calculations (Specific Impulse). Prepolymers in propellant binders keep the concentration of urethane groups small. Their effect on ballistic properties is therefore negligible and need not be considered in thermodynamic calculations. The contributions of the binder to specific impulse, density, etc., are determined by the chemical backbone structure of the prepolymer. [A more comprehensive treatment of interior ballistics can be found in References 37, 42.]

The specific impulse (I_s) of a propellant as a function of chemical parameters can be calculated according to:

$$I_s = K \sqrt{nT_c} = K' \sqrt{T_c/M}$$

where T_c is the chamber flame temperature; n is the moles of gas produced per unit weight of propellant; M is the average molecular weight of gaseous combustion products; K and K' are constants.

Consequently, a high I_s can be achieved by increasing n (or decreasing M) as well as T_c . The binder contributes mainly to n , which in turn is favored by a maximum hydrogen content in the prepolymer. On the other hand T_c increases with more exothermic ΔH and low heat capacities of the combustion products per unit weight. ΔH becomes more exothermic with more positive heats of formation of the propellant components and more negative heats of formation for its combustion products. Thus, binders with more positive heats of formation—*i.e.*, more energetic binders are preferred. Contributing to this are unsaturation (polybutadienes) and functional groups with carbon—nitrogen and nitrogen—nitrogen bonds, such as nitrile, amine, amine—oxide, hydrazine, nitramine,

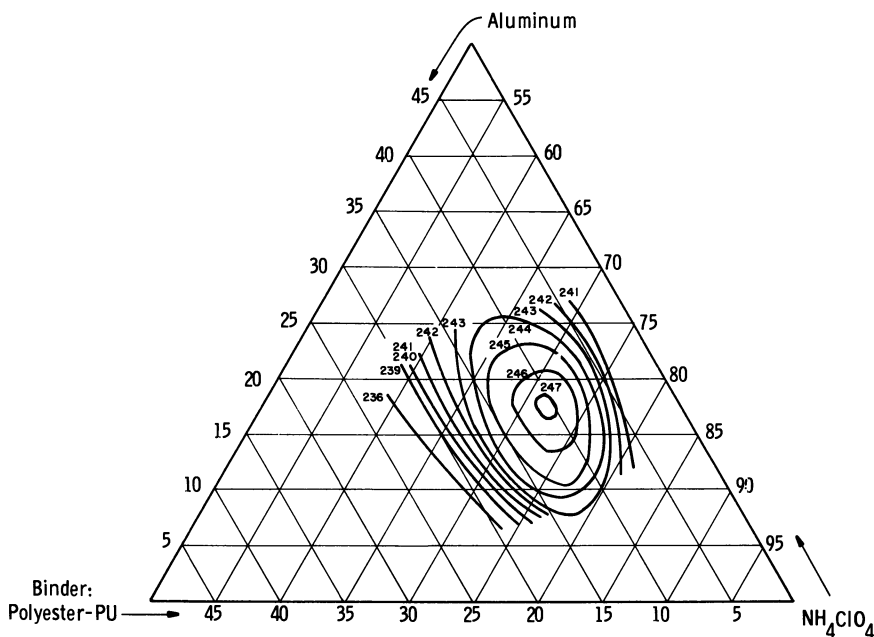


Figure 17. Composition diagram of expected specific impulse for ammonium perchlorate—aluminum—polyurethane (PU) propellant (polyester binder). $P_c/P_e = 1000/14.7$ p.s.i.a. 10KS-2500 motors

etc.). Carbon—oxygen bonds (such as carbonyl, carboxyl, hydroxyl, ether, and ester), carbon—halogen bonds, and carbon—sulfur bonds are undesirable because of their low energy contribution.

In combination with aluminum (high ΔH , but no combustion gases) and oxidizer (NH_4ClO_4) there exists a composition with maximum $I_s =$

$(I_s)_{\max}$ as shown in the diagrams of Figures 17–19 for the three pre-polymer types discussed before (polyester, polyether, and polybutadiene). In the examples shown $(I_s)_{\max}$ is about equal for a polyether (all polypropylene oxide) and a polyester (*ca.* 49 parts poly(neopentyl glycol) azelate, 35 parts poly(tripropylene glycol) azelate, 10 parts bis(2-ethylhexyl) azelate, 6 parts glycerolmonoricinoleate), and about 2 points higher for a polybutadiene binder (*ca.* 75 parts polybutadiene and 25 parts of a saturated hydrocarbon as plasticizer).

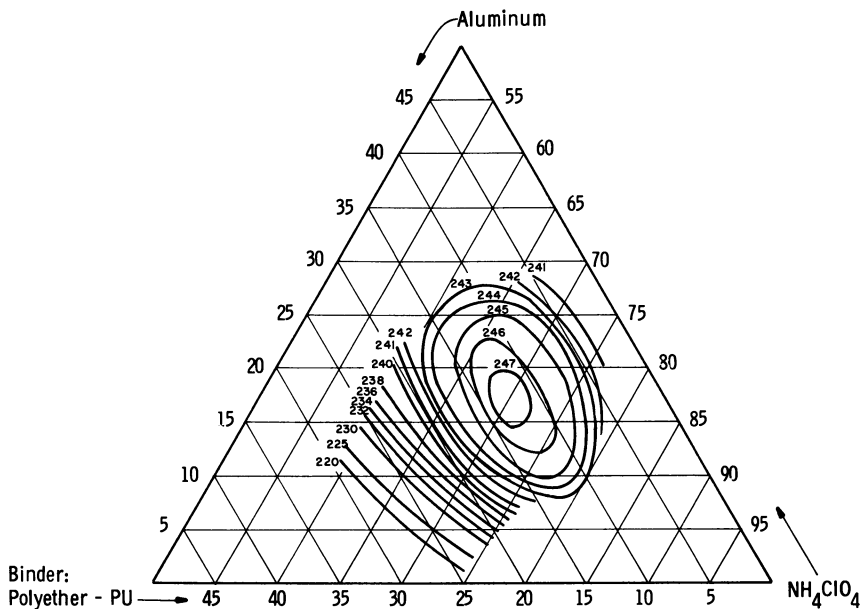


Figure 18. Composition diagram of expected specific impulse for ammonium perchlorate-aluminum-polyurethane propellant (polyether binder). $P_c/P_e = 1000/14.7$ p.s.i.a. 10KS-2500 motors

With only small differences in $(I_s)_{\max}$ the choice of the binder system is influenced by processability, physical properties, and propellant density. Thus, with the polyether binder an I_s of 247 is reached with about 14% binder, but with the polyester the same I_s is obtained with 11.5% binder, which is a definite disadvantage in terms of processability and mechanical properties. The higher I_s with the polybutadiene binder is realized only at high solids loadings, but owing to its lower density, processability is still satisfactory.

Density. For the performance of a rocket the I_s of the propellant is not the only factor to be considered. The burn-out velocity of the rocket (V_b) is given by the following equation:

$$V_b = gI_s \ln \left(\frac{M}{M - m} \right)$$

where g is the gravitational constant, M is the initial mass of rocket, and m is the initial mass of propellant. For a given volume of propellant as dictated by chamber dimensions and grain configuration, m is determined only by the propellant density, which enters as another important variable.

Compared at $(I_s)_{\max}$, polyether and polybutadiene propellants have nearly identical densities since the higher density of the polyether binder, $\rho = 1.0$ (polybutadiene $\rho \approx 0.9$), is offset by the lower solids content [$\rho(\text{NH}_4\text{ClO}_4) = 1.95$, $\rho(\text{Al}) = 2.7$]. At lower solids loadings the higher density of the polyether becomes a definite advantage. If nitroplasticizers are used [$\rho(\text{nitroplasticizer}) = 1.4$] the $I_{s \max}$ is shifted to appreciably lower solids loadings, so that the plasticizer is combined preferably with a polyether in order not to lose density.

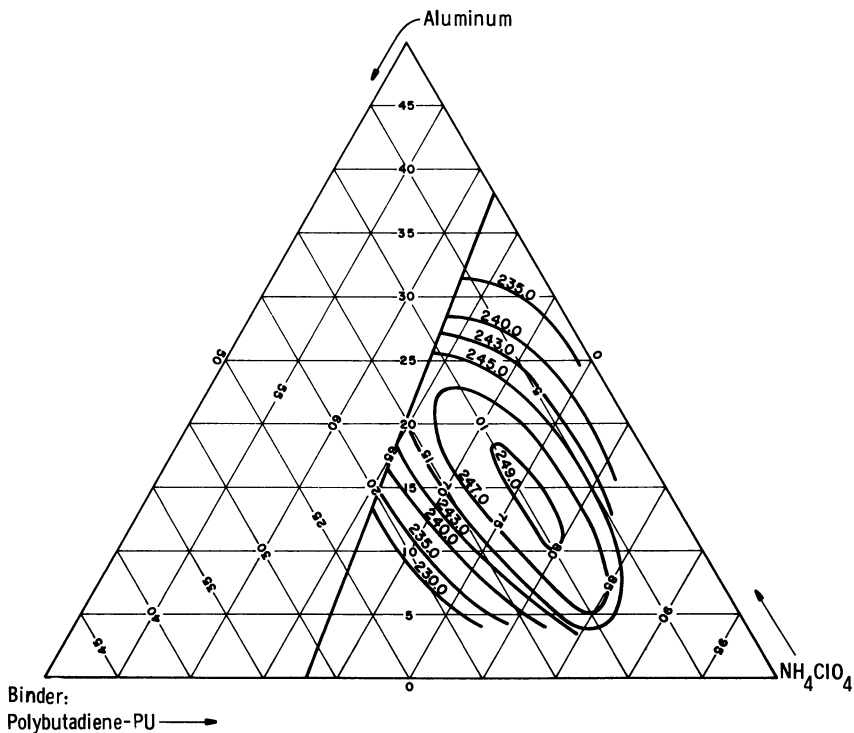


Figure 19. Composition diagram of expected specific impulse for ammonium perchlorate-aluminum-polyurethane propellant (polybutadiene binder). $P_c/P_a = 1000/14.7$ p.s.i.a. 10KS-2500 size motor. Optimum expansion, 15° half-angle

Burning Rate. The binder in polyurethane propellants has a relatively small influence on the burning rate compared with the effect of the type of oxidizer in such composites (*e.g.*, NH_4ClO_4 vs. NH_4NO_3). In general the urethane group, because of its low concentration, will have only a secondary effect on the burning rate, which is governed mainly by the type of prepolymer.

Literature Cited

- (1) Arendale, W. F., *ADVAN. CHEM. SER.* **88**, 67 (1969).
- (2) Baker, J. W., Gaunt, J., *J. Chem. Soc.* **9**, 19 (1949).
- (3) Baker, J. W., Holdsworth, J. B., *J. Chem. Soc.*, 713 (1947).
- (4) Bartley, C. E., U. S. Patent **2,997,376** (Aug. 22, 1961).
- (5) Blanchard, A. F., Parkinson, D., *Ind. Eng. Chem.* **44**, 799 (1952).
- (6) Bortwick, N. *et al.*, *J. Am. Chem. Soc.* **78**, 4358 (1956).
- (7) Bruenner, R. S., Oberth, A. E., *J. Org. Chem.* **31**, 887 (1966).
- (8) Bueche, A. M., *J. Polymer Sci.* **25**, 139 (1957).
- (9) Bueche, F., "Reinforcement of Elastomers," G. Kraus, Ed., p. 1, Interscience, New York, 1965.
- (10) Bueche, F., Halpin, J., *J. Appl. Phys.* **35**, 3147 (1964).
- (11) Dickinson, L. A., U. S. Patent **3,350,245** (Oct. 31, 1967).
- (12) Dyer, E. *et al.*, *J. Am. Chem. Soc.* **80**, 5495 (1958); **81**, 2138 (1959).
- (13) Eilers, H., *Kolloid Z.* **97**, 313 (1941).
- (14) Farkas, A., Strohm, P. F., *Ind. Eng. Chem. Fundamentals* **4**, 37 (1967).
- (15) Farris, R. J., *Trans. Soc. Rheol.* **12**, 281 (1968).
- (16) Farris, R. J., *CPIA Publ.* **61U**, **1**, 291 (1964); *Trans. Soc. Rheol.* **12**, 303 (1968).
- (17) Farris, R. J., *CPIA Publ.* **94U**, **1**, 105 (1965); *Trans. Soc. Rheol.* **12**, 315 (1968).
- (18) Frisch, K. C., Reegen, S. L., Floutz, W. V., *J. Polymer Sci.* **5A**, 35 (1967).
- (19) Gaylord, N. G., "Polyethers," Part III, "Polyalkylene Sulfides and Other Polythioethers," p. 59, Interscience, New York, 1962.
- (20) Gaylord, N. G., Sroog, C. E., *J. Org. Chem.* **18**, 1632 (1953).
- (21) Geckler, R. D., Klager, K., "Handbook of Astronautical Engineering," pp. 19-4 to 19-7, H. H. Koelle, Ed., McGraw-Hill, New York, 1961.
- (22) Johnson, D., Di Milo, A. J., *Rept. AFRPL-TR-66-40*, Contract AF 04(611)-10386 (Feb. 1966).
- (23) Jorczak, J. S., Fettes, E. M., *Ind. Eng. Chem.* **43**, 324 (1951).
- (24) Klager, K., Geckler, R. D., Parrette, R. L., U. S. Patent **3,132,967** (May 12, 1964); **3,245,849** (April 12, 1966).
- (25) Landel, R. F., Smith, T. L., *J. Am. Rocket Soc.* **31**, 599 (1961).
- (26) Oberth, A. E., Bruenner, R. S., *J. Phys. Chem.* **72**, 845 (1968).
- (27) Oberth, A. E., Bruenner, R. S., *Ind. Eng. Chem. Fundamentals*, in press.
- (28) Oberth, A. E., Smith, D. G., Bruenner, R. S., U. S. Patent **3,291,660** (Dec. 13, 1966).
- (29) Oberth, A. E., Van Ess, P., *CPIA Publ.* **158**, **II**, 93 (1968).
- (30) Oberth, A. E., Bruenner, R. S., *CPIA Publ.* **158**, **III**, 43 (1967).
- (31) Oberth, A. E., *Rubber Chem. Technol.* **40**, 1337 (1967).
- (32) Oberth, A. E., Bruenner, R. S., *Trans. Soc. Rheol.* **9** (2), 165 (1965).
- (33) Payne, A. R., "Composite Materials," L. Holliday, Ed., p. 300, Elsevier, New York, 1966.
- (34) Rehner, J., Jr., "Reinforcement of Elastomers," G. Kraus, Ed., p. 153, Interscience, New York, 1965.

- (35) Reilly, C. B., Orchin, M., "Abstracts of Papers," 130th Meeting, ACS, Sept. 1956, p. 15P.
- (36) Rogers, C. J., Smith, P. L., Bills, K. W., Dixon, J. D., *CPIA Publ.* 49, 223 (1964).
- (37) Sarner, S. F., "Propellant Chemistry," Reinhold, New York, 1966.
- (38) Saunders, J. H., Frisch, K. C., "Polyurethanes, Chemistry and Technology," Part I, p. 138, Interscience, New York, 1962.
- (39) *Ibid.*, p. 106.
- (40) *Ibid.*, p. 111.
- (41) Schwarzl, F. R., Bree, H. W., Struik, L. C., *CPIA Publ.* 119, I, 133 (1966).
- (42) Siegel, B., Schieler, L., "Energetics of Propellant Chemistry," Wiley, New York, 1964.

RECEIVED November 8, 1968.

6

Solid Propellants Based on Polybutadiene Binders

E. J. MASTROLIA and K. KLAGER

Aerojet-General Corp., Propulsion Division, P.O. Box 15847,
Sacramento, Calif. 95813

Butadiene prepolymers containing carboxyl functional groups are widely used to make the binder matrix for solid composite propellants. The prepolymers used most extensively are the copolymer of butadiene and acrylic acid (PBAA), the terpolymer of butadiene, acrylic acid and acrylonitrile (PBAN), and carboxyl-terminated polybutadiene (CTPB). These prepolymers are compared; the problems arising from side reactions of the curing agents used in these propellants are a major contribution to the postcuring and softening phenomena. CTPB propellants are the most desirable from the viewpoint of mechanical behavior and solids loading capability. PBAA has been replaced by PBAN or CTPB because of improvements in storage stability and mechanical behavior which they provide. The reproducibility of butadiene propellants is satisfactory when the lot qualification technique is used.

The most recent development in solid composite propellants makes use of liquid butadiene prepolymers which provide 2–3 seconds' higher specific impulse than is realized from most other ammonium perchlorate composites. Higher concentrations of solids and the greater fuel values of the butadiene binder are responsible for the increase in energy. Satisfactory mechanical properties over the temperature range -75° to $+180^{\circ}$ F. are obtained, and the propellants can also tolerate exposure to high levels of humidity for prolonged periods with minimum change in mechanical behavior. These attributes, plus the simplicity of compounding the propellants and the ready processability of these composites

containing between 82 and 88% solids have extended the capability of solid propellant technology markedly. A range of compositions for typical high energy propellants is shown in Table I.

This paper discusses the three butadiene prepolymers which have been used most extensively in solid rocket propellants—*i.e.*, the copolymer of butadiene and acrylic acid (PBAA), the terpolymer of butadiene, acrylic acid, and acrylonitrile (PBAN), and the carboxyl-terminated polybutadiene (CTPB). Since the chemistry of all of these carboxyl-containing prepolymers is essentially the same, the discussion of butadiene propellants in this paper is concerned mainly with those based on CTPB.

Table I. Compositions of High Energy Butadiene Propellants

<i>Ingredient</i>	<i>Weight %</i>
Ammonium perchlorate	60–84
Aluminum	2–20
Butadiene prepolymer	12–16
Stabilizers	0–1
Curing agent(s)	0.2–1.0
	<hr/> 100

Historical Development

PBAA. The first butadiene prepolymer to be used in a rocket motor application was the liquid copolymer of butadiene and acrylic acid (PBAA). It is synthesized by a free radical emulsion polymerization technique to an average molecular weight of 3000 and an average functionality of 2. Owing to the method of preparation, the functional groups are distributed randomly along the chain, and the number of functional groups per molecule varies over a wide range. The liquid prepolymer is therefore a mixture of nonfunctional, monofunctional, difunctional, and polyfunctional molecules which exhibits a range of molecular weights. As a result, the epoxide-cured binders and propellants prepared with PBAA show poor reproducibility of mechanical properties. The low viscosity of the liquid PBAA prepolymer at the propellant processing temperature permitted the preparation of propellants with higher solids than had been possible with other binders. However, the postcure during storage and the poor mechanical behavior of the propellants (caused by the poor spacing of functional groups and functionality distribution of the prepolymer) led to the discontinuation of this material in solid rocket propellants.

PBAN. The mechanical behavior and storage characteristics of butadiene propellants were improved by using terpolymers based on buta-

diene, acrylonitrile, and acrylic acid (PBAN). This liquid terpolymer was prepared by the same emulsion polymerization technique used for PBAA; however, the introduction of the acrylonitrile group probably improved the spacing of carboxyl species, which could be a factor in the more reproducible propellant cures and mechanical properties. Propellants based on PBAN also showed a lesser tendency to surface harden, which is caused by oxidative attack at the double bonds and is known to be suppressed in nitrile rubbers (1). Typical examples of the effects of surface hardening on the uniaxial tensile properties of solid propellants (JANAF-Instron (4) tensile specimens) can be seen in Table II. The propellant based on PBAN shows little change in hardness upon exposure to 220°F. in an oxygen atmosphere for 96 hours as opposed to the strong increase in hardness observed for propellants based on a non-nitrile containing prepolymer (CTPB).

Table II. Effect of 220°F. Storage on Propellant Properties^a

<i>Propellant Type</i>	<i>Storage Time, hrs.</i>	<i>Shore A Hardness</i>	
		<i>Internal Cut</i>	<i>Surface</i>
PBAN	0	40	40
	96	49	47
CTPB	0	47	47
	96	57	81

^a Oxygen atmosphere, 10 p.s.i.g.

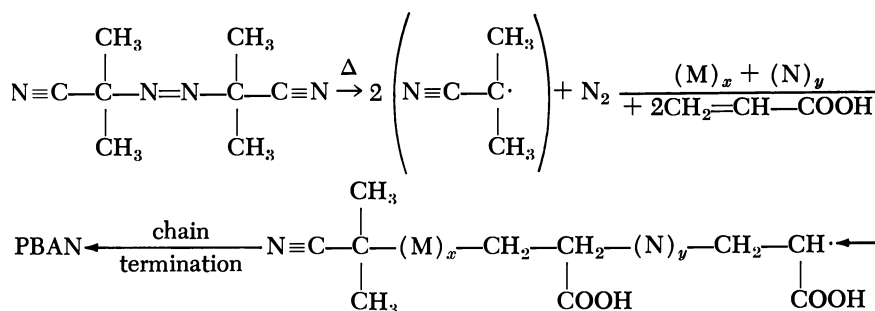
Since the development of this terpolymer in 1957, more solid composite rocket propellant has been produced from PBAN than from any other single prepolymer. Propellants based on this material have been used successfully in applications ranging from small tactical motors to the 260-in. diameter motor containing greater than 2,000,000 lb. of propellant. PBAN propellants, therefore, have been and are expected to be a major factor in making solid rocket motors during the next several years. The thermal stability which has been achieved, low temperature cycling characteristics, and low cost of propellants based on this prepolymer make this system attractive.

CTPB. Ultimately, prepolymers were developed with carboxyl groups in the terminal positions to take full advantage of the entire length of the polymer chain. These butadiene prepolymers were synthesized by a free radical- or lithium-initiation technique to an average molecular weight of 3500–5000 and a nearly bifunctional structure. These attributes provided for substantially improved mechanical behavior of highly loaded solid propellants, particularly at low temperatures. Pro-

pellants based on CTPB are therefore used in rocket motor applications in preference to PBAA or PBAN propellants, wherever stringent mechanical property requirements are imposed.

Chemistry of Carboxyl-Containing Polybutadiene Prepolymers

PBAA and PBAN. SYNTHESIS. PBAA and PBAN are prepared by an emulsion polymerization process initiated by a free radical mechanism. Using a quaternary ammonium salt as the emulsifier and azobisisobutyronitrile as the initiator, the reaction for the synthesis of PBAN proceeds according to:



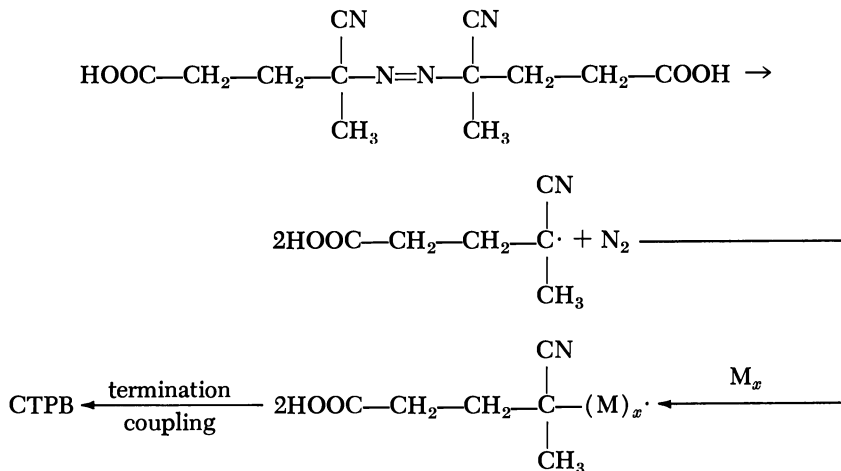
where $M_x = x$ moles of butadiene, $N_y = y$ moles of acrylonitrile, and for PBAA, $N_y = 0$. In this process, the butadiene-acrylic acid-acrylonitrile ratio can be varied over a wide range. In general, there is an average of two carboxyl groups per molecule and an average of 6% by weight of cyano groups. The acrylic acid and acrylonitrile are fed into the reactor containing the butadiene emulsion either intermittently or at a constant rate. The reaction is allowed to proceed until the molecular weight is in the range 2000-4000, at which time chain termination is effected, usually with a mercaptan. After termination of the polymer, the emulsion is broken, the antioxidant is added, and the product is purified by a water wash and vacuum drying. Typical properties of PBAA and PBAN are shown in Table III. [All materials are used as received unless otherwise noted.]

Table III. Physical Properties of PBAA and PBAN

	PBAN	PBAA
Molecular weight	3000-4500	2500-4000
Viscosity at 25°C., poise	300-350	275-325
Density, grams/cc.	0.93-0.94	0.90-0.92
ΔH_f , kcal./gram	9.9-10.1	10.2-10.4

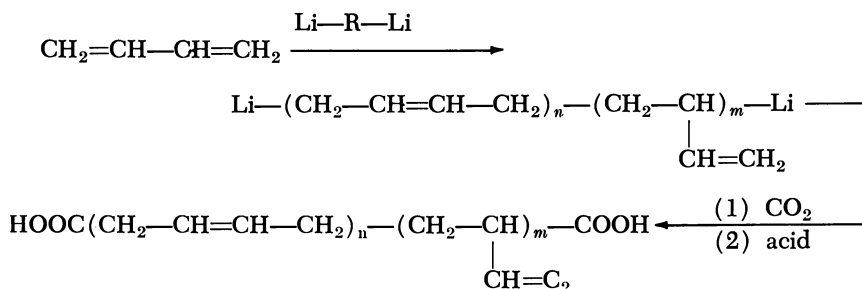
where M_x is x moles of butadiene, and $R = C_3H_6$. This polymerization technique may be extended to produce functionally terminated copolymers of butadiene and acrylonitrile.

The second method (12) uses 4,4'-azobis-4-cyanopentanoic acid as the initiator according to the following synthetic scheme:



where M_x is x moles of butadiene. So far, most propellant work has been conducted with the glutaric peroxide-initiated prepolymer.

Lithium-Initiated Prepolymers. The preparation of prepolymers by the organolithium technique (11) follows the reaction:

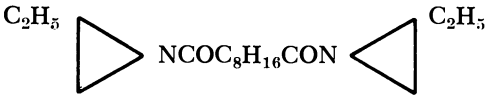
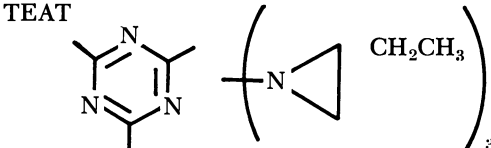


This process provides a prepolymer with a narrow molecular weight distribution, but the mean molecular weight can be varied over a wide range, and the process may also be adjusted to achieve various microstructures (cis, trans, and vinyl). On the other hand, prepolymers prepared by the free radical initiation technique generally exhibit a broad molecular weight range and a somewhat branched structure.

Table IV. Curing Agents for CTPB Propellants

Epoxides		Properties		
Name	Structure	Purity, %	Reaction Rate with Carbolic Acid 1/equiv.-hr. 80° C. 100° C.	
ERLA-0510		95	0.024	—
Epon X-801		81	—	0.0022
DER-332		96	—	0.0007
Aziridines				
MAPO		96	0.44	
BITA		92-94	0.9	

Table IV. (Continued)

Epoxides		Purity, %	Properties	
Name	Structure		Reaction Rate with Carbolic Acid 1/equiv.-hr. 80°C. 100°C.	
BISA		92-94	1.3	
TEAT		90-92	1.6	

CURING AGENTS FOR CARBOXYL-TERMINATED POLYBUTADIENE PREPOLYMERS. The types of curing agents used to prepare binders for CTPB propellants are the same as those for PBAN or PBAA. The bifunctionality of CTPB, however, requires that part of the curing agents be polyfunctional to provide for the formation of the tridimensional network. Almost without exception, the polyfunctional aziridines and epoxides used with CTPB undergo side reactions in the presence of ammonium perchlorate, which affects the binder network formation. Kinetic studies conducted with model compounds have established the nature and extent of the cure interference by these side reactions. The types and properties of some of the crosslinkers and chain extenders used to prepare solid propellants are summarized in Table IV.

Aziridines. Multifunctional aziridines have been used widely as curing agents for CTPB propellants. The desired chain extension and crosslinking are obtained by the formation of the amido-ester structure in the reaction with the carboxyl group. However, these materials are subject also to homopolymerization and rearrangement to oxazolines, which affects the equivalents balance of the reacting groups. The acidic ammonium perchlorate present in propellants promotes these side reactions which cause an undesirable shift in mechanical behavior and post-cure reactions. The known reactions of BITA (*see* Table IV) are shown in Figure 1. The rearrangement products of BITA (the mono-, di-, or trioxazoline) are still reactive with carboxyl groups but at a rate which is an order of magnitude (6) slower.

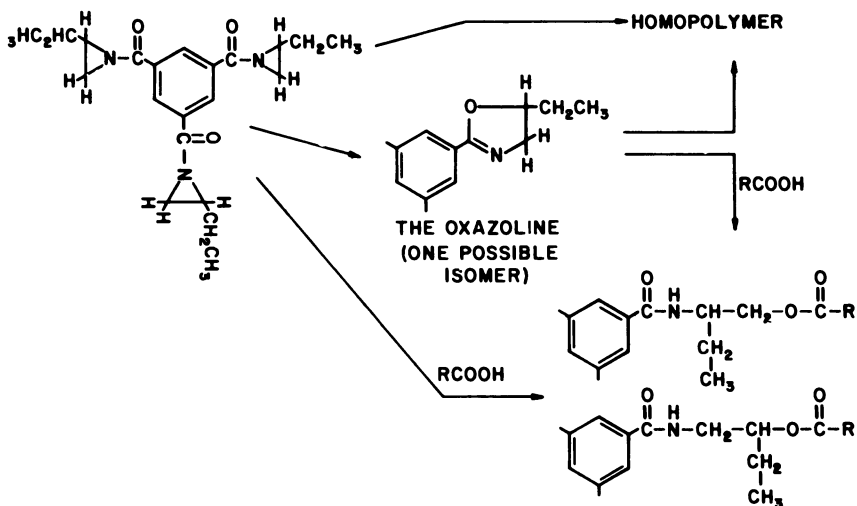


Figure 1. Reactions of BITA

The preceding conclusions were derived from model compound studies conducted to assess the reactions of aziridines and the carboxyl groups of CTPB (8). Propionic acid was used as the CTPB model, and the 1-benzoyl-2-ethyl aziridine was used as the curing agent model. The reaction was conducted in toluene and in the presence of ammonium perchlorate. Analyses by gas chromatography were conducted at periodic intervals to determine the species formed and the extent of the reactions. The results (Figure 2) showed that only *ca.* 50% of the aziridine curing agent forms the desired amide ester, 20% of the aziridine is converted to oxazolines, and the balance forms the homopolymer. Similar studies showed that higher concentrations of ammonium perchlorate (84.5%), with finer particle size of ammonium perchlorate and mixing action, increased the extent of the formation of the oxazolines (8). Additional model compounds tested with propionic acid and 1-benzoyl-2-ethyl aziridine have shown that zirconium acetylacetonate (ZrAA) is an effective polymerization catalyst for this cure reaction (Figure 3). The presence of the ZrAA catalyst not only increases the rate of reaction but promotes the desired primary reaction at the expense of the amount of homopolymer formed. Both the catalyzed and noncatalyzed reactions, however, produce about the same amount of the oxazolines.

MAPO (*see* Table IV) has also been used effectively as a curing agent for prepolymers containing carboxylic acid, and like BITA it undergoes homopolymerization and oxazoline formation, particularly in the presence of ammonium perchlorate. The polymer network formed, however, is unstable and softens rapidly when exposed to higher temperatures. This phenomenon is caused by the presence of three phosphorus—nitro-

gen bonds which cleave at high temperatures after the aziridine ring has reacted with the carboxylic acid. The mechanism and effects of the cleavage reaction on the physical properties of propellant are discussed under the section on aging of propellant.

The aziridine TEAT (*see* Table IV and Nomenclature section) exhibits the fewest side reactions in the presence of ammonium perchlorate of any aziridine used for curing carboxylic acid-containing prepolymers. Rate studies done with this curing agent and propionic acid in the presence of ammonium perchlorate have shown a uniform disappearance of both species without the formation of homopolymer (6). However, the rate of reaction of this compound with carboxylic acids is very high, which affects adversely the processing of solid propellants. This material, therefore, will not be useful as a curing agent until some means of moderating the reaction rate is found.

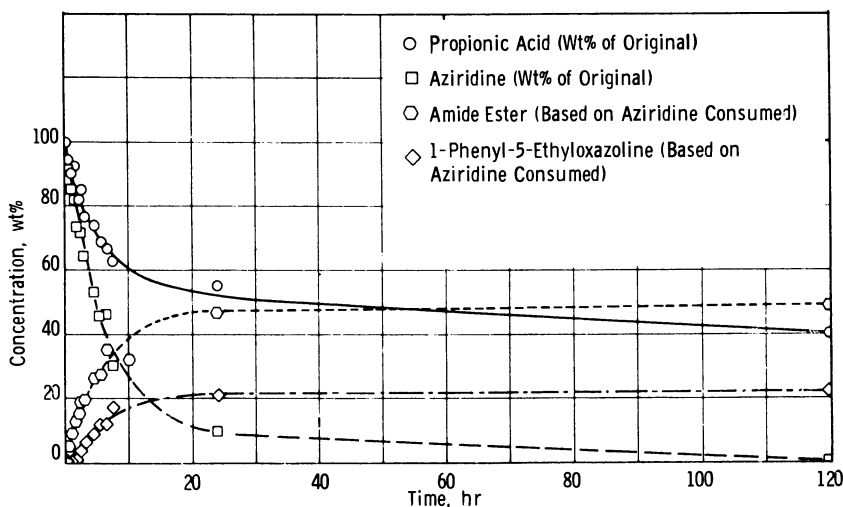


Figure 2. Change in concentration of reactants and products at 60°C. (140°F.) for agitated propionic acid (0.5M), 1-benzoyl-2-ethylaziridine (0.5M) in toluene with 18.5 wt. % ammonium perchlorate

Epoxides. Epoxy compounds react with the carboxyl groups of CTPB to form polyesters. The reaction rates and extent of reaction of a number of epoxides have been determined with the model compound hexanoic acid (6). It was found that most epoxides undergo side reactions (as evidenced by the more rapid consumption of epoxide species) but that at least one difunctional epoxide, DER-332 (Dow Chemical Co.) (Table IV), exhibits a clean reaction with carboxylic acids, even in the presence of ammonium perchlorate.

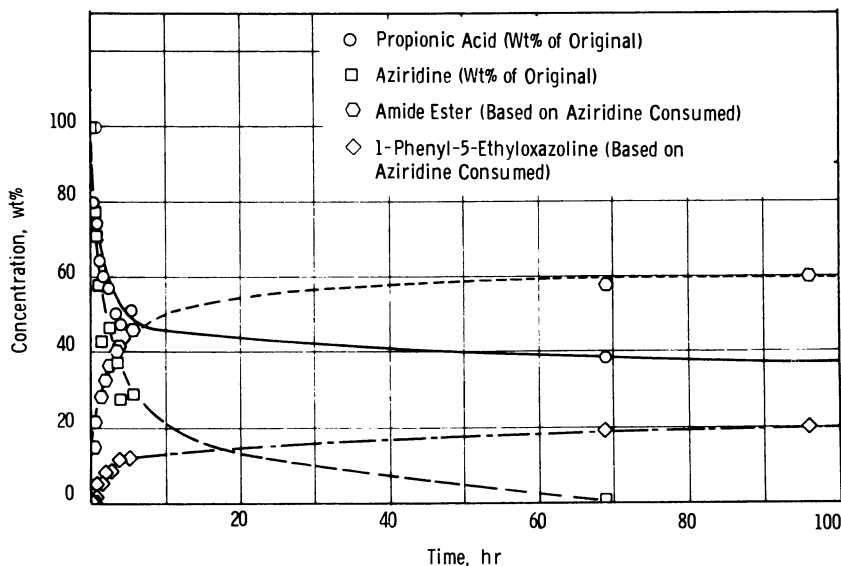


Figure 3. Change in concentration of reactants and products at 60°C. (140°F.) for agitated propionic acid (0.5M), 1-benzoyl-2-ethylaziridine (0.5M) in toluene solution with 18.5% ammonium perchlorate and 0.5 wt. % ZrAA

The results of model compound studies with three different types of epoxides, obtained in the presence and absence of ammonium perchlorate are shown in Figures 4, 5, and 6. The epoxide DER-332 shows a uniform rate of disappearance for the acid and epoxide species in this reaction. In the presence of ammonium perchlorate, the rate is increased, and a minimum of side reactions occur. Similar data but faster reaction rates are obtained with Epon X-801, but the consumption of epoxide species by side reactions is increased, particularly in the presence of ammonium perchlorate. On the other hand, the epoxide ERLA-0510 (Table IV), which contains a basic nitrogen, shows a reaction rate which is an order of magnitude greater than that for DER-332, accompanied by a substantial increase in side reactions. In the presence of ammonium perchlorate, the side reactions of ERLA-0510 predominate. In all probability, the side reactions of the multifunctional epoxides studied are homopolymerization.

The problems associated with the multifunctional curing agents for CTPB and the resultant aging behavior of the cured polymers have led to a practical solution for curing binders and propellants—*i.e.*, using mixed aziridines or a mixture of an aziridine and an epoxide. Such mixtures, when appropriately balanced, usually provide satisfactory mechanical behavior and high temperature stability. In dual curing systems such as MAPO and BITA or MAPO and a suitable multifunctional epoxide,

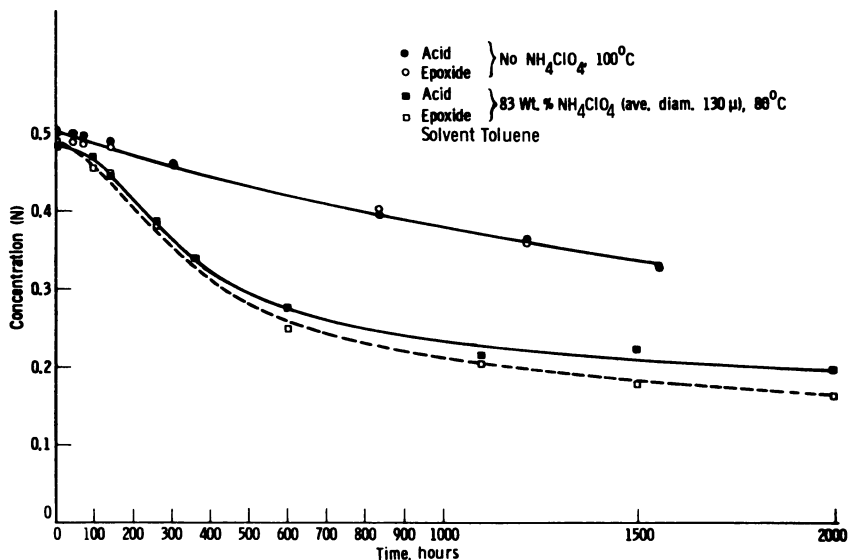


Figure 4. Rate of reaction of hexanoic acid with DER-332

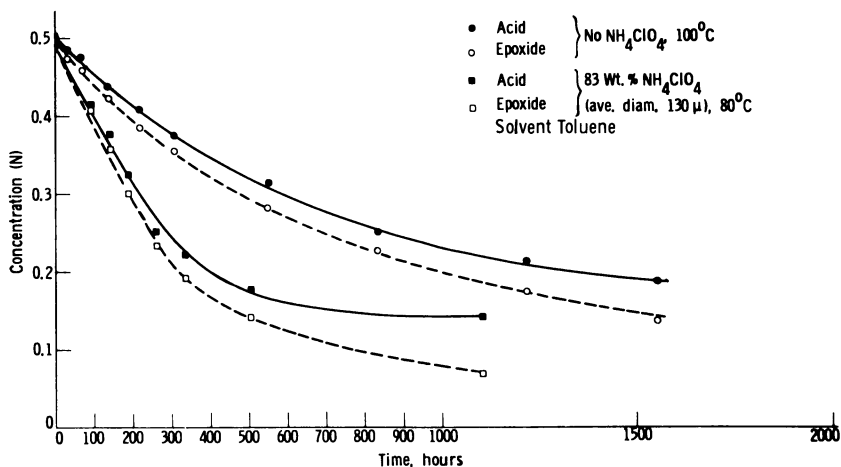


Figure 5. Rate of reaction of hexanoic acid with Epon X-801. Curves 1 and 2, no ammonium perchlorate; Curves 3 and 4, 83 wt. % ammonium perchlorate (average diameter = $130\ \mu$)

the latter material in each instance acts as the true crosslinker which does not experience cleavage and hence assures the integrity of the tri-dimensional structure. The softening caused by the P—N bond cleavage in MAPO-cured propellants is offset by the continued reaction of the oxazoline species resulting from the side reactions of BITA or the post-cure which is characteristic of most epoxides.

Mechanical Properties of Propellants

The use of carboxyl-terminated butadiene prepolymers has permitted an increase in the solids loadings of propellants while maintaining adequate mechanical properties over a wide temperature range. The uniaxial tensile properties—*e.g.*, elongation at break—over the temperature range -75° to $+180^{\circ}\text{F}$. are affected by the type of curing agent and plasticizer (Figure 7).

Effects of Curing Agent Type. EPOXIDE-CURED PROPELLANT. Carboxyl-terminated polybutadiene is a linear, difunctional molecule that requires the use of a polyfunctional crosslinker to achieve a gel. The crosslinkers used in most epoxide-cured propellants are summarized in Table IV and consist of Epon X-801, ERLA-0510, or Epotuf. DER-332, a high-purity diepoxide that exhibits a minimum of side reactions in the presence of the ammonium perchlorate oxidizer, can be used to provide chain extension for further modification of the mechanical properties. A typical study to adjust and optimize the crosslinker level and compensate for side reactions and achieve the best balance of uniaxial tensile properties for a CTPB propellant is shown in Table V. These results are characteristic of epoxide-cured propellants at this solids level and show the effects of curing agent type and plasticizer level on the mechanical properties of propellants.

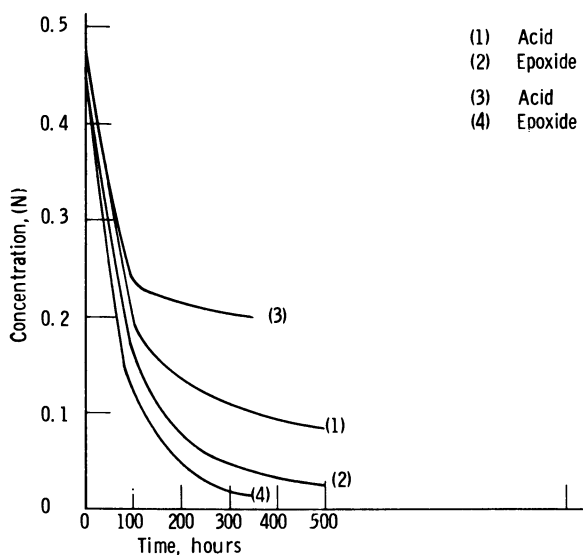


Figure 6. Rate of reaction of hexanoic acid with ERLA-0510 at 80°C .

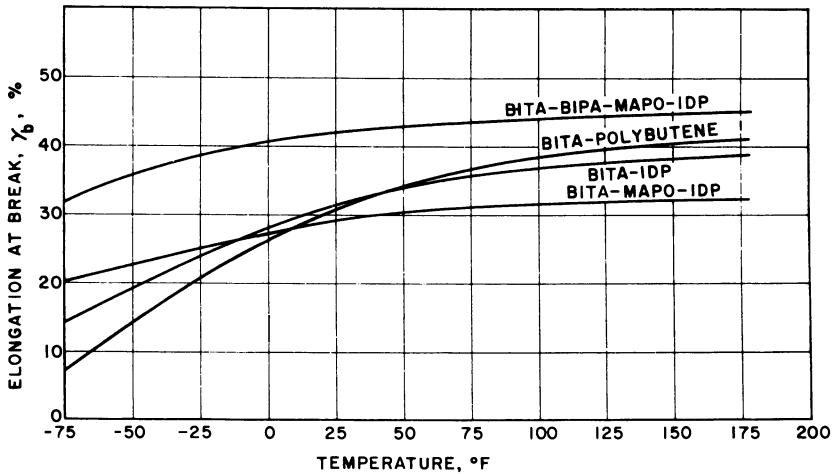


Figure 7. Effect of curing agent and plasticizer on the elongation of polybutadiene propellant

AZIRIDINE. Propellants cured with MAPO have excellent processing characteristics and satisfactory uniaxial tensile properties over a wide range of temperatures. However, the problems associated with the aging behavior of these propellants have led to the use of other types of curing systems which do not contain the P—N bond. These latter materials are di- and trifunctional aziridines, such as those shown in Table IV, and provide satisfactory propellants in which the uniaxial tensile properties can be tailored to a desired modulus. Such mixed aziridine-cured systems give satisfactory initial properties, reduce the postcure behavior, and improve the storage characteristics of CTPB propellants.

Table V. Mechanical Properties of Epoxide-Cured CTPB Propellants

		<i>Mechanical Properties at 77°F.^a</i>								
		<i>ERLA-0510/DER-332 Equivalents Ratio</i>								
<i>Plasticizer Level, % of Binder</i>	<i>Total Epoxide Equiv.</i>	<i>40/60</i>			<i>30/70</i>			<i>20/80</i>		
		σ_m , <i>p.s.i.</i>	ϵ_m , <i>%</i>	E_o , <i>p.s.i.</i>	σ_m , <i>p.s.i.</i>	ϵ_m , <i>%</i>	E_o , <i>p.s.i.</i>	σ_m , <i>p.s.i.</i>	ϵ_m , <i>%</i>	E_o , <i>p.s.i.</i>
25	100	128	27	753	—	—	—	75	25	511
	110	—	—	—	118	21	807	71	24	544
30	100	80	26	504	113	29	661	—	—	—
	110	—	—	—	121	24	768	—	—	—
35	100	61	34	302	—	—	—	—	—	—

^a Standard JANAF tensile specimens. Strain rate, 0.74 in./in./min.

MIXED AZIRIDINE-EPOXIDE CURES. An alternative method of achieving both thermal stability and satisfactory low temperature properties for CTPB propellants consists of using the combination of MAPO and a polyfunctional epoxide such as ERLA-0510, as the curing agent. Propellants in which the curing agent consists of 25% ERLA-0510 and 75% MAPO are shown in Table VI and indicate the marked influence of curing agent level on mechanical properties and the change of these properties over the temperature range -75° to $+180^{\circ}$ F.

Table VI. Mechanical Properties of MAPO/ERLA-0510-Cured Propellants

Batch No. 64-	Equivalents Ratio 75/25												
	1033				1035				1036				
Total Curing Agent Level, Equiv. ^a	90				100				110				
Test	Mechanical Properties ^b												
	Temp., °F.	σ_m , p.s.i.	ϵ_m , %	ϵ_b , %	e_o , p.s.i.	σ_m , p.s.i.	ϵ_m , %	ϵ_b , %	e_o , p.s.i.	σ_m , p.s.i.	ϵ_m , %	ϵ_b , %	e_o , p.s.i.
180	75	47	50	270	104	24	30	720	106	19	23	896	
110	87	46	50	384	119	26	43	823	121	19	23	1054	
77	102	47	50	405	156	33	36	936	159	24	28	1292	
0	147	50	59	800	221	37	49	1540	250	38	46	2010	
-40	204	49	76	2175	343	53	64	3470	364	50	57	3500	
-75	361	57	84	5330	569	50	67	9406	581	45	57	9549	

^a Per 100 equivalents of CTPB.

^b Standard JANAF tensile specimens. Strain rate, 0.74 in./in./min.

Effects of Prepolymer Molecular Weight. A marked effect on the uniaxial elongations of lithium-initiated CTPB propellants owing to the prepolymer molecular weight has been found. Analyses of the molecular weight distributions of several lots of CTPB prepolymer revealed that some lots showed a small fraction (10–15%) with a mean molecular weight in excess of 8000 (Figure 8). When propellants were prepared from these lots of material, the uniaxial elongations (when adjusted to the same modulus) appeared to correlate with the presence or absence of the high molecular weight fraction (Table VII).

Studies specifically designed to confirm this observation were conducted with prepolymer lots which were synthesized to molecular weights ranging between 10,000 and 15,000. These high molecular weight prepolymers and blends of the high molecular weight and normal production prepolymers were cured with BITA to produce binders and propellants. Table VIII shows that the high molecular weight (13,200) CTPB prepolymer resulted in binder with higher elongations at higher tensile

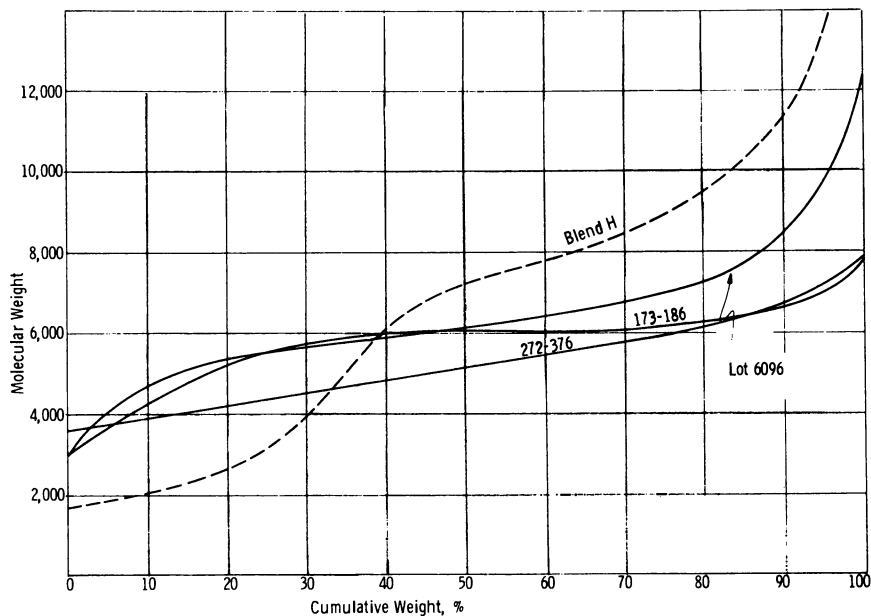


Figure 8. Molecular weight distribution of carboxyl-terminated polybutadienes

Table VII. Effect of CTPB Blend on the Mechanical Properties of Propellants

Mechanical Properties at 77°F.^b

CTPB Blend	σ_m , p.s.i.	ϵ_m , %	ϵ_b , %	$E_{0.2}$, p.s.i.	ϵ_b at Modulus of 450 p.s.i. %
H ^a	106	38	53	464	52.5
	103	34	49	498	52.5
	90	38	56	413	53.0
6096	94	42	52	439	51.0
173186	84	33	42	433	41.0
272376	83	31	41	486	43.3

^a Three curing agent lots.

^b Standard JANAF tensile specimens. Strain rate, 0.74 in./in./min.

strengths and higher moduli than binders prepared with production CTPB. These binders also showed a higher gel content, indicating that increased crosslinking occurred as the high molecular weight prepolymer was introduced. This implies a higher functionality for the higher molecular weight prepolymers, which is supported by the functionality distribution data for fractionated prepolymers (discussed later). The results of similar propellant studies are summarized in Table IX where it is shown again that improvements in tensile strength and elongation are

Table VIII. Properties of Binders Prepared with Blends of High Molecular Weight and Production CTPB

Batch No. B-	CTPB, %		Mechanical Properties at 77°F. ^b				Sol-Gel Fraction, %	
	High Molecular Weight ^a	Production	σ_m , p.s.i.	ϵ_m , %	ϵ_b , %	E_o , p.s.i.	Sol	Gel
	21	0	100	25	178	178	27	25.4
18	100	0	56	245	245	76	12.4	87.6
19	75	25	49	241	241	60	15.4	84.6
	50	50	43	263	263	46	16.8	83.2

^a Molecular weight, 13,200.

^b Standard JANAF tensile specimens. Strain rate, 0.74 in./in./min.

achieved on introducing the high molecular weight species (per 100 parts total CTPB), when compared at equivalent moduli.

The improvements in uniaxial tensile properties which can be achieved through higher molecular weight prepolymers clearly must be balanced against the deleterious effect that the higher prepolymer viscosity exerts on the propellant processing characteristics.

Effect of Solids Loading. CTPB propellants have been prepared over a wide range of solids loadings to establish the effects of filler concentration on the uniaxial tensile properties and processing characteristics. In agreement with Eilers and Van Dyck (5), the propellant modulus increases, and the elongation decreases with increased volume loading of solids (Figure 9). This behavior is consistent with the theory that the viscosity of liquids is increased by the presence of a filler and that propellant modulus is proportional to the ratio of the viscosities of the filled and unfilled systems (13). The trends observed are also in agreement with other studies which related the ratio of the moduli of filled and unfilled binders to the volumetric loading of the system (7).

Table IX. Uniaxial Tensile Properties of Propellants Prepared with Blends of High Molecular Weight and Production CTPB

CTPB, %		Mechanical Properties at 77°F. ^b				
High Molecular Weight ^a	Production	σ_m , p.s.i.	ϵ_m , %	ϵ_b , %	E_o , p.s.i.	ϵ_b at Modulus of 450 p.s.i., %
100	0	118	37	41	680	60
75	25	112	41	50	506	53
50	50	108	38	49	445	49
25	75	111	38	45	442	45
0	100	92	27	32	510	36

^a Molecular weight, 13,200.

^b Standard JANAF tensile specimens. Strain rate, 0.74 in./in./min.

Propellant Aging. Three structurally different chemicals and mixtures of these materials have been used to cure CTPB propellants. These are MAPO, other aziridines which do not contain the P—N bond, and epoxides. As stated in the discussion of curing agents, the aging behavior of CTPB propellants prepared with these materials is distinctly different, owing to the behavior of these compounds and their reaction products in the presence of ammonium perchlorate and at elevated temperatures.

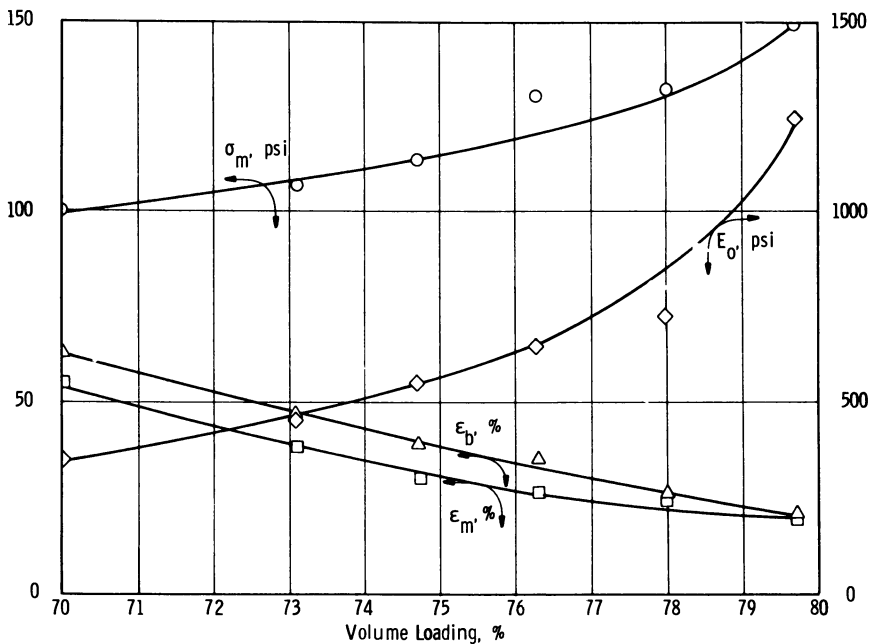


Figure 9. Relationship between volume loading and the uniaxial tensile properties of CTPB propellants

When MAPO-cured propellants are stored at elevated temperatures, the tensile strength and modulus decrease rapidly (Figure 10). This loss is also noticeable at room temperature, but the rate increases considerably as the temperature rises. The decrease in tensile strength is reversed with time, but the original rubbery properties of the binder are not recovered. This phenomenon can be explained by cleavage of the polymeric binder at the P—N bond with a resultant decrease in crosslink density and propellant softening. Model compound studies in which the reaction products were isolated and identified (Table X) have confirmed the mechanism (Figure 11) of softening.

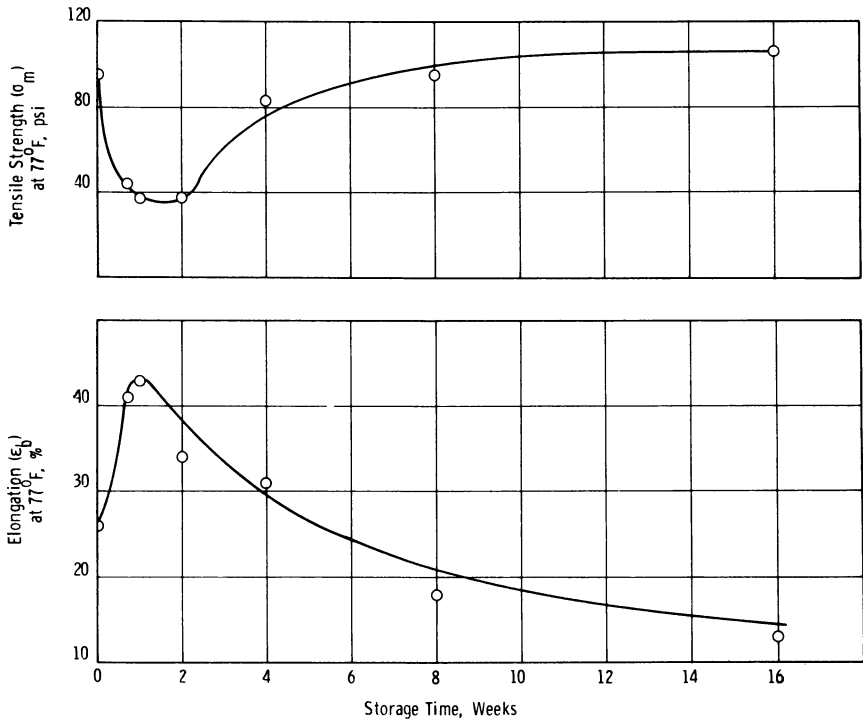


Figure 10. Effect of 180°F. storage on the tensile properties of a MAPO-cured CTPB propellant

The aging behavior of a BITA-cured propellant is shown in Figure 12, and is distinctly different from that of MAPO-cured propellants. Here, the modulus increases upon exposure to elevated temperatures, and the propellant is said to postcure. This behavior is in agreement with the known reactions of BITA, which includes the formation of oxazolines. These oxazolines which are formed are far less reactive with carboxylic acids than the original aziridines and, hence, the curing reactions continue in the propellant, particularly at elevated temperatures. Epoxy-cured propellants also postcure, owing to the side reactions revealed in

Table X. Identification of the

	% N (by Kjeldahl)	
	Theor.	Found
Base compound (dimethyloxazoline)	14.13	13.95
CH ₃ I derivative	5.80	5.80
Picrate derivative	—	—
Hexachloroplatinate derivative	—	—

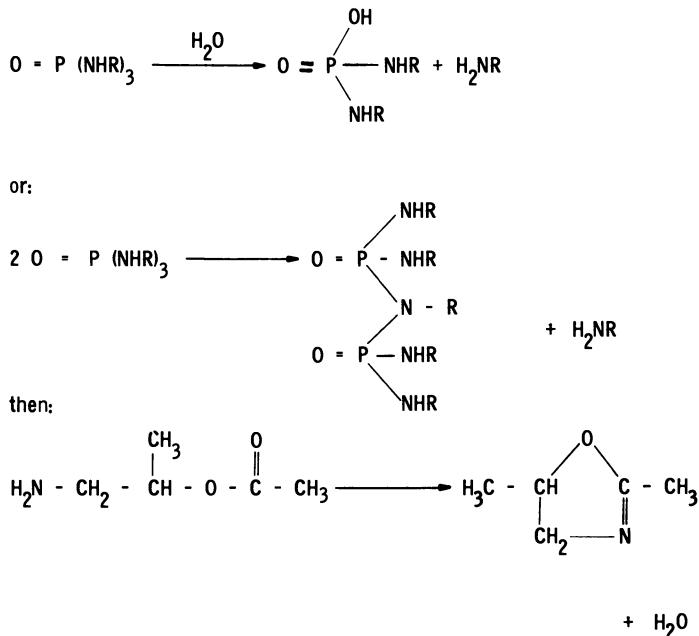


Figure 11. Rearrangement of the MAPO amide ester

kinetic studies, and are believed to be predominately homopolymerization of the curing agent.

Mixed aziridine or mixed epoxide-MAPO cures have been the practical solution to problems encountered with single curing agents. The mechanical properties of mixed aziridine or mixed epoxide-aziridine-cured propellants show less change on aging than those of propellants cured with MAPO or BITA alone. It appears that the BITA or the multifunctional epoxide (ERLA-0510 or Epon X-801) in the mixed curing systems provides stable crosslinks and a slight amount of postcure, which results

Rearrangement Product of MAPO Triacetate

% I (as AgI, gravimetrically)		M.P., °C.		B.P., °C.	
Theor.	Found	Theor.	Found	Theor.	Found
—	—	—	—	117	115
52.7	52.3	—	—	—	—
—	—	114-115	114-115	—	—
—	—	188-190	193	—	—

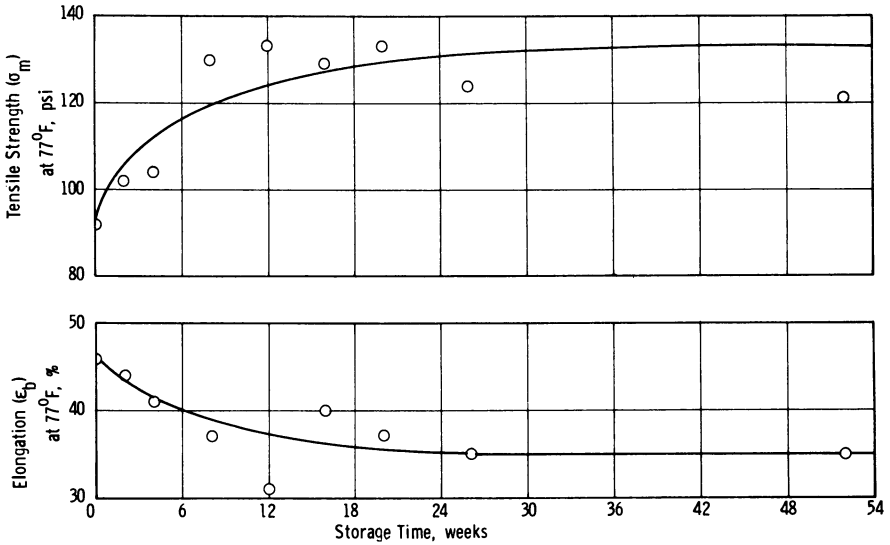


Figure 12. Effect of 150°F. storage on the tensile properties of a BITA-cured CTPB propellant

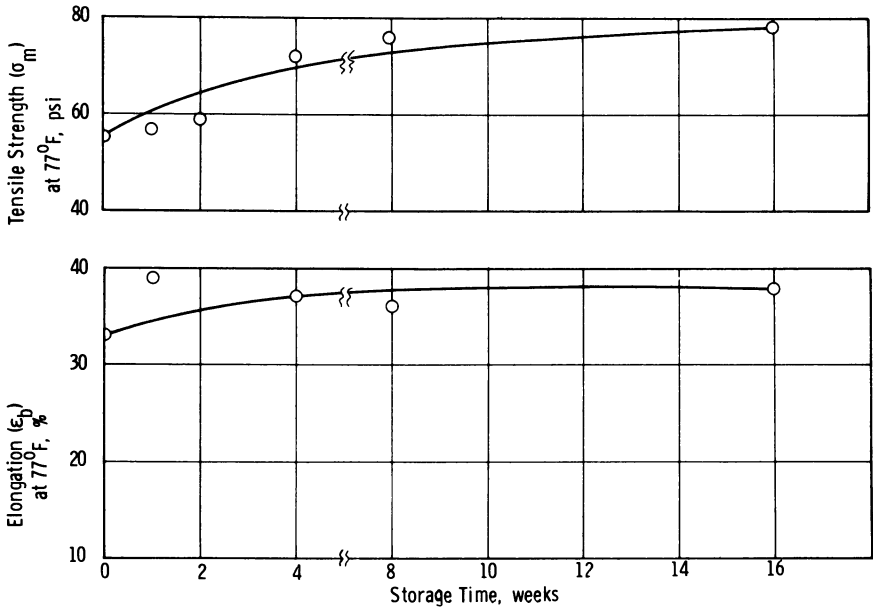


Figure 13. Effect of 160°F. storage on the tensile properties of a BITA-MAPO-cured CTPB propellant

in less change in the propellant uniaxial tensile properties upon storage at elevated temperatures. The effect of 160°F. aging on the uniaxial tensile properties of a BITA-MAFO-cured propellant are presented in Figure 13 and show little change over 16 weeks. Similar aging data for a MAPO-ERLA-0510-cured propellant aged at +180°F. are shown in Figure 14.

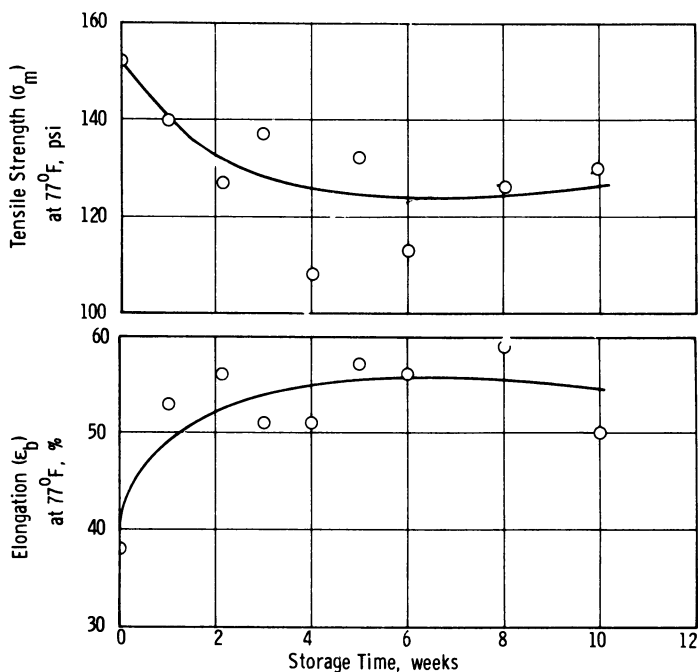


Figure 14. Effect of 180°F. storage on the tensile properties of an ERLA-0510-MAPO-cured propellant

A second mechanism in the aging of CTPB propellants also exists and proceeds concurrently with the reactions proposed above. It consists of an attack at the reactive points of unsaturation in the backbone polymer, which causes additional crosslinking and hence an increase in propellant modulus, particularly at the surface. The exposed surface of CTPB propellants changes, as indicated by an increase in hardness. Heavy metal ions are particularly harmful, and it was found that an increase from 10 to 80 p.p.m. of iron caused a significant increase in surface hardening by catalytic attack on the double bonds. Antioxidants in general provide sufficient protection for polymer storage. In CTPB propellants the antioxidant selected to protect the double bond is very important. Amine-type antioxidants have provided better surface stability than phenolic compounds.

Bonding. The three types of bonding required for solid propellants are (1) the bond between successive batches of uncured propellant being cast into a motor, (2) the bond between cured propellant and freshly cast propellant, and (3) the bond between the motor interior insulation/liner combination and the propellant. Methods have been developed to obtain satisfactory bonds for butadiene propellants in every instance.

PROPELLANT-TO-PROPELLANT BONDING. *Uncured Propellant.* The rheological characteristics, wetting properties, and extent of polymerization of CTPB propellants are continually changing from the point of completion of the mixing process until final cure. In a multiple batch motor, freshly prepared propellant is cast on propellant which is in a further state of cure. Since the state of cure (and hence the bonding characteristics) of the propellant depends on time, a time limit between batch castings must be established to assure grain integrity. The adequacy of the bond between castings can be tested by determining the strength and point of rupture of JANAF (4) tensile specimens which have been cut across the propellant-to-propellant (batch-to-batch) interface.

The results of one study to determine the maximum allowable time between casts are shown in Table XI. These data show that a change in the point of failure in the JANAF Instron tensile specimens occurred when the time between casts was changed from 48 to 72 hours. When the time between casts was increased to 96 hours, a marked change in the mechanical properties also occurred. Based on these data, the time between casts would be limited to 48 hours for this propellant.

Table XI. Effect of Time between Casts on the Bond between Batches of Butadiene Propellant

<i>Time between Casts, hours</i>	<i>Tensile Properties at 77°F.^a</i>				<i>Type of Break</i>
	σ_m , <i>p.s.i.</i>	ϵ_m , %	ϵ_b , %	E_o , <i>p.s.i.</i>	
1	66	33	41	266	propellant
24	62	29	30	273	propellant
48	60	26	27	261	propellant
72	66	30	34	275	interface
96	57	18	19	328	interface
168	56	20	21	293	interface

^a Standard JANAF tensile specimens. Interface approximately the midpoint of the gage section.

Bonding of Uncured to Cured Propellant. Uncured polybutadiene propellants do not normally bond satisfactorily when cast against cured propellants. Under these conditions, the sample usually ruptures at the propellant-propellant interface. Several techniques have been devised to improve this bond. The most satisfactory approach is to use a low viscosity curing agent containing the same functional groups that are present in the binder. This curing agent penetrates the cured propellant surface without leaving a finite layer which is oxidizer poor. A material which has performed satisfactorily for CTPB propellants is BISA, a difunctional aziridine which reacts with carboxyl species (Table IV). Bonding tests of propellant-to-propellant samples cast with the BISA washcoat on the surface of the cured propellant are shown in Table XII. Control samples (without BISA washcoat) break at the interface and exhibit a lower tensile strength than either of the two propellants used to prepare the propellant-to-propellant specimens. By contrast, those samples treated with the BISA washcoat break in the weaker of the two propellants.

Table XII. Propellant-to-Propellant Bonding

<i>Propellant</i>	<i>BISA Washcoat</i>	<i>Mechanical Properties at 77° F.^b</i>				<i>Break Location</i>
		σ_m , <i>p.s.i.</i>	ϵ_m , %	ϵ_b , %	E_o , <i>p.s.i.</i>	
Bipropellant ^a	Yes	71	31	42	378	First-cast (weaker) propellant
Bipropellant ^a	No	62	20	21	383	Interface
Single propellant (first-cast)		60	41	66	380	Interface
Single propellant (second-cast)		94	41	54	458	Interface

^a First propellant casting was cured 12 days at 110°F., washcoated with BISA, and subsequently cast with second propellant.

^b Standard JANAF tensile specimens tested at a strain rate of 0.74 in./in./min. Batch interface at approximately the midpoint of the gage section.

LINER PROPELLANT BONDING. The bonding properties of a typical CTPB liner and propellant system to a nitrile rubber insulation are shown in Table XIII. These data were obtained from 4-in. diameter "poker chip" (4) specimens with a diameter to thickness ratio of 20:1. The tensile bond values shown are approximately equal to the strength of the propellant.

Table XIII. Bond Strength between Insulation, SD-851-2 Liner and CTPB Propellant

<i>Mean</i>	<i>Peel Strength at 77°F., lb./in.</i>	<i>Double Plate^a Strength at 77°F., p.s.i.</i>	
		<i>Tensile</i>	<i>Shear</i>
	21.6 (L1)	86 (L1)	60 (L1)
Standard deviation	2.6	7.6	3.3
Samples	20	20	20

^a Square 2 in. × 2 in. specimens. Strain rate, 0.33 in./in./min. L1 failure within liner.

Since the bonding life of liner is influenced by age, bonding data must be developed by casting propellant against cured liner which has been allowed to stand at room or cure temperature for various times. The bonding life of the system is determined when a marked change in bond strength or the failure mode occurs. The results of a study of this type are shown in Table XIV. Based on the change in failure mode observed (liner to interface) the usable life of this liner is between 4–7 days standing time at 77°F. or less than 4 days at 110°F. Other liners exhibit up to 28 days of life under these conditions.

The relative humidity can also affect the usable life of the liner for many liner–propellant systems. However, studies to determine the usable life of a CTPB liner–propellant system (Table XV) would indicate that the bond is not affected significantly even upon exposure to 70% relative humidity for up to at least 8 days at 77°F.

Propellant Preparation

Processing Characteristics. To achieve the peak specific impulse for CTPB propellants requires a solids loading of 76% by volume. The viscosity characteristics of propellants containing up to and greater than this volume loading at 135°F. (the mixing and casting temperature) are shown in Figure 15. During the mixing and casting, the propellant viscosity increases steadily from the time of curing-agent addition. For propellants containing up to 76% by volume of solids, the potlife, determined by the flat portion of the viscosity–time curve, is greater than 12 hours at the processing temperature shown, which allows adequate time for most motor castings.

Casting of composite propellants is usually conducted under reduced pressure to eliminate air or other gases from the liquid propellant mix. Any voids caused by expanded gases will remain fixed in the propellant grain if gelation occurs before the vacuum is released. Hence, the vacuum must be released after volatiles are removed but before gelation

of the first batch, and cure is then completed at atmospheric pressure. A critical factor, therefore, in the propellant processability is the time between curing agent addition and gel formation. Noncatalyzed CTPB propellants cured with BITA or MAPO exhibit a gelation time (allowable cast time) usually greater than 60 hours at the curing temperature. For very large motors where the cast time is expected to exceed 60 hours, bayonet casting at ambient pressure with prior removal of gases has been successful. CTPB propellants are usually cured at 110°–150°F. for 6–12 days.

Table XIV. Effect of Cure Time on the Useful Life of SD-851-2 Liner

Cure Time at 110°F. hours	Bond Tensile Strength at 77°F., p.s.i.g. ^a					
	Holding Time at 77°F., days				Holding Time at 110°F., days	
	1	4	7	8	1	4
0	—	84(CPP,P2)	88(CPP)	69(CPP)	95(CPP)	97(CPP)
	90(L1)	90(L1)	79(CPP)	83(CPP)	77(L1)	98(CPP)
	90(L1)	94(L1)	92(CPP)	97(CPP)	90(L1)	79(CPP)
8	78(CPP)	78(P2,F)	84(CPP)	76(CPP)	88(CPP)	97(CPP)
	87(L1)	88(L1)	91(CPP)	94(CPP)	83(L1,P1)	107(CPP)
	89(CPP)	97(L1)	101(CPP)	100(CPP)	—	97(CPP)
16	81(F)	76(CPP,P2)	90(CPP,P2)	69(CPP)	85(F,P2)	97(CPP)
	89(L1)	89(CPP)	91(CPP)	72(CPP)	91(L1)	107(CPP)
	106(CPP,L1)	97(CPP)	97(CPP)	80(CPP)	104(L1)	97(CPP)
24	72(CPP)	—	87(CPP)	92(CPP)	65(CPP)	96(CPP)
	87(L1)	—	95(CPP)	79(CPP)	93(L1)	85(CPP)
	89(L1,CPP)	—	99(CPP)	94(CPP)	104(CPP)	103(CPP)

^a Square 2 in. × 2 in. tensile specimen. Strain rate, 0.33 in./in./min. Failure code:

(CPP) = clean peel at liner–propellant interface.

(L1) = failure in liner within 1 mm. of liner–rubber interface.

(P1) = failure in propellant within 1 mm. of liner–propellant interface.

(P2) = failure in propellant greater than 1 mm. from liner–propellant interface.

(F) = failure in adhesive at propellant–steel interface.

Prepolymer and Propellant Quality Control. PREPOLYMER CONTROL. The characterization of the functionally terminated prepolymers was an important factor in the control of these materials required to assure satisfactory reproducibility of solid propellant properties. To characterize these materials adequately, it was necessary to develop new analytical methods or to improve existing methods to provide the desired level of control. It was ultimately demonstrated that (1) propellant mechanical

properties depend strongly on the prepolymer functionality (which should approach 2), molecular weight, and molecular weight distribution, and (2) that the propellant processability is affected by the prepolymer molecular weight, microstructure, and the reactivity of the functional groups.

Table XV. Effect of Relative Humidity on the Bond Strength and Useful Life of SD-851-2 Liner^a

Storage Conditions, % Relative Humidity at 77° F.	Peel Strength at 77° F., lbs./in.				
	Initial (12 hours)	Storage Time at 77° F., days			
		1	4	6	8
30	19.0(L1)	—	—	—	—
0	—	22.7(L1)	15.1(L1,CPR)	16.0(L2,CPR)	12.7(CPP)
30	—	16.7(L1)	18.9(L1,L2)	20.4(L1)	17.1(CPP,L2)
50	—	17.8(CPR)	21.8(L1,L2)	19.9(L1)	16.6(CPP)
70	—	18.0(L1)	19.9(L1,L2)	18.1(CPR, CPP)	16.0(L2, CPP)

^a Failure code:

CPP = clean peel at liner-propellant interface.

CPR = clean peel at rubber-propellant interface.

L1 = failure in liner within 1 mm. of liner-rubber interface.

L2 = failure in liner greater than 1 mm. from liner-rubber interface.

Microstructure of Polybutadienes. Microstructure strongly influences the viscosity of the CTPB prepolymer. The viscosity of CTPB increases with increased vinyl content, but for CTPB prepolymers of the required molecular weight, an upper limit of 35% vinyl groups is satisfactory from the standpoint of propellant processing characteristics. It has also been found that the microstructure changes markedly with the synthesis process. Lithium-initiated polymerization yields prepolymers with slightly higher vinyl content than those produced by free radical initiation.

Infrared spectroscopy has been used successfully to determine the microstructure of CTPB prepolymers (10). Representative analysis for the microstructure of each of the four prepolymers presently available is shown below:

Polymer	Initiation	Typical Microstructure, %		
		Vinyl	Trans	cis
Butarez CTL	Li	27.0	39.0	34.0
Telagen CT	Li	25.7	40.7	33.6
Hycar CTPB	Free radical	19.8	50.9	29.3
HC-434	Free radical	20.4	51.5	28.1

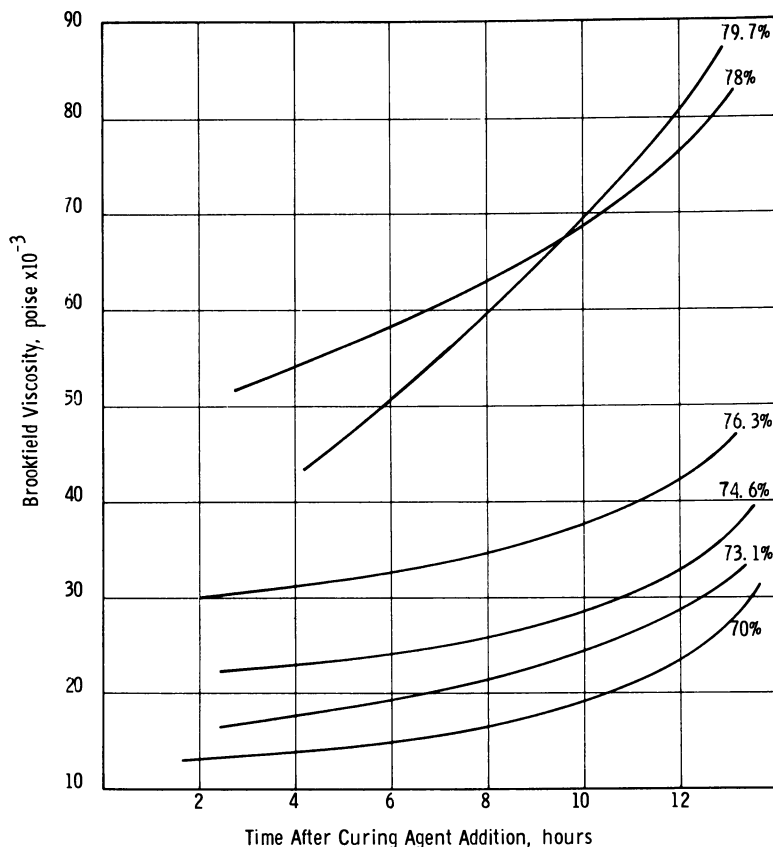


Figure 15. Effect of volume loading on the viscosity buildup of CTPB propellants. Measurements done at 135°F.

Equivalent Weight. Three reliable analytical methods are available to determine the equivalent weight of CTPB prepolymer: (1) titration by 0.1N sodium methylate in pyridine solution to the thymol blue end point, (2) infrared spectroscopy, and (3) nuclear magnetic resonance. Satisfactory agreement has been obtained between these instrumental analyses and the acid content as determined by titration (Table XVI).

Molecular Weight Determination. The techniques evaluated for determining the molecular weight of butadiene prepolymers have included freezing point depression, boiling point elevation, light scattering, intrinsic viscosity, and vapor phase osmometry. Although a certain degree of success has been achieved with most of these techniques, intrinsic viscosity and vapor-phase osmometry have provided the best results for prepolymers of this type.

Table XVI. Determination of Equivalent Weight

Prepolymer	End Group Analysis			
	Lot No.	Infrared	NMR	Wet Chemical
Butarez CTL	Blend H	2720	2897	2872
Telagen CT	228AM	3214	3159	2909
	259-325			
HC-434	Lot 23M	1920	2059	2000
Hycar CTB	Lot 13	2368	—	2250

The classical relationship between intrinsic viscosity and the molecular weight of prepolymers, where the end group theoretically does not influence the result is defined by the Mark-Houwink equation (9). Accurate values over a wide range of molecular weights can be obtained if the intrinsic viscosity is a function solely of the molecular weight of the compound and if reliable values of the constants are used. A plot of molecular weight (obtained by VPO) *vs.* the intrinsic viscosity of one lot of CTPB is shown in Figure 16. The constants in the Mark-Houwink equation are those calculated for nonfunctional prepolymers. The data points deviate appreciably from the curve at the high molecular weight end, where the constants are believed to deviate markedly from the values used. The Mark-Houwink relationship therefore, appears to be valid only over a limited molecular weight range when functional groups are present.

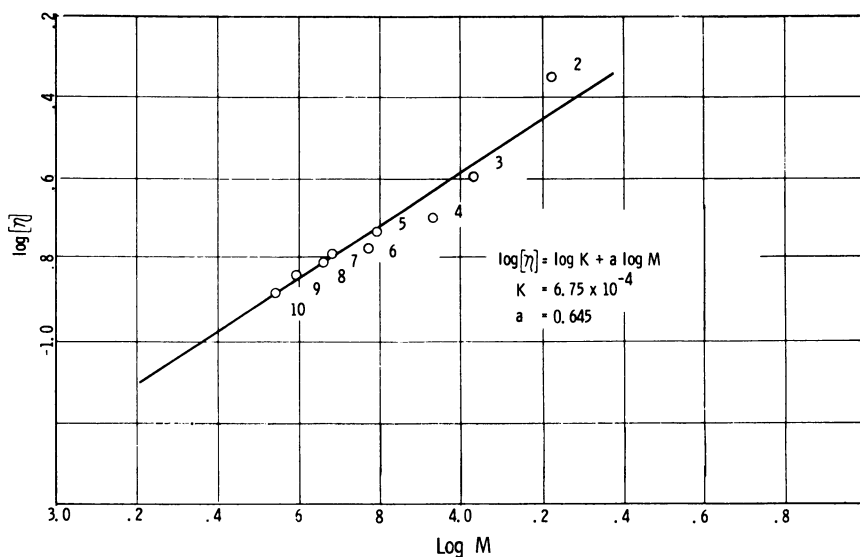


Figure 16. Relationship between intrinsic viscosity and molecular weight for Butarez CTL. Fractionation of blend H by gel chromatography

A more appropriate equation (3) for CTPB viscosity-molecular weight relationship which appears to apply over a wider molecular weight range is:

$$[\eta] = k_o + k_i M$$

This equation has been used successfully for low molecular weight species (up to 50,000) which contain polar groups. The constants k_o and k_i have been determined independently for CTPB's in the molecular weight range of interest (7). Using this relationship, the agreement between the points and the line for the same CTPB lot used in the previous example shows improvement at the high molecular weight end (Figure 17).

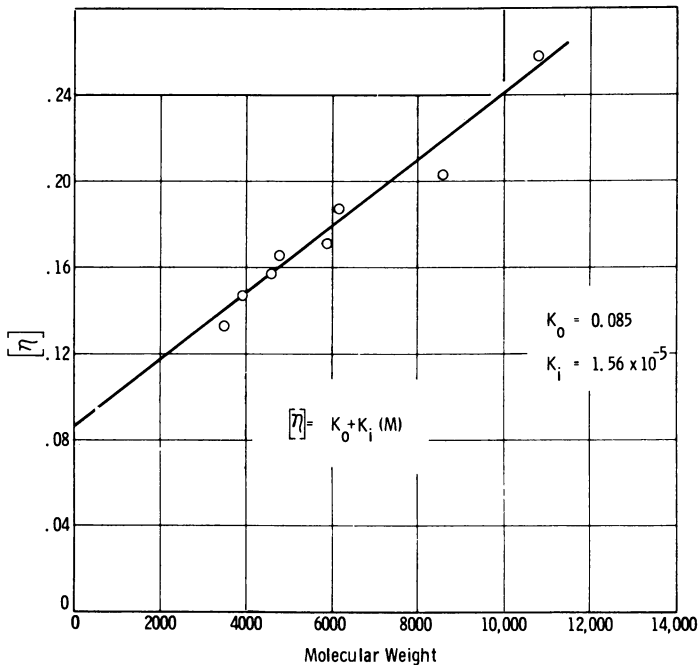


Figure 17. Linear relationship between intrinsic viscosity and CTPB molecular weight (Butarez CTL, blend H)

Of all the methods tested, the vapor-phase osmometry (VPO) method for determining the molecular weight of polybutadienes has proved to be the most satisfactory. Methyl ethyl ketone and chlorobenzene are the most widely used solvents for determining the molecular weight of CTPB owing to their polarity, which minimizes intermolecular association of the prepolymer. Robane (molecular weight 422) and selected other materials of higher molecular weight can be used to

calibrate the instrument. The reproducibility of the molecular weight determinations of a selected CTPB prepolymer (Butarez blend H), is shown in Table XVII. The values obtained show that the average deviation is approximately 1% of the mean value.

Table XVII. Reproducibility of Molecular Weight Determinations by Vapor-Phase Osmometry (Butarez CTL Lot 18)

<i>Test</i>	M_n	<i>Deviation from Average</i>
1	5462	0
2	5522	60
3	5462	0
4	5582	120
5	5393	69
6	5644	2
7	5462	0
8	5381	81
9	5376	86
10	5275	187
11	5404	58
12	5522	60
13	5462	0
15	5522	50
Av.	<hr/> 5462	<hr/> 56

Molecular Weight Distribution. The determination of prepolymer molecular weight distribution requires fractionation followed by the determination of the molecular weights of the individual fractions. The most satisfactory molecular weight fractionations have been achieved through either solvent precipitation or gel permeation chromatography.

The classical solvent precipitation fractionation technique provides reproducible fractionations for determining molecular weight distributions of CTPB and almost 100% recovery of the sample from the column. A solvent-nonsolvent combination which has been used effectively is the toluene-acetone-methanol system, where acetone and methanol are used as the nonsolvents. The precipitating fractions are required to stand approximately 24 hours to ensure complete separation. Each fraction is vacuum stripped of solvent at approximately 30°C., and the molecular weight of each fraction is then determined by either VPO or intrinsic viscosity.

A typical example of the reproducibility of molecular weight distribution when the fractions are separated by the solvent precipitation method is shown in Figure 18, where essentially identical results were achieved in replicate runs. In view of the degree of reproducibility of the

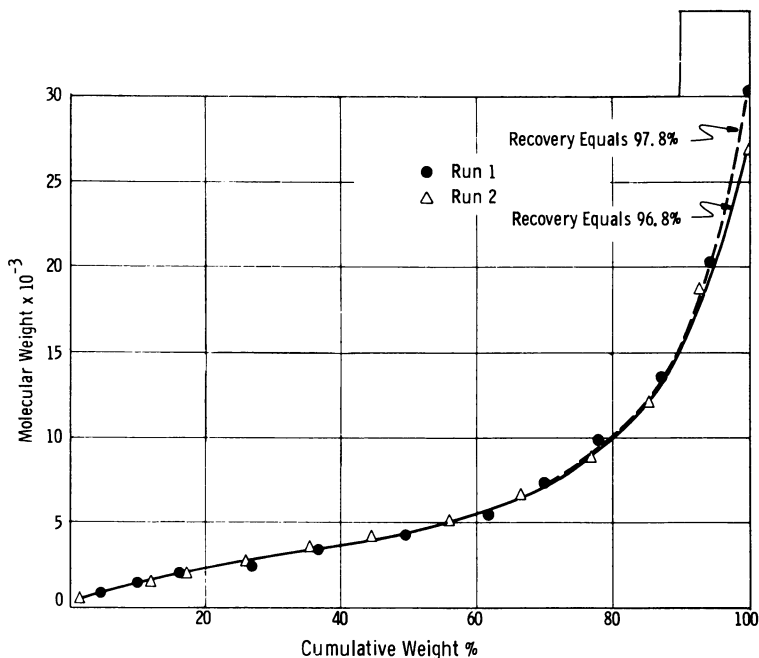


Figure 18. Reproducibility of the solvent precipitation fractionation technique for determining molecular weight distribution (molecular weights by intrinsic viscosity)

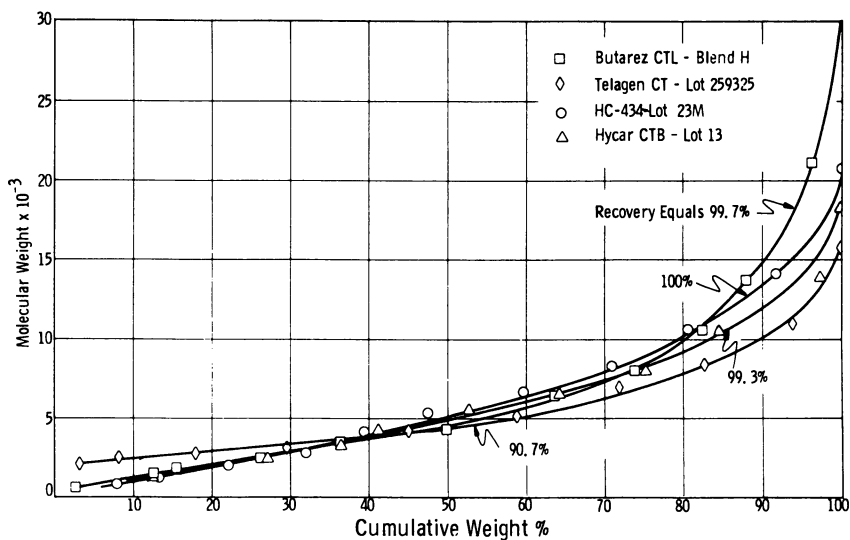


Figure 19. Comparison of molecular weight distributions of carboxyl-terminated polybutadienes by the solvent precipitation-intrinsic viscosity technique (representative lots)

method, small differences between prepolymers can be discerned, and the molecular weight distributions of different carboxyl-terminated polybutadienes can be compared. Typical distributions of various CTPB prepolymers are shown in Figure 19. It can be concluded that:

(a) The Telagen CT prepolymer exhibits a narrow molecular weight distribution.

(b) The Butarez CTL prepolymer contains a fraction which exhibits the highest molecular weight of any of the materials tested.

(c) The molecular weight distributions of the HC-434 and the Hycar CTB prepolymers are very similar and do not contain a high molecular weight fraction similar to that seen in the Butarez CTL.

Fractionation by gel permeation chromatography provides results similar to those obtained by solvent precipitation fractionation. For CTPB, satisfactory separation by molecular weight can be obtained with a column packed with polystyrene gel with a permeability limit of 1000 Å. Increments of the prepolymer are cycled twice through the column with toluene as the elution solvent; solvent stripping is accomplished by vacuum at room temperature. The molecular weight distribution of a single lot of CTPB obtained by the classified solvent precipitation and the gel chromatography techniques are compared in Figure 20.

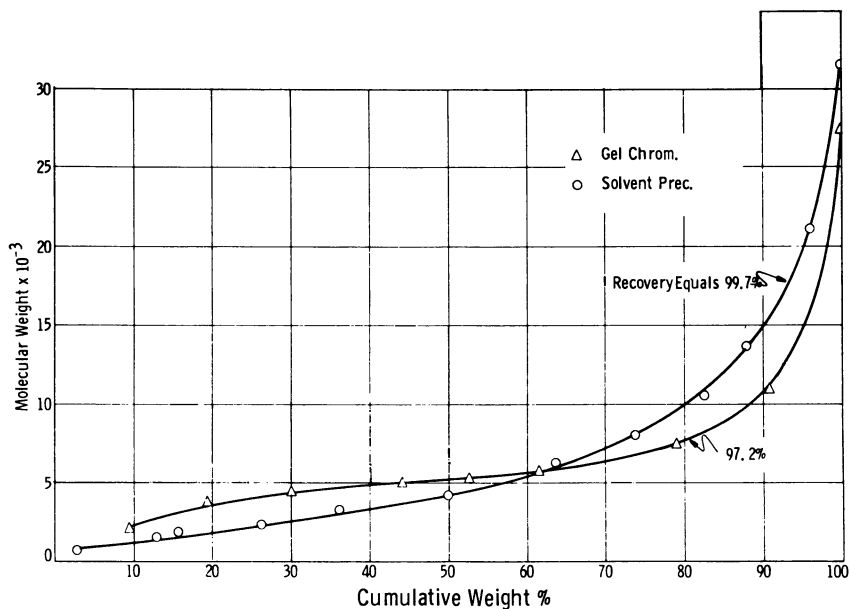


Figure 20. Comparison of molecular weight distributions of Butarez CTL blend H by solvent precipitation and gel chromatography fractionation (molecular weight by intrinsic viscosity)

Functionality. Functionality is the most important single parameter of liquid prepolymers because it determines the degree of chain extension, chain termination or crosslinking. The average functionality of a lot of CTPB is obtained by the relationship between molecular weight and equivalent weight and approaches the value of 2. The most reliable values of functionality which can be calculated from chemical analyses are obtained by comparing the VPO molecular weight and the end group analysis by wet chemical or instrumental methods. When the sample size is small, instrumental analysis is mandatory.

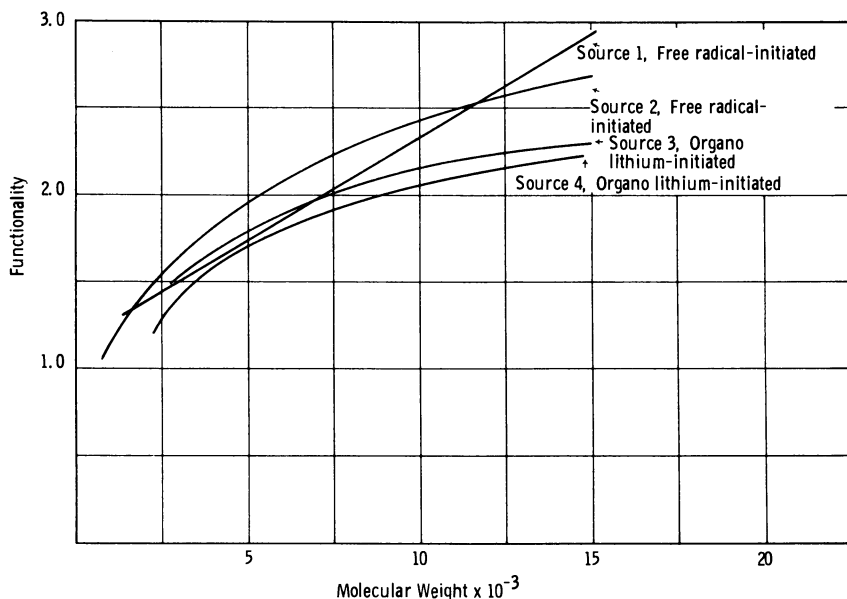


Figure 21. Functionality distributions of CTPB prepolymers (VPO-infrared technique)

The determination of functionality of a fractionated prepolymer lot permits the examination of smaller cuts of the material to determine whether functionality depends on molecular weight. Figure 21 shows this relationship for four representative prepolymer lots. Both types of prepolymers show an increase in functionality with increasing molecular weight. The functionality values for lithium-initiated prepolymers show a comparatively narrow range around the desired value of 2, whereas the free radical-initiated prepolymers generally show a wider range of functionalities over the molecular weight range and average functionalities which are greater than 2.

Reactivity of Functional Groups. The reactivity of the functional groups of liquid prepolymers significantly affects the processing, cure behavior, and the ultimate mechanical properties of the cured binder and propellant. The reactivity of carboxyl groups of CTPB can be determined by the rate of reaction with *n*-butyl alcohol. The rate of esterification is measured from the rate of water evolution from the alcohol-carboxylic acid reaction, and a plot of water evolved *vs.* time then permits the calculation of the corresponding rate constants.

For some prepolymers, it was found that two different types of carboxyl groups, which react at different rates, are present in CTPB. The data obtained are tabulated in Table XVIII, where the two different carboxyl species have been designated as Type I (more reactive) and Type II (less reactive). From these measurements, it was established that the Butarez CTL and Telagan CT are both made by a lithium-initiated process, contain approximately the same amount of the two types of carboxyl species. The Hycar CTB and the HC-434 prepolymers, however, appear to contain only (or predominately) the more reactive type of carboxyl groups. These differences in the reactivity are probably related to the structure of the prepolymer segment adjacent to the functional group, such that in some instance the carboxyl group is sterically hindered. For Butarez CTL and Telagen CT, these hindered structures probably arise during polymerization of the monomer while with Hycar CTB and HC-434 prepolymers, the initiating free radical may be the controlling factor. This difference in reactivity for the two different types of prepolymers is clearly reflected in the processing characteristics of the propellant prepared with these materials and requires appropriate adjustments to assure adequate potlife.

Table XVIII. Reactivity of Terminal Functional Groups of CTPB
Catalyzed Esterification with *n*-Butyl alcohol

CTPB Lot No.	Type I	$K_1, \text{sec.}^{-1}$ $\times 10^{-4}$	Type II	$K_2, \text{sec.}^{-1}$ $\times 10^{-5}$
	Carboxyl, % (Most Reactive)		Carboxyl, % (Least Reactive)	
Butarez CTL Blend H	49	4.1	51	4.5
Telagen CT	43	4.4	57	4.4
Lot 228 AM-259-325				
Hycar CTPB Lot 13	82	1.7	18	1.6
HC-434 Lot 23M	100	1.1	0	

PROPELLANT ACCEPTANCE. There are two principal areas in the control of CTPB propellants: (1) the preproduction tests which include raw material acceptance and the end product tests to determine the best prepolymer-curing agent ratio for a specific composition of solids, and

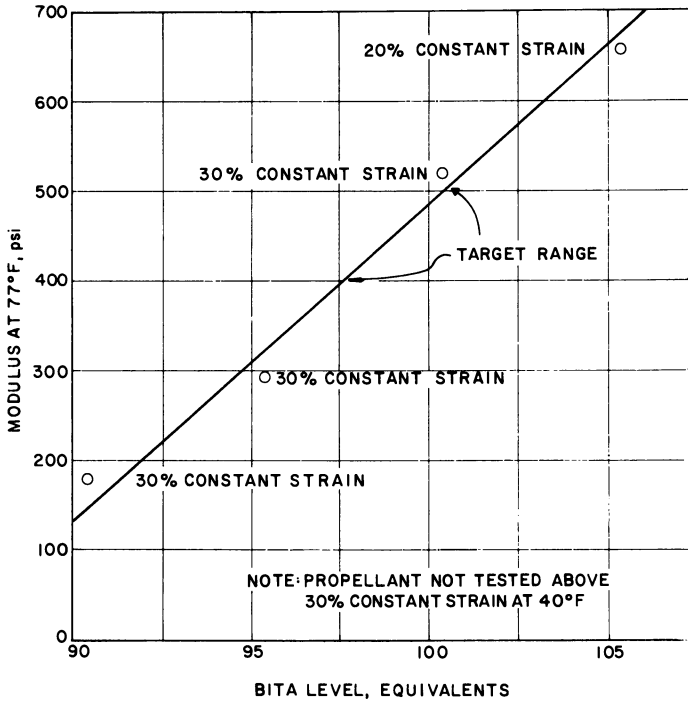


Figure 22. Effect of BITA level on the modulus of ANB-3066 propellant (2000-lb. batches)

(2) the in-process quality control tests to assure that the propellant will meet all requirements. Both types of controls are mandatory and are discussed separately in the succeeding paragraphs.

Raw Material Acceptance. The prepolymer and curing agent used in CTPB propellants are accepted by both analytical characterization and by qualification in the end product. Although many lots of CTPB prepolymer are blended to compensate for minor lot-to-lot differences (and thus assure satisfactory mechanical properties and reproducibility), it is still necessary to conduct these latter tests to confirm that the prepolymer is acceptable for use in propellant manufacture. This qualification consists of preparing and testing full-scale propellant batches which must meet certain mechanical property requirements established by specification. These batches are prepared over a range of curing agent levels, and the acceptance of the prepolymer depends on the demonstration of the required mechanical properties at a curing agent level which is within specified limits. A typical example of a qualification series prepared to determine the most satisfactory ratio of curing agent to prepolymer is shown in Figure 22, where 98 equivalents of BITA for 100 equivalents of

CTPB would be selected to achieve a target modulus of 450 p.s.i. A minimum propellant elongation is also usually specified to confirm that the propellant will tolerate the strains expected in the motor.

Using the above techniques, satisfactory reproducibility of CTPB propellant mechanical properties has been achieved. The reproducibility of the mechanical properties of a production CTPB propellant which is controlled by this method is shown in Table XIX. In this case, the standard deviations of the mechanical properties shown are 10% or less of the measured values. The data include differences arising from lot-to-lot variations in raw materials (27 lots of CTPB) and two sources for the prepolymer.

Table XIX. Reproducibility of Mechanical Properties of a Production CTPB Propellant

	<i>Mechanical Properties at 77°F.^a</i>			
	σ_m , p.s.i.	ϵ_m , %	ϵ_b , %	E_0 , p.s.i.
Mean	92	35	49	456
Standard deviation	6.6	3.1	5.3	45

^a Standard JANAF tensile specimens. Strain rate, 0.74 in./in./min. Number of batches, 3090.

Propellant Acceptance Testing. The acceptance of CTPB propellant for a given motor consists of two parts. These are the in-process controls or precasting acceptance tests and the testing of cured propellant samples to confirm that the propellant meets the specification requirements. Typical examples of the in-process control tests consist of liquid strand burning rate, liquid density, acid number of the liquid premix (polymer, plasticizer, and metallic fuel) and the total solids content. After propellant cure, the uniaxial tensile properties, subscale motor burning rate, and solid density may be tested also. The controls exercised on the liquid propellant are responsible largely for the reproducibility of the cured propellant. The reproducibility of burning rates and densities of liquid and solid propellants are compared in Table XX.

Ballistic Properties of CTPB Propellants

Propellants based on carboxyl-terminated polybutadiene characteristically exhibit the highest values of specific impulse which have been achieved for ammonium perchlorate-based composites. These propellants also exhibit satisfactory mechanical behavior over a wide range of temperatures and can be adjusted to meet the burning rate requirements of most applications.

Table XX. Reproducibility of In-Process Acceptance Tests and Cured Propellant Properties

	<i>Burning Rates at 500 p.s.i.a.</i>			
	<i>Density, grams/cc.</i>		<i>Liquid Strand</i>	<i>Subscale Motor^a</i>
	<i>Liquid</i>	<i>Solid</i>	<i>in./sec. at 80°F.</i>	<i>in./sec. at 80°F.</i>
Mean	0.00082	1.7713	0.3279	0.3211
Standard deviation	1.7702	0.0015	0.0025	0.0066
Number of batches	174	50	176	212

^a Six-pound grain.

Ballistic Properties. SPECIFIC IMPULSE AND DENSITY. A plot of the theoretical specific impulse of polybutadiene propellants over the range of solid loadings is shown in Figure 23. These calculations show that the peak value of theoretical specific impulse is 266 lbf.-sec./lbm. calculated at 1000 p.s.i.a. exhausting to 14.7 p.s.i.a. (0° half-angle). The highest values of specific impulse are obtained in the region 85–90% total solids and for compositions containing approximately 17–25% aluminum.

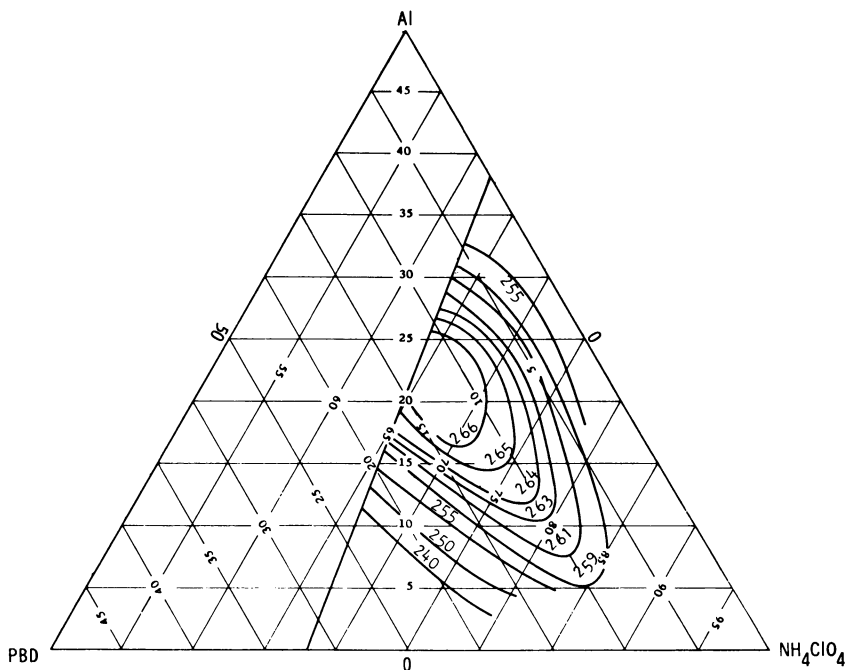


Figure 23. Theoretical specific impulse for an AP-Al-PBD propellant. $P_c/P_e = 1000/14.7$ p.s.i.a.; optimum expansion; 0° half-angle

The calculated flame temperatures and densities of the propellants of greatest interest are shown in Figures 24 and 25. For the highest specific impulse propellants, the calculated flame temperatures are in the region 5500°–6500°F. at 1000 p.s.i.a. The densities of these same propellants are in the region 0.062–0.066 lb./cu. in.

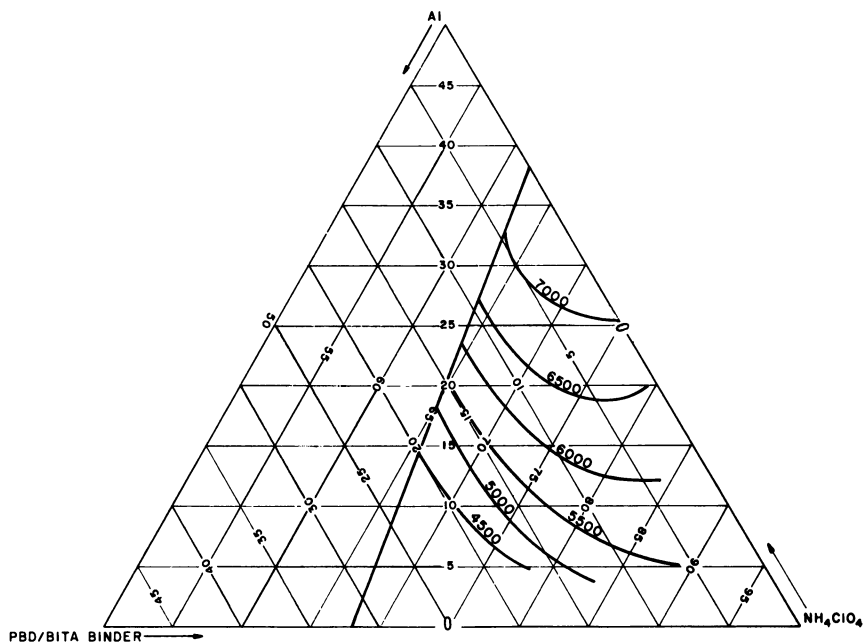


Figure 24. Composition diagram of chamber flame temperature, °F., for ammonium perchlorate–aluminum–polybutadiene/BITA propellant. $P_c = 1000$ p.s.i.a.; shifting equilibrium

BURNING RATES. Propellants based on butadiene prepolymers have been tailored to meet a wide range of burning rate requirements. A typical example of the range of burning rates available is shown in Figure 26 where the lowest burning rates were achieved with mixed ammonium perchlorate–ammonium nitrate oxidizers, the median range with a range of particle sizes of ammonium perchlorate oxidizer alone, and a higher range of burning rates with metal oxide catalysts. Propellants of this type can, therefore, be tailored to meet the burning rate requirements of a variety of applications.

Conclusions

Propellants based on carboxyl-terminated polybutadienes have been used successfully in many solid rocket motors. These propellants provide

the highest energy available from composite ammonium perchlorate propellants (Class I), can be prepared over a range of burning rates, are readily processable, and are suitable for use in multiple batch motors. Satisfactory reproducibility for the propellant mechanical properties and burning rates can be achieved with the lot-qualification technique.

The key problem with these propellants is related to the curing agents needed for the carboxyl species. These curing agents (difunctional or polyfunctional epoxides and aziridines) exhibit homopolymerization and other side reactions which are damaging to the polymer network and prevent CTPB propellants from achieving the best possible mechanical behavior. The side reactions of these curing agents, which cause poor aging behavior, result from the imbalance between the carboxyl groups and the curing agents, the further reaction of the carboxyl species with the products of side reactions (such as oxazolines) or cleavage at the crosslinks. Owing to the complexity of these reactions and an inability to characterize the prepolymer and curing agents adequately in labora-

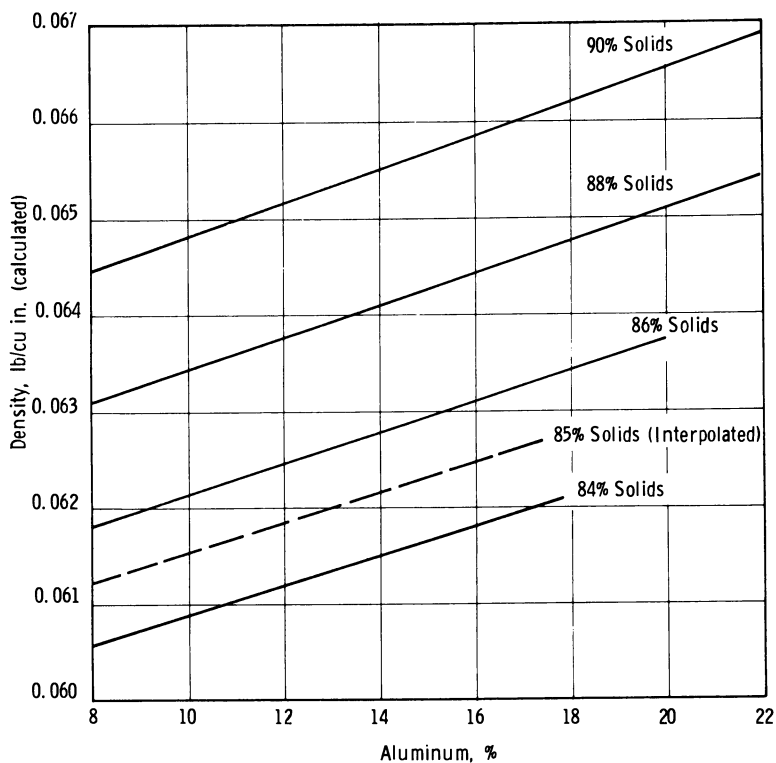


Figure 25. Effect of solids loading and aluminum content on the density of polybutadiene propellants (calculated)

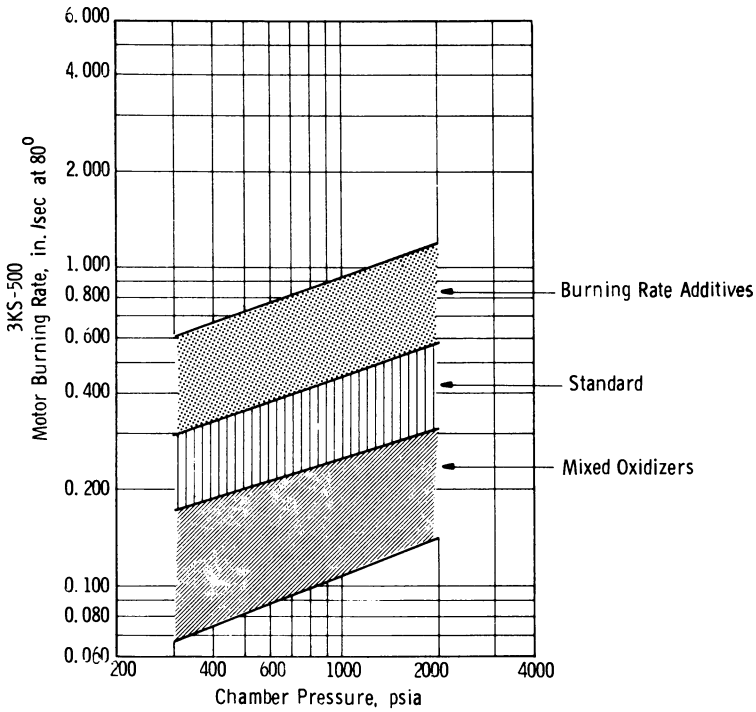


Figure 26. Burning rate range for polybutadiene propellants

tory acceptance tests, it is necessary to conduct the final acceptance by the lot-qualification technique, where the end product is tested for conformity to the specification.

Acknowledgments

We gratefully acknowledge the sponsorship of this work by the Ballistics Systems Division and the Rocket Propulsion Laboratory of the U. S. Air Force. Recognition is given to A. J. DiMilo, D. E. Johnson, C. B. Frost, and R. Putnam, who contributed a major portion of the experimental data.

Nomenclature

Prepolymers

- PBAA — Copolymer of butadiene and acrylic acid
- PBAN — Terpolymer of butadiene, acrylic acid and acrylonitrile
- CTPB — Carboxyl-terminated polybutadiene

- Telagen CT — Carboxyl-terminated polybutadiene
(General Tire & Rubber Co.)
- Butarez CTL — Carboxyl-terminated polybutadiene
(Phillips Petroleum Co.)
- Hycar CTB — Carboxyl-terminated polybutadiene
(B. F. Goodrich Co.)
- HC-434 — Carboxyl-terminated polybutadiene
(Thiokol Chemical Corp.)

Curing Agents

- MAPO — Tris(2-methyl aziridiny1)phosphine oxide
- BITA — 1,3,5-Tris(2-ethylaziridiny1) adduct of trimesic acid
- TEAT — 2,4,6-Tris(2-ethylaziridiny1)-S-triazine
- BISA — α,ω -Bis(2-ethylazirindyl-1) adduct of isosebasic acid
- BIPA — 1,4-Bis(2-ethylaziridiny1) adduct of isophthalic acid

Epoxides

- ERLA-0510 — Triepoxide of *p*-aminophenol and glycidyl ether
(Bakelite Division of Union Carbide Co.)
- Epon-X801 — Triepoxide of phenol and glycidyl ether
(Shell Development Co.)
- DER-332 — Diepoxide of bisphenol A (Dow Chemical Co.)

Plasticizers

- IDP — Isodecyl pelargonate
- Oronite-6 — Polybutene, MW about 300

Standards

- Robane — A saturated hydrocarbon— $C_{30}H_{62}$

Miscellaneous

- MW — Molecular weight
- Volume loading — Volume percent of solids
- Class I explosive — Fire hazard only
- NMR — Nuclear Magnetic Resonance
- VPO — Vapor Phase Osmometry
- σ_m — Tensile stress at maximum stress
- ϵ_m — Elongation at maximum stress
- ϵ_b — Elongation at break
- E_o — Initial modulus

Literature Cited

- (1) American Cyanamide Co., "The Chemistry of Acrylonitrile," 1959.
- (2) Berenbaum, M. B., *et al.*, U. S. Patent 3,235,589 (1966).
- (3) Braude, E. A., Nachod, F. C., "Determination of Organic Structures by Physical Methods," p. 61, Academic Press, New York, 1955.
- (4) "CPIA, IRCPG Solid Propellant Behavior Manual," Feb. 1968.

- (5) Eilers and Van Dyck, *Kolloid Z.* **97**, 313 (1941).
- (6) Johnson, D. E., DiMilo, A. J., Aerojet-General Corp., *Rept. AFRPL-TR-66-40* (Feb. 1966).
- (7) Landel, Robert F., *Solid Rocket Structural Integrity Abstr.* **2** (1), (Jan. 1965).
- (8) Mastrolia, E. J., Bills, K. W., Frost, C. B., Aerojet-General Corp., *Rept. BSD-TR-66-28, I*, 162-166 (1966).
- (9) Meyer, K. H., "Natural and Synthetic High Polymers," 2nd ed., Interscience, New York, 1950.
- (10) Silas, R. S., Yates, J., Thornton, V., *Anal. Chem.* **31**, 529 (1959).
- (11) Uraneck, C. A. *et al.*, U. S. Patent **3,135,716** (1964).
- (12) U. S. Naval Ordnance Test Station, Minnesota Mining and Manufacturing Co., *Final Rept.* 1 July 1964-30 June 1966, Contract N123 (60530) 50116A (June 1967).
- (13) Wieck, R. E., Jr., Moser, B. G., *Bull. 4th Meeting Interagency Chem. Rocket Propul. Working Group Mech. Behavior I* (Oct. 1965).

RECEIVED February 19, 1969.

Composite Solid Propellant Processing Techniques

GORDON A. FLUKE

Aerojet-General Corp., 9200 East Flair Dr., El Monte, Calif. 91734

The processing techniques for manufacturing composite solid propellants are described. The general operations of oxidizer preparation, binder and fuel preparation, propellant mixing, and chamber insulation and lining are illustrated by typical flow sheets and descriptions of the equipment used. Limited data on the performance of this equipment are presented. The importance of characterizing the processability of propellant is introduced together with an instrumental method for achieving this characterization on a comparative basis. New processing systems such as pneumatic mixing and inert diluent mixing are discussed with their apparent advantages and likely limitations.

Composite solid propellant processing has been reviewed in most chemical engineering and chemical society journals as well as the publications of the ordnance and propulsion industries (4, 5, 6, 7). Because the subject is closely associated with the investment rocket companies make in their manufacturing facilities and is related to the manufacturer's competitive position, the material usually presented is of a general nature. The actual details and controlling parameters of all the various propellant manufacturing methods is too lengthy to present in a single paper, and here again the description of the processes are generalized.

Noting that processability is an important factor in propellant formulation, a system is proposed for processability determination as a function of the rheology of the propellant. The instrumental analysis necessary to characterize the rheology by viscosity measurements, including the recommended viscosity measuring instruments, is suggested for various stages in propellant development and manufacture.

The discussion of manufacturing methods is divided into discrete operations and additionally separated by whether the method is a proved production technique or one which has been demonstrated but is not currently used as part of a significant production program.

Binder Requirements

The requirements for a good binder (5) are met by the ability to maintain the geometric integrity of the propellant charge when subject to conditions such as extreme temperatures from $+170^{\circ}$ to -75°F ., stresses resulting from thermal coefficient of expansion differences between the propellant and the case materials, stresses resulting from case pressurization, storage at elevated temperature, vibration and acceleration, and dead weight loads. In addition to these requirements, the binder must be a processable material which together with the solid additives can be mixed into a homogeneous mass and made to flow from the mixing vessel into the motor chamber where the bore mandrel may present a complex geometric pattern.

Current binder candidates are most likely to be materials typified by low glass-transition temperatures ranging well below -50°F . and high softening temperatures, above 200°F . Typical polymers whose chains are chemically crosslinked by the curative system are shown in Table I. The materials are generally of high molecular weight and are solids. To be processable, the starting binder ingredients must be liquid so that the oxidizer crystals and powdered metal fuels can be dispersed. The process is to start with low molecular weight liquid polymers, incorporate the solids, then chemically build the high molecular weight structure. Curing must take place with little or no exotherm that might lead to autoignition and with a low volume change to minimize stresses in the chamber-to-propellant bond. The binder material, aside from adding to the total energy of the system released through the formation of low molecular weight exhaust gases, is the fundamental structure on which the resultant mechanical properties are based. The resultant ballistic properties will be influenced to a greater degree by the oxidizer and its particle size distribution than by the metal fuel which increases the flame temperature.

A specific requirement of solid propellant binder polymers is the small tolerance allowed in the reproducibility of the product properties. As a result, some polymers that cannot be specified easily must be adjusted lot by lot in accordance with qualification tests. This is illustrated graphically by the data of Figure 1, where different lots of a carboxy-terminated polybutadiene procured to the same specification are compared with the different equivalents of the BITA (butylene imine adduct of trimesic

Table I. Molecular Structures and Glass-Transition Temperatures (T_g)

Name	Basic Structure	T_g , °F.
Polyisobutylene	$\begin{array}{c} \text{CH}_3 \\ \\ -\text{CH}_2-\text{C}- \\ \\ \text{CH}_3 \end{array}$	-97
Polysulfide	$\begin{array}{c} -\text{CH}_2-\text{CH}_2-\text{O}-\text{CH}_2-\text{O}-\text{CH}_2-\text{CH}_2-\text{S}-\text{S}- \\ (-\text{CH}_2-\text{CH}_2-\text{O}-\text{CH}_2-\text{CH}-\text{O}-)_x- \\ \\ \text{CH}_3 \end{array}$	-60
Polyether polyurethane	$\begin{array}{c} \text{O} \\ \\ \text{CH}_2-\text{CH}_2-\text{O}-\text{C}-\text{N}-\text{R}- \\ \\ \text{H} \end{array}$	-50
Polybutadiene	$-\text{CH}_2-\text{CH}=\text{CH}-\text{CH}_2-$	-120
Polybutadiene/ acrylonitrile	$\begin{array}{c} (-\text{CH}_2-\text{CH}=\text{CH}-\text{CH}_2-)_x \text{CH}-\text{CH}_2- \\ \\ \text{CN} \end{array}$	-70
Polybutadiene/ styrene	$\begin{array}{c} (-\text{CH}_2-\text{CH}=\text{CH}-\text{CH}_2-)_x \text{CH}-\text{CH}_2- \\ \\ \text{C}_6\text{H}_5 \end{array}$	-85
Polydimethyl- siloxane	$\begin{array}{c} \text{CH}_3 \\ \\ -\text{O}-\text{Si}- \\ \\ \text{CH}_3 \end{array}$	-180
Polybutadiene/ acrylic acid- acrylonitrile	$\begin{array}{c} (-\text{CH}_2-\text{CH}=\text{CH}-\text{CH}_2-)_x (-\text{CH}-\text{CH}_2-)_y- \\ \\ \text{CN} \\ (-\text{CH}_2-\text{CH}-)_z \\ \\ \text{COOH} \end{array}$	-110

acid) curing agent to gain a target modulus of 450 p.s.i.g. From these qualification data, proper equivalences are selected for each lot to produce a minimum tolerance around the target moduli. The standard deviation of moduli was decreased by one-half in changing from fixed formulation to lot adjustment for a typical CTPB system.

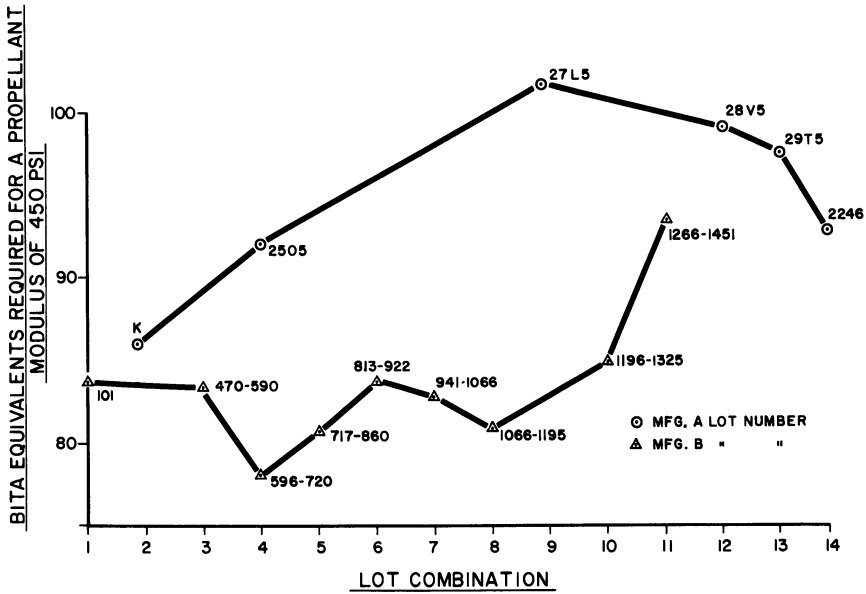


Figure 1. History of BITA requirements for production propellant

Processibility

The composite solid propellant manufacturing system can best be introduced by reference to the typical block flow diagram shown in Figure 2. Here the segregation of processing operations is clearly evident as well as the significance of intermediate materials handling operations. Of the materials encountered, the propellant system, once the oxidizer is incorporated into the binder, is the most rigorous processing and handling problem, and it is in this area that a good understanding of the mixture characteristics is mandatory. The rheological properties of the system are influenced by particle size distribution and shape of the oxidizer and other solids, viscosity of the binder polymer, temperature and time from addition of curing agent or accelerator. A rule of thumb encountered with polyurethane binders is that the viscosity doubled every hour after isocyanate addition. Figure 3 is a plot of propellant viscosity *vs.* temperature and is expressed in terms of varying flow rate. The data are

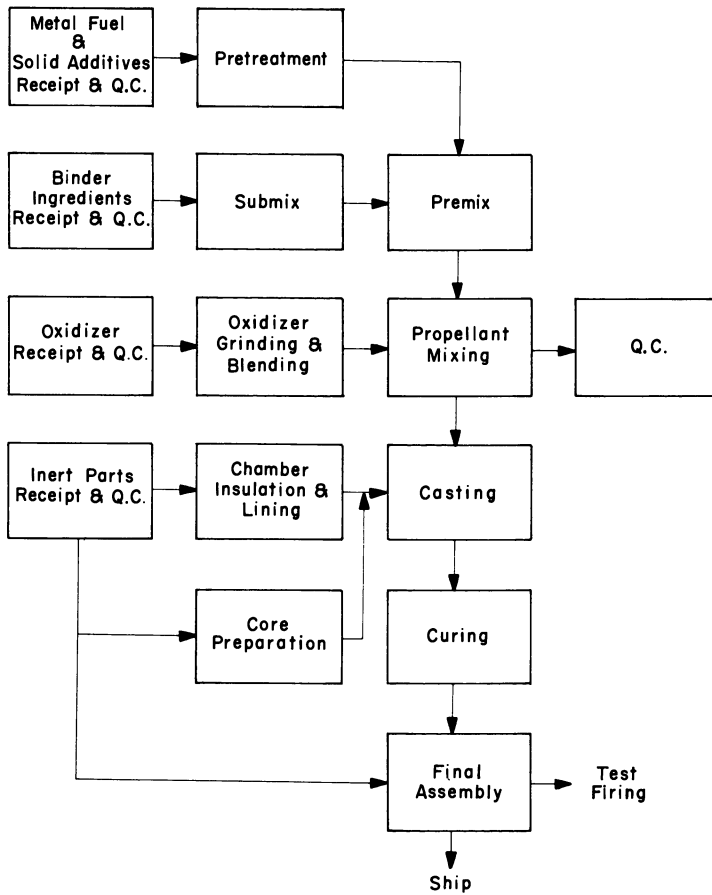


Figure 2. *Composite solid propellant processing*

for an uncatalyzed system and were determined by pressure drop measurements to demonstrate from a practical point of view the influence of propellant viscosity on such operations as casting.

The best measurement of polymer processability may be found in the rheological values associated with the system (8). Absolute values are rarely obtained from viscosity measuring equipment; however, knowing the relative abilities of each of the viscometers for measuring the rheological characteristics of uncured solid propellants, it is possible to predict which unit should be best applied for each measurement situation. Nine viscosity measuring systems—three rotational, three flow type, one vibrating reed, one capillary, and one visual flow—are shown for the research, development, and production of a propellant system. A systematic arrangement of these viscometers for the various applications

is given in Figure 4. The analysis is subdivided into the general applications of formulation characterization, formula optimization, line activities, and quality control.

(1) **Formula Optimization.** In formulating new propellants, it may be desirable for the research lab to optimize certain rheological characteristics by a quick-check method that can produce a full consistency curve.

(2) **Formulation Characterization.** Prior to using a new propellant formulation in pilot-plant or production studies, the material must be fully characterized and analyzed rheologically. Processability predictions may be extrapolated from this step.

(3) **Line Activities.** It is often necessary to make a quick check of the rheological flow properties of a specific sample in an in-process production line application. The equipment used may be either in-line flow apparatus or other simple characterization methods.

(4) **Quality Control.** In controlling the quality of production propellants, it is necessary to conduct various rheological tests on propellant samples in the laboratory.

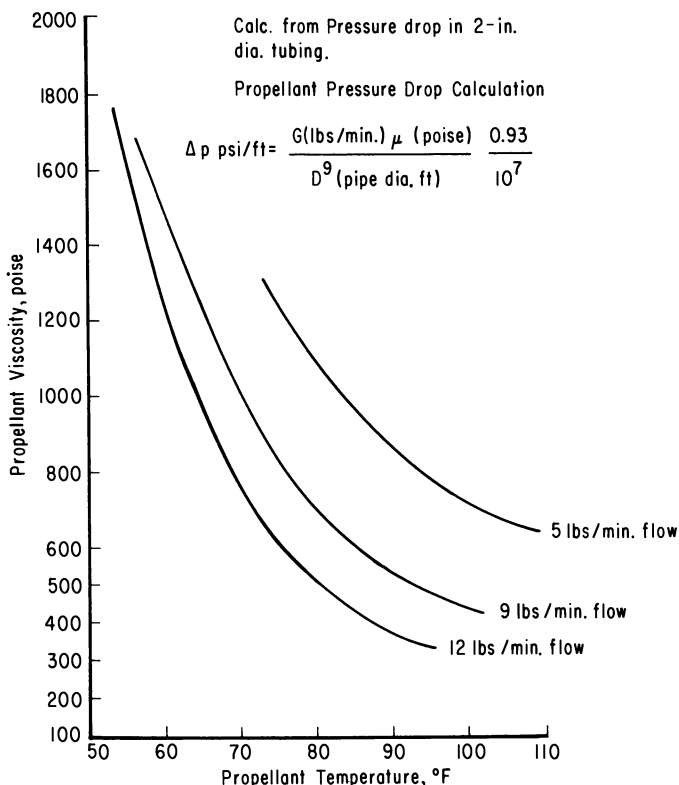


Figure 3. Uncatalyzed propellant viscosity vs. temperature

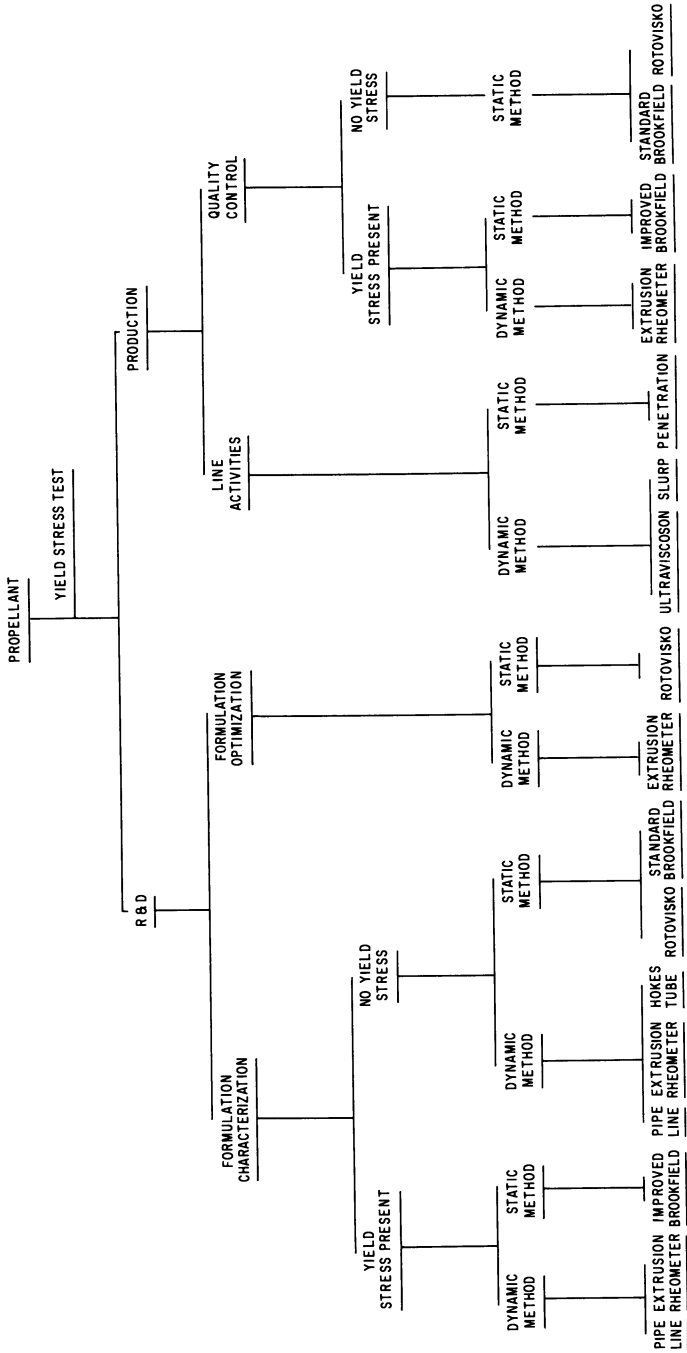


Figure 4. Viscometer applications

Figure 4 shows that the use of particular instruments depends upon whether or not the formulation exhibits yield stress—*i.e.*, there is stress necessary before material starts to shear. Most propellant formulations will either exhibit a true yield stress of certain magnitude or will not exhibit any yield stress at all. However, certain formulations may have a low shear rate exponent (n -value regression coefficient) of 0.6 or less. In this case, the material will perform as if there were true yield stress present even though it may not be measurable by the techniques presented. It is termed a pseudo-yield stress. Whenever the low exponent occurs, the material must always be treated as having a true yield stress.

Having performed the yield stress test, each category is then divided into static or dynamic methods. Dynamic methods indicate an actual flow test of a certain type, whereas the static methods indicate tests such as rotational flow between two cylinders.

There is good evidence that a single value derived from viscometer measurements is inadequate to describe whether a propellant is processable. In general, it appears that at least five values obtained by viscometer measurements are required:

- (1) Existence and magnitude of the yield stress.
- (2) Shear rate term exponent and shear rate range over which it can be considered valid.
- (3) Shear rate limits where the shear rate exponent changes value, becomes 1, or the consistence curve no longer follows a power law approximation.
- (4) Shear stress at a shear rate of 1.0 sec.^{-1} .
- (5) Estimated value of the cure rate and temperature dependence of the cure rate.

Since these are only suggestions and do not represent tested dependence, the use of viscometers for processability index can only be considered comparative.

Processing Methods

Having established the satisfactory or within-specification ballistics and mechanical properties of a new propellant system, a manufacturer is then faced with a reasonably limited choice of manufacturing methods. It is possible to generalize that the best manufacturing system is the one that has the greatest yield of raw materials mixed or combined in a manner which provides the designed ballistic and mechanical performance in the finished product. The high cost of these materials, as compared with the actual labor costs associated with propellant manufacture, emphasizes the need for a high yield operation.

First, discussing the established production methods, the steps in propellant processing are oxidizer preparation, fuel preparation, propellant mixing, cast, and cure. A standard practice in industries handling

pyrotechnic or explosive materials is to separate various operations involved in the manufacture to avoid performing different tasks in the same facility. Most facilities for producing solid propellants have been separated in accordance with these manufacturing steps, and each facility is operated independently outside of the scheduling necessary to transfer the materials from one operation to the subsequent operation.

Oxidizer Preparation

The oxidizer used for most solid propellants is ammonium perchlorate which is supplied to the propellant manufacturer in accordance with rigid specifications for impurities, surface and total moisture, and particle size distribution. Particle size distribution has an effect on the cured propellant mechanical properties and the burning rate. The rheological properties of liquid propellants are also influenced by the "packing" of the oxidizers. Establishment of a precise particle size distribution and maintenance of these sizes and shapes becomes the primary function of the oxidizer preparation process. The secondary functions are to screen agglomerates and tramp material from the oxidizer as received and to dispense the processed oxidizer in exact weights to meet the formulation specifications. The processing must be accompanied by a rigorous quality control program. Tyler screen sizing measurements, Fischer subsieve, and Micromerograph are some of the techniques used to establish that the appropriate particle size distribution has been obtained. These measurements may suffer from the difficulty in taking a representative sample and that the oxidizer crystal is readily friable and easily classified in subsequent handling.

A facility for preparing the oxidizer of a particle size distribution for the specific propellant ballistic and rheological properties must have capabilities to receive, screen, divide into fractions, grind, weigh, reblend, rescreen, and dispense into containers to transfer the oxidizer to the mixing facility. A typical oxidizer facility is shown on the process flow sheet of Figure 5. Since oxidizer is impact sensitive and forms a high explosive if contaminated with any hydrocarbon, the grinding operation is remotely controlled and segregated from the other handling operations. Figure 5 shows a facility designed to process five different fractions, three simultaneously. The grinding equipment consists of Mikro-Pulverizers (horizontal hammermills) and a Mikro-Atomizer, which is a horizontal hammermill followed by an air classification system. Another common type of oxidizer grinding equipment used in the industry is the Raymond mill, manufactured by Combustion Engineering, which is a vertical hammermill associated with an air classification system. The Mikro-Pulverizers are operated at different feed screw speeds and different hammermill speeds to yield different products.

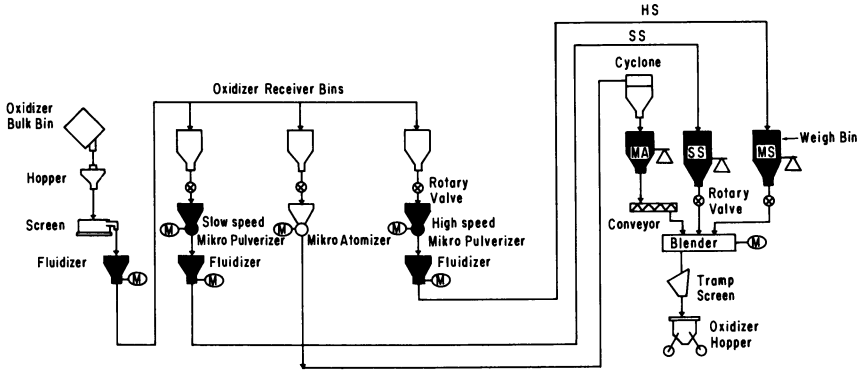


Figure 5. Oxidizer preparation

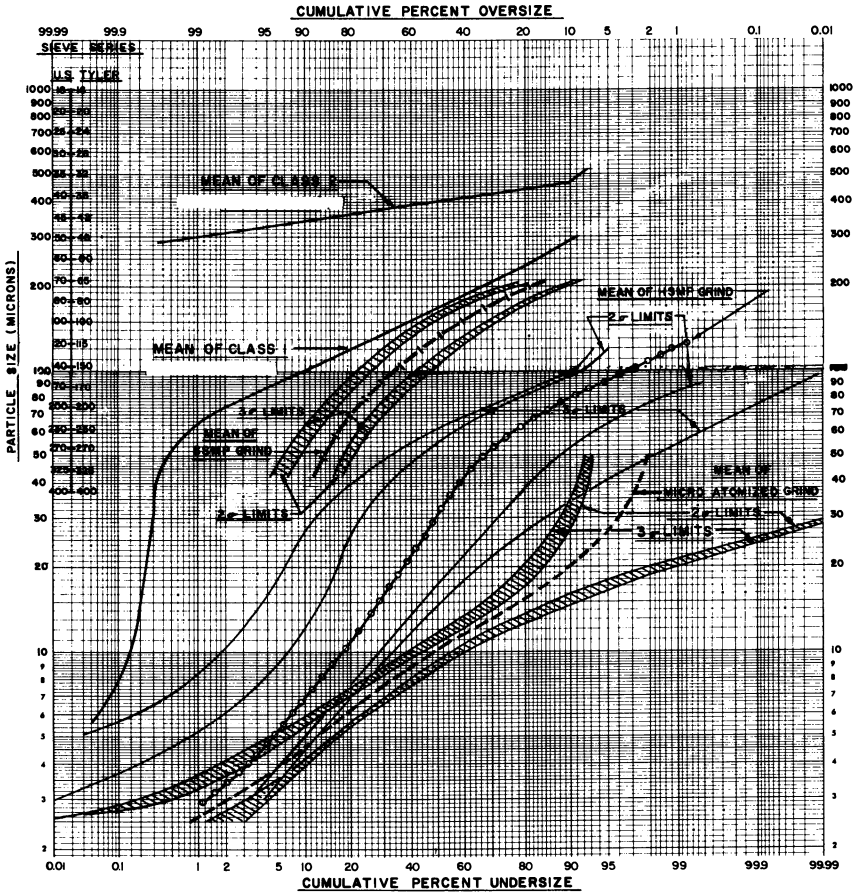


Figure 6. Particle size distributions of commercially used oxidizer grinds

Figure 6 indicates a typical particle size distribution of commonly used oxidizer grinds by one manufacturer. Shown here are the means and the two and three sigma limits of three different grinds: the Mikro-Pulverizer operated at a slow speed (*ca.* 2400 r.p.m.), and the Mikro-Atomizer. Also shown are two different particle size distributions of unground oxidizer as procured from the manufacturer. Selected operation of the Raymond mill will permit production of both oxidizers with a mean equivalent to that of the high speed Mikro-Pulverizer operation or the mean of the Mikro-Atomizer grind, and with proper calibration can be used interchangeably with these pieces of equipment. Recent demands for higher burning rate propellants have resulted in the use of fluid energy mills in preparing oxidizer for propellants. This equipment in which a high velocity gas stream causes the particles to impinge on each other and the container walls permits the production of submicron particle sizes over a limited range.

Fuel Preparation

The next operation is fuel preparation, often called premix preparation. Designing this process and the resulting facility requires the greatest degree of imagination to provide versatility for the system. The oxidizer system already discussed can produce a range of particle size distributions that will cover any expected requirement placed on solid propellant. The propellant mixing systems (discussed later) have demonstrated their ability to manufacture most types of composite propellants; however, modern fuel premix systems may contain from four to 13 different ingredients with a range of physical properties from a liquids to amorphous powders. Some of their functions are to act as basic polymers, metal fuels, defoaming agents, wetting agents, burning rate additives, cross-linkers, antioxidants, catalysts, opaquing agents, and polymerizing agents. Some compromises must be made, and space is reserved in the dispensing room of a premix facility for the manual addition of ingredients to the basic binder system.

The primary function of the fuel preparation system and facility is to prepare a homogeneous slurry of powdered metal fuel and any other solid except the oxidizer in the liquid polymer. The basic polymer, referred to as the liquid fuel, forms the backbone of the propellant binder system. The most important processing step is the fuel mixing operation. Materials are added to the mixer from storage tanks mounted on scales or from tared and weighed containers, as shown in Figure 7, which is a typical process flow sheet for a premixing or fuel preparation system. Similar systems have been designed and operated by the industry which are highly automated, even to the extent of programming the addition of various types of materials to intermediate mixers before being put

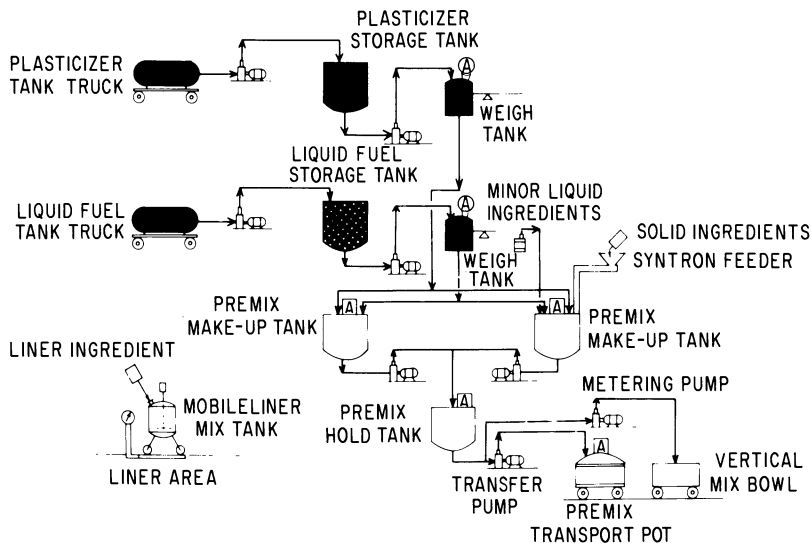


Figure 7. Fuel and liner preparation

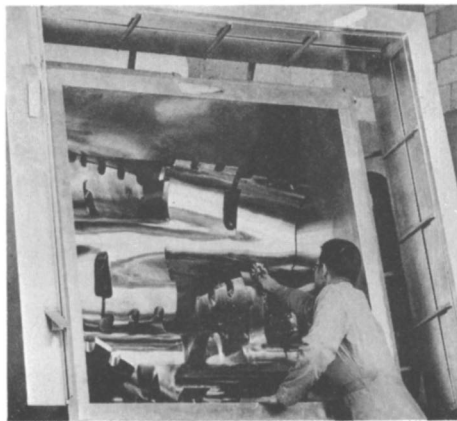


Figure 8. Overlapping bear claw blade

into the final fuel premix. Primary justification for this degree of automation is found in the elimination of human error in weighing out many small ingredients in preparation for the fuel premix. After the fuel premix batch has been made up, it is pumped to an agitated storage vessel or to a transport vessel which is used to transfer the premix to the mix station.

Propellant Mixing

The next operation is propellant mixing, and when most people think of solid propellant production, they envision a propellant mixing opera-

tion. There are five significantly different mixing systems that have seen production operation for solid composite propellants. The first is horizontal batch mixing. Two common horizontal batch mixers—the overlapping bearclaw blade (Figure 8) and the sigma blade dough mixer (Figure 9)—have been used to produce millions of pounds of castable propellant since 1944. These mixers are operated both with covers, in which a deaeration step takes place in the mixer to remove the air brought into the mixer through the entrainment with the oxidizer or other solids

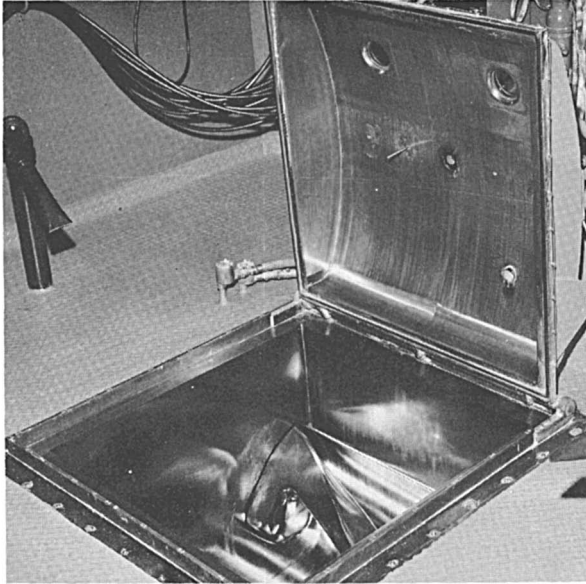


Figure 9. *Sigma blade dough mixer*

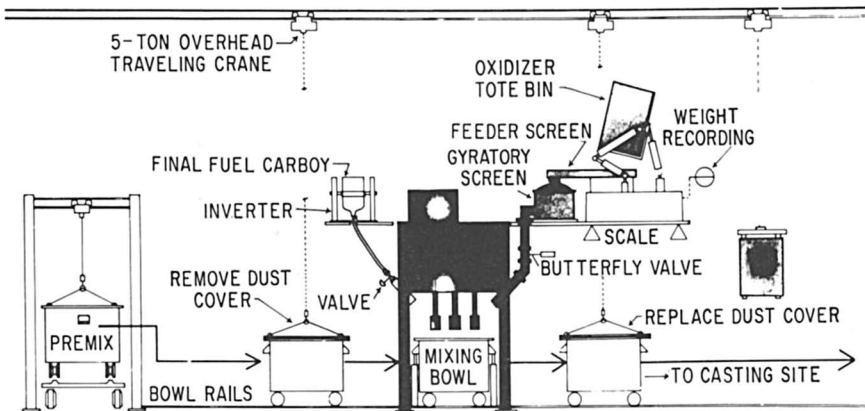


Figure 10. *Vertical batch mix*

as they are added, or the deaerating is done by use of a vacuum chamber in the line as the propellant is added to the motor in the casting station.

In the past few years there has been an increasing use of vertical change-can, planetary mixers. At least three different types have been used with significant success. Practically all of the most recent manufacturing facilities for propellant mixing that have been placed on stream have utilized large (up to 420-gallon) change-can, vertical, planetary mixers of either a two- or a three-blade design. A typical process flow sheet for a vertical batch mixer is shown in Figure 10. A three blade mixer is shown in Figure 11. The planetary mixers all depend upon a high shear, either between the blades or between the blades and the wall. This mixing action is similar to that experienced in the horizontal sigma

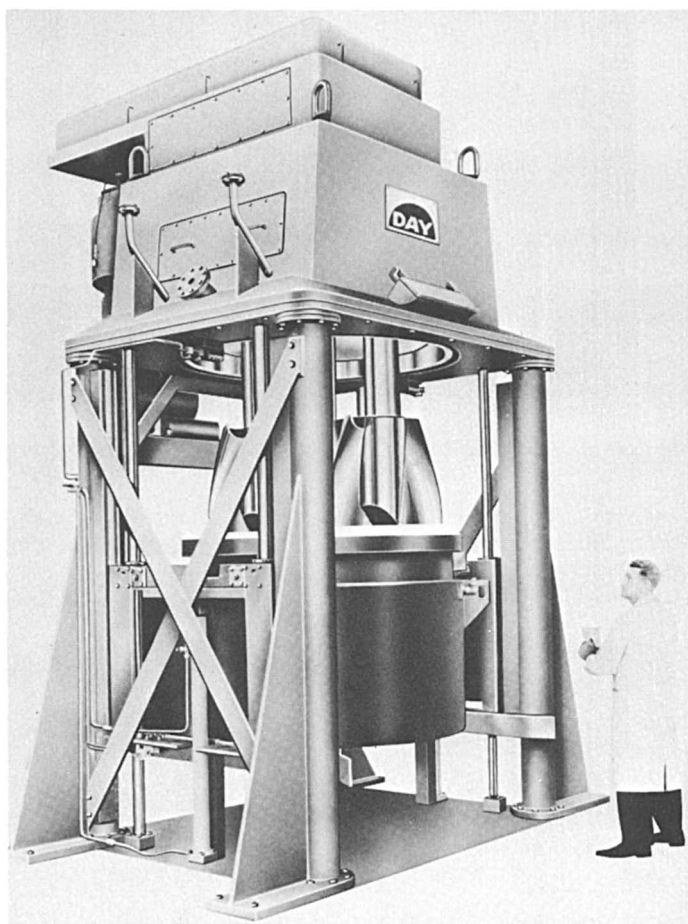


Figure 11. 300-Gallon vertical mixer with bowl in lowered position

blade mixers. The newest entry into the field of propellant mixing has been a vertical spiral mixer (3), shown in Figure 12. In this mixer, which uses a highly scalable mixing action, the propellant materials are lifted on the outside and allowed by gravity to settle through the middle of the spiral, to be lifted again on the outside. Incorporation of dry solids is rapid. The clearances between the blade and the bowl are large, and though the mixer has been used to date on propellant systems with fairly low yield stress, it has incorporated solids up to 88% satisfactorily in a homogeneous manner.

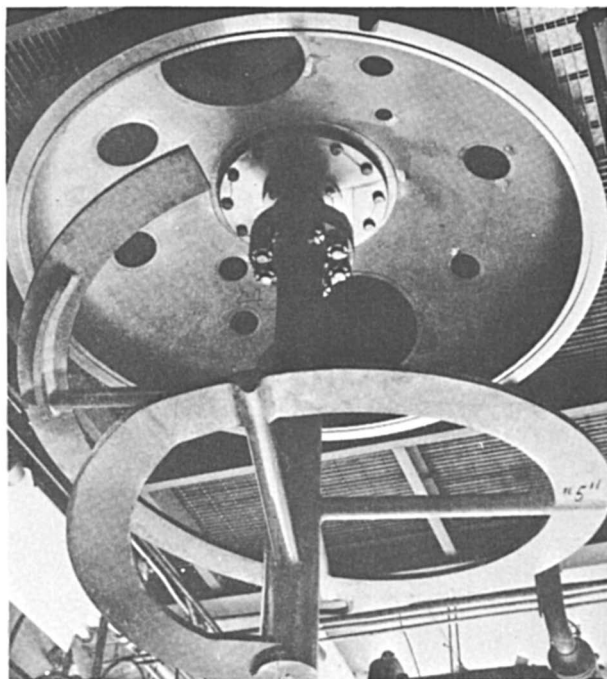


Figure 12. Spiral helix mixer

A final mixing system worthy of mention is that used by the Canadian Armament Research and Development Establishment and Bristol-Aerojet, which is a horizontal ribbon mixer. In this case, the blades carry the material from the center to the ends of the mixer and return it by internal spirals along the center shaft. This mixer is noted for its rapid incorporation of solids and the ease by which material is discharged as compared with the other fixed bowl, batch mixers. A comparison of typical batch mixers is shown in Table II.

The final production process of composite propellant mixing is that of continuous mixing. The continuous mixing system was demonstrated as a production process in 1958. The basic flow sheet for the Polaris

Table II. Mixer Comparisons

Item	Present 150-Gal. Horizontals		300-Gal. Baker-Perkins	
	Mfg. Rating	Use Condition	Mfg. Rating	Use Condition
	Mixer working volume			
gallons	150	164.5	420	377
cu. ft.	20.1	22.0	56.2	50.4
pounds propellant	2200	2400	6130	5500
Motor horsepower	40	40	75	75
estimated net hp./lb. propellant	—	0.0063 @ 29.6 r.p.m.	—	not known
Blade peripheral speed ft./min.		178 @ 29.6 r.p.m.		339 @ 58.8 r.p.m.
Blade diameter, inches		23		28.5
Blade and shaft area, sq. ft.		16.4		27.8
Blade and shaft weight, lbs.		cored blades		1646
Heat transfer area, sq. ft. at working level		63.5		60.0
sq. ft./lb. propellant		0.0265		0.0109
Propellant-gas inter- facial area, sq. ft.		10.56		22.3
sq. ft./lb. propellant		0.0044		0.0041
Blade pitch in blade diameters ^a		not applicable		13.2
Optimum experimental mixer				
Running time where heat transfer is not limiting, min.		60		50
lbs. propellant mixed/min.		40		110

^a A ratio of greater than 1 is inefficient for top to bottom flow.

continuous mixing production plant (9), which was activated in 1960, is shown in Figure 13. This process has successfully produced over nine million pounds of propellant for the Polaris motors. Here, three streams—the oxidizer, the premix, and the polymerizing agent—are accurately

Table II. Mixer Comparisons

<i>Planetary Mixers</i>		<i>500-Gal. Spiral or Helical</i>		
<i>Day Co.</i>		<i>Mixing Equipment Co.</i>		
<i>Mfg. Rating</i>	<i>Use Condition</i>	<i>Mfg. Rating</i>	<i>Use Condition</i>	<i>Small Batch</i>
300	377	500	652	377
40.1	50.4	66.9	87.2	50.4
4370	5500	7290	9500	5500
75	75	120	120	120
—	0.0043 @ 36 r.p.m.	—	0.0053 @ 60 r.p.m. 0.0018 @ 25 r.p.m.	0.0048 @ 60 r.p.m. 0.0016 @ 25 r.p.m.
	309 @ 36 r.p.m.		1056 @ 60 r.p.m. 440 @ 25 r.p.m.	1056 440
	27.7		67	67
	52.8		20	20
	4130		1400	1400
	65.9 0.0120		85 0.0090	60 0.0109
	23.75 0.0043		28.3 0.0030	28.3 0.0051
	10.8		0.5	0.5
	50		30	25
	110		317	220

metered at less than 1% rate deviation to the mixer, which is a rotating, reciprocating, interrupted screw-type, where the average residence time is about 1½ minutes. Propellant is discharged from the mixer at atmospheric pressure into a surge pot. Deaeration to remove the gas entrained

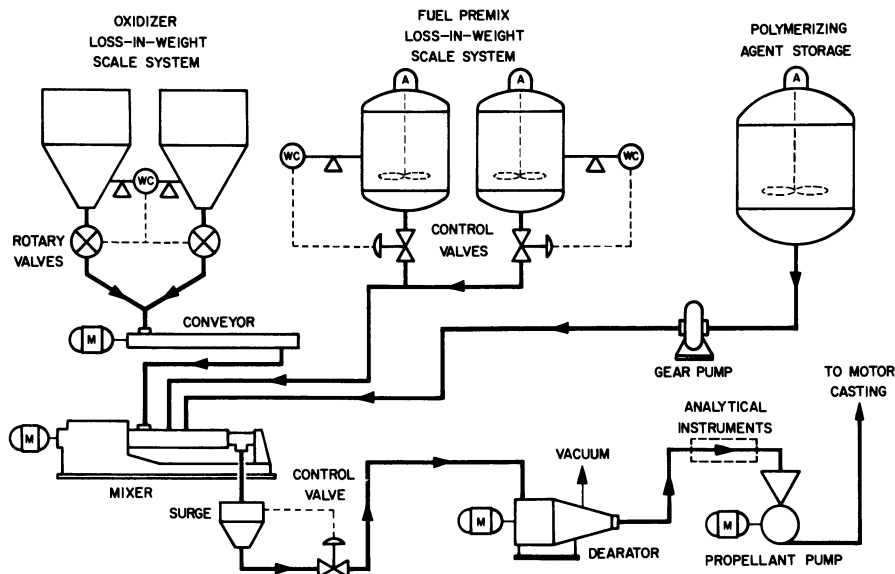


Figure 13. Continuous mixing system

by the solids entering the mixer and the gaseous products of the polymerization reaction is downstream from the mixer. A diaphragm valve controls the flow into the deaerator, so the vacuum can be maintained. The deaerator, which has a helical screw, pumps the propellant out of the remote controlled mixing area to the casting location or to an intermediate transport vessel which carries the material to the casting location. The screw configuration of the continuous mixer successfully used in composite propellant mixing systems is shown in Figure 14. Improvements in the use of the continuous mixing system have changed the flow sheet such that the premix fuel is now added by fuel metering pumps, and the oxidizer is metered into the mixer by a sensitive belt feeder with feedback control in lieu of the loss-in-weight duplex feeders shown in Figure 13.

Insulating and Lining

There are other polymer processing operations often encountered in the manufacture of solid propellant motors. In one of these—the application of insulation to the inside of the motor chamber—various methods have been tried, and to date production processes have been developed for applying thick layers of filled rubbers to the interior of the chamber by such methods as casting, automated troweling, and spraying. To provide an adequate bond between the insulation material installed in

the motor chamber and the propellant, it is often necessary to add a liner material which is cured to a tacky state just before the propellant is loaded into the chamber. Since this liner material adds no significant value to the total energy of the motor, it is ideally applied in the thinnest layer that would provide complete coverage.

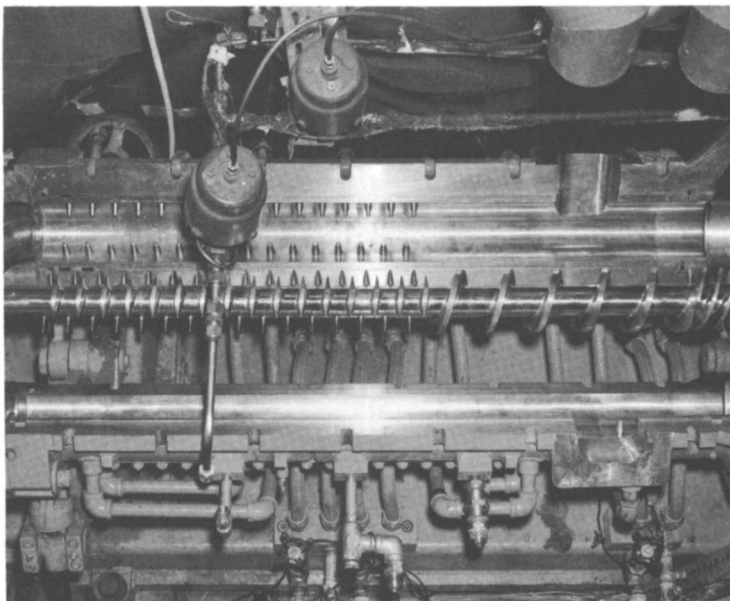


Figure 14. Continuous mix screw configuration

One method that has been developed for applying a liner material in the thinnest possible layer, but yet in a uniform coat, has been that of electrostatic liner application (1). In this system, variable speed volumetric metering pumps deliver the two liner ingredients—a catalyst and a resin—to an in-line ball bearing mixer. A spinning disc shown in Figure 15 receives a high voltage charge from a controlled d.c. output transformer, and the mixed liner is fed into this charged spinning device. The liquid is centrifugally distributed to the disc edge, and here it separates as droplets, each with a negative potential. The droplets are then directed to the chamber wall. In the case where a heat insulation has been applied on the chamber wall and acts also as an electrical insulator, it is possible to use a metallic shield on the outside of the case to provide the ground necessary to attract the droplets of liner uniformly to the insulation surface. The spinning disc is attached to a long vertically aligned hydraulic cylinder. This device, known as a reciprocator, serves to move the spray head at a controlled rate along the center line of the chamber, which is also vertically aligned. Through a multiswitch hydraulic system, the

reciprocator may be reversed, stopped or slowed at preset sequences. A minimum head potential of 50 to 60,000 volts above ground was found necessary for controlled deposition. Another lining method which has seen significant production use is the centrifugal spinning of the liner onto the case by rolling the chamber in a horizontal position while adding the liner materials by a distributor along the chamber axis.

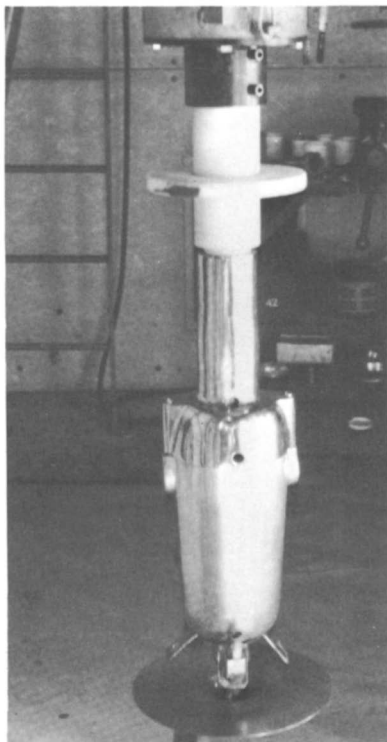


Figure 15. Electrostatic deposition head

Future Propellant Manufacturing Systems

There are two other mixing systems that should be considered as having progressed beyond the development stage and will likely be instituted as production systems for the manufacture of composite propellant. The first is a proprietary system developed by Rocketdyne and referred to as the "Quickmix system" (10). Here the solid ingredients, such as oxidizer and fuel additives, are placed in a dilute slurry with low viscosity, volatile, and immiscible carrier. These slurries, a minimum of two, and the fluid polymer and curing agent streams are metered to a continuous fluid mixer. The effluent from the mixer then flows to a separator and

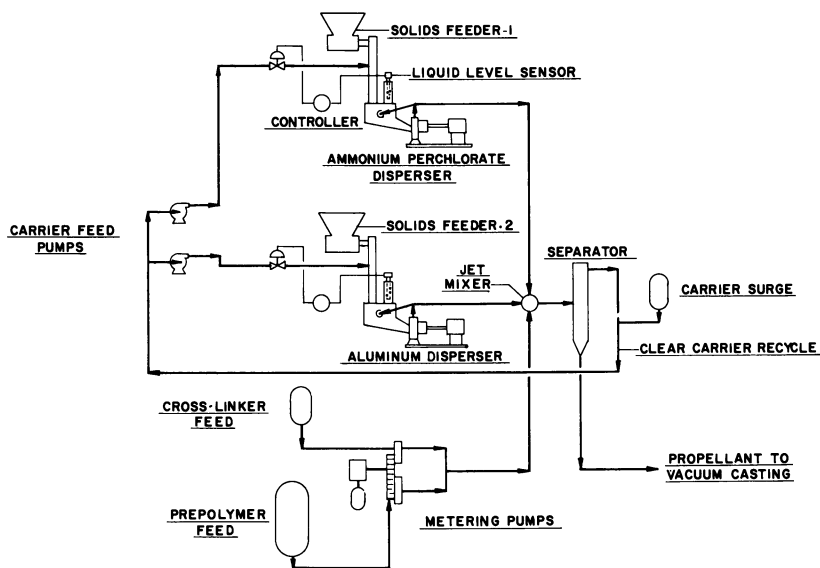


Figure 16. Basic quick mix process

vacuum casting site where the carrier must be removed from the diluted propellant (Figure 16). This process has the considerable advantage that the materials are at all times handled in highly dilute solutions and that the mixer which uses a jet impingement principle has no moving parts. It has the considerable disadvantage that the ingredients processed must in all cases be completely immiscible in the carrier, and it must also be possible to have a carrier with a high enough vapor pressure to be separated totally from the propellant at the casting site by flash evaporation or other vacuumizing techniques.

The second system has been developed by the personnel of the Naval Propellant Plant and is called the pneumatic mixing system (2). In this process, shown schematically in Figure 17, solid and liquid ingredients for the propellant are pneumatically conveyed through a porous tube. Air flows into the tube through the pores and provides turbulent mixing. The air is then removed from the solid-liquid dispersion by a centrifugal separator before vacuum casting and curing the propellant. It is claimed that by dispersing the solid particles and often viscous prepolymers in a gaseous carrier, materials can be processed at a very high rate. Therefore, only a small quantity of the material is present in the mixer at any given time. All the ingredients in the formulation come into contact in the fraction of a second allotted to mixing. The carrier gas moves solids and droplets randomly, providing intimate mixing. The gas also prevents the material from sticking to the tube wall. As the solid particles and associated liquid droplets move through the tube, uneven radial distribu-

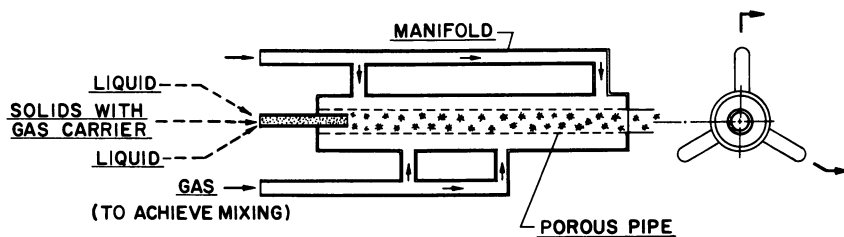


Figure 17. Continuous mixing of pneumatically conveyed solids and liquid

tion between the two phases disappears. Turbulent action and continuous acceleration of the material within the mixer tend to lessen the effects of short-term feed fluctuations. Both the polymer and the dry solids are metered into the gas stream with which it is conveyed into the device pictured in the flow sheet. This system again has the advantage of no moving parts in the mixer and the disadvantages inherent in maintaining an accurate flow rate during pneumatic conveying. Obviously, any solid additive with fragile crystals could suffer particle size change during the conveying.

Summary

The several solid propellant manufacturing systems have been reviewed along with two systems that have not reached routine production. A comparative system of establishing the processability of new propellants has been suggested along with the instrumental analysis plan. The requirements of the product systems from a mechanical properties standpoint are mentioned in terms of the environment, and special steps to insure minimum variation between batches are described to illustrate the stringent tolerances that are met.

Literature Cited

- (1) Anjier, J. L. *et al.*, "Chamber Lining by Electrostatic Deposition," AIChE, National Meeting, New Orleans, La.
- (2) Colli, A. J., *Chem. Eng. Progr.* **60** (10), 81 (1964).
- (3) Gahr, P. E., Madison, E. W., AIChE National Meeting, Atlantic City, N. J., September 1966.
- (4) Haite, W. F., AIChE, National Meeting, Las Vegas, Nev., September 1964.
- (5) Herty, C. H., III, *Chem. Eng.*, 85 (Feb. 3, 1964).
- (6) Holley, H. O., *Chem. Eng. Progr.* **57** (5) (1961).
- (7) Killian, W. P., *Chem. Eng. Progr.* **59** (9) (1963).
- (8) McKelvey, James M., "Polymer Processing," Wiley, New York, 1962.

- (9) Peterson, R. A., ARS, Missile and Space Vehicle Testing Conference, Los Angeles, Calif., March 1961.
- (10) Sheeline, R. D., AIChE, National Meeting, Las Vegas, Nev., September 1964.

RECEIVED April 14, 1967.

Solid Propellant Mechanical Properties Testing, Failure Criteria, and Aging

FRANK N. KELLEY

Air Force Rocket Propulsion Laboratory, Edwards, Calif.

Solid propellants are an integral part of the structure of solid rockets although their chemical composition and overall configuration are dictated by ballistic requirements. If the propellant is viewed as a material of construction, it must be characterized with respect to mechanical response, failure, and physical deterioration. The test techniques devised for such characterizations have undergone an evolutionary development in the direction of increased sophistication, if not usefulness. The JANAF uniaxial test specimen is still the most widely used for routine quality control testing, but a variety of improved uniaxial and multiaxial measurements are becoming commonplace. No completely general failure criterion has become available which may be used to evaluate either the propellant or the final grain design.

Solid propellants are structural materials. Today's rocket motors must be designed to meet a variety of mission applications, many of which place increasingly severe demands on the structural capability of the propellant grain. Although ballistic requirements generally dictate many aspects of the final grain configuration, structural limitations have become more apparent in recent years. Quantitative measurements of the propellant's physical and mechanical characteristics have become as important to the design engineer as the combustion laws may be to the ballisticsian. Unfortunately, the material is such that attempts to measure its mechanical properties have posed serious experimental and conceptual difficulties. Techniques of engineering structural analysis have developed to the state where reasonable predictions can be made of loads and deformations in such structures, which may be composed of 90% of this unusual material. On the other hand, analytical difficulties have been greatest in those regions where critical conditions are most likely, such as

grain discontinuities, corners, and bonded interfaces. That is, prediction of structural failure, where failure is most likely to occur, is often the least satisfactory result of the structural integrity analysis.

Substantial progress has been made in developing methods for solid propellant material characterization over the past decade, however. The propellant has been represented as a linear isotropic viscoelastic material with some success. The necessity for further sophistication is not always obvious, but in many instances large errors can be expected if assumptions of linearity and isotropic behavior are retained.

The loading environment which a propellant grain must survive includes thermal cycling, handling and vibration, ignition pressurization, and acceleration. Many of these conditions may prevail at the same time, such as the imposition of small oscillatory stresses on a grain which has been subjected to large thermal stresses. Since the resultant deformations may be much greater than a few percent, finite strains must be considered. The rate at which the material is deformed in some of these cases requires the recognition and proper accounting of its time- and temperature-dependent properties.

The generation of a practical propellant failure criterion has been the object of extensive study for several years. No completely general analytical criterion seems to be forthcoming, but significant advances in the experimental characterization of ultimate properties in multiaxial stress fields promise more reasonable empirical guidelines.

High speed computer techniques have provided the means by which material properties, loading environments, and geometry may be considered for a large number of grain configurations. Also, as an important adjunct, it must be recognized that propellant mechanical properties change with time and exposure, and any failure criterion or response characterization applicable to unaged material must also account for these changes to be significant in establishing operational design limitations. Many missile systems must undergo repeated exposure to thermal extremes as well as a wide range of vibrational frequencies and accelerations and are expected to survive for many years without intolerable changes in reliability or operational readiness.

The following discussion draws from many published documents and reports as well as private communications with individual investigators; however, only the unclassified literature has been surveyed. Several basic source documents have been used liberally. These include: the Interagency Chemical Rocket Propulsion Group's "(ICRPG) Mechanical Behavior Manual" (44), *Solid Rocket Structural Integrity Abstracts* and the bulletins of the Joint Army-Navy-Air Force (JANAF) Physical Properties Panel, the ICRPG Working Group on Mechanical Behavior and the JANAF Surveillance Panel.

Various tests are conducted to characterize the mechanical properties of solid propellants. The nature of the test, test mode, and environmental conditions used depend upon the end use of the data obtained. Certainly, a large portion of all testing is conducted for quality control—to determine batch variability and to check for gross formulation errors. Also, formulation chemists are guided by the recognition that some “standard” tests give reasonable indications of the practicability of experimental propellants. In general, these tests are used for relative comparisons of data rather than for precise values of stress and strain capability. On the other hand, if the tests are to provide data for engineering analysis, great care must be exercised in controlling test conditions and interpreting results. The specific tests described below are discussed in terms of their usefulness for both applications described above.

The Uniaxial Test

This is by far the most common test in use today. The so-called JANAF tensile specimen has received rather wide acceptance for constant strain rate testing since 1957 (67). Figure 1 shows this specimen with dimensions and a typical set of gripping jaws for use with any available tester. The specimen has been prepared by die-cutting, casting, or milling. The latter procedure usually provides a superior specimen, avoiding the irregularities in dimensions and composition normally produced by the other methods.

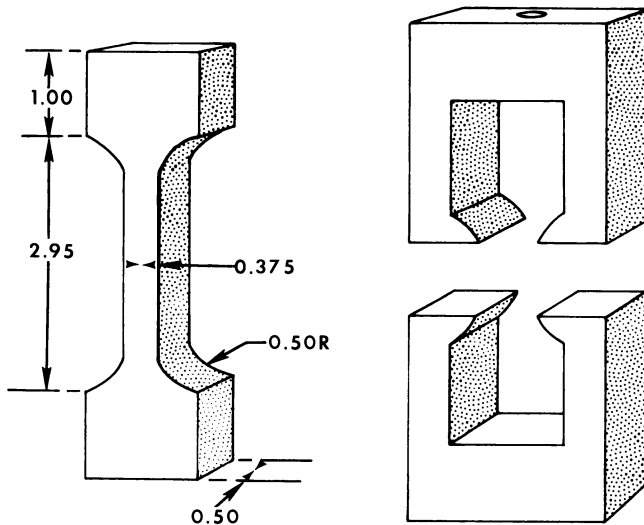
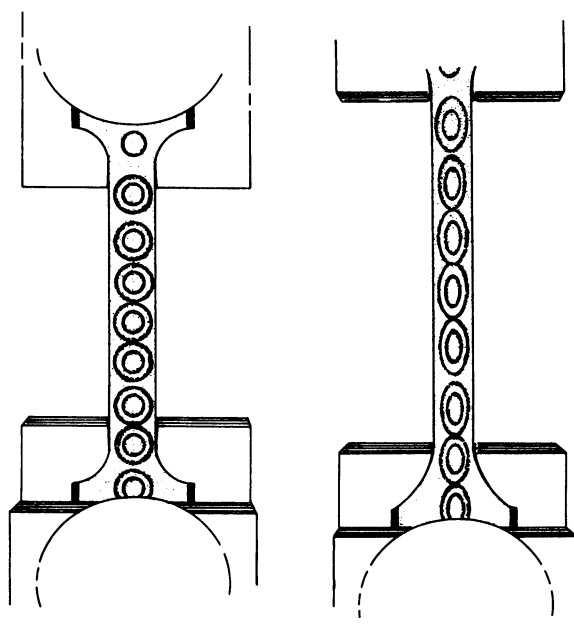


Figure 1. JANAF uniaxial solid propellant tensile specimen with typical gripping jaws. Dimensions are in inches

It was recognized early that although the JANAF specimen is easy to prepare in large quantities, certain precautions must be taken to provide meaningful property data. Since the specimen tends to extrude out of the jaws when a load is applied, strain data based on jaw displacement alone tend to include substantial errors. Figure 2 illustrates the extrusion phenomenon. Various techniques have been developed to provide a more accurate measure of strain in the JANAF specimen. One approach is to make a strain measurement which is independent of the jaw displacement, by optical or photographic methods, and to compute an effective gage length for the specific formulation of interest. Unfortunately, the effective gage length (EGL) varies with strain, and test conditions for most propellants, and a plot of EGL *vs.* strain must be used to correct for this variation.



—Transactions of the Society of Rheology

Figure 2. Schematic of the extrusion behavior of the JANAF specimen. The extended sample ($\lambda = 1.57$) on the right shows a displacement of the oval markings through the jaw area (11)

Other techniques for measuring strain more satisfactorily in the gage section of the JANAF specimen have been developed. One inexpensive and simple method is the use of a clear plastic film extensometer which is attached to the gage section of the specimen. A mark on the face of the specimen is pulled past evenly spaced lines on the clear film, and the

recorder chart is pipped manually as the mark passes each of the lines. Figure 3 illustrates this technique. Various other methods are also used, such as a spring clip strain gage (1) or the more elaborate extensometer designed by Farris (27) shown in Figure 4.

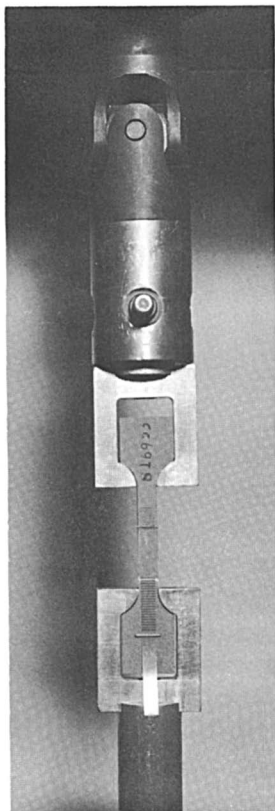


Figure 3. JANAF specimen with plastic film extensometer in place

At present there is considerable effort to develop a tensile specimen which does not exhibit a variable gage length. Most popular is some form of end-bonded sample. Figure 5 shows some of the specimen configurations presently used or under development. The end-bonded specimens have been quite satisfactory for response measurements in many cases, but the tendency to fail at one of the bonded joints makes many of the configurations unacceptable for ultimate property determinations. A specimen which has shown considerable promise is that developed by Saylak (81) (Figure 6). It is cast in a cylindrical mold, and steel washers are bonded to the ends with an epoxy glue. Figure 7 illustrates the

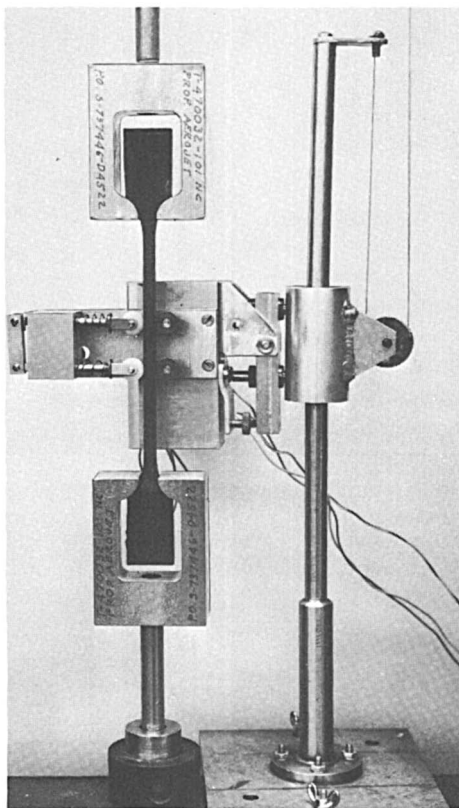


Figure 4. JANAF specimen with Farris (27) extensometer

improvement in the variation of effective gage length with strain when this configuration is compared with the JANAF specimen.

The uniaxial test is widely used for quality control and formulation testing for obvious reasons. The JANAF configuration is not likely to be replaced for these purposes, especially since the backlog of information relative to the formulation art is composed primarily of data from this specimen. Grain structural analysts require more precise information, however, and when uniaxial data are obtained for their purposes, more elaborate and time-consuming tests may be conducted.

Test Modes

This discussion applies to various test configurations whether uniaxial or multiaxial and is related, in general, to commercially available testing machines with controlled jaw displacement rates. The characteri-

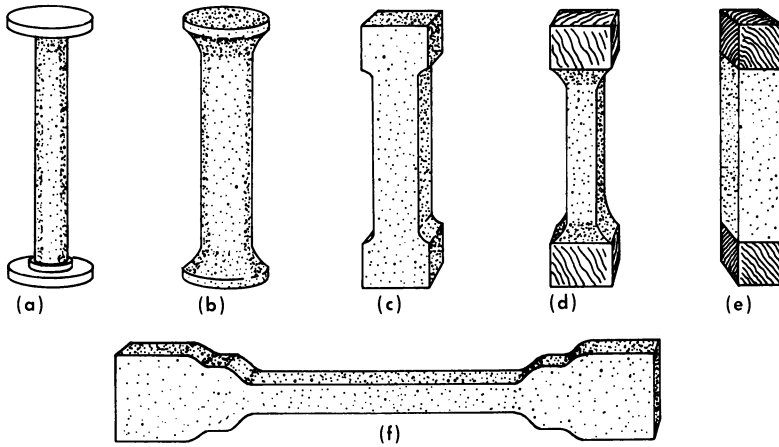


Figure 5. Several uniaxial specimen configurations: (a) Thiokol end-bonded, (b) cylindrical, (c) Stanford Research Institute configuration, (d) JANAF/Tab end hybrid, (e) rectangular tab end (f) flow reservoir (119) configuration

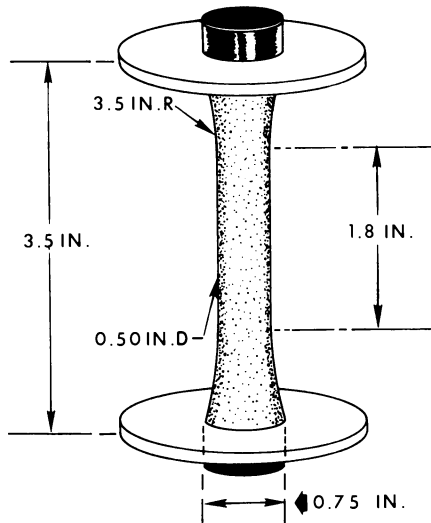


Figure 6. Saylak cylindrical specimen. Special jaws are required to fit the circular end plates

zation of viscoelastic materials requires testing conditions over wide temperature ranges and, at times, a range of strain rates. Although material properties are discussed in some detail later, the general applicability of time-temperature equivalence principles provides the convenience of temperature variation where very short or extremely long time testing would be impractical.

The constant-jaw displacement rate test mode is most frequently used. It meets most of the requirements for mass testing such as in the quality control situation, but various test analysis methods have made it quite suitable for design as well as research purposes. Displacement rates from 0.2 to 20 inches/min. are normally used, but some testing equipment provides reasonably controlled rates upwards of 10,000 in./min. Extremely low rate tests are time consuming, of course, but some specialized equipment has been designed to produce strain rates down to 8×10^{-7} inches/min. (1, 4).

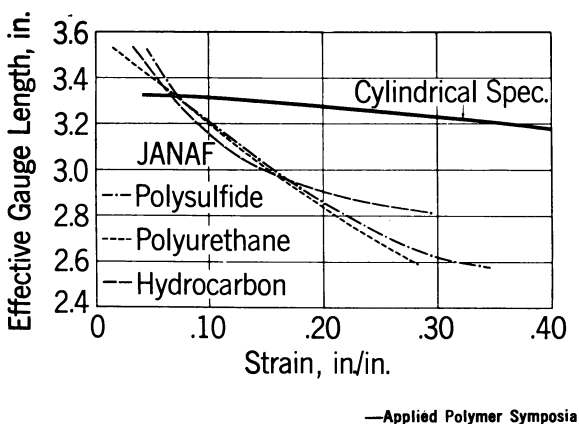
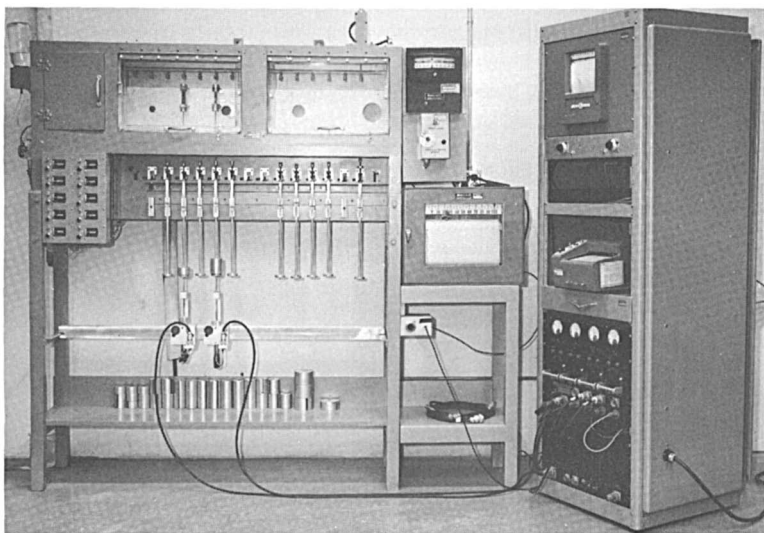


Figure 7. Plot of effective gage length (EGL) vs. strain comparing the Saylak cylindrical specimen with the JANAF specimen. Three propellant formulations were tested (83)

Constant strain for stress relaxation tests and constant load creep tests may be conducted in simple devices. Temperature control is critical since the results are usually applied as a spectral representation for structural analysis or research purposes. Figure 8 illustrates a multistation creep tester with automated data recorders. Strain and load endurance tests are conducted in similar devices, but the conditions existing at failure and time to failure are normally the only data required. The endurance tests are used frequently to supplement the constant displacement rate tests for routine evaluation.

Other test modes, such as constant loading rate and variable strain rate, have been used on a limited basis as research techniques to investigate such phenomena as the path dependence of failure, but no general description of these tests can be provided. Of course the entire area of dynamic testing and fatigue uses various specialized test conditions, but these are discussed later.



—Courtesy Stanford Research Institute

Figure 8. Stanford Research Institute multistation creep and stress relaxation tester with environmental conditioning and automated data recording system

Propellant Properties

Some of the unusual properties of a solid propellant results from its basic composition. The two general categories of double-base and composite rubber binder propellants have many subcategories, but no exhaustive compilation will be attempted here. Most modern propellants consist of a deformable binder phase and a crystalline salt filler, such as ammonium perchlorate and usually a powdered metallic fuel such as aluminum. Table I gives some typical compositions for both composite rubber-based and composite double-base systems.

A brief outline of manufacturing methods of the two general propellant categories is in order to provide a minimal background for following discussions. More detailed information may be found in the other chapters in this volume.

Composite rubber-based propellant ingredients are usually mixed together (under vacuum) at elevated temperatures (*ca.* 100°–160°F.), so that a reasonably fluid and uniform mixture results. The filler materials are dispersed in the low molecular weight polymer ($M_n = 2000\text{--}5000$) and other liquid ingredients, and the resultant mixture is poured through deaerating devices into an evacuated mold. Often the mold is the motor case itself, which is suitably fitted with a casting mandrel and lined with an insulating adhesive. The motor is then cured at similar temperatures

for several hours to several days. The propellant grain retains the geometry of the mold after cure and, therefore, many predetermined ballistic characteristics are built-in. The grain is somewhat rubbery over a wide temperature range and is dimensionally stable within certain physical limits. The ability to deform without rupture, and to recover is quite important since any cracks or unbonds which develop would result in additional burning surface and an unpredictable chamber pressure during motor operation.

Table I. Typical Solid Propellant Formulations

<i>Ingredient</i>	<i>Wt. %</i>
Hydrocarbon Binder Composite	
Ammonium perchlorate	70.00
Aluminum powder	16.00
Poly (butadiene-acrylic acid-acrylonitrile)	11.78
Epoxy curative	2.22
Polyurethane Binder Composite	
Ammonium perchlorate	65.00
Aluminum powder	17.00
Polyalkylene glycols	12.73
Diisocyanate	2.24
Triol	0.43
Additives and plasticizer	2.60
Composite Double Base	
Ammonium perchlorate	20.4
Aluminum powder	21.1
Nitrocellulose	21.9
Nitroglycerine	29.0
Triacetin	5.1
Stabilizers	2.5

The dimensional stability of the propellant grain is the result of the chemically crosslinked polymeric binder. Many of the mechanical properties of the final cured propellant will be dictated by binder characteristics. Another important consideration is the effect of filler, owing to its presence as well as its degree of interaction with the binder.

Composite double-base propellants are produced by allowing an energetic plasticizer, such as nitroglycerine, to swell and coalesce particles of a high molecular weight polymer such as nitrocellulose. The ingredients are dispersed by one of two processes in general use. The first is a casting technique, in which the basic ingredients are extruded and chopped into small granules and poured into the motor case or mold. The plasticizer (solvent) is introduced into the evacuated, granule-containing mold under pressure with some vibration to help eliminate bubbles. The second technique utilizes a slurry of small premixed granules

and plasticizer which is then poured into the grain mold. In each case, curing is accomplished at elevated temperature which helps to diffuse the plasticizer and to swell the polymer. The resultant molecular forces are sufficient to provide rigidity to the final propellant grain, but are secondary in nature and do not provide a continuous covalently bonded network such as that found in rubber-based systems. The individual granules in double-base propellants are identifiable even after swelling and curing, although their boundaries are somewhat diffuse. The precise curing mechanism is not completely understood for these propellants, but the material properties may be controlled by variations in the time-temperature curing cycles.

Obviously, typical composite propellants are highly filled polymers and, especially in the case of the rubber-based systems, are more nearly granular media than merely filled rubbers. Certain specific differences between the double-base binder and the elastomeric binder lead to some differences in behavior, but many of the resulting properties show similarities. The relationships between bulk properties and microstructure in the rubber-based systems are much better understood than those of the double-base propellants and, therefore, the following discussions focus primarily on the former category.

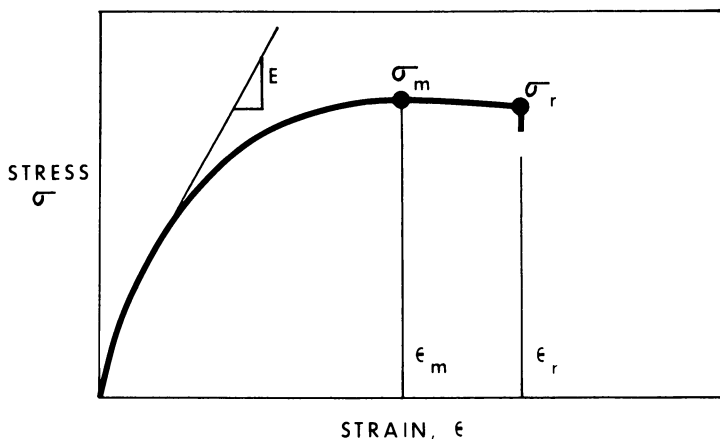


Figure 9. Typical stress-strain curve for solid propellants at 0.77 in./min. and 80°F. E is the slope of the tangent to the initial portion of the curve. A variety of curve shapes are possible depending on specific formulations and test conditions

Figure 9 is a schematic of a uniaxial stress-strain curve. The gradually decreasing slope and plateau region followed by diminishing stress just before rupture are typical features of the composite propellant stress-strain curve. This behavior is readily understood when one considers the

microstructural processes which occur when the material is deformed. Figure 10 illustrates the "dewetting" phenomenon which occurs in all composite solid propellants to some extent when a load is applied. The relative motion of particles imbedded in the matrix produces sufficiently high stresses near the binder–filler interface to cause rupture, and the binder–filler bonds may be pulled loose. The initial point of rupture appears to be in the binder phase, but in many cases the tear propagates to the filler surface, and the interface is separated unless the interface is chemically reinforced and particles are surrounded by a higher modulus polymeric shell (74).

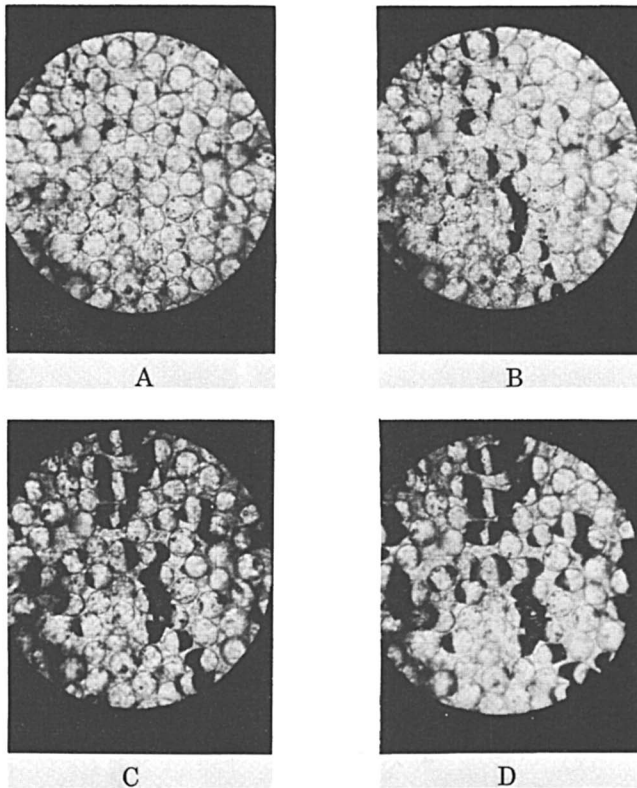


Figure 10. Dewetting behavior in a highly filled elastomer. Dark areas are vacuoles which form when the binder is pulled away from the solid inclusions. Direction of strain is indicated by arrow. Elongation: A, 5%; B, 10%; C, 15%; D, 25%

As dewetting takes place, the reinforcing effects of the filler are reduced, and a decreasing modulus results. When this process has proceeded as far as possible, any continued deformation is sustained by the binder until the sample breaks.

Propellant behavior is widely varied with respect to this process, however. Differences in formulation or even differences in test conditions may produce very localized dewetting and yielding, or the process may occur uniformly throughout the specimen. Obviously, a local yielding condition confuses the interpretation of test results based on force and jaw displacement curves.

When microscopic destruction occurs within propellant samples, whether by dewetting or by the formation of small cracks in the binder, the over-all volume increases (Figure 11).

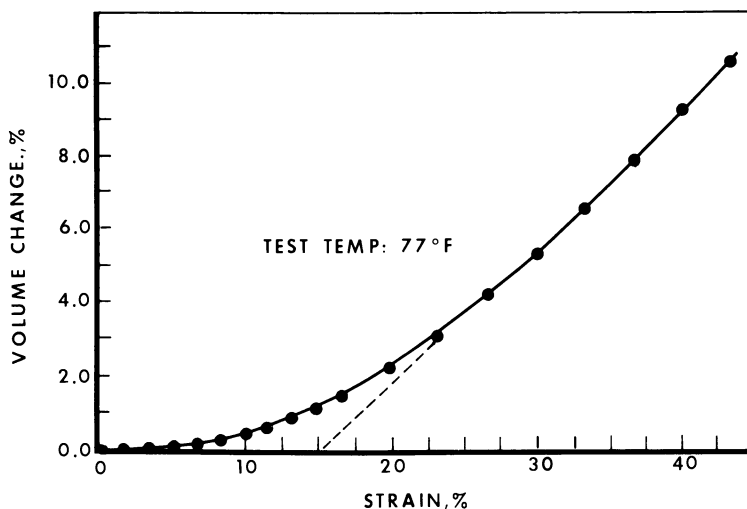


Figure 11. Volume change vs. strain for a polyurethane propellant (105). Volume change was determined by static buoyancy measurements

Dewetting may be observed with a microscope if some means is provided to strain the sample during the observation (74). Hilzinger (42) has produced many excellent photomicrographs using this technique. Various techniques have been used to monitor the volume change as a function of strain in propellant samples. Rainbird and Vernon (77), Smith (94), and Stedry *et al.* (101) have shown the general dependence of volume change on strain using simple dilatometers. Kruse (50) examined the rate and temperature effects on Poisson's ratio obtained from uniaxial tests conducted in a dilatometer, and Fishman and Rinde (29) extended this to include several propellant variations as well as humidity affects. Farris (26) has investigated dewetting extensively, providing many refinements of the strain dilatometer. Some of the basic design features are shown in Figure 12. Various media have been used as confining fluids, including silicone oils, air, and nitrogen. Some of the earlier

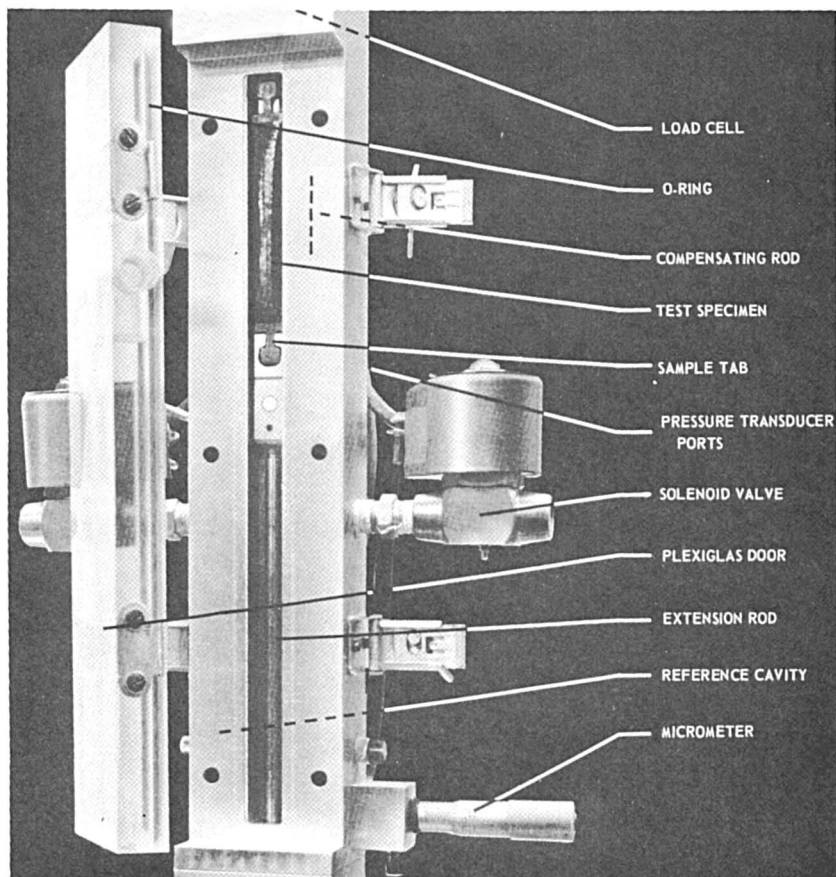


Figure 12. Gas dilatometer designed by Farris (26) has an aluminum body with two cavities, a test cavity, and a pressure reference cavity. The specimen is bonded to special tabs and is fitted into upper and lower sample holders. The upper jaw is attached to a load cell, and a compensating rod enters the cavity during extension

work in this area performed by Svob *et al.* (105) used simple static buoyancy measurements at various strain levels.

One approach which does not utilize a confining fluid has been developed by Saylak (83). This technique involves an optical system which continuously monitors the lateral strain in a uniaxial specimen. The specimen must be circular in cross section, and the volume change computation requires uniform dewetting throughout the sample. This method is not rate and temperature limited since no mechanical attachments or fluids are in contact with the sample. A schematic of the lateral strain device is shown in Figure 13. Surland and Givan (104) also describe an

electro-optic device which focuses on a rectangular patch on the test surface and reportedly provides lateral strain information.

Some efforts have been undertaken to study propellant dilatation in multiaxial stress fields and even in small motor configurations. Farris (25) has conducted limited investigations along this line and has made approximate correlations between uniaxial and multiaxial tests.

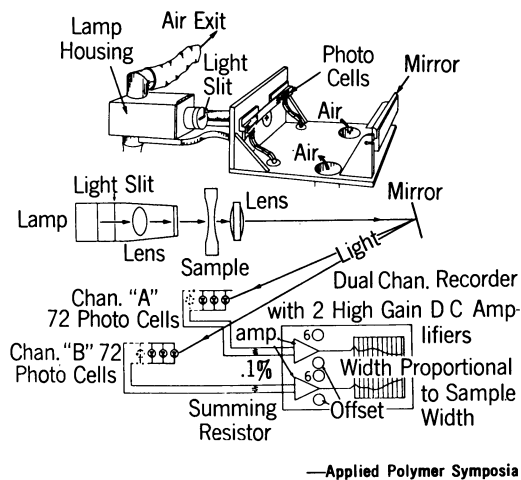


Figure 13. Optical scanning cross-sectional area recorder. Cylindrical sample shadow is magnified and monitored during extension by a bank of linearized photocells (83)

Generally applicable mathematical representations of the dilational behavior of propellants have not been developed, as might be expected; however, Fishman and Rinde (29) have derived empirical expressions for the formulations which they studied. These relationships give reasonable description of uniaxial behavior over wide ranges of strain, time, and temperature for several testing modes. Equation 1 is representative of one of the generalized expressions for the polyurethane and polybutadiene formulations studied.

$$\log V/V_o = A[\log W + B \log t/b_T - C(\log t/b_T)^2]^n \quad (1)$$

where V_o = initial sample volume, V = sample volume after time t , W = strain energy (area under stress-strain curve), b_T = time-temperature shift factor, and A , B , and C are constants for each formulation.

Figure 14 illustrates the relationships between volume change and test conditions for this formulation.

Although dewetting has been and currently is the subject of much discussion, its implications with respect to motor performance are not clear. In some cases the propellant burn rate appears to depend upon

the volume change-strain behavior as shown by Saylak (82). In other cases the onset of extensive dewetting has been considered an operational failure condition. Quite likely, repetitive environmental cycling may involve dewetting to the extent that the amount of dewetting per loading cycle may be a reasonable measure of damage to structural capability and may be applied to cumulative damage concepts. Colodny (21) has shown that low frequency stress-strain cycling below the failure limits of the material produces a general softening until some "equilibrium" exists. At somewhat elevated temperatures the relaxed cycled material appears to be "rehealed," and the original stress-strain curve may be regenerated. The implications of this to strength capability of the cycled material are not defined, but a general discussion and tentative approach are presented by Tormey and Britton (107), based on a first-order rate process assumption for the rehealing process.

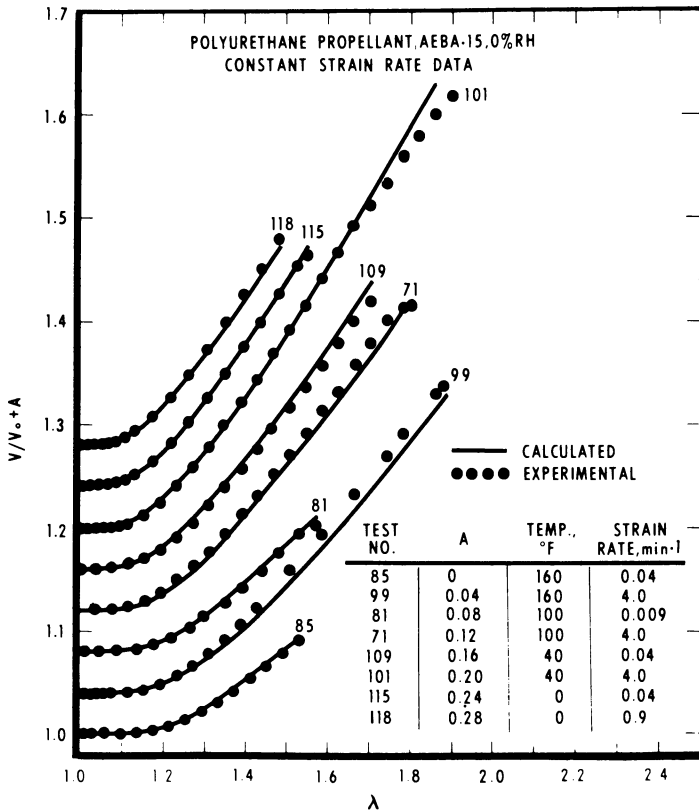


Figure 14. Calculated vs. experimental dilatometric data for a polyurethane composite propellant. Curves have been displaced by a constant A for convenience. The quantity V/V_0 is the ratio of sample volume to initial volume. Data from Ref. 29

Multiaxial Testing

Although the uniaxial test has traditionally received the most attention, such tests alone may be insufficient to characterize adequately the mechanical capability of solid propellants. This is especially true for ultimate property determinations where a change in load application from one axis to several at once may strongly affect the relative ranking of propellants according to their breaking strains. Since the conditions usually encountered in solid rocket motors lead to the development of multiaxial stress fields, tests which attempt to simulate these stress fields may be expected to represent more closely the true capability of the material.

Multiaxial test geometries and test conditions may be analyzed with reference to three orthogonal principal stresses as shown in Figure 15.

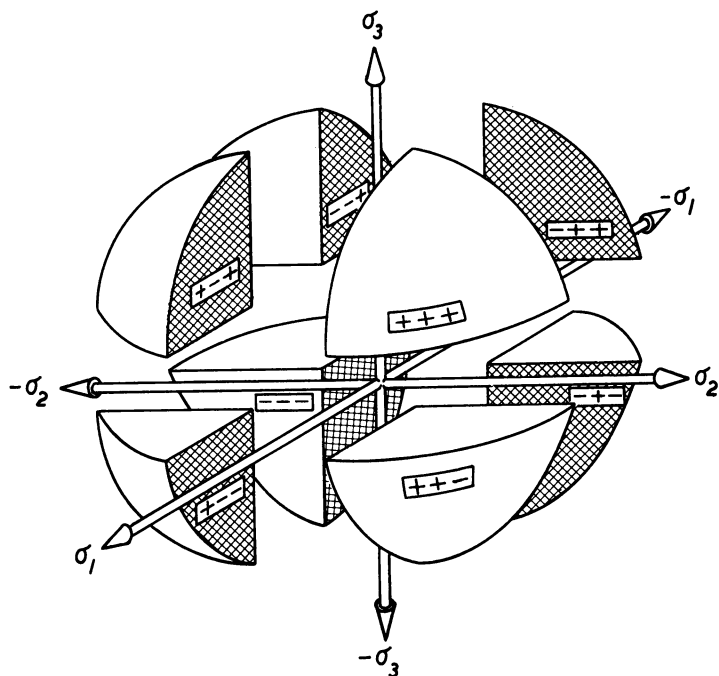


Figure 15. Schematic of the octants of principal stress space, where (+) indicates tension and (-) is compression

The various octants in principal stress space are described by considering conditions of tension (+) and compression (-) and their combination. Convention usually takes the upper right octant extending out from the page in Figure 15 to be the tension-tension-tension (++++)

octant, and similarly, going diagonally downward and backward through the origin, the (---) octant is reached.

Figure 16 illustrates several test specimens which have been used (46) in the multiaxial characterization of solid propellants. The arrows indicate the direction of load application. The strip tension or strip biaxial test has been used extensively in failure studies. It can be seen that the propellant is constrained by the long bonded edge so that lateral contraction is prevented and tension is produced in two axes simultaneously. The sample is free to contract normal to these axes. The ratio of the two principal tensile stresses may be varied from 0 to 0.5 by varying the bonded length of incompressible materials.

According to infinitesimal elastic theory, the stresses and strains which develop in the center of long strips are related as follows:

$$\sigma_1 = 2\sigma_2, \sigma_3 = 0$$

$$\epsilon_3 = -\epsilon_1, \epsilon_2 = 0$$

and

$$\tau_1 = \frac{\sigma_2 - \sigma_3}{2} = \frac{\sigma_1}{4}$$

$$\tau_2 = \frac{\sigma_3 - \sigma_1}{2} = \frac{-\sigma_1}{2}$$

$$\tau_3 = \frac{\sigma_1 - \sigma_2}{2} = \frac{\sigma_1}{4}$$

where τ_1 , τ_2 , and τ_3 are the principal shear stresses, and Poisson's ratio is 1/2.

The diametral compression test is performed by compressing a thick disc along a diameter of the specimen. A diameter-to-thickness ratio of approximately 3 is preferred. Figure 17 shows this test, including grid lines and gages for measuring the strains developed as the sample is compressed between the tester platens.

The stress field which is developed at the center of this test specimen is compression-tension, and taking the y axis to be the compression axis the compressive stress, σ_y , is given by (32, 44):

$$\sigma_y = \frac{-6 F_y}{\pi t d} \quad (2)$$

where d = sample diameter, t = thickness, and F_y = compressive force. The tensile stress normal to the axis of compression, σ_x , is given by

$$\sigma_x = \frac{2F}{\pi t d} \quad (3)$$

The corresponding strains are

$$\epsilon_y = \frac{-2 F_y (3 + \nu)}{\pi t d E} \tag{4}$$

and

$$\epsilon_x = \frac{2 F_y (1 + 3\nu)}{\pi t d E} \tag{5}$$

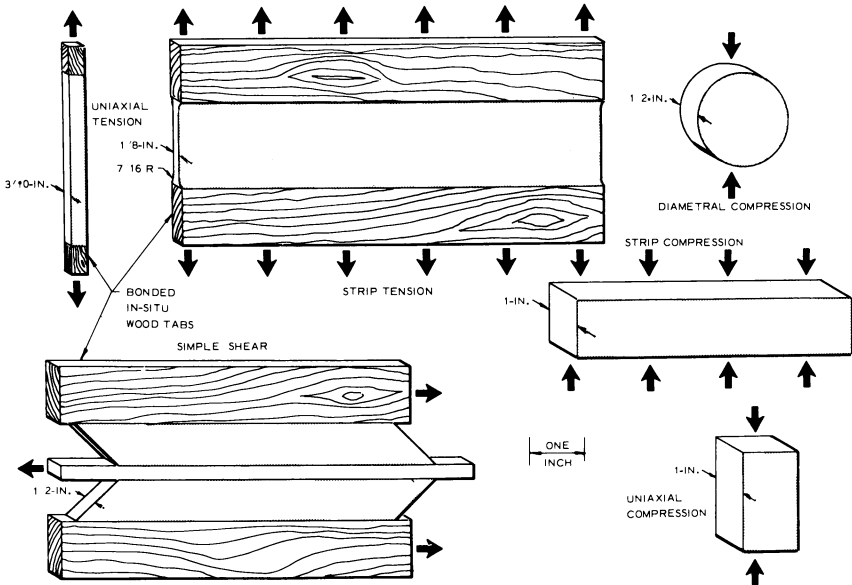
where ν is Poisson's ratio, and E is the modulus.

The total deformation U along the diameter in the x direction is given by

$$U = \frac{F_y}{\pi t E} [(1 - \nu)(2 - \pi) + 2(1 + \nu)] \tag{6}$$

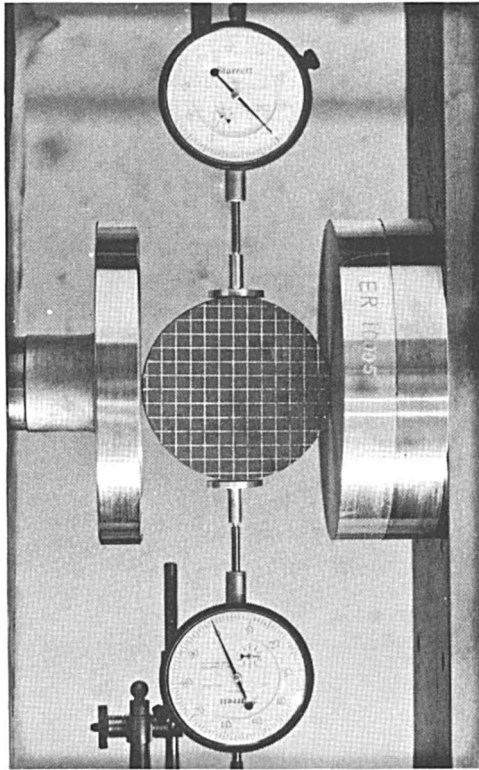
The simple shear test, also shown in Figure 16, was designed in the "chevron" configuration to eliminate premature tensile failure at the corner between the leading edge and the central plate. The propellant at these corners will be compressed during most of the test.

Another biaxial test, not shown here, utilizes a thin disc of material which is clamped around the edge and inflated by air. The pressure, p ,



—Courtesy Lockheed Propulsion Co.

Figure 16. Various specimens used in the multiaxial characterization of solid propellants



—Courtesy Lockheed Propulsion Co.

Figure 17. Diametral compression test. Deformations are followed by compression gages, cross head travel, and grid markings on the sample surface

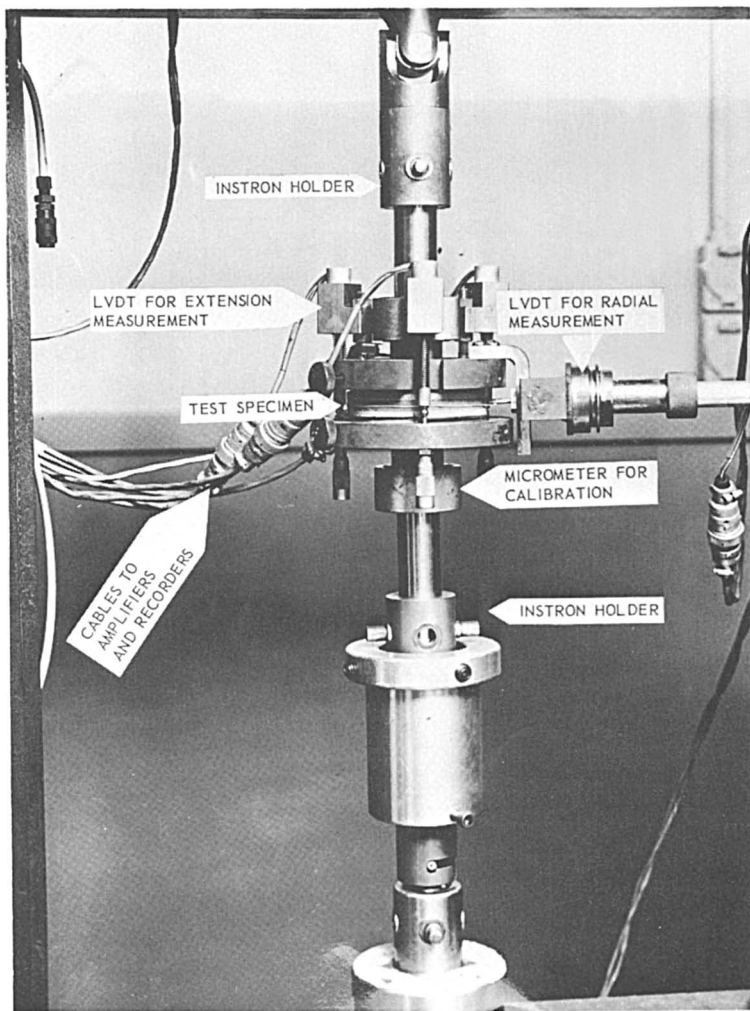
and the radius, r , are monitored, and if the disc is circular, the stress field is:

$$\sigma_x = \sigma_y = \frac{pr}{2t} \tag{7}$$

where t is the thickness. A complete description of this test and certain variations is given by Spangler (97, 98) and Long, Rainbird, and Vernon (60).

Triaxial tests usually involve more elaborate testing equipment and more precise measuring techniques than those normally used for uniaxial and biaxial measurements. In the “poker chip” test (33, 59) the faces of a thin circular disc are bonded to rigid plates (Figure 18). The speci-

men is loaded by axial displacement of the plates, normal to the face, and the lateral constraint induces a triaxial stress in the sample. The triaxial stress field approximates hydrostatic (equal triaxial) conditions near the center when (1) the grip plates are rigid, (2) the disc diameter to thickness is large (> 10), and (3) the ratio of shear to bulk modulus is small compared with unity (Poisson's ratio near $1/2$). The poker chip configuration has been analyzed by Lindsey *et al.* (58) and Brisbane (16) and by Messner (66), and the stress and displacement expressions will not be given here.



—Courtesy Rocketdyne, Division of North American Aviation, Inc.

Figure 18. "Poker chip" test assembly with indicated instrumentation

Refinement of the poker chip test to include a center load cell in one of the bonded plates is reported by Harbert (40). Figure 19 shows the stress-strain curves generated by external measurement as well as the failure point determined by the center load cell.

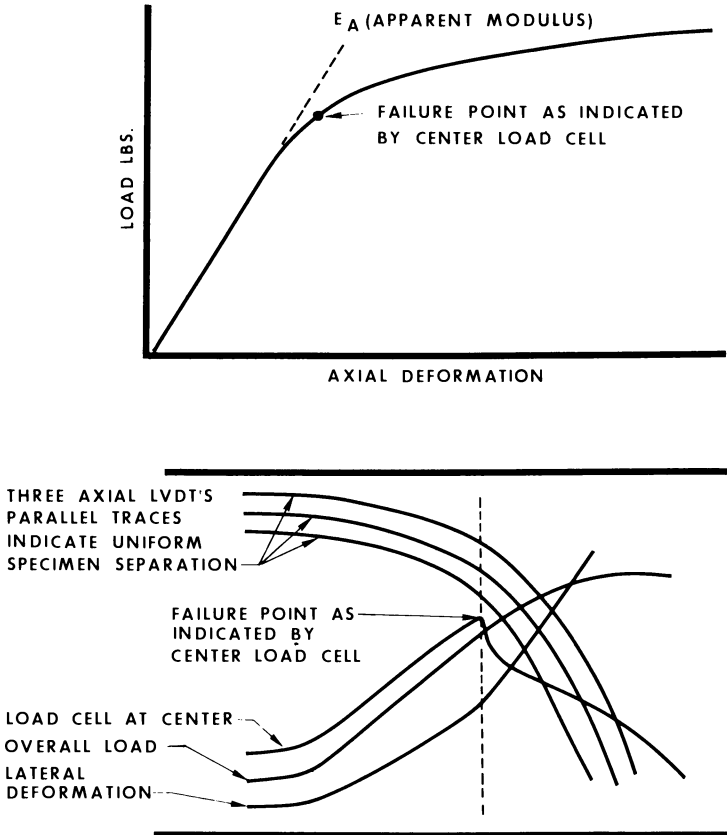
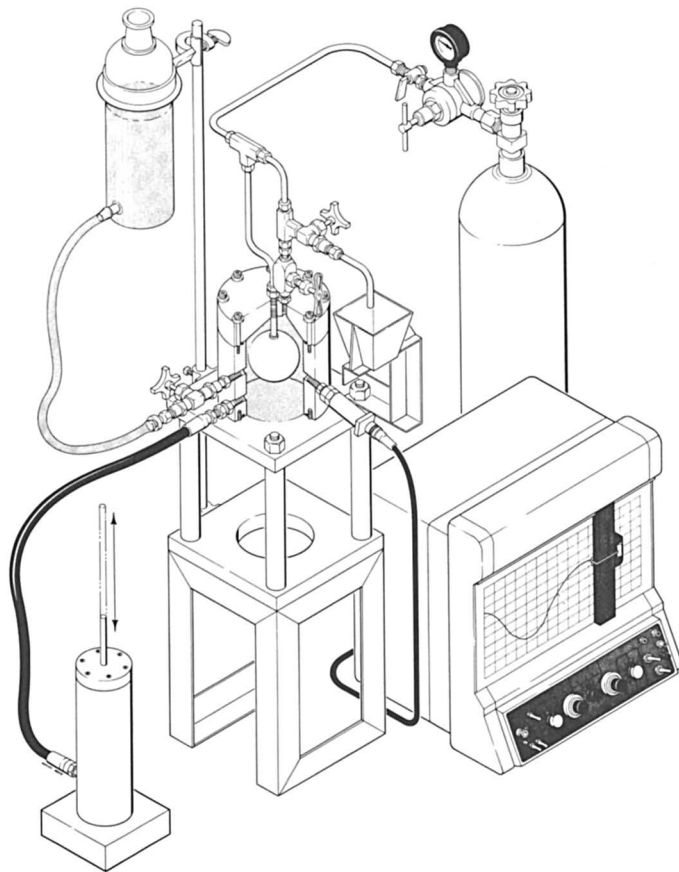


Figure 19. *Poker chip test data. Small center load cell in one of the bonded plates provides an indication of the rupture point which would not be obvious from over-all load recording instruments (40)*

A unique and considerably more elaborate multiaxial test employs a thick-walled hollow sphere test specimen which may be pressurized internally or externally with a nearly incompressible liquid. Figure 20 illustrates the essential features of the test device as described by Bennet and Anderson (5). The specimen is prepared by casting propellant in a mold fitted with a sand-poly(vinyl alcohol) mandrel inside the sphere which may be removed easily after curing. A constant displacement rate instrument drives the piston to pressurize the chamber and apply large deformations. The piston's total displacement volume is transferred to

the specimen. Simultaneous internal and external pressures may be applied and adjusted to provide a variety of stress fields. The force and displacement are measured in the hoop and radial directions at the internal boundary of the sphere.



—Courtesy Thiokol Chemical Corp., Wasatch Division

Figure 20. Spherical test assembly. Propellant sphere may be pressurized externally or internally, and wall thickness may be varied

For an externally applied pressure, a compression-compression stress field is obtained with a thick-walled sphere. If the sphere wall is thin, a biaxial field is produced. If the pressure is applied internally, a triaxial tension-tension-compression state is generated. A nearly uniform stress field is produced over the entire specimen. The supporting tube is surrounded with a low modulus material to avoid stress concentration and

premature rupture in this vicinity. The relative magnitudes of the stresses are varied by changing the thickness of the sphere. One additional feature is the ability to examine the effects of pressure on the mechanical properties of propellant. Obviously the various test modes such as constant strain and constant stress may be determined by regulating the pressurizing system.

Sharma (90) describes an apparatus which uses a tubular specimen which may be strained longitudinally with internal pressurization. Loading rate can be varied, and strains are measured by clip gages. This device permits characterization of propellant-like materials in various biaxial tension-tension and biaxial tension-compression stress fields. A schematic of the apparatus is shown in Figure 24.

Uniaxial tension testing with superposed hydrostatic pressure has been described by Vernon (111) and Surland *et al.* (103). Such tests provide response and failure measurements in the triaxial compression or tension-compression-compression octants.

Dynamic Testing

A variety of dynamic tests, testers, and specimen configurations have been used to measure solid propellant response to cyclic loading. Table II summarizes many of the techniques and characteristics. In most instances the loading is applied in a regular sinusoidal manner, although other nonsinusoidal time functions may be considered in some tests.

As pointed out by Britton (15), the measurements are useful in design and research studies pertaining to (1) vibration analysis of structure, (2) propellant viscoelastic behavior, (3) oscillating combustion, (4) internal attenuation of shock waves, and (5) fatigue life.

Test methods can be arranged according to two major categories:

(a) Relatively low amplitude tests ($< 1\%$ strain) for relatively short times, with response measured in terms of complex or dynamic modulus.

(b) Relatively high amplitude tests (strains approaching uniaxial rupture) for a time sufficient to cause deterioration and ultimate failure. Time to failure at a given applied stress or strain amplitude is determined.

A general description of the fundamental relationships governing the dynamic response of linear viscoelastic materials may be found in several sources (28, 37, 93). In general, sinusoidally applied strains (stresses) result in sinusoidal stresses (strains) that are out of phase. Measurements may be made under uniaxial, shear, or dilational loading conditions, and the resultant complex moduli or compliance and loss-phase angle are computed. Rotating radius vectors are usually taken to represent the

stress and strain behavior for graphical analysis on a complex plane. Complex stresses (σ^*) and strains (ϵ^*) may be written as:

$$\sigma^* = \sigma_a [\cos \omega t + i \sin \omega t] \quad (8)$$

$$\epsilon^* = \epsilon_a \cos(\omega t - \delta) + i \sin(\omega t - \delta) \quad (9)$$

where σ_a = stress amplitude, ϵ_a = strain amplitude, δ = loss-phase angle, ω = circular frequency, and t = time. The complex modulus may therefore be defined as:

$$E^*(\omega) = \frac{\sigma^*}{\epsilon^*} \quad (10)$$

and in terms of its components

$$E^*(\omega) = E'(\omega) + iE''(\omega) \quad (11)$$

where $E'(\omega)$ is called the storage modulus, and $E''(\omega)$ is the loss modulus. The ratio E''/E' is equal to the tangent of the loss angle. The dynamic compliance $D^* = \epsilon^*/\sigma^*$, and storage and loss compliance, $D'(\omega)$ and $D''(\omega)$ may be defined in a similar manner. These symbols are usually applied to uniaxial loading. The designations $G^*(\omega)$ and $J(\omega)$ are normally used for complex shear modulus and compliance, respectively.

Dynamic measurements can be made using either free or forced vibrations, and at resonance or outside of resonance conditions. Since the material depends on time and temperature, characterization over wide frequency ranges may be simplified by applying the WLF (118) equation for time-temperature equivalence. This relationship is generally useful in many propellant studies when used with caution under conditions which have established validity.

Sample shape and size are of considerable importance when selecting dynamic test methods for solid propellants. Preparation must take account of surface conditions and precise dimensions. Usually cast specimens retain a polymer-rich surface layer and should be avoided. Additionally, the sample dimensions should be large compared with the size of the largest solid particle inclusion in the propellant.

Forced vibrations at large amplitudes may result in propellant deterioration by several mechanisms. Tormey and Britton (107) examined this problem from the viewpoint of microstructural change as well as engineering mechanics. When a force is applied to the material and deformation results, the mechanical energy may be distributed in several ways, such as: (1) energy stored in recoverable elastic deformation; (2) interphase dewetting; (3) bond breakage; (4) viscous flow; (5) heat generation. New surfaces are formed internally owing to microfractures in the binder as well as binder-filler dewetting. Heat generation may be similar to that experienced in the repeated flexing of rubber tires. During

the application of cyclic loading, some of the mechanical energy of each cycle is lost as heat. If the heat cannot be transferred to the surroundings at a sufficient rate, the temperature of the material will rise.

The energy which is lost in each cycle when an alternating stress is applied to a viscoelastic material may be expressed as follows:

$$W' = \pi E'' \epsilon_a^2 \quad (12)$$

or

$$W' = \pi D'' \sigma_a^2 \quad (13)$$

Where D'' is the loss compliance or the out-of-phase component of the dynamic compliance. The rate is given by

$$W = 1/2 \omega D'' \sigma_a^2 \quad (14)$$

which for N cycles gives

$$W_N = N \pi D'' \sigma_a^2 \quad (15)$$

A vivid example of the resultant deterioration of a solid propellant grain is shown in the report by Torney and Britton (107), where a grain was subjected to a 5g input at resonant frequency for about 6×10^6 cycles. The propellant degraded so badly that it lost dimensional stability and flowed. Another example illustrated the tendency of vibration to propagate fracture in certain highly stressed regions of the grain. Although the energy loss per cycle may appear as a heat buildup in the material, this process is related to several governing factors. An increasing temperature in a viscoelastic material generally results in a decreasing modulus. This may lead to larger deformations at a given input vibrational force if the mass is not amplitude restricted. Since heat generation in a linear viscoelastic material increases in proportion to the second power of the strain, the process may tend to run away, unless there is a correspondingly large decrease in the loss modulus.

Schapery (86) has examined steady-state and transient temperature distributions resulting from energy dissipation in viscoelastic slabs and cylinders subjected to cyclic shear loading. The temperature dependence of the dissipation was introduced through the assumption of thermorheologically simple behavior. A nonlinear heat conduction equation resulted, and coupled processes for heat conduction and mechanical deformation were treated by two variational principles. Shapery and Cantey (87) studied thermomechanical phenomena, placing particular emphasis on the nature of thermal instabilities. An experimental examination of solid propellant subjected to steady-state sinusoidal shearing was conducted using specimens insulated so that heat transfer was one dimensional. Loading was accomplished in constant applied strain experiments and in forced vibration with inertia where the attached mass was

Table II. Dynamic Tests Used for

<i>Test and References</i>	<i>Stress/Strain Application</i>
Fitzgerald Transducer Fitzgerald <i>et al.</i> (28, 31) Landel (44, Sect. 4.6.2)	Forced sinusoidal nonresonant shear directly applied by pole pieces of electromagnet to sample disk
Oscillating Plate (FIL Tester) Phillipoff (76) Hoebel (43)	Forced sinusoidal shear strain imposed by mechanical drive of clamped annular plate of propellant
Vibrating Plate Baltrukonis (2) Layton <i>et al.</i> (44, Sect. 4.6.2)	Forced sinusoidal shear strain imposed by vibrating outer ring of annular plate of propellant on an electrodynamic shaker
Resonant Weighted Column Britton (107) Burton <i>et al.</i> (17)	Forced sinusoidal uniaxial tension and compression imposed by vibrating weighted rectangular column of propellant on electrodynamic shaker
LPC Large Deformation Dynamic Tester Jones <i>et al.</i> (45)	Forced sinusoidal uniaxial tension and shear imposed by mechanical drive to tensile bar or double-lap shear specimen
LPC Small Deformation Dynamic Tester Jones <i>et al.</i> (45)	Forced sinusoidal shear imposed by piezoelectric driver to single-lap shear specimen
Free Vibrating Reed Tester (AGC) Kostyrko (44, 49)	Free damped sinusoidal vibration of clamped thin rectangular specimen, free end set in motion by deflection and release
Forced Vibrating Reed Tester (HPC) Nicholson <i>et al.</i> (73)	Forced sinusoidal vibration of thin cantilever beam specimen by electrodynamic shaker
Dynamic Torsion Tester, Low Range (STL) Gottenberg <i>et al.</i> (35)	Forced sinusoidal oscillatory torsion imposed by mechanical drive to hollow cylindrical specimen through bell-crank arrangement
Dynamic Torsion Tester, High Range (STL) Gottenberg <i>et al.</i> (35)	Forced sinusoidal rotary vibration imposed by electrodynamic vibrator to hollow cylindrical specimen through bell-crank arrangement

free to move. Shapery's predictions of dynamic jump instabilities under certain critical conditions were qualitatively verified. Figure 21 shows a schematic of the large deformation sinusoidal test apparatus and specimen configuration which were used.

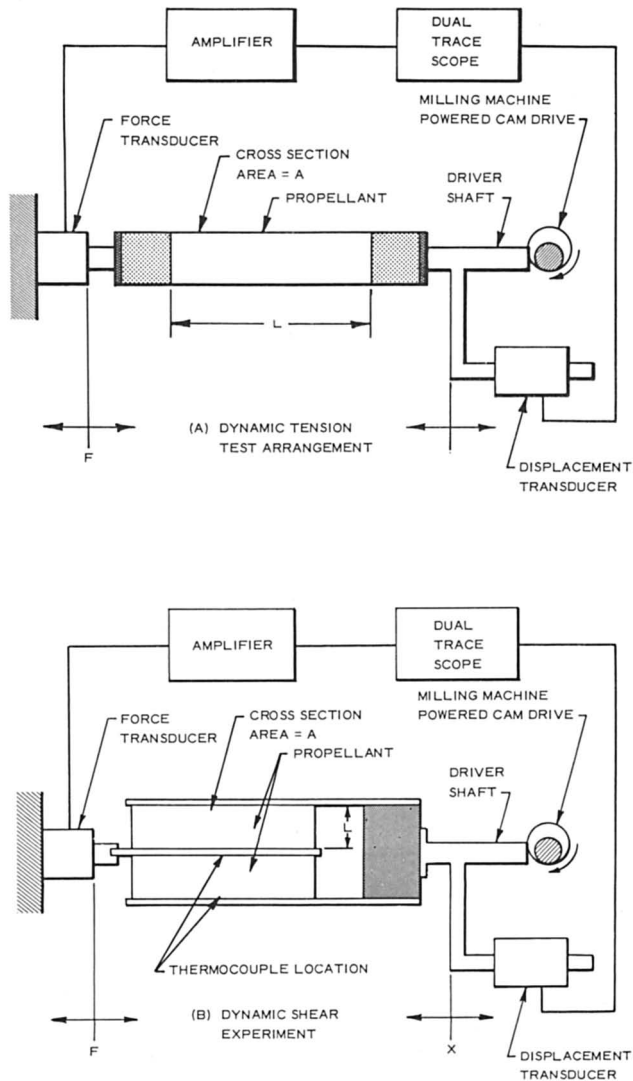
An important aspect is involved in large deformation cyclic tests; it is related to the amount of damage done in each cycle which may accumulate in a predictable fashion but which also depends on conditions which may allow recovery. These items will be discussed later.

Solid Propellant Characterization (15)

<i>Frequency Range, c.p.s.</i>	<i>Response Measured By</i>	<i>Data Usually Obtained</i>
25-3000	Changes in resistance and capacitance of electrical drive system	$G'(\omega)$ $G''(\omega)$
0.1-60	Deflection of center ring, applied force	$G'(\omega)$ $G''(\omega)$
75-1000	Amplitude ratio, phase angle from two accelerometers, frequency from electrical drive	$G'(\omega)$ $G''(\omega)$
30-1500	Amplitude ratio, phase angle from two accelerometers, frequency from electrical drive	$E'(\omega)$ $E''(\omega)$
1-45	Force and displacement by transducers in mounting arrangement	$E'(\omega)$ $E''(\omega)$ $G'(\omega)$ $G''(\omega)$
20-1000	Driving force from piezoelectric input voltage, transmitted force from piezoelectric monitor on clamped end of specimen	$G'(\omega)$ $G''(\omega)$
4-30	Deflection from strain gauge mounted on sample recorded against time, sample dimensions and mass. Time range extended by using time-temperature super-position	$E'(\omega)$ $E''(\omega)$
10-200	Free end displacement by optical displacement transducers. Input from shaker electrical measurements	$E'(\omega)$ $E''(\omega)$
0.0002-30	Angular displacement sensed by differential transformers; speed indication from electromagnetic sensor on output shaft of drive motor	$G'(\omega)$ $G''(\omega)$
30-1000	Angular displacement sensed by piezoelectric accelerometers; frequency from vibrator input	$G'(\omega)$ $G''(\omega)$

Physicochemical Characterization

While mechanical testing of all types provides a general description of the bulk properties of solid propellants, it is difficult to make generalizations or even extrapolations which may be used in a predictive fashion. When the content or type of solid filler is changed, or curative ratios are altered, there is no simple corresponding material property change which can be defined based on mechanical testing experience. If filler content



—Courtesy Lockheed Propulsion Co.

Figure 21. Schematic of large deformation dynamic tension and shear apparatus

and type are held constant, it may be expected that many mechanical properties are governed by binder crosslinking. Double-base formulations are particularly confounding with respect to variations in degree of “cure” because a continuous, chemically crosslinked network is not formed. Pseudo-equilibrium modulus measurements may be used to characterize

the extent of gelation in these materials, but only an "equivalent" crosslink density may be computed. It is not at all clear what benefit, in a predictive sense, is provided by such measurements.

Considerably more satisfactory results have been obtained with composite rubber-based propellants. The binder crosslink density and sol fraction may be determined by using modified swelling and extraction techniques common in polymer science. The complications introduced by measuring such parameters in the presence of very high filler volume fractions are significant, but nevertheless useful techniques have been worked out. The determination of crosslink density in composite solid propellants has been described (3, 48, 64) where both swollen tension and compression methods were employed. Previous efforts utilizing "equilibrium" modulus measurements or volume swelling techniques encountered some obvious difficulties. Equilibrium measurements are practically impossible to obtain since the gradual dewetting of the binder-filler composite structure contributes a relaxation mechanism with very stubborn and nonreproducible characteristics. When high temperatures and long times are used, some chemical changes are possible, but a significant factor is the change in moisture content. The moisture effects on solid propellant properties can be considerable and are discussed in the section on aging.

Volume swelling measurements have produced erratic results even under the most carefully controlled conditions. One important contribution in this regard is the work of Bills and Salcedo (8). These investigations showed that the binder-filler bond could be completely released with certain solvent systems and that the volume swelling ratio is independent of the filler content when complete release is achieved. Some thermodynamic problems exist, however, when such techniques are used to measure crosslink density quantitatively. First, equilibrium swelling is difficult to achieve since the fragile swollen gel tends to deteriorate with time even under the best conditions. Second, the solubility of the filler (ammonium perchlorate) and other additives tends to alter the solution thermodynamics of the system in an uncontrollable manner. Nonreproducible polymer-solvent interaction results, and replicate value of crosslink density are not obtained.

Swollen tensile and compression techniques avoid both of these problems since equilibrium swelling is not required, and the method is based on interfacial bond release and "plasticization" rather than solution thermodynamics. The technique relies upon the approach to ideal rubberlike behavior which results when lightly crosslinked polymers are swelled. At small to moderate elongations, the stress-strain properties of rubbers

have been described by a statistical theory of rubberlike elasticity (109) resulting in:

$$\sigma = \nu_e kT (\lambda - 1/\lambda^2) \quad (16)$$

where ν_e is the number of effective network chains per unit volume, k is Boltzmann's constant, T the absolute temperature, and λ is the extension ratio. Mooney (70, 71) and Rivlin (78) have developed expressions which result in a two-constant description which more nearly approximates real behavior. For simple tension, this is:

$$\sigma = (2C_1 + 2C_2/\lambda) (\lambda - 1/\lambda^2) \quad (17)$$

where $C_1 + C_2$ are empirical constants. C_1 has been related to $\nu_e kT$ of the statistical theory expression, and C_2 to various deviations from the model behavior such as chain entanglement and molecular interactions. A plot of $\sigma/(\lambda - 1/\lambda^2)$ against $1/\lambda$ usually results in a straight line, at small strains, with $2C_1$ as the intercept and $2C_2$ as the slope. This treatment is commonly referred to as a Mooney-Rivlin plot. Obviously, if the slope of the line is zero, the material may be represented by the expression for "ideal" rubbery behavior. Gumbrell, Mullins, and Rivlin (38) have examined the tensile properties of various rubbers in the swollen condition. They showed that a zero slope could be obtained in a Mooney-Rivlin plot, after only moderate swelling, independent of the swelling solvent.

Such techniques have been tried with solid propellants, but reproducible results depend on attaining complete binder-filler release and adequately measuring the binder sol fraction. Preliminary swelling studies to determine a solvent system and conditions which do not degrade the propellant are required. Common extraction techniques are used to determine the sol fraction. This determination is then applied as a correction when computing crosslink density. The force-deformation relationship for swollen rubbers is

$$F/A = \nu_e kT (\lambda - 1/\lambda^2) \nu_2^{-1/3} \quad (18)$$

where F is the force, A is the unstrained unswollen cross-sectional area, and ν_2 is the volume fraction of rubber in the swollen gel. A correction for ν_2 is required for large sol fractions as given by Bills and Salcedo (8):

$$\nu_2^{-1} = \frac{V_p - V_{st} - V_e}{V_p - V_e/V_r} \quad (19)$$

where V_p is the volume of sample; V_{st} , the volume of solvent in the swollen sample; V_e , the volume of extractable polymer (sol); and V_r , the volume fraction of rubber in the sample.

The average cross-sectional area of rubber in filled samples has been the subject of much discussion. In a filled system which swells to a foam-

like material, the average cross section of effective rubber is given by the initial sample area multiplied by the volume fraction of rubber in the sample and by the area fraction of gel. The volume fraction and area fraction are identical in multiphase solids (18).

Swollen tension methods using various sample-gripping techniques have been attempted, but none has been completely satisfactory. Compression methods, on the other hand, avoid the gripping problems, although it is difficult to attain parallel swollen sample faces, and errors occur in determining strain. Cluff, Gladding, and Pariser (19) have described compression techniques for swollen vulcanizates, and these methods have been used to characterize propellant crosslink density (48). Equation 20 was used

$$v_e = h_o S / 3A_o RT \quad (20)$$

where h_o is the height and A_o the cross-sectional area of the undeformed, unswollen sample, and S is the slope of the force deflection curve. Seeley and Dyckes (89) have performed compression tests on swollen cellular elastomers based on similar techniques.

Failure Criteria

Structural analysis of the solid rocket case-grain system using experimentally determined propellant response properties may permit a complete description of the combined stresses and resultant deformations, but a statement expressing the ability of the propellant to withstand these stresses is also required. Such a statement, which relates the physical state at which failure occurs to some material parameters, is called a failure criterion. The criterion for failure permits a prediction of safety margins expected under motor operation and handling and defines the loading regimes where abnormal operations will occur with intolerable frequency.

“Failure” may be defined in several ways. An operational definition might involve any deviation from the required motor ballistic performance such as motor pressure, total burn time, burning rate, etc. Several of these abnormalities may be related directly to grain structural integrity. Obviously, a crack or unbond of sufficient size, which is exposed to the hot combustion gases, may result in a catastrophic pressure increase or premature burn-through to the case wall. However, it is quite possible for small changes in burn rate or minor pressure fluctuations to cause mission failure. Since most solid rocket uses rely upon a preprogrammed thrust-time operation governed by the total burning surface, midcourse corrections may be impossible. Other definitions of failure might include: the first visual crack which forms, sample rupture into two or more pieces,

the maximum stress point on a stress-strain curve, a maximum acceptable volume increase, or perhaps a large modulus change resulting in grain slump or case bond release.

An important consideration in all failure studies is the influence of material variability. Statistical distributions of failure incidence must be known and properly accounted for if reliability limits are to be set. Wiegand and co-workers (14, 113) have discussed propellant sample and batch variability, and its effect on failure behavior, in numerous reports. These studies point out the statistical nature of failure and the fact that knowledge of the distributions is required to set conservative design values for motor stress and strain capability. Statistical distributions permit the prediction of the probability of failure, but mission considerations dictate the allowable failure frequencies.

Landel and Fedors (53, 54) have recently explored the usefulness of extreme value statistics applied to the statistical distribution of rupture in various unfilled polymer specimens. Both breaking stress and breaking strain of natural rubber (47) and styrene butadiene elastomers (53, 54) may be described by the double exponential distribution

$$\Phi = 1 - \exp[-\exp A (X - X^*)] \quad (21)$$

where Φ is the cumulative distribution of failures, A is the breadth of the distribution, and X and X^* are the value, and the most probable value, of stress (or strain), respectively. Therefore, although the following discussion may be concerned with rupture stress or rupture strain, the inherent variability in rupture processes as well as that of materials in general, requires that all discrete values be viewed as mean values of a distributed population.

The various approaches for establishing failure criteria for solid propellants may be divided roughly into two categories. First, simple relationships may be developed which relate actual motor failures to laboratory tests. This produces a pragmatic criterion which may be useful when the application is limited to the specific material, motor design, failure mode, and loading conditions which prevailed during the initial correlation testing. Secondly, an analytical criterion may be generated which may be represented in the geometrical form of a "failure surface." The surface represents a boundary, in some specifically defined space coordinate system, between safe mechanical states and unsafe states.

The first category is traditional in the solid rocket industry, and variations on this approach have been many and diverse. The second category is appealing its generality and possible mathematical rigor but has been hampered in its development by experimental difficulties. Until recently, however, most failure relationships have been based on a single loading history or "first stretch" conditions.

One of the simplest criteria specific to the internal port cracking failure mode is based on the uniaxial strain capability in simple tension. Since the material properties are known to be strain rate- and temperature-dependent, tests are conducted under various conditions, and a failure strain boundary is generated. Strain at rupture is plotted against a variable such as reduced time, and any strain requirement which falls outside of the boundary will lead to rupture, and any condition inside will be considered safe. *Ad hoc* criteria have been proposed, such as that of Landel (55) in which the failure strain ϵ_f is defined as the ratio of the maximum true stress to the initial modulus, where the true stress is defined as the product of the extension ratio and the engineering stress —i.e., $\sigma_m/E = \lambda_m \sigma_m/E = \epsilon_f$. This relationship breaks down at low strain rates and higher temperatures. Milloway and Wiegand (68) suggested that motor strain should be less than half of the uniaxial tensile strain at failure at 0.74 min.^{-1} . This criterion was based on 41 small motor tests.

The uniaxial failure envelope developed by Smith (95) is one of the most useful devices for the simple failure characterization of many viscoelastic materials. This envelope normally consists of a log-log plot of temperature-reduced failure stress *vs.* the strain at break. Figure 22 is a schematic of the Smith failure envelope. Such curves may be generated by plotting the rupture stress and strain values from tests conducted over a range of temperatures and strain rates. The rupture locus moves counterclockwise around the envelope as the temperature is lowered or the strain rate is increased. Constant strain, constant strain rate, and constant load tests on amorphous unfilled polymers (96) have shown the general path independence of the failure envelope. Studies by Smith (97) and Fishman (29) have shown a path dependence of the rupture envelope, however, for solid propellants.

Some investigators have shown a preference for plotting strain at maximum stress rather than rupture strain on solid propellant failure envelopes. This is based upon two considerations; first, the onset of cracking or localized blanching (dewetting) has been observed near the maximum stress point, and second, this value represents a more conservative design limit. Strain at maximum stress data generally show less scatter near the maximum strain portion of the failure envelope. Limited evidence indicates that the path dependence of the envelope generated this way may be somewhat less than that of a rupture boundary.

Uniaxial tensile criteria can lead to gross inaccuracies when applied to situations where combined stresses lead to failure in multiaxial stress fields. Often one assumes that combined stresses have no influence and that the maximum principal stress governs the failure behavior. An improved approach applied to biaxial tension conditions relies upon a pragmatic "biaxial correction factor" which is applied to uniaxial data,

modifying the strain values to account for the influence of combined stresses. Such factors are based upon extensive testing and comparisons for a single material using uniaxial, strip biaxial or, perhaps, analog motor tests.

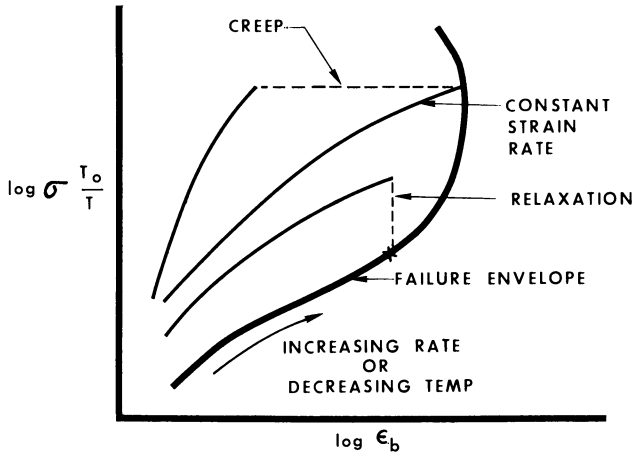


Figure 22. Schematic of the Smith failure envelope. Stress is corrected for kinetic theory temperature effects by the ratio of the reference temperature T_0 to the test temperature T

Majerus (61, 62) has approached the failure behavior of highly filled polymers by a thermodynamic treatment in which the ability to resist rupture is related to the propellant's ability to absorb and dissipate energy at a certain rate. An energy criterion which requires failure to be a function of both stress and strain was originally stated by Griffith (36) for brittle materials and later adapted to polymers by Rivlin and Thomas (80). Williams (115) has applied an energy criterion to viscoelastic materials such as solid propellants where appropriate terms are included for viscous energy dissipation.

A combination of an energy criterion and the failure envelope has been proposed by Darwell, Parker, and Leeming (22) for various double-base propellants. Total work to failure was taken from the area beneath the stress-strain curve, but the biaxial failure envelope deviated from uniaxial behavior depending on the particular propellant formulation. Jones and Knauss (46) have similarly shown the dependence of failure properties on the stress state of composite rubber-based propellants.

To visualize the stress states at which failure occurs, a failure surface may be constructed. The six stress components may be resolved into three orthogonal principal stresses. Plotting failure in principal stress space, any stress state which exists in the bounded space containing the

origin will not cause failure, and conversely, any state outside of this boundary will lead to failure. A mathematical description of the surface would greatly simplify matters since the most convenient stress field could be chosen for laboratory testing, and the entire surface could be described from a single failure locus. Such surfaces have been discussed at length by Blatz (12) and Williams *et al.* (114), and the failure surfaces associated with various failure criteria by several authors (39, 65, 108, 112). Nadai (72) has reviewed eight failure theories which have been proposed for materials (mainly metals), and Marin (63) discusses six of these in a more simplified manner. Simply listed, these are: (1) maximum principal stress or Rankine theory, (2) maximum shear or Coulomb-Tresca criterion, (3) maximum strain or St. Venant's theory, (4) maximum strain energy theory, (5) distortion energy or Von Mises-Hencky theory, and (6) the internal friction theory which is a special case of Mohr's theory.

Mehldahl (65) depicts several failure surfaces by photographs of various three-dimensional models. Figure 23 illustrates three such surfaces taken from Ref. 110, which shows geometries which are symmetrical about the space diagonal, $\sigma_1 = \sigma_2 = \sigma_3$, and containing the assumption that the triaxial compression octant should be open ("because hydrostatic compression cannot lead to failure in the ordinary sense").

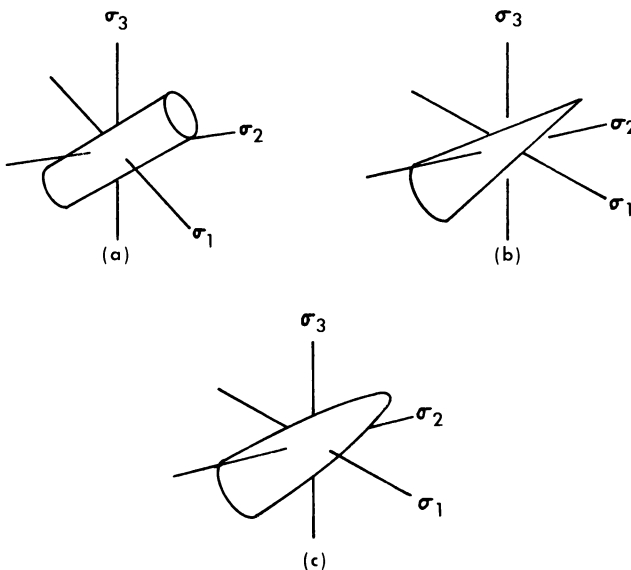


Figure 23. Various failure surfaces in principal stress space: (a) cylinder, (b) cone, and (c) paraboloid (110)

Although the concept of a failure surface in principal stress space seems to provide a descriptive definition of the ultimate capability of materials in any stress state, in reality there may not be one unique surface for each material. Failure in solid propellants is not only influenced by the stress state but also by the deformation history. Since a given stress state can be reached by any number of stress-strain paths, a given failure surface may exist for each specific loading history. Sharma (90) and Jones and Knauss (46) have produced traces of failure surfaces by maintaining the principal strain rates at equivalent values for the various tests conducted. Little has been said or done about the general problem of multiaxial strain rates and associated multiaxial stresses. Zak (120) has proposed a theory for polymeric materials in which both rate and multiaxial effects are included, but no experimental verification has been attempted. Figure 24 is a representation of parabolic failure surfaces in principal stress space, coaxial with the space diagonal. The two surfaces illustrate the possibility of several surfaces which might result from changes in the material or the test conditions. Such surfaces need not be concentric as shown; in fact, significant deterioration could change the basic failure mode of the material and therefore, the size and shape of the failure surface.

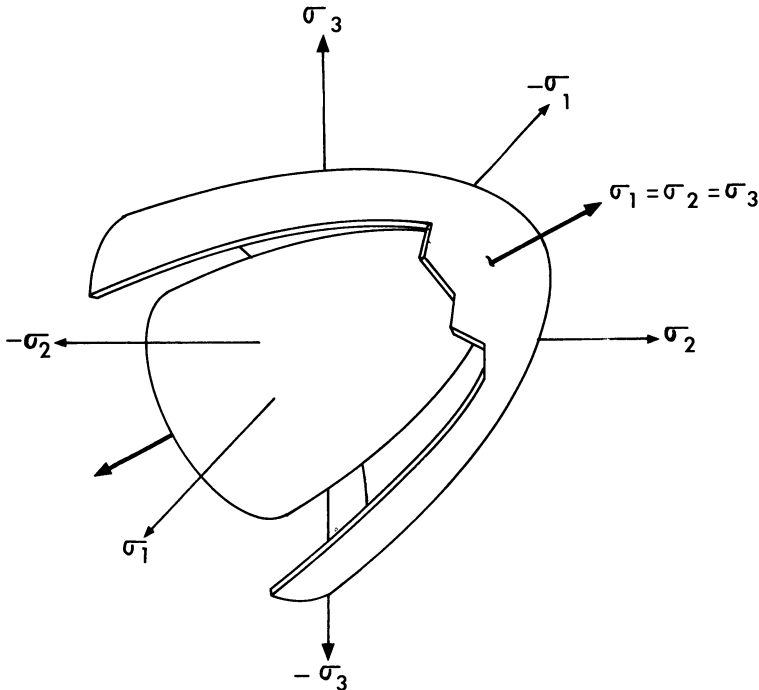
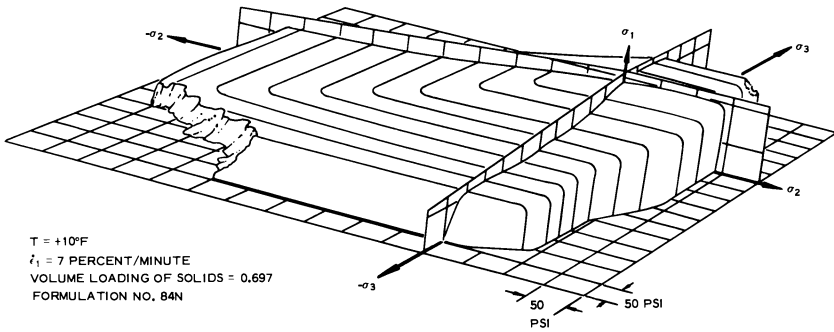


Figure 24. Parabolic failure surfaces coaxial to the hydrostatic axis

Other coordinate systems may be used for failure surface representations in addition to stress space. Blatz and Ko (11) indicate that either stress (σ_i) space, stretch (λ_i) space, or invariant (I_i) space may be appropriate. Stress space is most commonly used because the failure surface concept was originally applied to metals, for which stress and strain are more simply related. Viscoelastic materials, on the other hand, may show a multitude of strain values at a given stress level, depending on test conditions.

Some materials might produce a unique failure surface providing measurements could be conducted under "first stretch" conditions in a state of equilibrium. Tschoegl (110), at this writing, is attempting to produce experimental surfaces by subjecting swollen rubbers to various multiaxial stress states. The swollen condition permits failure measurements at much reduced stress levels, and the time dependence of the material is essentially eliminated. Studies of this type will be extremely useful in establishing the foundations for extended efforts into failure of composite materials.

The general inapplicability of the various classic failure theories to solid propellants has been noted by numerous investigators. Jones and Knauss (46) have shown approximate agreement with the maximum tensile stress theory in the triaxial tension stress octant, while data in other regions indicated an internal friction type of criteria. Figure 25 shows the surface constructed by these authors for a composite rubber-based propellant. Experimental mapping of failure surfaces for solid propellants has been attempted to a limited extent, but difficulties have been encountered, especially in the seven compressive octants. When various analytical criteria are compared to laboratory data, it becomes extremely difficult to distinguish the most appropriate criterion in the (+++) octant. Scatter in the failure data may be great enough to include several criteria at once since the differences in this octant are not large. In the other octants, however, there can be substantial divergences of the analytical failure boundaries, and the distinction should be much easier. A few investigators have conducted uniaxial and biaxial tests under superposed hydrostatic pressure. Vernon (111), Kruse (51), and Surland and co-workers (103) have discovered that certain composite propellants exhibit higher strain capability and tensile strength when tested under confining gas pressure. Hazelton and Planck (41) conducted uniaxial tension tests and simple shear tests on propellants and propellant liner bonds with gas pressures up to 800 p.s.i.g. They also found increased tensile properties under pressure and interpreted the behavior as caused by delayed dilation and to rate effects.



—AIAA Solid Rocket Propellant Conference

Figure 25. Failure surface in principal stress space for a composite solid propellant (46)

Sharma (90) has examined the fracture behavior of aluminum-filled elastomers using the biaxial hollow cylinder test mentioned earlier (Figure 26). Biaxial tension and tension-compression tests showed considerable stress-induced anisotropy, and comparison of fracture data with various failure theories showed no generally applicable criterion at the strain rates and stress ratios studied. Sharma and Lim (91) conducted fracture studies of an unfilled binder material for five uniaxial and biaxial stress fields at four values of stress rate. Fracture behavior was characterized by a failure envelope obtained by plotting the octahedral shear stress against octahedral shear strain at fracture. This material exhibited neo-Hookean behavior in uniaxial tension, but it is highly unlikely that such behavior would carry over into filled systems.

In a recent attempt to bring an engineering approach to multiaxial failure in solid propellants, Siron and Duerr (92) tested two composite double-base formulations under nine distinct states of stress. The tests included triaxial poker chip, biaxial strip, uniaxial extension, shear, diametral compression, uniaxial compression, and pressurized uniaxial extension at several temperatures and strain rates. The data were reduced in terms of an empirically defined constraint parameter which ranged from -1.0 (hydrostatic compression) to $+1.0$ (hydrostatic tension). The parameter (ϕ) is defined in terms of principal stresses and indicates the tensile or compressive nature of the stress field at any point in a structure—*i.e.*,

$$\phi = \frac{\sigma_I + \sigma_{II} + \sigma_{III}}{3 |\sigma_I|} \quad (22)$$

where σ_I , σ_{II} , and σ_{III} are the numerically maximum, intermediate, and minimum principal stresses, respectively. Tensile failure stress and tensile failure strain were plotted against the constraint parameter, and reason-

able correlation was shown for one temperature and strain rate. A preliminary comparison of the failure data with the maximum principal tensile stress, maximum principal tensile strain, maximum shear stress, and maximum distortional strain energy failure criteria showed no correlations for these propellants.

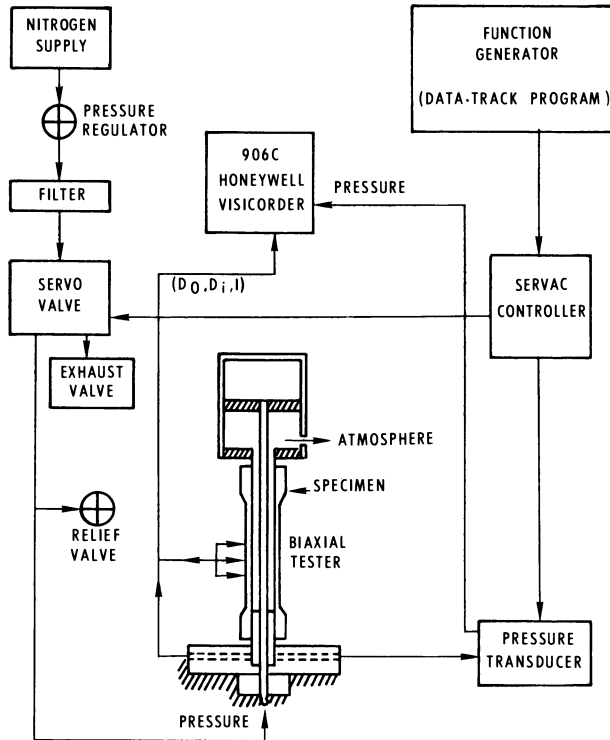


Figure 26. Schematic of hollow cylinder biaxial tester as given by Sharma (90)

Cumulative Damage

The conditions leading to damage accumulation are particularly relevant to the problems of solid rocket structural integrity. It is quite possible for a grain to "wear out" after repeated thermal cycling or vibration through the gradual development and propagation of microscopic tearing or molecular breakdown. If this process could be described analytically and formulated for complex motor geometries, a useful life prediction could be made based on the motor history.

Metal fatigue has been studied extensively for many years, and more recently, considerable attention has been given to fatigue in plastics and

rubbers (6, 24, 34, 52). Williams (116) has suggested that solid propellants might be examined on the basis of Miner's Law (69) which was developed for metal fatigue. This may be represented by the expression

$$\sum_{i=1}^M \left(\frac{N_i}{N_{fi}} \right)^n = 1.0 \quad (23)$$

where M is the number of load levels, N_i is the number of cycles at the i th load level, and N_{fi} is the number of cycles to failure at the i th load level. The exponent n can be determined experimentally but is usually taken to be 1.0, which indicates linear accumulation.

Miner's law has been used to predict failure for sequential loading of solid propellant at different strain rates. The linear form used here is:

$$\sum_{i=1}^M \left(\frac{t_i}{t_{fi}} \right) = 1.0 \quad (24)$$

where t_i is the time at i th strain rate, and t_{fi} is the time to failure at the i th strain rate. Various investigators have examined this relationship for application to solid propellants with only limited success. This is to be expected since the order of loading is not taken into account in Miner's law.

Bills (7) has applied an adaptation of this law to solid propellants and propellant-liner bonds for discrete, constantly imposed stress levels; considering t_i to be the time at the i th stress level and t_{fi} the mean time to failure at the i th stress level. A probability distribution function P was included to account for the statistical distribution of failures. For cyclic stress tests the time is the number of cycles divided by the frequency, and the i th loading is the amplitude. The empirical relationship

$$\left(\frac{\sigma}{\sigma_o} \right)^B = \frac{t_o}{t_f} f(t) \quad (25)$$

was employed to derive the integral expression

$$P \sum D_i = \frac{1}{\sigma_o^B t_o} \int_0^t \frac{\sigma(t)^B dt}{f[g(t)]} \quad (26)$$

where D_i = incremental damage, t_f = mean time to failure, t_o = unit time to failure, σ_o = stress required to cause failure at t_o , B = an empirical constant, and $f[g(t)]$ = viscoelastic time-temperature shift relation with temperature expressed as a function of time. The various constants were obtained from constant load tests at several temperatures and specific

temperature-stress-time cycles. Integration yields the mean damage per cycle or the number of cycles to failure, N . Figure 27 illustrates the correlation obtained for cyclic tests on propellant-liner bond specimens at temperatures of 40°, 77°, and 110°F. and sequential stress levels from 40 to 80 p.s.i.g. The degree of correlation is not completely satisfactory, but at least one can estimate the minimum number of cycles which will cause failure.

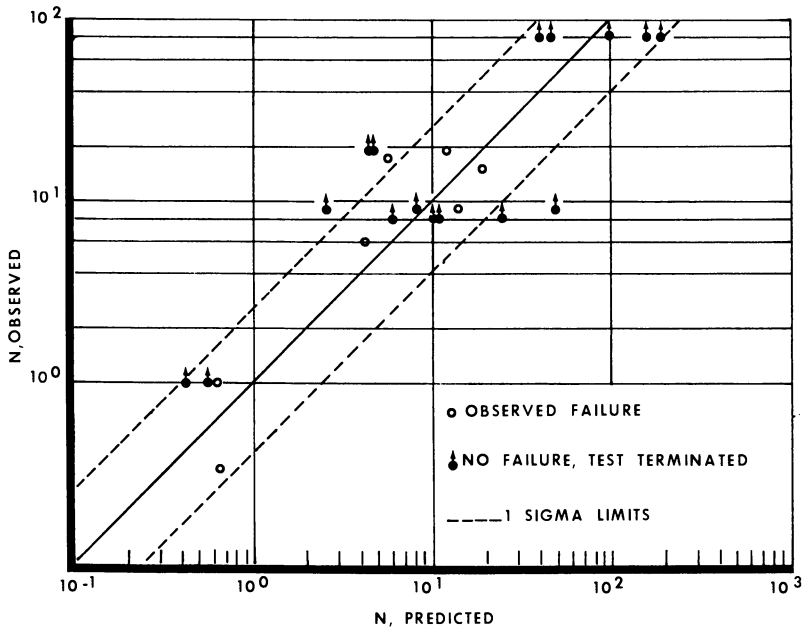


Figure 27. Comparison of predicted and observed number of cycles to failure for solid propellant-liner bond specimens, according to Bills et al. (7)

An approach suggested by Williams *et al.* (117) uses an energy balance equation for initiation of flaw growth in a linearly viscoelastic material. A spherical flaw geometry was selected for simplicity since the expressions for the critical values of applied stress to cause fracture were similar for several flaw geometries. The critical conditions are based on a power (energy rate) balance

$$\dot{I} = \dot{F} + 2\dot{D} + \dot{S}E \quad (27)$$

where I is the power input, F is the rate of increase of strain energy, $2D$ is the energy dissipated as heat, and SE is the rate of increase of surface energy. Dots over the symbols indicate differentiation with respect to time.

The thermodynamic conditions for spherical flaw growth were derived in Ref. 113 for a body with a sinusoidally displaced boundary. The final expression for the oscillatory displacement $u = u_o \sin \omega t$ is given as:

$$\begin{aligned} \frac{T}{2a} \left(\frac{a}{b}\right)^6 \left(\frac{b}{u_o}\right)^2 = & \frac{E_e}{4} (1 - \cos 2\omega t) + \sum E_i \left\{ \frac{\omega \tau_i}{1 + \omega^2 \tau_i^2} \right. \\ & + \left[\frac{\omega t}{2} + \frac{\sin 2\omega t}{4} + \frac{\omega^2 \tau_i^2}{1 + \omega^2 \tau_i^2} [\exp^{-t/\tau_i} \cos \omega t - 1] \right. \\ & - \frac{\omega^3 \tau_i^3}{(1 + \omega^2 \tau_i^2)^2} [\exp^{-t/\tau_i} \sin \omega t] \\ & \left. \left. + \frac{\omega^2 \tau_i^2}{4(1 + \omega^2 \tau_i^2)} [1 - \cos 2\omega t] \right\} \end{aligned} \quad (28)$$

where a = initial flaw radius, b = outer radius of the spherical body, and T = surface energy per unit surface area. A series expression was introduced for the relaxation modulus of an arbitrary material as given by Schapery (84). Figure 28 is a plot of flaw growth as a function of time according to Equation 28. Limited experimental results on a well characterized polyurethane elastomer showed a qualitative similarity to the predicted growth-rest cycle of crack propagation. This approach remains to be applied to filled materials such as solid propellants.

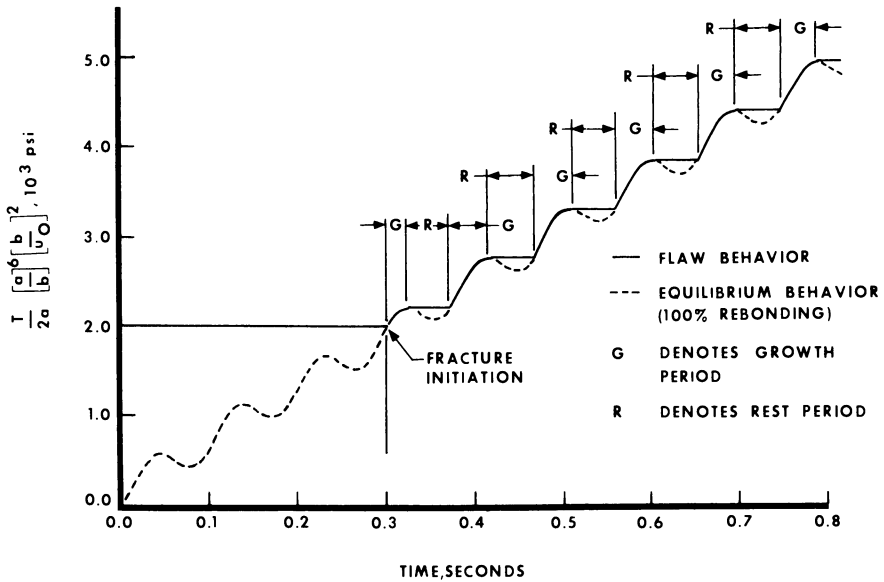


Figure 28. Spherical flaw growth caused by oscillatory displacement $u = u_o \sin \omega t$ for a polyurethane elastomer (5 c.p.s.). Curve generated by Equation 28

Aging

Since solid propellants are composed of a large percentage of energetic ingredients, it should be expected that prolonged storage might result in deterioration. Various ingredients may interact with each other or with the atmosphere to produce irreversible changes which can seriously affect both the ballistic and mechanical properties. Some ingredients may simply decompose, while others may react to produce chemical products which, by themselves, may degrade other materials in the system. Autocatalytic reactions are common, and frequently an ingredient which is a ballistic modifier may produce intolerable changes in the propellant during storage. Plasticizers may migrate and evaporate, gases may be generated, crosslinking and chain cleavage may occur simultaneously. Decomposition of primary ingredients to form products which increase the sensitivity of the propellant is a common problem in double-base systems. Any examination of aging should consider detailed formulations, expected operational environments, and failure modes. Since detailed formulations are generally revealed only in the classified literature, the following discussion is restricted to generalizations about typical aging mechanisms and useful test methods for following the aging behavior of solid propellants. Table III lists various interactions and resultant deterioration which must be considered (23).

This section deals with chemical aging and related physical phenomena, such as diffusion and embrittlement. Apart from the chemical problem there is mechanical deterioration which is also related to long term environmental effects, but this was covered briefly in the preceding cumulative damage discussion.

A prediction of useful life for solid propellant rockets is quite important, from the standpoint of operational readiness and economic considerations. The premature removal and replacement of deployed systems, based on inaccurate storage life estimates, can be costly. A specific missile system and propellant combination could become obsolete while long term storage data are being compiled. Accelerated aging tests are normally used to give qualitative indications of storability, but the deficiencies of these tests are obvious and are discussed later.

Chemical aging may be the result of thermal, oxidative or hydrolytic reactions. The changes observed may be softening, hardening, swelling, discoloration, and gas evolution. These changes may not constitute failure, as such, but should be examined in relation to possible failure modes. Hardening, which is usually accompanied by a decreased strain capability, may result from several conditions. Oxidation may produce discolored and hardened surfaces, continued cure reactions produce over-all modulus increases, and loss of volatile plasticizers also leads to higher modulus. Long term storage at low temperatures may cause embrittlement, whether

Table III. Factors Influencing Propellant Degradation during Aging (23)

<i>Factor</i>	<i>Manifestation</i>	<i>Failure Mode</i>
Change of Chemical State		
A. Chemical reactivity of propellant components singularly or in combination	Hardening, embrittlement, gassing, accumulation of degradation products, viscous flow enhancement, change of adhesivity.	Increased tendency to crack during storage, ignition, or temperature cycling; possible burning rate change, impulse loss, ignition problems, and liner separation.
B. Chemical interaction with environment		Same as A
1. Atmosphere		
a. Moisture		
b. Gaseous or solid decomposition products (autocatalysis)	Same as A; in addition, nonhomogeneity of propellant at surfaces and within bulk.	
c. Air (oxygen, ozone, contaminants in air)		
2. Other materials in motor (liner, metals, etc.)	Same as A	Same as A
C. Factors which may influence rate of change	Time scale of degradation	
1. Temperature		
2. Stress state		
D. Irradiation	Polymer crosslinking or degradation	Same as A
1. Background		
2. Induced		
E. Bacteriological action	Surface changes	Unknown
Change in Physical State		
A. Reversible physical changes		
1. Phase changes which depend on time and temperature	Hysteresis of temperature-dependent physical properties	Increased tendency to crack during storage, ignition, or temperature cycling.
2. Recoverable strains	Probably minor	Probably minor
3. Diffusion of materials	Nonhomogeneity of propellant properties; oxidizer-poor surfaces, porosity, shrinkage.	Crack development, increased tendency to crack during storage, ignition, or temperature cycling.
a. Gases		
b. Plasticizer		
c. Moisture		

Table III. (Continued)

<i>Factor</i>	<i>Manifestation</i>	<i>Failure Mode</i>
B. Irreversible physical changes		
1. Strain beyond reversible limit caused by:	Cracks at fillets, liner separation, viscous deformation, dewetting (blanching)	Increased burning areas and rates.
a. Gravity		
b. Acceleration (during transport)		
c. Thermal gradients		
d. Environmental temperature		

by binder crystallization or by other mechanisms. Softening is usually the result of binder chain scission or crosslink degradation, and may be produced by hydrolytic reactions or thermal decomposition. Moisture effects are particularly pronounced since they not only relate to hydrolysis but may interrupt the binder–filler interface. In some cases the solubility of ingredients in the binder may change with moisture content, and phase changes, solution, and precipitation may occur.

Within this morass of complex chemical and physical phenomena, there is little that has not been examined in some detail, but there is also much less which is sufficiently understood to permit predictive estimates of useful propellant life.

The aging characteristics of double-base and composite rubber binder propellants are substantially different. The primary changes which occur in double-base propellants relate to stability and are variously concerned with “safe storage life,” “safe use life,” and “useful life” (13). The first two categories attempt to define the time beyond which storage or use would constitute a hazard, while the useful life represents the time in which the rocket can be expected to perform reliably. Safe life tests usually consider such factors as the time to autoignition at a given temperature, or the time to the production of fumes of oxides of nitrogen. In some cases the rates of stabilizer depletion at high temperatures are measured and extrapolated to lower temperatures. The time to zero stabilizer concentration is then determined for normal storage temperatures. Depletion rates may be plotted for various temperatures in the form of an Arrhenius plot, and the energy of activation may be determined for a particular stabilizing agent.

So much concentrated effort has been expended on the stabilization of double-base formulations that stability is no longer a limiting factor in determining useful life. Some studies (102) have shown the safe storage life to be greater than 30 years under ordinary conditions.

Table IV. Non-destructive Testing

<i>Condition</i>	<i>Detection Technique</i>
Chemical State	Radiation Reflection or Diffraction Infrared attenuated total reflectance (ATR) Infrared reflectance Ultraviolet spectroscopy X-ray diffraction
	Resonant Response NMR EPR
	Evolved Gas Analysis Mass spectrometer Gas chromatography IR transmission Film sensors External sample analysis
Physical State	
A. Propellant Surface Condition	Visual (Photographic) Observation Boroscope Miniaturized T.V. Microscope Radiation Reflectance or Diffraction Photocell (visible) X-ray diffraction U.V. reflectance spectroscopy γ -Ray back-scatter Scintillation read out Infrared reflectance Radiation emission Infrared scan
B. Dimensional Stability	Profilometer

for Solid Propellants (23)*For Detection of**Other Considerations*

Chemical structural groups; quantitative compositional changes
 Same as above
 Same as above
 Appearance of crystalline degradation products

Poorer than ATR

Frequency of crystalline products occurrence unknown

Chemical structure and compositional changes
 Free radical concentration

Secondary effect; occurrence or correlation not established

Quantitative gases up to mol. wt. of C₆ hydrocarbons
 Same as above

All components

Does not measure grain

Surface cracks; migration products; roughness; accumulation of degradation products; oxidizer concentration owing to moisture; localized dewetting

Subjective observations; traveling mechanisms required

All surface and sub-surface changes that effect reflected radiation density

All physical changes of surface or sub-surface that effect local rate of heat transfer

Slump, liner separation, sub-surface voids, surface cracks

Requires internal traveling mechanism

Table IV.

<i>Condition</i>	<i>Detection Technique</i>
C. Propellant Homogeneity and Density	Radiation Transmission X-ray γ -Ray Scintillation read out Low Frequency Sonic Transmission or Scatter
D. Propellant Physical Properties	Hardness and Hardness Relaxation Sonic Transmission Reflection or Scatter Propellant Samples in Perforation or External to Motor X-ray Diffraction Microwave
E. Adhesive Interface Integrity	Ultra Sonic Reflection or Transmission Low Frequency Sonic Reflection or Transmission Infrared Emission Radiation Transmission X-ray γ -Ray Microwave transmission or reflection

Useful life determinations are similar for both general propellant types since they are primarily concerned with structural integrity. The decomposition or formation of relatively few chemical bonds will normally be undetectable from the viewpoint of ballistic characteristics. On the other hand, the formation of new crosslinks or the cleavage of polymer chains can strongly affect the mechanical properties of polymeric materials. Changes in strength or modulus may cause propellant capability to fall below the structural requirements of particular motor designs. However, some changes may not be deleterious but beneficial.

Many of the tests described earlier have been applied in surveillance studies of solid propellants. Both response and failure characteristics may be followed as a function of time during storage at various conditions. Physicochemical analysis of specimens before and after exposure to

Continued

<i>For Detection of</i>	<i>Other Considerations</i>
Porosity (dewetting) voids, cracks	
Porosity (dewetting) voids, cracks	
Propellant modulus and relaxation rate changes caused by chemical changes or compositional changes owing to migration or absorption	Good potential to provide monitoring of propellant condition at selected points on surface; semi-non-destructive
Propellant modulus	Establishment of correlation required
All physical properties	Correlation not established
Crystallinity changes	Occurrence and correlation of crystallinity not established
Modulus	At low temperature except for metal cases
Liner separations	Developed system
Liner separations	Very high energies required for large grains

determine sol content and crosslink density changes is particularly useful in correlating gross physical property variations. In conjunction with these tests, various nondestructive techniques may provide additional information. The summary in Table IV, taken from a compilation by DeFries and Johns (23), shows the many techniques and devices applied to solid propellant surveillance. Even this extensive list is not complete, and many variations and alternate methods have been proposed over the years. It is especially important to note that nondestructive tests only indicate that a *change* has taken place in the propellant. They do not evaluate the acceptability of the material for its intended application. Such decisions require a knowledge of material characteristics and a practical failure criterion. It has been suggested (30) that propellant aging which results in mechanical property changes may be examined in

reference to a changing failure surface. The aging material may have an associated failure surface which collapses around the origin similar to a deflating balloon. With the passage of time the structural requirements must be reviewed with respect to the new failure surface, and the tolerable limits established.

Laboratory measurements on stored samples are common, but many precautions must be observed. Samples must be representative of the propellant grain, enclosed in its case-liner insulation envelope. Since diffusion paths and exposed surface area may be germane to aging, these characteristics require duplication in aging samples. There is considerable evidence also that samples stored in sealed containers deteriorate much more rapidly and by different mechanisms than those exposed to the atmosphere.

The aging stability of solid propellants may be evaluated in a gross sense by measuring the change in some prominent property such as modulus or tensile strength at various temperatures. The temperature sensitivity of these changes may then be charted on an Arrhenius plot and extrapolated to normal storage temperatures. Such accelerated aging tests are useful in establishing degradation patterns and in guiding the production of propellants with superior aging characteristics. The temptation should be avoided, however, to use these tests in a quantitative, predictive, fashion to determine the useful life of propellant systems. In complex materials such as these some thermally activated mechanisms may prevail at high temperatures, which are relatively unimportant at lower temperatures (13). Used with caution, accelerated aging tests should be, therefore, an integral part of all propellant development efforts. Figure 29 is an example of the extrapolations which can be made from high temperature data. The critical storage time is defined in this case as the time to produce an associated change, by a factor of 2, in the initial maximum stress or in the initial strain at maximum stress.

Other conditions may be imposed upon stored propellant to increase the severity of the environment. In some cases the effects of ambient moisture may be exaggerated by exposure to high relative humidities, and low temperature embrittlement may be accelerated by the appropriate conditioning temperature. These techniques are particularly difficult to interpret owing to the variety of possible interactions and synergistic effects. High humidity can change the low temperature properties of propellants in various ways. Polyurethane propellants have undergone severe modulus increases and rupture strain decreases when tested at -40°F . after several days exposure to 90% relative humidity at 77°F . This has been interpreted (75) as being caused by the ion-dipole effects of dissolved ammonium perchlorate and related to the solubility of water in the binder phase. Other explanations hypothesize "rehealing" (20)

of broken binder-oxidizer bonds, or oxidizer dissolution and precipitation of small, high surface area crystals (56). Specialized techniques have been used to determine the nature of specific degradation reactions, and these have produced useful insight into the aging process. Chemorheological methods described by Colodny *et al.* (21) have been notable in establishing the relative amount of chain cleavage and crosslinking during exposure to various environments. In some cases the site of degradation may be determined, such as random chain or crosslink scission. These methods are based upon the procedures described by Tobolsky (106) in which both intermittent and continuous stress relaxation measurements are used. Tests conducted with unfilled binder materials are revealing, but when highly filled samples are examined, the relaxation process is confused by dewetting and granular interactions.

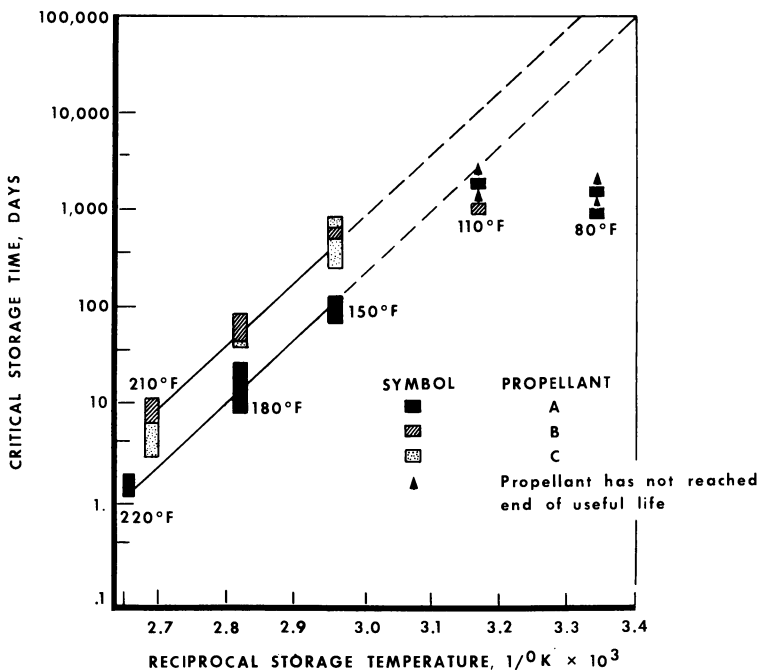


Figure 29. Plot of storage data for three propellant formulations at various temperatures. Critical storage time is defined as the time required for the strain at maximum stress or the maximum stress itself, to change by a factor of 2. Uniaxial constant strain rate data at 0.74 in./min. and 77°F. (44)

Many chemical and physical analysis techniques have been applied to the study of solid propellant aging. Valuable contributions have been made in improving formulations and in establishing confidence in the stability of propellants for a variety of applications. Fortunately, many

formulations have been developed with exceptional aging stability, and predictions of useful life have been exceeded in actual operations. As new, high energy propellants are developed and enter the inventory, degradation will be a more severe problem and improved predictive techniques will be required. Progress in structural integrity analysis, material characterization and failure criteria for solid propellants is continuing and holds the promise that such techniques will be available.

Summary

The preceding discussion has surveyed current approaches and techniques for solid propellant mechanical properties characterization. However, a number of related areas have not been mentioned. The various methods for determining propellant–liner bond strength and evaluating bond deterioration with environmental exposure have not been covered, although bond integrity is a critical requirement of solid rocket motors. Another omission is analog motor testing, an important area because it partially fills the large gap between laboratory and full scale motor tests. Determinations of bulk compressibility, thermal conductivity, and glass transition temperature are also not described. Certainly the topics included here are extensive, and the approaches vary according to discipline and viewpoint. Comprehensive treatments of most testing methods and data reduction techniques may be found in Ref. 44, the “ICRPG Mechanical Behavior Manual.” Review articles in the *Solid Rocket Structural Integrity Abstracts*, currently published by the University of Utah, provide up-to-date surveys of many related topics. These documents are limited in distribution, however, and are, generally, not available to the public.

Acknowledgment

The author expresses his appreciation to N. W. Tschoegl and Donald Saylak for many helpful suggestions and discussions during the manuscript preparation.

Literature Cited

- (1) Aerojet-General Corp. *Rept. 0411-10F* (1962).
- (2) Baltrukonis, J. H., Gottenberg, W. G., Schreiner, R. N., *Proc. U. S. Nat. Congr. Appl. Mechanics, 4th*, 867 (1962).
- (3) Beyer, R. B., *CPIA Publ. 119 I*, 83 (1966).
- (4) Beyer, R. B., *AIAA Solid Propellant Rocket Conf., 6th, Paper 65-169* (1965).
- (5) Bennett, S. J., Anderson, G. P., *CPIA Publ. 94u*, 121 (1965).
- (6) Beatty, J. R., *Rubber Chem. Technol. 37*, 1341 (1964).

- (7) Bills, K. W., Steele, R. D., Svob, G. J., *CPIA Publ.* **119, I**, 547 (1966).
- (8) Bills, K. W., Salcedo, F. S., *J. Appl. Phys.* **32**, 2364 (1961).
- (9) Blatz, P. J., *SPIA Publ.* **PP12**, 17 (1959).
- (10) Blatz, P. J., Bull., *SPIA Publ.* **PP13**, 165 (1960).
- (11) Blatz, P. J., Ko, W. L., *Trans. Soc. Rheol.* **6**, 223 (1962).
- (12) Blatz, P. J., *Rubber Chem. Technol.* **36**, 1488 (1963).
- (13) Boyars, C., *ARS J.* **29**, 148 (1959).
- (14) Briar, H. P., Wiegand, J. H., *CPIA Publ.* **61u**, 455 (1964).
- (15) Britton, S. C., *Solid Rocket Structural Integrity Abstr.* **2 (4)** (1965).
- (16) Brisbane, J. J., *CPIA Publ.* **27**, 337 (1963).
- (17) Burton, J. D., Jones, W. B., Frazee, J. D., *CPIA Publ.* **61u, I**, 191 (1964).
- (18) Chamot, E. M., Mason, G. W., Ed., "Handbook of Chemical Microscopy," pp. 483-488, Wiley, New York, 1958.
- (19) Cluff, E. F., Gladding, E. K., Pariser, R., *J. Polymer Sci.* **45**, 341 (1960).
- (20) Colodny, P. C., Delao, D., Svob, G. J., Lou, R. L., JANAF Surveillance Panel Meeting, San Francisco, Calif. (Dec. 1961).
- (21) Colodny, P. C., Waddle, L. A., Wood, J. S., *CPIA Publ.* **61A, III** (1965).
- (22) Darwell, H. M., Parker, A., Leeming, H., *AIAA Solid Propellant Rocket Conf., 6th, Paper 65-161* (1965).
- (23) DeFries, M., Johns, R. H., Atlantic Research Corp. *Rept.* **RTD-TDR-63-1106** (Aug. 1963).
- (24) Dillon, J. H., *Advan. Colloid Sci.* **3**, 219 (1950).
- (25) Farris, R. J., private communication.
- (26) Farris, R. J., *J. Appl. Polymer Sci.* **8**, 25 (1964).
- (27) Farris, R. J., Steele, R. D., *CPIA Publ.* **119, I, 1** (1966).
- (28) Ferry, J. D., "Viscoelastic Properties of Polymers," Wiley, New York, 1961.
- (29) Fishman, N., Rinde, J. A., *CPIA Publ.* **61u, I** (1964).
- (30) Fishman, N., *Solid Rocket Structural Integrity Abstr.* **III (1)** (1966).
- (31) Fitzgerald, E. R., Ferry, J. D., *J. Colloid Sci.* **8**, 1 (1953).
- (32) Fitzgerald, J. E., *SPIA Publ.* **pp-13/SPSP-8**, 155 (1960).
- (33) Gent, A. N., Lindley, P. B., *Proc. Roy. Soc.* **249A**, 195 (1959).
- (34) Gent, A. N., Lindley, P. B., Thomas, A. G., *J. Appl. Polymer Sci.* **8**, 455 (1964) [*Rubber Chem. Technol.* **38**, 292 (1965)].
- (35) Gottenberg, W. G., Christensen, R. M., Space Technology Laboratories *Tech. Rept.* **6121-6777-RU000**.
- (36) Griffith, A. A., *Trans. Roy. Soc. (London) Ser. A* **221**, 163 (1921).
- (37) Gross, B., "Mathematical Structure of the Theories of Viscoelasticity," Chap. 3, Hermann, Paris, 1953.
- (38) Gumbrell, L., Mullins, Rivlin, R. S., *Trans. Faraday Soc.* **49**, 1495 (1953).
- (39) Haigh, B. P., *Engineering* **190**, 158 (1920).
- (40) Harbert, B. C., *CPIA Publ.* **94u**, 217 (1965).
- (41) Hazelton, I. G., Plank, R. W., *CPIA Publ.* **94u**, 287 (1965).
- (42) Hilzinger, J. E., *CPIA Publ.* **119, I**, 169 (1966).
- (43) Hoebel, J. F., *SPIA Publ.* **PP/14u, II**, 13 (1961).
- (44) "ICRPG Solid Propellant Mechanical Behavior Manual," CPIA, Johns Hopkins Applied Physics Laboratory, Silver Spring, Md., 1963.
- (45) Jones, J. W., Cantey, D. E., *CPIA Publ.* **61u, I**, 203 (1964).
- (46) Jones, J. W., Knauss, W. G., *AIAA Solid Propellant Rocket Conf., 6th, Paper 65-157* (1965).
- (47) Kase, S., *J. Polymer Sci.* **11**, 425 (1953).
- (48) Kelley, F. N., *Appl. Polymer Symp.* **1**, 229 (1965).
- (49) Kostyrko, G. J., Aerojet-General Corp. *Rept.* **TN 229** (Aug. 1963).
- (50) Kruse, R. B., *CPIA Publ.* **2**, 337 (1962).

- (51) Kruse, R. B., Jones, T. M., *AIAA Solid Propellant Rocket Conf., 6th, Paper 65-156* (1965).
- (52) Lake, G. J., Lindley, P. B., *J. Appl. Polymer Sci.* **8**, 707 (1964) [*Rubber Chem. Technol.* **38**, 301 (1965)].
- (53) Landel, R. F., *Solid Rocket Structural Integrity Abstr.* **2**, (1) (1965).
- (54) Landel, R. F., Fedors, R. F., *Trans. Soc. Rheol.* **9**, 195 (1965).
- (55) Landel, R. F., Jet Propulsion Laboratory, *Rept. CB566* (Aug. 1958).
- (56) Landel, R. F., Moser, B. G., Jet Propulsion Laboratory *Tech. Rept.* **32-389** (1963).
- (57) Layton, L. H., *CPIA Publ.* **27A**, 155 (1964).
- (58) Lindsey, G. H., Shapery, R. A., Williams, M. L., Zak, A. R., *Rept. ARL 63-152* on Contract AF 33(616)-8399 to USAF Aerospace Research Laboratories (1963).
- (59) Lindsey, G. H., *Bull. CPIA Publ.* **61u**, 573 (1964).
- (60) Long, E. F., Rainbird, R. W., Vernon, J. H., *CPIA Publ.* **2**, 317 (1962).
- (61) Majerus, J. N., *J. Polymer Sci.* **3** (10) 3361 (1965).
- (62) Majerus, J. N., *J. Spacecraft Rockets* **2**, 883 (1965).
- (63) Marin, J., "Mechanical Behavior of Engineering Materials," Chap. 3, pp. 104-168, Prentice-Hall, New Jersey (1962).
- (64) Martin, D. L., *Bull. CPIA Publ.* **119, I**, 191 (1966).
- (65) Mehdahl, A., *Brown Boveri Rev.* **31**, 260 (1944).
- (66) Messner, A. M., *CPIA Publ.* **27**, 109 (1963).
- (67) "Method for Determining the Tensile Properties of Solid Rocket Propellants," *CPIA Publ. SPIA/PP8* (1956, 1957)
- (68) Milloway, W. T., Wiegand, J. H., *SPIA Publ.* **147, I**, 341 (1961).
- (69) Miner, M. A., *J. Appl. Mechanics* **12**, A159 (1945).
- (70) Mooney, M., *J. Appl. Phys.* **11**, 582 (1940).
- (71) *Ibid.* **19**, 434 (1948).
- (72) Nadai, A., "Theory of Flow and Fracture of Solids," Vol. I, Chap. 15, pp. 175-228, McGraw-Hill, New York, 1950.
- (73) Nicholson, D. E., Blomquist, D. S., Lemon, R. H., *SPIA Publ.* **14u, I**, 271 (1961).
- (74) Oberth, A. E., Bruenner, R. S., *Trans. Soc. Rheol.* **9** (2) 165 (1965).
- (75) Oberth, A. E., Bruenner, R. S., *CPIA Publ.* **119** (1966).
- (76) Phillippoff, W., *J. Appl. Phys.* **24**, 685 (1953).
- (77) Rainbird, R. W., Vernon, J. H. C., *SPIA Publ.* **PP-13**, 39 (1960).
- (78) Rivlin, R. S., *Trans. Roy. Soc. (London)* **A240**, 459, 491, 509 (1948).
- (79) *Ibid.*, **241**, 379 (1948).
- (80) Rivlin, R. S., Thomas, A. G., *J. Polymer Sci.* **10**, 291 (1952).
- (81) Saylak, D., *CPIA Publ.* **2**, 54 (1962).
- (82) Saylak, D., *CPIA Publ.* **27**, 423 (1963).
- (83) Saylak, D., *Appl. Polymer Symp.* **I**, 247 (1965).
- (84) Schapery, R. A., *U. S. Natl. Congr. Appl. Mech.*, **4th**, **2**, 1075 (1962).
- (85) Schapery, R. A., *Solid Rocket Structural Integrity Abstr.* **III** (4) (Oct. 1966).
- (86) Schapery, R. A., ASME Appl. Mechanics Fluids Eng. Conf. Paper **65-APM-15** (June 1965).
- (87) Shapery, R. A., Cantey, D., *AIAA J.* **4** (2) 255 (1966).
- (88) Schwarzl, F., Staverman, A. J., "Die Physik der Hochpolymeren," Springer, Berlin, 1956.
- (89) Seeley, R. D., Dyckes, G. W., *J. Appl. Polymer Sci.* **9**, 151 (1965).
- (90) Sharma, M. G., *CPIA Publ.* **94u**, 297 (1965).
- (91) Sharma, M. G., Lim, C. K., *CPIA Publ.* **119, I**, 625 (1966).
- (92) Siron, R. E., Duerr, T. H., *CPIA Publ.* **119, I**, 657 (1966).
- (93) Smith, T. L., *Trans. Soc. Rheol.* **2**, 131 (1958).
- (94) *Ibid.*, **3**, 113 (1959).

- (95) Smith, T. L., Stedry, P. J., *J. Appl. Phys.* **31**, 1892 (1960) [*Rubber Chem. Technol.* **34**, 897 (1961)].
- (96) Smith, T. L., *J. Polymer Sci.* **1**, 3597 (1963) [*Rubber Chem. Technol.* **37**, 777 (1964)].
- (97) Smith, T. L., Smith, J. R., Stanford Research Institute *Tech. Rept. NOw-61-1057-d* (Oct. 1962).
- (98) Smith, T. L., *J. Appl. Phys.* **35**, 27 (1964).
- (99) Spangler, R. D., *SPIA Publ.* **14c, II**, 23 (1961).
- (100) Spangler, R. D., *CPIA Publ.* **27**, 221 (1963).
- (101) Stedry, P. J., Landel, R. F., Shelton, H. T., *SPIA Publ.* **14c, II**, 43 (1961).
- (102) Steinberger, R., "The Chemistry of Propellants," Pergamon Press, New York, 1965.
- (103) Surland, C. C., Boyden, J. R., Givan, G. R., *SPIA Publ.* **14u, I**, 323 (1961).
- (104) Surland, C. C., Givan, G. R., *CPIA Publ.* **61A, III**, 85 (1965).
- (105) Svob, G. J., Colodny, P. C., Waddle, L. A., and Lefferdink, T. B., *SPIA Publ.* **14u, I**, 307 (1961).
- (106) Tobolsky, A. V., "Properties and Structure of Polymers," Wiley, New York, 1960.
- (107) Tormey, J. F., Britton, S. C., *AIAA J.* **1** (1963).
- (108) Torre, C., *Schweiz. Arch. Angew. Wiss. Tech.* **15**, 116, 145 (1949).
- (109) Treloar, L. R. G., "The Physics of Rubber Elasticity," 2nd ed., Chaps. IV and VII, Clarendon Press, Oxford, 1958.
- (110) Tschoegl, N. W., California Institute of Technology, *Materials Sci. Rept. MAT-SCIT PS 66-6, Quart. Rept.* **8**, Contract AF 04(611)-9572 (May 1966).
- (111) Vernon, J. H. C., *SPIA Publ.* **PP13**, 1 (1960).
- (112) Westergaard, H. M., *J. Franklin Inst.* **189**, 627 (1920).
- (113) Wiegand, J. H., *Am. Rocket Soc. J.*, 521 (April 1962) [*Rubber Chem. Technol.* **37**, 542 (1964)].
- (114) Williams, M. L., Blatz, P. J., Schapery, R. A., Graduate Aeronautical Lab., California Institute of Technology, *Rept. SM 61-5* (Feb. 1961).
- (115) Williams, M. L., "Fracture of Solids," p. 157, Interscience, New York, 1963.
- (116) Williams, M. L., *SPIA Publ.* (1959).
- (117) Williams, M. L., Knauss, W. G., Wagner, F. R., *CPIA Publ.* **119, I**, 681 (1966).
- (118) Williams, M. L., Landel, R. F., Ferry, J. D., *J. Am. Chem. Soc.* **77**, 3701 (1955).
- (119) Wise, J. S., *SPIA Publ.* **14u, I**, 209 (1961).
- (120) Zak, A. R., *CPIA Publ.* **61u**, 501 (1964).

RECEIVED April 14, 1967.

9

Low Pressure Burning of Composite Solid Propellants

JOHAN A. STEINZ and MARTIN SUMMERFIELD

Guggenheim Aerospace Propulsion Laboratories, Princeton University,
Princeton, N. J.

The granular diffusion flame theory is quantitatively valid for various AP propellants in the rocket pressure range 1–100 atm. and in good qualitative agreement with burning data at low pressures (to 0.05 atm.). The complete theory must include the pressure dependence of the kinetic rate of the first stage of the flame—i.e., the exothermic redox reaction between the gases produced by the dissociative sublimation of the solid AP. It is shown theoretically that above 10 atm. this first stage can be treated as having zero thickness, and one can disregard its pressure dependence. Generally, burning rate strands extinguish below 0.1 atm., apparently because unreacted AP escapes from the flame zone, and because convective cooling of the flame at the strand edges becomes dominant; radiation losses are not strong enough to account for the observed extinctions.

The ultimate aim of studying the steady-state burning characteristics and flame structure of composite solid propellants is to deduce enough information about the flame mechanism to be able to predict or modify the combustion performance of any propellant before deciding upon its use. Thus, expensive and time-consuming repetitive experimental testing can be avoided. In this context combustion performance includes erosive burning, dynamic burning rate under rapidly varying pressure, extinction by sudden depressurization, etc., as well as the steady-state burning rate. All these combustion characteristics should be deducible from a knowledge of the structure and internal processes of the flame.

An AP (ammonium perchlorate) composite propellant consists generally of finely divided ammonium perchlorate bonded in a matrix of some suitable plastic fuel. The burning mechanism of a composite solid propellant is quite complex. The flame wave is driven by several physical processes and many chemical reactions acting simultaneously or successively. Burning mechanism research aims to identify the most important physical processes and reaction steps in the flame and incorporate them into a theory of flame propagation that can predict burning rate behavior over the entire range of propellant parameters of interest. Experimental observations of the structural features of the flame and diagnostic measurements of various flame properties are essential for developing a theory based on a valid physical model. However, direct observations are not always possible; in such cases, inferences drawn from comparison between burning rate theory and experiment can help distinguish the roles played by various processes internal to the flame. This combination of flame structure observation and interpretation of rate data is the approach adopted here.

With a view to setting the basis for a valid theory of propellant burning, we summarize next all pertinent experimental information published on the flame structure and burning rate behavior of a composite propellant. The physical picture of propellant burning thus formed is used to evaluate the theories proposed to date.

Previous Studies of the Mechanism of Burning

Flame Structure and Surface Decomposition. Sutherland's (93) thermocouple and spectrographic emission traverses showed the gas flame thickness to be of the order 100μ in the range 1–5 atm. Repeating the spectrographic study of Sutherland with greater care, Povinelli (69) has since found that peak CN emission occurs about 200μ from the propellant surface for pressures from 1 to 4 atm. Neither Sutherland's (93), Cole's (23), nor Silla's (88) direct or schlieren photographs show any evidence of turbulent motion immediately near the regressing surface. However, Sutherland's spatial radiation emission surveys show an unsteadiness indicative of the unmixedness that obviously must be present in the gaseous flame zone. Similar unsteadiness was observed by Derr (26) with the same technique.

While Sutherland's photographs show that KClO_4 propellants have a movable liquid layer on the regressing surface, both his and Bastress' (9) studies indicate that the surface of AP propellants is dry, or at least so slightly molten, as to leave the surface geography rigid. Hightower's (41) observations of pure ammonium perchlorate, both during burning and after extinguishment, show that the pure AP surface is also molten,

but here again the layer is thin (order of microns) and there is no evidence to suggest that it is sufficiently mobile to disrupt the burning surface from a combustion mechanistic standpoint. As another surface feature, Bastress' photographs of extinguished propellants showed that the AP particles protrude above the fuel surface at low pressures during combustion while the opposite is true at high pressures. That the pyrolyzing oxidizer and fuel surfaces must generally lie in different planes is in accord with the "two-temperature" postulate proposed by Schultz and Dekker (83). This is based on the fact that for any given heat feedback situation, the two constituents pyrolyze at the same rate but at a different surface temperatures.

Thermocouple surveys by Sabadell (80) yielded approximate values of 620°C. for the mean surface temperature and 130 cal./gram for the net exothermic heat of decomposition at the regressing surface of PBAA (polybutadiene-acrylic acid) propellants containing 70% AP. Similar values for surface temperature have been given by Powling (71, 74), Beckstead (12), and Selzer (87) for various AP-containing propellants in the range 1-20 atm. As indicated in the Appendix, Sabadell's value of 130 cal./gram for the exothermic heat of decomposition at the surface of a typical AP propellant can be accounted for by assuming that the AP decomposes exothermally to the final products close to the surface and that the binder gasifies endothermally at the surface. No evidence of significant solid-phase reactions has yet been found. In fact, microscopic observations with spatial resolution of the order of 1-2 μ were made by Hightower (40) of the surface region of an AP composition propellant after it had been extinguished and sectioned, and clear visual evidence was reported to the effect that no significant subsurface reactions took place in the solid phase heatup zone. Similar observations were reported by McGurk (59).

It is generally agreed (32, 49, 97) that the heat of decomposition of pure AP is liberated very close to the AP surface. Jacobs' (48) results suggest that at least for temperatures above about 350°C., the exothermic part of the reaction occurs in the gas phase. Levy and Friedman (54) concluded that to account for their observed regression rates of pure AP, the gas-phase reaction zone must be less than 1 μ at 100 atm. and of the order of a few microns at atmospheric pressure. This is considerably less than the thickness of the fuel-oxidant flame found by Sutherland (93) and Povinelli (69). Others (45, 98, 100) have used test results obtained by differential thermal analysis to argue that exothermic solid-phase reactions could be significant in driving the flame. Wenograd (98, 100) stated that inserting his values for the exothermic heat release of pure AP (thought to be caused only by solid-phase reaction) and for the apparent kinetic rate of decomposition, both measured with a different thermal

calorimeter type apparatus, into a Semenov-type flame speed formula applied to the solid phase, yields a regression rate in agreement (factor of 2) with observed propellant burning rates at atmospheric pressure. However, it is not clear how such solid-phase reactions could cause the usual pressure dependences observed with pure AP and with AP-containing propellants. Also, the DTA curves are far from reproducible; the details of the calculations for all the curves have not been reported as yet. When the heat release rates obtained from the thermal decomposition results of Wise (77), Wenograd (100), and Coates (22) at low temperatures are extrapolated to near surface temperatures, whatever energy is released in the solid phase must occur within a relatively thin zone near the surface, only about 5μ thick (or less) at normal rocket operating pressures. However, Flanigan (28) calculated that even though the temperatures in the solid phase are high enough for condensed-phase reactions to occur, the stay time (compared with the reaction time) is too short to affect the over-all burning rate. Therefore, this solid-phase flame zone model does not make a logical physical model. It can't exist.

Bircumshaw and Newman (14) showed that the mode of degradation of pure AP depends on the prevailing pressure and temperature. *In vacuo* and below 300°C ., only 30% decomposition occurs. The remaining 70% is a porous solid residue which does not react further unless "rejuvenated" by exposure to a solvent vapor. Jacobs (48) found that moderate pressures of ammonia retarded this low temperature reaction. If only the temperature is raised to 280°C ., decomposition remains constant at 30%, but pure sublimation increases with increase in temperature. Beyond 280°C ., sublimation still increases with increase in temperature, but the amount of decomposition decreases with increase in temperature. Above 400°C ., no solid residue remains. Increased pressure retards pure sublimation and increases the extent of chemical reaction. Sublimation was hardly noticeable at atmospheric pressure. Neither infrared (55) nor mass spectroscopic (36) investigations could reveal the presence of the NH_4ClO_4 molecule in the gas phase. Thus, as is generally agreed (32, 49, 97), AP degradation involves as a first step dissociative sublimation of a loosely held $\text{NH}_3:\text{HClO}_4$ complex, physically adsorbed at the decomposing AP surface. Further chemical reaction between the gaseous NH_3 and HClO_4 is then possible, depending on the prevailing physical conditions.

Recently, Jacobs (48) proposed a unified mechanism incorporating this dissociative sublimation step. He imagines the step towards the adsorbed state to be accomplished by proton transfer. At low temperatures, both NH_3 and HClO_4 desorb but recombine in the gas phase to form gaseous NH_4ClO_4 —*i.e.*, pure sublimation occurs. At low temperatures and increased pressures, NH_3 does not desorb but remains physically

adsorbed and inhibits further desorption of the perchloric acid, which decomposes in the gas phase. As the temperature is increased, NH_3 is driven off the surface and reacts with the decomposed perchloric acid. Jacobs' pressure measurements show that here—*i.e.*, at significant pressure and above about 350°C .—the over-all decomposition, consisting of dissociative sublimation of AP followed by reaction between NH_3 and HClO_4 , has an activation energy of 39 kcal./mole. His weight loss measurements give 30 kcal./mole for the activation energy of the dissociative sublimation step. Sammons's (81) differential thermal analysis of commercial grade AP yielded the same result.

It can be calculated that the apparent activation energy during linear pyrolysis (as opposed to bulk degradation) would then be about 15 kcal./mole (*see below*). Thus, the value of 16 kcal./mole determined by Schultz and Dekker (85) and Coates (22) with their linear pyrolysis experiments agrees well with bulk degradation experiments.

[Consider decomposition to occur in a layer of thickness L_s below the surface regressing at rate r . Then the rate of decomposition below the surface is:

$$\dot{m} = \rho_c \epsilon L_s = \rho_c r$$

where $r =$ (regression rate) $\sim \exp(-E_s/RT_s)$

$$\epsilon = \text{(reaction rate)} \sim \exp(-E_B/RT_{eff})$$

and $L_s =$ (thermal wave thickness) $= (\alpha_c/r)$

From the above one obtains:

$$r \sim \exp(-E_s/RT_s) \sim \exp(-E_B/2RT_{eff})$$

Calculation of the rate of decomposition in the solid phase shows that it is significant only when T_{eff} approaches T_s . Thus, $T_{eff} \approx T_s$, and the apparent activation energy during linear pyrolysis is half of that measured in bulk degradation experiments. This conclusion can also be inferred from the relations given in Ref. 35.]

Although these low temperature bulk degradation experiments provide insight into the detailed mechanism of AP decomposition, it is doubtful whether kinetic rates obtained from such experiments can be extrapolated over many orders of 10 to the temperatures typically encountered at the propellant surface, especially since degradation in bulk is not the same as degradation at the surface of the sample.

Ammonium perchlorate is a monopropellant which is exothermic in its decomposition to the extent of 270 cal./gram (1, 30, 54), based on measured decomposition products, and has a measured adiabatic flame temperature of 950°C . (1, 54) (*see Table I*). The dissociative sublimation step is zero order and is endothermic to the extent of 500 cal./gram

(44, 73, 85). The exothermic gas phase reaction between NH_3 and HClO_4 is believed to be second order (97). Friedman (54) found that pure AP can not burn below 27 atm. and suggested that the growing importance of radiative heat loss from the burning solid surface of AP may cause this. However, a heat loss is required that is at least five times larger than can be accounted for by radiation alone (51). In fact, Horton and Price (42) found that minimizing radiative heat loss by using cylindrical grains instead of end-burning grains did not lower the extinction pressure of pure AP. However, the use of an epoxy resin surface inhibitor lowered the extinction limit from 23 to 3 atm. Thus, the burning process becomes more inefficient (2, 29) as the lower combustion limit is approached. Calculation of the heat liberated during AP combustion based on the composition measurements of Powling *et al.* (1) and Friedman *et al.* (54) (see Table I) shows that AP burns inefficiently (about 20% less heat liberated than for the case where the products of combustion are in equilibrium). These calculations also suggest that the inefficiency grows with decreasing pressure. Powling *et al.* (1) found that a minimum temperature of about 950°C . is necessary for continued steady burning of pure AP. For example, they found that the addition of only 3.85% paraformaldehyde depresses the lower limit to 1 atm. Here they measured the flame temperature to be 1000°C ., which compares well with Friedman's value of 950°C . at 27 atm. for pure AP. Therefore, the presence of the fuel assists the AP flame by providing a hotter environment which helps overcome the reaction's incompleteness.

Far less is known about the decomposition mechanism of the fuel constituent. Gasification at the surface involves scission or unzipping of the polymer chain to form generally a mixture of monomer units and chain fragments of varying sizes (31, 56). This process is assumed to be endothermic and zero order. In some cases, such as carboxyl-terminated polybutadiene (81), the decomposition can be exothermic. Activation energy for the surface decomposition appears to vary between 10 and 40 kcal./mole, depending on the polymer type (86) and decomposition temperature (21, 22, 86). A number of mechanisms have been proposed which consider the breaking of the chemical bonds to be the rate-determining step (86), but they differ as to the point of scission along the polymer chain. Unfortunately their predictions are too close to permit identification of the correct mechanism (86). Chaiken (21) suggested that monomer formation and diffusion in the surface substrate is rate controlling at low temperature but that at high temperature, desorption of the monomer is the rate-determining step. At this stage, interpretation of propellant burning behavior in terms of the detailed structure of the binder is extremely difficult. We must await more definitive results of further research on polymer degradation mechanisms.

Table I. Calculated and Measured Combustion

Mole Product per Mole AP	Equilibrium Calculations				Measurements ^a		
	<i>Beachell and Hackman (11)</i>				<i>Levy and Friedman (54)</i>		
	<i>P, atm.</i>	<i>1</i>	<i>34</i>	<i>64</i>	<i>100</i>	<i>1</i>	<i>68</i>
T _o , °K.	298	298	298				°
T _F , °K.	1375	1397	1403	1440			1203
H _R , kcal./mole ^b	38.3	39.2	39.5	39.5	31.4	32.7	
h _R , cal./gram ^b	326	334	336	336	267	278	
N ₂	0.50	0.50	0.50	0.50	0.13	0.27	
O ₂	1.24	1.22	1.20	1.16	0.68	1.02	
Cl ₂	0.02	0.07	0.09	0.08	0.50	0.12	
HCl	0.96	0.86	0.82	0.82	—	0.76	
H ₂ O	1.52	1.57	1.59	1.59	2.00	1.62	
NO	—	—	—	—	0.55	0.23	
N ₂ O	—	—	—	—	0.10	0.12	
NOCl	—	—	—	—	—	—	
HClO ₄	—	—	—	—	—	—	
Cl	0.01	—	—	—	—	—	

^a Mole fractions adjusted slightly to achieve mass balance.

^b Heat of reaction calculated from product gas composition using heats of formation (50).

The above observations lead to the following conclusions:

(1) The burning surface of an AP composite solid propellant with most fuels is effectively dry. Its character is rough, with the oxidizer particle surfaces protruding above or receding below the fuel surface, depending on the relative pyrolysis characteristics of these two constituents. A dry surface affords no opportunity for premixing of the issuing decomposition gases; these gases enter the gaseous reaction zone unmixed.

(2) The surface decomposition process of AP propellants is net exothermic, with heat absorbed at the AP and fuel surfaces by endothermic pyrolysis but with more heat liberated in the gas phase close to the AP crystals. In detail, decomposition at the AP surface consists of endothermic pressure-independent solid-to-gas phase dissociative sublimation, followed by exothermic pressure-dependent gas-phase oxidation. The over-all reaction for the AP decomposition is pressure dependent.

(3) Above the decomposing surfaces of AP crystals and exposed solid fuel a diffusion flame exists, which represents the reaction between fuel and oxidant vapors.

(4) Compared with the AP decomposition flame thickness, the fuel-oxidant redox flame extends a much greater distance from the propellant surface and depends on the rate of both chemical reaction and diffusional mixing.

Products and Heat of Reaction for Pure AP

Measurements ^a		Composition Claimed as Representative by Bircumshaw and Newman (14, 15); also Cited by Huggett (43)		Analysis of B&N (14, 15) Data by Geckler (30)
Aarden et al. (1)		T < 300°C.	T > 350°C.	
1	72			
550 ^d	293			
1243	1203			
28.7	32.4	°	°	29.4
244	276			250
0.09	0.14	—	—	—
0.73	0.98	0.75	0.50	0.60
0.35	0.18	0.50	0.50	0.20
0.30	0.65	—	—	0.30
1.85	1.67	2.00	2.00	1.80
0.54	0.16	—	1.00	0.40
0.15	0.23	0.50	—	—
—	—	—	—	0.20
—	—	—	—	0.10
—	—	—	—	—

[°] Radiative augmented burning at 1 atm.

^d Preheated at 1 atm.

^e Too inaccurate to calculate reliable heat of reaction.

These observations provide the basis for the physical model of the flame zone shown in Figure 1.

Composite Propellant Burning Rate Behavior. Figure 2 shows typical composite propellant burning rate data obtained to date. Generally, around 100 atm. the pressure exponent (n in the empirical equation $r = ap^n$) is about 0.3, and near 1 atm. it lies between 0.6 and 0.9, depending on the propellant type. Such burning rate data are best correlated by the equation:

$$1/r = a/p + b/p^{1/3} \quad \text{or} \quad p/r = a + bp^{2/3}$$

(where r = burning rate, p = pressure, and a and b are constants termed the chemical reaction and diffusion time parameters, respectively). The particle diameter d is contained in the parameter b . This expression is the result of the granular diffusion flame theory proposed by Summerfield in 1956 (93). (An improved version of this theory is presented in Ref. 92.) To test the validity of this theory, burning rate data are plotted as (p/r) vs. $(p^{2/3})$; they should fall on a straight line. Experimental work at Princeton commenced with Sutherland's (93) and Webb's (99) studies of the burning rate pressure dependence of AP-polystyrene propellants.

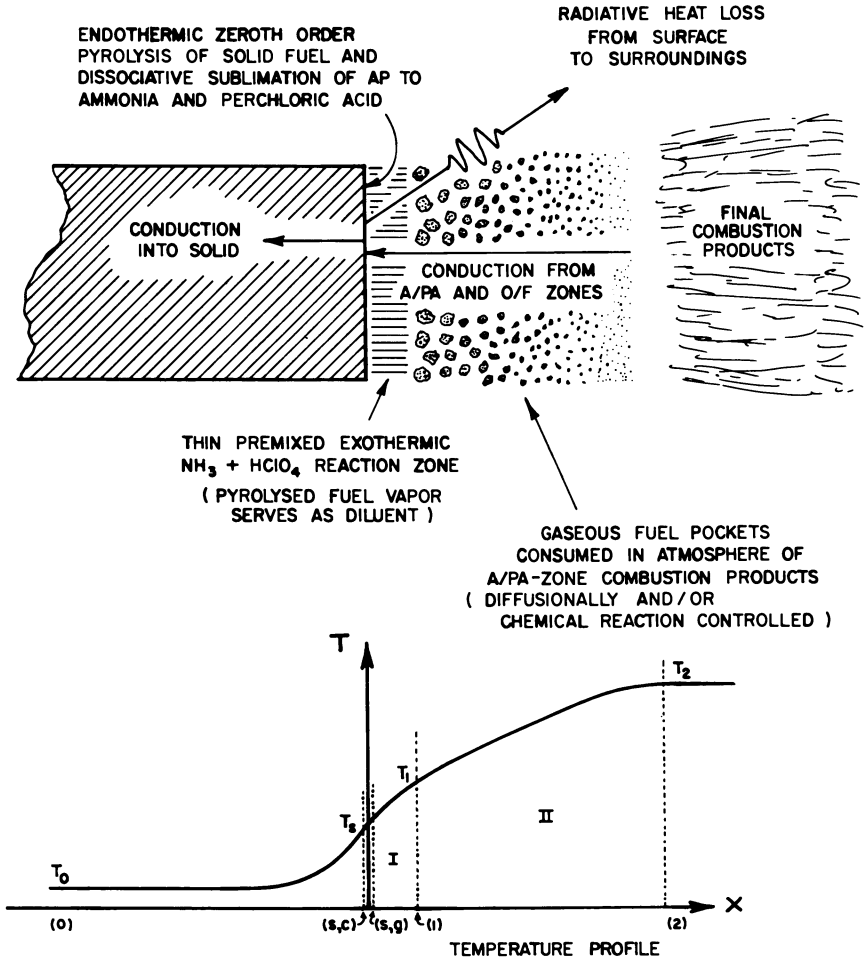


Figure 1. Two-stage granular diffusion flame model for ammonium perchlorate-type composite solid propellants

This was followed by Taback's (94) study of the effect of copper chromite catalyst additives. In general, the results of these investigations fitted the Summerfield relation remarkably well over the range 1–100 atm. (Figures 3 and 6). Moreover, the effects of propellant composition and oxidizer particle size on the constants a and b , respectively, were consistent with qualitative predictions from the theory. Similar results have since been obtained by Yamazaki (101), Marxman (18), and the group at ONERA (8, 52, 64) in France (Figure 7). An alternative to the above equation has been proposed by Penner *et al.* (68)—i.e., $(1/r)^2 = (a/p)^2 + (b/p^{1/3})^2$. A systematic survey (91) of all available data shows that when

this equation does fit the data, it is only for those values of (a/b) for which this equation is virtually identical to the equation:

$$1/r = a/p + b/p^{1/3}$$

Bastress (9) systematically studied the effect of oxidizer particle size on burning rate using narrow unimodal distributions. While his rate data for bimodal propellants and for highly loaded unimodal propellants with mean particle size between 20 and 200 μ fitted Summerfield's relation quite well over the range 1–100 atm., the rate data of his underoxidized propellants could not be correlated by this relation, especially for very small unimodal particle size distributions (*see also* Refs. 90 and 91). Here, a new phenomenon seemed to be taking over. Also, as predicted earlier (92), propellants with large particles did not obey the law because the scale of heterogeneity of the burning surface is no longer small compared with gas-phase flame thickness. One-dimensionality obviously breaks down.

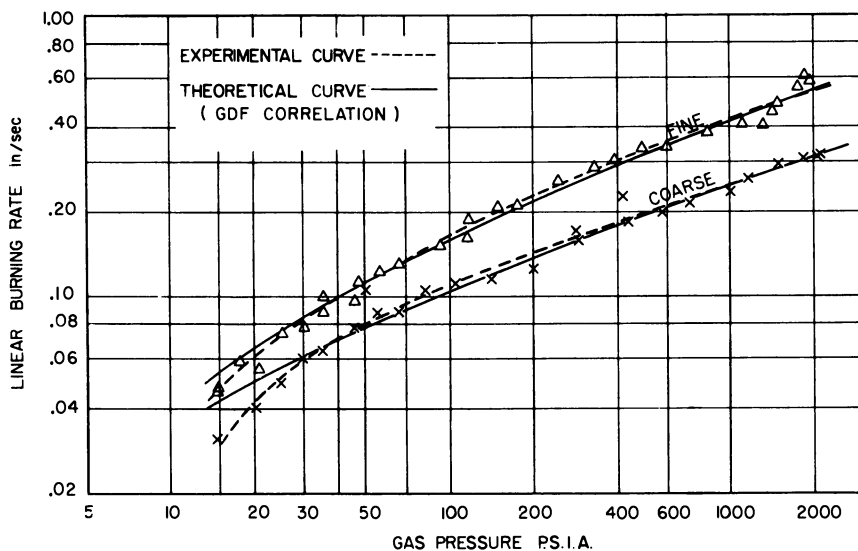


Figure 2. Pressure dependence of burning rate of a composite solid propellant with 75% AP + 25% polyester resin (99)

With the small mean particle sizes ($\sim 15\mu$ and less), it was found for underoxidized propellants that pressure increase would cause the burning rate to increase, reach a plateau, decrease, and then possibly extinguish at some critical pressure. Where extinction did not occur, the burning rate would continue to decrease after the plateau, reach a minimum and then again increase monotonically. Further reduction of oxidizer content accentuated the tendency toward plateau behavior. The

latter observation has also been reported by Rumbel *et al.* (78, 79). Reid (75) has shown that the pressure range over which extinction occurs depends on strand-size. Barrere's (8) photographic studies have demonstrated the existence of temporary localized extinctions in the plateau burning range. Bastress suggested that this behavior may be caused by intermittent random local deficiencies of oxidizer on the regressing surface, as a result of the peculiar individual pyrolysis characteristics of the fuel and oxidizer components. Obviously, such a mechanism could not have been deduced from the present granular diffusion flame (GDF) theory, which treated the solid propellant as a one-dimensional field and disregarded the known complexities of the surface as a secondary and therefore negligible aspect of the flame structure.

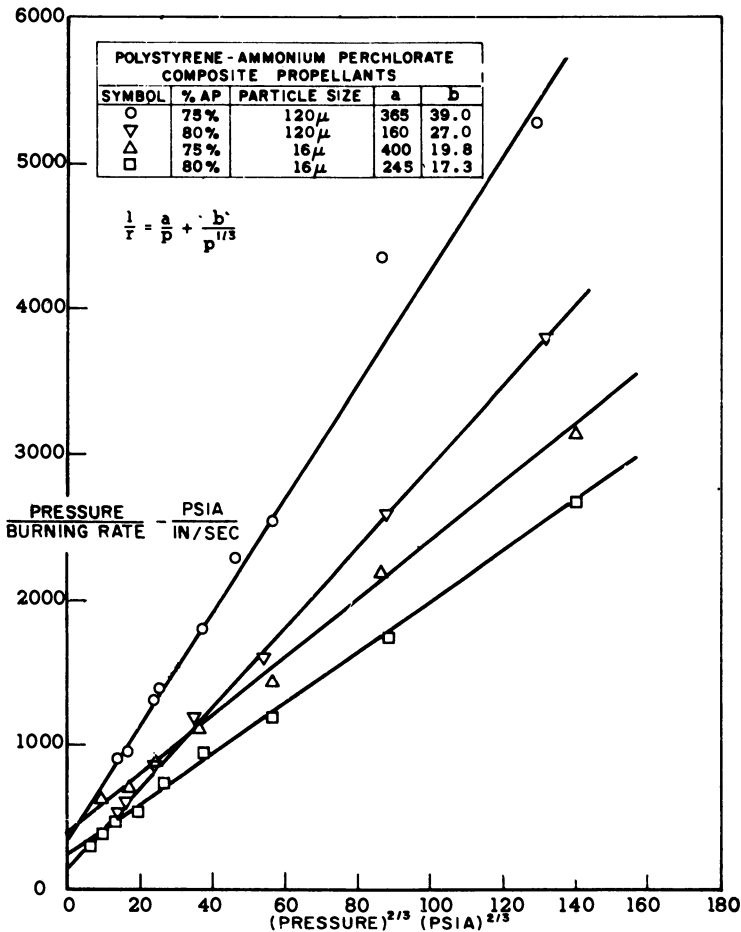


Figure 3. Burning rate data plotted to test validity of granular diffusion flame theory (93)

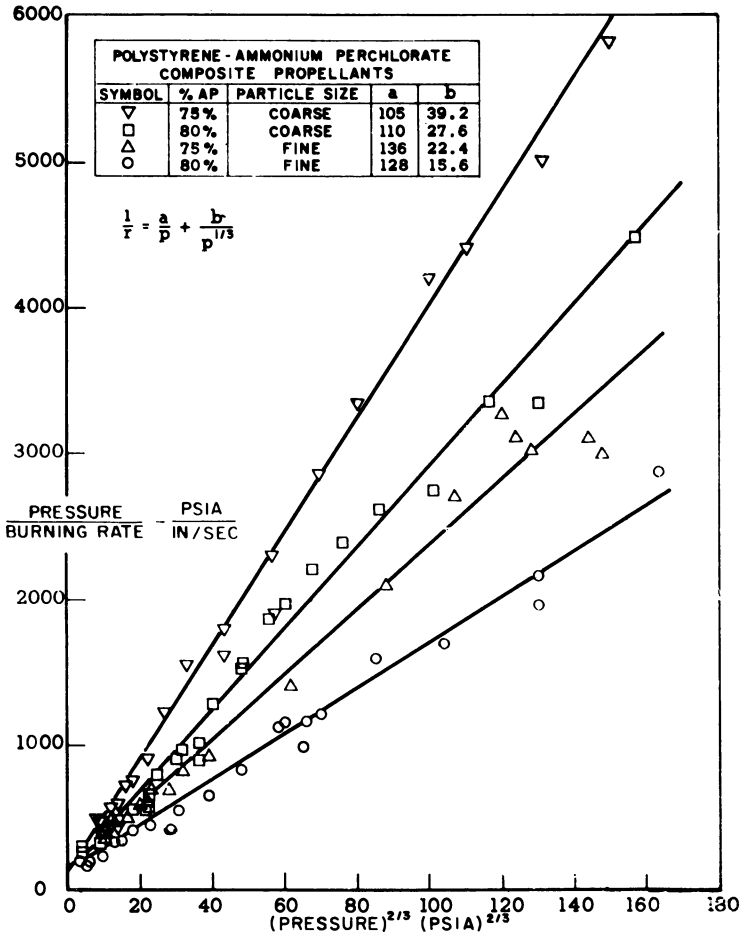


Figure 4. Burning rate data plotted to test validity of granular diffusion flame theory (99)

Further limitations of the GDF model were revealed by studies of burning rates at both high and low pressures. Above about 200 atm., various AP propellants display an increase in the pressure exponent with an increase in pressure (24, 33, 46). In the range 50–200 atm., it tends to be about 0.3–0.4 as predicted by the GDF theory, but in the range of 300–1000 atm. it is of the order 1.5–2.0. There is no good theory for this. One study (33) showed the tendency for the burning rate to become independent of binder properties and AP particle size in this high pressure range; no theory exists for this either.

The data of Webb (99) and Silla (88) for polystyrene propellants bear out the prediction of the GDF theory that the pressure exponent

approaches unity at 1 atm., whereas the exponent is about 0.3–0.4 at 100 atm. More careful experiments by Cole (23) and Most (60), however, showed that polysulfide and polybutadiene acrylic acid (PBAA) propellants have a pressure exponent of about 0.6 to 0.7 in this low pressure range (*see* Figure 15). They also revealed that some dependence of burning rate on oxidizer particle size persists to the lowest pressures at which burning rates could be measured. Feinauer (27) found that adding 2% carbon black to PBAA–AP propellant causes the burning rate *vs.* pressure curve to bend downward below about 0.2 atm. These low pressure phenomena have been unexplained until now; the GDF theory as previously published failed on these points. The work reported here was directed particularly at these questions.

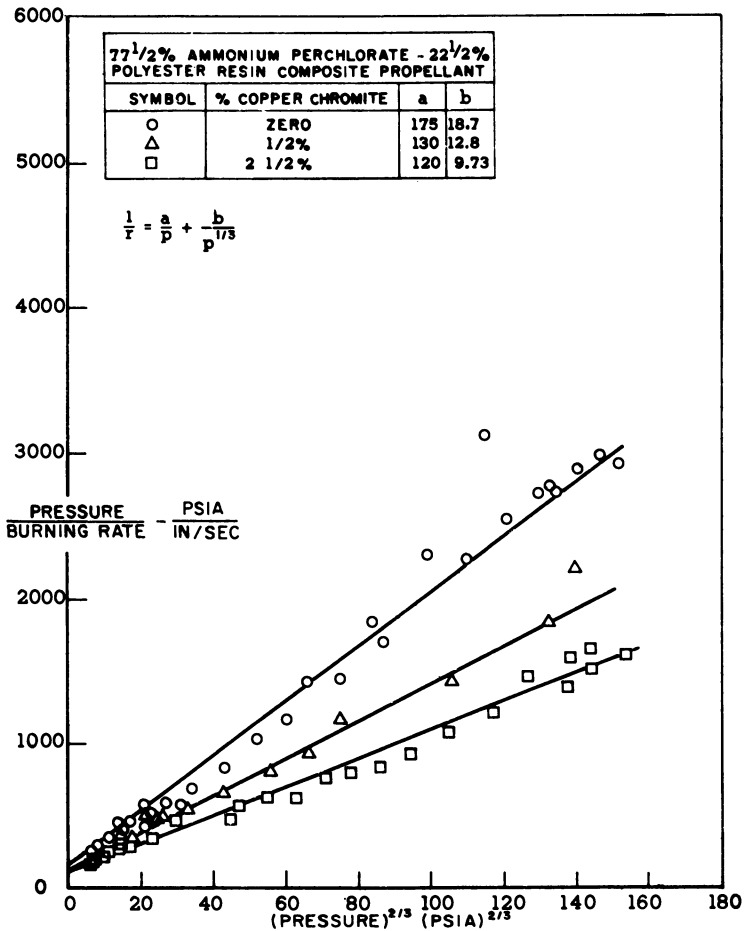


Figure 5. Burning rate data plotted to test validity of granular diffusion flame theory (95)

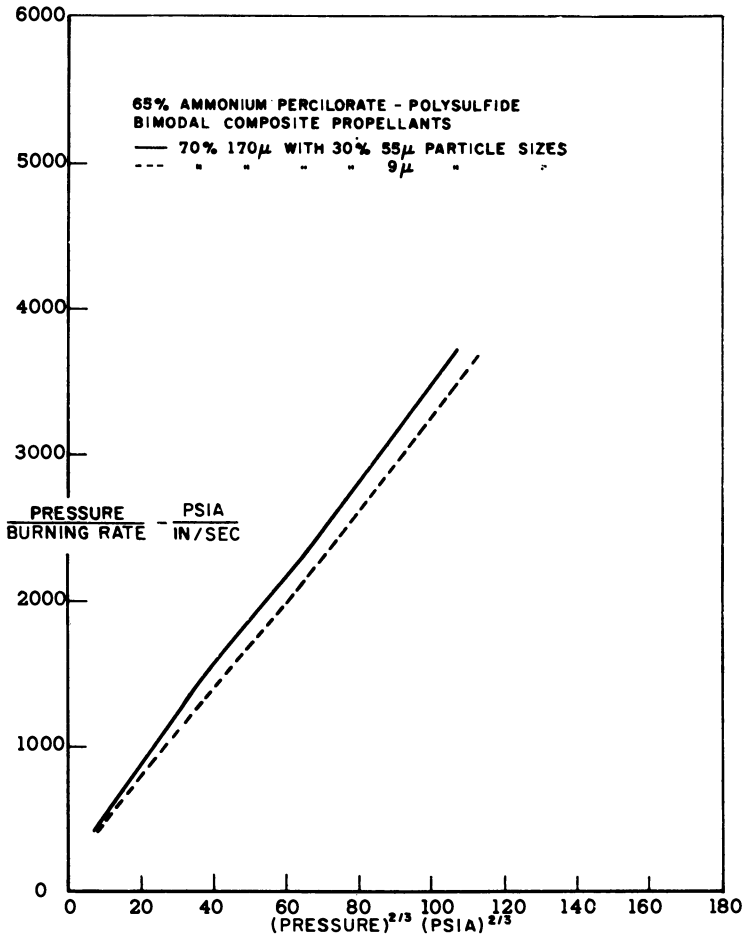


Figure 6. Burning rate data plotted to test validity of granular diffusion flame theory (10)

Theories of Burning of Composite Propellants. Experimental results such as those above have guided the development of various theories proposed to date. These results have also helped define the regions of validity of each theory. A primary requirement of any "true" theory of composite propellant burning is that it must take account of the initial "unmixedness" of the fuel and oxidizer gases emerging from the regressing surface. Such a theory must be able to predict the effect of such variables as propellant composition, temperature, and pressure. Unfortunately, the science has not yet progressed to the stage where predictions of the absolute magnitudes of burning rates can be made.

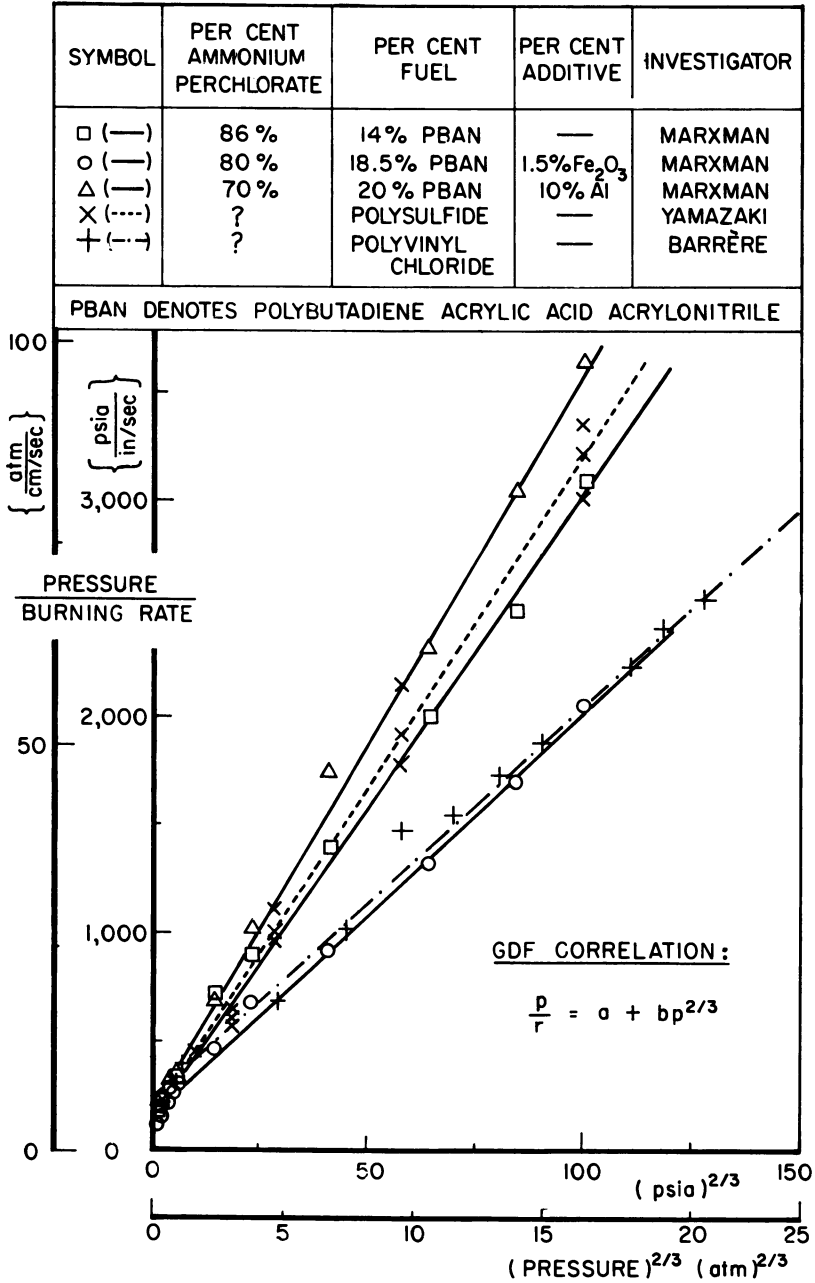


Figure 7. Burning rates plotted to test validity of granular diffusion flame theory

A number of diffusionally controlled flame models have been proposed. The first, a columnar diffusion flame model, was proposed by Rice (76) in 1945. Here the flame was assumed to occur at the interface between fuel and oxidizer streams pyrolyzing off the regressing surface. Although the model gives the correct qualitative dependence of burning rate on oxidizer particle size, neglect of finite reaction times and the assumption of a columnar flame geometry combine to cause the burning rate to be insensitive to pressure. The latter prediction is contrary to experimental observations. The theory was refined by Nachbar (61, 62, 63) in 1957. The burning rate was calculated for a geometrically simplified model consisting of alternate slabs of fuel and oxidizer. Owing to omission of finite gas-phase kinetics, this theory suffers from the severe shortcoming of having burning rate independent of pressure.

If finite chemical reaction times are put into the columnar diffusion flame theory (76), burning rates are predicted to be linearly proportional to pressure at low pressure and independent of pressure (plateau burning) at high pressure. Based on this model, von Elbe *et al.* (97) proposed the simple equation:

$$1/r = a/p + c$$

In a systematic survey of all available burning rate data, we have found that this equation does not fit well at all. These findings are reported in detail in Ref. 91. Further, it is known that normal burning propellants have a pressure exponent around 0.3 in the range 70–100 atm. (this model predicts much less) and that plateau burning is associated with the phenomenon of intermittent burning, which is not incorporated in this model. Thus, a different flame structure must be assumed, as Summerfield did in his GDF theory (92). He assumed that local surface disturbances during decomposition cause the fuel gases to leave the surface in tiny pockets which burn up in the surrounding atmosphere of oxidizer decomposition products; he also assumed that the average fuel vapor mass per pocket is independent of pressure. Based on the hypothesis that at low pressure the burning rate is a rate-controlled chemical reaction while it is diffusionally controlled at high pressure, two asymptotic forms for burning rate were obtained. The burning rate at intermediate pressure was then expressed in the simplest way by joining these two asymptotic forms as follows:

$$1/r = a/p + b/p^{1/3}$$

The theory has been remarkably successful concerning the effects of pressure and particle sizes over wide ranges of these variables.

This burning rate equation has been tested by McAlevy (58) with a so-called analog propellant. [The technique was first seriously exploited by Burger and van Tiggelen (17, 96).] In one form this propellant con-

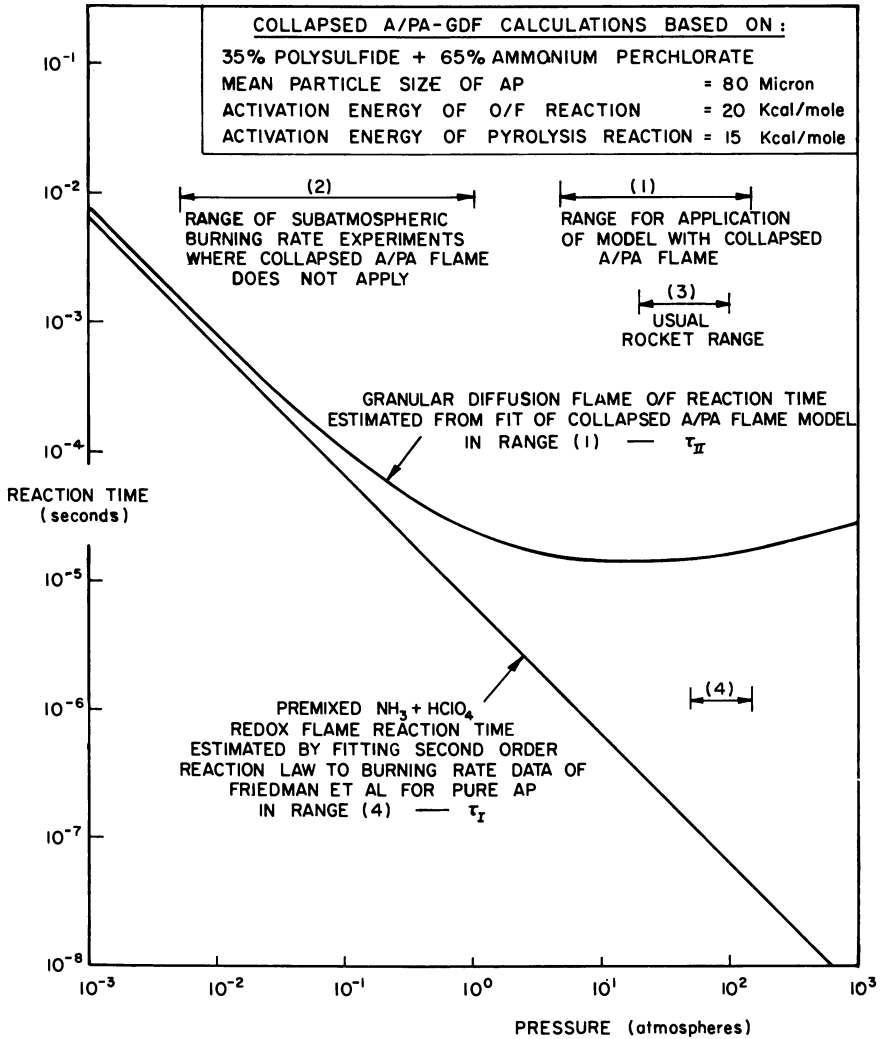


Figure 8. Pressure dependence of reaction times of ammonia-perchloric acid and oxidant-fuel reactions

sists of a permeable solid fuel made by lightly compacting a quantity of solid fuel spheres of submillimeter size; when a gaseous oxidizer flows through the resulting fuel body, a granular diffusion flame analogous to that of a composite solid propellant is formed. In another version, the permeable solid is made of ammonium perchlorate, and a fuel gas flowing through it supports the propellant-like flame. In McAlevy's experiments (58), measurements of mass burning rate as functions of pressure, mixture ratio, and particle size fell in line quantitatively with the above

equation. In addition, by studying the factors that affected the measured value of b , McAlevy concluded that b is directly proportional to the mean pore size between the oxidizer particles—*i.e.*, to the size of the fuel pockets. He showed that b would be somewhat sensitive, therefore, to mixture ratio as well as to oxidizer particle size.

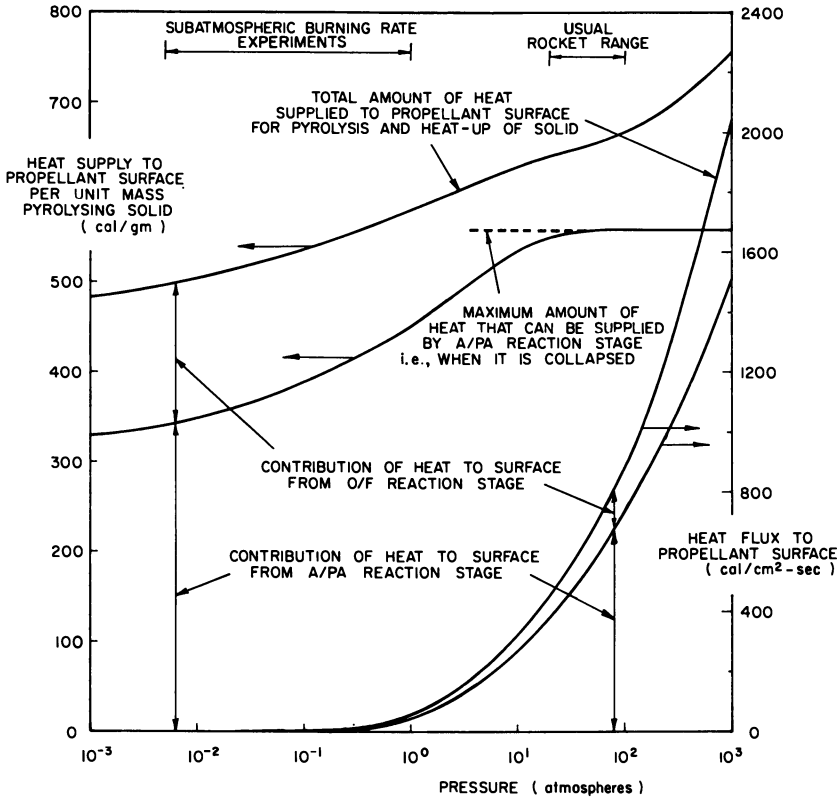


Figure 9. Heat supply to propellant surface by A/PA and O/F stages in the granular diffusion flame model

Arguing that the surface temperature of ammonium nitrate must be considerably less than that of typical binders during steady burning ($\sim 600^\circ\text{K}$. compared with $\sim 1000^\circ\text{K}$. respectively), Andersen (6) surmized that the fuel-oxidizer gas-phase reaction might be too far from the oxidizer surface to affect its regression rate. This idea of a burning rate controlled solely by an exothermic oxidizer decomposition reaction is the essence of the thermal layer theory developed by Chaiken (19). Although the physical picture might be roughly valid for ammonium nitrate propellants (the evidence is meager), the prediction that the burning rate depends linearly on pressure and is insensitive to fuel-

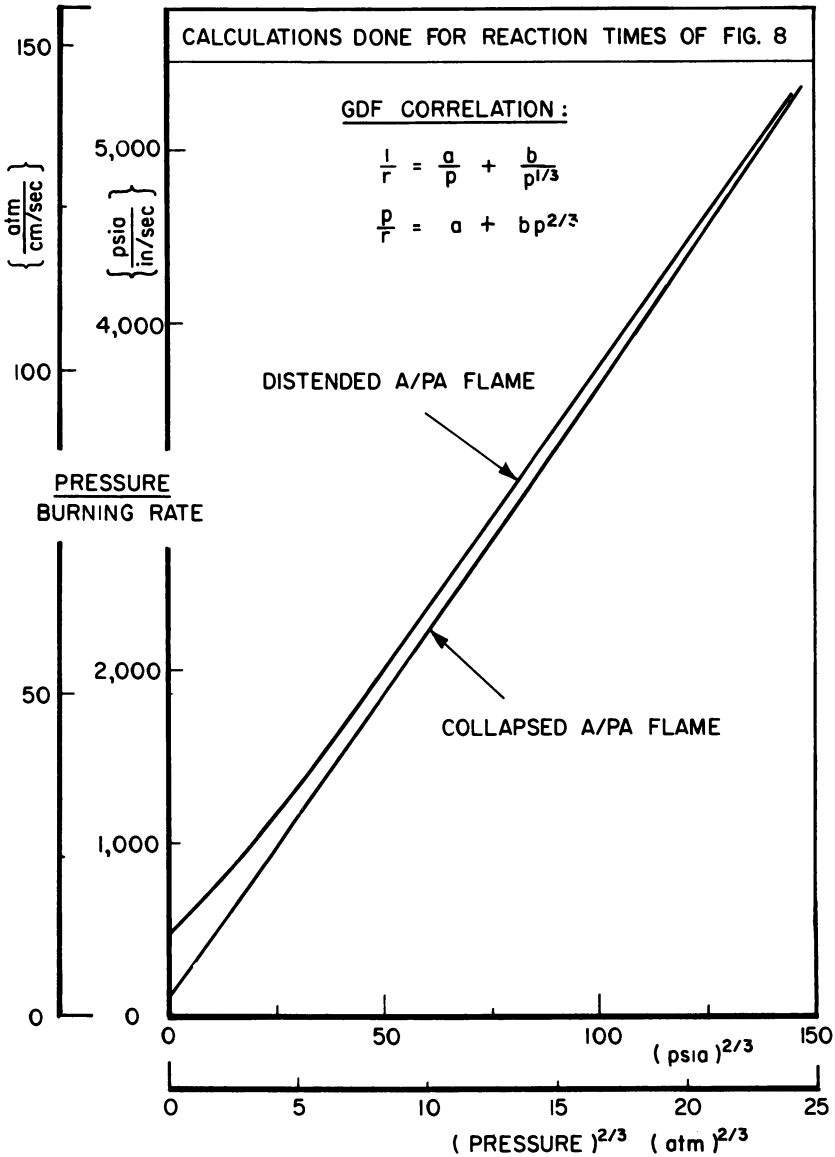


Figure 10. Granular diffusion flame theory predictions plotted as (p/r) vs. $(p)^{2/3}$ for collapsed and distended A/PA flames

oxidant mixture ratio renders it invalid for AP propellants from 1–100 atm. In the later revision (20) of the model, designed to correct the pressure effect and the mixture ratio effect, two adjustment parameters were included to allow for a small (unknown) amount of mixing of fuel and oxidizer decomposition products, supposedly microscopically close to

the AP particle surface. Unfortunately, these parameters then had to be made continuously variable functions of pressure to fit the measured rate *vs.* pressure curve. No burning rate predictions are possible with this theory until quantitative expressions are found for these two factors, even if they exist.

The fact that the pressure exponent of AP propellants at high pressures (200–1000 atm.) is of the order of 1.5 to 2.0 suggested to Irwin *et al.* (46, 47) that small cracks may be formed in the surface of the oxidizer, causing the exposed oxidizer surface area to increase progressively with increasing pressure. Then, on the assumption that the burning rate is controlled only by the oxidizer decomposition flame at these very high pressures, this exposure would increase the burning rate and the pressure exponent. The model has been translated into analytical form but has not been proved. In a parallel effort based on Bastress's earlier hypothesis, Hermance (37, 38) has formulated a model that emphasizes the role of the flame of the individual AP particle in determining the burning rate of the propellant, but it is difficult to reconcile his elaborate physical model or his detailed assumptions with experimental observations of the structure of the flame or of the surface. While the predictions can be made to fit Bastress's (9) underoxidized propellant burning rate data (near plateaus) over the range 5–100 atm. and 20–200 μ oxidizer particle size, the model does not include those features of the flame that are clearly responsible for the near plateaus—*i.e.*, intermittent burning at the surface. The concept of a flame around the individual oxidizer particle supported by fuel vapor from the surrounding fuel binder is probably important at very high pressures, instead of the quasi-one-dimensional flame; hence, for this regime the Hermance paper may be an interesting idea.

Other models of propellant burning, some of which have not been formulated mathematically, have also been advanced. Hicks (39) suggested that, at least during ignition, the burning process is driven by exothermic solid-phase reactions. Wenograd (98, 100) reported on the basis of differential thermal analysis measurements that the heat generated during pure AP decomposition at 1 atm., considered as caused by solid-phase reactions only, is roughly sufficient to account for observed propellant burning rates at 1 atm. However, it is not clear how such solid-phase reactions can produce the observed type of burning rate pressure dependence. Andersen and Brown (4, 5) proposed that heterogeneous reaction between the gaseous oxidizer decomposition products and solid fuel at the oxidizer interfaces is rate controlling. No burning rate equation has been derived for the model; hence, it must be regarded as an untested hypothesis.

Spalding (89) has developed a theory for the burning behavior of homogeneous propellants. Although his theory obviously is not applicable

to AP composite propellants and probably not applicable to the common homogeneous propellants based on nitrocellulose (whose flame structures are obviously complex), he showed that low pressure extinction could be caused by radiative heat loss to the surroundings from the hot, regressing surface.

Based on a literature survey, Powling (70) proposed that AP-based propellants burn with two gas-phase reaction stages—the first, a premixed reaction between the sublimed NH_3 and HClO_4 , and the second, an unmixed reaction between the pyrolyzed fuel vapors and the combustion products of the first stage. Diffusional mixing is important in the second flame stage. At high pressures (above about 70 atm.), he considers the $\text{NH}_3/\text{HClO}_4$ reaction zone to be confined close to the surface of the regressing AP crystal. The effect of fuel type on the burning rate of AP-based propellants at these pressures is explained by the existence of a fuel/oxidizer diffusion flame at the binder/oxidizer boundaries. At low pressures (subatmospheric), he considers the two stages of the flame to merge, forming a single premixed $\text{NH}_3/\text{HClO}_4/\text{fuel-vapor}$ stage. This representation would explain why most propellants have a pressure exponent near unity at subatmospheric pressures but does not account for the persistence of particle size effects at pressures as low as 0.1 atm.

The salient features of this picture of propellant burning have been incorporated into our theory below. However, in developing our theory, we assume a granular diffusion flame, and we retain the two-stage A/PA + O/F flame even at very low pressures.

Modified Granular Diffusion Flame Theory

In the original formulation of the granular diffusion flame theory, the premixed ammonia-perchloric acid (A/PA) reaction zone was considered so thin compared with the over-all temperature profile established by the oxidant-fuel (O/F) flame that it was identified as occurring entirely at the regressing propellant surface. (At normal rocket pressures the thickness of the $\text{NH}_3/\text{HClO}_4$ flame is estimated at *ca.* 0.5μ compared with *ca.* 20μ for the O/F flame). Since the A/PA reaction rate is pressure sensitive and since the thickness of the A/PA zone thus increases with reduction in pressure, the assumption that it is effectively collapsed must become invalid at some low enough pressure. Consequently, if the validity of the granular diffusion flame model is to be extended to very low pressures, the distributed nature of this reaction must be recognized. The model then possesses two gas-phase reaction stages, the second stage, the fuel oxidation stage, still retaining its original proposed character of a granular diffusion flame. The theory is further modified by the fact that low pressure burning rate behavior depends critically on the sensitivity

of the pyrolysis rate (*i.e.*, burning rate) to surface temperature. Therefore, the variation of surface temperature with pressure must be accommodated. The following two-stage GDF theory is developed (1) to extend its validity to very low pressures, and (2) to check *a posteriori* the validity of assuming an infinitely fast A/PA reaction at normal rocket pressures.

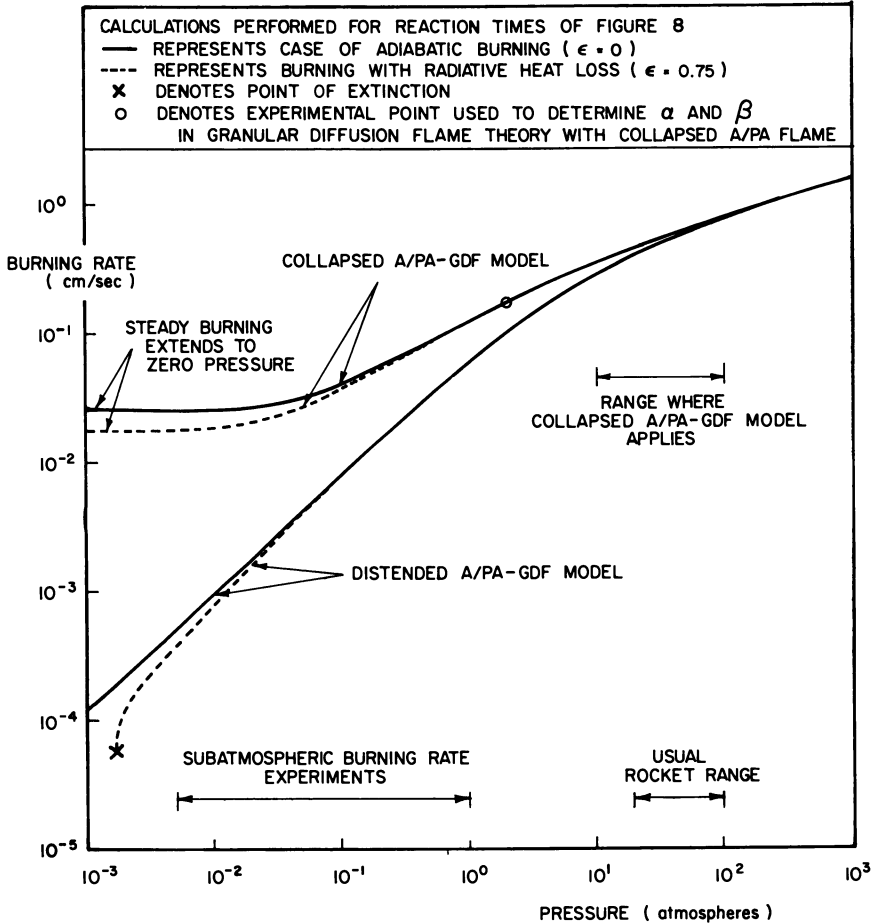


Figure 11. Pressure dependence of burning rate predicted by the granular diffusion flame theory for the case (1) where premixed ammonia/perchloric acid flame is distended and (2) where it is collapsed

Physicochemical Model. In constructing the GDF model, it is assumed that gasification at the solid regressing surface is driven by conductive heat feedback from a two-stage flame occurring in the gas phase (*see* Figure 1). This solid-to-gas phase step is generally endo-

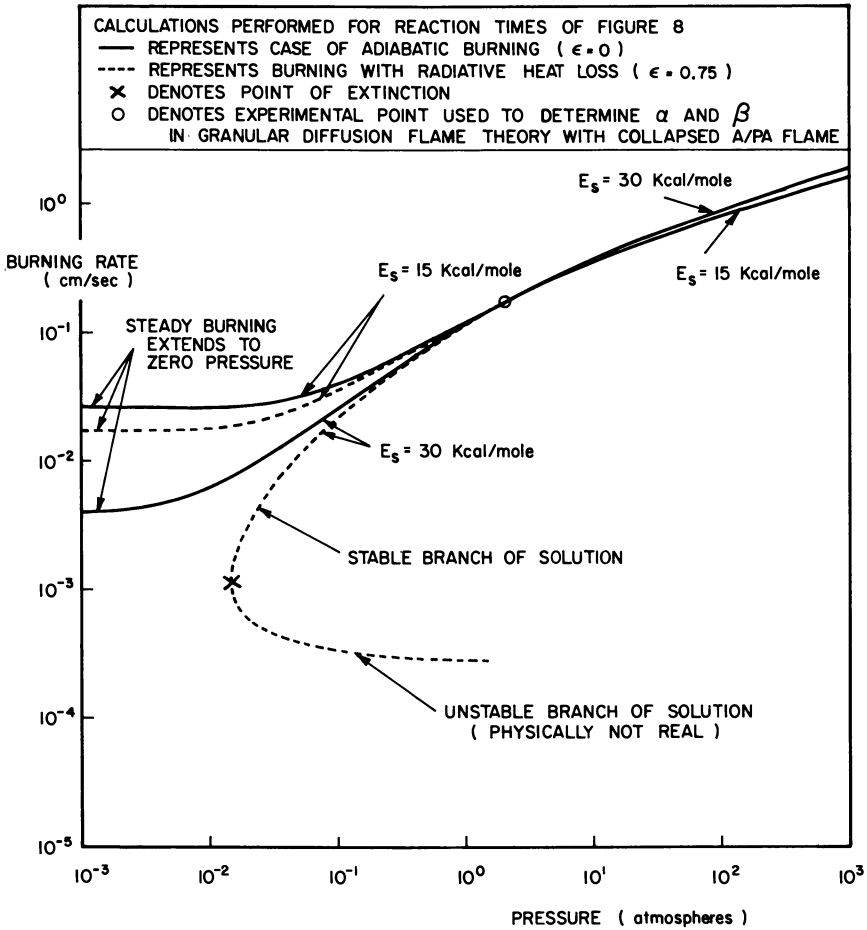


Figure 12. Effect of activation energy of surface reaction on burning rate behavior of granular diffusion flame theory with collapsed A/PA flame zone

thermic for both the fuel and oxidizer constituents. For ammonium perchlorate, this step is dissociative sublimation, yielding hot gaseous ammonia and perchloric acid (*see text above*). These products become the reactants for a vigorous premixed exothermic gas-phase reaction occurring close to the surface of the AP crystal (less than 1μ at normal rocket pressures). The products of this reaction, which are rich in oxygen and oxygen-containing compounds, now serve as reactants in the ensuing fuel-oxidant gas-phase reaction which extends much further from the regressing propellant surface (about 20μ at normal rocket pressures). Up to this point (the beginning of the O/F flame) the pyrolyzed fuel gases are considered dispersed in the oxidant stream but still unmixed

(pockets). In the one-dimensional energy equation below, the fuel vapor is an energy diluent in this first stage. Since a composite propellant is heterogeneous and the fuel and oxidizer gases therefore are unmixed when they emerge from the propellant surface, both the rates of diffusional mixing and of chemical reaction determine the over-all reaction rate of fuel-oxidant redox reaction in the second stage. In the GDF model it is presumed that the fuel enters this flame zone as tiny gas pockets whose mass is independent of pressure. These pockets burn up in an atmosphere of oxidizer decomposition products. Composite propellant burning is thus viewed as a three-step process in which the endothermic solid-to-gas phase step, the exothermic premixed $\text{NH}_3/\text{HClO}_4$ reaction, and exothermic fuel-oxidant reaction occur sequentially; the diffusional mixing and chemical reaction processes in the O/F flame zone occur simultaneously.

The granular diffusion flame is a one-dimensional model which assumes that the A/PA and O/F reaction zones are planar and parallel to the regressing propellant surface. This is valid provided the depth of the thermal wave L_s in the solid phase and the O/F flame thickness L_{II} are large compared with the effective roughness dimension of the regressing propellant surface. The roughness scale of the surface is not known accurately, but based on Bastress' (9) photographic study which shows the surface to be relatively smooth at normal rocket pressures, it could be of the order of 10μ (this varies with particle size). Based on this value, calculation of the pressure dependence of L_{II} and L_s (see Figure 13) shows that the assumption of one dimensionality will break down only when the pressure exceeds *ca.* 100 atm. At high pressures especially, the A/PA flame hugs the exposed AP crystal, leaving the fuel surface exposed only to the O/F flame. However, we can still represent this zone as a planar wave in the energy equation provided the temperature, T_1 , at the point of completion of the A/PA reaction, is obtained from mass flux average enthalpy, including both the gases in the A/PA reaction zone and the as-yet unreacted fuel vapors. If we define T_1 this way, by definition the enthalpy term in the $1 - D$ energy equation is satisfied. The same is true for the choice of the average surface temperature, T_s . (The average T_1 and the T_s selected to satisfy the one-dimensional energy equation may differ appreciably from measured average values). Finally, the energy equation contains one-dimensional heat conduction terms for the solid phase and for the O/F flame. We assume that the microscopic three-dimensional heat flow processes smooth out the temperature profile to validate these one-dimensional heat conduction terms.

The relative roles played by diffusional mixing and chemical reaction in determining the reaction rate of the O/F flame are difficult to analyze. Consequently, as was done in the original formulation (92), expressions

will be derived for the burning rate in the extremes of low and high pressure where chemical reaction and diffusional mixing rates, respectively, are known to be controlling; the burning rate at intermediate pressure is then taken as the simplest empirical formula which has these high and low pressure asymptotes and which has been found to fit experimental burning rate data best over the range 1–100 atm.

General Equations for a Two-Stage Gaseous Flame Model. The complete three-stage model depicted in Figure 1 can be solved by setting up integrated steady-state $1 - D$ energy equations for various stations in the flame zone—*viz.*, in the solid just below the surface, in the gas just

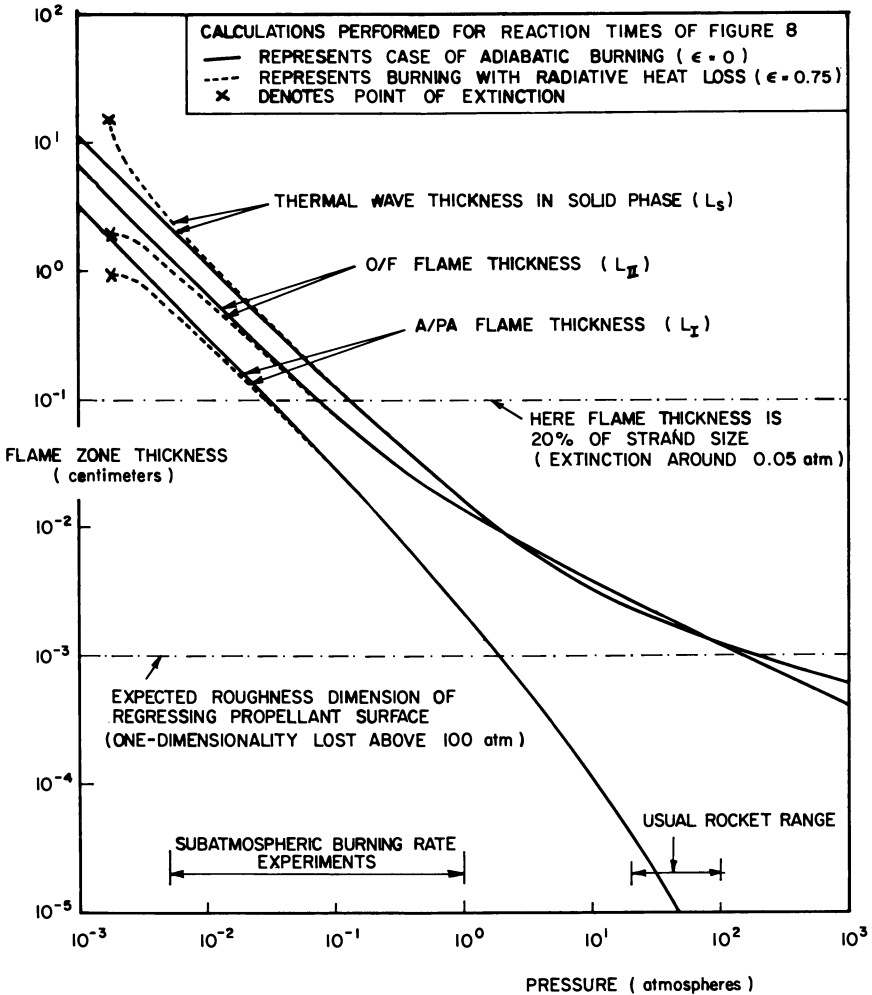


Figure 13. Pressure dependence of flame zone thicknesses predicted by granular diffusion flame theory with distended A/PA flame

SURFACE TEMPERATURE MEASUREMENTS					
CURVE	PER CENT FUEL	AP PARTICLE SIZE	PER CENT ADDITIVE	MEASURING TECHNIQUE	WORKER
○ (---)	3-24% PARAFORMALDEHYDE	?	—	INFRA-RED RADIOMETER	POWLING
△ (---)	18% POLYURETHANE	5-75 μ	2 %	DEPTH OF THERM. WAVE	SELZER
□ (.....)	—————	SINGLE CRYSTAL	—	DEPTH OF THERM. WAVE	BECKSTEAD
▽ (---)	29% POLYBUTADIENE ACRYLIC ACID	9 μ	0-1 %	TH.-COUPLE	SABADELL
◇	35% POLYSULFIDE	15 μ	—	TH.-COUPLE	MOST

— DEPICTS SURFACE TEMPERATURE PREDICTION OF GDF MODEL WITH DISTENDED A/PA REACTION ZONE (FOR REACTION TIMES OF FIG. 8)

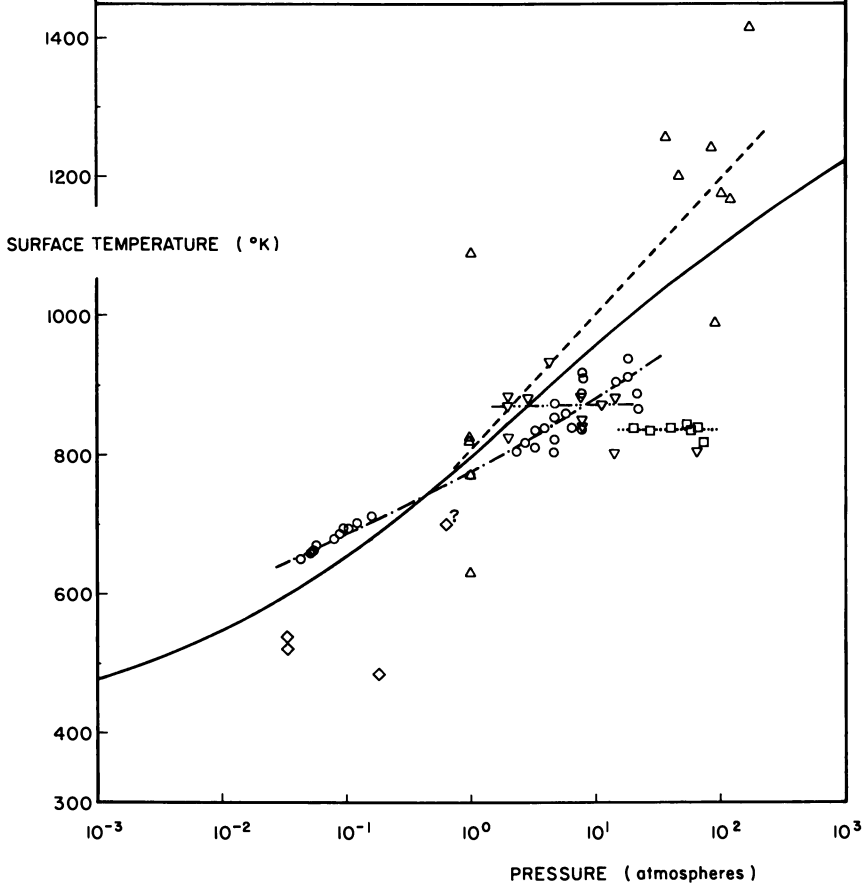


Figure 14. Comparison of GDF theory predicted surface temperature with measurements for AP-based propellants

above the surface, at the point of completion of the $\text{NH}_3/\text{HClO}_4$ reaction, and at the point of completion of the fuel-oxidant reaction. The reference state will be considered as the energy of the unburned solid at the initial temperature T_o . Since radiative heat loss has been suggested as a possible cause for low pressure extinction behavior (51, 54, 89), a term accounting for radiation from the hot propellant surface to the surroundings is included. Simple calculation has shown that provided no free carbon or other radiating solid particles are present in large amounts in the flame zone, radiation from the gas-phase flame is negligible.

With reference to Figure 1 and the list of symbols in the Nomenclature section, the integrated energy equations are:

$$0 = \rho_c r [c_c(T_s - T_o) + \Delta h_{tr}] - \lambda_c \left. \frac{dT}{dx} \right|_{s,c} \quad (1)$$

$$= \rho_c r [c_g(T_s - T_o) + \Delta h_{tr} + \Delta h_s] + \epsilon \sigma T_s^4 - \lambda_g \left. \frac{dT}{dx} \right|_{s,g} \quad (2)$$

$$= \rho_c r [c_g(T_1 - T_o) + \Delta h_{tr} + \Delta h_s + \Delta h_{I1}] + \epsilon \sigma T_s^4 - \lambda_g \left. \frac{dT}{dx} \right|_{1,g} \quad (3)$$

$$= \rho_c r [c_g(T_2 - T_o) + \Delta h_{tr} + \Delta h_s + \Delta h_{I1} + \Delta h_{II}] + \epsilon \sigma T_s^4 - \lambda_g \left. \frac{dT}{dx} \right|_{2,g} \quad (4)$$

where r satisfies the Arrhenius expression for a pyrolysis reaction, *i.e.*,

$$r = A \exp(-E_s/RT_s) \quad (5)$$

Introducing the Mallard-Le Chatelier approximation (57) that the local temperature gradients in the conduction terms are equal to the average gradients and recognizing that the temperature gradient is zero when the final flame temperature T_2 is reached, these energy equations reduce to:

$$0 = \rho_c r [c_c(T_s - T_o) + \Delta h_{tr}] - \lambda_c \left. \frac{dT}{dx} \right|_{s,c} \quad (1a)$$

$$= \rho_c r [c_g(T_s - T_o) + \Delta h_{tr} + \Delta h_s] + \epsilon \sigma T_s^4 - \lambda_g \left(\frac{T_1 - T_s}{L_I} \right) \quad (2a)$$

$$= \rho_c r [c_g(T_1 - T_o) + \Delta h_{tr} + \Delta h_s + \Delta h_{I1}] + \epsilon \sigma T_s^4 - \lambda_g \left(\frac{T_2 - T_1}{L_{II}} \right) \quad (3a)$$

$$= \rho_c r [c_g(T_2 - T_o) + \Delta h_{tr} + \Delta h_s + \Delta h_{I1} + \Delta h_{II}] + \epsilon \sigma T_s^4 \quad (4a)$$

$$= \rho_c r c_g [T_2 - T_{2(ad)}] + \epsilon \sigma T_s^4 \quad (4b)$$

Equations 1a-4b can be solved simultaneously provided expressions for L_I and L_{II} can be inserted. In general, the flame zone thickness L and the reaction time τ are related by:

$$L = (\rho_c r / \rho_g) \tau \quad (6)$$

Thus, the pressure dependence of τ_I and τ_{II} must be estimated quantitatively. This is done below.

Pressure Dependence of the Reaction Times of the Gas-Phase Reaction Zones. AMMONIA-PERCHLORIC ACID REACTION ZONE. Since we assumed that the premixed $\text{NH}_3/\text{HClO}_4$ reaction is bimolecular and hence second order, τ_I is inversely proportional to pressure. Friedman (54) shows that since the final flame temperature of pure burning AP is low and since its linear burning rate is fairly high, the thickness of the $\text{NH}_3/\text{HClO}_4$ flame must be a fraction of a micron at about 50 atm. Owing to the heating effect of the fuel-oxidant flame, the thickness of the $\text{NH}_3/\text{HClO}_4$ reaction zone in a burning propellant will be still less, say 0.1μ at 50 atm. This implies that the first gas-phase stage has a reaction time of 1.3×10^{-7} sec. at 50 atm.; for other pressures we may write:

$$\tau_I = 6.5 \times 10^{-6} p^{-1} \quad (7)$$

τ_I is plotted as a function of pressure in Figure 8.

FUEL-OXIDANT REACTION ZONE. An expression giving the quantitative pressure dependence of τ_{II} can not be obtained directly. However, since the GDF theory with a collapsed $\text{NH}_3/\text{HClO}_4$ reaction correlates experimental burning rate data remarkably well over the range 10–100 atm. and since it is known that $\tau_I \ll \tau_{II}$, a reasonable estimate of τ_{II} can be inferred from the GDF model with a collapsed A/PA flame. This approach implies that the calculated O/F reaction time is insensitive to neglect of the resistance to heat conduction of the A/PA flame. This is reasonable because the calculated value of τ_{II} will be much larger than τ_I above *ca.* 10 atm. Because we will extrapolate τ_{II} to low pressures, variation of surface temperature with pressure must be allowed for; low pressure burning rate behavior is quite sensitive to this variation. The derivation of the GDFT with a collapsed A/PA flame presented below is an improvement over that originally presented in Ref. 92. Note that Equation 2a states that if the first gaseous reaction stage is collapsed to the surface—*i.e.*, $L_I = 0 = \tau_I$ —then $T_1 = T_s$ if the burning rate is to remain finite. (This is not to be confused with T_s measured, say, by a radiometer directed at the surface; the effective surface temperature here is defined in terms of total energy flux at the surface.)

As in Ref. 92 for a second-order gas-phase reaction where the prevailing pressure is sufficiently low for the O/F flame (Zone II of Figure 1) to be chemical-reaction rate controlled (high diffusional mixing rate), the chemical mass conversion rate in a zone of length $L_{II, ch}$ at temperature T_g may be expressed as:

$$\rho_c r_{ch} = L_{II, ch} B \rho_g^2 \exp(-E_2/RT_g)$$

Assuming as an approximation that the effective gas temperature is close to the flame temperature—*i.e.*, $T_2 = T_g$ —then the perfect gas law simplifies the expression for $L_{II, ch}$ to:

$$L_{II, ch} = \alpha^2 \frac{\rho_c r_{ch} T_2^2}{p^2} \exp(E_2/RT_2) \quad (8)$$

where $\alpha = \text{constant}$.

An implicit relationship for the burning rate at low pressure may now be found by substituting $L_{II, ch}$ from Equation 8 for L_{II} in the heat balance (Equation 3a). Inherent in this step is the assumption that the pyrolyzed fuel and oxidizer gases start to react immediately on leaving the propellant surface. When $T_1 = T_s$ (*e.g.*, where the first gaseous reaction stage is very fast) the burning rate at low pressure where it is chemical-reaction rate controlled can be written as:

$$\frac{1}{r_{ch}} = \alpha \sqrt{\frac{c_g(T_s - T_o) + \Delta h_{tr} + \Delta h_s + \Delta h_I + \frac{\epsilon \sigma T_s^4}{\rho_c r_{ch}}}{\lambda_g(T_2 - T_s)}} \frac{\rho_c T_2^2}{p} \exp\left(\frac{E_2}{2RT_2}\right) \quad (9)$$

Again, as in Ref. 92, the burning rate at high pressure, where it is diffusively controlled, may be found. It is assumed that the mass (μ) of each of the fuel gas pockets, of effective diameter d_g , is independent of pressure but directly related to the size of the solid oxidizer crystals d , through the size of the fuel elements between the crystals—*i.e.*,

$$\mu = f(d) \sim \rho_g d_g^3 \quad (10)$$

It is expected that the functional relationship $f(d)$ and hence μ , increases with increasing particle size d .

The over-all flame thickness of the fuel-oxidant stage may be obtained from the average gas velocity V_{II} and the fuel pocket life time $\tau_{II, f}$, which is determined by the rate of supply of both fuel and oxidizer gases to the flame front enveloping each of the fuel pockets, *i.e.*,

$$L_{II, df} = V_{II} \tau_{II, f} \sim \frac{r_{df} \rho_c}{\rho_g} \frac{d_g^2}{D_g} \sim \frac{r_{df} \rho_c \mu^{2/3}}{\rho_g^{5/3} D_g} \quad (11)$$

While chemical reaction rates were identified with T_2 in the previous case, it would be more reasonable to identify diffusion rates with T_s here. Thus, use of the perfect gas law and the empirical relationship (67):

$$D_g \sim T_g^{7/4}/p = T_s^{7/4}/p$$

yields

$$L_{II, df} = \beta(d) \frac{\rho_c r_{df} T_2^{5/3}}{T_s^{7/4} p^{2/3}} \quad (12)$$

where $\beta(d)$ is some function only of d [includes $f(d)$].

Again, when $T_1 = T_s$, substitution of $L_{II, \text{diff}}$ for L in the heat balance equation gives the asymptotic value for burning rate at high pressures:

$$\frac{1}{r_{\text{diff}}} = \beta(d) \frac{\rho_c T_2^{5/6}}{p^{1/3} T_s^{7/8}} \sqrt{\frac{c_g(T_s - T_o) + \Delta h_{tr} + \Delta h_s + \Delta h_1 + \frac{\epsilon \sigma T_s^4}{\rho_c r_{\text{diff}}}}{\lambda_g(T_2 - T_s)}} \quad (13)$$

With these two asymptotic forms for burning rate, the burning rate at intermediate pressure can be expressed by some relation which reduces to these forms at the extremes of pressure. Many relations are possible, but

$$1/r = 1/r_{ch} + 1/r_{\text{diff}}$$

originally proposed, has been successful to date and is simple. Thus:

$$\frac{1}{r} = \rho_c \sqrt{\frac{c_g(T_s - T_o) + \Delta h_{tr} + \Delta h_s + \Delta h_1 + \frac{\epsilon \sigma T_s^4}{\rho_c r}}{\lambda_g(T_2 - T_s)}} \left\{ \frac{\alpha T_2}{p} \exp\left(\frac{E_2}{2RT_2}\right) + \frac{\beta(d) T_2^{5/6}}{p^{1/3} T_s^{7/8}} \right\} \quad (14)$$

If we consider T_s constant and radiative heat loss negligible, Equation 14 reduces to the earlier law:

$$\frac{1}{r} = \frac{a}{p} + \frac{b(d)}{p^{1/3}} \quad (15)$$

where a = chemical reaction time parameter, and b = diffusion time parameter. Numerical values of a and b can be evaluated by fitting Equation 15 to experimental burning rate curves. Since Equations 14 and 15 display the same behavior in the range 1–100 atm. (*see* discussion below), α and β can be evaluated from a and b using a measured surface temperature at a particular pressure.

The variation of τ_{II} with pressure predicted by this model can now be found. Again noting that $T_1 = T_s$, Equations 3a and 14 lead to:

$$L_{II} = \sqrt{\frac{\lambda_g(T_2 - T_s)}{c_g(T_s - T_o) + \Delta h_{tr} + \Delta h_s + \Delta h_1 + \frac{\epsilon \sigma T_s^4}{\rho_c r}}} \left\{ \frac{\alpha T_2}{p} \exp\left(\frac{E_2}{2RT_2}\right) + \frac{\beta(d) T_2^{5/6}}{p^{1/3} T_s^{7/8}} \right\} \quad (16)$$

Substituting Equations 14 and 16 into Equation 6 and using the perfect gas law, one obtains:

$$\tau_{II} = \frac{\rho_2}{\rho_c} \frac{L_{II}}{r} = \frac{pM_2}{RT_2} \left\{ \frac{\alpha T_2}{p} \exp\left(\frac{E_2}{2RT_2}\right) + \frac{\beta(d) T_2^{5/6}}{p^{1/3} T_s^{7/8}} \right\}^2 \quad (17)$$

The low and high pressure asymptotes for τ_{II} are proportional to p^{-1} and $p^{1/3}$, respectively, as expected for this model.

An implicit relationship between T_s and p can be found by substituting Equation 5 into Equations 14 and 4b:

$$\frac{\exp\left(\frac{E_s}{RT_s}\right)}{A} = \rho_c \sqrt{\frac{\left[c_g(T_s - T_o) + \Delta h_{tr} + \Delta h_s + \Delta h_1 + \frac{\epsilon\sigma T_s^4}{\rho_c A} \exp\left(\frac{E_s}{RT_s}\right) \right]}{\lambda_g(T_2 - T_s)}} \left\{ \frac{\alpha T_2}{p} \exp\left(\frac{E_2}{2RT_2}\right) + \frac{\beta(d)}{p^{1/3} T_s^{7/8}} \right\} \quad (18)$$

where

$$T_2 = T_{2(ad)} - [\epsilon\sigma T_s^4 \exp(E_s/RT_s)] / (\rho_c c_g A) \quad (19)$$

The pressure dependence of τ_{II} can be obtained by solving Equation 18 for T_s (by trial and error) for every p and inserting these values into Equation 17. The pressure dependence of the burning rate is calculated by inserting the value of T_s for every p obtained from Equation 18 into Equation 5. The numerical values assumed as typical for the physical constants are listed in the Appendix.

Figure 8 shows that in the range 10–100 atm., the first stage A/PA flame is more than 20 times faster than the second stage O/F flame. Our *a priori* assumption that the A/PA flame is collapsed in this pressure range is consistent with this finding although not yet proved. For this, the complete two-stage GDF theory must be developed. Figure 8 shows also, that the assumption of a collapsed A/PA flame breaks down below 1 atm.; τ_I and τ_{II} become comparable in magnitude in this range. Thus, also to extend the validity of the GDF theory to very low pressure, the distended A/PA–GDF theory is treated below.

The treatment of the complete two-stage GDF theory will be based on extrapolations of the functional relationships $\tau_{I,II}(p)$ to low pressures. Similar extrapolation cannot be carried out indefinitely to high pressures for τ_{II} because L_{II} would become small and soon approach the effective roughness dimension of the propellant surface. The one-dimensional character of the O/F flame would then be lost.

Two-Stage Granular Diffusion Flame Theory. The complete two-stage gas-phase reaction granular diffusion flame theory can now be solved using $\tau_I(p)$ and $\tau_{II}(p)$ given in Figure 8. However, owing to the complexity of the equations, burning rate can not be written directly as a function of p , $\tau_I(p)$ and $\tau_{II}(p)$. Therefore, the equations had to be solved by numerical iteration. The equations rewritten in a form convenient for iteration are:

From Equation 6 and the perfect gas law we obtain:

$$L_I = \left(\frac{R\rho_c}{M_1} \right) \frac{rT_1}{p} \tau_I \quad (6a)$$

$$L_{II} = \left(\frac{R\rho_c}{M_2} \right) \frac{rT_2}{p} \tau_{II} \quad (6b)$$

Equation 5 is:

$$r = A \exp(-E_s/RT_s) \quad (5)$$

Equation 4b rewritten becomes:

$$T_2 = T_{2(od)} - (\epsilon\sigma T_s^4)/(\rho_c c_g r) \quad (4a)$$

Rearrangement of Equation 2a and substitution of 6a yields:

$$T_1 = T_s / \left\{ 1 - \frac{r^2 \tau_I}{p} \left(\frac{R\rho_c^2}{\lambda_g M_1} \right) \left[c_g(T_s - T_o) + \Delta h_{tr} + \Delta h_s + \frac{\epsilon\sigma T_s^4}{\rho_c r} \right] \right\} \quad (2b)$$

Rearrangement of Equation 3a and substitution of Equation 6b gives:

$$r^2 = \frac{p}{\tau_{II}} \frac{M_2 \lambda_g (T_2 - T_1)}{\rho_c^2 RT_2 \left[c_g(T_1 - T_o) + \Delta h_{tr} + \Delta h_s + \Delta h_1 + \frac{\epsilon\sigma T_s^4}{\rho_c r} \right]} \quad (3b)$$

This set of equations is solved at any particular pressure by assuming a trial value of T_s and then in sequence, determining τ_I and τ_{II} from Figure 8, r from Equation 5, T_2 from Equation 4a, T_1 from Equation 2b, r from Equation 3b, and T_s from Equation 5. If the finally calculated value of T_s does not correspond to the initially assumed value, the procedure is repeated with another trial value of T_s until they do agree.

These calculations were performed for the assumed physical constants listed in the Appendix. The results are shown in Figures 9–14, together with the predictions of the collapsed A/PA granular diffusion flame model of the previous section.

Theoretical Predictions: Collapsed A/PA–GDF Model Compared with Distended A/PA–GDF Model. One of the main objectives for carrying out the complete two-stage GDF theory, aside from its application to low pressure burning rates, is to determine theoretically the range of validity of the earlier approximate version, the collapsed A/PA stage-GDF model. Figure 8 shows that the assumption $\tau_I = 0$ in the collapsed model is reasonable above *ca.* 10 atm. ($\tau_I \ll \tau_{II}$). Figure 9 shows that the distended model does behave like the collapsed model at all pressures above 10 atm.—*i.e.*, the energy per unit mass of unburned propellant arriving at the regressing surface by conduction from the A/PA stage

becomes independent of pressure above 10 atm.; this is the essence of the collapsed A/PA-GDF model. The collapsed A/PA flame assumption is therefore justified for pressure levels above 10 atm. [The conductive heat feedback per unit mass of unburned propellant coming from the A/PA flame is given by: $q_1 = (\dot{q}_1/\dot{m}) = [(T_1 - T_s)/L_1 - (T_2 - T_1)/L_{II}]/(\rho_0 r)$.]

An interesting point of the two-stage GDF theory (Figure 9) is that the pressure dependence of the heat flow into the interior and hence of the propellant burning rate is almost entirely governed by the kinetics of the O/F granular diffusion flame at pressures above 10 atm., even though the heat feedback from this source is considerably less than the heat contributed by the AP-monopropellant reaction. This is because compared with the O/F flame the A/PA layer has a small impedance to conductive heat feedback above 1 atm. In effect, the A/PA layer is so thin at these pressures (particularly above 10 atm.) that the requirement of finite heat conduction through the layer (only a finite amount of heat is available) forces the temperature difference ($T_1 - T_s$) across the layer to be small also. Calculations show that this temperature difference is several hundred degrees at subatmospheric pressure, but above 10 atm. it goes below 100°C. and is even less than 10°C. at 100 atm. This occurs despite the fact that the heat generated by the A/PA reaction is sufficient to produce a temperature rise of *ca.* 300°C. (54) in the gas evolved in pure AP monopropellant combustion. Thus, it is the pressure sensitivity of the "trigger" and not of the main source of heat feedback that is important in determining the pressure dependence of composite propellant burning rate at normal rocket pressures.

Figure 8 shows that the assumption $\tau_1 = 0$ in the collapsed model starts to break down below 10 atm. (τ_1 becomes comparable with τ_{II}). Figure 10 shows that this partial breakdown of the assumption does not jeopardize our graphical test for the validity of the GDF theory—*i.e.*, determining whether data taken in the usual 1–100 atm. experimental range fall on a straight line when plotted as (p/r) vs. $(p^{2/3})$. In fact, this graphical test will never distinguish between the collapsed and the distended A/PA stage models since the predictions of both models fall on straight lines on the (p/r) vs. $(p^{2/3})$ plot. (The line for the two-stage flame falls higher on this plot because all physical constants were left the same but τ_1 was increased from zero to a finite value; in effect, the thermal resistance to heat flow was increased when going to the two-stage model.) Data taken in the 0.001–0.1 atm. range, where $\tau_1 \approx \tau_{II}$ (and hence the models most dissimilar), cannot distinguish between the collapsed A/PA flame or the distended A/PA flame when plotted this way $(p/r-p^{2/3})$ because all data points will cluster at the low pressure end of this graph; a different kind of plot (*e.g.*, log-log) would distinguish them.

These findings validate the approach of Krier *et al.* (53) when they adopted the collapsed A/PA-GDF model to predict low frequency instability behavior of composite solid propellants at normal rocket pressure. Since $\tau_{II} = 1.5 \times 10^{-5}$ sec. at these pressures, their quasi-steady treatment of the O/F flame reaction time is valid for low frequencies; above about 5000 c.p.s., the dynamic lag of the O/F flame must be taken into account—the dynamic lag of the A/PA flame need be considered only when frequencies approach 100 k.c.p.s.

The above findings also show that the assumption of a collapsed A/PA flame breaks down at subatmospheric pressure. To discern the role played by the AP/A flame, therefore, burning rate data must be taken in this low pressure range where the A/PA stage of the gas-phase flame represents a large part of the total reaction time. Figure 11 compares the burning rate *vs.* pressure predictions of the two models on a log-log plot. As expected, their behavior is drastically different at subatmospheric pressures. Where τ_I is non-zero and where there is no radiative heat loss, the $(\log r)$ *vs.* $(\log p)$ plot tends to follow a straight line with slope slightly less than unity. [The pressure exponent would have been unity because the two stages are essentially second order reaction rate controlled at these pressures, but, because the surface temperature decreases with reduction in pressure, the pressure exponent comes out less than unity.] For small activation energies of the surface reaction E_s , the collapsed A/PA flame model predicts that the burning rate curve will bend concave upward as the pressure is reduced and will level out asymptotically to some non-zero burning rate at zero pressure, regardless of radiative heat loss. Only the fact that the surface reaction is exothermic over-all makes the burning rate non-zero at zero pressure. The transition from a finite pressure exponent to a zero pressure exponent denotes the region where the second stage O/F flame, the only pressure-sensitive process, becomes so distended that its heat flux to the pyrolyzing surface(—*i.e.*, its contribution towards establishing the burning rate) becomes negligible; below *ca.* 0.01 atm., only the exothermic A/PA surface reaction (effectively of zero order when $\tau_I = 0$) controls the burning rate. This behavior would not exist in practice without some “artificial” means of ensuring that $\tau_I = 0$ or at least be independent of pressure. This possibility will be referred to later.

The low pressure behavior predicted by the collapsed model is very sensitive to the choice of E_s (*see* Figure 12); when E_s is large and when there is radiative heat loss, extinction will occur at some low pressure because the surface reaction for large E_s is a more sensitive function of surface temperature than is radiative heat loss. Thus, at some low pressure, where the O/F flame is weak, the surface reaction, which is almost the entire source of heat, cannot overcome the heat loss. This is the

pressure at which extinction occurs. For the distended A/PA flame model, radiative heat loss will always cause extinction because the surface pyrolysis is taken to be an endothermic process in this case and behaves in the same way as the O/F stage, the heat feedback declining as the pressure is reduced. This model predicts extinction at 0.002 atm. (see Figure 11).

Radiative heat loss has been proposed as a factor responsible for low pressure extinction of solid propellants. Theoretical predictions characteristically state that radiative heat loss becomes more important as pressure is reduced. Consequently, just before the extinction point is reached, the burning rate pressure curve starts to bend downward with reduction of pressure. Two other factors more likely to be responsible for extinction are cooling of the gas-phase flame by dilution with the entrained ambient gases (in a strand burner, not in an internal burning grain), and reduction of the amount of heat produced in the flame owing to increased combustion inefficiency (seen in both gaseous and solid products) with reduction in pressure. A propellant strand, typically 5 mm. square, will be particularly susceptible to cooling by dilution with the surrounding ambient gases at about 0.05 atm. because the calculated flame thicknesses of the A/PA and the O/F stages are of the order of millimeters (Figure 13). This is a full order of magnitude above the pressure at which extinction can be accounted for by radiative heat loss alone; hence, convective heat loss is more likely to cause extinction at low pressures. The significance of combustion inefficiency in determining low pressure extinction behavior cannot be calculated theoretically. One must rely on actual measurements of the heat generated as a function of pressure. Product analyses will be useful for this purpose.

At the high pressure end of the burning rate curve, propellant burning can be considered one dimensional only if the O/F gas-phase flame thickness and the thermal wave thickness in the solid are large compared with the effective roughness dimension of the propellant surface (this is more nearly the size of the crevice between the particles of oxidizer, not the mean particle diameter). [The solid-phase thermal wave thickness is defined as the depth below the propellant surface at which $(T - T_o) = 1/e(T_s - T_o)$ and is calculated from the usual equation for the temperature profile in a moving medium with conductive and convective heat flow: $(T - T_o)/(T_s - T_o) = \exp(-rx/\alpha_c)$.] If the significant dimension is of the order of 10μ , then Figure 13 shows that one-dimensional considerations break down above about 100 atm. Therefore, agreement with the GDF one-dimensional theory must break down above 100 atm., and generally this is true.

As a final prediction, the GDF model with a distended A/PA flame predicts a steady rise of surface temperature with increased pressure. Figure 14 shows that the slope of the theoretical T_s vs. p curve agrees

well with experimental measurements, especially when it is realized (72) that both the infrared radiometer and thermocouple techniques are expected to record a lower pressure dependence than is actually the case. This arises from the fact that the temperature profile becomes steeper with increased burning rate and hence pressure. Bobolev *et al.*'s (16) thermocouple measurements have been omitted from the figure because they report low values (600° – 700° K. in the range 50–200 atm.), and moreover they report a decrease in T_s with increased p . Selzer's (87) measurements for particle sizes larger than 100μ have also been omitted because of unduly large scatter. Beckstead and Hightower (12) indicate that the actual value of surface temperature could be 200° C. higher than they reported because of the presence of a thin molten layer on the AP crystal.

The previous theoretical considerations lead to the following conclusions:

(a) The collapsed A/PA–GDF model is a valid representation of propellant combustion behavior at normal rocket pressures.

(b) The reaction time of the O/F stage can be inferred from the collapsed flame model when fitted to experimental data taken in the range 10–100 atm.

(c) The reaction times of the A/PA and O/F gas-phase stages become comparable in magnitude at subatmospheric pressures; hence, the two-stage model must be used to predict low pressure burning behavior.

(d) Subatmospheric burning rate data will distinguish between the validity of either the collapsed or distended A/PA–GDF models.

(e) Radiative heat loss could explain low pressure extinction of a solid propellant, but cooling of the flame with the ambient gases and increased combustion inefficiency with reduction in pressure could be equally important. The importance of either factor can be tested only by experiment.

Low Pressure Burning Rate Studies

Low pressure burning behavior gives information concerning the detailed structure of the flame zone. It is known that the fuel–oxidant reaction zone becomes very weak at very low pressures. Thus, the nature of any remaining exothermic reactions occurring at or near the propellant surface is more obvious in the over-all propellant burning behavior. Burning rates and extinction behavior have been measured for a number of propellant systems and are reported below. These results are then interpreted in terms of the theoretical predictions made previously.

Experimental Procedure. All propellants used in this investigation were produced at this laboratory and were quality tested before use. These tests were the measurement of uncured propellant viscosity, fin-

ished propellant hardness, and density. Density proved to be the most critical test since, when compared with theoretical density, it can be used to detect void content, oxidizer particle settling during curing, and possible composition errors. Density values deviating by more than 1% from theoretical were generally considered unacceptable for the program. Oxidizer particle size, being an important parameter, was measured in every case using the microscopic technique of Dallavalle (25). The values obtained agreed to within 10% of those given by the manufacturer (3), also using the microscopic method.

A finished propellant block (of precisely known properties) was then cut into strands 0.25 in. square and approximately 4 in. long. All strands were inhibited by leaching in water for 10–15 sec. When the burning surface could not be made to burn straight and perpendicular to its direction of travel, the strands had to be inhibited with three coats of 5% vinyl plastic (VYLF) in dichloromethane solution in addition to leaching in water. Preliminary tests showed that this inhibition had no significant effect on the burning rate but did increase the extinction pressure from 0.045 to 0.060 atm.

The apparatus used to measure burning rates is a modified version of that described by Cole (23). It consists of a bell jar connected to a vacuum pump through a large surge tank. The bell jar which serves as the combustion chamber is fitted with a window behind which a propellant strand is mounted vertically. A system of beamsplitters, lenses, and a 35 mm. automatic sequencing camera, triggered by an electronic timer, is aligned so that the camera simultaneously records the propellant strand, a steel rule, and a stopwatch. By taking a number of photographs during an actual test at constant pressure, the progress of the burning surface with time, and hence burning rate, can be determined. Before such a test, the bell jar was purged with nitrogen for 3–5 min. and evacuated to the desired pressure. The pressure during the test was read from a mercury manometer or McLeod gage, depending on the test pressure in the bell jar.

At pressures below *ca.* 0.05 atm. it was not possible to photograph the propellant strand through the bell jar window because white fumes evolved during the burning and coated the window (recall the discussion about combustion inefficiency at very low pressure). The problem was alleviated by washing a thin film of oil (silicone diffusion pump fluid) down the inside of the window.

Results. BURNING RATES. Burning rates were measured for a number of propellant systems. These results, together with those from the literature (*see* Review Section and Figure 15), show that subatmospheric burning rates tend to follow a straight line on the ($\log r$) *vs.* ($\log p$) plot; the slope is usually around 0.7, but for some binder types such as

CURVE	PER CENT FUEL	AP PARTICLE SIZE	PER CENT ADDITIVE	INVESTIGATOR
A (—)	35% POLYSULFIDE	5 μ	—	THIS STUDY
B (—)	35% POLYSULFIDE	45 μ	—	THIS STUDY
C (-----)	25% POLYBUTADIENE ACRYLIC ACID	5 μ	—	THIS STUDY
D (-----)	25% POLYBUTADIENE ACRYLIC ACID	13 μ	—	COLE
E (-----)	25% POLYBUTADIENE ACRYLIC ACID	188 μ	—	COLE
F (-----)	25% PB (CARBOXYL-TERMINATED)	5 μ	—	THIS STUDY
G (-----)	25% PB (HYDROXYL-TERMINATED)	5 μ	—	THIS STUDY
H (-----)	25% PB (HYDROXYL-TERMINATED)	5 μ	0.75% CC	THIS STUDY
I (-----)	20% POLYESTER RESIN	20 μ	—	WEBB
J (-----)	20% POLYESTER RESIN	100 μ	—	WEBB
K (-----)	20% POLYESTER RESIN	?	—	SILLA
L (-----)	POLYVINYL CHLORIDE	50 μ	ALUMINUM	BARRÈRE
M (-----)	POLYVINYL CHLORIDE	50 μ	—	BARRÈRE
N (-----)	24.3% PARAFORMALDEHYDE	?	—	POWLING
O (-----)	10% PARAFORMALDEHYDE	?	3% CC	POWLING
P (-----)	11% POLYISOBUTYLENE	?	—	POWLING
Q (-----)	18% PB ACRYLIC ACID (1/1 BIMODAL)	15μ + 230μ	—	FEINAUER
R (-----)	20% PB ACRYLIC ACID (1/1 BIMODAL)	15μ + 230μ	2% CARBON	FEINAUER
S (-----)	20% PB ACRYLIC ACID (1/1 BIMODAL)	15μ + 230μ	2% CC	FEINAUER

PB DENOTES POLYBUTADIENE ; CC DENOTES COPPER CHROMITE .

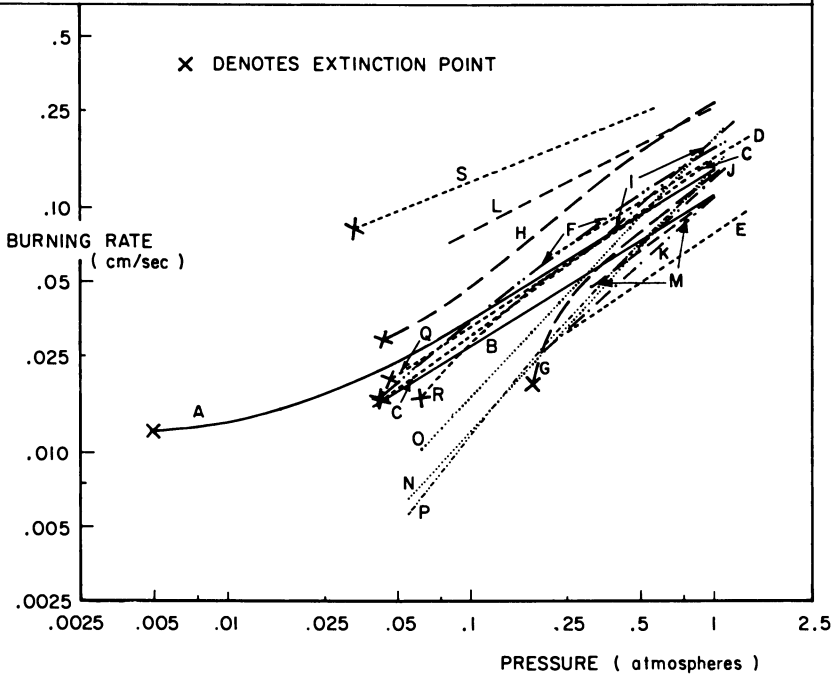


Figure 15. Burning rate–pressure dependence at subatmospheric pressures for ammonium perchlorate with different binders

polyesterstyrene, paraformaldehyde, and polyisobutylene, it is close to unity. The reason for this is unknown.

Figure 16 shows our results for the effect of several binders on the burning rate at subatmospheric pressures. This set of curves represents propellants loaded as highly as practical with 5- μ mean particle size unimodal "spherical" AP. [This particular set of parameters was chosen

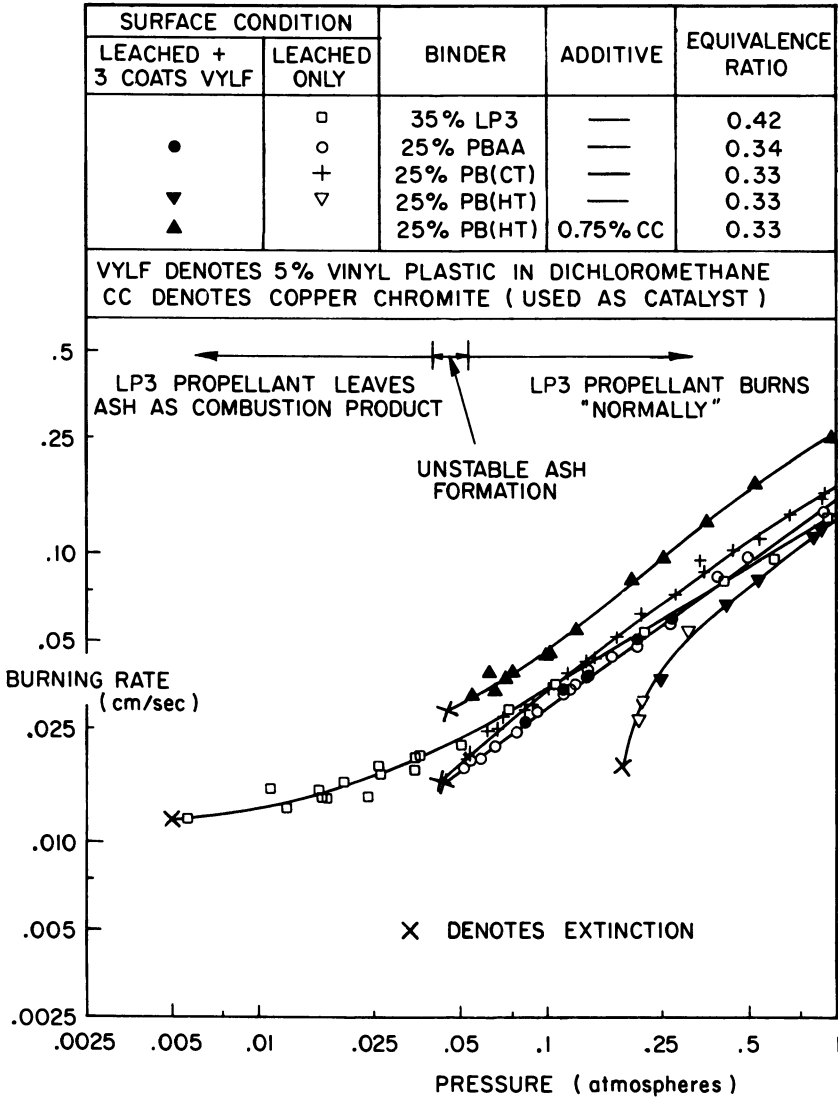


Figure 16. Effect of binder type on burning rate of ammonium perchlorate propellants. Mean particle size of AP is 5 μ

because preliminary tests have shown that propellants with the highest possible loading of very fine AP burn to lower pressures than propellants more highly loaded with coarse AP; it is very low pressure burning behavior that is of primary interest here.] (The equivalence ratio for each propellant is listed in the figure. Equivalence ratio ψ is defined here as the mass fraction of oxidizing species (O, Cl, F . . .) present in the propellant (oxidizer and fuel) divided by the mass of oxidizing species present in the same propellant mixed to stoichiometric proportions. The stoichiometric ratio is that which leads to the products H_2O , CO_2 , SO_2 , HCl , N_2 .) Figure 16 shows that propellants with polybutadiene acrylic acid (PBAA) (cured with 14.4% Epon 828 epoxide obtained from Shell Chemical Co.) and carboxyl terminated polybutadiene (PB(CT)) (cured with 5.2% ERL-0500 epoxide obtained from Union Carbide Plastics Co.) binder behave in the usual way—*i.e.*, follow straight lines on the $(\log r)$ vs. $(\log p)$ plot. This is also true of the hydroxyl terminated polybutadiene (PB(HT)) (cured with 6.0% Hylene-T toluene-2,4-diisocyanate (TDI) obtained from E. I. du Pont de Nemours & Co. (Inc.)) when copper chromite is added [PB(HT) cured with TDI is a polyurethane (13)]. The pressure exponents for all three propellants lie between 0.68 and 0.78, and they all extinguish at about 0.045 atm.

As seen from Figure 15, our results agree fairly well with those obtained by others for similar propellant systems. The most marked difference is that our curves extend to lower pressures. The propellants we tested could be made to burn at very low pressures only by first igniting the strand above about 0.3 atm. and then slowly reducing the pressure to the desired test pressure; if the pressure is reduced too rapidly, extinction will inevitably occur. In this study, the extinction pressure for a particular propellant was taken as the lowest value (out of a number of tests) at which the propellant could be made to burn. Extreme care was used to reduce the pressure as slowly as possible. The extinction pressures determined in each test generally fell within 10% of each other. Some tests done with the PBAA propellant showed that the extinction pressure is strand-size dependent—*i.e.*, it was lower by almost a factor of 2 when the strand size was increased from 0.25 to 0.6 inch square cross section. The burned surface of extinguished samples of all three propellants (PBAA, PB(CT), and PB(HT) with copper chromite) looked porous and dull black when observed through a microscope; it appeared as though it were dry during burning.

Contrary to the general trend described above, hydroxyl terminated polybutadiene (a polyurethane) has a burning rate curve which bends concave downward below 0.3 atm. (Figure 16), and the extinction pressure of this propellant is rather high (0.18 atm.). The burned surface of extinguished samples of this propellant had a glistening black appearance.

It had many depressions of about 1 mm. diameter, whose bottoms were the same color as the unburned propellant (white). Little conical flamelets of about 1 mm. base diameter and about 1 mm. height could be seen darting about the propellant surface when the propellant was burning at a low pressure near the extinction pressure. These observations suggest that a mass of molten fuel containing solid AP particles is present on the burning propellant surface and that globules of this mixture periodically erupt from the surface. [Polyurethanes generally melt at temperatures lower than that for which decomposition (as detected by weight loss measurements) becomes significant (13, 91). However, Ref. 91 shows that this particular polyurethane melts less readily than, say, polypropylene glycol cured with TDI; the latter appears to extinguish around 1 atm.] (The exothermic $\text{NH}_3/\text{HClO}_4$ reaction is severely inhibited because of encapsulation of the AP particles by the molten fuel.) These globules are presumably carried into the afterburning zone where they burn up and thus contribute little toward the heat needed for gasification at the propellant surface. This inefficiency during burning can explain the drooping of the burning rate curve at low pressures as well as the observation that the extinction pressure is higher than that of the PBAA-AP and PB(CT)-AP propellants.

Adding 0.75% copper chromite to PB(HT) propellant increases the burning rate at all pressures (Figure 16), but more important, the burning rate curve now follows a straight line all the way to the extinction pressure which is the same as that of the PBAA-AP and PB(CT)-AP propellants. Moreover, the burned surface of extinguished samples of the PB(HT)-AP-copper chromite propellant had the same appearance as that of PBAA-AP and PB(CT)-AP propellants—*i.e.*, it appeared dry during burning. These observations concerning the effect of copper chromite on the burning behavior of PB(HT)-AP propellant are reasonable because copper chromite is a good catalyst for AP decomposition (32, 49); it is conceivable copper chromite addition will allow the same or more AP decomposition at a surface temperature lower than the melting temperature of PB(HT) binder.

Figure 17 shows that a polysulfide (LP3) (cured with 6% *p*-quinone-dioxime and 1% sulfur) propellant behaves completely differently: the burning rate curve bends concave upward below 0.05 atm., and there is a strong tendency for the burning rate to become independent of pressure at very low pressure (~ 0.005 atm.); the extinction pressure is an order of magnitude lower than that of the PBAA-AP and PB(CT)-AP propellants. It is significant that the burning rate curve starts bending up at about the pressure below which the propellant leaves a porous but very firm solid residue as a combustion product. The peculiar characteristic that polysulfide propellant forms an "ash" was discovered by

Most (60). He found that the ash starts forming unstably below 0.053 atm., but then a firm layer of solid residue builds up on the regressing interface to a thickness of 1–2 mm. and then suddenly burns away. Below about 0.040 atm., the propellant burns in cigarette fashion, leaving the solid residue intact. There is no evidence of a visible flame. The rate of progress of the interface into the unburned propellant here is taken as the burning rate of the propellant. The scatter in our burning rate results is large ($\pm 5\%$) in the range 0.005–0.05 atm. because the burning is somewhat irregular at these pressures, and an oil film which produces small random distortions had to be used to prevent coating of the window by the excessive amounts of white fumes produced. Our burning rates compare well with those obtained by Most (60) in the 0.2–1.0 atm. pressure range.

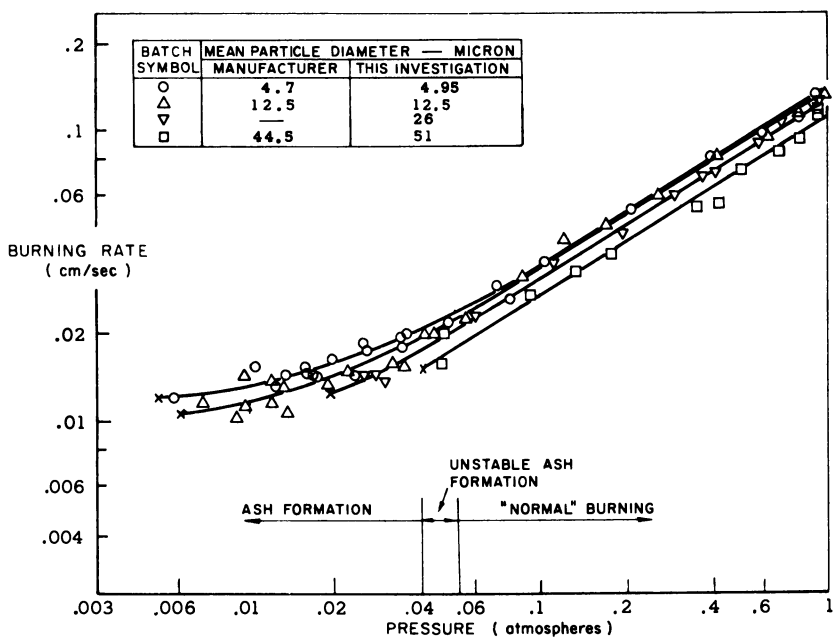


Figure 17. Burning rate of 35% polysulfide + 65% NH_4ClO_4 with varying mean oxidizer particle size

The effect of oxidizer particle size on the burning rate of LP3-AP propellant (with $\psi = 0.42$) was investigated (Figure 17). Although the scatter is large, increase of particle size does appear to depress the burning rate. The effect of particle size appears to be larger in the 0.005–0.05 atm. than the 0.1–1.0 atm. pressure range. In view of the fact that both the 15- and 25 μ propellants had densities within 1% of theoretical, it seems unlikely that the large void content (5%) of the 5 μ propellant

caused its higher rate. The pressure at which extinction occurs increases with increasing particle size. Particle size has no effect on the pressure at which the transition to ash formation occurs.

SUBSIDIARY SEMIQUANTITATIVE OBSERVATIONS. When the pressure is around 0.05–0.06 atm., the flame of a “normal-burning” propellant (*i.e.*, PBAA–AP) has the appearance of a two-stage flame. The first stage is a dark zone with no visible radiation and is 0.5–1.0 mm. thick. This is followed by a very thin blue layer which marks the beginning of a long (several centimeters) yellow-to-orange zone. (The latter zone is blue when copper chromite has been added to the propellant.) At about 0.06 atm., the blue envelope is still largely planar and parallel to the propellant surface, but upon further reduction in pressure, especially near the extinction pressure, it takes on a bulbous form. The dark region can be as thick as 3–5 mm. when the pressure is near the extinction pressure. When the dark zone is thick, white smoke (probably AP sublimate) leaves its edges. When extinction is slow enough, extinction starts from the edges of the propellant strand. These observations suggest that the dark zone is the $\text{NH}_3/\text{HClO}_4$ reaction zone (NH radiates in the ultraviolet at 3360 Å. (93)) and that the blue envelope marks the onset of the premixed fuel–oxidant reaction (probably CH or perhaps C_2 emission). Low pressure extinction seems to be caused by convective heat loss at the flame periphery together with inefficient combustion associated with the escape of sublimed AP at the edges of the dark zone. This would explain the effect of strand size on the extinction pressure.

On burning LP3–AP propellant, whenever the ash broke (under the influence of gravity) within about 2 mm. from the regressing interface, then regression would immediately cease. This, together with the fact that the burning rate curve changes character as soon as the ash starts forming, suggests that the presence of the ash is an important aspect of the burning process. Ash formation is not a peculiarity of the mixture ratio because the same phenomenon was observed for polysulfide propellant containing 75% bimodal AP. The pressure at which the transition to ash formation occurs is independent of the nature of the ambient gas (nitrogen or air). The ash itself is combustible; it is totally consumed when ignited in nitrogen or air above about 0.1 atm. Chemical analysis of the ash obtained from 35% LP3 + 65% 5μ AP propellant ($\psi = 0.42$) has shown that it contains about 60% NH_4ClO_4 and about 10% NH_4Cl . Microscopic observation of the ash obtained from 25% LP3 + 75% bimodal AP (5μ and 80μ in the ratio 30/70) revealed the presence of large unburned AP particles in the ash. The weight of ash obtained from the 35% LP3 + 65% 5μ AP propellant at 0.03 atm. amounted to about 30% of the original weight of the propellant. No accurate deter-

mination of the effect of pressure and particle size on this quantity could be made.

Burning at subatmospheric pressure is accompanied by the evolution of white fumes which solidify upon contact with a cold surface. For the LP3 propellant, it is larger in quantity and increases considerably as soon as the ash starts forming. This smoke was found to contain 25% ammonium perchlorate and 55% ammonium chloride. A trap was installed to determine the amount of smoke evolved per unit mass of propellant as a function of pressure and oxidizer particle size, but the results were inconclusive. The weight of sublimate caught was approximately 20% of the original weight of the propellant.

The presence of large amounts of AP in the ash as well as in the smoke constitute large sources of combustion inefficiency at low pressures. Another possible source could be the ejection of AP particles from the regressing propellant surface. These would be carried into the after-burning zone where they burn up but contribute little toward the heat needed for gasification of the solid-phase propellant constituents at the regressing propellant surface. Microscopic examination of extinguished propellant surfaces revealed many deep holes, giving the impression that the oxidizer particles had been ejected from these holes. Those particles still intact were covered by a thin transparent yellow layer, like molten fuel. With 600μ particle size propellants many small particles were found lying at the bottom of the bell jar after burning. Ohlemiller (65) has photographed particle tracks in the flame zone of PBAA-AP propellants. He calculated from the number of streaks that under conditions of radiative-augmented burning or with 1% copper chromite additive, the AP ejection rate could be as high as 50% of that originally in the propellant at low subatmospheric pressures. [A group of Russian workers, led notably by Bakhaman, believe that there are regimes in which the dominant mode of heat release in the flame arises from the oxidizer particles burning up in the vaporized fuel gas stream as they are carried away from the surface. They consider this to be the normal, not the anomalous mode (as we do), but they do concede that under some circumstances such particle transport can lead to severe combustion inefficiency (7)].

General Discussion

“Normal-burning” propellants such as PBAA-AP and PB(CT)-AP are in qualitative agreement with the behavior predicted by the granular diffusion flame theory when the $\text{NH}_3/\text{HClO}_4$ reaction is considered distended. Quantitative comparison between theory and experiment is not

possible because combustion inefficiency, not accounted for by the theory, is an important factor in low pressure combustion.

The pressure at which extinction occurs depends on the size of the strand. Both theoretical predictions and our observations of the flame indicate that the A/PA and O/F flame zones are thick enough (order of millimeters) at the extinction pressure for the flame to be susceptible to convective cooling by the entrained ambient gases as well as to a significant loss of available heat owing to escape of unreacted AP from the A/PA flame zone. No evidence has been found to show that radiative heat loss from the propellant surface is a major factor. However, Feinauer's (27) results indicate that it is a contributory factor when carbon black has been added to the propellant.

Ohlemiller (65) measured the regression rate of PBAA/AP propellant under conditions of radiative augmented burning at about 0.005 atm., almost one-tenth the extinction pressure of the propellant. He found, by comparing burning rates with radiative flux that the over-all burning process is endothermic to the extent of several hundred calories per gram of propellant. This is consistent with our deductions from our burning rates based on a distended A/PA-GDF flame model.

The mere presence of the ash seems responsible for the ability of the LP3-AP propellant to undergo self-sustained combustion to pressures as low as 0.005 atm., an order of magnitude less than PBAA-AP and PB(CT)-AP propellants, and to maintain a relatively high burning rate at such low pressures. Two questions are of interest: why does it form, and how does it sustain the burning rate? It is not clear why the ash forms. It may be related to Bircumshaw and Newman's (14, 15) discovery that only 30% of the original AP decomposes when the temperature is below *ca.* 350°C. and that the remaining 70% is unreacted solid AP, and to the fact that the surface temperature and the temperature in the ash were measured by Most (60) as 250°-300°C. (The GDF theory with a collapsed A/PA flame indeed predicts a low surface temperature, *ca.* 400°C. below 0.01 atm.)

The LP3-AP burning-rate curve is similar in shape to that predicted by the GDF theory with a collapsed A/PA flame, when the activation energy of the surface reaction is 15 kcal./mole (as indicated in the Review Section, this value for E_s is reasonable). Working backward from the measured asymptotic zero-pressure burning rate, the surface pyrolysis heat (including the endothermic dissociative sublimation step as well as the exothermic gas-phase A/PA reaction step) turns out to be exothermic to the extent of 90 cal./gram. This is 35% short of the previously assumed value of 130 cal./gram (based on the heats of transition of the various reaction steps and in rough agreement with the value measured at elevated pressure by Sabadell (80)). Considering the in-

accuracies involved, it is indeed surprising that this defect is approximately the percentage of original AP found as undecomposed AP in the combustion product at these pressures. We therefore speculate that the A/PA reaction zone is the major source of heat in the pressure range where the ash forms. If so, the shape of the burning rate curve implies that the reaction time of this zone τ_1 becomes independent of pressure below 0.05 atm., in the ash formation regime, just like the theoretical burning rate curve for the collapsed A/PA model. We may then infer that the ash serves as a hot porous bed which ignites the desorbed NH_3 and HClO_4 vapors a short but fixed distance from the regressing interface and that this is the role of the ash in determining the unusual rate-pressure curve.

Pearson (66) found that hot solid surfaces drastically accelerate the ignition of these vapors. In line with our identification of the A/PA reaction zone as the major heat source, it is expected that both burning rate and extinction pressure depend on the total surface area of AP particles exposed to the A/PA reaction occurring in the pores of the ash. Thus, as observed experimentally, both burning rate and extinction pressure depend upon oxidizer particle size. However, this interpretation is obscured by the fact that combustion inefficiency, an important parameter, is also expected to be particle size dependent. [Total AP surface area exposed to A/PA reaction zone = $A = na$, where n = (number of AP particles exposed), \sim (volume of each AP particle) $^{-1} \sim d^{-3}$, a = (exposed surface area of each AP particle) $\sim d^2$. Therefore, $A \sim d^{-1}$.]

Before leaving this account of this two-stage gas-phase flame propagation theory and its predictions we must concede that solid-phase interfacial reactions and heterogeneous reaction between the HClO_4 vapor or products and the solid fuel cannot be ruled out on the basis of the experimental evidence at hand. However, there is no evidence that includes them as major contributory heat sources. The gas-phase driving source seems to account for all the known facts.

Conclusions

The major conclusions of this study are:

(a) The granular diffusion flame theory with a collapsed A/PA reaction zone is a valid representation of composite AP propellant burning rate behavior in the usual rocket motor pressure range, 10–100 atm.

(b) The A/PA reaction zone must be considered distended at pressures below 1 atm., and this affects the theoretical burning rate curve greatly.

(c) Normal-burning propellants such as PBAA-AP and PB(CT)-AP conform in burning rate to the GDF theory at subatmospheric pres-

tures (to about 0.05 atm.), but only when the A/PA reaction zone is considered distended in the theory.

(d) Combustion inefficiency in the form of unreacted AP in the combustion product is significant at low subatmospheric pressures.

(e) The dominant cause of low pressure extinction (at *ca.* 0.05 atm.) in normal burning propellants in strand form appears to be convective cooling by the entrained ambient gases in the combustion chamber together with loss of available heat owing to escape of unreacted AP from the edges of the A/PA flame zone. In motors under more nearly adiabatic conditions, these losses might be avoidable, and still lower pressures might be attainable.

(f) The peculiarities in burning rate at very low pressure burning for the case of PB(HT)-AP propellant are caused by the fact that hydroxyl terminated polybutadiene (a polyurethane) melts at the temperature of the regressing propellant surface.

(g) LP3-AP propellant is able to burn to extremely low pressures (0.05 atm.) because it forms a protective ash that retains the heat of the exothermic A/PA flame close to the solid surface.

Nomenclature

a: Chemical reaction time parameter in Summerfield Equation 15

b: Diffusion time parameter in Summerfield Equation 15

c: Specific heat

d: Mean oxidizer particle size

d_g: Effective diameter of gaseous fuel pockets

p: Pressure

r: Burning rate

x: Distance from propellant surface (Figure 1)

A: Pre-exponential factor for surface reaction

B: Pre-exponential factor for gas phase reaction

D: Diffusion coefficient

E: Activation energy

L: Thickness of zones in propellant flame (Figure 1)

M: Molecular weight

R: Universal gas constant

T: Absolute temperature

V: Average gas velocity

h: Enthalpy required to affect a change of state

α_c : $(\lambda/\rho c)_c$ = thermal diffusivity of solid phase

α : Constant related to *a* through Equations 14 and 15

β : Constant related to *b* through Equations 14 and 15

ϵ : Emissivity of propellant surface

λ : Thermal conductivity

μ : Average mass of gaseous fuel pockets

ρ : Density

σ : Boltzmann constant

τ : Reaction time

ψ : Equivalence ratio

Subscripts

- I: First-stage gas-phase reaction zone (A/PA flame)
 II: Second-stage gas-phase reaction zone (O/F flame)
 1: Condition at end of first-stage gas-phase reaction zone (A/PA flame)
 2: Condition at end of second-stage gas-phase reaction zone (O/F flame)
ad: Adiabatic condition
c: Solid phase
ch: O/F flame, chemical reaction rate controlled
dif: O/F flame, diffusional mixing rate controlled
eff: Effective value of parameter
f: Gaseous fuel pocket
g: Gas phase
o: Initial condition
s: Propellant surface
tr: Lattice phase transition

The following numerical values were assumed typical of AP composite propellants in the calculations:

$$\begin{array}{ll}
 c_c = 0.3 \text{ cal./gram, } ^\circ\text{C.} & E_g = 20 \text{ kcal./mole} \\
 c_g = 0.3 \text{ cal./gram, } ^\circ\text{C.} & E_s = 15\text{--}30 \text{ kcal./mole} \\
 \alpha_c = 10^{-3} \text{ sq. cm./sec.} & M_1 = M_2 = 30 \\
 \epsilon = 0 \text{ or } 0.75 \text{ (estimated)} & T_{2(ad)} = 2000^\circ \text{K.} \\
 \lambda_g = 2 \times 10^{-4} \text{ cal./cm.-sec.-}^\circ\text{C.} & (\Delta h_{tr} + \Delta h_s) = 430 \text{ cal./gram} \\
 \rho_c = 1.66 \text{ gram/cc.} & \Delta h_1 = -560 \text{ cal./gram}
 \end{array}$$

The values chosen for the various enthalpies of transition have been obtained by drawing the respective values for pure AP and typical fuels from the indicated references and converting them to their equivalent values for a typical propellant containing 70% AP—*i.e.*, for pure AP, we assumed,

$$\begin{aligned}
 \Delta h_{tr} &= 20 \text{ cal./gram (82)} \\
 \Delta h_s &= 520 \text{ cal./gram (44, 73, 85)} \\
 \Delta h_1 &= (\Delta h_{tr} + \Delta h_s) - \Delta h_s \\
 &= -280\text{--}520 = -800 \text{ cal./gram (see Table I)}
 \end{aligned}$$

and for typical binders, we assumed,

$$\begin{aligned}
 h_{tr} &= 0 \text{ cal./gram} \\
 h_s &= 175 \text{ cal./gram (34)} \\
 h_1 &= 0 \text{ cal./gram}
 \end{aligned}$$

In accord with Ref. 80, the net heat liberated at the regressing propellant surface when the A/PA flame is collapsed to the surface is: $(\Delta h_s + \Delta h_1) \approx 140 \text{ cal./gram}$.

The above values have been used in conjunction with the measurement (80):

$$T_s = 615^\circ\text{C.} \approx 900^\circ\text{K. at } p = 30 \text{ p.s.i.a.}$$

and typical values of a and b for an 80μ mean oxidizer particle size propellant (9, 92), namely,

$$a = 190 \text{ p.s.i.a. sec./in.} = 32.8 \text{ atm. sec./cm.}$$

$$b = 25 (\text{p.s.i.a.})^{1/3} \text{ sec./in.} = 25.9 (\text{atm.})^{1/3} \text{ sec./cm.}$$

to evaluate α and β from the identical Equations 14 and 15 and to evaluate A from Equation 5.

Acknowledgment

The authors thank Victor S. Natiello for his effective assistance in obtaining the burning rate data used for this paper; we acknowledge also the excellent work of C. R. Felsheim in preparing the many propellant specimens of good quality used in this program. This work was sponsored by the Power Branch, Office of Naval Research, Department of the Navy under contract NONR 1958(32).

Literature Cited

- (1) Arden, E. A., Powling, J., Smith, W. A. W., *Combust. Flame* **6**, 21 (1962).
- (2) Adams, G. K., Newman, B. H., Robins, A. B., *Symp. Combust., 8th, Pasadena, Calif., 1960*, 693 (1962).
- (3) American Potash & Chemical Corp., Los Angeles, Calif., *Bull.* Dec. 14.
- (4) Andersen, R., Brown, R. S., Shannon, L. J., *AIAA Preprint* **64-156** (Jan. 1964).
- (5) Andersen, R., Brown, R. S., Shannon, L. J., *AIAA J.* **2**, 179 (1964).
- (6) Andersen, W. H., Bills, K. W., Mishuck, E., Moe, G., Schultz, R. D., *Combust. Flame* **3**, 301 (1959).
- (7) Bakhman, N. N., Belyaev, A. F., "Combustion in Heterogeneous Condensed Systems," Nauka, Moscow, 1967 (*RPE Transl.* **19**, G. S. Pearson, Ed., Rocket Propulsion Establishment, Westcott, England, 1967).
- (8) Barrere, M., Nadaud, L., *Rech. Aerospatiale* **98**, 15 (1964).
- (9) Bastress, E. K., Ph.D. Thesis, Princeton University (Jan. 1961).
- (10) Bastress, E. K., unpublished results (1961).
- (11) Beachell, H. C., Hackman, E. E., University of Delaware, *AFOSR Interim Sci. Rept.* **AFOSR 67-2419** (Sept. 1967).
- (12) Beckstead, M. W., Hightower, J. D., *AIAA J.* **5**, 1785 (1967).
- (13) Billmeyer, F. W., "Textbook of Polymer Science," Interscience, New York, 1965.
- (14) Bircumshaw, L. L., Newman, B. H., *Proc. Roy. Soc. (London)* **A227**, 115 (1954).
- (15) *Ibid.*, p. 228.
- (16) Bobolev, V. K., Glazkova, A. P., Zenin, A. A., Leipunskii, O. I., *Proc. Acad. Sci., USSR, Phys. Chem. Sect.* **151**, 644 (1963).
- (17) Burger, J., van Tiggelen, A., *Mem. Roy. Belg.* **34**, 3 (1964).
- (18) Capener, E. L., Dickinson, L. A., Marxman, G. A., Stanford Research Institute, *Quart. Rept.* **1** (Oct. 1965).
- (19) Chaiken, R. F., *Combust. Flame* **3**, 285 (1959).

- (20) Chaiken, R. F., Andersen, W. H., *Progr. Astronautics Rocketry* **1**, 227 (1960).
- (21) Chaiken, R. F., Andersen, W. H., Barsh, M. K., Mishuck, E., Moe, G., Schultz, R. D., *J. Chem. Phys.* **32**, 141 (1960).
- (22) Coates, R. L., *AIAA J.* **3**, 1257 (1965).
- (23) Cole, R. B., Wenograd, J., Princeton University, *Aerospace Mech. Sci. Rept.* **446-o** (June 1965).
- (24) Cole, R. B., Rohm and Haas Co., *Spec. Rept.* **S-68** (1965).
- (25) Dallavalle, M., "Micromeritics: The Technology of Fine Particles," 2nd ed., p. 68, Pitman, New York, 1948.
- (26) Derr, R. L., Osborne, J. R., *CPIA Publ.* **162**, 491 (Dec. 1967).
- (27) Feinauer, L. R., *AIAA Student J.* **3**, 125 (1965).
- (28) Flanigan, D. A., Thiokol Chemical Corp., *Progr. Rept.*, Appendix A (Sept. 1967).
- (29) Friedman, R., Nugent, R. G., Rumbel, K. E., Scurlock, A. C., *Symp. Combust.*, 6th, *Yale Univ.*, 1956, 612 (1957).
- (30) Geckler, R. D., "Selected Combustion Problems," p. 289, Butterworth, London, 1954.
- (31) Grassie, N., "Chemistry of High Polymer Degradation Processes," Interscience, New York, 1956.
- (32) Hall, A. R., Pearson, G. S., *R.P.E. Tech. Rept.* **67/1** (Jan. 1967).
- (33) Hall, K. P., Wenograd, J., Cole, R. B., *Aeron. Eng. Rept.* **446 k**, **446 l**, Princeton University (March 1962).
- (34) Hansel, J. G., Ph.D. Thesis, Stevens Institute of Technology, p. 99 (1964).
- (35) Hart, R. W., McClure, F. T., *J. Chem. Phys.* **30**, 1501 (1959).
- (36) Heath, G. A., Majer, J. R., *Trans. Faraday Soc.* **60**, 1783 (1964).
- (37) Hermance, C. E., *AIAA J.* **4**, 1629 (1966).
- (38) Hermance, C. E., *CPIA Publ.* **141**, 89 (June 1967).
- (39) Hicks, B. L., *J. Chem. Phys.* **22**, 414 (1954).
- (40) Hightower, J. D., Price, E. W., *CPIA Publ.* **105**, 421 (1966).
- (41) Hightower, J. D., Price, E. W., *Symp. Combust.*, 11th, 463 (1967).
- (42) Horton, M. D., Price, E. W., *ARS J.* **32**, 1745 (1962).
- (43) Huggett, C., "High Speed Aerodynamics and Jet Propulsion," Vol. 2, p. 514, Princeton University Press, Princeton, N. J., 1956.
- (44) Inami, S. H., Rosser, W. A., Wise, H., *J. Phys. Chem.* **67**, 1077 (1963).
- (45) Inami, S. H., Rosser, W. A., Wise, H., *Combust. Flame* **12**, 41 (1968).
- (46) Irwin, O. R., Salzman, P. K., Andersen, W. H., *Symp. Combust.*, 9th, *Cornell Univ.*, Ithaca, N. Y., 1962, 358 (1963).
- (47) Irwin, O. R., Salzman, P. K., Andersen, W. H., *AIAA J.* **1**, 1178 (1963).
- (48) Jacobs, P. W. M., Russell-Jones, A., *AIAA J.* **5**, 829 (1967).
- (49) Jacobs, P. W. M., Whitehead, H. M., University of Western Ontario, Final Report, Contract No. N60530-12591, U. S. Naval Weapons Center, China Lake, Calif. (Feb. 1968).
- (50) "JANAF Thermochemical Data," Dow Chemical Co., Midland, Mich.
- (51) Johnson, W. E., Nachbar, W., *Symp. Combust.*, 8th, *Pasadena, Calif.*, 1960, 678 (1962).
- (52) Kling, R., Brulard, J., *Rech. Aeron.* **80**, 3 (1961).
- (53) Krier, H., T'ien, J. S., Sirignano, W. A., Summerfield, M., *AIAA J.* **6**, 278 (1968).
- (54) Levy, J. B., Friedman, R., *Symp. Combust.*, 8th, *Pasadena, Calif.*, 1960, 663 (1962).
- (55) Mack, J., Wilmot, G., *Symp. Molecular Structure Spectroscopy*, Ohio State University (1962).
- (56) Madorsky, S. L., "Thermal Degradation of Organic Polymers," Interscience, New York, 1964.

- (57) Mallard, E., le Chatelier, H., *Ann. Mines* 8, Ser. 4, 274 (1883).
- (58) McAlevy, R. F., Lee, S. H., Lastrina, F. A., Samurin, N. A., *AIAA Preprint* 67-101 (Jan. 1967).
- (59) McGurk, J. L., *CPIA Publ.* 68, 345 (1965).
- (60) Most, W. J., Wenograd, J., Princeton University, *Aerospace Mech. Sci. Rept.* 446-p, (June 1965).
- (61) Nachbar, W., Parks, J. M., Lockheed Missile Systems Division, *Rept. LMSD-2191, AFOSR-TN 57-418* (Sept. 1957).
- (62) Nachbar, W., *Progr. Astronautics Rocketry* 1, 207 (1960).
- (63) Nachbar, W., Cline, G. B., *AGARD Colloq.*, 5th, 551 (1963).
- (64) Nadaud, L., *Recherche Aeron.* 85, 3 (1961).
- (65) Ohlemiller, T. J., Summerfield, M., Princeton University, *Aerospace Mech. Sci. Rept.* 799, (July 1967).
- (66) Pearson, G. S., Sutton, D., *AIAA J.* 5, 344 (1967).
- (67) Penner, S. S., "Chemistry Problems in Jet Propulsion," p. 246, Macmillan, New York, 1957.
- (68) Penner, S. S., "Chemical Rocket Propulsion and Combustion Research," p. 132, Gordon and Breach, New York, 1962.
- (69) Povinelli, L. A., *AIAA J.* 3, 1593 (1965).
- (70) Powling, J., *E.R.D.E. Rept.* 15/R/65 (July 1965).
- (71) Powling, J., *Symp. Combust.*, 11th, 447 (1967).
- (72) Powling, J., Smith, W. A. W., *Combust. Flame* 6, 173 (1962).
- (73) *Ibid.*, 7, 269 (1963).
- (74) Powling, J., Smith, W. A. W., *Symp. Combust. 10th, Univ. Cambridge, Cambridge, Engl.* 1964, 1373 (1965).
- (75) Reid, D. L., M.S.E. Thesis, Princeton University (July 1957).
- (76) Rice, O. K., *OSRD Rept.* 5574 (1945).
- (77) Rosser, W. A., Fishman, N., Wise, H., *AIAA J.* 4, 1615 (1966).
- (78) Rumbel, K. E., *ADVAN. CHEM. SER.* 88, 36 (1969).
- (79) Rumbel, K. E., *et al.*, Atlantic Research Corp., *Quart. Repts.* (1952-1969).
- (80) Sabadell, A. J., Wenograd, J., Summerfield, M., *AIAA J.* 3, 1580 (1965).
- (81) Sammons, G. D., *CPIA Publ.* 139, 75 (1967).
- (82) Sarner, S. F., "Propellant Chemistry," p. 296, Reinhold, New York, 1966.
- (83) Schultz, R. D., Dekker, A. O., Aerojet-General Corp. *Rept.* 576 (Confidential) (1952).
- (84) Schultz, R. D., Dekker, A. O., *Symp. Combust. 5th, Pittsburgh, 1954*, 260 (1955).
- (85) Schultz, R. D., Dekker, A. O., *Symp. Combust.*, 6th, *Yale Univ.*, 1956, 618 (1957).
- (86) Schultz, R., Green, L., Penner, S. S., *AGARD Collog.* 3rd, 367 (1963).
- (87) Selzer, H., *Symp. Combust.*, 11th, 439 (1967).
- (88) Silla, H., *ARS J.* 31, 1277 (1961).
- (89) Spalding, D. B., *Combust. Flame* 4, 59 (1960).
- (90) Steinz, J. A., Stang, P. L., Summerfield, M., *CPIA Publ.* 162, 499 (1967).
- (91) Steinz, J. A., Stang, P. L., Summerfield, M., *AIAA Preprint* 68-658 (June 1968).
- (92) Summerfield, M., Sutherland, G. S., Webb, M. J., Taback, H. J., Hall, K. P., *Progr. Astronautics Rocketry* 1, 141 (1960).
- (93) Sutherland, G. S., Ph.D. Thesis, Princeton University (May 1956).
- (94) Taback, H. J., *Aeron. Eng. Rept.* 429, Princeton University (Sept. 1958).
- (95) Taback, H. J., M.S.E. Thesis, Princeton University (1958).
- (96) Van Tiggelen, A., Burger, J., *Rev. Inst. Franc. Petrole* 11 (5) 816 (1966).

- (97) von Elbe, G., King, M. K., McHale, E. T., Macek, A., Atlantic Research Corp., *Rept. 66307* (Jan. 1967).
- (98) Waesche, R. H. W., Wenograd, J., *CPIA Publ. 162*, 481 (1967).
- (99) Webb, M. J., M.S.E. Thesis, Princeton University (May 1958).
- (100) Wenograd, J., *CPIA Publ. 138*, 89 (1967).
- (101) Yamazaki, K., Hayashi, M., Iwama, A., *Intern. Chem. Eng.* **5**, 186 (1965).

RECEIVED April 14, 1967.

Hazards and Hazard Testing

HENRY M. SHUEY

Rohm and Haas Co., Redstone Research Laboratories, Huntsville, Ala. 35807

The identification and evaluation of hazards in manufacturing solid propellants are being brought to a semiquantitative state of the art. Indiscriminate use of routine "approved" tests is being supplanted by analysis of the processes and operations to be used. By identifying the principal stresses involved (as thermal, friction, impact, electrostatic), one can design specific "use" tests, resulting in numerical values broad enough to distinguish discrete differences in stimuli necessary to ignite materials tested. Consideration of the consequences of such ignition allows tests to assess the worst catastrophe probable and suggests modifications of process conditions or plant construction to minimize risk to personnel, facilities, and product.

Throughout the history of industrial development man has generally adopted a new invention, process, or product and attempted quickly to adapt it to a particular need for which adequate data are unavailable. In aerospace propulsion many of the prior arts and processes were those of the explosives industry, an industry characterized by intensive employee training and considerable reluctance toward change. In the expansion caused by utilization of many of the processes in solid propellant manufacture, adaptation was necessarily performed by personnel not experienced in the rationale of the prior art, occasionally leading to disastrous results.

The operations involved in the manufacture and handling of solid propellants involve grinding of oxidants, blending of fuel and additives, loading of mixers, incorporation, discharge of the blended material, casting, curing, disassembly of tooling, and trimming of the final product. The materials are exposed at the various stages to mechanical stimuli, such as impact and friction, electrostatic discharge, thermal environment, and—under some conditions—shock. Considerable experience has been obtained as to the probability of occurrence and the results of ignitions

in these various stages of manufacture with subsequent modification of the procedure to reduce both the ignition probability and its effect.

Recently, attempts have been made to analyze hazards on a sound, predictive basis, not only to eliminate the risk involved in handling a new material or changing a process but to allow the process itself to be designed to produce the desired material at the lowest risk to personnel, property, and product—a sort of before-the-fact value engineering.

Attempts to estimate the probable hazard of handling a new compound were generally based on correlation of available test data with that of materials which had been processed successfully. Unfortunately, many of the test techniques used were designed for reproducibility of result rather than for interpretation of hazard, and they applied primarily to correlation within the industry where they were developed.

Hazards Analysis

Although the basic principles of explosives safety—the minimization of personnel exposure, of material quantity, and of possible ignition sources—could be transferred from the explosives industry, only minimization of personnel exposure could be accomplished efficiently without additional knowledge. An understanding of the physical chemistry of ignition and propagation of combustion and of the physics of heat generation as they relate to the processing and handling of propellants was necessary. The application of this knowledge as quantitatively as possible is regarded as “hazards analysis.”

Solid propellants are formulated to contain both a fuel and an oxidizer so that on ignition they will deflagrate uniformly and efficiently. They must also possess adequate physical properties to maintain structural integrity over a wide range of stress and strain rates. High explosives are generally formulated of materials which contain both fuel and oxidant moieties so that upon shock stimulus the material will detonate uniformly and efficiently. Herein lies a primary difference between a solid propellant and a high explosive: one must be cohesive and maintain essentially theoretical density under fairly high stresses; the other will fracture easily and is purposely manufactured at less than theoretical density in a prestressed state so that the shock stimulus necessary for initiation is not too great.

The reaction of the two systems to an ignition stimulus is markedly dissimilar; the cohesive material presents a combustible surface wherein the rate of regression is controlled by thermal diffusivity into the propellant; the non-cohesive system offers flame paths of convection into the explosive bulk, which if ignited produce gases to fracture the ma-

terial further and in many cases cause transition from a deflagrative reaction to detonation, often referred to as DDT.

Hazard Tests

Tests made on explosives for "sensitivity" by impact or friction, although in reality only ignition tests, should correlate well with the hazard of detonating the material. On the other hand, the same tests on a cohesive solid propellant would indicate only its ignitability under that particular stimulus and would not correlate prior experience in the explosives industry.

A typical example is interpretation of impact testing, generally expressed as the height of fall of a hammer onto a specially prepared sample which should produce ignition 50% of the time. Composition B, a high explosive often taken as a reference for a "safe" material, has a test height of 25 cm. on a particular machine. The same test run on a rubbery binder, ammonium perchlorate-oxidized propellant, yields the value of 11 cm., indicating at first that the propellant was much more hazardous than the high explosive. Yet the propellant in conventional test size shows little reaction in response to a high energy shock, while Composition B may be initiated by a detonator. Actually, the test only indicates that in thin films under impact loading, ignition temperature is reached in the solid propellant at a lower height of fall, and even this may be misleading since the test sample size enhances the effect of converting mechanical impact into thermal stress by the hardness of the ammonium perchlorate and the closeness of approximation of the film thickness to the particle size of the ammonium perchlorate.

On the other hand, if we consider the processing steps in making an ammonium perchlorate-oxidized solid propellant, the same test data would indicate a significant hazard of explosion or detonation when the propellant was unconsolidated and porous, particularly from impact or frictional stimulus in thin films such as might happen in shear-mixing. The test results would also indicate an ignition and fire hazard greater than the high explosive in machining or trimming operations of the final consolidated product where mechanical stimulus is applied to thin films. Hence, normal safety practices dictate remote operations during mixing and trimming, good hazards analysis practice would require conversion of the impact fall into kinetic energy units to compare with possible measured and predicted stresses which may be encountered in processing.

Explosive Liquids

Handling of explosive liquids has for years been based on a comparison of various test data with that obtained for nitroglycerine since

that compound has had the most production experience. The results have not correlated well when standard impact or thermal tests were used. More recently work at the Bureau of Mines (1, 3, 4) has shown that initiation of liquids to a low velocity reaction at low stimulus is a function of the material properties of both the liquid and its container and allows a more rational assessment of hazards to be made.

Instead of providing stimulus only to thin films of liquid in an impact test (which still has predictive use), testing may be done at levels and conditions comparable with that which may be accomplished in practice. Analysis of probable stimuli in the handling of discrete quantities of liquids shows a highly probability of dropping. Tests may therefore be designed to drop the material in question in the proper containers from various heights until an initiation occurs and until there is some statistical certainty of non-initiation at some finite height below this. Since heights may be compared, an assessment of the safety margin may be obtained for this handling operation.

More in line with the predictive use of hazards analysis, however, is the experimental and theoretical assessment that the viscosity of the liquid significantly affects this mode of initiation. Such information allows redesign of the process to eliminate handling of low viscosity liquid explosives, and quantitative measurement of the sensitivity of the system to mild shocks as a function of viscosity may allow the optimum level to be selected. This is not necessarily a new concept, only quantified in a different manner. Thirty years ago transporters of neat nitroglycerine in the oil fields were paid \$25 a day. The stipend for transporting jellied nitroglycerine was seven dollars, a practical comment on the understood difference in hazard.

Another type of testing, that of electrostatic sensitivity, has been demonstrated in some cases to be more properly a delicate test of the ignitability of the material under localized thermal stress which correlates best to the friction sensitivity of the system under test rather than to electrostatic hazards. On the other hand, electrostatic tests done in the supposed atmosphere above a propellant mixer were reduced in absolute value by more than an order of magnitude when the ammonium perchlorate dust actually present was introduced in the test since this altered the potential path for spark discharge within the system.

Another favored test for the past few years has been a form of gap testing, usually cards, whereby the explosive stimulus necessary to initiate the material to detonation is determined. Again, as for impact testing, the results are presented in terms of inches or numbers of cards which attenuate the donor shock wave to non-initiation. The results are much more valuable if expressed in terms of the minimum initiation pressure necessary to initiate the system since a quantitative assessment

of hazards in terms of flight malfunction or high speed impact may be made. In many cases it is also important to determine the minimum donor which can initiate the material since the potential hazard of handling can be shown to be small if insufficient energy is available to initiate it.

The previous examples demonstrate the need for an over-all understanding of manufacturing operations, ignition and combustion, and analytical test methods to perform a hazards analysis on a new material or process or even to define more accurately the safety margins of existing systems. The investigator should determine, in order and before the fact, the stresses imposed upon materials during processing, their reaction to such stresses and subsequent propagation at that degree of consolidation, altering the process or the physical state of the material such that a reasonably positive margin of safety exists. When this is not plausible, the investigator should provide such data to management that a logical decision may be made regarding the economic aspects of taking certain negative margins of safety.

An excellent attempt to formalize such an investigative procedure has been presented by Richardson (2) who summarized hazards analysis as "essentially an accident investigation before it happens."

Literature Cited

- (1) Hay, J. E., Watson, R. W. *et al.*, *N.Y. Acad. Sci. Conf. Prevention Protection Against Accidental Explosions Munitions, Fuels, Other Hazardous Mixtures* (Oct. 13, 1966).
- (2) Richardson, R. H. *et al.*, *N.Y. Acad. Sci. Conf. Prevention, Protection Against Accidental Explosions Munitions, Fuels, Other Hazardous Mixtures* (Oct. 13, 1966).
- (3) *Symp. Detonation, 4th, Naval Ordnance Lab., White Oak, Md.*, 1, A121 (1965).
- (4) Van Dolah, R. W., ASES, *Explosives Safety Seminar High-Energy Solid Propellants, 5th, Santa Monica, Calif., Minutes (S)*, 1963, 344-360.

RECEIVED May 4, 1967.

Current Liquid Propellant Systems

JACOB SILVERMAN and MARC T. CONSTANTINE

Rocketdyne, A Division of North American Rockwell Corp.,
Canoga Park, Calif. 91304

The requirements for selecting a fuel and oxidizer as a liquid bipropellant system are usually a compromise between the demands of the vehicle system, the propulsion system, and the propellants themselves. The vehicle and propulsion system will determine performance levels, physical property requirements, thermal requirements, auxiliary combustion requirements, degree of storability and packageability, hypergolicity, etc. The final propellant selection must not only satisfy such requirements but is also dictated by thermochemical demands which the fuel and oxidizer make on each other. Frequently, specifically required properties are achieved through the use of chemical additives and/or propellant blending.

From the initial application of the liquid rocket propulsion system concept in the V-2 rocket to the present development of various systems used to perform the Apollo missions, a variety of elements, compounds, and mixtures have been utilized as liquid rocket propellants. Since there has been no single liquid chemical or combination of liquids suited to all requirements of the present spectrum of rocket propulsion systems, a number of liquid propellants have been developed from various chemical families. Significantly, the hydrocarbons, amines, hydrazines, boranes, nitrogen oxides, nitric acids, halogens, and oxygen have all contributed to the growing technology of liquid rocket propellants.

The physical and chemical characteristics of these candidate liquid propellants vary widely. However, all of the liquids which have found application as rocket propellants have one common characteristic—they are designed to fit the particular requirements of at least one particular rocket engine and vehicle system. Obviously, few liquids initially fulfill the requirements of a propulsion system designed to perform a particular mission. Thus, various compromises must be undertaken between the

requirements of the system and the inherent characteristics of the available candidate propellants. Sometimes the propellant is modified, or some of the desirable design or operational features of the systems are changed, but in the end the resultant compromise between the system and propellant will perform the originally conceived mission.

To establish the relationship between current liquid propellant applications and the available propellant technology, this paper has been divided into three sections. A section on basic propellant considerations describes the normal parameters used to evaluate propellant candidates and their influence on the propulsion system. Although such considerations have been thoroughly discussed in many previous publications (*e.g.*, Ref. 3), their importance in establishing the basic criteria for propellant system selection requires a limited review in this text as a background aid to the reader. Current liquid propellants and propellant candidates are discussed in a second section in terms of capabilities and limitations as well as potential application areas (the compositions of all propellants discussed are defined in the Nomenclature section at the end of this article). Finally, a section of propellant tailoring illustrates examples of propellant formulation and describes propellant problem-solving techniques. In conclusion, the results of these considerations are illustrated by the current liquid propellant systems.

Basic Propellant Considerations

Theoretical Performance Requirements. Each propulsion system has a minimum performance level that must be achieved to conduct its required mission. After careful analysis of the mission profile, this required performance level is usually related in terms of required specific thrust or specific impulse (I_s). This nomenclature defines the pound of thrust produced per pound per second of propellant flow:

$$I_s = \frac{F}{\dot{W}} \quad (1)$$

where I_s = specific impulse (sec.), F = engine thrust (lbs.), and \dot{W} = total weight flow rate of propellant feed (lbs./sec.). This propellant system figure of merit represents the work done by the enthalpy drop in the rocket engine system:

$$I_s = k \sqrt{\frac{H_c - H_e}{\text{mass}}} \quad (2)$$

where k = dimensional constant; H_c = enthalpy of incoming propellants; and H_e = enthalpy of the combustion products at the exit plane of the rocket engine.

The calculation of a propellant system's theoretical I_s is a complex process which involves a number of different assumptions and estimations. Most standard computations, which are described thoroughly in a number of texts (1), involve a model which assumes instantaneous adiabatic combustion at a constant pressure or volume in the chamber section of a rocket engine, followed by one-dimensional isentropic expansion of the gases in the nozzle section to an assigned pressure or nozzle area. The model further assumes gas ideality, kinetic and thermal equilibrium between condensed and gaseous phases, and a negligible volume of condensed phase. The typically reported I_s assumes that chemical equilibrium is achieved in the chamber and maintained throughout the expansion process (shifting equilibrium).

Specific impulse, calculated by this technique, represents a 100% conversion of chemical energy to mechanical energy, and, therefore, is an upper limit to the performance available from a real rocket engine. However, regardless of the technique utilized, the theoretical I_s of each of the systems are compared on a common basis (*e.g.*, at the same combustion chamber pressure, nozzle geometry, exit pressure, etc.) with the desired performance level dictated by the mission and engine system requirements.

In systems in which the vehicle configuration is volume limited, theoretical performance comparisons, using density impulse ($I_s d$) are also necessary. This nomenclature, which is the product of the I_s and the bulk density of the propellants, defines the amount of thrust available in a unit volume of the propellant. The relative importance of $I_s d$ to I_s must be defined in the mission analysis.

Desirable Physical Characteristics. A number of physical characteristics are important in evaluating and selecting a liquid propellant system. Among these is the normal liquid range of the propellants. This should conform to the operating range of the vehicle system. In most cases, thermal regulation is usually undesirable or impossible; therefore, matching low temperature properties of the propellant to the system's operating environment is more feasible. Conversely, the desirability of a high boiling point and high critical temperature is obvious for those systems exposed to high temperatures.

Another desirable physical property is high propellant density. One requirement for high propellant density has already been noted in the discussion of performance ($I_s d$) requirements. The density of the propellant controls the size of the propellant tankage. Even in systems in which the volume of the vehicle is not critical, the smaller tankage results in a reduction in structural weight and aerodynamic drag of the vehicle. In addition, the change in density with temperature variation should be

low to limit propellant system design and operational problems attendant to expansion and contraction of the liquid during temperature changes.

In systems where the propellants are used for thrust chamber cooling, properties related to heat transfer are important. Candidate propellants should have high specific heats, high thermal conductivities, high boiling points, high decomposition temperatures, etc.

Mass transfer requirements dictate low propellant viscosity. In addition to the excessive work required to transfer a viscous propellant from the tank to the combustion chamber (either through pumping or pressurization), the injection problems associated with viscous propellants have often compromised efficient combustion. Low propellant vapor pressure allows a more efficient pump design and avoids one problem area in fluid pumping.

Engineering Properties. Engineering properties usually include storability, thermal stability, materials compatibilities, shock and thermal sensitivity, and toxicity. Failure in any of these areas would eliminate the propellant from further consideration.

Storability is the physical and chemical stability of the liquid propellant during storage either in propellant handling or in missile systems. This property is always related to various materials of construction and at temperature ranges normally associated with potential storage conditions. The complete absence of decomposition or chemical reaction of the propellants in the presence of various types of materials, common system contaminants (*i.e.*, moisture), and maximum storage temperatures is normally preferred; however, some minimum rates or levels are permitted in various applications.

Because propellants are constantly subjected to abnormally high temperatures in various parts of the propulsion system during operation, high thermal stability is desirable. Decomposition of the propellant at temperatures experienced in the combustion chamber cooling jacket, the injector, and/or the gas film on the combustion chamber wall, can cause undesirable product deposition (resulting in local "hot spots" and burn-out), explosion in the cooling jacket and/or injector, undesired reaction chains in the combustion chamber, etc.

Materials compatibility is the resistance of materials of system construction to chemical or physical attack by the propellants or the products of propellant combustion. In addition to destroying the integrity of the pertinent structural member, corrosion of the material by the propellant results in contamination of the propellant with the corrosion products, which in turn deteriorates the propellant's physical and chemical properties. As in storability, materials compatibility is related to usage temperatures, as well as to special materials handling, cleaning, and/or passivation techniques. Although limited materials compatibility of a

propellant may not necessarily eliminate the propellant from consideration, it imposes restrictions on the ultimate mission.

The propellants should be stable with respect to initiation and propagation of deflagration or detonation. Because of their energetic nature and high reactivity, most propellants are sensitive to compression or thermal shock under certain conditions (*i.e.*, contamination, high temperature, incompatible materials); however, many of these propellants can be utilized if the pertinent conditions are well characterized and avoided. Of course, there are some chemicals (*i.e.*, ozone) whose sensitivities are beyond present handling technology; thus, their use as propellants is presently precluded.

Although toxicity of a propellant candidate (or its combustion products) is important in all propellant selections, emphasis varies on this factor. Toxicity is usually of passing interest in upper stage or space vehicles, which can utilize specialized handling techniques and controlled launch sites to eliminate the possibility of contamination during launch. However, where the application involves the handling of the propellant system by a large number of personnel in the field or a potential launch over a populated area, high toxicity eliminates a propellant from further considerations.

Economic Factors. Economic factors are related to the availability and cost of the propellant as well as the cost of the equipment required to transport, store, and supply the propellant. Generally, low cost is a prime requisite for a propellant which will be utilized in large quantities and/or in multiunits (*i.e.*, booster stages of launch vehicles and in military weapons). However, where utilization of a high-cost propellant may be required to complete the mission, the cost factor can be of secondary importance. This situation is usually associated with upper stages of a space launch vehicle.

Combustion Characteristics. Ignition, combustion efficiency, and combustion stability are the principal combustion-related considerations in liquid propellants. Hypergolic ignition, defined as the spontaneous ignition upon contact of fuel and oxidizer, is a distinctly advantageous property. Although hypergolicity is not a prime requisite of all propulsion systems, this desirable feature eliminates the complexity and weight of auxiliary ignition systems. In systems requiring pulsing operation and/or several restarts, hypergolicity is a necessity.

Combustion efficiency is usually described in terms of specific impulse efficiency (percentage of theoretical specific impulse achievable). Specific impulse efficiencies depend greatly on both chemical composition of the propellant and the physical design of the injector, combustion chamber, and nozzle configuration. Efficiencies can thus vary from 90–98%.

Under certain conditions, propellants may exhibit high frequency vibratory combustion. Such vibration can cause extensive hardware damage and/or a mission abort. In most instances, however, combustion instability is related principally to the physical design of the combustion chamber rather than the chemical properties of the propellants.

Current Liquid Propellants and Propellant Candidates

Current liquid propellants are reviewed from two points of view. First, the current application areas are described in terms of their requirements. Secondly, the capabilities and limitations of various liquid propellant candidates are indicated with a few descriptive illustrations.

Application Areas. Applications can be divided into two general groupings—space exploration and military applications. Space exploration may range from a sounding rocket into the upper atmosphere to manned exploration of the moon. Military applications range from small air-to-air missiles to ICBM requirements. Although many of the requirements between the two may be similar, the primary difference is that the space systems are designed to be handled by a relatively few highly specialized and trained personnel in well-controlled environments, while military systems are designed to be handled by a large number of personnel under various situations in the field.

Space exploration application areas can be further subdivided—namely, booster propulsion, upper stage propulsion, and spacecraft control propulsion. The requirements in each of these general areas are different.

Propellants that are comparatively easy to handle in large quantities, have unlimited availability, and are relatively cheap are normally the choice for booster application. Although only moderate performance levels are required, the bulk density of the propellant should be fairly large to preclude unreasonably sized vehicles. The propellant system need not be hypergolic, although this is obviously desirable. The propellants can have almost any liquidus range as long as they can be handled within the available technology. Because these systems are usually pump fed and regeneratively cooled, both propellants should have good mass transfer properties, and at least one of the propellants (usually the fuel) should have good heat transfer properties.

Upper stage propellant applications are usually based primarily on performance—*i.e.*, high specific impulse. If the upper stage is a multistart vehicle, hypergolicity is usually required. Careful consideration is also given to the propellant physical and chemical stability as well as to the matching of the propellant's liquidus range to the space environmental temperature if the propellant system is to remain operational in space

for an extended period. Such factors as toxicity, cost, density, etc., are of much lesser importance.

Selection of propellants for spacecraft control propulsion usually depends on factors related to long term reliability and ease of operation. Spacecraft control propulsion systems include reaction control systems, attitude control systems, orbital altitude, maneuvering systems, etc. All require hypergolic propellants for multirestart and/or pulsing modes of operation. Although specific impulse is not of primary importance, reasonably high bulk density (weighted average of fuel and oxidizer) is usually required because of the limited volume configuration. These systems are usually pressure fed and utilize ablative, film, or radiation cooling for the combustion chamber.

Military applications can be subdivided into two distinct types—fixed launch site systems and mobile systems. Both types place emphasis on specific impulse, density impulse, excellent storability and stability, and instant readiness. Fixed-site systems, which include most of the long range ballistic missiles, are systems whose launch facilities are well established and are usually environmentally controlled. These vehicles are usually pump fed and regeneratively cooled. Hypergolicity is preferred, but not necessarily required.

Mobile weapon systems include the ordnance weapon systems, such as the air-to-air, air-to-surface, surface-to-air, and short-range, surface-to-surface missile. Because of the limited volume requirements, heavy emphasis is placed on density impulse. These systems are completely prepackaged (including propellants) and require complete storability of the propellant as a liquid over a temperature range -65° – 160° F. Because of personnel proximity at all times, toxicity is sometimes an important factor. The large number of units which are utilized usually imposes restrictions on propellant cost.

Current Propellant Capabilities and Limitations. In selecting a propellant system for any application, the various considerations and factors briefly outlined above are weighted for each of the propellant candidates against the requirements of the proposed system. Initially, the potential candidates are screened by evaluating their performance potential (I_s and/or $I_s d$, as required). Some insight into the performance of different combinations can be obtained by utilizing a generalized performance criteria chart such as shown in Table I.

This table illustrates the performances that may be achieved through combination of various oxidizer and fuel types. The numbers in the table represent theoretical calculations of I_s (seconds) at standard conditions of 1000 p.s.i.a. and shifting equilibrium with optimum expansion to sea level conditions (using the "typical procedure" previously described). The thermodynamic properties of the propellants and the potential reac-

tion products, which are required for these calculations, were established by the JANAF Thermochemical Working Group (2). The propellants in the top row of Table I represent the highest performing members of the various halogen, oxyhalogen, nitrohalogen, hydroxyl, nitrogen oxide, and interhalogen oxidizer families, respectively. The left-hand column represents various fuels of the hydrogen, beryllium, borane, hydrocarbon, hydrazine (and amine), aluminum, and lithium families.

Table I. Generalized Performance Criteria

Specific Impulse at 100 p.s.i.a. Chamber Pressure, Shifting Equilibrium, Optimum Expansion to Sea Level

Fuel	Oxidizer						
	F_2	OF_2	O_2	N_2F_4	H_2O_2	N_2O_4	ClF_5
H_2	411	401	391	361	314	341	343
BeH_2	378	360	351	350	357	332	329
B_2H_6	363	365	343	340	332	321	317
CH_4	344	347	311	314	281	283	293
N_2H_4	364	339	313	334	282	292	312
AlH_3	348	322	309	327	318	301	304
LiH	365	332	269	333	268	253	313

Such a table is indicative of the performance potential of these propellant groupings, although the performances will vary slightly from member to member in each propellant family. Table I shows that the highest performance is realized from systems containing F_2 (in particular, the F_2/H_2 system). In general, maximum performance is achieved with various combinations of the cryogenic propellants, H_2 , B_2H_6 , CH_4 , F_2 , OF_2 , O_2 , N_2F_4 . One exception are those combinations involving BeH_2 . Typical performances of earth-storable propellants are noted in the combinations of H_2O_2 , N_2O_4 , and ClF_5 with BeH_2 , N_2H_4 , AlH_3 , and LiH .

An expansion of Table I is shown in Table II to illustrate the performances available in combinations of other members of the various chemical families. These differences are noted through the examples of two different propellant system groupings. The upper section of Table II utilizes two different members of the nitrogen oxide oxidizer family, N_2O_4 and IRFNA (inhibited red fuming nitric acid), with several members and mixtures of the hydrazine and amine fuel family, N_2H_4 , NH_3 , $CH_3N_2H_3$ (monomethylhydrazine, MMH), $(CH_3)_2N_2H_2$ (*unsym*-dimethylhydrazine, UDMH), $N_2H_4-(CH_3)_2N_2H_2$ (50-50), and MAF-4 (UDMH-diethylenetriamine, 60-40). As noted, there is an 8-10-second difference in I_s between the N_2O_4 - and IRFNA-oxidized systems. The I_s performance range between various fuels is 23 seconds.

Table II. Theoretical Specific Impulse of Selected Propellant Systems

1000 p.s.i.a. Shifting Equilibrium, Optimum Expansion to Sea Level

Oxidizer	Fuel					
	N_2H_4	NH_3	$CH_3N_2H_3$	$(CH_3)_2N_2H_2$	50% N_2H_4 - 50% $(CH_3)_2N_2H_2$	MAF-4
N_2O_4	292	269	289	286	289	282
IRFNA	283	260	279	277	280	274

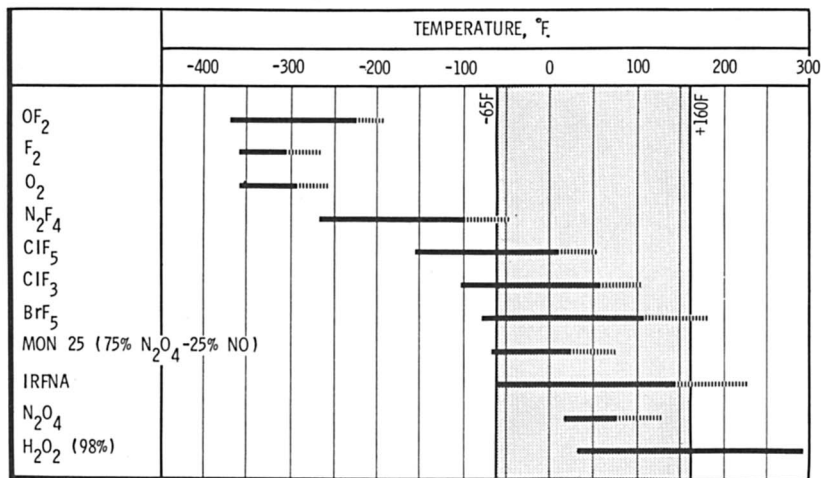
Oxidizer	Fuel	
	CH_4	RP-1
O_2	311	300
Flox-30	325	317
Flox-70	350	344
OF_2	347	341
F_2	344	318

The lower half of Table II demonstrates the performance differences between two members of the hydrocarbon family, CH_4 and RP-1 (a kerosene cut), with various oxidizer selections. The oxidizer selections are designed to demonstrate the change of performance between the oxygen and fluoride groups with various intermediate mixtures, flox 30 (F_2 - O_2 , 30-70), flox 70 (F_2 - O_2 , 70-30), and an oxyfluoride compound, OF_2 . The difference between CH_4 and RP-1 performance, as F_2 is added to O_2 , is particularly noteworthy. This difference is fairly consistent between the two as F_2 is added; however, after reaching a maximum in each system (345 seconds at 71% F_2 with RP-1, and 353 seconds at 83% F_2 with CH_4), the performance dropoff with additional F_2 content occurs at lower F_2 concentrations and is more rapid with the RP-1 fuel. This difference is a result of the RP-1, which has a hydrogen/carbon ratio (H/C) of ~ 2 , requiring more oxygen than CH_4 (H/C = 4).

In addition to the use of tables such as these to establish the theoretical performance potential (a like comparison can be made of $I_s d$) of various propellant systems under the desired operating conditions, the individual propellants are compared with respect to the other considerations. An example of a comparison of liquid range of various propellants to a specific set of required conditions is shown in Table III. In this example, the operating temperature environment of the particular vehicle is -65° to $+160^\circ F$. With this information, the liquidus ranges of various oxidizers and fuels are plotted under these conditions. (In the table, the solid line represents the range between the normal freezing and boiling points, with the end of the broken line representing the boiling point at 50 p.s.i.a.) Those propellants with liquid ranges entirely within the shaded area fulfill the initial liquid range requirements.

Table III. Normal Liquid Range

Oxidizers

**Propellant Tailoring**

In many situations, the propulsion and vehicle system requirements cannot be met by the available propellant combinations. Such problems are often solved by tailoring. This involves the formulation of a desirable set of characteristics by mixing selected ingredients. Several examples of new propellants that have been developed in this manner are noted below.

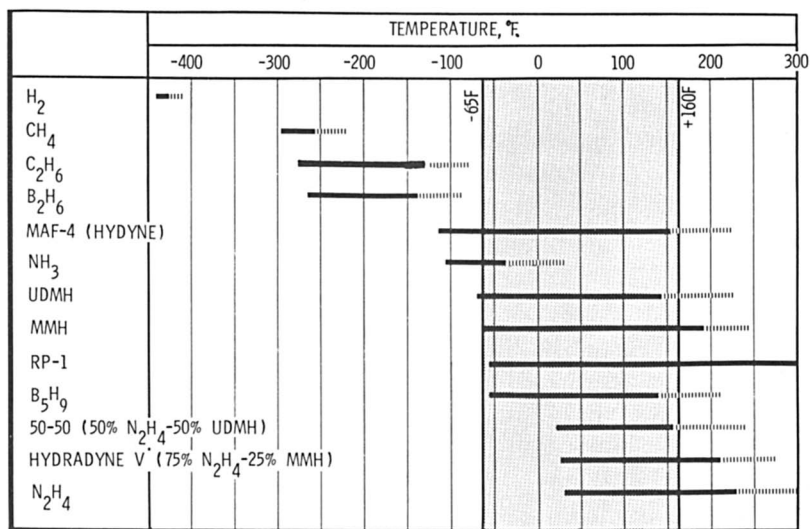
An example of propellant tailoring is the fuel used to launch the first U. S. satellite into orbit. The original fuel for the launch vehicle was ethyl alcohol. MAF-4 (also known as hydne or U-DETA), a mixture of 60% UDMH and 40% diethylenetriamine (DETA), was formulated to simulate the physical properties of C₂H₅OH but provide the increased propellant performance (using liquid oxygen as the oxidizer) requirements of the mission.

Other MAF fuels, MAF-1 (DETA-UDMH-acetonitrile, 50-40-10), and MAF-3 (UDMH-DETA, 20-80) were formulated primarily to increase density. These formulations were based on density impulse requirements of various prepackaged propulsion systems as well as to maintain the freezing point and viscosity characteristics of the UDMH.

Formulation of the N₂H₄-UDMH (50-50) blend provided a relatively high performance but thermally stable hydrazine-type fuel suitable for regenerative cooling of large thrust chambers.

of Selected Propellants

Fuels



The current RP-1 hydrocarbon fuel used in high thrust boosters is an example of a special kind of tailoring. This hydrocarbon blend or distillation cut was selected to meet a series of special property and combustion requirements for liquid oxygen-oxidized high thrust systems.

Propellant tailoring has also been studied as a means of upgrading the performance of present liquid oxygen systems by adding F₂. This potential performance improvement (indicated in Table II) would apply to both hydrocarbon- and hydrogen-fueled systems. Experimental studies with both systems have verified the propellant system performance increases which can be realized.

Conclusions

As a result of this constant evaluation and compromise between the demands of the vehicle and propulsion systems and the current propellant technology, various liquid propellant systems have been developed and are being applied in current vehicle systems (Table IV). In Table IV thrust level is used to demonstrate the size of the propulsion system. Some of the systems in this table have been phased out, while others are still in development. However, Table IV does represent the current status of operational liquid bipropellant systems.

Table IV. Current Liquid Bipropellant Applications

<i>Propellant System,</i>	<i>Engine System, Common Designation</i>	<i>Thrust Level, lbs.</i>	<i>Application Area</i>
LO ₂ /RP-1	Thor	170,000	Space booster, IRBM (Delta 1st stage)
	H-1	200,000	Up-rated Saturn I
	Blue Streak	300,000	Space booster
	Titan I	300,000 (1st stage)	ICBM
		80,000 (2nd stage)	
	Atlas	370,000–390,000	Space booster, ICBM
LO ₂ /H ₂	F-1	1,500,000	Saturn V, S-IC
	Centaur	15,000	Up-rated Saturn I, SIII (2 engines)
			Saturn I, SII (6 engines)
J-2	200,000	Saturn V, SII & SIII	
LO ₂ /NH ₃	X-15	15,000–58,000	Experimental rocket plane
LO ₂ /C ₂ H ₅ OH H ₂ O ₂ /JP-4, JP-5	Redstone AR-2, 3	75,000	SRBM
		3300–6600	Auxiliary rocket engine for aircraft
	Warrior	3500–10,200	Auxiliary rocket engine for aircraft
IRFNA/UDMH	AJ10-118	7500	Space booster (Delta 2nd stage)
	Lance		Surface-to-sur- face missile
	Agena	16,000	Space booster (2nd stage)
IRFNA/MAF-1	Bullpup		Air-to-surface missile
IRFNA/MAF-3	TD-174		Air-to-air missile
IRFNA/MAF-4	P4	550 (booster) 106 (sustainer)	Target drone

Table IV. Continued

<i>Propellant System,</i>	<i>Engine System, Common Designation</i>	<i>Thrust Level, lbs.</i>	<i>Application Area</i>
IRFNA/JP-4	Aerobee 100 sustainer	2600 (total)	Sounding rocket
IRFNA/aniline-furfuryl alcohol	Aerobee 150 and 150A sustainer	4100 (total)	Sounding rocket
IWFNA/turpentine	Emeraude	62,700	Space booster
N_2O_4/N_2H_4 -UDMH (50-50)	Apollo service module RCS	100	Reaction control
	Ullage rocket	1750	Saturn V, S-IVB Ullage control
	AJ10-131	2200	General purpose space engine
	F750 L2. 2K	2200	Multiple restart space engine
N_2O_4/N_2H_4 -UDMH (50-50)	Lunar module ascent engine	3500	Lunar module liftoff (moon)
	F720 L8. 0K	8000	Multiple restart space engine
	Transtage	8000	Upper stage propulsion
	Lunar module descent engine	1050-10,500	Lunar landing engine
	Apollo service module	21,900	Space propulsion
	YLR113-AJ-1	50,000-150,000	Rocket sled
	Titan II	430,000 (1st stage) 100,000 (2nd stage)	Space booster, ICBM
N_2O_4/MMH	Advanced Syncom RCS	5	Reaction control
	Gemini RCS	25 (two 8-engine sets)	Reaction control
	Transtage ACS	25 (4 engines) 45 (4 engines)	Attitude control
	Apollo command module	93 (two 6-engine sets)	Attitude control
N_2O_4/MMH	Gemini OAMS	25 (8 engines) 85 (2 engines) 100 (6 engines)	Orbital change
	Radiomic	85-100	General purpose attitude control

Table IV. Continued

<i>Propellant System,</i>	<i>Engine System, Common Designation</i>	<i>Thrust Level, lbs.</i>	<i>Application Area</i>
N ₂ O ₄ /N ₂ H ₄ -MMH	Advent RCS	22	Reaction control Agena secondary propulsion
	SE-5	48 (2 engines)	
N ₂ O ₄ /JP-X MON/MMH	Air turbo rocket	500	Drone
	Surveyor vernier engine	30-104	Attitude and velocity control
MON/UDMH		16 (2 engines)	Agena secondary propulsion
		200 (2 engines)	

Table IV shows that the LO₂/RP-1 and N₂O₄/N₂H₄-UDMH (50-50) propellant combinations have emerged as the current workhorse propellant systems for first stage or booster applications. These systems are relatively inexpensive, have good physical and engineering properties, and reflect a high degree of development. Both have been and are systems being used in ICBM applications, although the former is a nonhypergolic cryogenic system, while the latter is a hypergolic storable combination.

Current upper stage systems are based on propellant combinations with performances ranging from those of the IRFNA/UDMH and the N₂O₄/N₂H₄-UDMH (50-50) systems, to the high levels achieved with the LO₂/H₂ system. The development of the nitrogen oxide-type oxidizer/hydrazine-(or amine)-type fuel propellant system for second-stage application was based on the need for wide liquid ranges and hypergolicity, whereas the development of the LO₂/H₂ system for upper stage application responded to the need for high performance.

The spacecraft control propulsion systems utilize primarily moderate performing nitrogen oxide/hydrazine systems. These systems are reliably hypergolic with good storability and stability under the programmed environmental conditions. The present ICBM system requirements are identical to those of the large boosters. The present performance and prepackageable requirements of the ordnance systems are well suited to the combination of IRFNA with various prepackageable hydrazines and amines.

Nomenclature

Fuels

DETA: Diethylenetriamine, (NH₂C₂H₄)₂NH

MMH: Monomethylhydrazine, CH₃N₂H₃

UDMH: *unsym*-Dimethylhydrazine, (CH₃)₂N₂H₂

50-50 Fuel blend: 50% N₂H₄-50% UDMH

Hydradyne V: 75% N_2H_4 –25% MMH

MAF-1: 50.5% DETA–40.5% UDMH–9.0% CH_3CN

MAF-3: 80% DETA–20% UDMH

MAF-4 (Hydyne, U–DETA): 60% UDMH–40% DETA

JP-4, JP-5: Hydrocarbon fuels (kerosene cut) developed for jet propulsion applications

JP-X: 60% JP-4–40% UDMH

RP-1: A hydrocarbon fuel blend (kerosene cut) developed for rocket propulsion applications

Oxidizers

Flox: Various mixtures of liquid fluorine and liquid oxygen (*e.g.*, flox 30 is 30% F_2 –10% O_2 ; flox 70 is 70% F_2 –30% O_2)

IRFNA (inhibited red fuming nitric acid): 84.4% HNO_3 –14% N_2O_4 –1% H_2O –0.6% HF

IWFNA (inhibited white fuming nitric acid): 97.5% HNO_3 –1.5% H_2O –0.3% N_2O_4 –0.7% HF

Lox (LO_2): Liquid oxygen, O_2

MON: Mixtures of NO and N_2O_4 (*e.g.*, MON 10 is 10% NO–90% N_2O_4 ; MON 30 is 30% NO–70% N_2O_4)

Literature Cited

- (1) Huff, V. N., Gordon, S., Morrell, V. E., *NACA Rept. 1037* (1951).
- (2) Stull, D. R. *et al.*, "JANAF Thermochemical Tables," Dow Chemical Co., Midland, Mich., Aug. 1965.
- (3) Sutton, G. P., "Rocket Propulsion Elements, An Introduction to the Engineering of Rockets," Wiley, New York, 1963.

RECEIVED April 14, 1967.

Advanced Fuels and Oxidizers

CLAIR M. BEIGHLEY, WILLIAM R. FISH, and ROGER E. ANDERSON

Aerojet-General Corp., P. O. Box 15847, Sacramento, Calif. 95813

Guidelines for developing advanced liquid fuels and oxidizers are outlined from theoretical considerations of the reaction principle of rocket propulsion. Advanced oxidizers are based on oxygen and, increasingly, on fluorine. The potential of these elements, their blends, intercompounds, and compounds with nitrogen, chlorine, noble gases, and other carrier elements in advanced chemical propulsion is discussed. Fuel research and development are oriented largely toward incorporating metal additives into liquid fuels to form chemically and mechanically stable heterogeneous gels and emulsions of high heating value and/or density. Factors pertinent to this relatively new area of liquid propellant technology are discussed.

October 4, 1967 was the decennial of the Space Age (Sputnik I was launched October 4, 1957). Chemical propulsion, more specifically, liquid rocket propulsion, has been the pacing technology which dictated progress and eventually permitted the existing record of achievements in space. The liquid rocket engineer, working with selected sources of liquid propellant energy, has been primarily responsible for the space achievements to date. What does the future hold for the liquid rocket engine and liquid propellants as a source of propulsive energy?

All rocket propulsion systems are based on the reaction principle in which reaction thrust is imparted by the momentum of matter ejected through a nozzle. In a chemical propulsion system such as a liquid propellant rocket, gases generated by chemical reactions are ejected as high velocity gas streams through a nozzle. In essence, propulsive thrust is achieved by converting thermal energy of chemical reactions into directed translational energy of the combustion products.

The primary parameter which indicates the merit of a chemical propellant is the specific impulse, I_s , which is defined as the ratio of the

thrust, F , lb.(f), produced to the rate of propellant consumption, w , lb.(m)/sec. Thus,

$$I_s = F/w \quad (1)$$

An elementary analysis, based on the simplifying assumptions that the generated combustion product gases are ideal and that their heat capacities and composition are independent of temperature and pressure, yields the following expression for specific impulse:

$$I_s = \left\{ \frac{2J}{g} \frac{\gamma R T_c}{(\gamma - 1)M} \left[1 - \left(\frac{P_e}{P_c} \right)^{\frac{\gamma-1}{\gamma}} \right] \right\}^{1/2} \quad (2)$$

where the adiabatic coefficient, γ , is defined as

$$\gamma = \left(\frac{\delta \ln P}{\delta \ln \rho} \right)_s \quad (3)$$

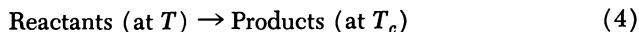
and where

- | | |
|---|---|
| g = gravitational constant, ft./sec. ² | R = universal gas constant, cal./mole-°K. |
| J = mechanical equivalent of heat, erg/cal. | s = constant entropy |
| P = pressure, p.s.i.g.; P_e , at chamber; P_e , at exit plane | T_c = chamber temperature, °K. |
| M = molecular weight, grams/mole | ρ = density, grams/cc. |

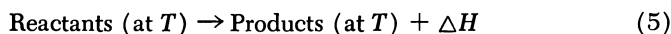
[This elementary analysis is presented to emphasize the factors that guide the search for advanced propellants. Equation 2 is no longer used to calculate specific impulse. Refs. 37 and 43 contain more rigorous analyses and the thermodynamic basis for the modern computational methods for obtaining the specific impulse of rocket propellants.] Examination of Equation 2 reveals three variables that are functions of the propellant chemistry, T_c , M , and γ . The parameter γ is *ca.* 1.2 for most propellant combinations and cannot be significantly altered. Therefore, the search for higher specific impulse, I_s , must start with propellant combinations which react to yield high temperature combustion products with a low average molecular weight.

In practical applications the weight and size of the tanks which must carry the propellant are important. Therefore, propellants with a high bulk density are preferred and in some cases are essential to minimize these factors.

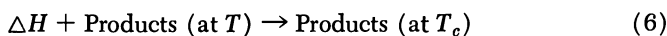
In a rocket combustion chamber the chemical reaction is essentially adiabatic. This has been expressed by Siegel and Schieler (37) as follows:



Thermodynamically this can be divided into an isothermal step:



and an adiabatic step



Because most propellant reactants are endothermic or only slightly exothermic, a high chamber temperature results from selecting propellants which react to yield highly exothermic products. However, from Equation 2 it is apparent that low average molecular weight is just as important as high T_c . Therefore, our search through the periodic table of the elements rapidly narrows to those which yield (a) high exothermicity (negative of the heat of formation per gram of the primary product species), (b) low molecular weight products, (c) high density reactants.

Figure 1 presents a graphical comparison of the exothermicity of the first 40 elements in the periodic table. Compounds formed with oxygen and fluorine have the highest specific exothermicities. Chlorine and nitrogen compounds are considerably lower. Carbides of the light elements, not shown in the graph, are lower than the corresponding nitrides. Clearly, both the oxides and fluorides merit serious considerations as desirable propulsion combustion products. Because hydrogen has the lowest atomic weight, propellants rich in hydrogen—*e.g.*, N_2H_4 and light metal hydrides—provide high specific impulse. However, hydrogen itself has a low density which is a disadvantage for certain specific applications. Liquid–solid mixtures of hydrogen, called slush hydrogen, are being investigated to alleviate the density disadvantage and to increase the heat capacity and lower losses caused by evaporation (6).

Li, Be, and B, metallic elements of the second row of the periodic table, along with hydrogen-rich compounds of these metals, carbon and nitrogen are of primary interest. In the third row of elements, Mg, Al, and Si have some potential. Interest in elements with atomic numbers greater than 16 rapidly decreases because of the high molecular weight of the resulting combustion products. Ti and Zr are potential fuels for systems requiring very high performance on a volumetric basis.

Unfortunately, most of the elements chosen as promising propellant ingredients are metals and hence solids rather than liquids. The endeavor to incorporate solid-phase metals and metal compounds into liquid propellants has led to a whole new area of propellant technology. Heterogeneous fuels are discussed in detail later.

The metals also present an additional problem in that the product oxide, fluoride, or nitride species may be a solid phase at the combustion temperature or condense during expansion through the rocket nozzle. Figure 2 presents a graphical comparison of the phase properties of the

primary product species for the elements of interest. The range of typical rocket combustion temperatures and exhaust temperatures reveals that in most cases a condensed phase will be present in the exhaust. The energy exchange which occurs during a phase change must be considered. Liquid or solid combustion products cannot expand through the nozzle and must transfer their energy to a working gas during expansion. If the condensed phase grows to large particle diameter, a lag in the transfer of both thermal and kinetic energy occurs, representing a loss in the attainable specific impulse from the system.

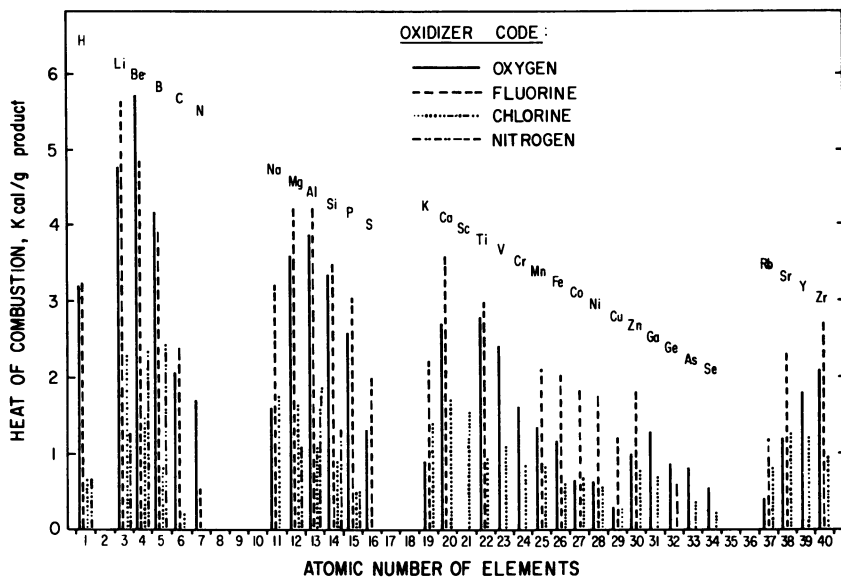


Figure 1. Heat of combustion of the low atomic number elements with oxygen, fluorine, chlorine, and nitrogen

An additional consideration is the extent of dissociation of the product species. Rocket combustion temperatures range from 3000° to 5000°K. At these temperatures, many of the product species dissociate, tying up energy in atomic and free radical species. Figure 3 shows the dissociation which occurs in typical product gases at a pressure of 50 atm. (37). The oxygen-oxidized propellant systems generally produce temperatures toward the lower end of the range, 3000°K., where dissociation of species such as CO₂ and H₂O becomes important. The fluorine-oxidized propellant systems produce temperatures toward the upper end of the range, 4000°–5000°K., where the dissociation of species such as H₂, HF, and metallic fluorides must be considered. Pressure has a significant effect on dissociation: lower pressure increases dissociation. A combination of low pressure and high combustion temperature can result

in considerable energy being tied up in dissociated species. Conversion of this energy into useful kinetic energy for propulsion presents a design compromise. Rocket nozzles are normally made as short as possible, resulting in very rapid expansion of the product gases. The recombination of the various dissociated product species may not be rapid enough to occur within the nozzle, thus representing a loss in the theoretically attainable specific impulse.

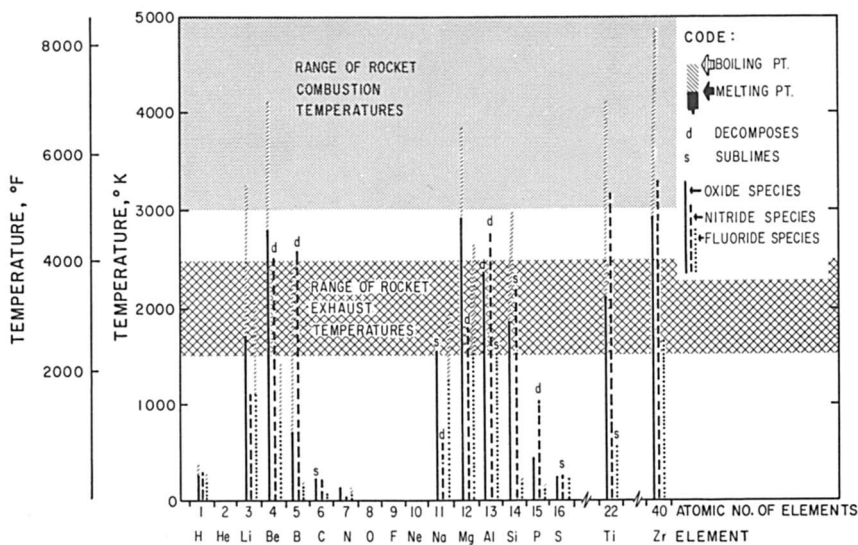


Figure 2. Phase properties of the oxides, fluorides, and nitrides of the low atomic number elements

A liquid propellant must satisfy many additional criteria to be considered for a specific application. Rocket engineers have divided propellants roughly into two general types: storable and cryogenic. Storable refers to those which are liquid near standard conditions and can be stored in simple containers for long periods without serious deterioration or loss. Cryogenic refers to propellants which are gaseous at standard conditions and, therefore, must be handled under refrigerated conditions to remain liquid. A detailed discussion of all the criteria which must be satisfied for specific applications can be found in Silverman and Constantine's chapter (38).

Many compounds have been evaluated as propellants in the past, but only a small percentage of these are currently being used in operational liquid rocket engines. Current operational propellants are based on hydrogen and hydrogen-rich compounds of carbon and nitrogen as fuels and oxygen or oxygen-based oxidizers. Obviously, fuels based on the low atomic number elemental metals, metal hydrides, and organo-

metallic compounds and oxidizers based on fluorine and oxygen offer the highest specific impulse potential. They are, therefore, most significant in advanced propellant research and development. Some of the metal-containing fuels such as B_2H_6 , B_5H_9 , $Al(BH_4)_3$, and $Al(CH_3)_3$ are liquids whose properties are quite well known and documented (25). The liquid metal compounds are not discussed here because they do not demand radically new fuel technology and because of their limited applicability stemming from a combination of certain disadvantages in cost/availability, toxicity/handling, and logistics/storability. On the other hand, the application of solid metals and metal compounds to liquid systems depends upon new heterogeneous fuel technology. This technology is the basis for the development of most advanced fuels and is discussed in the last section of this chapter.

The advanced oxidizers are based almost entirely on oxygen and fluorine chemistry, and increasingly on fluorine. The utility of various types of oxygen- and fluorine-bearing materials that have been and/or are being considered in rocketry is discussed in detail. This discussion points up the relative usefulness of a broad range of materials in terms of properties and performance and provides insight into the direction future oxidizer research may be most fruitful. For convenience, the discussion of oxidizers is separated into two sections. The first section covers those materials which derive their oxidative capabilities primarily from oxygen. The second section deals with those materials which derive their oxidative capabilities from either fluorine or a combination of fluorine and oxygen.

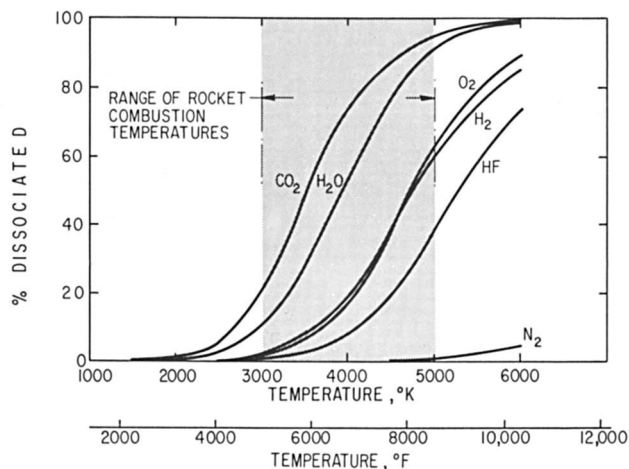


Figure 3. Dissociation of typical combustion products at a pressure of 50 atm. (37)

Oxygen-Based Oxidizers

Oxygen and Ozone. Elemental oxygen exists in two allotropic forms—*i.e.*, as the normal diatomic molecule, O_2 , and the more energetic, less stable triatomic molecule ozone, O_3 . The normal molecular form in the liquid state has been in use in rocketry for more than 20 years and, even today, is used in larger quantity than any other oxidizer. Its widespread use is of course readily understandable in view of its high performance capabilities, low cost, and ready availability. Liquid oxygen does, however, present handling problems because of its very low boiling point, sensitivity to shock when contaminated with a variety of organic materials, and its capacity for supporting or intensifying fires. The solution of these problems has been largely responsible for present-day capabilities to handle routinely a broad range of industrially important gases as cryogenic liquids, for the ability to maintain new levels of cleanliness, and for advancements in the prevention and control of fires and explosions.

Ozone has a number of obvious advantages over normal oxygen, including higher performance, boiling point, and density, and the suggestion of its use as an oxidizer for rocket fuels dates back to 1929 (26). Unfortunately, ozone is both unstable and toxic. Its instability in gaseous and liquid states and in solution in oxygen has been the subject of several studies (1, 2, 9, 30, 32) and presents the major impediment to its practical application to rocketry. Although the presentation of the results of such studies is beyond the scope of this paper, some of the more significant conclusions are: (1) extremely pure gaseous ozone is relatively stable, but its decomposition is accelerated by various agents, and it can decompose explosively; (2) pure liquid ozone detonates at a rate near that of TNT (~ 7000 meters/sec.), has a critical diameter of less than 1 mm., and is sensitive to contaminants in the oxygen from which it is produced; (3) oxygen-ozone solutions containing up to at least 33 wt. % ozone do not detonate in diameters up to at least 38 mm. (1.5 in.).

The question of the practical use of ozone in liquid rocket engines is still open, and its resolution will require much more research. On the basis of the existing knowledge it would appear, however, that a relatively dilute solution of ozone could be made a workable advanced oxidizer to replace oxygen. The over-all attractiveness of using ozone to improve rocket capabilities can be judged, however, only after the necessity of such an improvement is established and the alternatives presented by other advanced propellants and engine concepts are carefully considered. A comparison of some pertinent properties of oxygen and ozone is presented in Table I.

Nitrogen-Oxygen Compounds. When considering nitrogen-oxygen bonded compounds as oxidizers it should be recognized that the nitrogen serves only as a carrier for the oxygen and, therefore, the nitrogen content

Table I. Properties of Oxygen and Ozone (25)

	<i>Oxygen</i>	<i>Ozone</i>
Freezing (melting) point, °C.	-218.9	-192.8
Boiling point, °C.	-183.0	-111.9
Critical temperature, °C.	-118.8	-12.1
Critical pressure, atm.	49.7	54.6
Critical density, grams/cc.	0.430	0.437
Density at NBP, grams/cc.	1.140	1.460
Heat capacity, cal./gram, °C.		
liquid at NBP	0.406	0.354
gas at 25°C. (1 atm.)	0.220	0.196
Viscosity at NBP, centipoise	0.190	—
Thermal conductivity at NBP, cal./cm. sec., °C.	0.00050	(0.00056) ^a
Heat of formation gas at 25°C., kcal./gram-mole	0	34.2
Maximum theoretical specific impulse, lb.(f) sec./lb.(m) ^b with liquid H ₂	391	422

^a Extrapolated value.

^b Values calculated by Aerojet-General Corp. assuming shifting equilibrium and optimum expansion from 1000 to 14.7 p.s.i.a.

should be kept small. [Nitrogen itself is important as an oxidizer for the peculiar propellants that depend upon metal nitride (particularly BN_(s) and AlN_(s)) formation for the release of energy; however, in such propellants the introduction of oxygen (or fluorine) is thermodynamically detrimental to metal nitride formation.] The nitrogen-oxygen compounds of greatest interest include the nitrogen oxides; nitric acid and nitrates; nitrosyl, nitryl, and nitronium compounds; and nitro organics.

NITROGEN OXIDES. Among the various nitrogen oxides known (N₂O, NO, N₂O₃, NO₂, N₂O₄, N₂O₅, NO₃, N₂O₇) only the equilibrium mixture of N₂O₄ ⇌ 2 NO₂, commonly referred to as nitrogen tetroxide, has been utilized extensively in pure form. Nitrous oxide (N₂O) is of little interest to rocketry because of its low boiling point and poor performance capability as an oxidizer. Nitric oxide (NO) and dinitrogen trioxide (N₂O₃) similarly are of little interest as pure components; however, they have been utilized as additives to N₂O₄ to depress its freezing point. NO or N₂O₃ utilized in this manner actually form complex mixtures of nitrogen oxides in accordance with the following reactions:



Such mixtures are commonly referred to as mixed oxides of nitrogen (MON) in the rocket industry and are normally prepared from NO(g)

Table II. Properties

	NO (8, 22, 25)
Freezing (melting) point, °C.	-163.6
Boiling point, °C.	-151.8
Critical temperature, °C.	-93.0
Critical pressure, atm.	64.0
Critical density, grams/cc.	0.52
Density, grams/cc.	1.269 (-152.2°)
Heat capacity, cal./gram, °C.	
liquid	0.622 (-152.6°)
gas	0.238 (25°)
Viscosity (liquid), centipoise	—
Thermal conductivity (liquid), cal./cm. sec., °C.	—
Heat of formation at 25°C., kcal./gram-mole	21.58 (gas)

and $N_2O_4(l)$ (the equilibrium yields of NO_2 and N_2O_3 are spontaneously achieved upon mixing according to Equations 7 and 8).

The extensive application of N_2O_4 in pure form to rocketry is a fairly recent development; however, its use as a stabilizer and freezing point depressant for HNO_3 dates back more than 15 years. Mixtures of HNO_3 , N_2O_4 , and small amounts of water and HF are referred to as inhibited red fuming nitric acid (IRFNA) or without the HF (a corrosion inhibitor) as merely red fuming nitric acid (RFNA).

Dinitrogen pentoxide (N_2O_5) offers a theoretical performance advantage over N_2O_4 , but its marked instability presents significant problems as an oxidizer for rockets. Studies of its stability show a rather strong temperature dependence and the stabilizing influence of H_2SO_4 , HNO_3 , and $HClO_4$ as solvents. While temperature control and/or use of a solvent such as HNO_3 reduces the instability problem, these remedial approaches severely compromise its performance advantage.

Higher oxides of nitrogen have been reported (NO_3 , N_2O_6 , N_2O_7); however, their isolation has been difficult or impossible because of their rapid decomposition. Such materials are theoretically attractive from a performance standpoint, but their use as oxidizers appears remote at present. The properties of NO, N_2O_3 , N_2O_4 , and N_2O_5 are presented for comparison in Table II.

NITRIC ACID AND NITRATES. The use of nitric acid as a major component in liquid oxidizers dates back to at least World War II when it was used in a mixture with oleum (88 wt. % white fuming nitric acid and 12 wt. % oleum) and was denoted as "mixed acid." In later years its use as white fuming nitric acid (WFNA) and inhibited white fuming nitric acid (IWFNA) developed because of its higher performance capabilities in these forms. These acids are fairly pure nitric acid; WFNA contains a maximum of 2 wt. % H_2O and 0.5 wt. % NO_2 ; IWFNA addi-

of Nitrogen Oxides

N_2O_3 (18, 22)	N_2O_4 (22, 25, 33, 34, 35)	N_2O_5 (18, 22)
-102	-11.23	30
3.5 (decomp.)	21.15	47 (decomp.)
—	158.0	—
—	100.0	—
—	0.56	—
1.447 (2°)	1.433 (25°)	1.642 (18°)
—	0.370 (25°)	—
0.206 (25°)	0.201 (25°)	0.213 (25°)
—	0.39 (25°)	—
—	0.00031 (25°)	—
—	-4.676 (liquid)	—
19.80 (gas)	2.17 (gas)	2.7 (gas)

tionally contains approximately 0.7 wt. % HF to inhibit corrosion. Both acids tend to decompose unless maintained in sealed vessels able to withstand their high equilibrium decomposition pressures (*ca.* 100 atm. under temperature and ullage conditions of interest in rocketry). This instability stimulated research which led to the development of IRFNA containing approximately 14 wt. % NO_2 , 2 wt. % H_2O , and 0.7 wt. % HF. This composition reduces the equilibrium decomposition pressure to the point that sealed storage vessels are practical and, in addition, depresses the freezing point, increases density, and improves performance capabilities. Nitric acid solutions containing even higher concentrations of NO_2 (up to *ca.* 50 wt. %, the limit of solubility at room temperature) have been studied and appear both practical and attractive. These latter compositions are more dense than IRFNA, have low freezing points except near the limit of NO_2 solubility, and have a performance advantage. The use of these solutions as replacements for WFNA, IFWNA, or IRFNA appears quite likely in a few specialized cases.

A number of other compounds have been considered as additives to HNO_3 to improve its properties and/or performance capabilities. Among the more important are N_2O_5 , NO_2ClO_4 (nitronium perchlorate), and $HClO_4$. While each of these systems theoretically provides increased performance, their use presents some technical and operational problems. Only careful consideration of the magnitude of these problems *vs.* potential benefits and alternatives can resolve the question of their role as advanced oxidizers.

In general, the salts, esters, and halogen derivatives of nitric acid represent a poor compromise between performance and stability, and their future use in liquid systems appears limited. Several salts or esters of nitric acid have, however, achieved some prominence as oxidizers or monopropellants. The most important are the nitrates of alkali metals,

N—H bases, and a few alcohols or polyhydroxy compounds. The nitrates of Li, Na, and K are largely of interest in solid propellant formulations but have been considered to some extent as solutes in liquid propellants (particularly in HNO_3). The low performance of such oxidizers does, however, limit their use to those systems where their other properties are of major interest. The nitric acid salts of N—H bases such as NH_3 , N_2H_4 , NH_2OH , CH_3NH_2 , etc., are similarly of more interest as solid propellant ingredients, but their use as solutes in other liquid propellants has been considered. The sensitivity of these materials, even in solution, limits their applicability to special circumstances. Ethyl and propyl nitrates have been utilized as liquid monopropellants, and trinitrate and cellulose nitrate are the principal ingredients of double base solid propellants. The halogen nitrates (NO_3Cl and NO_3F) although intriguing from the standpoint of theoretical performance are so unstable that their use as oxidizers appears very remote.

NITROSYL, NITRYL, AND NITRONIUM COMPOUNDS. The nitrosyl, nitryl, and nitronium compounds are of only moderate interest as oxidizers for liquid rockets. There has been sufficient interest in them, however, to warrant discussion of some of the more prominent members. Among the nitrosyl and nitryl compounds, NOF and NO_2F are most important. Both are cryogenic, however, and present handling problems not too different from those of liquid oxygen. Theoretically, their performance is intermediate between that of N_2O_4 and O_2 . The most important nitronium compounds are the nitrate (N_2O_5) and perchlorate, both of which are solids. The possible use of these materials as solutes in HNO_3 is discussed in the sections on nitrogen oxides and nitric acid and nitrates, respectively.

NITROPARAFFINS. Nitro-organics as a class of compounds are of greater interest in solid than liquid propellants. However, some nitroparaffins have been utilized in liquid systems. Nitromethane has been used as a monopropellant, while tetranitromethane, hexanitroethane, nitroform, and nitroform salts have been considered as oxidizing components in bipropellant systems. The high melting points of the latter and their sensitivity restrict their use to solutes in lower freezing, insensitive liquids. A solution of 70 wt. % $\text{C}(\text{NO}_2)_4$ in N_2O_4 is an example of such a system and has been proposed as an oxidizer (3).

Halogen—Oxygen Compounds. In halogen—oxygen bonded materials other than those containing fluorine—oxygen bonds it should be recognized that while Cl, Br, and I are strong oxidizers, they are not desirable in rocketry because of their high molecular weights and the strong tendency of their reaction products with rocket fuels to dissociate. For these reasons, the content of Cl, Br, and I must be minimized if the oxidizer is to be of interest to rocketry.

CHLORINE OXIDES. The halogens, like nitrogen, form several oxides. The more important oxides of chlorine include Cl_2O , ClO_2 , Cl_2O_6 , and Cl_2O_7 , but each has a strong tendency to explode. Cl_2O_7 is the most stable of the chlorine oxides, has a low freezing point (-91.5°C ., (18)), high density, and is of most interest to rocketry. Unfortunately, even Cl_2O_7 is so shock sensitive that its utilization in rocket engines appears unlikely.

PERCHLORIC ACID AND PERCHLORATES. Pure perchloric acid is not subject to explosion as is its anhydride, Cl_2O_7 . Hence, its consideration in rocketry has been somewhat stronger. From the standpoint of properties, HClO_4 is very attractive [f.p., -112°C .; b.p., 39°C . at 56 mm. Hg; density, 1.764 grams/cc. at 22°C .] (18)]. However, it tends to decompose on standing, and the decomposition products are catalysts which autoaccelerate the reaction. The future of HClO_4 in rocketry, therefore, depends upon the ability to control this decomposition. The fact that $\text{HClO}_4\text{-H}_2\text{O}$ solutions are much more stable than pure HClO_4 is reason to believe that HClO_4 may be sufficiently stable in more desirable solvents to be acceptable for rockets.

A number of salts of perchloric acid are stable; in fact, NH_4ClO_4 is one of the most commonly used oxidizers in solid propellants. In general, the perchlorates are of most interest as solid propellant ingredients, but some have been considered as solutes in liquid systems. Those of most importance in tailoring liquids include the light metal perchlorates, perchlorates of N—H bases such as NH_3 , and N_2H_4 , and nitronium perchlorate. The low boiling material, ClO_4F , sometimes called fluorine perchlorate, is of only theoretical interest because of its extremely explosive nature.

BROMINE- AND IODINE-OXYGEN COMPOUNDS. The oxidizers containing Br—O and I—O bonds are of little interest to liquid rocketry because of poor performance and properties. The bromine oxides are particularly unstable, and I_2O_5 is the only stable iodine oxide. While I_2O_5 has poor performance potential on a weight basis, its high density [4.799 grams/cc. at 25°C . (18)] theoretically predicts high performance on a volumetric basis. Because it is a high melting solid, its use in hybrid or solid propellant systems would be more easily realizable. Some consideration has, however, been given to finding ways to incorporate it into liquid systems.

Peroxides, Superperoxides, and Ozonides. Among this group of materials, H_2O_2 is the only compound to see actual use as a propellant. Its use in concentrations of 80–85 wt. % in water dates back to World War II. It is currently used in approximately 90 wt. % concentration in several systems, and considerable effort has been devoted toward the use of material of purity greater than 98%. The stability of H_2O_2 has been studied over many years (37), and a good understanding and control of

decomposition have resulted. Although it has not been possible to eliminate decomposition completely, stabilizers and handling techniques have advanced to the point that extended periods of closed storage appear practical, and its application to new fields of liquid propulsion appears possible. The performance of H_2O_2 is not better than that of N_2O_4 with conventional fuels, but with metal-containing fuels it can be significantly superior. The advancements made in metallized fuels in recent years are largely responsible for the renewed interest in H_2O_2 . Although well-accepted as a monopropellant, the future of H_2O_2 as an oxidizer will probably depend upon the acceptability of these advanced fuels.

Many metal peroxides, superoxides, organic peroxides, and hydroperoxides are known, but they are not expected to be significant because of their inferiority to H_2O_2 in terms of performance, properties, or stability.

The credibility of the existence of superperoxides of hydrogen has been the subject of considerable controversy in recent years. Ghormley (15) summarized the evidence for H_2O_3 existence, indicating it is unstable above $\sim -60^\circ\text{C}$., and Czapski, *et al.* (11) found that the half-life of H_2O_3 at 23°C . reaches a maximum of 2 sec. in $0.02M$ (H^+) solution. On thermodynamic grounds, Benson (4) indicates that the alkyl and hydrogen trioxides should be reasonably stable, while the corresponding tetroxides appear unlikely of being produced or isolated above $80^\circ\text{--}100^\circ\text{K}$. Skokhodov *et al.* (39) report yields of H_2O_4 of $\sim 25\%$ (based on O_3) from O_3 and atomic H reaction in the presence of a film of liquid O_3 , and Csejka *et al.* (10) have determined the heat of decomposition of H_2O_4 at -196°C ., from which they calculate a heat of formation of -27.9 kcal./mole. Thus, the existence of H_2O_3 and H_2O_4 appears established. While these materials are theoretically of interest, their instability creates doubt that they can be used in rocketry.

Alkali metals can form ozonides, and an ozonide is formed when O_3 is bubbled into liquid NH_3 . Although such ozonides have theoretical interest, their instability makes their practical use in rocketry also appear remote.

Noble Gas-Oxygen Compounds. Since the discovery in 1962 that the noble gases are not truly chemically inert, propellant chemists became intrigued with the possibility that they could serve as excellent carriers of oxygen (and fluorine) and thus generate a new family of chemical propellants. While the importance of this discovery to chemistry cannot be underestimated, so far it has not led to the preparation of new compounds as significant rocket oxidizers.

Of the noble gas-oxygen compounds, XeO_3 and XeO_4 are known best. Both are unstable and explode easily. Despite their large positive heats of formation (ΔH_f of $\text{XeO}_3 = 96$ kcal./mole) (20), the high molecu-

lar weight of Xe severely detracts from their theoretical propellant performance potential. Xenic acids and their salts are also known. These materials are more stable than the oxides, but again low performance potential excludes them from serious consideration as oxidizers. Krypton oxides, particularly as kryptic acid and its salts, are known and are theoretically more desirable than corresponding xenon compounds. These materials are, however, less stable than the xenon analogs and still offer poor performance because of relatively low oxygen content and the high molecular weight of krypton. Although the oxides of the light noble gases would be theoretically desirable, the likelihood of their being sufficiently stable for use in rockets is poor.

Fluorine-Based Oxidizers

Fluorine is the most energetic oxidizing element and as such is of prime importance in advanced oxidizers. The fluorine-based oxidizers discussed here include elemental fluorine, compounds containing oxygen and fluorine, nitrogen-fluorine compounds, halogen fluorides, and noble gas fluorides.

Elemental Fluorine. Fluorine is the highest performing, stable oxidizer available to rocketry (ozone theoretically can provide higher performance with some fuels but is highly unstable). Although the performance potential of elemental fluorine has been recognized for many years, some of its properties pose severe problems to rocket application. Basically these problems arise from its low boiling point ($-188.14^{\circ}\text{C}.$), the extreme reactivity and toxicity of it and its reaction products, and the high combustion temperatures it produces. The cryogenic nature of fluorine does not present problems too different from those encountered with oxygen for which solutions are available from modern cryogenic technology. The combination of extreme reactivity of the oxidizer and reaction products and the extremes in the temperatures encountered, however, create problems much more difficult to solve than those encountered with oxygen. These extremes necessitate a thorough knowledge of the capabilities of materials in such adverse environments and careful design to insure that the materials are not exposed to conditions beyond their inherent capabilities. The problem is further compounded because trace contaminants on hardware can initiate a reaction of sufficient intensity to cause burning of primary structures. While the materials problems and their solutions are known, the ability to pre-recognize problems and properly apply the solutions in hardware as complex as a rocket engine becomes the real crux to fluorine usage. Obviously, the high toxicity and cost concomitant with fluorine further impede its application to rocketry. Despite these difficulties, the interest in fluorine and fluorine-

Table III. Properties of

OF_2	
Freezing (melting) point, °C.	-223.8
Boiling point, °C.	-144.8 (-145.3°)
Critical temperature, °C.	-58.0
Critical pressure, atm.	48.9
Critical density, grams/cc.	0.553
Density, grams/cc.	1.521 (-145°)
Heat capacity, cal./gram, °C.	
Gas at 25°C. and 1 atm.	0.192
Liquid at -145°C.	0.345
Viscosity, centipoise	0.283 (-145°)
Thermal conductivity (liquid), cal./cm. sec., °C.	0.00061 (-183°)

oxygen blends (flox) for rocket engines is demonstrated by the fact that a bibliography published in 1964 (5) lists approximately 350 reports which deal with F_2 and F_2 - O_2 oxidizers for space applications. It seems safe to assume that fluorine can and will be used in the future if a real need for its superior performance capabilities exists.

Compounds Containing Oxygen and Fluorine. OXYGEN FLUORIDES. Four oxygen fluorides are well known (OF_2 , O_2F_2 , O_3F_2 , and O_4F_2) and are the subject of an excellent review by Streng (41). Of these, OF_2 is the most stable and important to rocketry. It is cryogenic and requires handling much like fluorine but does have a sufficiently high boiling point (-144.8°C.) to be considered storable in a closed system in space. Its performance with H_2 is intermediate between that obtainable with O_2 and F_2 but is superior to either with many carbon-containing fuels. The combination of high performance and in-space storability is the strongest basis for its possible future use.

Although the other oxygen fluorides are far less stable than OF_2 , O_3F_2 is moderately stable in liquid O_2 when stored in darkness. Despite its low solubility (0.110 wt. % at 90°K.), undersaturated solutions have been shown to be hypergolic with many fuels nonhypergolic with pure liquid oxygen (24, 41). This ability to impart hypergolicity is significant to rocketry and could bring about its future use. The properties of the oxygen fluorides are compared in Table III.

FLUOROXY COMPOUNDS. The desirable oxidizing capabilities of oxygen and fluorine and the energy of the O—F bond make compounds containing the fluoroxy group (—OF) of considerable interest to rocketry. Unfortunately, much of the interest is academic because most of the known fluoroxy compounds (except for OF_2) are either unstable or contain other bonds which drastically reduce their performance potential. Among the better known inorganic fluoroxy compounds, NO_3F and ClO_4F are violently explosive, and the sulfur compounds SF_5OF and

Oxygen Fluorides (13, 21, 22, 41)

O_2F_2	O_3F_2	O_4F_2
-163.5	-189 to -190	> -196 < -183
-57 (decomp.)	-60 (decomp.)	(decomp.)
—	—	—
—	—	—
—	—	—
1.736 (-157°)	1.573 (-157°)	—
—	—	—
—	—	—
—	—	—
—	—	—

FSO_2OF also contain S—F bonds which are undesirable in rocket oxidizers. The organic fluoroxy compound CF_3OF is known and is stable to relatively high temperatures, but the strong C—F bonds degrade performance to the point that it is of no direct practical interest in rocketry. While it seems reasonable that other fluoroxy compounds can and will be prepared, the low strength of the O—F bonds may well limit the number of O—F bonds per molecule and/or necessitate the presence of other strong bonds to such an extent that high performance and stability are not simultaneously possible.

CHLORINE AND NITROGEN OXYGEN FLUORIDES. Most of the more important compounds containing O, F, and N or Cl (*i.e.*, NOF , NO_2F , NO_3F , and ClO_4F) have already been discussed. However, one additional compound deserves consideration—*i.e.*, ClO_3F , perchloryl fluoride. In view of its remarkable stability compared with ClO_2F , chloryl fluoride, and ClO_4F , fluorine perchlorate, it is surprising that it was first synthesized in 1952. This compound is more stable than the chlorine oxides and yields some of the performance advantage of fluorine. Unfortunately, its performance gain over more common oxidizers, such as N_2O_4 , is small, and its low boiling point ($-46.8^\circ C.$) creates added handling problems. These factors, plus the toxic nature of its combustion products, have generally caused it to be considered as an additive to other oxidizers rather than as a primary oxidizer.

Nitrogen-Fluorine Compounds. NITROGEN FLUORIDES. Four nitrogen fluorides are quite well known (NF_3 , N_2F_4 , N_2F_2 , and N_3F) but only NF_3 and N_2F_4 are of real interest to rocketry. N_3F is extremely sensitive to shock and light, and N_2F_2 , being unsaturated, is less stable and lower in performance than NF_3 or N_2F_4 .

Both NF_3 and N_2F_4 are cryogenic, boiling at -129° and $-73^\circ C.$, respectively. Their high fluorine contents and densities lead to performance capabilities generally intermediate to those obtainable with

liquid oxygen and OF_2 but lower than both O_2 and OF_2 with H_2 or high carbon-content fuels such as kerosene. Compared with OF_2 and F_2 , NF_3 and N_2F_4 are relatively inert and easier to handle. Like OF_2 , both appear capable of closed storage in space. These characteristics plus the fact that they are available in limited quantities at high cost and produce toxic exhaust products would appear to limit their future use largely to the specialized field of in-space propulsion. The properties of NF_3 and N_2F_4 are given in Table IV.

Table IV. Properties of NF_3 and N_2F_4 (22, 29)

	NF_3	N_2F_4
Freezing (melting) point, °C.	-208.5	-163
Boiling point, °C.	-129	-73
Critical temperature, °C.	-39.1	36
Critical pressure, atm.	44.7	77
Density, grams/cc.	1.54 (-129°)	1.5 (-100°)
Heat capacity (gas) at 25°C., cal./gram, °C.	0.180	0.182
Heat of formation (gas) at 25°C., kcal./gram mole	-30.4 ± 2.0	-2.0 ± 2.5

FLUOROAMINO COMPOUNDS. A few inorganic derivatives of NF_3 are known (other than the N, O, F compounds previously mentioned) and are commonly referred to as fluoroamines. Two of these, difluoroamine (HNF_2) and chlorodifluoroamine (ClNF_2), are moderately well characterized. While the physical properties of HNF_2 are desirable (b.p., -23.6°C .; critical temp., 130°C .) (23), its extreme sensitivity virtually eliminates it from serious consideration as a future rocket oxidizer. ClNF_2 is more stable than HNF_2 , but its low boiling point (-67°C .) and low performance potential compared with NF_3 practically negate its usefulness in rocketry.

Many organic N—F compounds are known (19), and the perfluoro derivatives of many different organic nitrogen-containing compounds are possible. However, the fluorine in the known compounds is mostly C—F rather than N—F bonded fluorine even though some of the starting materials were rich in nitrogen (*e.g.*, urea). Thus, it appears that organic N—F compounds are sufficiently stable to isolate only when the carbon is highly fluorinated and when the ratio of N—F to C—F bonds is low. Certainly much more of the chemistry of organic N—F compounds must be elucidated before the true relationship between structure and stability can be defined unambiguously, but if the apparent relationship is true, organic fluoroamines with high contents of N—F bonded fluorine will be relatively unstable. It is easily shown on a theoretical basis that only

organic fluoroamines having a large content of N—F bonded fluorine are capable of providing a performance advantage over more common oxidizers.

Halogen Fluorides. The halogen fluorides have long been recognized as promising oxidizers. Interest in these compounds is based on their high densities, storability under earth (and perhaps space) conditions, and good performance capabilities. They do, however, suffer some of the same drawbacks as other fluorine-containing oxidizers—*i.e.*, high toxicity and cost and handling problems.

Of the known halogen fluorides, most interest has been paid to the higher fluorides of chlorine (ClF_3 and ClF_5) and, secondarily, to BrF_3 and BrF_5 . The exceptionally high density of the iodine fluorides does, however, give them the theoretical capacity to deliver high performance on a volumetric basis and creates some interest in specialized cases. Except for ClF_5 , these compounds have been known for many years and are well characterized. Greatest attention has been given to ClF_3 , but discovery of ClF_5 in 1963 (40) caused attention to be refocused on this most interesting new member of the halogen fluoride family. The importance of this new oxidizer to rocketry is obvious merely from its theoretical performance potential and reasonably attractive physicochemical properties, and we would expect this material to receive more attention in the future. Some pertinent properties of the halogen fluorides are presented in Table V.

Noble Gas Fluorides. Since the discovery of XeF_4 in September 1962, several fluorides and oxygen fluorides of the three heaviest noble gases have been reported. As previously mentioned, the existence of such compounds intrigued propellant chemists with the possibility of gaining a new family of propellants.

Among the noble gas compounds, those of xenon are best known and are the subject of an excellent review by Malm *et al.* (27). The xenon fluorides (XeF_2 , XeF_4 , XeF_6) are solids, and compared with the oxides they have a high degree of stability. From the stability standpoint, they are attractive as propellants; however, the high molecular weight of xenon results in low performance and virtually eliminates them from serious consideration. The xenon oxygen fluoride, XeOF_4 , is also well known and is apparently a stable liquid. This material, like the fluorides, has poor performance potential.

The krypton fluorides, KrF_2 and KrF_4 , are moderately stable, but the combination of the relatively high molecular weight of krypton and low fluorine content (< 50 wt. %) results in performance capabilities of little real interest. The fluorides of the light noble gases have not been isolated although some spectroscopic evidence for their existence has

Table V. Properties of the

	ClF_3	ClF_5
Freezing (melting) point, °C.	-76.32	-93
Boiling point, °C.	11.75	-12.9
Critical temperature, °C.	153.5	—
Density at 25°C., grams/cc.	1.81	—
Heat capacity (gas) at 25°C., cal./gram °C.	0.165	0.178
Heat capacity (liquid) cal./gram °C.	0.303 (5.09°)	—
Heat of formation (gas) at 25°C., kcal./gram mole	-37.97 ± 0.7	-57 ± 15

been found. Theoretically, these materials would be good oxidizers, but present knowledge indicates that they may be too unstable to use as rocket propellants or perhaps even to isolate.

Conclusions Regarding Oxidizers. Much effort has gone into developing advanced oxidizers. While much of the earlier work was devoted to oxygen-based oxidizers, the later work has become increasingly oriented toward fluorine-based oxidizers. In both cases we seem to be reaching the point where the chemical structures required to achieve higher levels of propellant performance are thermodynamically so unstable that they cannot be applied to conventional rocketry. Thus, we need breakthroughs in the stabilization of very energetic materials and in the conversion of this stored chemical energy into propulsive force without allowing the materials to pass through intermediate conditions conducive to the uncontrollable release of the energy.

Heterogeneous Fuels

The heterogeneous fuels are a class of liquid propellants that has been considered for propulsion for many years. Over 30 years ago Eugen Sänger suggested the use of suspensions of powdered aluminum in liquid hydrocarbons, and fuels of this type were investigated for air-breathing propulsion systems by the National Advisory Committee for Aeronautics two decades ago. The current interest in heterogeneous fuels began in 1958 and led to significant advances in the technology of these two-phase fuels. This recent work is the subject of this discussion.

Theoretical Basis. Heterogeneous fuels are suspensions of finely divided metals or metal compounds in appropriate liquid fuels and represent one approach for using the low molecular weight metals (and certain of their derivatives) that have high heats of combustion with typical rocket oxidizers. The theoretical basis for the interest in metal-containing fuels is discussed in the introduction. Glassman (16) showed that all

Halogen Fluorides (7, 14, 18, 22)

BrF_3	BrF_5	IF_5	IF_7
8.77	-62.5	9.43	5.5
127.6	40.3	100.5	Subl.
~327	~197	~283	—
2.797	2.465	3.186	2.8 (6.0°)
0.116	0.139	0.111	0.125
0.217 (22.64°)	—	—	—
-61.1 ± 0.7	-102.5 ± 0.5	-196.35 ± 1.0	-224 ± 1.5

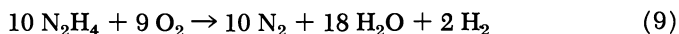
the metallic elements of molecular weight less than 30 (atomic numbers lower than 15), except sodium, have heats of combustion with oxygen that exceed the heat of combustion of gasoline with oxygen. All these metals, including sodium, have heats of combustion with fluorine that exceed that of hydrazine with fluorine. Of these seven elements, however, lithium, sodium, and silicon are poorly suited for use in heterogeneous fuels because of the reactivity of the first two and the marginal performance potential of the third. Interest has therefore been focused principally on four metals—aluminum, boron, beryllium, and magnesium—and some of their solid hydrides. A discussion of aluminum, beryllium, boron, and lithium as fuels in multicomponent propellants is presented in a paper by Gordon and Lee (17) which includes data from Dobbins (12) on the hydrides of aluminum, beryllium, and lithium. The theoretical specific impulse values of several heterogeneous hydrazine-based fuels oxidized with N_2O_4 are compared in Table VI; the specific impulse of the N_2O_4/N_2H_4 system is included for reference. For a discussion of the utilization of heterogeneous fuels in propulsion systems, the reader is referred to the article by Wells (42).

Table VI. Maximum Theoretical Specific Impulse Values of Heterogeneous Fuels with Nitrogen Tetroxide

<i>Fuel</i>	<i>Specific Impulse^a</i> <i>lb.-sec./lb.</i>
$BeH_2 + N_2H_4$	346
$Be + N_2H_4$	327
$AlH_3 + N_2H_4$	318
$Al + N_2H_4$	303
$B + N_2H_4$	296
N_2H_4	292

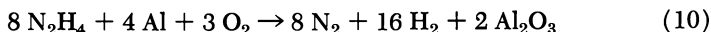
^a P_c/P_e , 1000/14.7 p.s.i.a.; shifting equilibrium.

Mechanism for Deriving Energy. The mechanism by which propulsive energy is derived from propellant systems containing metals and their compounds is somewhat different from that of conventional liquid propellant systems. For hydrazine and nitrogen tetroxide, for example, their combustion leads to the formation of N_2 , H_2O , and H_2 through a relatively simple series of intermediate species:



In this reaction most of the energy released is derived from the formation of water, and the fuel-oxidizer ratio is adjusted to leave some of the hydrogen unoxidized to achieve an appropriate balance between the release of heat and the molecular weight of the combustion products.

On the other hand, when a metal such as aluminum is added to this system, some energy is derived from the decomposition of the hydrazine, but the principal source is the formation of the metal oxide:



In this case the hydrazine is the sole source of the working gas, which is expanded by the heat released by the oxidation of aluminum, whereas in the unmetallized system a significant part of the hydrogen from hydrazine decomposition furnishes energy by oxidation as well as part of the working gas in the form of water.

During the combustion of the metallized system in a rocket chamber, it is unavoidable that part of the oxygen is involved first in the oxidation of hydrazine to form N_2 and H_2O , leaving an equivalent amount of the metal unoxidized. A loss of propulsive energy would occur if this situation were to persist throughout the entire length of the combustor and nozzle because the flame temperature would be lower and the average molecular weight of the working gas higher than theoretically possible. The full potential of this type of propellant system can be realized, therefore, only if the conditions in the combustor and nozzle permit the transfer of oxygen from the water to the aluminum and the absorption by the hydrogen of the heat released by this transfer before the products pass the throat of the nozzle. The construction and operation of combustion chambers and nozzles for use with metal-containing propellants must take into account the "stay time" required for the occurrence of these processes that do not take place in unmetallized systems.

Utilization of Multicomponent Propellants. One approach to the utilization of a metallized system such as that involving hydrazine, aluminum, and oxygen is to inject the three components separately into the combustion chamber (tripropellant system). This avoids the problems associated with the suspension of the metal in the fuel or oxidizer (and is therefore not a heterogeneous propellant), but it imposes other prob-

lems. A method must be available for the transport and precise metering of the dry powdered metal, and a third tank and associated hardware must be incorporated into the propulsion system. The latter increases the weight and volume of the system and is likely to reduce the reliability—factors that must be weighed against the gain in propulsive energy.

A second approach is to incorporate the metal into a small amount of solid binder (hydrazine is not utilized in a system of this kind) and to burn the metal and the binder with oxygen in a combustion chamber similar to that of a solid rocket motor. A working gas such as hydrogen is then mixed with the hot reaction products in a secondary chamber in which the heat of metal oxidation is transferred to the gas before its entrance into the nozzle. Because this type of system involves both liquids and a solid grain that contains the metal, it is called a tribrid propellant system. It also involves a vessel for containing the metal-containing grain but avoids the transport and metering problems associated with the tripropellant approach. In this case, however, one of the principal problems is the efficient mixing of the hydrogen with the hot metal oxides to effect the high degree of heat transfer desired.

The use of a heterogeneous fuel, in which the metal compound is suspended in a liquid fuel, avoids a third storage vessel because it is used with the oxidizer as in a conventional bipropellant system. The technical problems are then associated only with the stabilization of the suspension, with the rheological properties of the stabilized fuel, and with the reactivity of the suspended solid with its carrier.

Mechanical Stabilization. Four methods may be considered for stabilizing heterogeneous fuels mechanically. The use of the metals in the form of sols is not practical because the powders, when subdivided to the required degree, are expensive and hazardous to handle. If they are allowed to become coated with the metal oxide, to eliminate their pyrophoricity, their metal content is reduced to an unacceptable level. Another approach involves the use of a liquid whose density equals that of the solid phase. Such an approach is also impractical because there are few liquid materials that have appropriate densities, and those that do are inappropriate as fuel components for chemical or thermodynamic reasons. Furthermore, the density equivalence is lost at reduced and elevated temperatures, causing settling or floating of the solid phase.

A third approach is emulsification. Most emulsified commercial products are the oil-in-water type, in which the oil is suspended in the form of small spheres in the water. The oil is the discontinuous or internal phase, and the water is the continuous or external phase. Stabilization of these systems is effected by surface-active compounds that prevent the oil drops from coalescing and by proportioning the two phases so that the lighter phase cannot separate to the top. In applying the emulsion ap-

proach to heterogeneous fuel technology water-in-oil types are used because of the nature of the liquid fuels that are desirable as carriers for the solid-phase fuel components. In a sense, they are inverted oil-in-water types of emulsions.

Theoretically, the internal phase of an emulsion can constitute as much as 74% of the total volume without distorting the suspended spheres. To produce emulsions having proportions of internal phase greater than this, the spheres must be distorted to accommodate them in the highly packed condition. The continuous phase, then, is no more than an interstice filler and a barrier to the direct contact of neighboring units of the internal phase. Thermodynamically, this is a highly unstable situation because of the large surface area of the internal phase. There is a tendency for the small volume of external phase to become the internal phase to effect a significant reduction in interfacial surface. If such an inversion can be prevented, however, the internal phase can be used to suspend a large amount of a powdered solid. The solid particles can settle to the bottom of each of the units but no farther, unless the interface between the unit and the continuous phase is broken.

Significant progress has been made in investigating metal-containing fuels stabilized by the emulsion approach. The studies have been confined, of course, to the storable fuels because of the obvious barriers to the emulsification of cryogenic liquids. In addition, the choice of suitable combinations for the phase pairs is limited because not only must they have adequate fuel value and be chemically compatible, they must also be essentially immiscible—*e.g.*, hydrazine and rocket propellant kerosene. Emulsions containing more than 90% by weight of hydrazine dispersed as a phase internal to the kerosene are possible, so that when a powdered light metal is added, the content of combined emulsifier and kerosene is no more than 5%. Although fuel formulations of this type are moderately viscous, they thin as the shear rate is increased and become relatively fluid under the shear conditions of operating propulsion systems. The emulsion approach may ultimately be the favored one for stabilizing heterogeneous fuels, but additional work is required, especially to formulate fuels having proved, long term stability and to establish the storage and use conditions to which they can be subjected without inducing inversion.

The fourth approach to the stabilization of heterogeneous fuels—by gelation of the liquid carrier—has been developed more thoroughly than the emulsification method. Hence, the gelled fuels are discussed in greater detail than emulsified fuels. However, some aspects of heterogeneous fuels are not related to mechanical stabilization; when these are discussed in connection with gelled fuels, it will be apparent that the comments apply also to emulsified fuels.

It is possible to reduce the rate of settling of solids suspended in a liquid by using either a viscous Newtonian liquid or by making a viscous Newtonian liquid by adding a thickener to one of low viscosity. The utility of suspensions made this way would be very brief, for settling would commence immediately upon preparation, the duration of utility depending upon the degree of nonuniformity of distribution that could be tolerated by the application. Their utility in propulsion systems would be limited further because of the magnitude of the pressure differentials required to flow them at high velocities. It is apparent, therefore, that a viscous heterogeneous fuel must satisfy two criteria. The viscosity must be produced by a colloidal structure that has a yield value upon deformation and that is reversible when subjected to shear—*i.e.*, the liquid must be a gel that shear thins. When the yield value is high enough for the colloidal structure to resist the shearing forces of suspended particles acting on the gel under the influence of gravity, the suspended material should remain uniformly distributed indefinitely. If, in addition, the colloidal structure is made up of units loosely united by bonds that are easily broken and reformed, thinning will occur under shear and the gel will recover when the shearing stress is removed—*i.e.*, the system is thixotropic. These, however, are only the minimum requirements of a gelled fuel suitable for use in rocket propulsion. The yield value must be high enough to withstand the shearing forces of particles under many times the force of gravity, depending upon the mission in which the propulsion system will be utilized. The colloidal structure must exhibit sufficient capillarity to hold the liquid phase without bleeding, it must not change appreciably with age either chemically or physically, and these characteristics must be attainable with sufficiently small concentrations of the colloid so that the energy content of the fuel is not adversely affected.

Types of Gelling Agents. Two general types of gelling agents have been extensively used in the development of heterogeneous fuels—the particulate agents such as silica and acetylene black, and the natural and synthetic hydrophilic polymers. Since they do not involve solubilization in the medium to be gelled, the particulate agents have been used to gel a variety of fuel carriers, including some for which suitable hydrocolloid gelling agents have not been found. The particulate gelling agents depend largely on electrical charges for the attraction between dispersed particles that hold them in the chain network which constitutes the colloid structure. Consequently, the electrically charged particles are strongly agglomerated in the dry state, and their dispersion in the liquid fuel requires high shear mixers and long mixing times. In addition, relatively large quantities of these inert materials are required to produce gels of adequate yield value and sufficient capillarity to prevent exudation

of the carrier. In many cases the gel structure appears to change with age, causing its deterioration and the eventual appearance of supernatant carrier. Although these defects can be remedied to some degree by a hydrocolloid gelling agent in combination with the particulate colloid, the long term storability of such formulations remains to be proved.

Hydrocolloid Gelling Agents. The hydrophilic polymers (28, 31) are generally more effective for gelling the carriers which are most appropriate in heterogeneous fuel formulations. Dozens of such materials, most of which are commercially available, have been evaluated during the past several years for gelling hydrazine, 1,1-dimethylhydrazine, methylhydrazine, other hydrazine derivatives, and mixtures of these materials. They include the natural gums such as guar gum, locust bean gum, and gum arabic; alginates; and gelatin among the natural vegetable and animal products. From the class of modified natural products, various hydroxyalkylcellulose and carboxymethylcellulose products have been evaluated. Poly(vinyl alcohol), poly(vinyl pyrrolidone), sulfonated poly(vinyl toluene), polyacrylamide, poly(acrylic acid), and poly(methylacrylic acid) are examples of the synthetic commercial hydrophilic polymers that have been investigated. Some derivatives of poly(acrylic acid) that are not commercially available have also been studied.

The search for effective gelling agents from among the large number available as commercial products has been undertaken by many research and development laboratories interested in heterogeneous fuels. There has been little agreement, however, with respect to which materials are best suited to the applications, even among those who are investigating the same metal-carrier combinations. This is caused partly by differences in the criteria by which the gelled fuels are evaluated and the absence of standardization of methods and instruments for measuring their properties, but the most important barrier is the competitive spirit that exists among the various industrial, governmental, and research institute laboratories conducting these investigations. At present the gelling agents being used in various fuel formulations based on hydrazine and its derivatives include silica, acetylene black, hydroxyalkylcellulose, alginic acid, and poly(acrylic acid). Certain combinations of these are in use, and in some cases aluminum octonate is used with alginic acid and with the cellulose derivatives.

Chemical Stability of Fuels. Although the principal problem associated with the development of a gelled heterogeneous fuel is the mechanical stabilization of the suspended solids, the solid phase must be chemically compatible with the carrier fuel. The hydrazine-type carriers utilized in these fuels are thermodynamically unstable and decompose to produce gaseous products by mechanisms that are sensitive to catalysts. Special attention must therefore be given to the problem of decomposi-

tion because of the large surface areas involved. In many cases it is necessary to investigate the contribution of the solid phase to the gas-producing reactions and to take measures to reduce them to tolerable levels by selecting materials carefully or by treating them by appropriate chemical or physical processes. In most cases, decomposition rates are not large enough to cause significant loss of the propellant itself, but the pressure developed in the fuel tank may reach an intolerable level, and the insoluble gaseous decomposition products are held suspended in the gel structure, causing an undesirable increase in the specific volume of the fuel.

Importance of Rheology. Even though gelling agents are selected on the basis of their capacity (at acceptable concentrations in the fuel) to provide long term mechanical stability of the suspended solids, other factors are of equal importance, and many secondary criteria are used to determine the utility of a heterogeneous fuel in propulsion systems. These factors vary, of course, with the application of the propulsion system. The rheological properties are as important as mechanical stability in view of the influence the flow properties have on the design of propulsion systems. In addition, the effect of temperature on the rheological properties should be as small as possible, and the gel structure should not deteriorate during repeated transfer and other handling operations.

These considerations have resulted in the introduction into liquid propellant research and development laboratories of instruments and techniques not previously used there; further, the production of heterogeneous fuels requires processes and control methods unnecessary in producing conventional propellants. Although some innovation has occurred, for the most part propellant chemists have satisfied their requirements by adopting instruments and methods from various segments of industry involved in the development of commercial products utilizing gel technology. They have found, however, in drawing upon industrial experience, that propellants must be developed to much higher standards of quality and uniformity than ordinary commercial products because the high levels of reliability demanded in missile and rocket propulsion systems cannot be jeopardized by even small changes in the physical and chemical properties of the propellants during storage. The realization of the performance improvements that can be obtained by using heterogeneous fuels in rocket propulsion depends largely on whether or not the propellant chemists can meet these high standards of quality.

Status of Technology. At present only one heterogeneous fuel, aluminum in gelled hydrazine (42), has been thoroughly developed and evaluated extensively in a static propulsion system. Other metal-containing fuels are being developed, but fuels based on the metal hydrides are

still in the research and exploratory development stages. Many problems associated with the development of heterogeneous fuels have been solved, and the obstacles to the development of the more advanced systems are expected to be overcome. The technology of heterogeneous fuels is certainly ahead of the capability of propulsion engineers to use them.

Literature Cited

- (1) Apin, A. Ya., Pshezhetskiy, S. Ya., Pankratov, A. V., *Zh. Fiz. Khim.* **34**, 1935 (1960).
- (2) Axworthy, A. E., Jr., Benson, S. W., *ADVAN. CHEM. SER.* **21**, 388 (1959).
- (3) Behrens, H., *Z. Electrochem.* **55**, 425 (1951).
- (4) Benson, S. W., *J. Am. Chem. Soc.* **86**, 3922 (1964).
- (5) Cabaniss, J. H., "Bibliography on Fluorine Oxygen Oxidizers for Space Applications," NASA-TM-X-53145 (Oct. 16, 1964).
- (6) *Chem. Eng. News* **43**, 41 (Sept. 6, 1965).
- (7) "Chlorine Trifluoride and Other Halogen Fluorides," Allied Chemical Corp., *Tech. Bull.* TA-8532-2.
- (8) Cole, L. G., Jet Propulsion Laboratory, *Progr. Rept.* 9-23 (Oct. 18, 1948).
- (9) Cook, G. A., Spadinger, E., Kiffer, A. D., Klumpp, C. V., *Ind. Eng. Chem.* **48**, 736 (1956).
- (10) Csejka, D. A., Martinez, F., Wojtowicz, J. A., Zaslowsky, J. A., *J. Phys. Chem.* **68**, 3878 (1964).
- (11) Czapski, G., Bielski, B. H. J., *J. Phys. Chem.* **67**, 2180 (1963).
- (12) Dobbins, T. O., "Thermodynamics of Rocket Propulsion and Theoretical Evaluation of Some Prototype Propellant Combinations," WADC TR-59-757 (1959).
- (13) Fang, F., Allied Chemical Corp., *Tech. Bull.* 65-62 (Nov. 15, 1965).
- (14) Gatti, R., Krieger, R. L., Sicre, J. E., Schumacher, H. J., *J. Inorg. Nucl. Chem.* **28**, 655 (1966).
- (15) Ghormley, J. A., *J. Chem. Phys.* **39**, 3539 (1963).
- (16) Glassman, I., *Am. Scientist* **53**, 508 (1958).
- (17) Gordon, L. J., Lee, J. B., *ARS J.* **32**, 600 (1962).
- (18) "Handbook of Chemistry and Physics," 46th ed., The Chemical Rubber Co., Cleveland, Ohio, 1965-1966.
- (19) Hoffman, C. J., Neville, R. G., Lockheed Aircraft Corp., *Tech. Rept. LMSD-703005* (August 1960).
- (20) Hyman, H. H., *Science* **141**, 61 (1963).
- (21) "Investigations of Space Storable Propellants (OF₂/B₂H₆)," Thiokol Chemical Corp., NASA CR-54741 (*Rept. RMD 6039-F*) (June 10, 1966).
- (22) "JANAF Thermochemical Data," Dow Chemical Corp., Midland, Mich.
- (23) Kennedy, A., Colburn, C. B., *J. Am. Chem. Soc.* **81**, 2906 (1959).
- (24) Kirschenbaum, A. D., Stokes, C. S., Grosse, A. V., U. S. Patent 3,170,282 (Feb. 23, 1965).
- (25) Kit, B., Evered, D. S., "Rocket Propellant Handbook," MacMillan, New York, 1960.
- (26) Kondratyuk, Yu. V., "Zavoyevaniye Mezhplanetnykh Prostranstv" (The Conquest of Interplanetary Space), Novosibirsk, 1929.
- (27) Malm, J. G., Selig, H., Jortner, J., Rice, S. A., *Chem. Rev.* **65**, 199 (1965).
- (28) "Natural Plant Hydrocolloids," ACS Monograph 11, Reinhold, New York, 1954.

- (29) "Nitrogen Trifluoride, Tetrafluorohydrazine," Stauffer Chemical Co., *Tech. Bull.* (Feb. 1960).
- (30) Paushkin, Ya. M., "Khimya Reaktivnykh Topliv" (The Chemistry of Reaction Fuels), Izdatel'stvo Akademii Nauk SSSR, Moskva, 1962.
- (31) "Physical Functions of Hydrocolloids," ACS Monograph 25, Reinhold, New York, 1960.
- (32) Platz, G. M., Hersh, C. K., *Ind. Eng. Chem.* **48**, 742 (1956).
- (33) Reamer, H. H., Sage, B. H., *Ind. Eng. Chem.* **44**, 185 (1952).
- (34) Richter, G. N., Sage, B. H., *Chem. Eng. Data Series* **2** (1), 61 (1957).
- (35) Richter, G. N., Reamer, H. H., Sage, B. H., *Ind. Eng. Chem.* **45**, 2117 (1953).
- (36) Schumb, W. C., Satterfield, C. N., Wentworth, R. L., "Hydrogen Peroxide," Reinhold, New York, 1955.
- (37) Siegel, B., Schieler, L., "Energetics of Propellant Chemistry," Wiley, New York, 1964.
- (38) Silverman, J., Constantine, M. T., *ADVAN. CHEM. SER.* **88**, 301 (1969).
- (39) Skorokhodov, I. I., Nekrasov, L. I., Kobozev, N. I., *Zh. Fiz. Khim.* **38**, 2198 (1964).
- (40) Smith, D. F., *Science* **141**, 1039 (1963).
- (41) Streng, A. G., *Chem. Rev.* **63**, 607 (1963).
- (42) Wells, W. W., *Space/Aeronautics* **45**, 76 (1966).
- (43) Wilkins, R. L., "Theoretical Evaluation of Chemical Propellants," Prentice-Hall, Englewood Cliffs, N. J., 1963.

RECEIVED April 14, 1967.

Characterization, Chemical Compatibility, Storability, and Hazard Testing of Liquid Propellants

STANLEY TANNENBAUM and ANTHONY J. BEARDELL

Thiokol Chemical Corp., Reaction Motors Division, Ford Rd.,
Denville, N. J. 07834

Primary attention has recently been directed to those liquid fuels, oxidizers and monopropellants that are storable. The goal has been to obtain maximum energy fuels either as liquids or as dispersions of dense metals in liquid carriers and oxidizers of optimum energy. Although these materials may be thermodynamically unstable or highly reactive, they must meet rigid specifications of storage and safety for military applications. Various laboratory tests are used to establish physical properties, burning properties for monopropellants, chemical compatibility, thermal and mechanical stability, rheological properties (where needed), and shock sensitivity. Field tests are also needed to examine long term storage (pressure/time studies), mechanical stability of metal loaded systems, and shock sensitivity characteristics.

The liquid rocket engine can be considered a chemical reactor with an extremely large throughput rate. The primary purpose of the reactor is to generate a large quantity of hot, low molecular weight exhaust gas that can be used to propel the rocket engine (and the rest of the missile) at great speeds. The reactions that occur in these reactors are primarily oxidation, although in many cases the oxidation is not caused by an oxygen-containing species. Fluorine is a more energetic oxidizing agent than oxygen, and oxidizers containing active fluorine atoms—*i.e.*, oxygen difluoride (OF_2) and chlorine trifluoride (ClF_3)—are considerably more reactive and energetic than some of the standard oxygen-containing liquid oxidizers—*i.e.*, nitric acid, concentrated hydrogen peroxide (98% H_2O_2) and nitrogen tetroxide (N_2O_4).

Much has been written on the drawbacks and benefits of various fuel/oxidizer systems. The purpose of this report is to discuss the efforts of chemist and engineer in developing a new liquid propellant system ready for use in a tactical mission.

We think it is valuable to consider the techniques and approaches used in the rocket propulsion areas since many of the concerns, and the devices and approaches developed to cope with these concerns, can be used by the chemical industry. This is perhaps particularly true when one considers hazard evaluation. The procedures developed in the propellant industry to assess explosive and fire hazards are directly applicable to the chemical process industry. In addition, some of the techniques developed for measuring the properties of liquid propellants, particularly at elevated temperatures and pressures (and frequently on materials which can decompose or even detonate), can be used in similar studies with actual commercial chemicals.

Storable liquid propellants have received greater attention from the chemist than have cryogenic liquid propellants. Storable generally refers to a liquid which can be kept for long times at ambient temperatures in standard containers without any significant loss of material. Although the most energetic propellants are those which are cryogenic (boil well below room temperature), these cannot be used in tactical missions because of cooling requirements. Also, at ambient temperatures, cryogenic materials are above their critical temperatures, and their densities are so low that they have unacceptably low energy/unit volume for use in a tactical weapon.

There is relatively little chemical effort devoted to cryogenic propellants although they are important for non-military space missions where there is little concern with difficulty in handling. These are also the simplest molecules such as hydrogen, oxygen, and fluorine about which a great deal of information is already available. The relative merit of a propellant system is normally presented in terms of specific impulse (I_s) which is the thrust developed (F) by a given flow of propellant per unit time (\dot{W}); $I_s = F/\dot{W}$. Table I gives several typical theoretical specific impulse values to illustrate the differences in performance between typical cryogenic and storable propellant systems. The use of storable propellants, however, introduces a host of chemical considerations for the reasons outlined below.

First, attempts are made to tailor the properties of the fuels to be optimum for the application. This requires the use of mixtures of materials. Many of the tactical fuels currently in use are actually mixtures selected to have the highest energy possible while retaining certain required physical properties. The specific requirement differs in each case, but it frequently includes (1) a freezing point sufficiently low so

that the weapon can be used over a divergent climatic region, (2) a high density so that one can maximize volumetric energy in a tactical (volume limited) system, (3) a moderately low vapor pressure at high ambient condition so that tank materials need not be too heavy, (4) a viscosity which is relatively low or at least will not vary greatly with temperature and, (5) a high heat capacity if the propellant is to cool the engine walls before entering the combustion chamber (regenerative cooling). In addition, it is important that, where possible the propellant not be excessively toxic, corrosive, reactive with air or moisture, thermally unstable, or detonable. In many cases, it is not possible to meet these goals and still provide performance, but frequently improvements can be effected by using a mixture of propellants. Typical of the blends developed are the 50/50 hydrazine/*unsym*-dimethylhydrazine (UDMH) fuel in the Titan II, and the mixed amine fuel (UDMH, acetonitrile and diethylene triamine), that is used in the air to ground "Bullpup" missile. The former was developed to overcome the detonation hazard associated with using neat N_2H_4 , and the latter was developed to provide an energetic fuel that could meet certain specific freezing point, density, and viscosity requirements.

Table I. Typical Propellant Systems

<i>Type of System</i>	<i>Fuel</i>	<i>Oxidizer</i>	I_s
Cryogenic	Hydrogen	Fluorine	410
	Hydrogen	Oxygen	391
Storable	Hydrazine	Nitrogen tetroxide	292
	Monomethyl- hydrazine	Chlorine trifluoride	284

Secondly, storable propellants should be energetic, and therefore the molecules and systems are frequently difficult to handle. Scientists involved in rocket propellant research have attempted to use increasingly energetic materials. As mentioned above, the figure of merit for the potential performance of a rocket propellant combination is the specific impulse ($I_s = F/\dot{W}$). F depends directly on the heat generated in the reaction, and therefore the larger the heat of reaction of fuel and oxidizer, the larger the potential energy release and the higher the specific impulse. Naturally, there are other considerations, but generally the greater the heat release, the higher the potential performance of the combination. Ideally then, one wants to maximize the heat of reaction, and this leads to attempts to use oxidizers and fuels with as large a positive heat of formation as possible and whose products of reaction have as large a negative heat of formation as possible. Because of the available type of fuel molecules this frequently results in efforts to use fuels that are thermodynamically unstable and hence subject to catalytic decomposition.

Two prime examples are hydrazine ($\Delta H_f = 12.05$ kcal./mole and penta-borane ($\Delta H_f = +7.7$ kcal./mole). Both materials have been considered for many rocket engine applications, and hydrazine is currently used as an ingredient in several operational systems.

Most of the available storable energetic oxidizers are unfortunately very reactive, toxic, and/or unstable (*i.e.*, ClF_3 , N_2O_4 , 98% H_2O_2). The property of reactivity is one that is a benefit when the propellant is performing its mission in the propulsion system, but it greatly complicates its handling properties.

One method of minimizing liquid propellant handling problems is to "prepackage" them so that the entire rocket motor can be assembled and welded shut at the plant, thus reducing the possibility of contamination or spillage when the units are handled in the field. This is precisely what has been done in Thiokol's family of Bullpup missiles. While the hermetic sealing of the propellants at the factory minimizes handling problems, it makes substantial demands on the stability of the system. Clearly the propellants in such a system must meet rigid requirements of thermal stability and compatibility.

Within the last five years the desire to raise the volumetric energy contained in a propulsion system has led to an intensive effort to prepare and use two-phase systems consisting of a dispersion of solids in a gelled or emulsified liquid fuel vehicle. The solids are most often metals such as aluminum or boron although an effort has also been made to introduce solids that are more energetic than elemental metals. The introduction of such unorthodox propellant systems has resulted in the propellant chemist and engineer becoming involved with the problems inherent in the flow and combustion of non-Newtonian liquids and slurries. Previously, only the unique properties of a homogeneous system had to be determined, but the introduction of non-Newtonian systems involves time- and history-dependent properties of heterogeneous systems such as consistency curves, yield stress, and mechanical stability under a variety of conditions.

One final problem area related to the use of energetic molecules is that of determining whether the material is detonable. Monopropellants such as hydrazine and concentrated hydrogen peroxide can detonate under certain conditions. In addition, efforts are continually being made to use more energetic monopropellant molecules which may consist of either a single molecule type such as ethylene oxide or a multicomponent monopropellant such as a solution of nitropropane in nitric acid (6). Monopropellants are considered inherently unstable and must be studied carefully to establish conditions of their safe usage. When they can be used, these propellants greatly simplify the combustion process by eliminating needs for proper fuel/oxidizer mixing, and this significantly reduces

equipment complexity. The methods used to evaluate the sensitivity of propellants will be discussed in some detail in this report.

Thirdly, if new molecules could be synthesized which were to maximize properties and energy, such molecules could be useful even if costly. Much effort has been expended toward synthesizing new compounds for use as liquid propellants. Since that area of the propellant industry is the subject of two other chapters in this volume, I will avoid any detailed discussion of this area. However, in many tactical weapons systems, propellants can be used whose costs would normally be considered prohibitive for a propulsion application. This results from the fact that the rest of the missile propulsion, guidance, and warhead systems are so expensive and the amount of propellant so small that propellant costs become unimportant. The larger the missile becomes, and the more propellant it contains, the greater becomes the consideration of propellant cost. However, the fact that propellant cost may not be crucial has justified much research to prepare new propellants. In fact, several new propellant or propellant ingredients have been synthesized and will find their way into propulsion systems.

A much larger number of new molecules were synthesized whose properties were found to be unacceptable for use in rocket engines. Many were rejected because they had unsuitable energy, others had poor densities, viscosities, or vapor pressures and still others were too reactive, unstable, or detonable. The remainder of this paper will deal with the methods used to determine the properties which determine whether or not a new material could be used as a rocket propellant.

Determining Physical Properties of Potential Propellants

Homogeneous Liquids. The physical properties important in determining the suitability of a liquid for propellant application are the freezing point, vapor pressure, density, and viscosity. To a lesser extent, other physical properties are important such as the critical temperature and pressure, thermal conductivity, ability to dissolve nitrogen or helium (since gas pressurization is frequently used to expel propellants) and electrical conductivity. Also required are certain thermodynamic properties such as the heat of formation and the heat capacity of the material. The heat of formation is required for performing theoretical calculations on the candidate, and the heat capacity is desired for calculations related to regenerative cooling needs.

Generally, all of these properties are required over a temperature range broad enough to include those likely to be encountered any place on the globe. It is also necessary to conduct measurements over a range

of compositions when mixed fuels are of interest, so that a chart of properties *vs.* composition can be plotted and an optimum region selected.

The equipment used to determine these properties is fairly standard, although, when highly corrosive or sensitive materials are employed it is necessary to conduct the operation in specially designed, remotely operated apparatus rather than glass. In many cases it is necessary to use Kel-F or Teflon equipment—this is particularly true in working with highly energetic fluorine oxidizers (such as tetrafluorohydrazine (N_2F_4) or ClF_3).

Non-Newtonian Systems. Although the determination of the required properties is straightforward for liquids, the situation is much more complex for non-Newtonian systems such as gels, emulsions, and slurries. As indicated earlier, there is a significant effort under way to prepare slurries of solids in liquid fuels to increase the volumetric energy of such fuels. These slurries must be stabilized as gels or emulsions to prevent solid separation. It therefore seems worthwhile to discuss the preparation of such slurries as well as the techniques used to measure some of the properties required to characterize these systems.

The slurry propellant consists of a liquid carrier such as hydrazine or a hydrocarbon in which a solid powder is dispersed. The solid powders of greatest interest are boron and aluminum since these two substances produce relatively low molecular weight products and high heat release during combustion with either oxygen-containing oxidizers (*e.g.*, N_2O_4) or interhalogen (*e.g.*, ClF_3). To maintain the particles in stable suspension, a gelling agent is required for the liquid medium (1). It is also possible to use emulsifying agents. Such dispersions have actually been prepared and tested (3) although they have not been studied as extensively as gelled slurry systems.

A number of factors must be considered in formulating a slurry propellant. The particle size of the solid powder must not be too large, or the residence time required to effect complete combustion could be too long, and inefficient energy release would result. On the other hand, if the particle size is extremely small, it may not be possible to formulate a slurry of the requisite solid content (25–50 vol. %).

Another consideration is the type and concentration of gellant required to produce a stable suspension. Sufficient gellant to impart some rigidity to the gel is necessary to avoid solid settling but if the concentration of the gellant is too high, it may be difficult to flow the mixture at pressure drops (~ 250 p.s.i.g.) which can produce a linear velocity of 70–100 ft./sec., which is required in many rocket systems. Ultimately the concentration of the gellant has a most important effect on the rheological characteristics of the slurry. Of course, the process of slurry mixing will influence the degree of deaggregation of the solid particles and the

uniformity of dispersion of the gellant, and this will influence the rheological characteristics of the system. The equipment used to mix high solid loaded fuel slurries and to measure their rheological properties may be commercially available or might require special designs because of the corrosive, toxic, or air-reactive nature of the ingredients.

The following discussion details some of the recommended procedures used to prepare slurry fuels and to measure their rheological properties.

MIXING STUDIES. The typical steps in preparing a gelled slurry system may be summarized as follows:

- (1) Preparation of the solid components (gellant and/or metal powder)
- (2) Addition of slurry components
- (3) Mixing of the slurry
- (4) Addition of the gellant
- (5) Final mixing of the gelled slurry

Many processors utilize the metal powders and gellants as received from the manufacturer. For certain specific systems, however, these components must be pretreated. For example, some powders must be cleaned to provide a surface that will not react with the liquid substrate, and other powders must be ball milled to provide proper rheological properties to the slurry. Degassing of the metal powder, drying of the gellant, or preblending the metal additive and gellant are also required occasionally. Degassing the metal removes adsorbed air which may be subsequently entrapped in the gel, and drying the gellant removes moisture that can adversely effect the properties of many gelled slurries.

Most gelled systems require that the metal be dispersed in a slurry before the gellant is added. If this is not done, the higher viscosity of the gelled system hinders the dispersion of the metal particles resulting in added shear energy. Since most gel systems are shear sensitive, only a limited amount of work can be performed on the system following the gellant addition without destroying its properties.

The liquid phase is added to the mix vessel before solids addition to minimize the formation of solid agglomerates. Various methods of adding the fine metal particles have been used varying from hand-scoop to elaborate hopper facilities. In many cases, these additions must be accomplished in an inert atmosphere to avoid deterioration of the resultant slurry.

In preparing the slurry, high shear mixing combined with thorough circulation of the vessel contents are the basic requirements: high shear mixing to break up aggregates of solid particles, and thorough circulation to attain homogeneous and reproducible gels. At high solids loadings, slurries are so thick that obtaining efficient mixing is difficult. This

preparation of slurries with reproducible composition and rheological characteristics remains very difficult.

The mixing requirements for gellant incorporation into the slurried propellant are more stringent than those for dispersing the slurry. Whereas there is no indication that it is possible to overshear the slurry, this is certainly not true once the gelling agent has been added. Most gels shear thin irreversibly and, therefore, the amount of shear work used during this mix duty becomes significant. As in the dispersion of the solid phase, there is an advantage in high shear mixing to break up agglomerates of gellant and metal powder and thus homogenize the resultant gel. The requirement for mixing in the gellant is to provide sufficient shear and circulation to ensure a homogeneous gel but not so much that it will irreversibly shear the gellant structure and result in too low a viscosity.

When choosing a mixer for gel preparation, the common approach is to test available mixers until one is found which adequately performs the tasks described previously. Although this is largely a hit-or-miss approach, it is apparently not too critical, and many suitable candidate fuel slurries have been prepared. Similar end products can be obtained with different mixing devices. At present non-Newtonian fluid mixing remains more of an art than a science, and the outlook is that it will remain as such in the near future.

RHEOLOGICAL PROPERTIES. *Yield Stress.* The idealized slurry fuel must have a yield stress (defined as the minimum stress required to initiate flow) which imparts the necessary rigidity to the gel to prevent solid settling and shear thin to a value approaching the viscosity of the liquid. The yield stress needed to prevent settling of solid particles such as used in propellants is not definite, but certain values are reported (1). The classical way to measure yield stress involves the extrapolation of the shear-stress rate curve (*e.g.*, as obtained from a rotational type viscometer) to zero shear rate. This method generally does not apply to the gelled slurries with a high volume percent of solids because of the great difficulty encountered in obtaining the consistency curve. The rising sphere method is frequently used to measure the minimum stress needed to produce flow (4).

The instrument consists of a steel sphere (2.063 cm. in diameter) attached by a length of thin steel wire to a load cell. The slurry sample rests on a horizontal cross arm which can be raised or lowered at controlled speeds. The load cell and cross arm which are part of an Instron Model TT-C testing instrument may be used. The sphere is placed in the lower third of the slurry sample, and the cross arm is lowered at a constant speed (8.5×10^{-4} cm./sec.). The resulting force on the load

cell is recorded *vs.* time until the force reaches a constant value. The yield stress is then calculated using the equation:

$$\text{Yield stress} = \frac{(F - W_s) g}{4\pi r^2}$$

where F = maximum recorded force in grams, W_s the weight of the sphere in the slurry, r is its radius, and g is the force of gravity.

The magnitude of the yield stress depends on the type of gellant used, its concentration, and the solids content. If the gellant is of the particulate type, such as finely divided carbon or pyrogenic silica, the yield stress will be quite low, even with 5–10% of gellant. If the gellant is a polymeric thickening agent, such as polystyrene in hydrocarbons which simply forms a viscous solution, it may have no yield stress. The presence of the solid powder fuel even at a high concentration in the gel, appears to have only a small effect ($< 10\%$) on the yield stress.

Slurry Viscosities. In addition to the yield stress, the characteristic shear stress–shear rate relation of the fuel slurry should be known since the shape of the shear rate–shear stress curve (consistency curve) is an indication of the gel characteristics. Low shear rate data (10^2 sec^{-1}) are useful mainly in determining batch-to-batch reproducibility, while high shear rate data (10^4 to 10^6 sec^{-1}) are required to assess the flow characteristics in engine hardware.

The gelled slurry fuels that are being studied are often referred to as “thixotropic” although many of them are not. A material which is thixotropic undergoes time-dependent shear thinning at a fixed shear rate. What is really important in the rocket propellant application is that the material has an essentially rigid structure at rest so that it can support the suspended solid, but that it break under shear and flow as nearly like a liquid as possible—*i.e.*, it should be a pseudoplastic material with yield stress. The extent to which a typical fuel slurry displays the property is shown in Figure 1. In this case the viscosity of the gel decreases continuously with increasing shear rate, and the process is essentially reversible.

Various methods are used to examine the viscosity characteristics of metallized gels. Two types that have received extensive application are the cone and plate viscometer and the capillary viscometer. Both instruments can measure rheological characteristics at high shear rates, and the former is useful for low shear rate measurements as well.

A cone and plate rotational type viscometer is used to obtain rheological data in the low-to-medium shear rate range. It gives a constant rate of shear across a gap, and therefore, equations for this instrument are simple when the angle is small (less than 3°). For this reason the cone and plate viscometer has become a standard tool

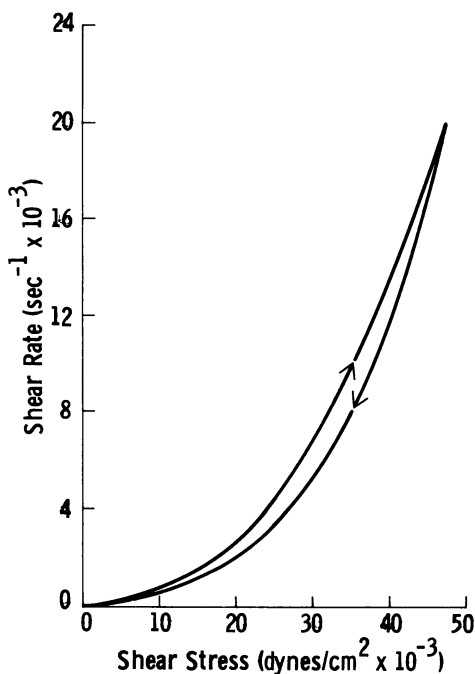


Figure 1. Typical consistency curve of a high solid loaded fuel slurry

with research investigators studying non-Newtonian fluids. The instrument used at TCC-RMD is a commercial device called the Ferranti-Shirley cone and plate viscometer. This instrument is provided with six cones (insulated for use up to 200°C.). Three are "standard" cones which will measure slurries with particles up to 36 μ . The other three are "special" truncated cones for slurries containing particles up to 100 μ . By means of this cone angle, r.p.m.-range and torque spring adjustment, shear rates from 0–20,000 sec.⁻¹ and shear stresses from 0–562,500 dynes/sq. cm. can be obtained. Figure 2 shows a curve obtained with a 13 vol. % slurry of 4 μ graphite in water containing 1% gelling agent. The curve shows that the slurry is thixotropic and shear thins from an apparent viscosity of 2 poise at a shear rate of 10³ sec.⁻¹ to a viscosity of 0.36 poise at a shear rate of 10⁴ sec.⁻¹.

Since capillary viscometers are usually made at the laboratory using them, they are all somewhat different although their general construction is the same. A typical capillary viscometer consists of a heavy walled stainless steel cylinder of 500-ml. capacity, which is fitted with a capillary adapter plug, a nitrogen pressurization port, and a large cap to facilitate ready access for sample loading and cleaning. By means of different

sized capillaries, shear rates to 10^6 sec.^{-1} can be obtained. In use, the cylinder body is filled with the sample to be tested. Nitrogen is admitted at a given pressure, and a sample of the exudate is collected over a specified period of time, and its mass is determined. The shear rate (SR) is calculated from the equation:

$$SR = 32Q/\pi D^3$$

where Q is the flow rate of the material (cc./sec.) and, D is the diameter of the tube (cm.). The shear stress (SS) is calculated as follows:

$$SS = \frac{\Delta P}{L} \times \frac{D}{4}$$

where ΔP is the pressure drop across the tube (dynes/sq. cm.), D is the diameter, and L is the length of the tube (cm.).

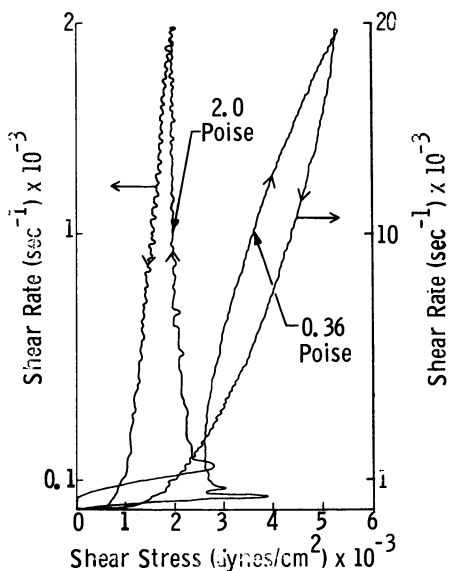


Figure 2. Consistency curve of 13 vol. % graphite dispersed in a water gel using a cone and plate viscometer

Figure 3 shows a curve of the 13 vol. % 4μ graphite slurry in water as determined with a capillary viscometer. This is the same material examined on the cone and plate unit. The apparent viscosity is 1.6 poise at a shear rate of 10^3 sec.^{-1} and decreases to a value of 0.39 poise at a shear rate of 10^4 sec.^{-1} , the viscosity data being corrected for the true wall shear rate. The flow curves obtained from both instruments agree quite closely.

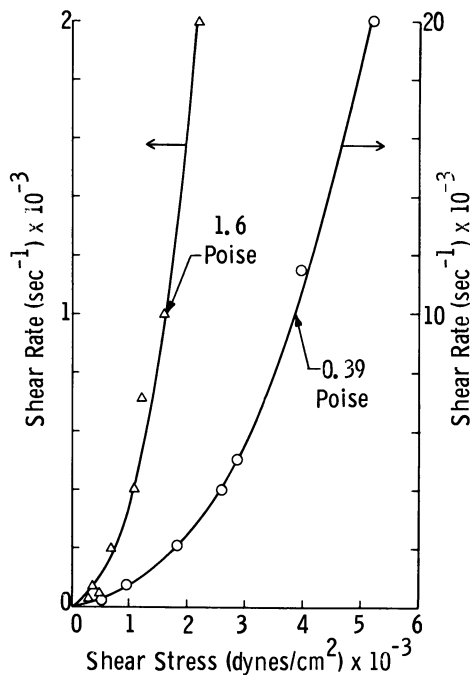


Figure 3. Consistency curve of 13 vol. % graphite dispersed in a water gel using a capillary viscometer

Burning Rates. One additional non-routine property that is determined in studying certain propellants is the burning or deflagration rate. This determination is a measure of the rate of consumption that a propellant can be expected to undergo in an engine. Originally, this measurement was developed for use with solid propellant samples, and it provides useful quantitative data as to the consumption rate expected in a solid propellant motor. It can also provide useful, although relative information, for monopropellants since the main factor that controls the rate of consumption of a monopropellant is its rate of introduction into the rocket motor.

There is reason to believe that the measurement of burning rate should be of interest to the chemical industry. A number of materials that are handled can deflagrate, particularly if subjected to elevated temperature and pressure; certain organic material containing nitrate, nitro, peroxide, and certain other oxidizing species are examples. It is important to know what these rates are and how they depend on temperature and/or pressure in order to know whether or not they constitute an industrial hazard.

The strand burner used generally for studies of the burning rate of solid propellant strands is easily adapted for use in studying the burning rate of liquid monopropellants. A sample tube (usually 0.2–0.5 inch in diameter and 4 inches long) is placed within the bomb and wired as shown in Figure 4 so that it can measure not only burning rate but the uniformity of rate throughout the sample length. The ignition wire is placed 1 inch above the first of three mechanical switches which are activated as the flame burns past them. The burning pattern is traced out on an oscilloscope and recorded photographically. Pressures (usually 200–2000 p.s.i.g.) are kept constant by using a large surge tank in line with the bomb, and the temperature of the experiment can be varied over a wide range.

The effect of pressure on the burning rate of a new, experimental monopropellant is shown in Figure 5. Note that the greater the pressure,

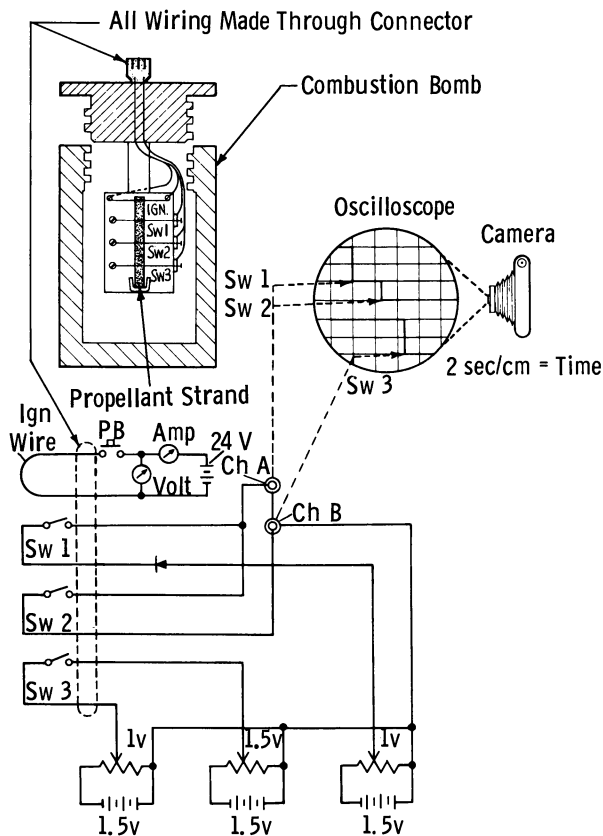


Figure 4. Schematic of modified strand burner circuit employing three-wire timing circuit

the higher the burning rate—*i.e.*, this is normally observed for both solid and liquid monopropellants. This dependence can be expressed as $K = AP^n$ or its logarithmic form $\log K = n \log P + \log A$ where K is the burning rate (inches/sec.), P is the bomb pressure (p.s.i.g.), and n and A are constants characteristic of the propellant composition and indicative, respectively, of the pressure dependence and magnitude of the burning rate. Figure 5 is in good agreement with this relationship where $n = 0.64$ and $\log A = -2.66$.

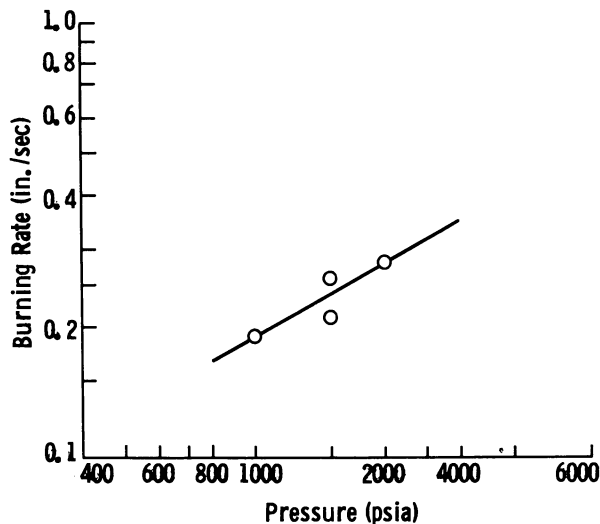


Figure 5. Effect of pressure on the burning rate of an experimental monopropellant

Storability and Compatibility of Liquid Propellants

The use of hermetically sealed tanks greatly reduces the complexity of a rocket engine and increases the reliability. It is, therefore, advantageous to use propellants which are sufficiently stable to be packageable, but this is not always possible. Many of the fuels used in current rocket engines contain at least a sizeable fraction of hydrazine which is either packageable or not depending on the other fuel ingredients present and/or the selection of the container material. This fuel is thermodynamically unstable, and its rate of decomposition is therefore sensitive to the presence of foreign ingredients.

A second consideration concerned with propellant storage and which applies specifically to slurried propellants is its mechanical stability. The suspended particles must remain in stable suspension in the gelled liquid for long times, and the mixture must not exude liquid (syneresis). To

avoid solid settling, the gel structure must remain intact as it ages, and it must remain rigid enough to prevent solid settling when the slurried propellants are exposed to the long term vibration conditions that may occur during land or sea transportation and the short term acceleratory forces that may occur under actual operational conditions.

Chemical Stability. Chemical stability as defined by TCC-RMD refers to the ability of a material to be stored for long periods without undergoing self-decomposition or chemical reaction. If this occurs, it can produce gaseous products which can cause a dangerous buildup of pressure within the storage container.

The importance of a chemically stable system can be illustrated with hydrazine. This compound has an extremely high computed specific impulse with interhalogen oxidizers, and its physical properties are excellent except for its freezing point. This freezing point can be modified by adding other ingredients that do not significantly degrade the energy. However, hydrazine is exothermic and susceptible to both thermal and catalytic decomposition by a variety of materials including metals and metal oxides. Therefore, extreme care must be taken in choosing storage tanks for the fuel, especially since it is desirable to fill the tank to its full capacity. A typical propellant tankage system requirement is that the free vapor space (ullage) be no more than 5%. Hydrazine decomposes according to the following stoichiometry.



If 1% decomposition were to occur, a pressure buildup of 4350 p.s.i.g. would develop in such a tank. The extent of the decomposition will result in little or no performance loss, but the weight of the tank required to contain the propellant would be prohibitive and negate any advantage in the use of hydrazine. In addition, if the fuel is a slurried propellant, gas bubbles will form and will be trapped in the gel structure causing an over-all bulk growth of the mixture. The effective density of the slurry will then be lowered, resulting in a change in the designed expulsion rate of the fuel into the combustion chamber. The rocket motor is designed to eject the fuel and oxidizer at a specific O/F ratio, and the density change will disturb this balance.

Since chemical reactions are accelerated by temperature increases, the recommendation is to store materials at the highest possible temperature consistent with practical limits—*i.e.*, 165°F., for the longest possible storage period. Storage data generated for liquid and slurry propellants are of two types: (1) laboratory controlled experiments, and (2) field tests in hermetically sealed containers. The laboratory experiments provide for rapid and convenient determinations and are used primarily for comparing one propellant with another or for comparing the relative

effects of container materials. In the laboratory experiments, gas evolution rates are measured by either gas volume produced or increase in pressure. The field tests represent actual tankage conditions closely since they are performed in sealed containers with propellant volume-to-container surface areas comparable to power plant tankage. To minimize the possibility of gas loss, these test tanks have a minimum area of non-welded closures.

Mechanical Stability. Mechanical instability in a slurry propellant can occur in two ways. For a polymer-thickened fuel, low temperatures can reduce the solubility of the polymer and result in separation into two phases. A relatively quick test in the laboratory can confirm the presence or absence of this problem. For the solid powder dispersed on the gelled fuel, exposure to temperature cycling, vibration, or acceleration could possibly cause settling of the solid phase. Considerable work has been done on fuel slurries which must be mechanically stable for periods of three to five years. It is our belief that "accelerated" mechanical stability tests are not recommended. There have been instances where short term accelerations at high g forces (500 g for 30 minutes) in a centrifuge were used to predict the mechanical stability of slurries during long term storage. It would seem that the demonstration of stability under high g forces would be more difficult than during long term storage at 1 g . However, samples which do not settle during acceleration can settle drastically during extended storage. Since long term storage tests are usually conducted using vessels nearer in size to an end-use container, they have a lower surface-to-volume ratio than unaccelerated test containers, thus giving the slurry less surface on which to cling. Another factor may be an extremely low particle settling rate which is not observable during a short duration of acceleration tests.

However, short term acceleration tests may simulate randomly occurring shocks that the propellant will be exposed to during road transportation or transonic buffeting and sudden gusts during flight. It is therefore necessary to perform both short and long term testing on a slurry system to demonstrate the resistance to settling of the solid powder. In short term tests effects of acceleration and vibration are relatively easy to study.

Many types of procedures are used to perform these tests, and a variety of equipment is used. Some of the recommended tests are discussed below.

SHORT TERM TESTS. Centrifuge Tests. Samples of the slurries are syringed into tubes which are capped at both ends. The tubes are then centrifuged (International Centrifuge Type SB) at a force of 50 g for 30 minutes. After the acceleration, samples from the top and bottom of

the tube are analyzed for solids content. Other conditions of acceleration or time can also be used.

Vibration Tests. Vibration tests are conducted in metal tubes (1-3/8 inches by 7/16 inch) which are capped at both ends. The vibration tester used is a model SAC vibrator from MF Manufacturing Co. In each test, duplicate samples are vibrated for 24 hours while a third is kept stationary for the same period as a control. Tests are usually performed at 300 c.p.s. and 5 g and 1000 c.p.s. and 3 g although these conditions can be varied. At the conclusion of each test, samples of the slurry are removed from the top and bottom of each tube and analyzed for solids content.

LONG TERM TESTS. In studying long range mechanical stability various tests are used—*e.g.*, static tests, actual transportation tests, and vibration tests. The first is the easiest to arrange, but it provides the least useful data. Normally many containers are set aside for a year, and periodically, a pair of containers will be examined for settling and change of rheological characteristics of their contents. It is better, however, to expose samples of the slurry to transportation modes it will see in use. This was done recently with a large number of samples of material being considered for use by the Navy. Samples were actually kept in the magazine of a ship for nine months under typical end-use conditions. Then the containers were sacrificed, and the homogeneity and rheology were examined. In this case the results indicated no significant change in either property.

Another recommended test is to expose samples of propellant to testing on a vibration unit for weeks to months. The specific device we use is a model 100 HLA-D (horizontal) vibration fatigue tester made by All American Tool and Manufacturing Co. Samples, 1 liter in size, are tested, and temperatures can be adjusted easily from below 0° to above 100°F.

Material Compatibility. Many of the oxidizers used as propellants are extremely reactive and can attack a variety of metals and non-metals. In addition, fuels can also attack the non-metallic components in the system and even, in some rare cases, cause stress corrosion of certain metal alloys. However, more normally the fuel/materials problem is one that is observed as an instability produced in the fuel rather than an attack on the materials of the engine system.

All oxidizers being evaluated for use in rocket engines are carefully examined to determine their compatibility with the materials with which they will be in contact. In some cases elaborate steps are necessary to develop passivation techniques that permit extended storage of these oxidizers. One of the classical cases in recent years was the development of inhibited red fuming nitric acid (IRFNA) for use in aluminum tanks.

It was found that the addition of 0.5% hydrogen fluoride to red fuming nitric acid (RFNA) removed the large pressure increase observed when normal RFNA was stored in the aluminum tanks used in certain rocket engine systems. Apparently this small amount of HF "passivated" the surface of the metal and prevented it from reacting with RFNA to generate decomposition gases.

In studying compatibility of oxidizers, both static and dynamic tests are conducted. An oxidizer such as chlorine trifluoride is particularly troublesome under flow conditions, although it can be stored under static conditions rather easily because of the firm fluoride film it forms. If this film is cracked so that continuity no longer exists, burnout under high flow conditions can occur.

The problem is somewhat different with an oxidizer such as N_2O_4 . While N_2O_4 is compatible with aluminum and many stainless steels, the presence of a small amount of water as an impurity can increase its corrosive characteristics considerably. In addition, if a leak, even of micron size, is present in the propellant tank, a corrosive condition occurs, caused by reaction of the metal with nitric acid, which formed when the N_2O_4 contacts water from the surrounding atmosphere.

Hazard Testing of Liquid Propellants

Establishing the hazard associated with a given propellant is a difficult but essential part of any propellant development and improvement study. When handling known energetic rocket fuels, a fire hazard unquestionably exists, and precautions are taken to minimize the mixing of fuel vapors with air. Likewise, when handling known energetic oxidizers, great care is used to avoid skin contact or excess inhalation since these materials are known to be strong irritants and toxicants. However, even more complex problems exist when first attempting to synthesize a new high energy propellant because the propellant might be shock sensitive or the method of preparation might result in explosion. Also, when handling any monopropellant system, the possibility of detonation must always be considered. Determining this possibility, either during synthesis or application studies, receives a good deal of attention by propellant chemists, and this area of hazard testing will be discussed in detail here. A second reason for the emphasis given here to safety testing, is the applicability of the concerns and methods to the chemical industry.

The development of a liquid propellant advances through many stages. Initial synthesis or formulation of high energy materials is usually performed on a small scale. Somewhat larger quantities are required for complete laboratory characterization. Engineering evaluation and field testing require still larger quantities. The safety and handling prob-

lems associated with each phase of the development program are different, and a realistic appraisal of the hazards involved at each step requires a different approach. On a small scale, materials of extreme sensitivity can be readily handled for preliminary screening studies, with a minimum of precaution and hazard. Simple qualitative sensitivity tests are adequate when working at this level. However, the degree to which an explosive propellant can be scaled depends on how easily it can be initiated and the force with which it reacts. The larger the quantities to be handled, the more sophistication is required in the test methods. It is a great error to accept the results of small scale qualitative testing to assess the larger scale handling problems. This is a dangerous practice for the ultimate result can be catastrophic.

All test procedures are limited in the amount of impulse they deliver to the sample. The sample size, geometry, confinement, temperature range, and pressure range are also fixed within specific limits for any given test. The susceptibility of a material which gives positive results in several tests can usually be readily defined; however, a propellant that continues to exhibit negative results requires a more stringent analysis. A negative result in any given test is not necessarily indicative of a non-detonable material. Assuming the use of an initiator or booster of sufficient energy, a material may fail to propagate a detonation because it is below its critical diameter, or if above its critical diameter, it may fail to propagate because of improper intrinsic or extrinsic conditions. Intrinsic conditions refer to the chemical and physical properties of the propellant environment. Thus, it is important not only to distinguish between a non-detonable and a detonable material but also to define the conditions under which a detonation will occur. It is impractical to test propellants under every conceivable condition which can occur; however, the broader the range of extrinsic and intrinsic factors covered, the greater is the degree of confidence which can be obtained for any material.

Lab Scale Testing. When handling propellants on a laboratory scale, it is important to know how easily they can be initiated and the extent of damage to be expected from a given sample size. Such information is helpful in determining the quantity of any given material that can be handled safely within the shielded laboratory facilities available.

Many tests have been used to estimate or evaluate the explosive power of materials by assessing the damage done to the surroundings. At TCC-RMD we have adopted a modified version of the well-known Trauzl test. This test gives a relative measure of the power of an explosive and a qualitative indication of its sensitivity. In our modification of the test, the lead block used is a cylinder 2-1/2 inches high, 2 inches outer diameter with a cavity bored out so that the walls and bottom are 1/2-inch thick.

Between 0.5 and 2.0 grams of the test material are sealed into a glass vial and placed into the lead cylinder along with a No. 8 blasting cap which is used as the initiator. The cap is electrically detonated, and the lead cylinder is examined. An indication of initiation and an estimate of the explosive power of the test sample are obtained from the amount of deformation experienced by the lead cylinder. Figure 6 shows a cross section of three cylinders. In the center is an unused cylinder. The one on the right was used in a control experiment to demonstrate the effect of the initiating source by itself. On the left is one in which 0.5 grams of an explosive mixture was tested. The deformation is reported in terms of the increased volume of the cylinder in excess of that obtained in control experiments. The units used are cc./gram of test sample. This test is extremely simple to conduct and is of great use to the synthetic chemist when he first prepares a new material. It is also useful for investigating small quantities of material, chemical combinations that could be considered hazardous. However, while the small sample size is an advantage in terms of initial testing, it may lead to erroneous conclusions because of the effect of size in sensitivity testing. A steady state detonation may not develop, and the results could appear less severe than those obtained in larger containers. For this reason, negative Trauzl tests are always followed by larger scale tests. Typical results obtained with this device are shown in Table II.

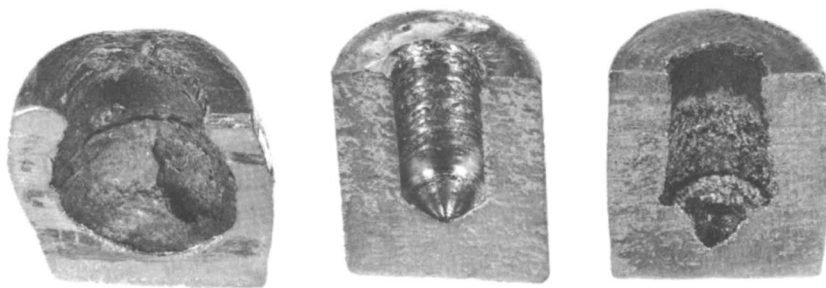


Figure 6. Damage to lead cylinder vs. criteria of detonation

Left: positive detonation

Center: original cylinder before test

Right: no detonation, damage caused by initiator

The shock sensitivity of materials are also frequently evaluated in a drop weight test. A variety of drop weight testers have been developed, but the standard device used to evaluate the sensitivity of liquid propellants is test No. 4 of the Joint Army-Navy-Air Force Panel on Liquid Propellants (2). A sample of material (usually less than 0.1 gram) is confined in an enclosed volume, and a calibrated weight is allowed to

Table II. Modified Trauzl Test

<i>Material</i>	<i>Expansion Caused by Sample (cc./gram)</i>
Hydrazine	0
Trinitrotoluene	0.5
Hydrogen peroxide (98%)	15
Nitroglycerine	27

drop on the sample from a given height. Both weight and height can be varied, and the results must be handled as a statistical presentation since exact experimental results are hard to reproduce. The sensitivity is normally reported as the height and weight at which the probability of explosion is 50%. This test, like the Trauzl test, can be useful as a guide to the synthetic chemist, but it is even further removed from a practical case. Therefore, completely negative results or even relative sensitivities should not be given undue merit. Typical data obtained with this equipment are shown in Table III.

Table III. Drop Weight Test

<i>Material</i>	<i>50% Height with a 2-kg. Weight (cm.)</i>
<i>n</i> -Propyl nitrate	1
Nitroglycerine	1
Ethyl nitrate	4
Hydrazine	>100

Another laboratory scale test that is conducted in many propellant laboratories although not at TCC-RMD is the adiabatic-compression sensitivity test. In a sense, the drop weight tester also measures the sensitivity of a liquid to compression, but other devices have been developed which attempt to determine this sensitivity more directly. In all these tests, a sample of liquid in contact with a vapor space is rapidly compressed, and the kinetic energy introduced into the system is assumed adiabatically to heat the vapor bubble above the liquid. In test No. 5 recommended by the Joint Army-Navy-Air Force Panel on Liquid Propellants (2) a piston is used to compress rapidly a gas bubble above the liquid propellant sample, and the measurement is then made as to whether this adiabatic heating of the bubble can initiate a detonation in the liquid sample. The energy input to the test sample is calculated from the mass and velocity of the piston. This tester is quite similar in action to that expected in the actual use of a fuel owing to rapid closing of valves in propellant lines containing entrained air bubbles. Typical values are shown in Table IV.

Table IV. Adiabatic-Compression Sensitivity Test

<i>Material</i>	<i>Sensitivity</i> (kg.-cm./ml. of sample)
<i>n</i> -Propyl nitrate	6.7
Nitromethane	10.5
Hydrazine	>144
UDMH	>144

Thermal initiation of an explosion as well as the temperature of decomposition of propellants are measured by standard test No. 6 developed by the Joint Army-Navy-Air Force Panel on Liquid Propellants (2). The primary purpose of this test is to determine at what temperature an unstable material will undergo rapid exothermic decomposition. If the rate at which the heat is generated is greater than the rate at which it can be dissipated, an explosion will be likely. This test attempts to predict the result of conditions that can exist in the regenerative heating section of a rocket engine as well as at the propellant injector. Both of these sections experience relatively rapid local temperature rises owing to combustion.

The sample is enclosed in a heavy walled bomb with an internal volume of approximately 1 to 1½ ml. Although similar to a differential thermal analysis (DTA) test, the samples used are much larger, and the conditions of confinement allow the liquid to remain in contact with any decomposition products that form as vapors. Heat is applied so that the bath temperature increases at a constant rate and the temperature of both the heating bath and the sample are recorded continuously. When the temperature of the sample exceeds that of the bath, an exothermic reaction must be occurring in the sample, and this process is frequently accompanied by a detonation. (The bomb is equipped with a blow out disc to avoid any major damage to the equipment). In the more usual case the discrepancy between sample temperature and bath temperature increases with temperature, and the point at which this deviation is 5°F./min. is called the self-heating temperature. Typical values for some liquid materials of interest in the propellant field are listed in Table V.

Table V. Standard Test No. 6

<i>Material</i>	<i>Self-Heating Temperature</i> (°F.)
<i>n</i> -Propyl nitrate	330
Hydrazine	400
Nitromethane	530
UDMH	590

Larger Scale Testing. The standard card gap test (2) is test No. 1 of a series of larger scale tests designed to determine the sensitivity of liquid propellants to hydrodynamic shock. In this test, relative sensitivities of various propellants are determined in terms of the number of 0.01-inch thick cellulose acetate cards required to attenuate a standard shock sufficiently just to prevent initiation in the test sample. When performed according to the exacting conditions of apparatus and procedure, the results are very reproducible from one laboratory to another. However, small variations in the apparatus or procedure can cause major variations in the resulting data, and therefore the test can be considered only relative. A major drawback of the standard test is that it cannot accommodate materials that are volatile under the test condition. At TCC-RMD some special equipment has been developed that allows tests to be made on confined samples at elevated temperature and pressure.

Another major drawback to this test is that a sensitive material must be energetic enough so that when a sample of 40 cc. is initiated it can blow a hole in a 3/8-inch steel plate mounted atop the sample container. This criteria for detonation is not useful in those cases of low order detonation where considerable energy would be released, but the test plate would indicate that no detonation had occurred.

In the tests conducted at TCC-RMD, more severe experimentation is conducted than required in the standard test, and more sensitive techniques have also been developed to detect a detonation. When a propellant is found to propagate in the standard card gap container or in any diameter up to two inches, its critical diameter is determined by performing detonation tests in containers of consecutively smaller diameter until a detonation fails to propagate. To ensure that the negative observation is caused by propagation failure rather than by some initiation problem, the detonation is led into the smaller tube from a larger one which is known to be above the critical diameter. The detonation is then monitored throughout both tubes. A high-order detonation is observed in the large tube, enters the small tube, and fails after a short distance (usually less than an inch) if the small tube is below the critical diameter.

The criterion used at TCC-RMD to detect the detonation is to measure the velocity of the detonation wave. The constant current resistance wire method, originally developed at the U.S. Naval Ordnance Laboratory (7), is the technique used. This method depends on the high degree of ionization existing in the reaction zone of a detonation. The advancing detonation front completes the circuit between a central resistance wire and another conductor, which may be the metal test container or a separate wire, maintained at ground potential. The method provides a permanent record of a complete and accurate history of a detonation as it passes through a container of any size or shape. Needless

to say, the absence of a detonation can also be demonstrated by this method. While the test is precise (detonation velocities can be measured to $\pm 3\%$), the utility of the method for evaluating propellants does not depend on a high degree of precision. Rather, the greatest utility stems from the fact that it is an unambiguous criterion of detonation propagation. It is used with those systems whose detonability has not been clearly established in the tests described previously. The test is well suited for examining the effects of various extrinsic variables such as composition of confining material, temperature, and geometry. This type of testing can provide interesting data. The results of tests on several candidate propellant materials in the standard card gap tests are given in Table VI.

Table VI. Standard Card Gap Test

<i>Material</i>	<i>Card Gap Value for a 1-inch Diameter Sample</i>
Nitroethane	0 ^a
Nitromethane	20
Hydrazine	0 ^a
Hydrazine (65%) + hydrazine nitrate (35%)	15

^a Negative test even with 0 cards.

In a series of tests on a monopropellant (structure is classified information), the particular type of tubing used to hold the material was found to have a significant effect on the critical diameter of the system. The data in Table VII present the results of critical diameter studies on six different materials. These data have proved useful in sizing pipes to handle sensitive propellants safely.

Table VII. Critical Diameter Studies

<i>Material</i>	<i>Critical Diameter (in.)</i>
Aluminum	0.18–0.36
Stainless steel	0.18–0.38
Alumina	0.43–1.0
Zircon-mullite	0.50–1.0
Borosilicate glass	0.92–1.9
Lucite	0.92–2.0

One interesting application is included to show how these testing techniques can be used to evaluate hazards caused by handling operations. The example presented here involves the use of methylene chloride or other chlorinated hydrocarbons, as solvent cleaners for transfer lines, processing equipment, etc.

Methylene chloride is generally considered inert and is often used indiscriminately as a solvent cleaner in many operations. It was recognized, however, that solutions with oxidizers might be potentially hazardous. Preliminary compatibility testing with nitrogen tetroxide did not reveal any reaction at room temperature. In addition impact tests on mixtures containing 50% methylene chloride and 50% N_2O_4 gave negative results at 36-inch drop heights using a 2-kg. weight.

In the Trauzl test, the mixture produced an expansion of 24 cc./gram, which is indicative of a high energy reaction. Card gap tests were also positive; the value at room temperature is approximately 25 cards. From these results it was concluded that a mixture of methylene chloride with nitrogen tetroxide constitutes a definite explosive hazard. This conclusion was not immediately apparent as a result of compatibility and impact testing alone. Methylene chloride was not recommended as a solvent for cleaning N_2O_4 systems; instead, a water flush is used for this operation.

The correctness of the conclusions reached in this study were confirmed by a recent report on the explosions of mixtures containing halogenated solvents (such as methylene chloride) and nitrogen tetroxide.

Literature Cited

- (1) Beerbower, A., Philippoff, W., *Proc. Aircraft Fluids Fire Hazard Symp.* 86 (1966).
- (2) "Liquid Propellant Test Methods," Chemical Propulsion Information Agency, Applied Physics Laboratory, The Johns Hopkins University, Silver Spring, Md., March 1960.
- (3) *Ibid.*, p. 165.
- (4) McVean, D. E., Mattocks, A. M., *J. Pharm. Sci.* 50, 785, 1961.
- (5) Wells, W. W., *Space/Aeronautics*, 76 (June 1966).
- (6) Whittaker, A., Greenville, *J. Phys. Chem.* 62, 267 (1958).
- (7) U. S. Naval Ordnance Laboratory, *NAVORD Rept.* 6280 (March 16, 1959).

RECEIVED May 4, 1967.

Combustion of Liquid Propellants and the Use of Similarity Principles in Theoretical Combustion Research

S. S. PENNER

Department of the Aerospace and Mechanical Engineering Sciences,
University of California, San Diego, La Jolla, Calif.

Injector design determines the physicochemical processes occurring in liquid propellant rocket engines. A complete quantitative description of the processes in liquid rockets is impossible because of our limited understanding of chemical reaction mechanisms and rates. The use of similarity principles simplifies the solution of theoretical combustion problems and is described for channel flow with chemical reactions and for diffusion flames over liquid droplets involving two coupled reaction steps. We find the new result that the observed burning rate of a liquid droplet is substantially independent of the relative rates of the coupled reactions.

Injector design determines combustion efficiency, engine stability, heat transfer, and performance reproducibility (4). The injector, in turn, is described by orifice construction and location and by the injector feed passage and supply system. Baffles may help to improve engine stability.

In conventional rocket engines, propellant distribution tends to be non-uniform across the injector face. Furthermore, relatively large changes in flow velocity may be associated with small fluctuations in supply pressures (4). Improved distribution of fuel and oxidizer across the injector face may be achieved by using orifice designs in which fully turbulent flow is attained reproducibly (4, 18).

Heat transfer across the injector face is also controlled by the judicious design of propellant injection. Such fuels as hydrogen and hydrazine (50%)—UDMH (50%) have been used as film coolants on the periphery of injector plates. Alternately, non-stoichiometric mixture

ratios may be used at favored locations to limit the combustion temperatures. Programmed mixture and mass ratio distributions across the injector face may help to minimize coupling between the combustion reactions and high frequency instabilities since it is known, for example, that optimum coupling with the first and second tangential modes occurs at large radial distances from the center. Similarly, coupling of oscillations with the feed system may occur unless the injector pressure drop is carefully controlled.

The detailed injector element design profoundly affects atomization and combustion rates. Among the more widely used configurations is the like-on-like design. Showerhead and splash-plate injectors have been used less frequently in recent years. Various special techniques have also been used to improve liquid-phase mixing and/or atomization and reaction rates.

In summary, all features of the liquid rocket engine combustion processes are extensively affected by injector design, and any simplified combustion model, in which the essential three-dimensional nature of the flow processes is ignored, can only be of qualitative significance. Nevertheless, these simplified models are useful in giving us some insight into the nature of the physicochemical phenomena that determine engine performance. In this connection, steady-state combustion rates and overall combustion efficiencies in propellant utilization are far less important practical problems than are control or elimination of instabilities, excessive heat transfer, and hard starts.

Fundamental Combustion Research Relating to Liquid Fuel Rocket Propellants

Fundamental combustion studies on liquid fuel rocket components have been a favorite subject for experimental and theoretical combustion research for some years (11). Among representative problems that have been studied extensively are the following:

(a) Burning of single fuel or oxidizer droplets in a gaseous atmosphere of oxidizer or fuel, respectively, without and with natural or forced convection. The observed burning rates are fairly well described by a (spherical) diffusion-flame approximation. Some relation has been noted between the magnitude of the evaporation constant, which measures the rate of droplet burning, and the required rocket chamber length for complete combustion (11, 22).

(b) Burning of monopropellant droplets without or with natural or forced convection (11, 22).

(c) The burning of simple geometric arrays of two to nine droplets has been studied with natural and with forced convection. Depending on droplet composition and on the nature of the surrounding atmosphere,

interference during droplet burning (*i.e.*, heat conduction from adjacent flamelets, removal of oxygen by adjacent regions of burning, supplementary induction of convection currents, etc.) may lead either to increased or decreased local burning rates (11).

(d) The mechanism and rate of flame propagation have been investigated in one-dimensional droplet arrays, with and without forced convection (11, 22).

(e) An enormous amount of experimental and theoretical work has been carried out on chemical reaction rates and mechanisms involving gaseous propellants or gaseous products derived from chemical reactions involving propellants.

(f) Simple, one-dimensional models describing spray burning have been developed and extended for empirical comparisons with studies performed on idealized rocket engine configurations (11, 22).

(g) Ignition phenomena involving liquid propellants have been investigated at various levels of sophistication (1, 11, 16, 22).

The specified investigations have all contributed to our qualitative understanding of combustion phenomena in liquid fuel rocket engines and have provided insight into the many facets that determine over-all propellant conversion rates and combustion efficiencies. However, no quantitative *a priori* predictions of the performance of practical propulsion systems appear to be in sight. The final successful development of a new engine, or even of the scaled version of an existing engine, must still be achieved empirically.

Energy Addition to Expanding Gas Flows. In connection with the analyses of optimal rocket engine cycles, it is of interest to develop generalized solutions for the equations of motion with heat addition. An efficient technique is to write the fraction of reaction completed (ϵ), at any station, as a function of the square of the local Mach number (M^2), in the form

$$\epsilon = [(M^2 - M_o^2)/(M_e^2 - M_o^2)]^{1/n}$$

where the subscripts o and e denote, respectively, inlet and exit conditions, and the parameter $0 \leq n \leq \infty$ measures the heat addition rate in the flow channel. Using this approach, we may develop generalized steady-flow solutions relating the channel area first to M^2 and then to ϵ . Subsequently, we determine, for given values of $A(x)$, the heat release profiles as functions of the distance coordinate x for which the flow equations have been solved (14).

Similarity Principles in Theoretical Combustion Research

The use of similarity principles in theoretical combustion research is justified because of our inadequate present and expected future knowl-

edge of chemical reaction mechanisms and rates (7) and of the nature of turbulent flow phenomena with chemical reactions (5, 9, 19). In the following sections, we describe the basic phenomenology of the similarity procedures and illustrate their utility by considering chemical reactions during flow in a constant-area channel and the burning of hydrazine droplets in oxygen.

Chemical Reactions Involving Liquid Propellants. All liquid mono- and bipropellants undergo chain reactions in producing reaction products. The elementary steps involved in the decomposition or combustion reactions are not well understood, except possibly for some of the hydrogen-halogen mixtures. Specific reaction rates are generally unknown and are defined only within about an order of magnitude for the simplest processes (*e.g.*, recombination of hydrogen atoms in the presence of a third body). An effective over-all rate law for the production of reaction products has sometimes been determined for a limited range of experimental conditions.

The steady-state approximation is often used for the atomic and free radical intermediates occurring in combustion processes. The validity of this approximation has been examined in connection with the theoretical calculation of laminar flame velocities (3, 20, 21) in premixed gaseous systems. The steady-state approximation is occasionally useful for obtaining first-order estimates for flame-propagation velocities but should probably not be used in estimating concentration profiles for reaction intermediates. Some additional observations on the steady-state approximation are contained in Appendix I.

In summary, combustion processes generally involve unknown reaction steps with unknown rates in complex systems for which no generally useful simplification procedure in analysis is applicable. Furthermore, judging from the painfully slow progress that has been made in elucidating the relatively simpler problem of air reactions, it is unrealistic to believe that this situation will change materially in the foreseeable future. In fact, agreement between theory and experiment is generally achieved by repetitive iterations which ultimately lead to the selection of particular, non-unique sets of reactions and rate laws that yield "predictions" which are in agreement with very limited experimental data and usually require readjustment as soon as new measurements are performed.

Our past and expected future lack of progress in the quantitative understanding of reaction rates and mechanisms has forced us, for all practical purposes, to formulate analyses for "real" combustion processes at such an unsophisticated level that detailed reaction mechanisms and rate laws are not required. The conclusions derived from procedures of this type are then likely to be only of qualitative or, at best, of semi-quantitative significance. Among the schemes that are most useful for

avoiding immediate confrontation with the complexities resulting from unknown or inadequate kinetic information are techniques leading to similarity solutions, as introduced by Penner and Williams (17) for one-step reactions into the Western literature and identified as the Shvab-Zeldovich procedure. This methodology has been generalized to multistep reactions by Penner and Libby (for studies of boundary-layer heat transfer) (15) in a manner that is related to an earlier modification of the Penner-Williams procedure by Lees (8). As new illustrations of results derivable from application of this technique, we shall consider the problems of chemical changes occurring during flow in a channel of constant cross section and of droplet burning controlled by a two-step reaction mechanism.

Similarity Relations for One-Dimensional, Constant-Area Channel Flow with Chemical Reactions. Similarity relations between stagnation temperature and mass fractions obtain during flow in a channel of constant cross section, provided a binary mixture approximation is used for the diffusion coefficient, the Lewis number is set equal to unity, the Prandtl number is set equal to $3/4$, and a constant value is employed for the species and average isobaric specific heats. [The assumption that the species $(c_{p,i})$ and average $(\bar{c}_p = \sum_1 Y_i c_{p,i})$ isobaric specific heats are equal may be deleted without difficulty by a slight modification in procedure, as described in Appendix II.] For the sake of simplicity, we illustrate the applicable procedure for the one-step chemical reaction



with specific reaction rate constant k_f when molar concentrations are used in the equations of chemical kinetics. The final results may be generalized easily to multistep reactions [see Ref. 15 and the following section for details]

For steady, one-dimensional flow without body forces, with local mean velocity $v(x)$ in a channel of constant cross-sectional area A , the energy conservation equation becomes, approximately (13):

$$v \frac{d}{dx}(\rho u) + \rho u \frac{dv}{dx} + v \frac{d}{dx} \left(\frac{1}{2} \rho v^2 \right) + \left(\frac{1}{2} \rho v^2 \right) \frac{dv}{dx} = \frac{d}{dx} (-pv) + \frac{4}{3} \frac{d}{dx} \left(\mu \frac{dv}{dx} v \right) + \frac{d}{dx} \left(\lambda \frac{dT}{dx} \right) - \frac{d}{dx} \left(\rho \sum_i Y_i h_i V_i \right) \quad (2)$$

where ρ is the mixture density, u equals the specific internal energy of the gas mixture $= \sum_1 u_i Y_i$ if Y_i is the mass fraction of species i , p is the pressure, μ represents the mixture viscosity coefficient, λ equals the thermal conductivity of the gas mixture, T is the temperature, h_i stands for

the specific enthalpy of species i , and V_i is the diffusion velocity of species i . For a binary mixture approximation, without pressure diffusion,

$$V_i = - \frac{D}{Y_i} \frac{dY_i}{dx} \quad (3)$$

whence

$$\begin{aligned} \frac{d}{dx} \left(\rho \sum_i Y_i h_i V_i \right) &= - \frac{d}{dx} \left(\rho D \sum_i h_i \frac{dY_i}{dx} \right) \\ &= - \frac{d}{dx} \left(\rho D \sum_i h_i^\circ \frac{dY_i}{dx} \right) \end{aligned} \quad (4)$$

where

$$\begin{aligned} h_i &= h_i^\circ + \bar{c}_p T = h_{i,s} - (v^2/2), \\ h_{i,s} &= h_i^\circ + \bar{c}_p T_s = h_i^\circ + \bar{c}_p [T + (v^2/2 \bar{c}_p)] \end{aligned} \quad (5)$$

is the specific stagnation enthalpy at the temperature T , h_i° is the standard specific enthalpy at 0°K ., and T_s denotes the stagnation temperature. Here we have used the relation, $\sum_i Y_i = 1$. In view of Equations 3–5, Equation 2 may be rewritten as:

$$\frac{d}{dx} (\rho v h_s) - \frac{d}{dx} \left(\frac{\lambda}{\bar{c}_p} \sum_i h_i^\circ \frac{dY_i}{dx} \right) = \frac{d}{dx} \left(\lambda \frac{dT_s}{dx} \right) \quad (6)$$

where we have employed the relations

$$\begin{aligned} h_s &= u + \frac{1}{2} v^2 + \frac{p}{\rho} = \sum_i h_i^\circ Y_i + \bar{c}_p T_s, \\ \rho D &= \lambda / \bar{c}_p \text{ (i.e., Lewis Number = Le = 1),} \\ \frac{4}{3} \mu &= \lambda / \bar{c}_p \text{ (i.e., Prandtl Number = Pr = } \frac{3}{4} \text{).} \end{aligned} \quad (7)$$

After substituting for h_s from the first relation given in Equation 7, Equation 6 becomes

$$\frac{d}{dx} (\rho v \bar{c}_p T_s) - \frac{d}{dx} \left(\lambda \frac{dT_s}{dx} \right) = - \frac{d}{dx} \left(\rho v \sum_i h_i^\circ Y_i \right) + \frac{d}{dx} \left(\frac{\lambda}{\bar{c}_p} \sum_i h_i^\circ \frac{dY_i}{dx} \right). \quad (8)$$

Similarly, the continuity equation for species i is readily shown (12) to reduce to the form

$$\frac{d}{dx} (\rho v Y_i) - \frac{d}{dx} \left(\frac{\lambda}{\bar{c}_p} \frac{dY_i}{dx} \right) = \dot{w}_i \quad (9)$$

where \dot{w}_i is the mass production rate of species i per unit volume. From Equations 8 and 9 it follows immediately that

$$\frac{d}{dx} (\rho v T_s) - \frac{d}{dx} \left(\frac{\lambda}{c_p} \frac{dT_s}{dx} \right) = - \frac{1}{c_p} \sum_i h_i^\circ \dot{w}_i \quad (10)$$

Proceeding in the usual manner (15, 17), we note for the reaction described by Equation 2 that $\dot{w}_i = Y_i^* w$ and

$$- \frac{1}{c_p} \sum_i h_i^\circ \dot{w}_i = w T_0^* \quad (11)$$

where Y_i^* equals the mass of species i involved in the reaction of Equation 1 per gram of reactant mixture, T_0^* is the temperature rise per unit mass of reacting mixture which is initially at 0°K ., and w represents the product of the molar removal rate of one of the reactant species with the total mass of the reactant mixture per mole of O or F—*i.e.*,

$$w = (W_O + W_F) k_f \rho^2 (Y_O Y_F / W_O W_F), \quad (12)$$

where W_i equals the molecular weight of species i .

We now note that, if

$$L(\) = \frac{d}{dx} [\rho v(\)] - \frac{d}{dx} \left[\frac{\lambda}{c_p} \frac{d}{dx}(\) \right], \quad (13)$$

then

$$L\left(\frac{T_s}{T_0^*}\right) = w = L(\widetilde{T}_s) \quad (14)$$

$$L\left(\frac{Y_i}{Y_i^*}\right) = \pm w = L(\widetilde{Y}_i),$$

where the $+$ sign in the second relation of Equation 14 is to be used for a reaction product, and the $-$ sign applies for one of the reactant species; quantities identified by tilde refer to the dependent variables divided by the corresponding starred quantities. The differential equations are seen to be of the form,

$$L(\alpha_i) = 0 \quad \text{for } i = 1, 2, \dots, 10, \quad (15)$$

where

$$\begin{aligned} \alpha_1 &= \widetilde{T}_s + \widetilde{Y}_O, \\ \alpha_2 &= \widetilde{T}_s + \widetilde{Y}_F, \\ \alpha_3 &= \widetilde{T}_s - \widetilde{Y}_P, \\ \alpha_4 &= \widetilde{T}_s - \widetilde{Y}_P', \\ \alpha_5 &= \widetilde{Y}_O + \widetilde{Y}_P, \end{aligned}$$

$$\begin{aligned}\alpha_6 &= \widetilde{Y}_O + \widetilde{Y}_P', \\ \alpha_7 &= \widetilde{Y}_F + \widetilde{Y}_P, \\ \alpha_8 &= \widetilde{Y}_F + \widetilde{Y}_P', \\ \alpha_9 &= \widetilde{Y}_O - \widetilde{Y}_F, \\ \alpha_{10} &= \widetilde{Y}_P - \widetilde{Y}_P'.\end{aligned}$$

Of course, only four of the parameters α_1 to α_{10} are independent.

Equation 15 may be integrated with the result

$$\dot{m} \alpha_i + c_1 = \frac{\lambda}{\bar{c}_p} \frac{d}{dx} (\alpha_i) \quad (16)$$

where

$$\dot{m} = \rho v \quad (17)$$

is the constant mass flow rate per unit area, and c_1 represents an integration constant. Equation 16 may be integrated readily a second time with the result

$$\alpha_i = \frac{\alpha_{i, \text{ex}} [(\exp \dot{m} \bar{c}_p x / \lambda) - 1] + \alpha_{i, \text{en}} [(\exp \dot{m} \bar{c}_p \xi / \lambda) - (\exp \dot{m} \bar{c}_p x / \lambda)]}{(\exp \dot{m} \bar{c}_p \xi / \lambda) - 1} \quad (18)$$

where $\alpha_{i, \text{en}}$ and $\alpha_{i, \text{ex}}$ denote, respectively, the values of α_i at the channel entrance ($x = 0$) and exit ($\xi = 0$) locations.

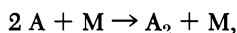
The similarity laws summarized by Equation 18 may be useful, in conjunction with experimental measurements of temperatures and flow velocities, for determining (over-all) composition changes during flow for complex chemical reactions described by an effective, one-step, over-all process. Needless to say, however, the similarity relations are no substitute for the solution of kinetic equations. Rather, the use of similarity principles is complementary to the use of kinetic equations since it serves to uncouple the energy and species conservation equations from each other. As has been emphasized before (15) for a one-step reaction, we must solve one kinetic equation of the form,

$$L(\widetilde{Y}_i) = w,$$

solve the equation for momentum conservation, use the mass balance condition $\sum_i Y_i = 1$, employ three of the similarity relations to determine two of the mass fractions and T_b , and finally utilize the equation of state for the determination of mixture density ρ .

Generalization to multistep reactions may be accomplished readily by following the procedure of Penner and Libby (15) and is best deferred to the discussion of a specified chemical system.

SELECTED APPLICATIONS OF EQUATION 18. Equation 18 does not provide useful information for similarity variables that are constants during flow, as is the case, for example, for the composition variables in mixtures containing only a single species A_2 and its dissociation product A. Thus, for the reaction



where the molar concentrations are related through the expression $(M) = (A) + (A_2)$, it is readily seen that the only meaningful composition similarity variable is

$$\alpha = \widetilde{Y}_A + \widetilde{Y}_{A_2} = (Y_A + Y_{A_2})/Y_{A_2}^*, (Y_A^* = Y_{A_2}^*),$$

with

$$Y_A + Y_{A_2} = (Y_A + Y_{A_2})_{en} = \text{constant}$$

since the total atomic mass of A must be conserved. In this special case, the differential relation given in Equation 16 should be replaced by the relation $\alpha = \text{constant}$, and Equation 18 reduces to an identity since $\alpha_i = \alpha_{i, ex} = \alpha_{i, en}$. On the other hand, when the species A and A_2 are coupled to other reaction processes in a complex gas mixture, application of Equation 18 may provide useful expressions between selected mass fractions and stagnation temperature. As a representative example, when we consider the variable α_3 , we find the following coupling function between \widetilde{T}_s and \widetilde{Y}_P :

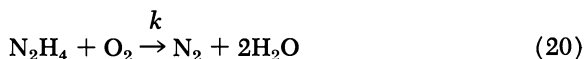
$$\widetilde{T}_s - \widetilde{Y}_P = \frac{(\widetilde{T}_{s, ex} - \widetilde{Y}_{P, ex}) [(\exp \dot{m} \bar{c}_p x/\lambda) - 1] + \widetilde{T}_{s, en} [\exp (\dot{m} \bar{c}_p \xi/\lambda) - \exp (\dot{m} \bar{c}_p x/\lambda)]}{(\exp \dot{m} \bar{c}_p \xi/\lambda) - 1} \quad (19)$$

where we have assumed that pure reactants are injected at the entrance section. Equations 18 and 19 thus yield simplified expressions for the complete composition and temperature profiles from a measurement of either $\widetilde{T}_s(x)$ or of $\widetilde{Y}_i(x)$, where $i = O, F, P$, or P' . Corresponding relations can be derived only with considerable difficulty for a flow problem with axial heat conduction and diffusion when the essential simplifications introduced by setting $Le = 1$, $Pr = 3/4$, are not made.

The practical utility of the coupled assumptions of unit Lewis number and a single, over-all reaction step in complex reaction processes is unknown. The use of relations derivable from Equation 18, in conjunction with an experimental study, should help in providing some insight concerning the utility of these coupled approximations for representative combustible gas mixtures.

Burning of Hydrazine Droplets in Oxygen. As a simple illustration of the use of similarity procedures for studying droplet burning, we consider the burning of a liquid hydrazine droplet in pure oxygen.

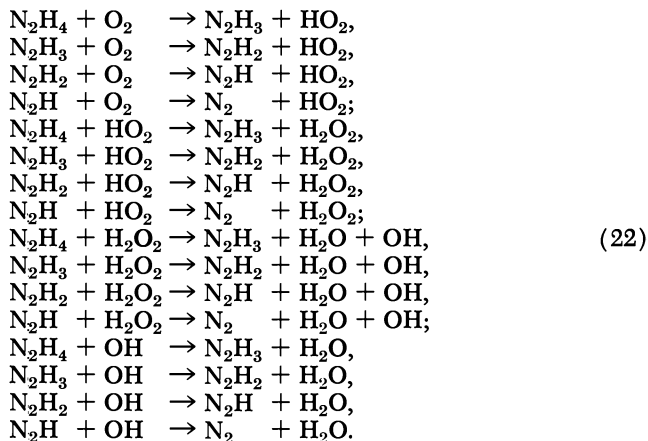
The reaction mechanism for the over-all process



with the over-all rate law

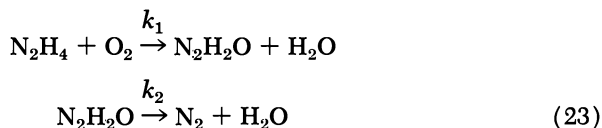
$$-d(\text{N}_2\text{H}_4)/dt = k (\text{N}_2\text{H}_4) (\text{O}_2) \quad (21)$$

has not been studied adequately to allow construction of a complete oxidation mechanism. In particular, no allowance is usually made (10) for the possible production of oxygen-containing compounds of nitrogen. The following simplified reaction scheme contains a description of some of the elementary reaction steps that are expected to occur:



The proposed scheme, in addition to neglecting the possible transient occurrence of nitrogen-oxygen compounds, does not include N, O, and H as reaction intermediates, an assumption which may constitute a reasonable approximation at relatively low temperatures.

The use of the complete similarity relations for the specified 16 reaction steps appears excessively laborious in view of our lack of real knowledge concerning the dominant reaction paths. For this reason, we content ourselves with discussing the expected differences in estimated droplet burning rates when "Reaction" 20 is replaced by the following artificially concocted, highly simplified reaction scheme:



For this two-step process, the basic differential equations are those shown below (Equations 24–29). [The differential equations for the limiting case of the one-step reaction corresponding to Equation 20 may be obtained from Equations 24–29 by making the following identification:

$$w_1 = w_2 = w, Y^*_{N_2H_2O, 2}/Y^*_{N_2H_2O, 1} = Y^*_{H_2O, 2}/Y^*_{H_2O, 1} = 1, T_1^* = T_2^* = T^*/2.]$$

$$L \left(\frac{Y_{N_2H_4}}{Y^*_{N_2H_4, 1}} \right) = -w_1 \tag{24}$$

$$L \left(\frac{Y_{O_2}}{Y^*_{O_2, 1}} \right) = -w_1 \tag{25}$$

$$L \left(\frac{Y_{N_2H_2O}}{Y^*_{N_2H_2O, 1}} \right) = w_1 - w_2 \frac{Y^*_{N_2H_2O, 2}}{Y^*_{N_2H_2O, 1}} \tag{26}$$

$$L \left(\frac{Y_{H_2O}}{Y^*_{H_2O, 1}} \right) = w_1 + w_2 \frac{Y^*_{H_2O, 2}}{Y^*_{H_2O, 1}} \tag{27}$$

$$L \left(\frac{Y_{N_2}}{Y^*_{N_2, 2}} \right) = w_2 \tag{28}$$

$$L \left(\frac{T}{T_1^*} \right) = w_1 + w_2 \left(\frac{T_2^*}{T_1^*} \right) \tag{29}$$

The subscripts 1 and 2 refer to the reaction processes with rate constants k_1 and k_2 , respectively. Representative applicable similarity relations are the following:

$$L \left(\frac{Y_{O_2}}{Y^*_{O_2, 1}} - \frac{Y_{N_2H_4}}{Y^*_{N_2H_4, 1}} \right) = 0 \tag{30}$$

$$L \left[\left(\frac{Y_{H_2O}}{Y^*_{H_2O, 1}} + \frac{Y_{O_2}}{Y^*_{O_2, 1}} \right) \frac{Y^*_{H_2O, 1}}{Y^*_{H_2O, 2}} - \frac{Y_{N_2}}{Y^*_{N_2, 2}} \right] = 0 \tag{31}$$

$$L \left[\left(\frac{Y_{N_2H_2O}}{Y^*_{N_2H_2O, 1}} \right) + \left(\frac{Y_{N_2H_4}}{Y^*_{N_2H_4, 1}} \right) + \left(\frac{Y^*_{N_2H_2O, 2}}{Y^*_{N_2H_2O, 1}} \right) \left(\frac{Y_{N_2}}{Y^*_{N_2, 2}} \right) \right] = 0 \tag{32}$$

and

$$L \left\{ \frac{T}{T_1^* + T_2^*} + \frac{Y_{O_2}}{Y^*_{O_2}} + \left[\frac{Y_{N_2H_2O}}{Y^*_{N_2H_2O, 1}} \frac{T_2^*}{(T_1^* + T_2^*)} \right] - \frac{Y_{N_2}}{Y^*_{N_2, 2}} \left[\frac{T_2^*}{T_1^* + T_2^*} \left(1 - \frac{Y^*_{N_2H_2O, 2}}{Y^*_{N_2H_2O, 1}} \right) \right] \right\} = 0 \tag{33}$$

Here it is easily shown that

$$L() = \frac{d}{dr} [r^2 \rho v()] - \frac{d}{dr} \left[r^2 \rho D \frac{d()}{dr} \right] \tag{34}$$

for a problem with spherical symmetry. Hence, it follows that

$$r^2 \rho v (\eta_i - \eta_{i,r_l}) = r^2 \rho D \frac{d\eta_i}{dr} - \left(r^2 \rho D \frac{d\eta_i}{dr} \right)_{r_l} \text{ for } i = 1, 2, 3, 4, \quad (35)$$

where we have integrated the quantities

$$\begin{aligned} \eta_1 &= \frac{Y_{O_2}}{Y_{O_2,1}^*} - \frac{Y_{N_2H_4}}{Y_{N_2H_4,1}^*} \\ \eta_2 &= \left(\frac{Y_{H_2O}}{Y_{H_2O,1}^*} + \frac{Y_{O_2}}{Y_{O_2,1}^*} \right) \frac{Y_{H_2O,1}^*}{Y_{H_2O,2}^*} - \frac{Y_{N_2}}{Y_{N_2,2}^*} \\ \eta_3 &= \frac{Y_{N_2H_2O}}{Y_{N_2H_2O,1}^*} + \frac{Y_{N_2H_4}}{Y_{N_2H_4,1}^*} + \left(\frac{Y_{N_2H_2O,2}^*}{Y_{N_2H_2O,1}^*} \right) \left(\frac{Y_{N_2}}{Y_{N_2,2}^*} \right) \end{aligned} \quad (36)$$

and

$$\begin{aligned} \eta_4 &= \frac{T}{T_1^* + T_2^*} + \frac{Y_{O_2}}{Y_{O_2,1}^*} + \left[\frac{Y_{N_2H_2O}}{Y_{N_2H_2O,1}^*} \frac{T_2^*}{(T_1^* + T_2^*)} \right] \\ &\quad - \frac{Y_{N_2}}{Y_{N_2,2}^*} \left[\frac{T_2^*}{T_1^* + T_2^*} \left(1 - \frac{Y_{N_2H_2O,2}^*}{Y_{N_2H_2O,1}^*} \right) \right] \end{aligned}$$

between the fuel-droplet surface at $r = r_l$ and an arbitrary station. It is now convenient to replace $r^2 \rho v$ by $\dot{m}_F/4\pi$, where \dot{m}_F is the fuel flux rate at steady burning, whence it follows that Equation 35 may be rewritten in the form

$$\frac{\dot{m}_F}{4\pi} (\eta_i - \eta_{i,r_l}) = r^2 \rho D \frac{d\eta_i}{dr} - \left(r^2 \rho D \frac{d\eta_i}{dr} \right)_{r_l} \text{ for } i = 1, 2, 3, 4. \quad (37)$$

To permit derivation of simplified relations, we introduce the following applicable asymptotic relations:

$$\begin{aligned} \lim_{r \rightarrow \infty} Y_{N_2H_4} &= \lim_{r \rightarrow \infty} (dY_{N_2H_4}/dr) = \lim_{r \rightarrow \infty} Y_{N_2H_2O} = \lim_{r \rightarrow \infty} (dY_{N_2H_2O}/dr) = \\ \lim_{r \rightarrow \infty} Y_{H_2O} &= \lim_{r \rightarrow \infty} Y_{N_2} = \lim_{r \rightarrow r_l} Y_{O_2} = \lim_{r \rightarrow r_l} (dY_{O_2}/dr) = 0. \end{aligned} \quad (38)$$

USEFUL COUPLING FUNCTIONS. For η_1 we find from Equations 36, 37, and 38 the relation

$$\frac{\dot{m}_F}{4\pi} \left(\eta_1 + \frac{Y_{N_2H_4,r_l}}{Y_{N_2H_4,1}^*} \right) = r^2 \rho D \frac{d\eta_1}{dr} + \left(\frac{r^2 \rho D}{Y_{N_2H_4,1}^*} \frac{dY_{N_2H_4}}{dr} \right)_{r_l}.$$

Here the last term is determined by the usual surface boundary condition

$$- \left(r^2 \rho D \frac{dY_{N_2H_4}}{dr} \right)_{r_l} = \frac{\dot{m}_F}{4\pi} (1 - Y_{N_2H_4,r_l}). \quad (39)$$

Therefore, the differential equation for η_1 reduces to the form

$$\frac{\dot{m}_F}{4\pi} \left(\eta_1 + \frac{1}{Y_{N_2H_4,1}^*} \right) = r^2 \rho D \frac{d\eta_1}{dr}. \tag{40}$$

Equation 40 may now be integrated between r_l and $r = \infty$ with the result

$$\dot{m}_F = \frac{4\pi \lambda r_l}{\bar{c}_p} \ln \frac{1 + Y_{N_2H_4,1}^* (Y_{O_2,\infty}/Y_{O_2,1}^*)}{1 - Y_{N_2H_4,r_l}} \tag{41}$$

where we have introduced explicitly the condition $\rho D = \lambda/c_p$ of unit Lewis number. For a known fuel burning rate—*i.e.*, for a known value of \dot{m}_F , Equation 41 determines the hydrazine mass fraction at the droplet surface, $Y_{N_2H_4,r_l}$. It is apparent from Equation 41 that the unobservable limiting case of $Y_{N_2H_4,r_l} = 1$ corresponds to infinite fuel flow rate \dot{m}_F .

A relation between hydrazine and oxygen mass fractions at any radial distance r is obtained from Equation 40 by integrating from r_l to r . The resulting expression is

$$\frac{\dot{m}_F}{4\pi} \left(\frac{1}{r_l} - \frac{1}{r} \right) = \frac{\lambda}{\bar{c}_p} \ln \frac{[(1/Y_{N_2H_4,1}^*) + (Y_{O_2}/Y_{O_2,1}^*) - (Y_{N_2H_4}/Y_{N_2H_4,1}^*)]}{[(1 - Y_{N_2H_4,r_l})/Y_{N_2H_4,1}^*]}. \tag{42}$$

It is apparent from Equations 36, 37, and 38 that

$$\frac{\dot{m}_F}{4\pi} [(\eta_2 - \eta_{2,r_l}) + (Y_{H_2O,r_l}/Y_{H_2O,2}^*) - (Y_{N_2,r_l}/Y_{N_2,2}^*)] = \frac{\lambda}{\bar{c}_p} r^2 \frac{d\eta_2}{dr}$$

whence

$$\dot{m}_F = \frac{4\pi \lambda r_l}{\bar{c}_p} \ln \frac{[(Y_{O_2,\infty}/Y_{O_2,1}^*) (Y_{H_2O,1}^*)]}{(Y_{H_2O,r_l}) - (Y_{N_2,r_l}/Y_{N_2,2}^*) (Y_{H_2O,2}^*)}. \tag{43}$$

Here we have used one of the boundary conditions

$$\left(r^2 \rho D \frac{dY_j}{dr} \right)_{r_l} = Y_{j,r_l} \frac{\dot{m}_F}{4\pi} \text{ for } j = N_2, H_2O \text{ or } N_2H_2O, \tag{44}$$

which apply for the chemical species that are not injected through the interface. Next we integrate the differential equations in η_3 and η_4 with the following results:

$$\dot{m}_F = \frac{4\pi \lambda r_l}{c_p} \times \ln \left\{ \frac{(Y_{N_2H_2O,1}^*/Y_{N_2H_4,1}^*)}{(1 - Y_{N_2H_4,r_l})(Y_{N_2H_2O,1}^*/Y_{N_2H_4,1}^*) - (Y_{N_2H_2O,r_l}) - Y_{N_2,r_l}(Y_{N_2H_2O,2}^*/Y_{N_2,2}^*)} \right\} \tag{45}$$

and

$$\dot{m}_F = \frac{4\pi \lambda r_l}{\bar{c}_p} \ln \left\{ \left[\frac{\Delta l}{\bar{c}_p (T_1^* + T_2^*)} + \frac{T_2^*}{(T_1^* + T_2^*)} \frac{Y_{N_2H_2O, r_l}}{Y_{N_2H_2O, 1}^*} \right. \right. \\ \left. \left. + \frac{T_2^*}{T_1^* + T_2^*} \left(\frac{Y_{N_2H_2O, 2}^*}{Y_{N_2H_2O, 1}^*} - 1 \right) \frac{Y_{N_2, r_l}}{Y_{N_2, 2}^*} \right]^{-1} \left[\frac{T_\infty - T_l}{\bar{c}_p (T_1^* + T_2^*)} \right. \right. \\ \left. \left. + \frac{Y_{O_2, \infty}}{Y_{O_2, 1}^*} + \frac{\Delta l}{\bar{c}_p (T_1^* + T_2^*)} \right] \right\}, \quad (46)$$

respectively. Equation 46 was derived by using the applicable surface boundary condition for the chemical species, as well as the relation

$$\left(4\pi r^2 \lambda \frac{dT}{dr} \right)_{r_l} = \dot{m}_F \Delta l \quad (47)$$

where Δl is the heat of evaporation per unit mass of hydrazine.

Equations 41, 43, 45, and 46 constitute four expressions for the five unknowns \dot{m}_F , $Y_{N_2H_4, r_l}$, $Y_{N_2H_2O, r_l}$, Y_{H_2O, r_l} , and Y_{N_2, r_l} if we assume that the surface temperature T_{r_l} is known or else use the approximation $T_{r_l} \ll T_\infty$. The required fifth relation for solution of the problem is obtained by solving one of the kinetic relations. However, it is possible without completing this difficult program to obtain reasonable bounds on \dot{m}_F , as is shown in the following section.

DROPLET BURNING RATE. The droplet burning rate is derived most conveniently from Equation 46. Here $Y_{O_2, \infty} = 1$ for burning in pure oxygen and T_∞ may be identified with the adiabatic flame temperature, in first approximation. Equation 46 differs from the result obtained for the one-step reaction through the occurrence of the terms involving $Y_{N_2H_2O, r_l}$ and Y_{N_2, r_l} . [The correct limiting case for the one-step reaction is readily obtained from Equation 46 by making the substitutions $Y_{N_2H_2O, r_l} = 0$ and $Y_{N_2H_2O, 2}^* = Y_{N_2H_2O, 1}^*$.]

We may obtain from Equation 46 reasonable bounds on \dot{m}_F for interesting limiting cases in which the chemical reactions go to completion (*i.e.*, $T_1^* + T_2^*$ is fixed). For example, if the first step in the two-step reaction is very fast and the second step is very slow, then $Y_{N_2, r_l} \sim 0$ and $Y_{N_2H_2O, r_l} < 46/64 \simeq 0.72$; similarly, if both the first and the second steps are exceedingly fast, then $Y_{N_2H_2O, r_l} \sim 0$ and $Y_{N_2, r_l} < 28/64 \simeq 0.44$; finally, if the first step is very slow, then $Y_{N_2H_2O, r_l} \sim Y_{N_2, r_l} \sim 0$.

Using, for example, the numerical values $\Delta l = 314$ cal./gram, $\bar{c}_p = 0.36$ cal./gram-°K., $T_1^* = T_2^* = 2000^\circ\text{K.}$, $(T_\infty - T_{r_l})/T_2^* = 2$, $Y_{O_2, \infty} = 1$, we obtain the following results:

$$(\dot{m}_F \bar{c}_p / 4\pi \lambda r_l):$$

3.13 for $Y_{N_2, r_l} = Y_{N_2H_2O, r_l} = 0$, corresponding to an upper bound for very small values of w_1 (with or without small values of

w_2) and to the limiting result (which is altogether independent of w) for the one-step reaction of Equation 20, with equivalent heat release;

- 2.21 for $Y_{N_2, r_l} = 0$ and $Y_{N_2H_2O, r_l} = 0.72$, corresponding to a lower bound for the limiting case in which the first step is very fast and the second step is very slow;
- 2.63 for $Y_{N_2H_2O, r_l} = 0$ and $Y_{N_2, r_l} = 0.44$, corresponding to a lower bound for the limiting case in which both the first and the second steps are exceedingly fast.

Thus, we find a remarkable lack of sensitivity for the calculated burning rates of an adiabatic droplet-burning process in which the reactions go to completion. This observed lack of sensitivity to reaction rates may well be related to the known successes (11, 12, 22) of simplified diffusion-flame theories in theoretical "predictions" of droplet burning rates.

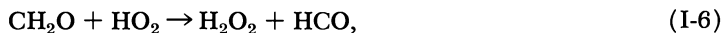
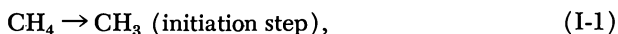
Acknowledgments

This work was supported by Grant No. DA-ARO(D)-31-124-G747 from the Chemistry Branch of the U. S. Army Research Office. The author is indebted to F. A. Williams for making helpful critical comments on a preliminary version of this manuscript.

Appendix

I. Some Observations on the Use of the Steady-State Approximation in Complex Reactions

Methane oxidation is among the more widely studied combustion reactions. Based largely on the work of Semenov *et al.* (6) the following summary mechanism has recently been proposed by a group of knowledgeable authors (2):

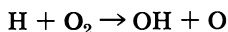




The over-all rate of removal of methane is said to be determined largely by Process I-3; Reactions I-9 and I-10 determine the rate of production of CO_2 ; Reactions I-5, I-6, and I-7 determine the consumption rate of formaldehyde. The sum of the production rates of CO and CO_2 may then be expressed in terms of a relation involving the concentrations of CH_2O , O_2 , CO_2 , CH_4 , and various rate coefficients. Removal of H atoms is stated to occur by the third-order process:



(where M is any third body) rather than by the chain-branching process



at least in the interesting temperature range.

For analytical studies involving the interplay of flow processes and chemical reactions, we require a set of chemically balanced equations that lead from the known reactants to the measured reaction products. For the *complete* oxidation of CH_4 , this last statement implies that we need a reaction scheme producing only H_2O and CO_2 . This requirement is incompatible with Equations I-1 to I-10. To achieve consistency, we first replace Equation I-1 by the balanced process



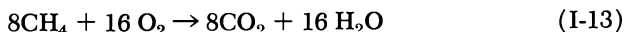
and then add arbitrarily the following "over-all" reactions for the removal of H_2O_2 and H:



and



We may now inquire if Reactions I-1 to I-12 may be made compatible with the over-all reaction



by introducing a steady-state approximation for all of the other chemical species, which are then considered to be reaction intermediates. A simple procedure for testing this idea involves the imposition of conditions leading to zero net change for all intermediates. For example, if Reaction 1a occurs a times, and Reactions 2 to 12 are taken to occur b , c , d , e , f , g ,

i , j , k , l , and m times, respectively, the condition that no net production of CH_3 occurs leads to the relation

$$b = a + c + d + 2l \quad (\text{I-14})$$

Similarly, the conditions that no net production or removal occur for CH_2O , OH , HO_2 , H_2O_2 , HCO , H , and CO , lead to the following equations:

$$e + f + g = b, \quad (\text{I-15})$$

$$c + e + j = b + k, \quad (\text{I-16})$$

$$d + f + k = g + i, \quad (\text{I-17})$$

$$l = d + f, \quad (\text{I-18})$$

$$i = e + f + g, \quad (\text{I-19})$$

$$4m = a + j \quad (\text{I-20})$$

$$j + k = i; \quad (\text{I-21})$$

finally, Equations I-1a and I-2 to I-12 are consistent with Equation I-13 only if the following additional constraints are met:

$$a + c + d + 2l = 8, \quad (\text{I-22})$$

$$b + g + i + m = 16, \quad (\text{I-23})$$

$$j + k = 8, \quad (\text{I-24})$$

$$c + 2l + 2m + e = 16. \quad (\text{I-25})$$

Equations I-14 to I-25 constitute a set of 12 equations in 12 unknowns for which no positive definite values exist, except for an unacceptable solution in which we set $a = d = f = g = j = l = 0$.

II. Extension of Similarity Analyses to Gas Mixtures with Large Differences in $c_{p,i}$

Flows with Chemical Reactions in Constant-Area Channels. For gas mixtures containing chemical species with highly variable values of $c_{p,i}$, it is desirable to modify the analysis given in the main text by replacing Equation 5 by the following expressions:

$$h_s = (v^2/2) + \sum_i Y_i (h_i^\circ + c_{p,i} T) = h_i^\circ + \left(\sum_i Y_i c_{p,i} \right) T + (v^2/2), \quad (\text{II-1})$$

$$T_s = T + v^2 \left(2 \sum_i Y_i c_{p,i} \right)^{-1},$$

where

$$\lambda/\rho \bar{c}_p D = 1, \lambda/\mu \bar{c}_p = 4/3, \rho D =$$

$$\lambda/\bar{c}_p = \text{constant}, \bar{c}_{p,i} = \text{constant}, \quad (\text{II-2})$$

$$\bar{c}_p = \sum_i Y_i c_{p,i} \neq \text{constant}.$$

Proceeding now as in the derivation of Equation 8, this expression is replaced by the relation

$$\frac{d}{dx} [\rho v (\sum_1 Y_i c_{p,i}) T_s] - \frac{d}{dx} \left\{ \frac{\lambda}{\bar{c}_p} \left[\frac{d}{dx} (\sum_1 Y_i c_{p,i}) T_s \right] \right\} = - \frac{d}{dx} \{ \rho v \sum_1 h_i^\circ Y_i [1 + (V_i/v)] \} \quad (\text{II-3})$$

while the continuity equation (*cf.* Equation 9) becomes

$$\frac{d}{dx} \{ \rho v Y_i [1 + (V_i/v)] \} = \dot{w}_i \quad (\text{II-4})$$

Combining Equations II-3 and II-4 then leads to the result

$$\frac{d}{dx} [\rho v (\sum_1 Y_i c_{p,i}) T_s] - \frac{d}{dx} \left\{ \frac{\lambda}{\bar{c}_p} \frac{d}{dx} [(\sum_1 Y_i c_{p,i}) T_s] \right\} = - \sum_1 h_i^\circ \dot{w}_i \quad (\text{II-5})$$

The use of Equations 12 and 13 now allows us to rewrite Equation II-5 in the form

$$L \{ (\sum_1 Y_i c_{p,i}) T_s \} = - \sum_1 h_i^\circ \dot{w}_i \equiv w \Delta l^* \quad (\text{II-6})$$

where

$$\Delta l^* = (h_{O^\circ} Y_{O^*} + h_{F^\circ} Y_{F^*} - h_{P^\circ} Y_{P^*} - h_{P'^\circ} Y_{P'^*}) \quad (\text{II-7})$$

for the one-step reaction described in Equation 1. The applicable similarity relations given in Equation 14 become, therefore,

$$L \{ \sum_1 Y_i c_{p,i} T_s / \Delta l^* \} = w, \quad L(\tilde{Y}_i) = \pm w, \quad (\text{II-8})$$

i.e., the parameter T_s is to be replaced everywhere by the quantity $\sum_1 (Y_i c_{p,i} T_s / \Delta l^*)$ for gas mixtures containing constituents with greatly different values for the isobaric specific heats $c_{p,i}$.

Droplet Burning. An analysis completely analogous to that described in Appendix IIA leads to the conclusion that the terms T/T_j^* ($j = 1, 2$) in Equations 29 *et seq.* should be replaced by $\sum_1 Y_i c_{p,i} T_j / \Delta l_j^*$ where j ($j = 1$ or 2) refers to either of the chemical processes described by Equation 22 or 23. Also

$$\Delta l_1^* = h^\circ_{N_2H_4} Y^*_{N_2H_4} + h^\circ_{O_2} Y^*_{O_2} - h^\circ_{N_2H_2O} Y^*_{N_2H_2O} - h^\circ_{H_2O} Y^*_{H_2O} \quad \text{and} \quad (\text{II-9})$$

$$\Delta l_2^* = h^\circ_{N_2H_2O} Y^*_{N_2H_2O} - h^\circ_{N_2} Y^*_{N_2} - h^\circ_{H_2O} Y^*_{H_2O}$$

Literature Cited

- (1) Altman, D., Penner, S. S., "Combustion Processes," pp. 470-488, Princeton University Press, Princeton, N. J., 1956.
- (2) Blundell, R. V., Cook, W. G. A., Hoare, D. E., Milne, G. S., *Symp. Combust. 10th, Univ. Cambridge, Cambridge, Engl., 1964*, 445-452 (1965).
- (3) Campbell, E. S., Hirschfelder, J. O., Shalit, L. M., *Symp. Combust. 7th, London, Oxford, 1958*, 332-338 (1959).
- (4) Harje, David T., *AGARD Colloq. Advan. Tactical Rocket Propulsion*, pp. 267-286, Technivision Services, Maidenhead, England, 1968.
- (5) Jost, W., "Explosion and Combustion Processes in Gases," McGraw-Hill, New York, 1946.
- (6) Karmilova, L. V., Enikolopyan, N. S., Nalleandyan, A. B., Semenov, N. N., *Zh. Fiz. Khim.* **34**, 1176 (1960).
- (7) Kondrat'ev, V. N., "Chemical Kinetics of Gas Reactions," Pergamon Press, Ltd., London, 1964.
- (8) Lees, L., "Combustion and Propulsions: Third AGARD Colloquium," pp. 451-498, Pergamon Press, New York, 1958.
- (9) Lewis, B., von Elbe, G., "Combustion, Flames and Explosions of Gases," Academic Press, New York, 1951.
- (10) Minkoff, G. J., Tipper, C. F. H., "Chemistry of Combustion Reactions," pp. 196-197, Butterworths, London, 1962.
- (11) Penner, S. S., "Chemical Rocket Propulsion and Combustion Research," Chap. 3, Gordon and Breach, New York, 1962.
- (12) Penner, S. S., "Chemistry Problems in Jet Propulsion," Chap. XXI-XXVI, Pergamon Press, London, 1957.
- (13) *Ibid.*, p. 239, Equation 23.
- (14) Penner, S. S., Davidor, W., *Proc. Heat Transfer Fluid Mechanics Inst.*, 1967, 233.
- (15) Penner, S. S., Libby, P. A., *Astronautica Acta* **13**, 75 (1967).
- (16) Penner, S. S., Mullins, B. P., "Explosions, Detonations, Flammability, and Ignition," Chap. VII, IX-XIV, Pergamon Press, London, 1959.
- (17) Penner, S. S., Williams, F. A., "Explosions, Detonation, Flammability and Ignition," pp. 101-107, Pergamon Press, London, 1959.
- (18) Rupe, J. H., *Progr. Rept.* **20-195**, **20-209**, **20-299**; *Tech. Rept.* **32-207**, Jet Propulsion Laboratory, California Institute of Technology, Pasadena (1956-1962).
- (19) Semenov, N. N., "Some Problems in Chemical Kinetics and Reactivity," transl. by N. Boudart, Vols. I, II, Princeton Univ. Press, Princeton, N. J., 1958.
- (20) Von Kármán, Th., Penner, S. S., "Selected Combustion Problems, Fundamentals and Aeronautical Applications," pp. 1-41, Butterworths, London, 1954.
- (21) Von Kármán, Th., *Symp. Combust. 6th, Yale Univ., 1956*, 1-11 (1957).
- (22) Williams, F. A., "Combustion Theory," Chap. II, Addison-Wesley, Reading, Mass., 1965.

RECEIVED May 4, 1967.

INDEX

A	
Accelerated aging	115
tests	231
Activation energy	248
Additives for altering burning rate	54
Additives and modifiers	91
Adhesives	34
Adiabatic-compression sensitivity test	365
Adiabatic flame temperature	45
Advanced fuels and oxidizers	316
Advanced oxidizers	321
Agglomerates, mixing time <i>vs.</i> breakup of	7
Aggravated aging	76
Aging	231
accelerated	115
aggravated	76
humidity	113
propellant degradation during ..	232
of solid propellants	188
stability of polyurethane propellants	112
thermal	114
Air dispersion powder filling apparatus	15
Aluminum	31, 51
Ammonia-perchloric acid	264
reaction zone	271
Ammonium perchlorate	3, 30
decomposition of	246
Analog propellant	259
Anisotropy	226
A/PA	264
Arcite	38
Arrhenius plot	233, 238
Asphalt	84
Autoignition temperature	59
Aziridines	129, 135
B	
Ballistics	116
properties of CTPB propellants ..	158
Beryllium	31
Biaxial correction factor	221
Binder	166
components, propellant	87
crosslinked polymeric	197
decomposition of	249
effect of elastic modulus of	101
-filler interaction	106
-filler interface	199
Binders	84
chemistry of propellants based on chemically crosslinked	67
Binders (Continued)	
solid propellants based on polybutadiene	122
Biot's theory	22
BIPA	163
BISA	163
BITA	163
Blending	10
Bonding agent on propellant mechanical properties, effect of ..	112
Bonding of propellants	144
Booster application	306
British detergent	38
Brittle temperature	75
Bromine-oxygen compounds	327
Bulk degradation	248
Burning	
of hydrazine droplets	378
mechanism of	245
rate .. 46, 120, 251, 272, 277, 279,	355
additives for altering	54
low pressure	275
metal wires to increase	56
particle size <i>vs.</i>	253
of PVC plastisol propellant ..	48
Butadiene propellants, compositions of high energy	123
Butarez CTL	163
C	
Carboxyl groups, prepolymer containing	81
Card-gap test	59, 367
Case bonding	34
Cast double-base propellant, manufacture of	1
Casting	16
powder	
composite-modified	2
double-base	2
manufacture of	4
parameters	12
single-base	2
theory of	18
Cavity formation	111
Centrifuge tests	359
Characterization of liquid propellants	344
Charge manufacture, propellant ..	14
Chemical	
compatibility of liquid propellants	344
crosslinking	31
reaction rate	271
stability	358
of fuels	340

Chemistry of propellants based on chemically crosslinked binders	67	Detonation, deflagrative reaction <i>vs.</i>	298
Chemorheological methods	239	Dewetting	199
Chlorine oxides	327	Dielectric heating	42
Chlorine oxygen fluorides	331	Diffusional mixing	264
Classed propellant explosive	59	Diffusion equation	374
Colloided spheroidal nitrocellulose	30	Diffusion flame	250
Columnar diffusion flame model	259	model, columnar	259
Combustion		Dilatometer	200, 201, 203
characteristics	305	dual	24
efficiency	249	Dissociative sublimation	247, 266
of liquid propellants	369	Double-base	
products	58	casting powder	2
research, similarity principles in theoretical	369	propellant, composite	197
Compatibility of liquid propellants	357	propellant, manufacturing of cast	1
Complex shear modulus	212	Droplet burning	370, 386
Composite		rate	382
double-base propellants	197	Drop weight test	364
-modified casting powder	2	Drying	9
propellant	67	Dynamic lag	277
solid propellant processing techniques	165	Dynamic testing	211, 214
solid propellants, low pressure burning of	244		
Compositions, typical propellant	2	E	
Constraint parameter	226	Effective bulk	24
Copper chromate	55	Elastic modulus of binder, effect of	101
Coupling functions	377, 380	Electrostatic liner application	183
Critical diameter	367	Electrostatic sensitivity	299
Crosslink density	71, 217	Elongations, ultimate	79
Crosslinked binders, chemistry of propellants based on chemically	67	Embrittlement	231
Crosslinked polymeric binder	197	End-bonded specimens	192
Crosslinkers	89	End-burning grains	57
Crosslinking	78	Energetic fuels	31
Cryogenic propellants	320	Energy equation	267
Crystallization of polymer	75	Energy, mechanism for deriving	336
CTPB	123, 162	Engineering properties	304
propellants, ballistic properties of	158	Epon-X801	163
propellants, curing agents for	128	Epoxides	131, 134
Cumulative damage	227	Equivalence ratio	283
Curing	17, 20, 37, 60	ERLA-0510	163
agents for CTPB propellants	128	Evacuation	16
theory of	18	Exothermic curing reactions	73
Cyclic methylene nitramines	30	Expanding gas flows	371
		Explosive liquids	298
D		Extensometer	191
DDT	298	Extinction	278, 283
Decomposition of ammonium perchlorate	246		
Deflagrative reaction <i>vs.</i> detonation	298	F	
Deformation history	224	Failure criteria	219
Degradation during aging, propellant	232	of solid propellants	188
Densities by various mold-filling techniques	16	Failure strain	221
Density	12	Failure surface	220, 226
of casting powders, solvent <i>vs.</i>	6	parabolic	224
impulse	303	Filler interaction, binder-	106
Depolymerization	79	Filling apparatus, air dispersion powder	15
DER-332	163	Finishing	9
		Fixed launch site systems	307
		Flame	
		propagation	371
		structure	245
		theory, granular diffusion	264
		thickness	272
		gas-phase	278
		Flow, steady one-dimensional	373

Fluorine-based oxidizers	329
Fluoroamino compounds	332
Fluoroxo compounds	330
Formulation of PVC plastisol propellant	44
Formulations, solid propellant ...	197
Fuel, decomposition of	249
Fuels, energetic	31
Fuels and oxidizers, advanced ...	316

G

Gap testing	299
Gasification	265
Gas mixtures, similarity in	385
Gas-phase flame thickness	278
Gelation	338
Gelling agents	339
hydrocolloid	340
Glass transition temperatures	167
Grain design, propellant	4
Granulating	8
Grinding	173-4
Granular diffusion flame theory ..	251, 264

H

Halogen fluorides	333
Halogen-oxygen compounds	326
Hazard testing of liquid propellants	296, 344
HC-434	163
Heat of combustion	319
Heat of polymerization	73
Heat generation	213
Heterogeneous fuels	334
Heterogeneous reaction	263
High energy butadiene propellants, composition of	123
High explosive, solid propellant vs.	297
Humidity aging	113
Hycar CTB	163
Hydrocolloid gelling agents	340
Hydrolytic cleavage	87
Hydrostatic pressure	225
Hydrazine	369
droplets, burning of	378

I

IDP	163
Ignition	371
Impact testing	298
Inert diluent process	33
Inhibitor	63
Injectors	369
Instability behavior	277
Insulating	182
Iodine-oxygen compounds	327
Isocyanates	90

J

Jacketed compressibility	25
JANAF specimen	191

K

Kinetic rates	248
---------------------	-----

L

Lab scale testing	362
Larger scale testing	366
Lewis number	374
Limiting molecular weight	71
Liner application, electrostatic	183
Liners	34, 115
Lining	182
Liquid bipropellant applications ..	312
Liquid propellants characterization, chemical com- patibility, storability, and hazard testing of	344
combustion of	369
prepackaged	347
storability and compatibility of systems	357
Liquid ranges	309, 310
Long term tests	360
Loss modulus	212
Low pressure burning of composite solid propellants	244
Low pressure burning rates	275

M

Macaroni operation	7
Magnesium	51
MAPO	163
Matrix, influence of	100
Mechanical properties	99
effect of bonding agent on propellant	112
stability	359
stabilization	337
strength	73
Mechanism for deriving energy ..	336
Metal as an ingredient	51
Metal hydrides	31
Metals, finely divided	81
Metal wires to increase burning rate	56
Methane oxidation	383
Microstructure data for prepolymers	89
Military applications	306
Miner's Law	228
Mixer comparisons	180-1
Mixing	5
pneumatic	185
propellant	176
time vs. breakup of agglomerates	7
Mobile weapon systems	307
Modifiers and additives	91
Moisture embrittlement	102
Moisture and volatiles	12
Mold filling	14
techniques, densities by various	16
Molten fuel	284
Molten surface	245
Monomer formation	249

Rheological properties	351	Stress-strain cycling	203
Rheology	341	Strip biaxial test	205
Robane	163	Structural failure of solid propellants	189
Rocket propellants, liquid	301	Subatmospheric pressures	282
S			
Safe storage life	233	Sublimation, dissociative	266
Safety characteristics of PVC plastisol propellant	58	Superperoxides	327
Screen loading density	13	Surface decomposition	245
Screw extrusion	61	Surface temperature	278
cure	40	Swelling	14, 217
Second-order transition	75	T	
Shvab-Zeldovich procedure	373	TEAT	163
Silver wires	56	Telagen CT	163
Similarity in gas mixtures	385	Temperature, physical properties <i>vs.</i>	44
Similarity principles in theoretical combustion research	369	Terpolymer	80
Similarity relations	373, 378	Testing, hazard	296
Simple shear test	206	Testing solid propellants	188
Single-base casting powder	2	Thermal aging	114
Slurry	29	cleavage	86
viscosities	352	cycling	227
Sol fraction	217	layer theory	261
Solid composite propellants	82	wave thickness	278
Solid-phase reactions	246, 263	Time-temperature equivalence ..	212
Solid propellant based on polybutadiene binders	122	Trauzl test	364
formulations	197	Two-temperature postulate	246
<i>vs.</i> high explosive	297	U	
low pressure burning of composite	244	UDMH	369
mechanical properties	188	Ultimate elongations	79
plasticizers used in	90	Uniaxial failure envelope	221
processing techniques	165	Uniaxial test	190
Solvent pressures	17, 24	Uniformity	13
Solvent <i>vs.</i> density of casting powder	6	Unmixedness	257
Spacecraft control	307	Unsaturated polyester	77
Space exploration	306	Upper stage propellants	306
Specific impulse	45, 116, 302, 316	Urethane reaction	85
of selected propellant systems, theoretical	309	Useful life	231
theoretical	335	V	
Spherical flaw growth	230	Vibration tests	360
Spheroidal nitrocellulose	32	Viscoelastic materials	194
colloided	30	Viscometers	169, 171
Spray burning	371	Viscosity	31, 299
Stability of fuels, chemical	340	of PVC plastisol	39
Stability of polyurethane pro- pellants, aging	112	Volatile component	76
Stabilizer, PVC	39	Volatiles, moisture and	12
Stabilizers	30	Volume change	26
Steady one-dimensional flow	373	W	
Steady-state approximation	372	Weight average particle size	47
Storability of liquid propellants ..	344, 357	Wetting agent	39
Storable propellants	320	Y	
Storage characteristics	76	Yield stress	351
Storage modulus	212		
Strand burner	356		